Common Diagnostic Pitfalls in Thyroid Cytopathology

Adebowale J. Adeniran
David Chhieng

Springer

Common Diagnostic Pitfalls in Thyroid Cytopathology

Adebowale J. Adeniran • David Chhieng

Common Diagnostic Pitfalls in Thyroid Cytopathology

Springer

Adebowale J. Adeniran
Department of Pathology
Yale University School of Medicine
New Haven, CT, USA

David Chhieng
Department of Pathology
Mount Sinai Health System
New York, NY, USA

ISBN 978-3-319-31600-0 ISBN 978-3-319-31602-4 (eBook)
DOI 10.1007/978-3-319-31602-4

Library of Congress Control Number: 2016937359

Printed on acid-free paper

This Springer imprint is published by Springer Nature
The registered company is Springer International Publishing AG Switzerland

To my parents, for their unfailing love and constancy and all the sacrifice during the days of little beginning. To my wife, Olabisi, for her unwavering support, patience and enduring love. To my precious children, Oluwademilade, Temiladeoluwa and Titiladeoluwa, for their understanding.

– Adebowale J. Adeniran

Contents

Aspirates with Macrophages and/or Colloid Only

1

Case Study

A 63-year-old male presented for evaluation of primary hyperparathyroidism. He had recurrent kidney stones for several years and was noted to have hypercalcemia 4 years prior. His presenting symptoms included fatigue and muscle pain. He had no complaints of hoarseness, dysphagia, or difficulty breathing. He had no history of radiation treatment to the head or neck. He had no family history of kidney stones. Examination revealed a normal thyroid gland with no palpable mass. There was no cervical or supraclavicular lymphadenopathy. His serum calcium and parathyroid hormone levels were 10.7 mg/dL and 109 pg/mL, respectively. Ultrasonographic examination revealed a thyroid with normal echotexture. The left thyroid lobe contained a 1.2 cm heterogeneous cystic and solid nodule. Fine needle aspiration of the left lobe cyst showed abundant colloid and macrophages and no follicular epithelial cells. Patient was later scheduled for parathyroidectomy with intraoperative PTH measurements and showed an uneventful postoperative course.

Discussion

The National Cancer Institute (NCI) Thyroid Fine Needle Aspiration State of the Science Conference concluded that thyroid FNA specimens with abundant histiocytes and few to no follicular cells should be interpreted as "cyst fluid only," under the category of "nondiagnostic" [1, 2]. Numerous histiocytes can be seen in a variety of hyperplastic and neoplastic benign and malignant thyroid nodules undergoing cystic degeneration. Typically, such cystic degeneration is seen on smears of fine needle aspiration as numerous foamy macrophages, hemosiderin-laden macrophages, and scant colloid (Figs. 1.1, 1.2, 1.3, 1.4, 1.5, and 1.6). The frequent hemorrhage and cyst formation in benign colloid nodules most likely reflect a fundamental difference in the organization of the vasculature of benign colloid nodules, when compared to follicular neoplasms [3]. The rate of malignancy in thyroid cysts is low.

A.J. Adeniran, D. Chhieng, *Common Diagnostic Pitfalls in Thyroid Cytopathology*, DOI 10.1007/978-3-319-31602-4_1

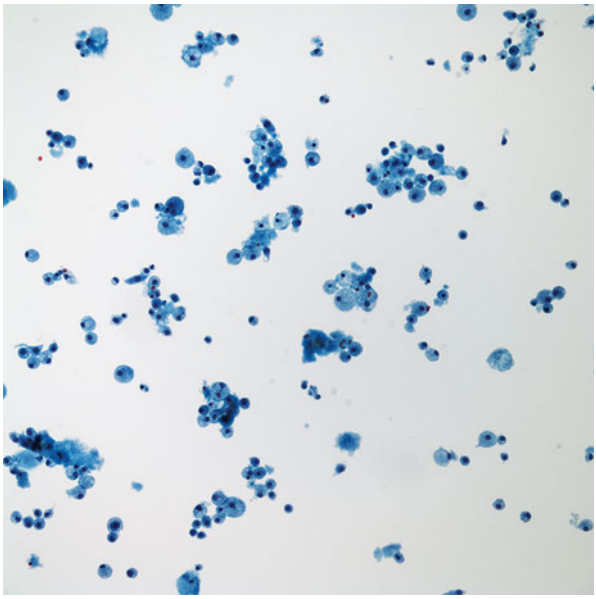

Fig. 1.1 Cystic degeneration in a hyperplastic nodule. Numerous foamy macrophages (Papanicolaou stain, X200)

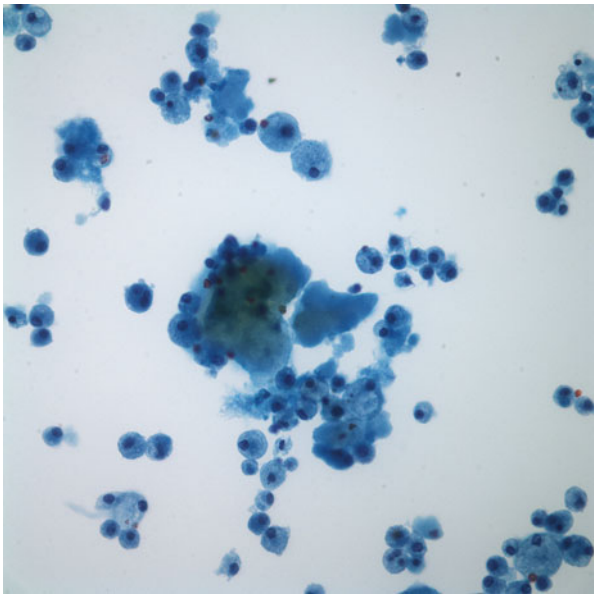

Fig. 1.2 Cystic degeneration in a hyperplastic nodule. Numerous foamy macrophages and scant colloid (Papanicolaou stain, X400)

This rate increases with size and complexity. Given the extremely low potential of malignancy in such FNA, it has been suggested that a diagnosis of "cyst fluid only" is more informative than unsatisfactory, as this indicates that a cyst has been aspirated even though the etiology is uncertain. An optional recommendation for

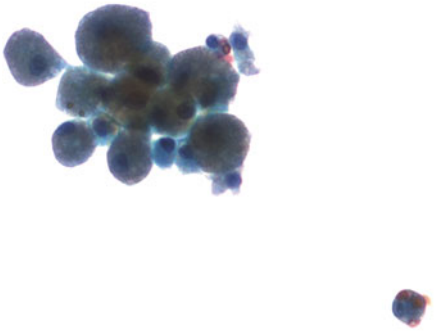

Fig. 1.3 Cystic degeneration in a hyperplastic nodule. Hemosiderin-laden macrophages (Papanicolaou stain, X400)

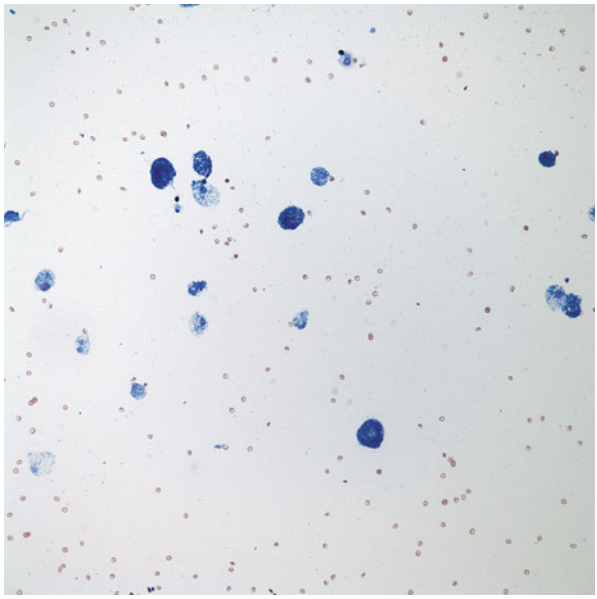

Fig. 1.4 Cystic degeneration in a hyperplastic nodule. Hemosiderin-laden macrophages (Diff-Quik stain, X200)

correlation with the cyst size and complexity and a disclaimer that a cystic carcinoma cannot be entirely excluded may be added [4]. In such cases, the decision for surgical intervention is based on factors such as clinical and imaging findings, cyst recurrence after aspiration, surgeon's judgment, and patient's preference.

Thyroid cysts are mostly benign. However, cysts are well-known causes of false-negative results. Risk factors for malignancy include large cysts (>3 cm), recurrent cysts, cysts in young males, and history of radiation [5].

It is recommended that stringent criteria be used for the interpretation of cyst fluid only. The use of this term should be restricted to cases that present with abundant macrophages and/or pigmented macrophages and inadequate number of follicular cells [1, 6].

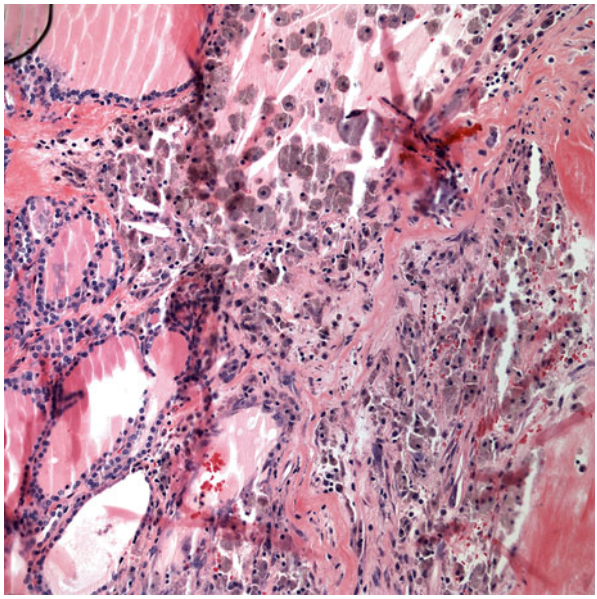

Fig. 1.5 Abundant macrophages in cystic degeneration in a hyperplastic nodule (H&E stain, X200)

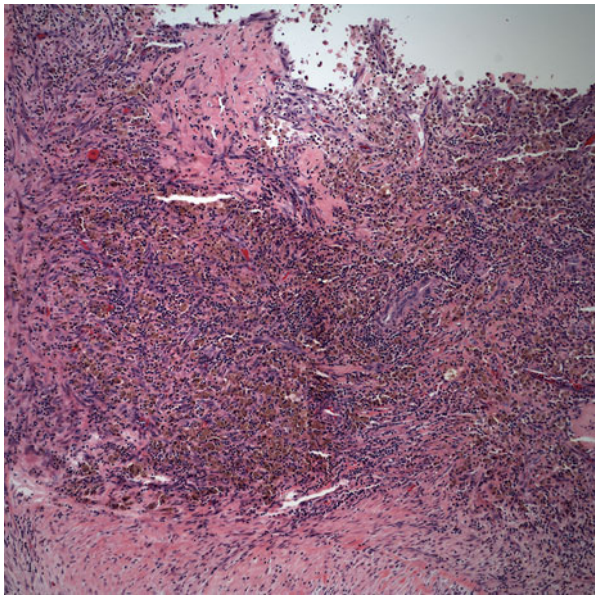

Fig. 1.6 Abundant macrophages and granulation tissue in cystic degeneration in a hyperplastic nodule (H&E stain, X200)

The amount of colloid and the number of macrophages are not predictive of a malignant histologic outcome. The sole morphologic feature of malignancy is the presence of atypical features in follicular epithelium [1]. This follicular epithelium atypia can often be confused with atypia in cyst lining cells, which resemble classic epithelial repair [7] (Figs. 1.7 and 1.8). Cases with the presence of atypical follicular

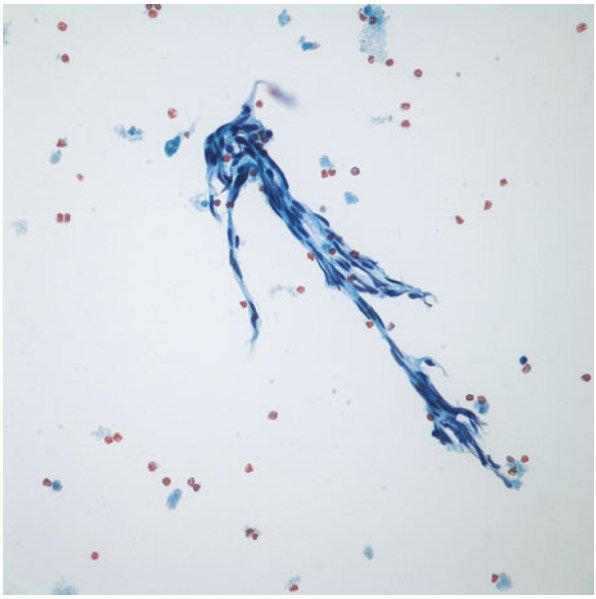

Fig. 1.7 Cyst lining cells with reparative changes (Papanicolaou stain, X400)

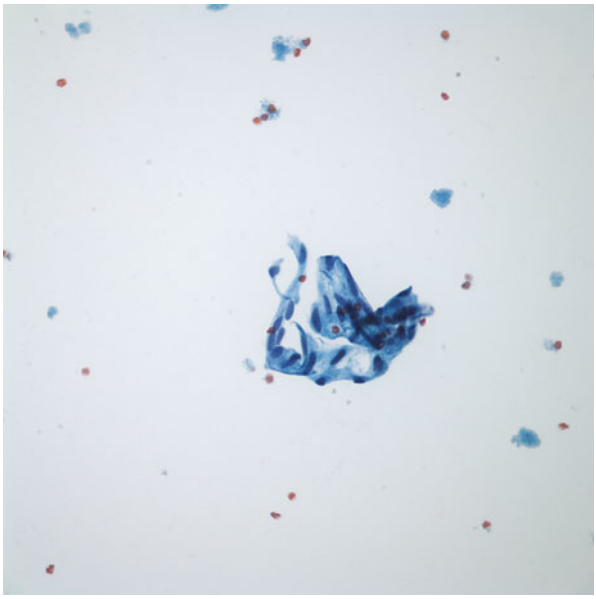

Fig. 1.8 Cyst lining cells with reparative changes. This may be confused with follicular epithelial cell atypia (Papanicolaou stain, X400)

epithelial cells even in the absence of adequate cellularity should be called atypical or suspicious rather than nondiagnostic or cyst fluid only [1]. The majority of thyroid cysts are in fact pseudocysts because they lack an epithelial lining. These pseudocysts result from degeneration in goiters. Large collections of colloid can also form cystic colloid nodules or colloid cysts (Figs. 1.9, 1.10, 1.11, and 1.12).

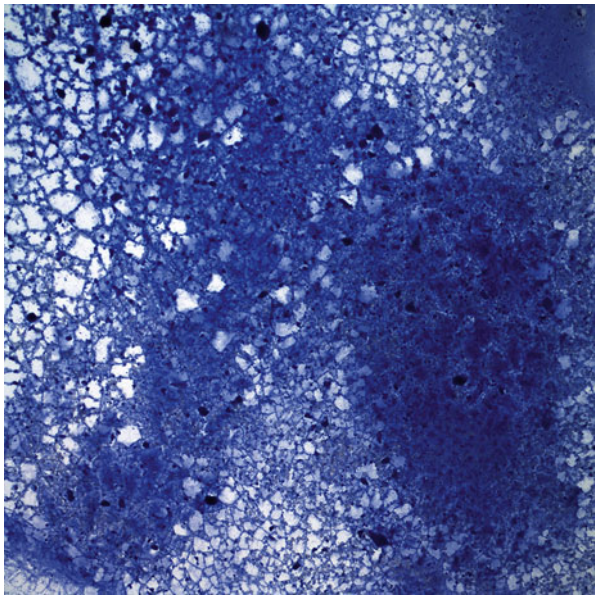

Fig. 1.9 Abundant colloid in a colloid cyst (Diff-Quik stain, X100)

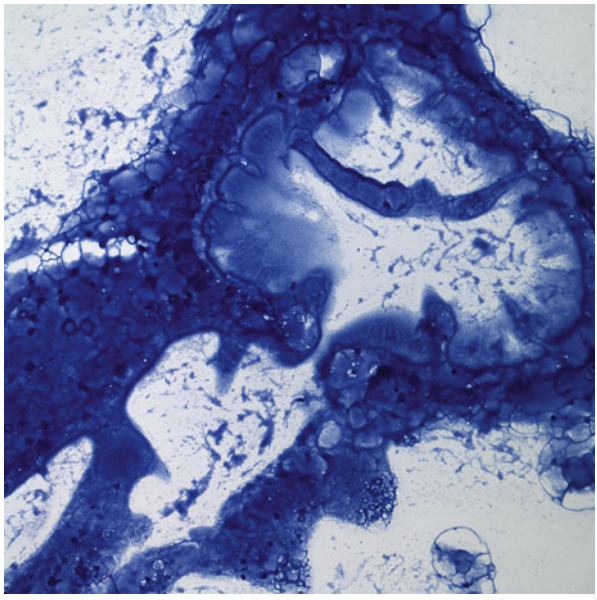

Fig. 1.10 Abundant colloid in a colloid cyst (Diff-Quik stain, X200)

An interpretation of a colloid nodule in which there is abundant, thick colloid present does not require a minimum number of follicular cells [8].

If macrophages only are present on a smear, it is imperative that other causes of cystic neck mass such as branchial cleft cyst, epidermal inclusion cyst, lymphoepithelial cyst, and thyroglossal duct cyst be excluded. Thyroglossal duct cyst is the

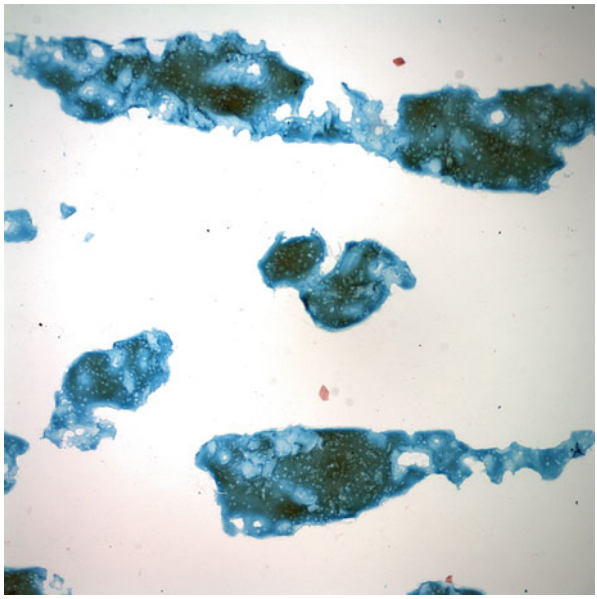

Fig. 1.11 Abundant colloid in a colloid cyst (Papanicolaou stain, X100)

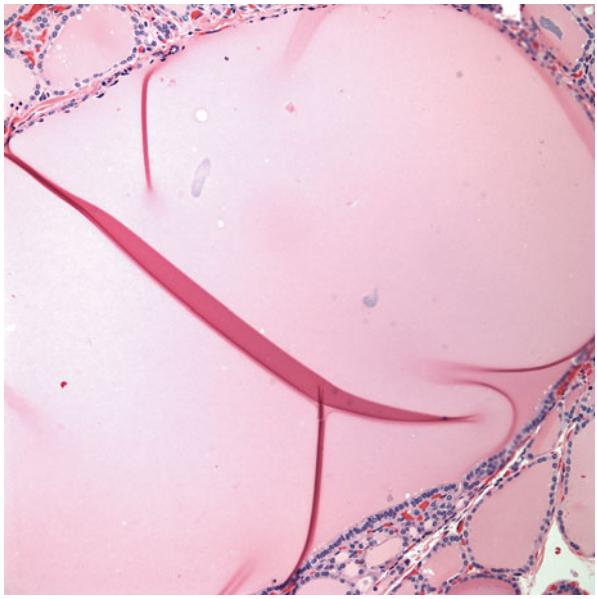

Fig. 1.12 Histologic appearance of a colloid cyst (H&E stain, X200)

most common congenital abnormality in the neck [9, 10]. It occurs in or near the thyroid gland, and it can present as a solitary nodule. Histologically, it contains an epithelial lining of squamous or pseudostratified ciliated columnar epithelium (Fig. 1.13) and ectopic thyroid gland tissue, which is usually found in the duct wall. The FNA specimen typically consists of cystic fluid containing macrophages,

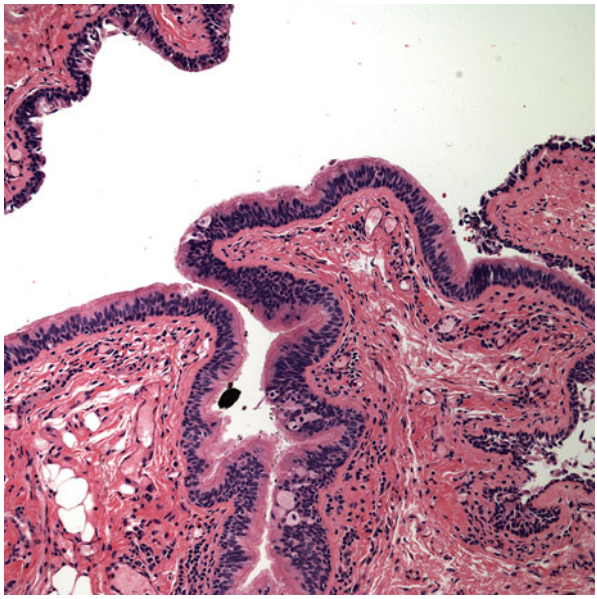

Fig. 1.13 Thyroglossal duct cyst is lined by pseudostratified ciliated columnar epithelium (H&E stain, X200)

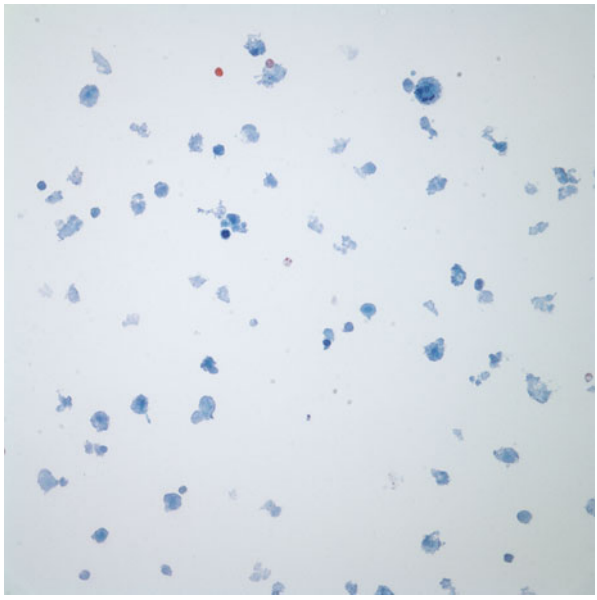

Fig. 1.14 Thyroglossal duct cyst, FNA. Foamy macrophages, lymphocytes, and cystic debris (Papanicolaou stain, X400)

neutrophils, and scant epithelial cells in a mucoid or proteinaceous background [9] (Fig. 1.14). Squamous cells are the most frequent epithelial cells seen, and ciliated columnar cells are occasionally found [11]. Rare thyroid follicular cells may be seen. The absence of epithelial cells may lead to underdiagnosis of this entity as the macrophages and proteinaceous background are only interpreted as being

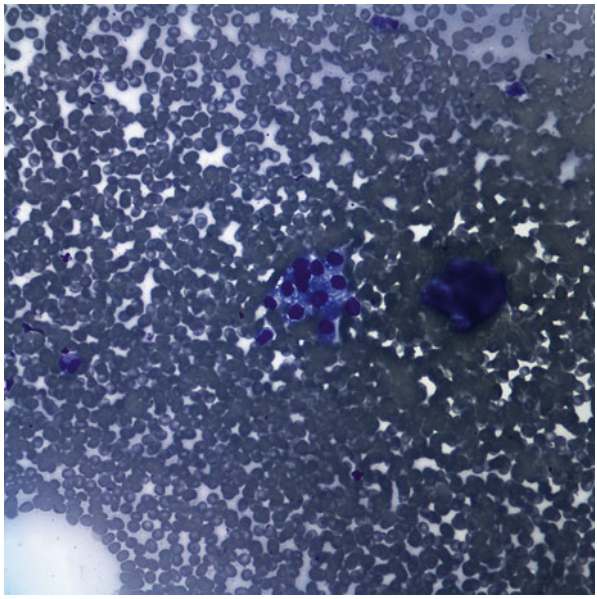

Fig. 1.15 Cluster of atypical histiocytoid cells including cells with vacuolated cytoplasm (Diff-Quik stain, X400)

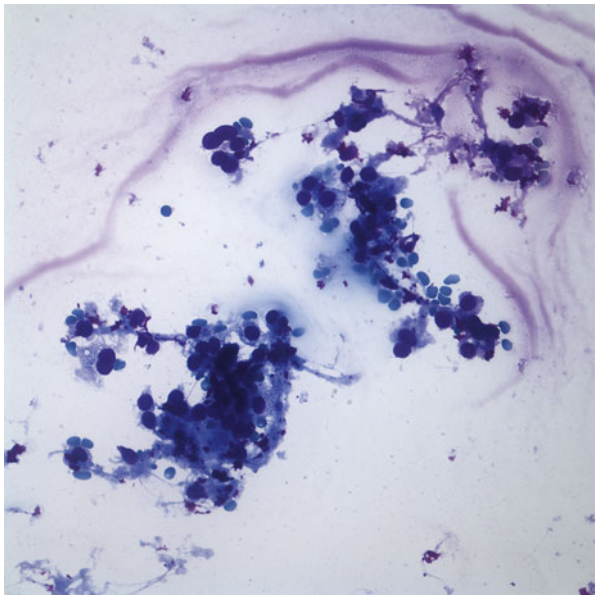

Fig. 1.16 Clusters of atypical histiocytoid cells including cells with vacuolated cytoplasm and enlarged, irregular nuclei (Diff-Quik stain, X400)

consistent with cystic debris. It is essential that the correct diagnosis is made and the lesion excised, as secondary carcinoma has been reported in the background of thyroglossal duct cyst [9, 12].

Papillary carcinoma is the most common cystic thyroid cancer. Cells typically have a histiocytoid appearance with vacuolated cytoplasm (Figs. 1.15 and 1.16) and

usually have the typical nuclear features of papillary carcinoma. Follicular neoplasms such as follicular adenoma, follicular carcinoma, and Hürthle cell neoplasms can also be cystic [5, 13, 14]. Initially, the fluid is grossly bloody and appears red. Later there is degeneration of the blood into a chocolate brown fluid containing hemosiderin. It subsequently becomes green and turbid, and finally the fluid becomes clear and yellow. The gross appearance of the cysts fluid is not helpful to determine whether the lesion is malignant or not [5, 15–17]. Giant cells with foamy cytoplasm are also relatively common. Inflammatory cells may also be present, so also are cholesterol crystals and granular debris.

In patients with PTC, the presence of a cystic lymph node by ultrasonographic examination is highly suggestive of locally metastatic disease. In our experience, a cystic neck lymph node in a patient with a history of PTC even in the absence of follicular epithelial cells by FNA is almost always metastatic disease. Confirmation of metastatic PTC may sometimes be achieved with thyroglobulin aspirate from cystic lymph nodes when cytologic findings are negative. Clinicians should strongly consider surgical lymph node resection of cystic lymph nodes regardless of the preoperative cytologic findings by FNA.

The measurement of thyroglobulin levels in the washout fluid from FNA (FNA-Tg) is now widely used for the early detection of neck lymph node metastases in patients with differentiated PTC [18, 19]. FNA-Tg is 100 % sensitive in detecting lymph node metastasis in patients who have been treated previously, whereas cytology alone is only 85 % sensitive [18]. It's been found that FNA-Tg could contribute to the diagnosis of the poor cellular material obtained from cystic metastasis [20]. Several studies have reported FNA-Tg to be more sensitive than FNA cytology for detecting metastasis, and the sensitivity of FNA cytology is increased when combined with FNA-Tg [18–22]. FNA-Tg in addition to cytology should be considered the standard for investigating neck node metastasis in patients with thyroid malignancy. Considering the high sensitivity and accuracy of the suggested FNA-Tg threshold values, neck node dissection should be considered when FNA-Tg is higher than the suggested threshold values, despite a negative cytology.

References

1. Jaragh M, Carydis VB, MacMillan C, Freeman J, Colgan TJ. Predictors of malignancy in thyroid fine-needle aspirates "cyst fluid only" cases: can potential clues of malignancy be identified? Cancer. 2009;117:305–10.
2. Baloch Z, LiVolsi V, Asa S, et al. Diagnostic terminology and morphologic criteria for cytologic diagnosis of thyroid lesions: a synopsis of the National Cancer Institute thyroid fine-needle aspiration state of the science conference. Diagn Cytopathol. 2008;36:425–37.
3. Jaffar R, Mohanty SK, Khan A, Fischer AH. Hemosiderin laden macrophages and hemosiderin within follicular cells distinguish benign follicular lesions from follicular neoplasms. Cytojournal. 2009;6:3.
4. Bishop-Pitman M, Abele J, Ali S, et al. Techniques for thyroid FNA: a synopsis of the National Cancer Institute thyroid fine-needle aspiration state of the science conference. Diagn Cytopathol. 2008;36:407–24.
5. DeMay RM. The art and science of cytopathology: superficial aspiration cytology. Chicago: ASCP Press; 2012.

6. Cibas ES, Sanchez MA. The National Cancer Institute thyroid fine-needle aspiration state-of-the-science conference. Cancer. 2008;114:71–3.
7. Faquin WC, Cibas ES, Renshaw AA. “Atypical” cells in fine-needle aspiration biopsy specimens of benign thyroid cysts. Cancer. 2005;105:71–9.
8. Guidelines of the papanicolaou society of cytopathology for the examination of fine-needle aspiration specimens from thyroid nodules: The Papanicolaou Society of Cytopathology Task Force on Standards of Practice.
9. Wei S, LiVolsi VA, Baloch ZW. Pathology of thyroglossal duct: an institutional experience. Endocr Pathol. 2015;26:75–9.
10. Chou J, Walters A, Hage R, Zurada A, Michalak M, Tubbs RS, Loukas M. Thyroglossal duct cysts: anatomy, embryology and treatment. Surg Radiol Anat. 2013;35:875–81.
11. Yang YJ, Haghir S, Wanamaker JR, Powers CN. Diagnosis of papillary carcinoma in a thyroglossal duct cyst by fine-needle aspiration biopsy. Arch Pathol Lab Med. 2000;124:139–42.
12. Shahin A, Burroughs FH, Kirby JP, Ali SZ. Thyroglossal duct cyst: a cytopathologic study of 26 cases. Diagn Cytopathol. 2005;33:365–9.
13. Goellner JR, Johnson DA. Cytology of cystic papillary carcinoma of the thyroid. Acta Cytol. 1982;26:797–808.
14. Hammer M, Wortsman J, Folse R. Cancer in cystic lesions of the thyroid. Arch Surg. 1982;117:1020–3.
15. Cusick EL, McIntosh CA, Krukowski ZH, Matheson NA. Cystic change and neoplasia in isolated thyroid swellings. Br J Surg. 1988;75:982–3.
16. de los Santos ET, Keyhani-Rofagha S, Cunningham JJ, Mazzaferri EL. Cystic thyroid nodules. The dilemma of malignant lesions. Arch Intern Med. 1990;150:1422–7.
17. McHenry CR, Slusarczyk SJ, Khiyami A. Recommendations for management of cystic thyroid disease. Surgery. 1999;126:1167–71.
18. Pacini F, Fugazzola L, Lippi F, Ceccarelli C, Centoni R, Miccoli P, Elisei R, Pinchera A. Detection of thyroglobulin in fine needle aspirates of nonthyroidal neck masses: a clue to the diagnosis of metastatic differentiated thyroid cancer. J Clin Endocrinol Metabol. 1992;74:1401–4.
19. Kim MJ, Kim EK, Kim BM, Kwak JY, Lee EJ, Park CS, Cheong WY, Nam KH. Thyroglobulin measurement in fine-needle aspirate washouts: the criteria for neck node dissection for patients with thyroid cancer. Clin Endocrinol (Oxf). 2009;70:145–51.
20. Cignarelli M, Ambrosi A, Marino A, Lamacchia O, Campo M, Picca G, Giorgino F. Diagnostic utility of thyroglobulin detection in fine-needle aspiration of cervical cystic metastatic lymph nodes from papillary thyroid cancer with negative cytology. Thyroid. 2003;13:1163–7.
21. Frasoldati A, Toschi E, Zini M, Flora M, Caroggio A, Dotti C, Valcavi R. Role of thyroglobulin measurement in fine-needle aspiration biopsies of cervical lymph nodes in patients with differentiated thyroid cancer. Thyroid. 1999;9:105–11.
22. Snozek CL, Chambers EP, Reading CC, Sebo TJ, Sistrunk JW, Singh RJ, Grebe SK. Serum thyroglobulin, high-resolution ultrasound, and lymph node thyroglobulin in diagnosis of differentiated thyroid carcinoma nodal metastases. J Clin Endocrinol Metabol. 2007;92:4278–81.

Usefulness of Subclassification of Follicular Lesion of Undetermined Significance

2

Case Study

A 43-year-old male presented to his primary care physician for routine checkup and was found to have a thyroid nodule on examination. He had no complaints of difficulty swallowing or hoarseness. He had no symptoms of hyperthyroidism, no history of radiation to the neck, and no previous history of neck surgery. Patient had a family history of thyroid cancer. Ultrasonographic studies revealed a $3.2 \times 2.8 \times 2.5$ cm nodule in the left lobe of the thyroid. In addition, there were scattered smaller nodules in the same lobe. Fine needle aspiration cytology revealed a follicular lesion of undetermined significance, as cells showed nuclei with chromatin clearing and minimal nuclear enlargement and elongation. FNA lavage fluid was sent for *BRAF* mutation analysis, and *BRAF* gene V600E was not detected. Based on the size and the family history, patient underwent a left thyroid lobectomy, which revealed a 3.5 cm, encapsulated follicular variant of papillary thyroid carcinoma. Tumor was limited to the thyroid, and the margins were negative. He subsequently had a completion lobectomy, and the postoperative course was uneventful.

Discussion

The diagnosis category "follicular lesion of undetermined significance" is a controversial category in thyroid fine needle aspiration (FNA), not only for its questionable clinical utility but also for its existence as an expression of uncertainty [1, 2]. Various names have been used to describe lesions in this category, which include atypical follicular lesion, atypical cellular lesion, and atypical epithelial cells. Because of a lack of well-defined diagnostic criteria, the atypical category has poor reproducibility and is associated with high interobserver variability [3, 4]. The 2007 National Cancer Institute State of the Science Conference discussed diagnostic terminology and related diagnostic criteria. A category of follicular lesion of undetermined significance (FLUS) or atypia of unknown significance (AUS) was proposed

A.J. Adeniran, D. Chhieng, *Common Diagnostic Pitfalls in Thyroid Cytopathology*, DOI 10.1007/978-3-319-31602-4_2

for lesions that are characterized by too great a degree of architectural or cytologic atypia for definitive assignment to the benign category but insufficient findings for a diagnosis of follicular neoplasm or suspicious for carcinoma. The committee suggested that this category was optional, and its usage should not exceed 7 % of thyroid FNA diagnoses [5, 6]. Specific morphologic criteria do not exist for this category, but smears are characterized by relatively low cellularity, at least some background colloid, and in many cases the presence of microfollicles according to a multicenter study [5].

Several studies have documented that atypical cases with focal features of papillary carcinoma have an elevated risk of malignancy when compared with other "atypical" cases [7–9]. This has proven to be true in our experience [10]. Hence in our laboratory, we routinely subclassify lesions in the FLUS category into two, and we have defined uniform criteria for both subcategories. The first subcategory is for cases that demonstrate low cellularity as well as a predominantly microfollicular pattern and no or minimal colloid (Figs. 2.1, 2.2, 2.3, and 2.4). These features elicit concern for a follicular neoplasm. The second subcategory is used for cases that show nuclear atypia (Figs. 2.5, 2.6, 2.7, and 2.8), which elicit concern for a papillary carcinoma. Little data exist in the published literature to support the recommendation that the category should not exceed 7 % of all thyroid FNA diagnoses; hence, the frequency with which the FLUS terminology is used varies widely between institutions. The wide range may be a direct result of the nonuniformity of the criteria used in these various institutions. The risk of malignancy for all AUS cases, including those patients with benign results in follow-up and in whom surgery was not performed, presumably is up to 5–15 % [11]. The malignancy rates in recently

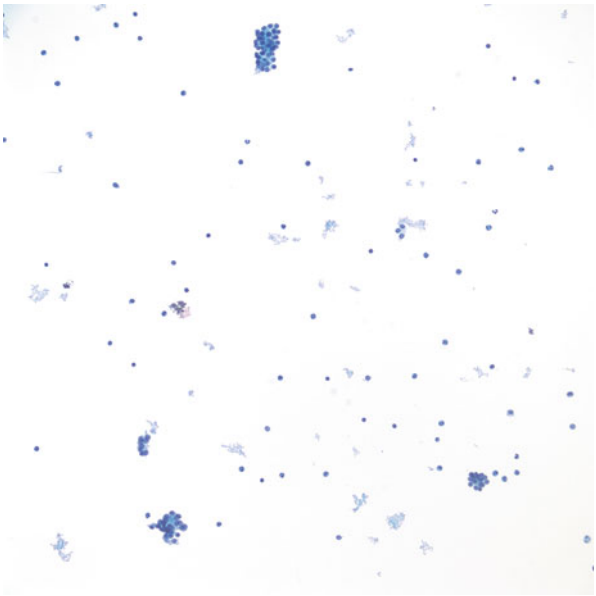

Fig. 2.1 Low cellularity with microfollicular architecture and the absence of colloid (Papanicolaou stain, X200)

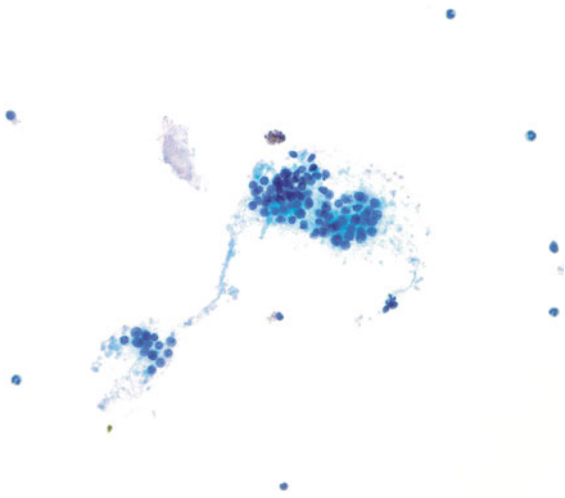

Fig. 2.2 Aggregate of microfollicles with scant colloid (Papanicolaou stain, X400)

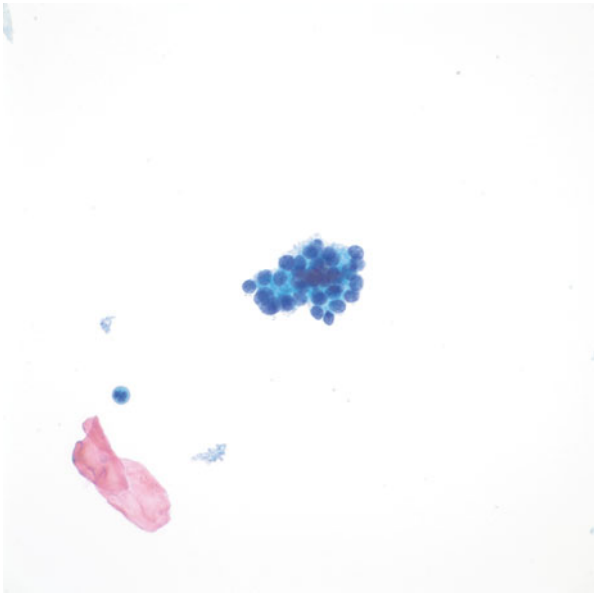

Fig. 2.3 Cluster of microfollicles. The cells have round, uniform nuclei, with no evidence of nuclear atypia (Papanicolaou stain, X600)

published studies using the Bethesda reporting system show a wide range of 6–48 % of resected cases [12, 13] and 5–27 % of all cases [14, 15]. The results are sometimes confusing as the percentages may reflect all cases or only resected cases, and the percentages may differ for malignancy rates and neoplastic rates [16].

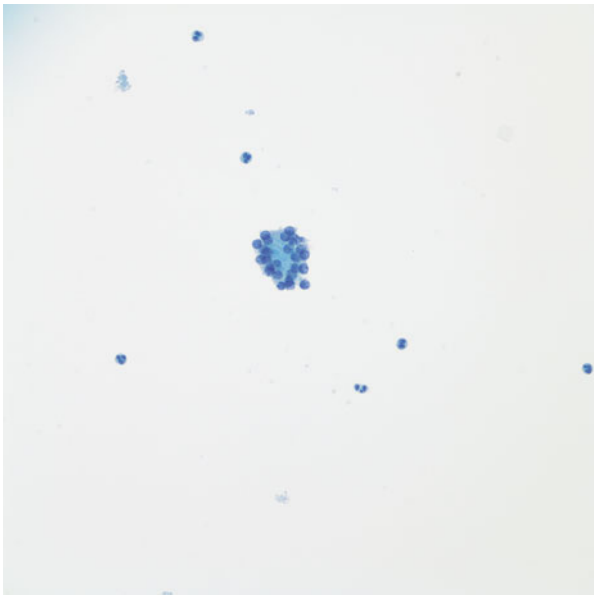

Fig. 2.4 Low cellularity with small cluster of microfollicles (Papanicolaou stain, X400)

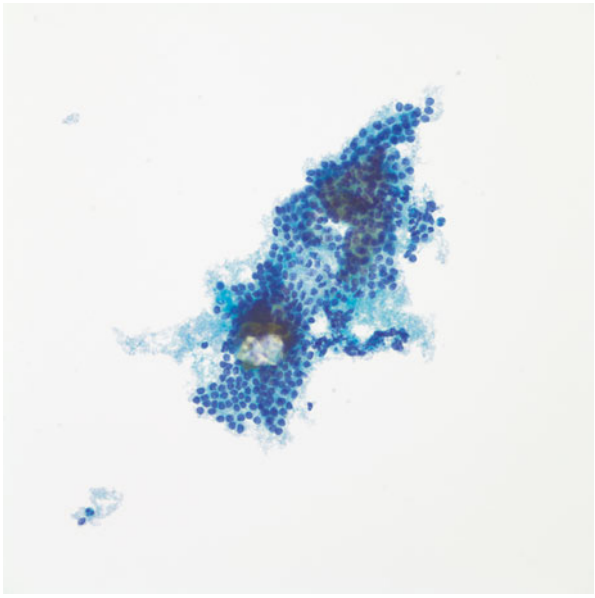

Fig. 2.5 Sheet of follicular cells. The nuclei of the cells are small and uniform but show nuclear membrane irregularity (Papanicolaou stain, X400)

Although the findings of "atypical follicular cells" is separated from other "indeterminate" cases in thyroid FNA by the most recent Bethesda system for reporting thyroid cytopathology [17], whether the overall risk of malignancy for this group of patients is truly different than that of patients with other indeterminate diagnoses is not clear. Other authors have suggested that the risk of malignancy for patients with

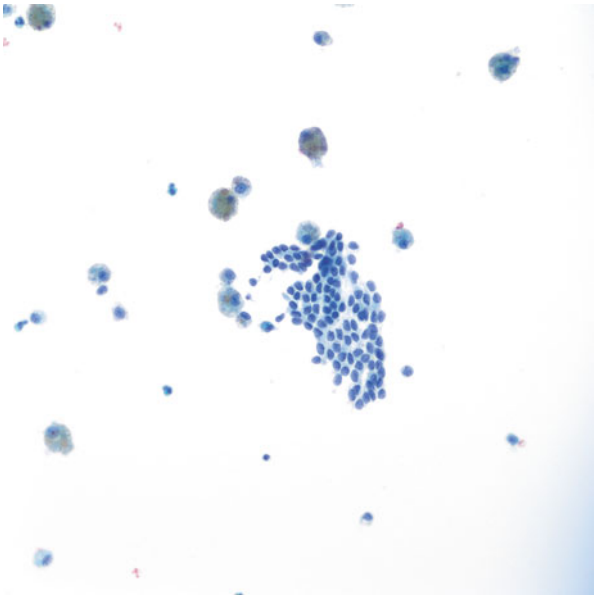

Fig. 2.6 Subset of cells in an otherwise cystic degeneration in a goiter. The cells demonstrate nuclear atypia, which includes nuclear membrane irregularity and rare grooves (Papanicolaou stain, X400)

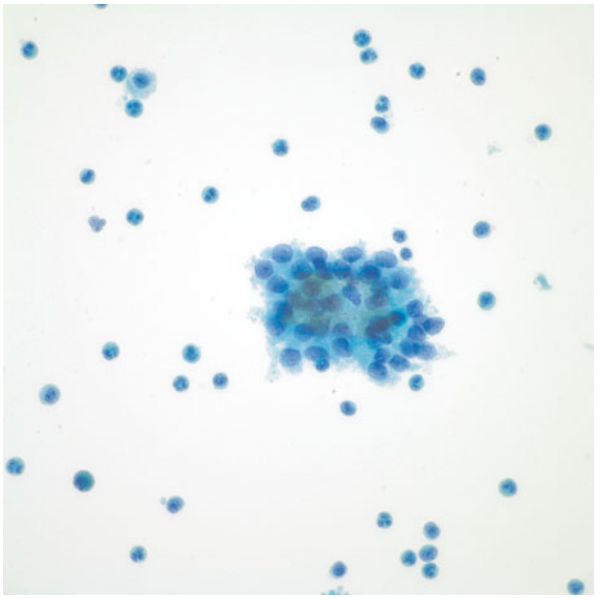

Fig. 2.7 Nuclear atypia. Nuclei with powdery chromatin and rare nuclear grooves (Papanicolaou stain, X600)

a diagnosis of "atypical follicular cells" is similar to that of patients with diagnoses of "suspicious for a follicular" or "Hürthle cell neoplasms" [5, 10, 18]. These authors have suggested that patients with these diagnoses should be grouped together into one group with a similar risk of malignancy.

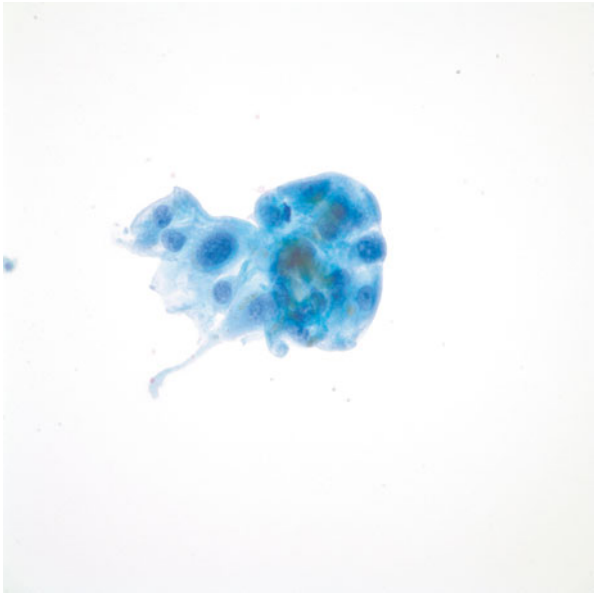

Fig. 2.8 Reactive atypia in cystic degeneration of a hyperplastic nodule. Cells with nuclear enlargement, nuclear membrane irregularity, and occasional small nucleoli (Papanicolaou stain, X600)

Renshaw [9] found at least four groups of cases within the diagnosis of "atypical follicular cells" that can be separated based on distinct cytologic criteria, and at least two of these groups have significantly different risks of malignancy. These different risks of malignancy may be important for both cytopathologists and clinicians. He found that the risk of malignancy for atypical follicular cells subclassified as "rule out papillary carcinoma" was significantly higher than the other atypical cells, while the risk of "rule out Hürthle cell neoplasm" was significantly lower than the other cases of atypical follicular cells. In our experience, we have found two groups of cases within the diagnosis of FLUS that can be separated based on distinct cytologic criteria, and we have been able to prove that these two groups have significantly different risks of malignancy [10].

While suggested follow-up of FLUS cases was re-aspiration, a good number of indeterminate cases also have surgical exploration. While it is uncertain what clinical or ultrasonographic features help in triage of patients for surgical exploration, such factors such as family history of thyroid carcinoma, history of radiation exposure, multiple nodules, a rapidly increasing size of nodules, nodules >4 cm in size, and symptomatic nodules (e.g., those causing compression symptoms) certainly play some role.

In a particular study, surgical resections and repeat FNAs following a FLUS diagnosis revealed a benign diagnosis in up to two-thirds of patients [10]. The diagnosis of malignancy was disproportionately more in patients with smears showing nuclear atypia. The majority (up to 83 %) of malignancies detected following a FLUS cytologic diagnosis were papillary carcinoma. Follicular variant of papillary thyroid carcinoma (PTC-FV) accounted for the majority of cases in this group. The predominance of PTC-FV in patients with PTC is supported by previous reports that

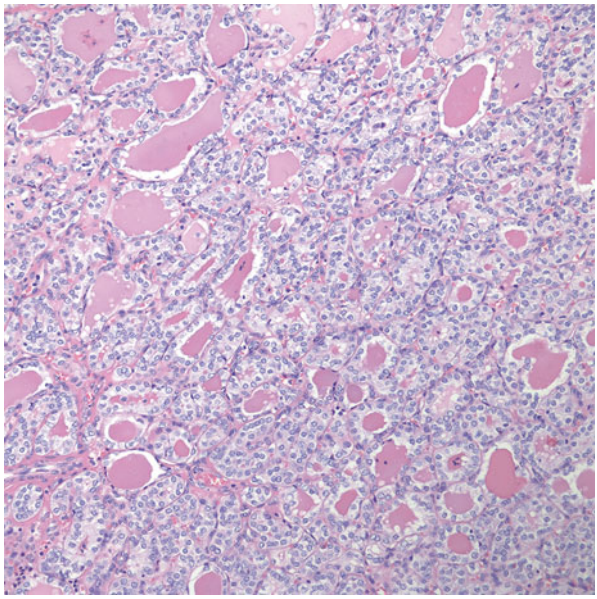

Fig. 2.9 Follicular variant of papillary thyroid carcinoma. Cells show nuclear membrane irregularity and rare grooves. Other nuclear features of papillary thyroid carcinoma are not well developed (H&E stain, X200)

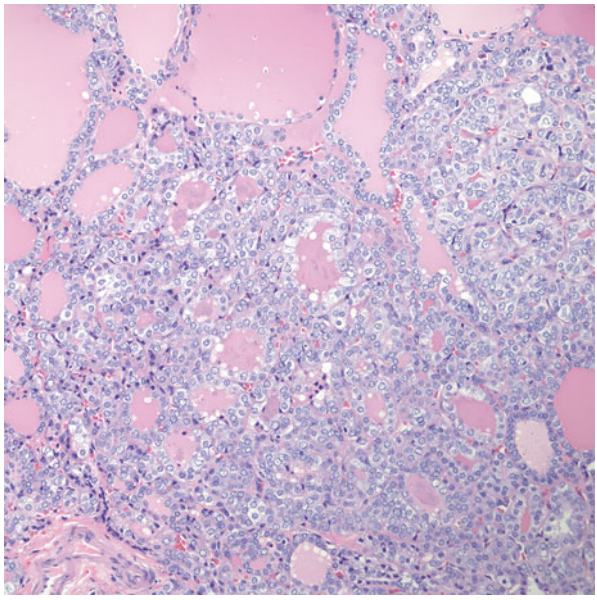

Fig. 2.10 Follicular variant of papillary thyroid carcinoma. Cells show nuclear enlargement and powdery chromatin. Other nuclear features of papillary thyroid carcinoma are not well developed (H&E stain, X200)

the nuclear features in PTC-FV are less pronounced and typically observed only focally. This is particularly true for chromatin clearing, nuclear grooves, and nuclear inclusions (Figs. 2.9 and 2.10). This clearly indicates that the presence of nuclear atypia is an independent risk factor for patients with FLUS FNAs. Kelman et al.

[19] reported a similar finding. They noticed that up to 60 % of the indeterminate thyroid nodules showing nuclear atypia on cytologic examination went on to develop malignancy, whereas only 7 % of the nodules without nuclear atypia were malignant. These observations prove that further subclassification of cases in this category based on nuclear atypia may give an added predictive value.

In the last decade, investigators have increasingly studied the potential for clinical, radiological, and molecular markers to predict nodule benignity or malignancy. American Thyroid Association and European Thyroid Association have broadly recommended partial or near total thyroidectomy for patients with indeterminate nodule cytology [20]. Another group suggested clinical correlation and re-FNA [21]. Patients diagnosed with AUS would undergo close follow-up with repeat biopsy in 3–6 months [4]. Several investigators have documented that repeat FNA is cost-effective for evaluating atypical thyroid smears [22, 23]. There is an increased likelihood that subtle evidence of malignancy on the initial FNA may become obvious during the second FNA, and the exuberant reactive changes on the initial smear may diminish after several months [1]. Currently, we believe that nodules with a FLUS FNA diagnosis should be rebiopsied and not be surgically resected unless other clinical and/or radiological risk factors exist. Given the often-borderline specimen adequacy in the subcategory with low cellularity and microfollicular pattern, we reason that a targeted, well-sampled re-FNA with a non-equivocal benign diagnosis is reassuring and hence should be followed up by conservative management. However, those cases in the nuclear atypia subcategory need a more aggressive follow-up, and the re-biopsy should be sooner than those in the first subcategory. Patients in this subcategory with nuclear atypia may also undergo surgical resection (hemithyroidectomy) especially if other risk factors coexist.

Given the very high specificity of BRAF V600E mutation as a marker for PTC in thyroid nodules with an indeterminate diagnosis and the very high positive predictive value of PTC in thyroid nodules with an indeterminate diagnosis and with positive *BRAF* mutation, *BRAF* mutation analysis has become a useful adjunct test that helps to stratify cases in the FLUS category, thus allowing better planning of surgical treatment. Patients with nodules that have a diagnosis of FLUS on FNA and are positive for *BRAF V600E* mutation would be strong candidates for total thyroidectomy [24]. This eliminates the need for a second surgery in up to 40 % of patients [25]. Patients with nodules that have a FLUS cytologic diagnosis and negative *BRAF* mutation may be followed up conservatively with repeated FNAs in 6–12 months if there are no other concomitant risk factors. However, patients may be considered for surgical exploration if there are other concomitant risk factors such as a family history of thyroid carcinoma, a history of radiation exposure, rapidly increasing size of nodules, nodules greater than 4 cm in size, and symptomatic nodules. Since the cases in the nuclear atypia subcategory tend to have a higher risk of malignancy, and given that the majority of the cases that harbor the *BRAF* mutation are in this category, there should be a shorter follow-up with repeat FNA for the cases with nuclear atypia that are negative for *BRAF* mutation.

Other test modalities have emerged in the management of thyroid lesions in the indeterminate categories, and this is the future of management of thyroid nodules.

There are tests utilizing gene expression or miRNA profiling to triage indeterminate thyroid FNAs [26]. These tests have a high negative predictive value, similar to the probability of malignancy for an initial benign diagnosis. There are other genetic tests based on a comprehensive panel of point mutations and gene fusions occurring in thyroid cancers. This analysis is performed on a proprietary sequencer using the targeted ThyroSeq next-generation sequencing panel, which simultaneously tests for point mutations in 13 genes and for 42 types of gene fusions that occur in thyroid cancer [27]. This has led to increasing the sensitivity of cancer detection to 90 % and a negative predictive value of 96 %. All these tests can be performed on FNA samples by using lavage fluid obtained from washing the needles after preparation of direct smears.

References

1. Shi Y, Ding X, Klein M, et al. Thyroid fine-needle aspiration with atypia of undetermined significance: a necessary or optional category? Cancer Cytopathol. 2009;117:298–304.
2. Weber D, Brainard J, Chen L. Atypical epithelial cells, cannot exclude papillary carcinoma, in fine needle aspiration of the thyroid. Acta Cytol. 2008;52:320–4.
3. Pitman MB, Cibas ES, Powers CN, et al. Reducing or eliminating use of the category of atypical squamous cells of undetermined significance decreases the diagnostic accuracy of the Papanicolaou smear. Cancer. 2002;96:128–34.
4. Layfield LJ, Cibas ES, Gharib H, et al. Thyroid aspiration cytology: current status. CA Cancer J Clin. 2009;59:99–110.
5. Marchevsky AM, Walts AE, Bose S, et al. Evidence-based evaluation of the risks of malignancy predicted by thyroid fine-needle aspiration biopsies. Diagn Cytopathol. 2010;38: 252–9.
6. Renshaw AA. Reporting risk of malignancy/dysplasia in cytology: a potential way to improve communication, if not reputation. Cancer. 2007;111:465–6.
7. Renshaw AA. Focal features of papillary carcinoma of the thyroid in fine-needle aspiration material are strongly associated with papillary carcinoma at resection. Am J Clin Pathol. 2002;118:518–21.
8. Wu HH, Jones JN, Grzybicki DM, et al. Sensitive cytologic criteria for the identification of follicular variant of papillary thyroid carcinoma in fine-needle aspiration biopsy. Diagn Cytopathol. 2003;29:262–6.
9. Renshaw AA. Should "atypical follicular cells" in thyroid fine-needle aspirates be subclassified? Cancer Cytopathol. 2010;118:186–9.
10. Horne MJ, Chhieng DC, Theoharis C, Schofield K, Kowalski D, Prasad ML, Hammers L, Udelsman R, Adeniran AJ. Thyroid follicular lesion of undetermined significance: evaluation of the risk of malignancy using the two-tier sub-classification. Diagn Cytopathol. 2012;40: 410–5.
11. Krane JF, Nayar R, Renshaw AA. Atypia of undetermined significance/follicular lesion of undetermined significance. In: Ali SZ, Cibas ES, editors. The Bethesda system for reporting thyroid cytopathology. New York, NY, USA: Springer; 2010. p. 37–49.
12. Nayar R, Ivanovic M. The indeterminate thyroid fine-needle aspiration: experience from an academic center using terminology similar to that proposed in the 2007 National Cancer Institute Thyroid Fine Needle Aspiration State of the Science Conference. Cancer. 2009; 117:195–202.
13. Theoharis CG, Schofield KM, Hammers L, Udelsman R, Chhieng DC. The Bethesda thyroid fine-needle aspiration classification system: year 1 at an academic institution. Thyroid. 2009;19:1215–23.

14. VanderLaan PA, Marqusee E, Krane JF. Clinical outcome for atypia of undetermined significance in thyroid fine-needle aspirations: should repeated FNA be the preferred initial approach? Am J Clin Pathol. 2011;135:770–5.
15. Layfield LJ, Morton MJ, Cramer HM, Hirschowitz S. Implications of the proposed thyroid fine-needle aspiration category of "follicular lesion of undetermined significance": a five-year multi-institutional analysis. Diagn Cytopathol. 2009;37:710–4.
16. Dincer N, Balci S, Yazgan A, Guney G, Ersoy R, Cakir B, Guler G. Follow-up of atypia and follicular lesions of undetermined significance in thyroid fine needle aspiration cytology. Cytopathology. 2013;24:385–90.
17. Ali SZ, Cibas ES. The Bethesda system for reporting thyroid cytopathology. New York: Springer; 2010.
18. Redman R, Yoder BJ, Massoll NA. Perceptions of diagnostic terminology and cytopathologic reporting of fine-needle aspiration biopsies of thyroid nodules: a survey of clinicians and pathologists. Thyroid. 2006;16:1003–8.
19. Kelman AS, Rathan A, Leibowitz J, et al. Thyroid cytology and the risk of malignancy in thyroid nodules: importance of nuclear atypia in indeterminate specimens. Thyroid. 2001;11: 271–7.
20. Alexander EK. Approach to the patient with a cytologically indeterminate thyroid nodule. J Clin Endocrinol Metab. 2008;93:4175–82.
21. Layfield LJ, Abrams J, Cochand-Priollet B, et al. Post-thyroid FNA testing and treatment options: a synopsis of the National Cancer Institute Thyroid Fine Needle Aspiration State of the Science Conference. Diagn Cytopathol. 2008;36:442–8.
22. Yang J, Schnadig V, Logrono R, et al. Fine-needle aspiration of thyroid nodules: a study of 4703 patients with histologic and clinical correlations. Cancer. 2007;111:306–15.
23. Baloch Z, LiVolsi VA, Jain P, et al. Role of repeat fine-needle aspiration biopsy (FNAB) in the management of thyroid nodules. Diagn Cytopathol. 2003;29:203–6.
24. Adeniran AJ, Hui P, Chhieng DC, Prasad ML, Schofield K, Theoharis C. BRAF mutation testing of thyroid fine-needle aspiration specimens enhances the predictability of malignancy in thyroid follicular lesions of undetermined significance. Acta Cytol. 2011;55:570–5.
25. Adeniran AJ, Theoharis C, Hui P, Prasad ML, Hammers L, Carling T, Udelsman R, Chhieng DC. Reflex BRAF testing in thyroid fine-needle aspiration biopsy with equivocal and positive interpretation: a prospective study. Thyroid. 2011;21:717–23.
26. Alexander EK, Schorr M, Klopper J, Kim C, Sipos J, Nabhan F, Parker C, Steward DL, Mandel SJ, Haugen BR. Multicenter clinical experience with the Afirma gene expression classifier. J Clin Endocrinol Metab. 2014;99:119–25.
27. Nikiforov YE, Carty SE, Chiosea SI, Coyne C, Duvvuri U, Ferris RL, Gooding WE, Hodak SP, LeBeau SO, Ohori NP, Seethala RR, Tublin ME, Yip L, Nikiforova MN. Highly accurate diagnosis of cancer in thyroid nodules with follicular neoplasm/suspicious for a follicular neoplasm cytology by ThyroSeq v2 next-generation sequencing assay. Cancer. 2014;120: 3627–34.

Cytologic Atypia in Toxic Goiter

3

Case Study

This patient who was a 55-year-old female presented with incidental thyroid nodules in both the isthmus and the left lobe of her thyroid gland during a routine ultrasound examination. She has been diagnosed with hyperthyroidism secondary to Grave's disease for approximately a year. She was otherwise completely asymptomatic with no signs and symptoms of hyperthyroidism except for an 8 lb weight loss within a month. She did not complain of any hoarseness or voice changes and difficulty in swallowing or breathing. Her laboratory workup was significant for a low TSH level (0.14 mIU/L) and elevated level of antibodies to thyroid peroxidase (764 IU/ml) and TSH receptor (188 % above baseline). She did not have a history of radiation to the head and neck area or a family history of thyroid cancer. Physical examination of the neck revealed a 3 cm firm and fixed mass to the left of the midline. There was no cervical adenopathy.

The thyroid ultrasound demonstrated an isthmus nodule $1.3 \times 1.2 \times 0.8$ cm and a left lower nodule $1.1 \times 1.0 \times 0.9$ cm. No cervical lymphadenopathy was noted by ultrasound. Fine-needle aspiration biopsy was performed on both nodules. The aspirates of both nodules displayed similar findings. Both specimens were markedly cellular and consisted of numerous crowded groups admixed with loosely cohesive groups and single cells (Fig. 3.1). Individual cells appeared large and polygonal in shape with abundant granular eosinophilic cytoplasm and distinct cell borders (Fig. 3.2). The nuclei were enlarged with nuclear grooves and frequent intranuclear inclusions (Fig. 3.3). The background showed a mixed lymphoid infiltrate and bland-appearing Hürthle cells (Fig. 3.4). The cytologic diagnosis was papillary thyroid carcinoma arising in a background of lymphocytic thyroiditis.

The patient underwent a total thyroidectomy and left central neck dissection. The thyroid gland was of normal size and weight. Serial sectioning revealed two nodules: a nodule in the isthmus, measuring $1.2 \times 0.8 \times 0.8$ cm, and a left middle nodule, measuring $1.5 \times 1.2 \times 0.7$ cm. The remaining thyroid gland appeared pale with vague nodularity. Microscopic examination of both nodules demonstrated a neoplastic

A.J. Adeniran, D. Chhieng, *Common Diagnostic Pitfalls in Thyroid Cytopathology*, DOI 10.1007/978-3-319-31602-4_3

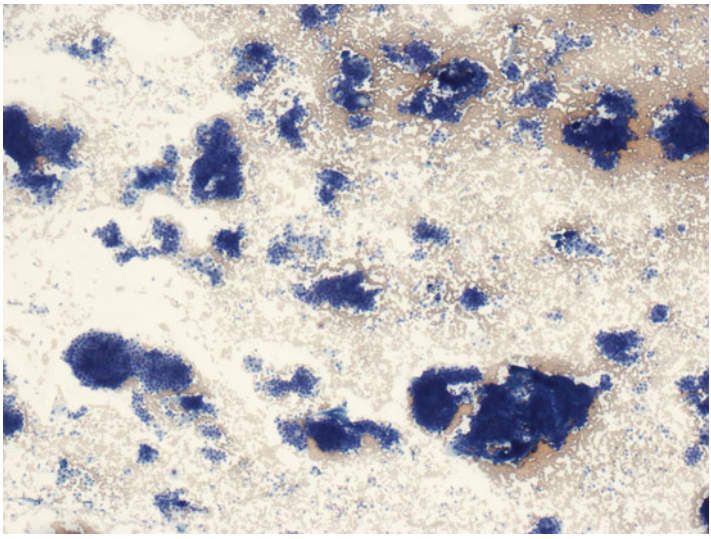

Fig. 3.1 Thyroid FNA papillary thyroid carcinoma in a patient with treated Graves' disease. The aspirate is moderately cellular and consists of numerous large cellular clusters of varying sizes and shapes (Diff-Quik stain, low power)

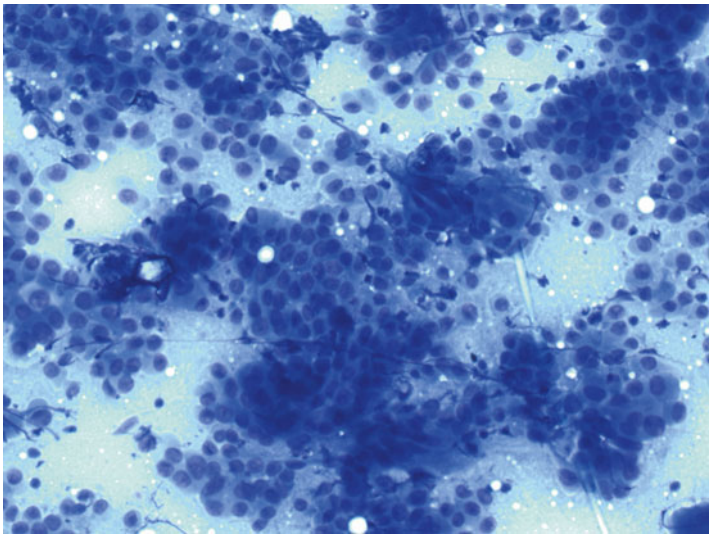

Fig. 3.2 Thyroid FNA papillary thyroid carcinoma in a patient with treated Graves' disease. The follicular cells are arranged in loosely cohesive crowded groups (Diff-Quik stain, high power)

cellular population with predominant papillary growth pattern in a lymphocytic stroma (Fig. 3.5). The papillae were lined by tall columnar cells with abundant eosinophilic cytoplasm (Fig. 3.6). Nuclear evidence of papillary thyroid carcinoma, such as nuclear grooves and inclusion, was readily apparent (Fig. 3.7). The

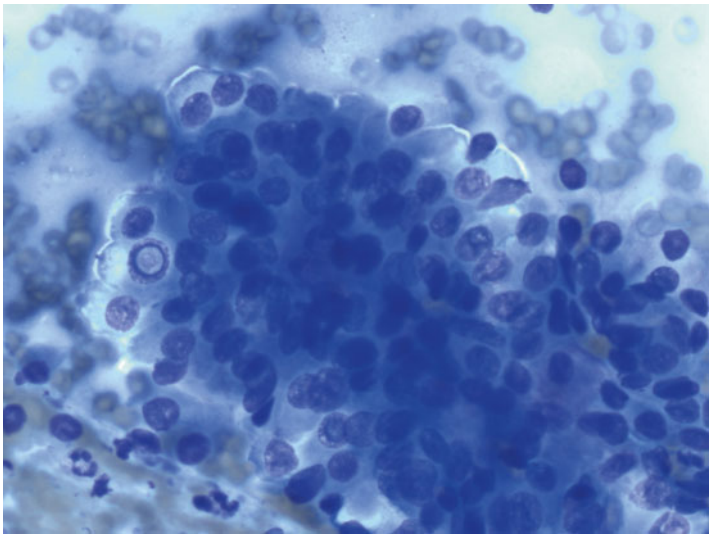

Fig. 3.3 Thyroid FNA papillary thyroid carcinoma in a patient with treated Graves' disease. The follicular cells possess moderate amount of cytoplasm with enlarged nuclei. Nuclear grooves and intranuclear inclusions are readily apparent (Diff-Quik stain, high power)

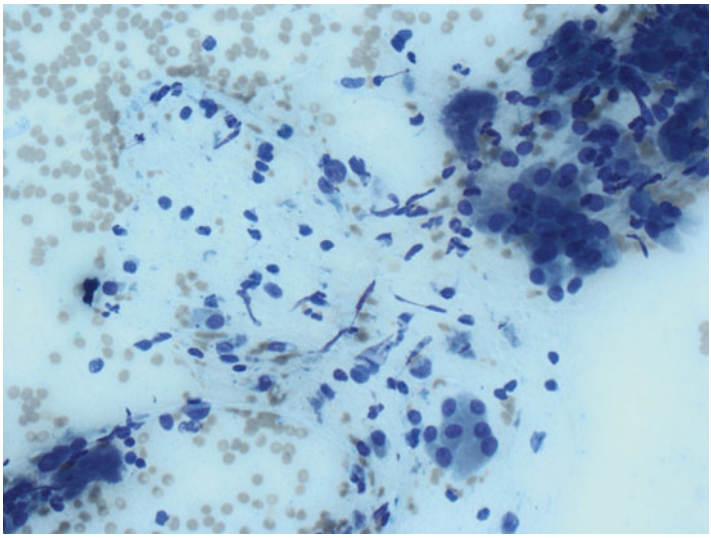

Fig. 3.4 Thyroid FNA papillary thyroid carcinoma in a patient with treated Graves' disease. A group of nonneoplastic Hürthle cells admixed with scattered lymphocytes, indicating the presence of lymphocytic thyroiditis in the background (Diff-Quik stain, high power)

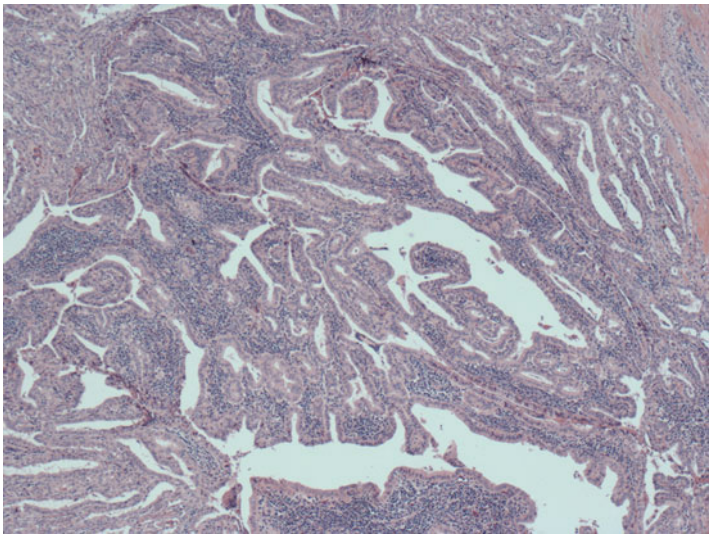

Fig. 3.5 Papillary thyroid carcinoma, tall-cell variant. The 1.5 cm nodule in the left thyroid lobe demonstrates a predominant papillary growth pattern (H&E, low power)

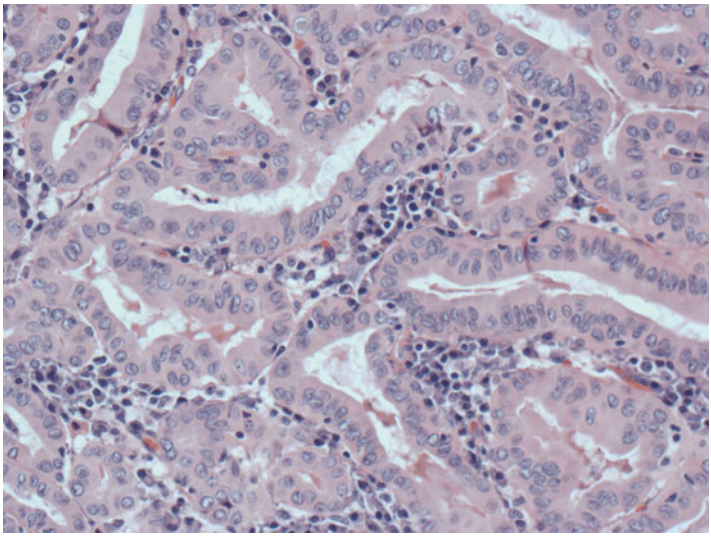

Fig. 3.6 Papillary thyroid carcinoma, tall-cell variant. The majority (>90 %) of the papillae are lined by tall columnar cells with abundant eosinophilic cytoplasm. There is also a striking lymphocytic infiltrate in the fibrovascular core of the papillae (H&E, high power)

nonneoplastic thyroid parenchyma showed chronic lymphocytic thyroiditis with extensive fibrosis (Figs. 3.8 and 3.9). The final diagnosis was papillary thyroid carcinoma, tall-cell variant. Three out of 13 lymph nodes were positive for metastatic papillary thyroid carcinoma.

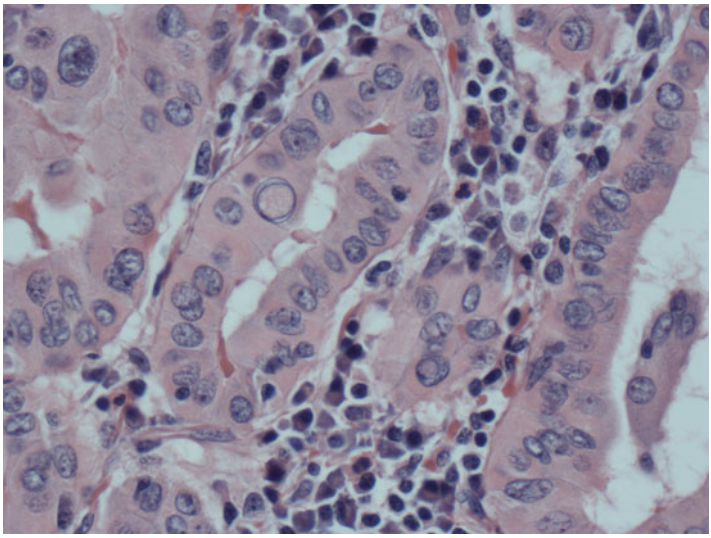

Fig. 3.7 Papillary thyroid carcinoma, tall-cell variant. The height of the columnar follicular cells is at least twice their width. The nuclear features of the follicular cells include nuclear enlargement, powdery chromatin with clearing, nuclear grooves, and readily apparent intranuclear inclusions (H&E, high power)

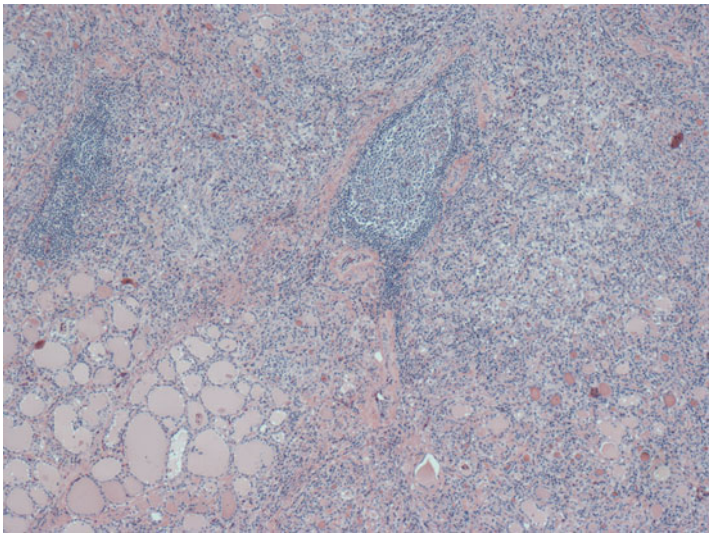

Fig. 3.8 Background lymphocytic thyroiditis. The nonneoplastic thyroid parenchyma shows both micro- and macro-follicular structures with an intense lymphoid infiltrate and formation of lymphoid aggregates (H&E, low power)

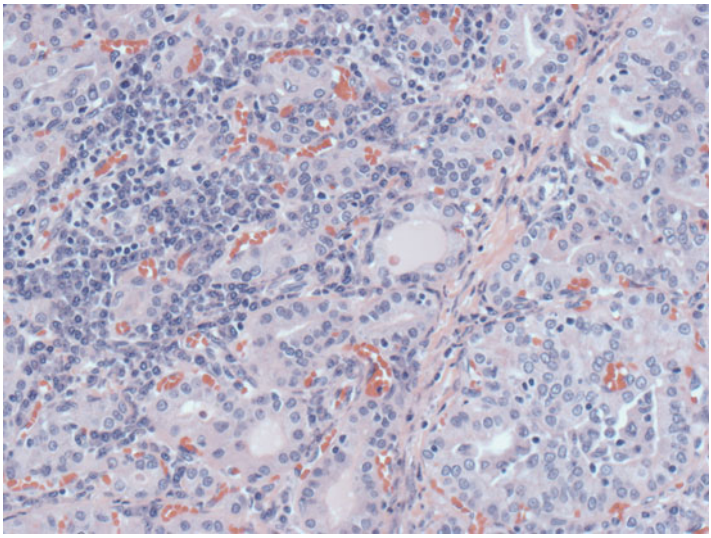

Fig. 3.9 Background lymphocytic thyroiditis. High magnification showing a lymphoplasmacytic infiltrate among follicles lined by nonneoplastic Hürthle cells (H&E, high power)

Discussion

Graves' disease is an autoimmune disorder characterized by hyperthyroidism and a diffuse toxic goiter. This disease is fairly common and is said to affect up to 2 % of adult women in the USA. Management of patients with Graves' disease aims to maintain an euthyroid state through the lowering of thyroid hormone levels. The latter can be achieved by antithyroid medication, radioactive iodine (^{131}I), and surgery. ^{131}I therapy leads to the destruction of thyroid cells and an associated reduction of thyroid hormone output and is the preferred treatment of choice in the USA.

The typical presentation is a diffusely enlarged thyroid gland. However, it is not infrequent to find nodular lesions in patients with Graves' disease, especially in patients with long-standing disease and/or post ^{131}I therapy. The frequency of thyroid nodules detected in patients with Graves' disease is approximately 15 % by palpation [1] but can be up to 35 % by ultrasound examination [2–4]. Nodular lesions in patients with Graves' disease should be evaluated by fine-needle aspiration (FNA) biopsy, similar to those without this disorder.

Cytomorphologic changes associated with ^{131}I therapy in patients with Graves' disease have been well described [5–8]. Some of these changes, which include nuclear and cytoplasmic enlargement, anisonucleosis, hyperchromasia, pale chromatin and cytoplasmic vacuolation, can be seen in both the acute and chronic periods following ^{131}I administration (Fig. 3.10). In addition, squamous and/or oncocytic metaplasia and variable degree of nuclear changes including pale chromatin, nuclear grooves, and rare nuclear inclusions have been described as part of late cytologic changes post-^{131}I therapy (Figs. 3.11 and 3.12). Calcified debris and, rarely,

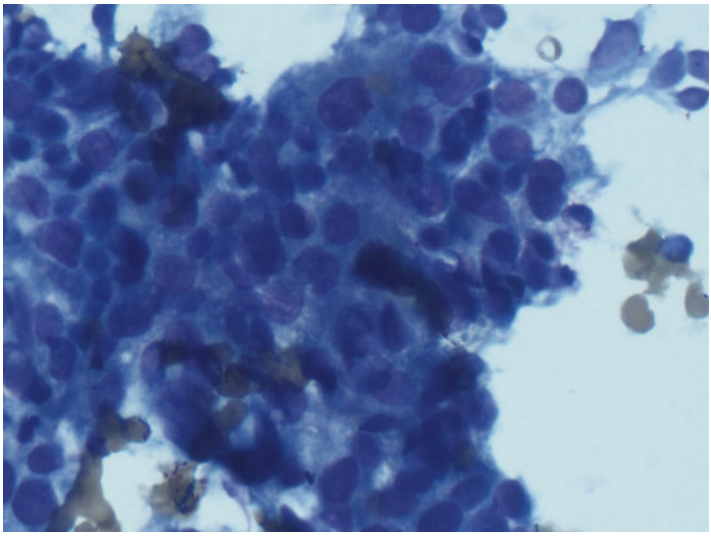

Fig. 3.10 Thyroid FNA atypia associated with treated Graves' disease. Group of follicular cells with mild nuclear crowding. Individual cells demonstrate both cytoplasmic and nuclear enlargement and considerable anisonucleosis (Diff-Quik stain, high power)

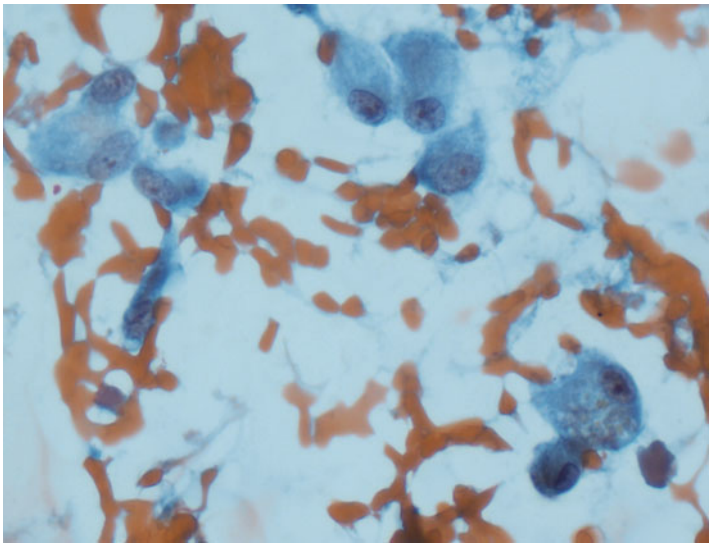

Fig. 3.11 Thyroid FNA atypia associated with treated Graves' disease. Loosely cohesive and single follicular cells with both cytoplasmic and nuclear enlargement. The cytoplasm is abundant and granular and sometimes vacuolated. The nuclei demonstrate pale chromatin and infrequent nuclear grooves (Diff-Quik stain, high power)

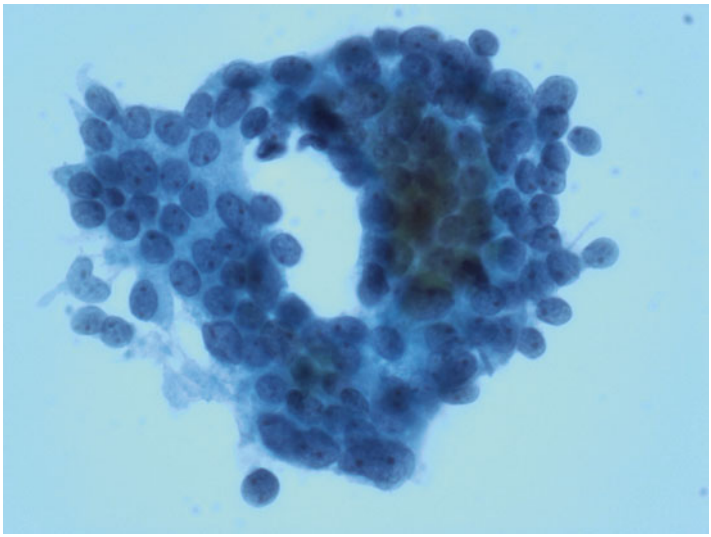

Fig. 3.12 Thyroid FNA atypia associated with treated Graves' disease. Cohesive group of follicular cells with considerable crowding and overlapping. The follicular cells demonstrate powdery chromatin and infrequent nuclear grooves (Papanicolaou stain, high power)

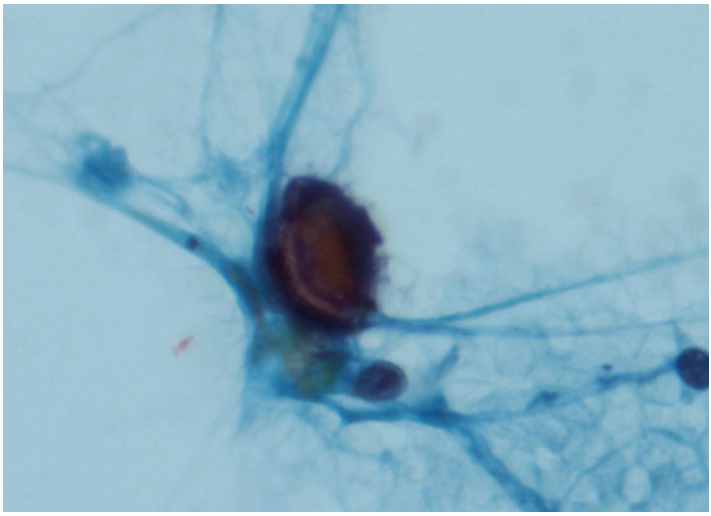

Fig. 3.13 Thyroid FNA atypia associated with treated Graves' disease. Calcified debris, sometimes in the form of psammoma bodies, can be seen in patients with Graves' disease treated with radioactive iodide (Papanicolaou stain, high power)

psammoma bodies have been described [9] (Fig. 3.13). Based on the descriptions from the literature, cytologic changes associated with post-^{131}I therapy are variable and nonspecific but can occasionally be confused with malignancy when the

changes are significant. The cytologic clues to the benign nature of these nodules include cohesive flat sheets and the presence of lymphocytes, histiocytes, colloid, and cytoplasmic vacuoles [6]. However, the knowledge of a clinical history of Graves' disease treated with ^{131}I is of paramount importance in minimizing overdiagnosis of malignancy.

Although there is not a well-documented causal relationship between ^{131}I therapy and subsequent development of thyroid malignancies, many studies have reported a higher incidence of thyroid malignancy in patients with Graves' disease than those without [1, 10, 11]. According to a population-based study, the authors reported an incidence of thyroid carcinoma in patients with Graves' disease of 4.92 per 1000 person-years, which was 1.37-fold higher than those without the disease [10]. The reported incidence of papillary thyroid carcinoma in patients with Graves' disease ranged from 2 to 17 % [12–15]. The most common thyroid carcinomas arising in patients with Graves' disease are papillary thyroid carcinomas, with the majority of them being conventional type [11]. It is important to note that the tall-cell variant of papillary thyroid carcinoma, which is associated with aggressive clinical features and poor prognosis, has been found to have a higher prevalence in patients with Graves' disease [11, 16]. One study showed that the prevalence of tall-cell variant of papillary thyroid carcinoma accounted for 18 % of papillary thyroid carcinoma in patients with Graves' disease and only 6 % of those without Graves' disease [16]. As mentioned earlier, ^{131}I therapy can result in cytologic atypia; therefore, it is equally important to avoid underdiagnosing malignancy which might lead to a delay in diagnosis and treatment and, in turn, a decrease in survival opportunity.

References

1. Pellegriti G, Mannarino C, Russo M, et al. Increased mortality in patients with differentiated thyroid cancer associated with Graves' disease. J Clin Endocrinol Metab. 2013;98:1014–21.
2. Cantalamessa L, Baldini M, Orsatti A, Meroni L, Amodei V, Castagnone D. Thyroid nodules in Graves disease and the risk of thyroid carcinoma. Arch Intern Med. 1999;159:1705–8.
3. Kraimps JL, Bouin-Pineau MH, Mathonnet M, et al. Multicentre study of thyroid nodules in patients with Graves' disease. Br J Surg. 2000;87:1111–3.
4. Kim WB, Han SM, Kim TY, et al. Ultrasonographic screening for detection of thyroid cancer in patients with Graves' disease. Clin Endocrinol (Oxf). 2004;60:719–25.
5. Oz F, Urgancioglu I, Uslu I, Dervisoglu S, Oz B, Kanmaz B. Cytologic changes induced by 131I in the thyroid glands of patients with hyperthyroidism; results of fine needle aspiration cytology. Cytopathology. 1994;5:154–63.
6. Centeno BA, Szyfelbein WM, Daniels GH, Vickery Jr AL. Fine needle aspiration biopsy of the thyroid gland in patients with prior Graves' disease treated with radioactive iodine. Morphologic findings and potential pitfalls. Acta Cytol. 1996;40:1189–97.
7. Granter SR, Cibas ES. Cytologic findings in thyroid nodules after 131I treatment of hyperthyroidism. Am J Clin Pathol. 1997;107:20–5.
8. Anderson SR, Mandel S, LiVolsi VA, Gupta PK, Baloch ZW. Can cytomorphology differentiate between benign nodules and tumors arising in Graves' disease? Diagn Cytopathol. 2004;31:64–7.

9. Sturgis CD. Radioactive iodine-associated cytomorphologic alterations in thyroid follicular epithelium: is recognition possible in fine-needle aspiration specimens? Diagn Cytopathol. 1999;21:207–10.
10. Chen YK, Lin CL, Chang YJ, et al. Cancer risk in patients with Graves' disease: a nationwide cohort study. Thyroid. 2013;23:879–84.
11. Wei S, Baloch ZW, LiVolsi VA. Thyroid carcinoma in patients with Graves' disease: an institutional experience. Endocr Pathol. 2015;26:48–53.
12. Ozaki O, Ito K, Kobayashi K, Toshima K, Iwasaki H, Yashiro T. Thyroid carcinoma in Graves' disease. World J Surg. 1990;14:437–40. discussion 440–431.
13. Gerenova J, Buysschaert M, de Burbure CY, Daumerie C. Prevalence of thyroid cancer in Graves' disease: a retrospective study of a cohort of 103 patients treated surgically. Eur J Intern Med. 2003;14:321–5.
14. Chao TC, Lin JD, Chen MF. Surgical treatment of thyroid cancers with concurrent Graves disease. Ann Surg Oncol. 2004;11:407–12.
15. Tamatea JA, Tu'akoi K, Conaglen JV, Elston MS, Meyer-Rochow GY. Thyroid cancer in Graves' disease: is surgery the best treatment for Graves' disease? ANZ J Surg. 2014;84: 231–4.
16. Boutzios G, Vasileiadis I, Zapanti E, et al. Higher incidence of tall cell variant of papillary thyroid carcinoma in Graves' disease. Thyroid. 2014;24:347–54.

Hürthle Cell Lesions

4

Case Study

The patient was an 83-year-old woman who was recently diagnosed with a primary lung adenocarcinoma of the right lower lobe. During her metastatic workup, her PET scan revealed several mediastinal lymphadenopathies and a 4 cm left thyroid nodule with substernal extension. Her complaint included intermittent difficulty in swallowing and breathing. Physical examination was unremarkable except for a palpable left thyroid nodule. There was no personal history of radiation to the neck and no family history of thyroid cancer. Ultrasound examination showed a 3.8 cm nodule in the left thyroid lobe and multiple sub-centimeter nodules in the right lobe. There was no airway compression.

Fine needle aspiration biopsy of the left thyroid nodule was performed. The aspirate was cellular and consisted of both loosely cohesive groups and three-dimensional crowded clusters (Figs. 4.1 and 4.2). Individual follicular cells were predominantly Hürthle cells with moderate amount of granular cytoplasm (Fig. 4.3). The nuclei appeared round to oval and were centrally or slightly eccentrically located; nuclear enlargement and frequent prominent nucleoli were apparent (Figs. 4.4 and 4.5). No evidence of nuclear features of papillary thyroid carcinoma was noted. There was minimal amount of colloid in the background. The cytologic diagnosis was Hürthle cell neoplasm. FNA of mediastinal lymph nodes station 2R, 4R, 7, and 11L was performed under endobronchoscopic ultrasound guidance. All mediastinal lymph nodes demonstrated mixed lymphoid population consistent with benign lymph node; there was no evidence of metastatic disease.

The patient underwent total thyroidectomy followed by mediastinoscopy. Gross examination revealed an enlarged left thyroid lobe. Serial sectioning revealed a 3.9 cm dominant nodule in the left thyroid lobe; the cut surface appeared tan brown with a hemorrhagic center. Several sub-centimeter nodules were also noted in the right lobe. Microscopic examination revealed an encapsulated nodule composed of a neoplastic proliferation of Hürthle cells in both solid and microfollicular growth pattern (Figs. 4.6 and 4.7). Individual cells demonstrated moderate to abundant

A.J. Adeniran, D. Chhieng, *Common Diagnostic Pitfalls in Thyroid Cytopathology*, DOI 10.1007/978-3-319-31602-4_4

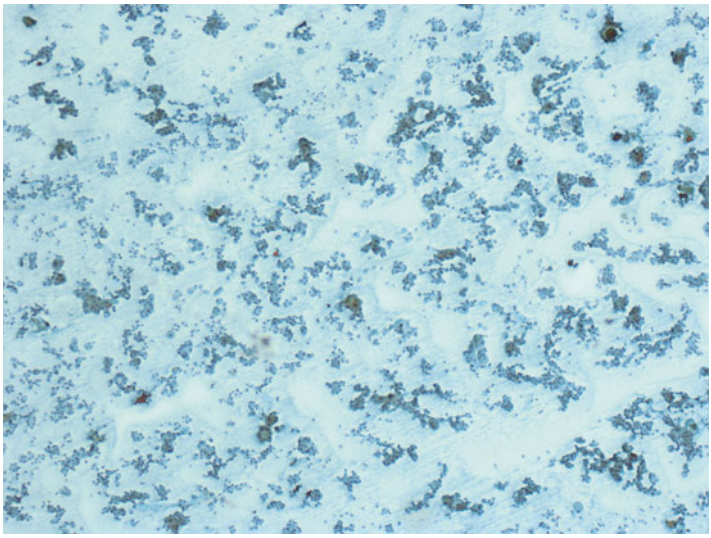

Fig. 4.1 Thyroid FNA-Hürthle cell neoplasm. The aspirate is markedly cellular and consists of follicular cells singly and in groups. There is no colloid or lymphocytes in the background (Papanicolaou stain, low power)

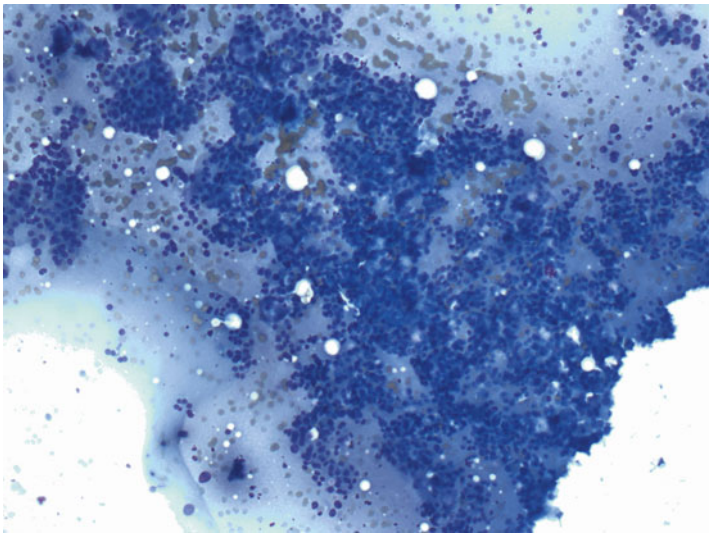

Fig. 4.2 Thyroid FNA-Hürthle cell neoplasm. Predominantly crowded clusters of follicular cells are noted. No colloid is noted in the background (Diff-Quik stain, low power)

eosinophilic granular cytoplasm with round to oval nuclei, nuclear enlargement, and prominent nucleoli (Fig. 4.8). Nuclear features of papillary thyroid carcinoma were absent. Multiple foci of capsular invasion with mushroomlike growth pattern were identified (Fig. 4.9); however, there was no evidence of vascular invasion. In

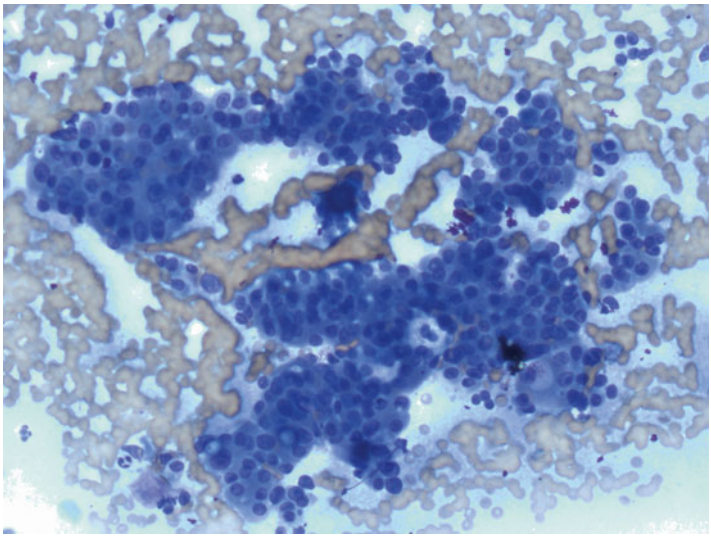

Fig. 4.3 Thyroid FNA-Hürthle cell neoplasm. The follicular cells are arranged in crowded groups and demonstrate moderate amount of granular cytoplasm (Diff-Quik stain, high power)

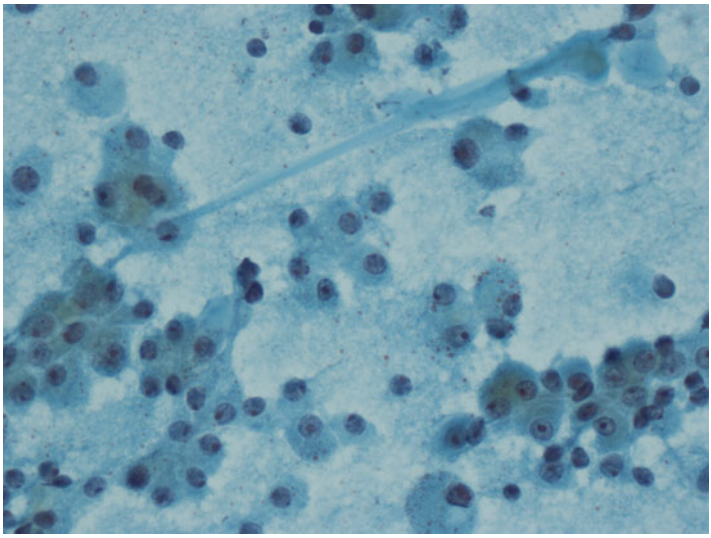

Fig. 4.4 Thyroid FNA-Hürthle cell neoplasm. Loosely cohesive and single Hürthle cells with abundant granular cytoplasm. The nuclei are eccentrically placed and appear round to oval with prominent nucleoli. Occasional binucleated Hürthle cells are noted (Papanicolaou stain, high power)

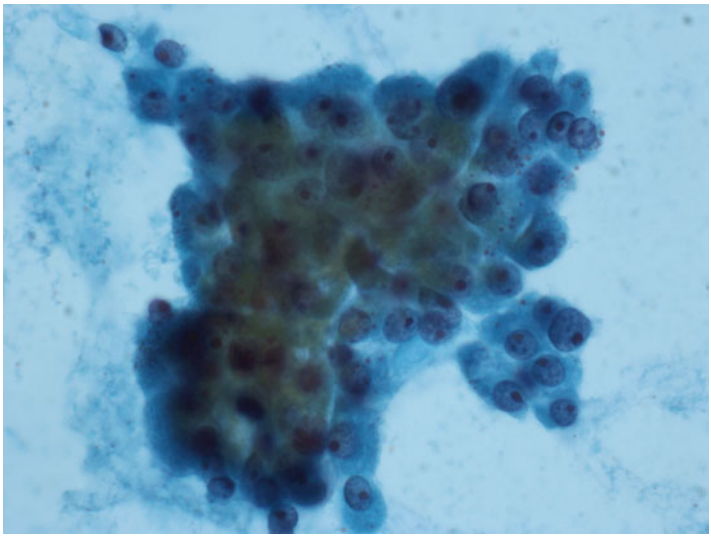

Fig. 4.5 Thyroid FNA-Hürthle cell neoplasm. This group of Hürthle cells shows considerable nuclear crowding and overlapping. There is also considerable nuclear pleomorphism with features such as nuclear enlargement, anisonucleosis, and prominent macronucleoli (Papanicolaou stain, high power)

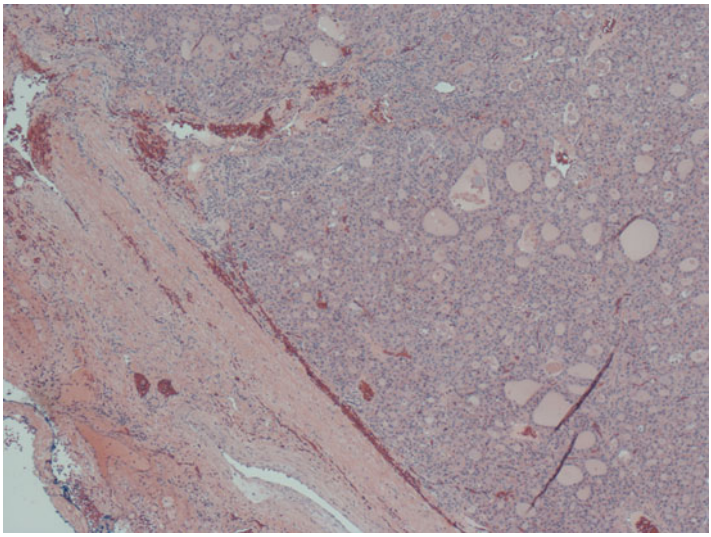

Fig. 4.6 Hürthle cell carcinoma. The tumor is surrounded by a thick fibrous capsule and is composed of neoplastic Hürthle cells arranged in predominantly follicular pattern (H&E stain, low power)

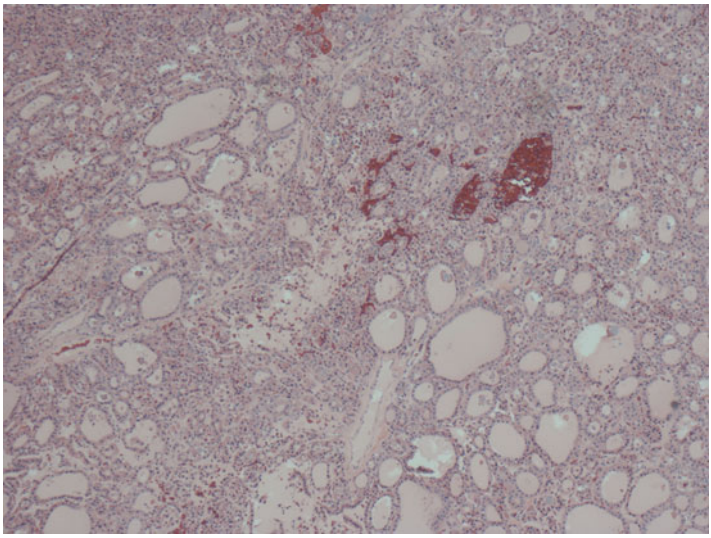

Fig. 4.7 Hürthle cell carcinoma. Follicles of varying sizes and shapes are noted. The neoplastic cells are composed of entirely Hürthle cells (H&E stain, low power)

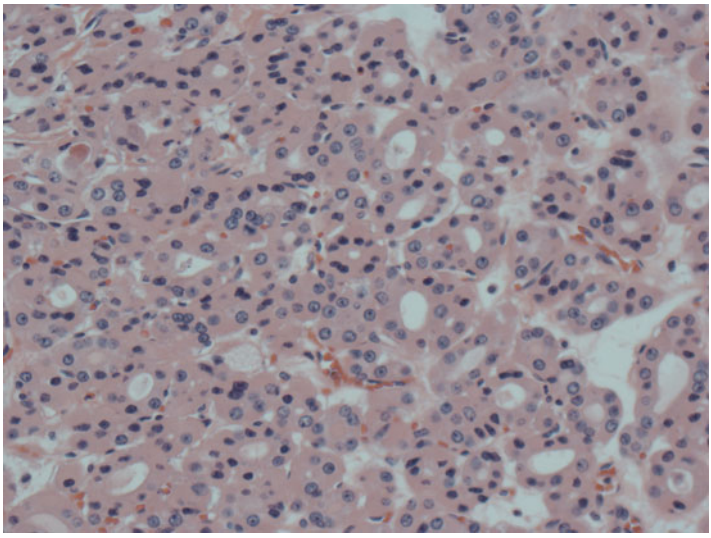

Fig. 4.8 Hürthle cell carcinoma. The neoplastic Hürthle cells demonstrate abundant granular eosinophilic cytoplasm, round to oval nuclei. Nuclear anisonucleosis, hyperchromasia, and prominent nucleoli are noted (H&E stain, high power)

addition, there was no extrathyroidal extension. The remaining thyroid showed features of multinodular goiter. The final diagnosis was Hürthle cell carcinoma. Level 7 and 4R mediastinal lymph nodes were sampled via mediastinoscopy and found to be negative for carcinoma.

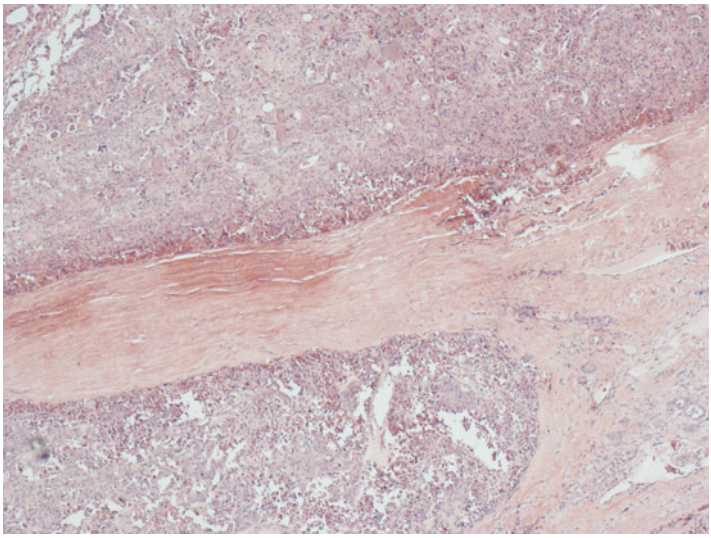

Fig. 4.9 Hürthle cell carcinoma. The tumor nodule (*left lower half*) invades the thick tumor capsule separate from the main tumor (*upper half*), denoting capsular invasion (H&E stain, low power)

Discussion

Hürthle cells, also called Askanazy cells, oxyphilic cells, and oncocytes, are altered follicular cells. They are arranged in two-dimensional flat sheets, and are typically described as large polygonal cells with abundant granular cytoplasm, enlarged round to oval nucleus, and, sometimes, prominent nucleolus (Figs. 4.10 and 4.11). They are frequently seen in reactive/hyperplastic conditions like lymphocytic or Hashimoto's thyroiditis, Graves' disease, and multinodular goiter, where they are considered metaplastic and nonneoplastic in nature. Not infrequently, Hürthle cell changes can be extensive, resulting in the formation of nodules that can be detectable on ultrasound. The challenge for cytologist is to distinguish these nonneoplastic Hürthle cell nodules from their neoplastic counterparts such as Hürthle cell adenomas and Hürthle cell carcinoma. According to the World Health Organization (WHO), Hürthle cell adenoma and carcinoma are classified as variants of follicular adenomas and carcinomas, respectively [1]. However, the Bethesda system for reporting thyroid cytology (TBSRTC) distinguishes Hürthle cell neoplasms from follicular neoplasms because the cytology is strikingly different between the two entities, and there is evidence suggesting that follicular and Hürthle cell carcinomas may be genetically different [2]. As a screening tool, thyroid FNA is highly sensitive at detecting Hürthle cell carcinomas. However, the specificity of thyroid FNA in diagnosing Hürthle cell carcinomas is fairly low because of the inability of cytology to establish the presence of capsular and/or vascular invasion. Approximately 14–30 % of patients with a cytologic diagnosis of Hürthle cell neoplasm are found to have a Hürthle cell carcinoma on subsequent surgical resection.

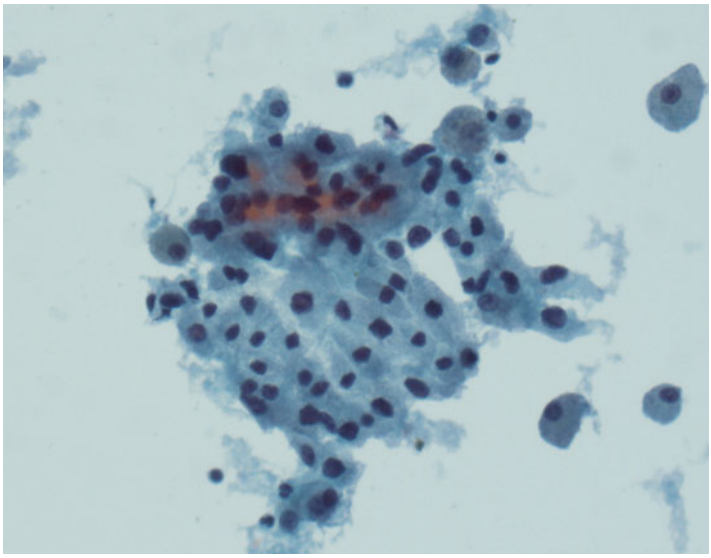

Fig. 4.10 Thyroid FNA-Hürthle cells. A two-dimensional sheet of Hürthle cells with abundant bluish gray granular cytoplasm. The nuclei are round to oval with mild anisonucleosis (Papanicolaou stain, high power)

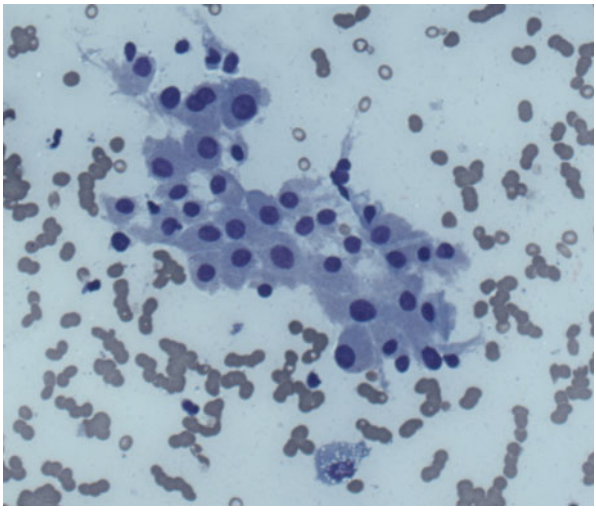

Fig. 4.11 Thyroid FNA-Hürthle cells. A two-dimensional sheet of Hürthle cells with abundant bluish magenta granular cytoplasm. The nuclei are round to oval and slightly eccentrically located with mild anisonucleosis (Diff-Quik stain, high power)

Hürthle cell adenomas are benign thyroid neoplasms and are composed entirely or predominantly (>75 %) of Hürthle cells. Their incidence is difficult to estimate because they are often considered as a variant of follicular adenoma. Hürthle cell adenomas are usually solitary, but multiple and bilateral tumors have been reported

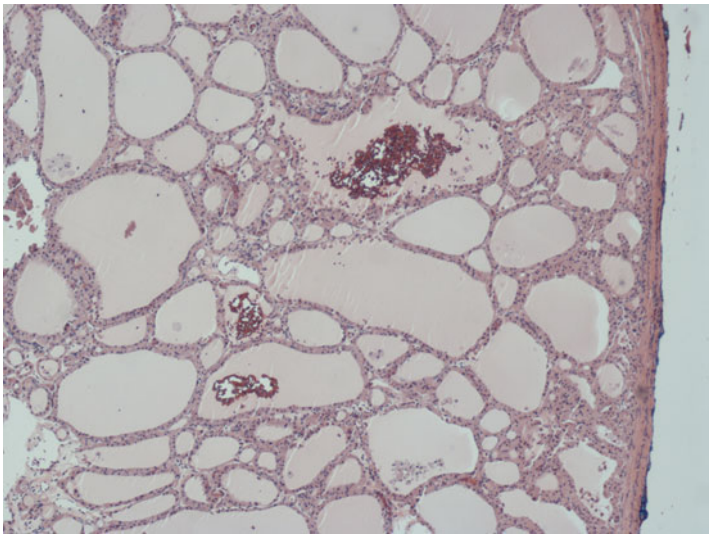

Fig. 4.12 Hürthle cell adenoma. A well-circumscribed neoplastic proliferation of Hürthle cells completely encapsulated by a thin fibrous capsule. The Hürthle cells are arranged in follicles of varying sizes and shapes (H&E stain, low power)

[3]. Histologically, Hürthle cell adenomas are completely encapsulated by a capsule of variable thickness (Fig. 4.12). The neoplastic Hürthle cells demonstrate growth patterns ranging from follicular, solid, trabecular, to occasional papillary (Figs. 4.13 and 4.14). Cystic changes have been described. Individual Hürthle cells can display significant nuclear pleomorphism including nuclear enlargement, anisonucleosis, hyperchromasia, and binucleation (Fig. 4.15).

Hürthle cell carcinomas are relatively uncommon, accounting for 2–3 % of all thyroid malignancies and 20 % of follicular carcinomas [3]. They are large and bulky and frequently replace the entire lobe. Histologically, Hürthle cell carcinomas can be completely encapsulated with evidence of capsular and/or vascular invasion (Figs. 4.16 and 4.17); however, widely invasive examples have also been described. Increased mitotic activities and apparent nuclear pleomorphism, such as increased N/C ratios, anisonucleosis, and prominent nucleoli, are frequently observed (Fig. 4.18). The distinction between Hürthle cell carcinoma and Hürthle cell adenoma is entirely based on demonstrating invasive characteristics such as capsular and/or vascular invasion, invasion of surrounding parenchyma, and metastatic lesions. Other primary thyroid malignant neoplasms such as papillary carcinoma and medullary carcinoma can also occasionally demonstrate diffuse Hürthle cell changes.

The primary goal of thyroid FNA in the management of Hürthle cell nodules is to separate those for which surgery is indicated, i.e., Hürthle cell adenomas and carcinomas, from those that can be managed conservatively, i.e., adenomatous

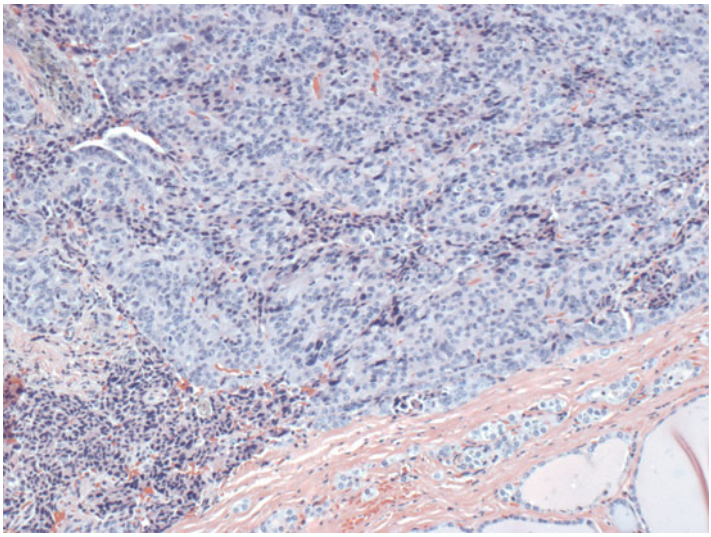

Fig. 4.13 Hürthle cell adenoma. Another example of Hürthle cell adenoma that is surrounded completely by a thick fibrous capsule and demonstrates a more solid growth pattern (H&E stain, low power)

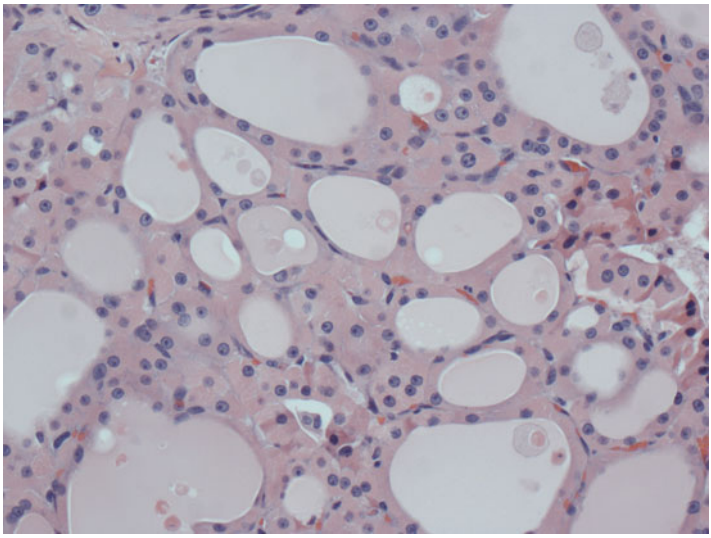

Fig. 4.14 Hürthle cell adenoma. High magnification shows that the follicles are lined by Hürthle cells with abundant granular cytoplasm. The nuclei are round and oval with considerable anisonucleosis and prominent nucleoli (H&E stain, high power)

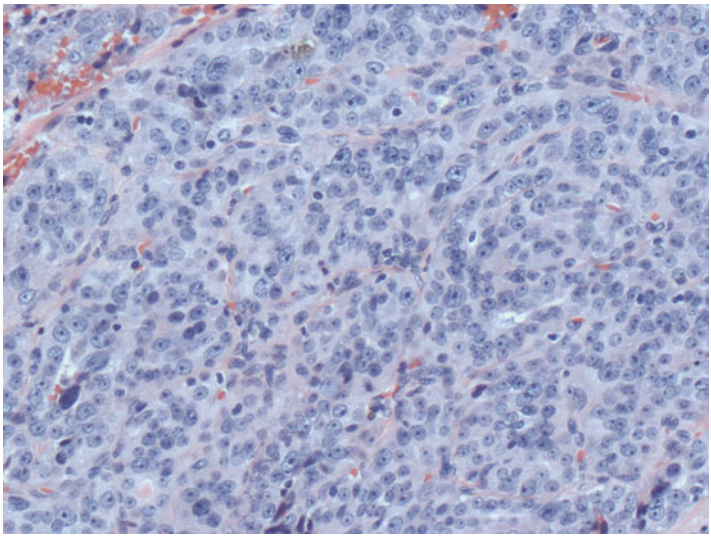

Fig. 4.15 Hürthle cell adenoma. This Hürthle cell adenoma is composed of solid proliferation of Hürthle cells with relatively less amount of granular cytoplasm, resulting in an increased nuclear to cytoplasmic ratio. There are also considerable nuclear crowding, anisonucleosis. Prominent nucleoli are frequent (H&E stain, high power)

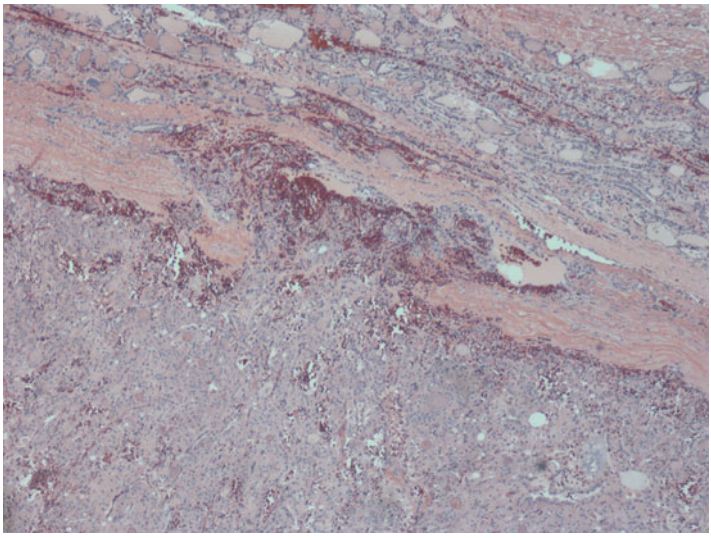

Fig. 4.16 Hürthle cell carcinoma. Low magnification showing a mushroomlike outgrowth of the tumor into the tumor capsule, i.e., capsular invasion (H&E, low power)

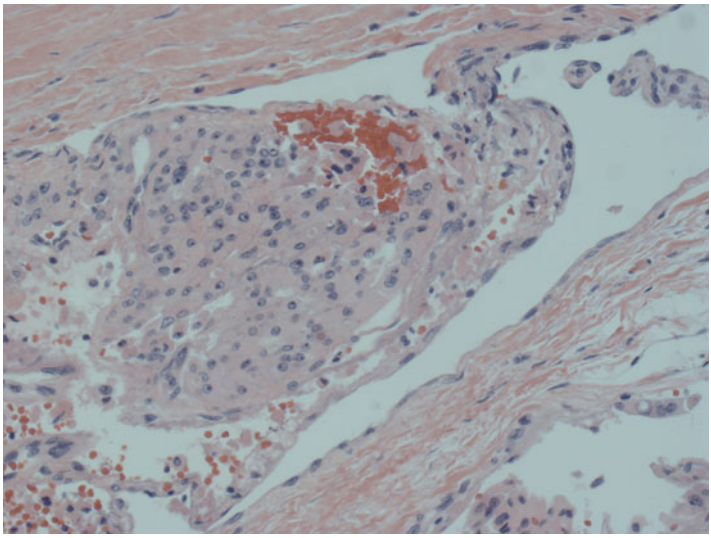

Fig. 4.17 Hurthle cell carcinoma. A tumor thrombus is noted in the lumen of a vessel within the tumor capsule, denoting vascular invasion. The tumor thrombus is lined by small, spindle-shaped endothelial cells (H&E stain, high power)

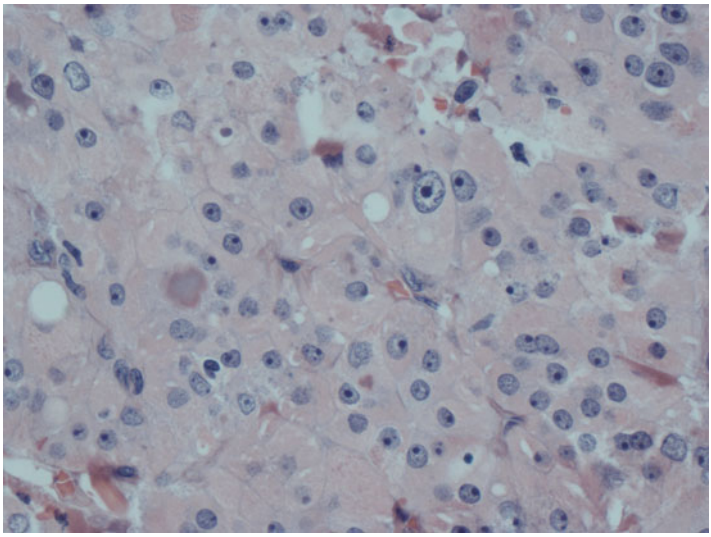

Fig. 4.18 Hürthle cell carcinoma. The neoplastic cells demonstrate abundant granular cytoplasm. The nuclei are round to oval with nuclear enlargement, marked anisonucleosis, and prominent nucleoli (H&E stain, high power)

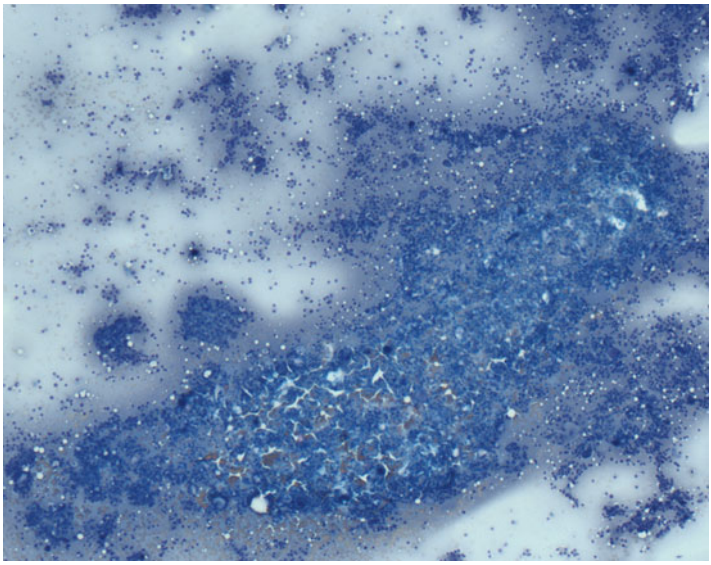

Fig. 4.19 Thyroid FNA-Hürthle cell neoplasm. The aspirate is highly cellular and consists of single and clusters of Hürthle cells in a bloody background. Subsequent follow-up revealed a Hürthle cell carcinoma (Diff-Quik stain, low power)

nodules with oncocytic changes and Hashimoto's thyroiditis. According to TBSRTC, the former group of Hürthle cell nodules would be classified under the diagnostic category "follicular neoplasm, Hürthle cell type" or "suspicious for a follicular neoplasm, Hürthle cell type" [2]. As mentioned earlier, the distinction between Hürthle cell adenomas and carcinomas is not possible on cytology because of the inability of cytology to establish the presence of capsular and/or vascular invasion. Therefore, rendering a diagnosis of Hürthle cell neoplasm implies these lesions should be excised to exclude a malignancy.

According to TBSRTC, the criteria for diagnosing "follicular neoplasm, Hürthle cell type" or "suspicious for a follicular neoplasm, Hürthle cell type" are moderately to markedly cellular aspirate that consists exclusively or predominantly (>75 %) of Hürthle cells with little or no colloid and lack of background lymphocytes [2] (Fig. 4.19). Hürthle cells with nuclear features of papillary thyroid carcinoma are excluded from this category. The Hürthle cells characteristically demonstrate abundant finely granular cytoplasm, which appears blue or bluish magenta with Diff-Quik stain, green, orange, or bluish gray with Papanicolaou stain, and pink with H&E stain (Figs. 4.20 and 4.21). Individual cells can be either small with high N/C ratio (≥50 %) (small cell dysplasia, Fig. 4.22) or large with at least 2× variability in nuclear size (large cell dysplasia, Fig. 4.23) [4]. Other nuclear atypia, such as nuclear crowding/overlapping, hyperchromasia, irregular nuclear membrane, and prominent nucleoli, can be seen in some cases (Fig. 4.24). The typical arrangement is loosely cohesive/single-cell pattern but crowded, syncytial tissue fragments can be seen sometimes (Figs. 4.25 and 4.26).

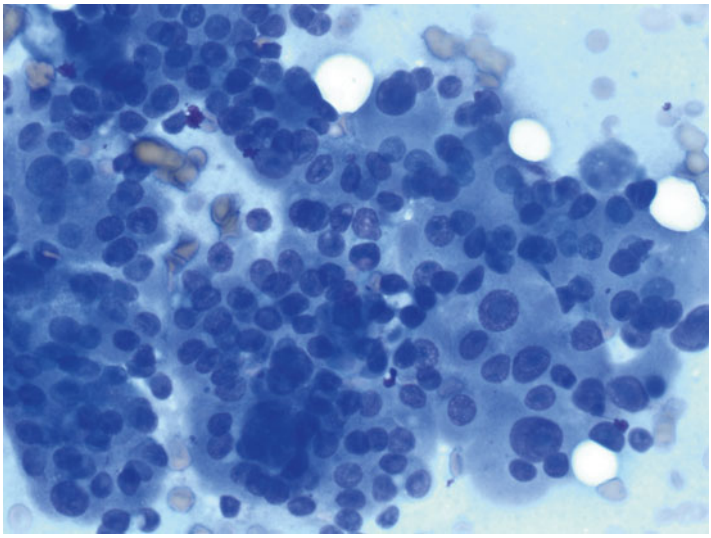

Fig. 4.20 Thyroid FNA-Hürthle cell neoplasm. A large cluster of Hürthle cells with considerable crowding and overlapping. Individual cells have abundant granular cytoplasm and demonstrate considerable anisonucleosis with more than 2× variability in sizes. Subsequent follow-up revealed a Hürthle cell carcinoma (Diff-Quik stain, high power)

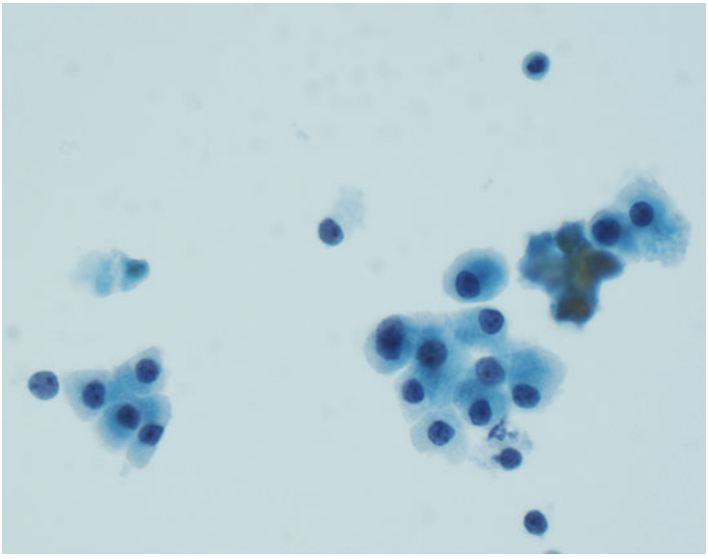

Fig. 4.21 Thyroid FNA-Hürthle cell neoplasm. Loosely cohesive groups of Hürthle cells with abundant granular cytoplasm and centrally or eccentrically located nuclei. Subsequent follow-up revealed a Hürthle cell carcinoma (Papanicolaou stain, high power)

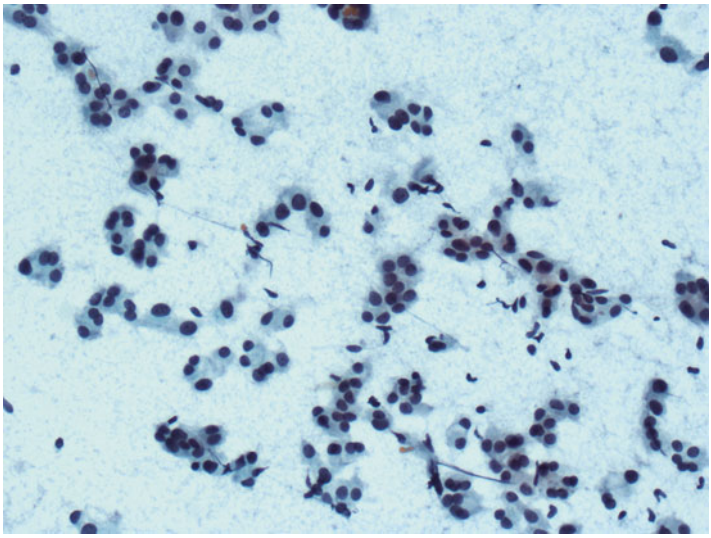

Fig. 4.22 Thyroid FNA-Hürthle cell neoplasm (small cell dysplasia). Loosely cohesive groups of Hürthle cells with scanty to moderate amount of granular cytoplasm, resulting in increased nuclear to cytoplasmic ratio. Nuclei are hyperchromatic and demonstrate mild degree of anisonucleosis. Subsequent follow-up revealed a Hürthle cell adenoma (Papanicolaou stain, high power)

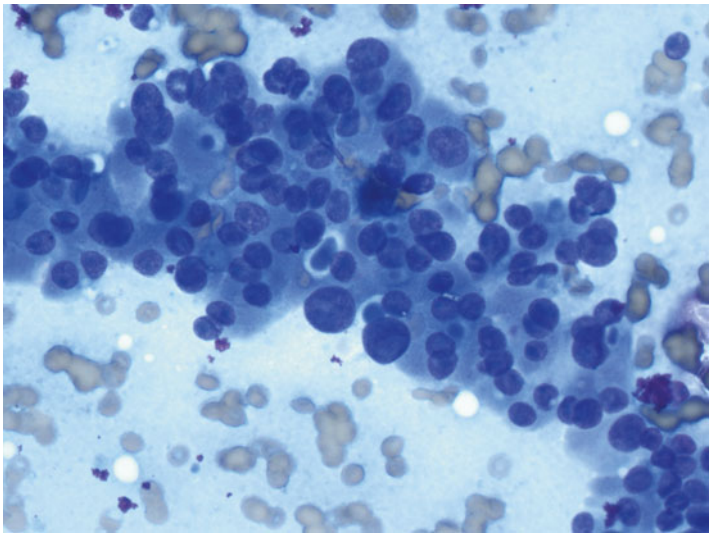

Fig. 4.23 Thyroid FNA-Hürthle cell neoplasm (large cell dysplasia). Cohesive groups of Hürthle cells with moderate to abundant amount of cytoplasm. The nuclei demonstrate considerable anisonucleosis with more than 2× variability in sizes. Subsequent follow-up revealed a Hürthle cell carcinoma (Diff-Quik stain, high power)

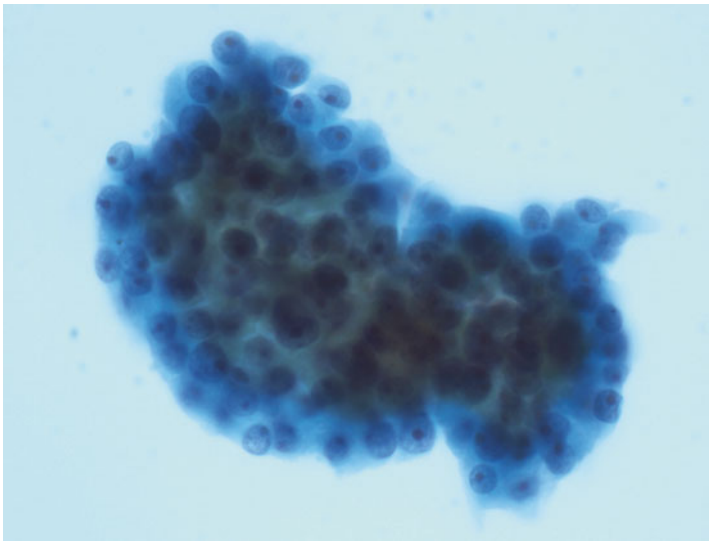

Fig. 4.24 Thyroid FNA-Hürthle cell neoplasm. A tightly cohesive group of Hürthle cells with considerable nuclear crowding and overlapping. The nuclei are large with prominent macronucleoli. Subsequent follow-up revealed a Hürthle cell adenoma (Papanicolaou stain, high power)

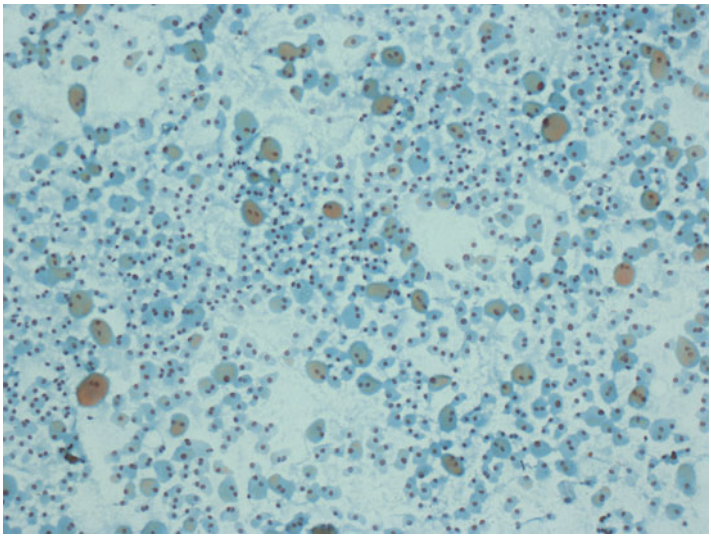

Fig. 4.25 Thyroid FNA-Hürthle cell neoplasm. This aspirate is cellular and consists of predominantly single Hürthle cells. Subsequent follow-up revealed a Hürthle cell adenoma (Papanicolaou stain, low power)

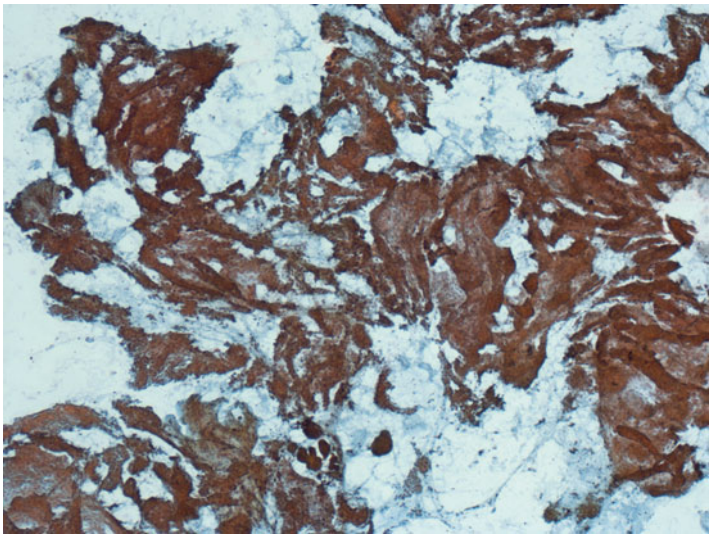

Fig. 4.26 Thyroid FNA-Hürthle cell neoplasm. This aspirate is cellular and consists of predominantly large syncytial tissue fragments of Hürthle cells. Subsequent follow-up revealed a Hürthle cell adenoma (Papanicolaou stain, low power)

When all the cytologic criteria are present, the diagnosis of "follicular neoplasm, Hürthle cell type" or "suspicious for a follicular neoplasm, Hürthle cell type" is straightforward. However, when only some of the criteria are present, the diagnosis can be challenging. One problematic scenario is the finding of sparsely cellular specimens composed entirely of Hürthle cells and little colloid (Fig. 4.27). Most cytologists would agree that a diagnosis of "follicular lesion of undetermined significance" (FLUS) would be more appropriate than a diagnosis of "follicular neoplasm, Hürthle cell type" or "suspicious for a follicular neoplasm, Hürthle cell type." A repeat biopsy would frequently offer a more definitive diagnosis since many of these cases are due to poor sampling.

Another diagnostic challenge is the finding of a moderately to markedly cellular aspirate consisting of a pure population of Hürthle cells and a conspicuous amount of colloid (Fig. 4.28). Most cytologists would prefer to interpret the sample as benign, particularly in the absence of any cytologic and/or architectural atypia. A variation of this scenario is the finding of a cellular aspirate of Hürthle cells without both architectural and cytologic atypia as well as little or no colloid (Figs. 4.29 and 4.30). Many cytologists would diagnose such sample as "follicular neoplasm, Hürthle cell type" or "suspicious for a follicular neoplasm, Hürthle cell type." However, some cytologists advocate classifying such case as "benign" since recent studies have shown that only very small percentages of aspirates with this presentation were found to be malignant on subsequent follow-up [4, 5].

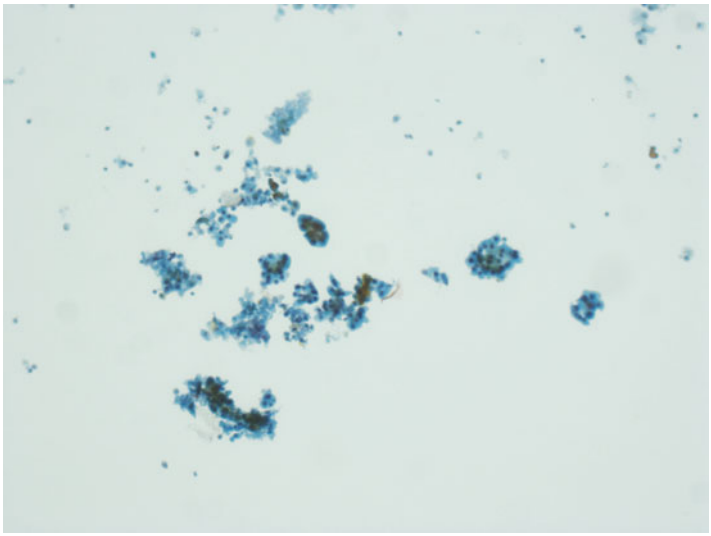

Fig. 4.27 Thyroid FNA-follicular lesion of undetermined significance (FLUS). The aspirate is of low cellularity and consists of scattered small groups of Hürthle cells. No colloid is noted in the background. Subsequent follow-up revealed a Hürthle cell carcinoma (Papanicolaou stain, low power)

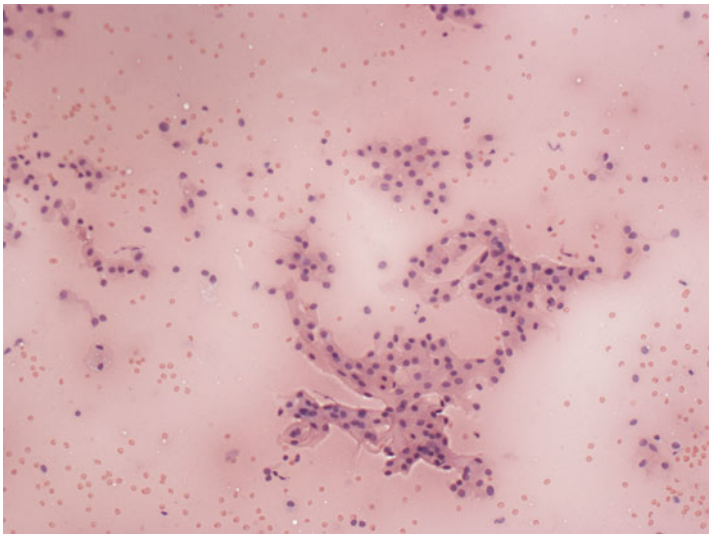

Fig. 4.28 Thyroid FNA-goiter. This aspirate is moderately cellular and consists of monolayer flat sheets of predominantly Hürthle cells in a background of abundant colloid (Papanicolaou stain, low power)

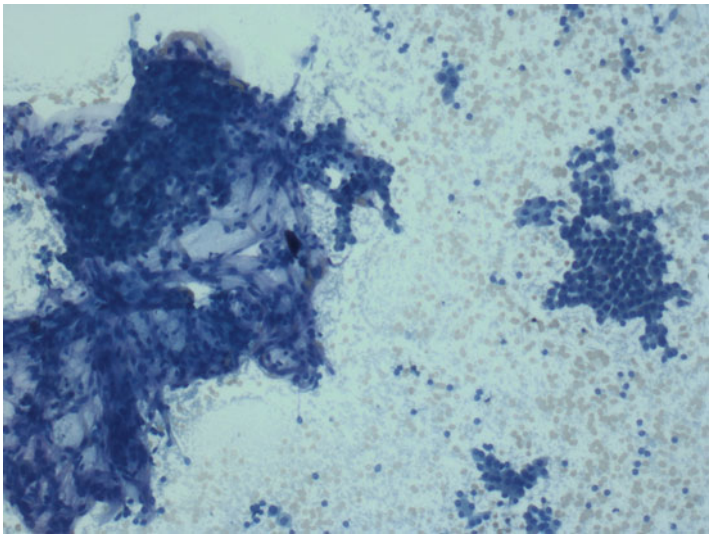

Fig. 4.29 Thyroid FNA-Hürthle cell neoplasm. Cellular aspirate with sheets of Hürthle cells. No colloid is noted in the background. Subsequent follow-up revealed a nodular goiter with adenomatous hyperplasia (Diff-Quik stain, low power)

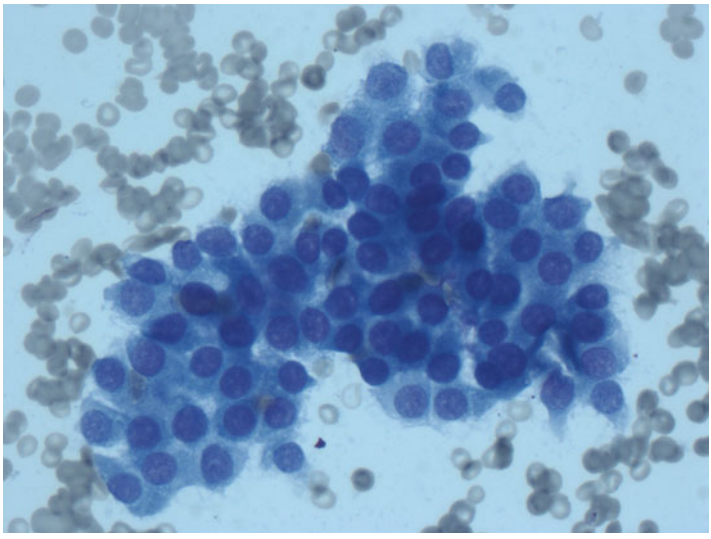

Fig. 4.30 Thyroid FNA-Hürthle cell neoplasm. High magnification shows a flat sheet of relatively uniform Hürthle cells without any significant cytologic atypia. Subsequent follow-up revealed a nodular goiter with adenomatous hyperplasia (Diff-Quik stain, high power)

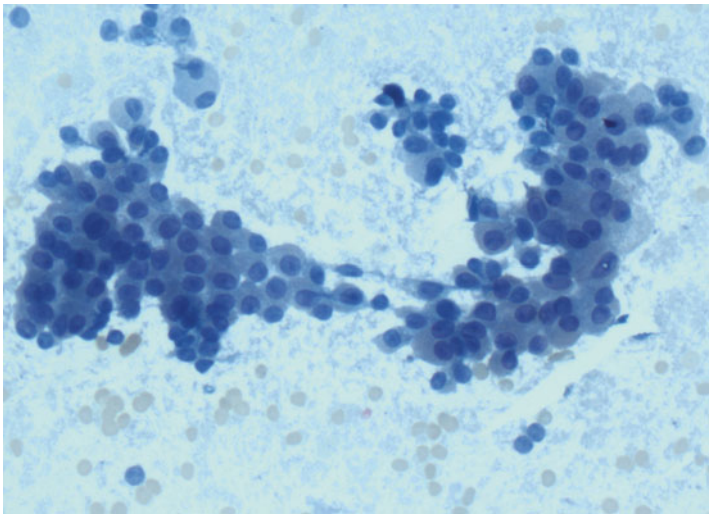

Fig. 4.31 Thyroid FNA-goiter. Monolayer sheets of Hürthle cells with minimal cytologic atypia. Features of small cell or large cell dysplasia are absent (Diff-Quik stain, high power)

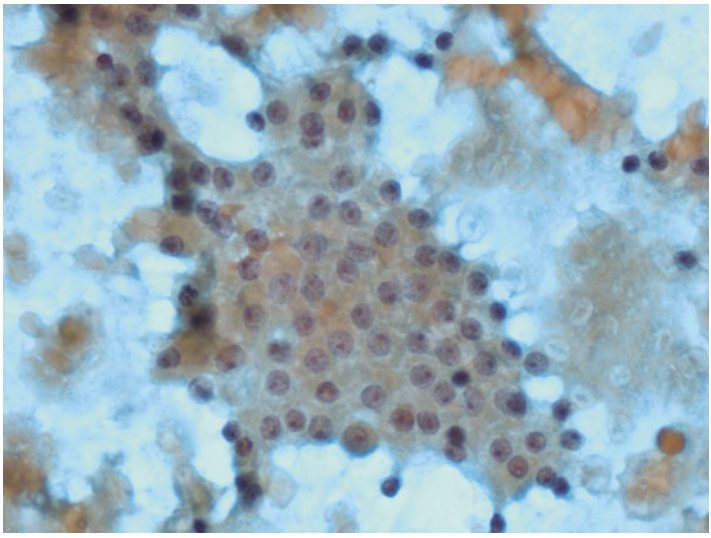

Fig. 4.32 Thyroid FNA-goiter. Monolayer sheet of Hürthle cells with minimal cytologic atypia. Features of small cell or large cell dysplasia are absent (Papanicolaou stain, high power)

Nonneoplastic nodules composed of entirely or predominantly Hürthle cells can occur in nodular goiters, Hashimoto's thyroiditis, and sometimes Graves' disease. These nodules are indistinguishable from neoplastic Hürthle cell nodules clinically

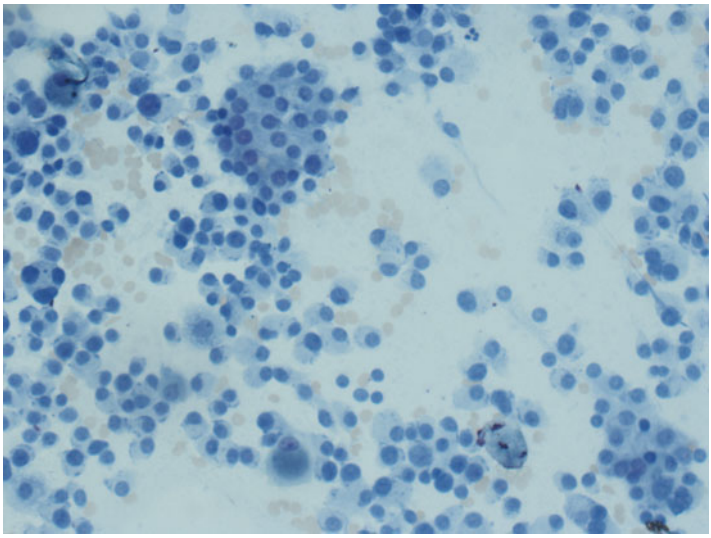

Fig. 4.33 Thyroid FNA-medullary carcinoma. Cellular aspirate consisting of loosely cohesive and single neoplastic cells. Individual cells have moderate amount of granular cytoplasm, eccentrically located nuclei, resulting in a plasmacytoid appearance. Moderate degree of anisonucleosis is noted (Diff-Quik stain, low power)

and radiologically. Hürthle cells aspirated from these nonneoplastic Hürthle cell nodules tend to be cohesive and arranged in two-dimensional sheets with a honeycomb appearance (Figs. 4.31 and 4.32). Hürthle cells with features of small cell or large cell dysplasia are usually not apparent. However, other nuclear atypia, such as hyperchromasia, nuclear enlargement, and anisonucleosis, can be identified in some nonneoplastic Hürthle cell nodules and can be confused with their neoplastic counterparts. Colloid and/or a mixed lymphoid population are frequently present, but they are variable and can be inconspicuous. The finding of groups and tissue fragments of regular type follicular cells that are often present in the background would further support a nonneoplastic process.

The differential diagnosis of Hürthle cell neoplasm includes other neoplasms such as oncocytic and tall cell variant of papillary thyroid carcinoma, medullary carcinoma, parathyroid adenoma, and metastatic renal cell carcinoma. Both Hürthle cell neoplasm and medullary carcinoma are characterized by a loosely cohesive/single cell pattern of neoplastic cells with moderate to abundant amount of granular cytoplasm and eccentrically located nuclei (Fig. 4.33). Nuclear atypia such as binucleation and anisonucleosis can be seen in both tumors. One helpful feature is the presence of a prominent central nucleolus, which is frequently present in Hürthle cell neoplasms but rarely in medullary thyroid carcinomas (Fig. 4.34). The finding of "a conspicuous" population of spindle neoplastic cells would not favor a diagnosis of Hürthle cell neoplasm (Fig. 4.35). Since the management of these two entities is quite different, the use of immunocytochemical staining for calcitonin and

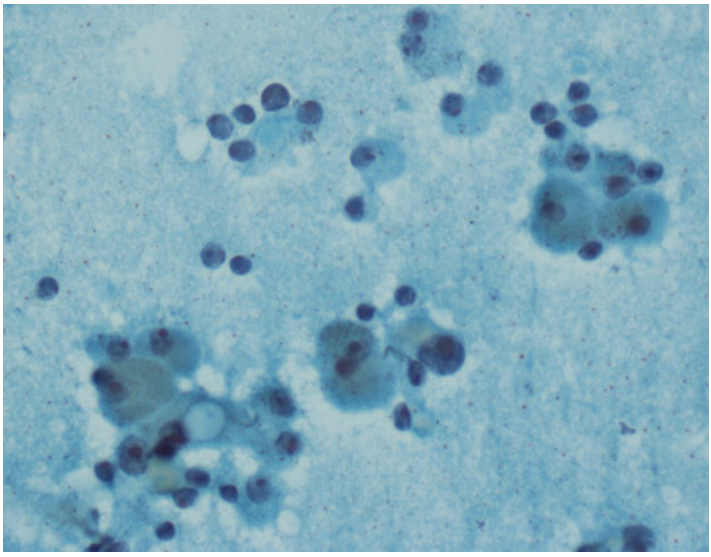

Fig. 4.34 Thyroid FNA-Hürthle cell neoplasm. In contrast to medullary carcinoma, the presence of prominent central nucleoli would favor a diagnosis of Hürthle cell neoplasm (Papanicolaou stain, high power)

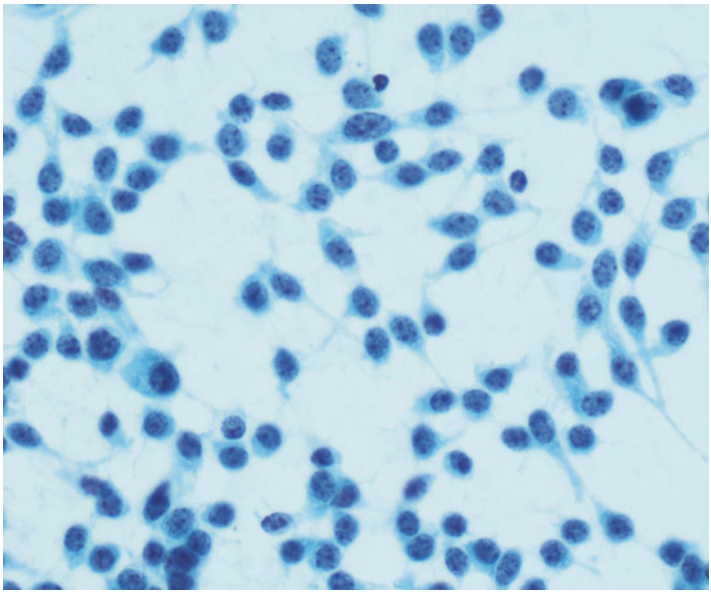

Fig. 4.35 Thyroid FNA-medullary carcinoma. This aspirate consists of a mixture of epithelioid and spindle-shaped cells. The latter would not favor a diagnosis of Hürthle cell neoplasm. The nuclei demonstrate the "salt and pepper" chromatin which is characteristic of medullary carcinoma (Diff-Quik stain, low power)

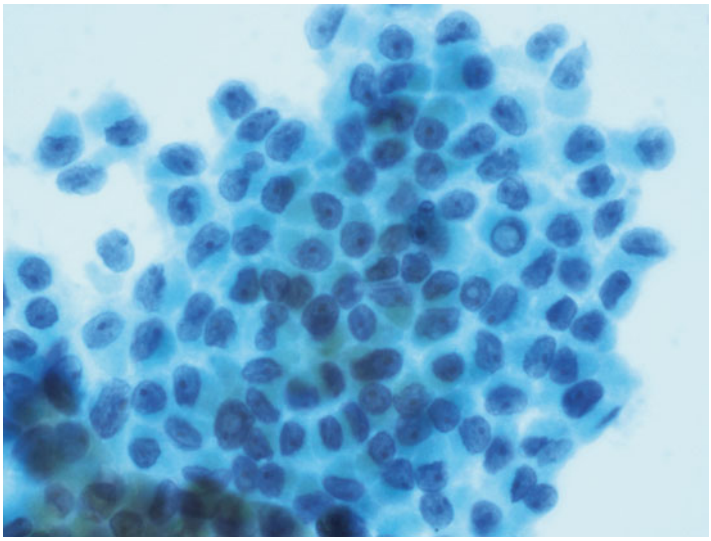

Fig. 4.36 Thyroid FNA-papillary thyroid carcinoma, oncocytic variant. Mildly crowded sheets of follicular cells with moderate amount of granular cytoplasm, resembling Hürthle cells. Individual cells show powdery chromatin, irregular nuclear membrane, nuclear grooves, and intranuclear inclusions—changes typical of papillary thyroid carcinoma (Papanicolaou stain, high power)

thyroglobulin for the differential diagnosis is highly recommended when possible. Alternatively, serum calcitonin level can be recommended to rule out a medullary carcinoma when additional cytologic material is not available for ancillary studies or when result of the immunohistochemical staining is noncontributory. Keep in mind that thyroid transcription factor-1 (TTF-1) would not be helpful in the differential diagnosis since both tumors would demonstrate positive staining with TTF-1.

Because the neoplastic cells of both oncocytic and tall cell variants of PTC have abundant granular cytoplasm, they may be mistaken for Hürthle cell neoplasms (Fig. 4.36). Occasionally, papillae can be seen in Hürthle cell neoplasms, making the distinction from PTC more challenging (Fig. 4.37). The most salient feature distinguishing Hürthle cell neoplasms from PTC is the lack of classic nuclear features diagnostic of PTC such as extensive nuclear grooves, pseudo-nuclear inclusions, and pale chromatin. Additionally, the dispersed, isolated cell pattern of Hürthle cell neoplasm differs from the crowded, overlapping cellular groups found in PTCs (Fig. 4.38).

Parathyroid adenomas with oncocytic features may be mistaken for a Hürthle cell neoplasm. The latter usually presents with loosely cohesive or isolated neoplastic cells with much larger nuclei and prominent nucleoli when compared to parathyroid adenomas. Immunohistochemical stains for thyroglobulin/TTF-1 and parathyroid hormone will separate these two entities. Alternatively, the aspirate can

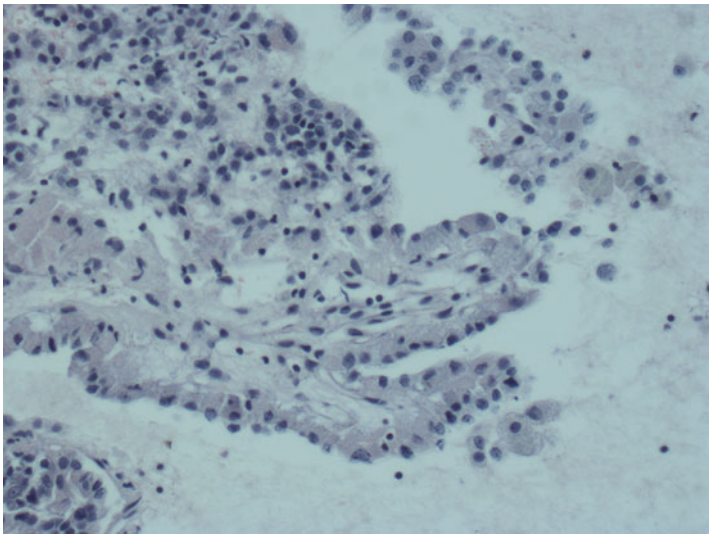

Fig. 4.37 Thyroid FNA-goiter. Cell block preparation showing papillae lined by oncocytic follicular cells. Nuclear features of papillary thyroid carcinoma are not present (H&E stain, high power)

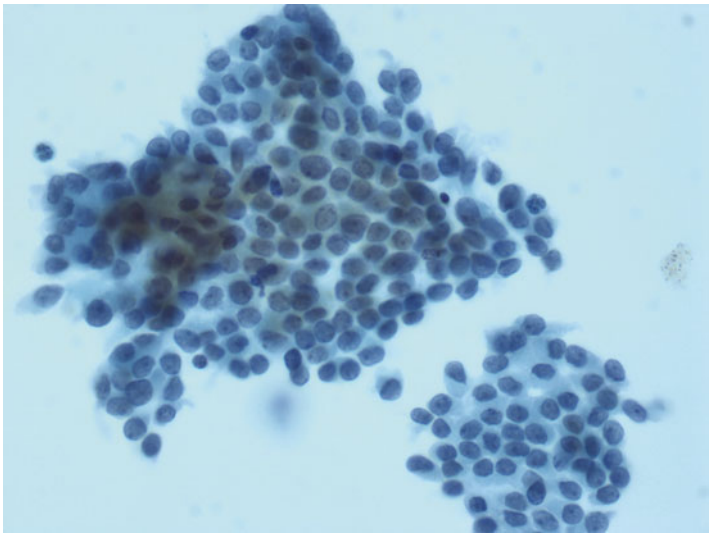

Fig. 4.38 Thyroid FNA-papillary thyroid carcinoma, oncocytic variant. Clusters of oncocytic follicular cells with considerable overlapping and crowding. The latter is more frequently observed in papillary thyroid carcinoma when compared to Hürthle cell neoplasm (Papanicolaou stain, high power)

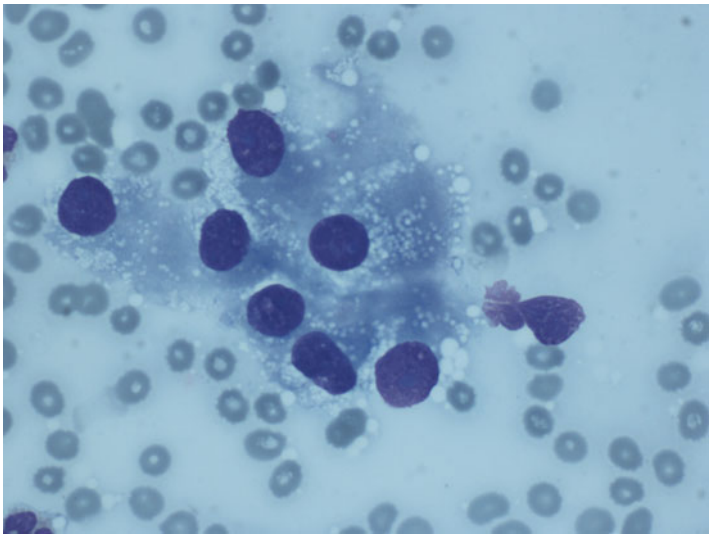

Fig. 4.39 Thyroid FNA-metastatic renal cell carcinoma. A small cluster of neoplastic cells with abundant granular cytoplasm. Multiple fine cytoplasmic vacuoles are also noted. Nuclei are markedly enlarged (Diff-Quik stain, high power)

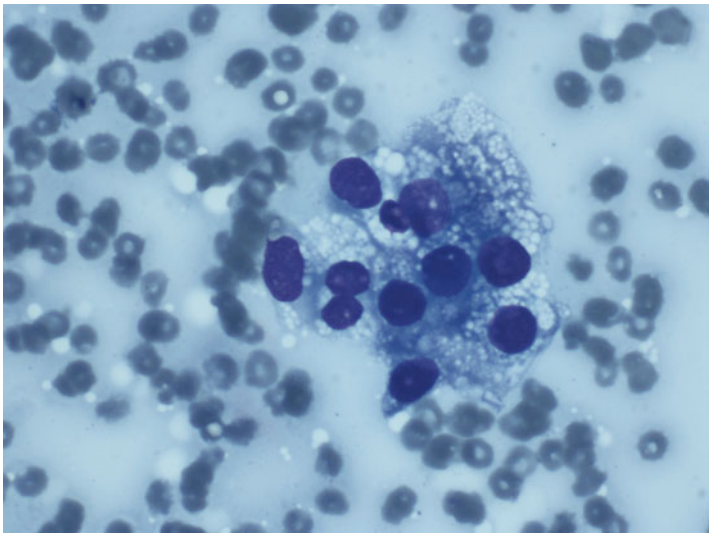

Fig. 4.40 Thyroid FNA-metastatic renal cell carcinoma. A small cluster of neoplastic cells with abundant cytoplasmic vacuoles, resulting in a "clear" cell appearance (Diff-Quik stain, high power)

be submitted for parathyroid hormone level analysis when a parathyroid lesion is suspected clinically or on imaging prior to FNA.

Metastatic renal cell carcinomas, especially those with a more granular cell pattern (Fig. 4.39), should be included in the differential diagnosis of a Hürthle cell

neoplasm. A prior history of malignancy should alert the cytologists to the possibility of a metastasis, although this is not always the case. The finding of neoplastic cells with clear cell changes or vacuolated cytoplasm would favor a metastatic renal cell carcinoma (Fig. 4.40). A panel of antibodies including TTF-1 and thyroglobulin would be helpful in the differential diagnosis.

References

1. DeLellis RA, Lloyd RV, Heitz PU, Eng C. Pathology and genetics of tumours of endocrine organs. Lyon, France: IARC Press; 2004.
2. Ali SZ, Cibas ES. The Bethesda system for reporting thyroid cytopathology. New York, NY: Springer; 2010.
3. Watson RG, Brennan MD, Goellner JR, van Heerden JA, McConahey WM, Taylor WF. Invasive Hürthle cell carcinoma of the thyroid: natural history and management. Mayo Clin Proc. 1984;59:851–5.
4. Renshaw AA. Hürthle cell carcinoma is a better gold standard than Hürthle cell neoplasm for fine-needle aspiration of the thyroid: defining more consistent and specific cytologic criteria. Cancer. 2002;96:261–6.
5. Wu HH, Clouse J, Ren R. Fine-needle aspiration cytology of Hürthle cell carcinoma of the thyroid. Diagn Cytopathol. 2008;36:149–54.

Hashimoto Thyroiditis

5

Case Study

A 40-year-old female presented with a bilateral thyroid enlargement, which was noted 3 years ago. She complained of hoarseness and difficulty in swallowing, but she had no complaints of difficulty in breathing or compressive symptoms. She had no symptoms of hyperthyroidism and no history of radiation to the head or neck. Her past medical history was significant for primary hypothyroidism. She was on synthroid, 0.88 mg/day. The patient was a known smoker, but she had no history of alcohol intake and no recreational drug use. Her mother had a history of unspecified thyroid disease while her sister had a history of papillary thyroid carcinoma. Her thyroid function tests were as follows: TSH, 5.49 μU/mL; total T3, 91 ng/dL; total T4, 5.6 μg/dL; and free T4, 0.8 ng/dL. Ultrasonographic examination showed an $8.1 \times 3.5 \times 2.5$ cm right thyroid lobe and a $7.7 \times 3.4 \times 3.2$ cm left thyroid lobe. There were no discrete thyroid nodules. Fine needle aspiration of right thyroid demonstrated follicular lesion of undetermined significance in a background of lymphocytic thyroiditis. Patient underwent total thyroidectomy, which revealed florid Hashimoto thyroiditis. Her postoperative course was unremarkable.

Discussion

Chronic lymphocytic (Hashimoto) thyroiditis is a common autoimmune disease, which is characterized by the destruction of thyroid follicles by marked lymphoid infiltrate. This condition more commonly occurs in women, with a peak incidence in the fourth and fifth decades of life, but affected individuals range from children to older adults [1, 2]. Some individuals have a genetic predisposition to develop Hashimoto thyroiditis. The susceptibility genes appear to include both immune modifying genes, in particular HLA-DR and cytotoxic T lymphocyte factor 4 (*CTLA-4*) and thyroid-specific genes such as thyroglobulin [3, 4]. This condition is generally thought to result from a complex interaction of these genes and

A.J. Adeniran, D. Chhieng, *Common Diagnostic Pitfalls in Thyroid Cytopathology*, DOI 10.1007/978-3-319-31602-4_5

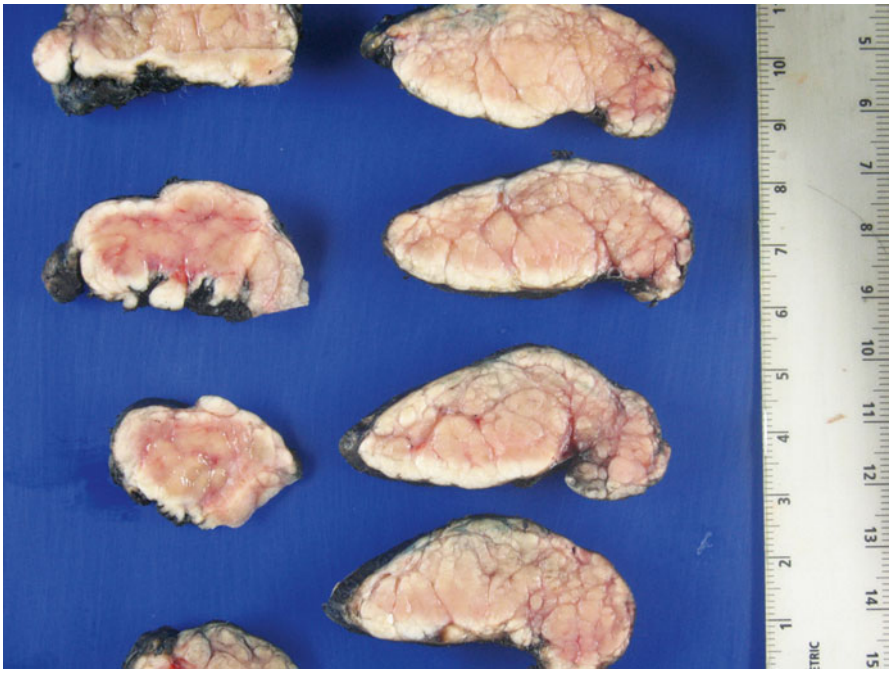

Fig. 5.1 Gross appearance of the thyroid. Uniform enlargement with pale cut surface and accentuated lobular pattern

environmental factors. The diagnosis is usually established by a constellation of clinical features and serologic test results. One or more of a variety of circulating autoantibodies are identified in almost all patients, the most common of which are anti-thyroglobulin and antithyroid peroxidase. Patients with Hashimoto thyroiditis are at increased risk of developing malignant lymphoma [5–7], and this risk has been estimated to be up to 80-fold.

Thyroid glands with Hashimoto thyroiditis typically show diffuse enlargement, which is usually symmetrical, but some variation in the size of the lobes may be seen, leading to asymmetrical and massive enlargement of the gland. The gland feels firm and rubbery. The cut surface is usually paler than the normal red-brown color, reflecting the infiltration by lymphocytes and loss of follicular tissue [8, 9] (Fig. 5.1). Intense and patchy infiltration of the gland by lymphocytes and plasma cells with formation of germinal centers is the most characteristic feature on histologic examination (Fig. 5.2). The lymphoplasmacytic infiltration is diffuse but variable in its intensity and effacement of the follicles [10, 11]. There is significant variation in the lymphoid infiltrate from gland to gland and also in different areas of the same gland. In extreme cases, it can be florid with markedly enlarged lymphoid follicles containing large, expanded germinal centers (Figs. 5.3, 5.4, and 5.5). Epithelial changes seen in Hashimoto thyroiditis include follicular atrophy and Hürthle cell metaplasia, which can be focal, diffuse, and sometimes extensive, with

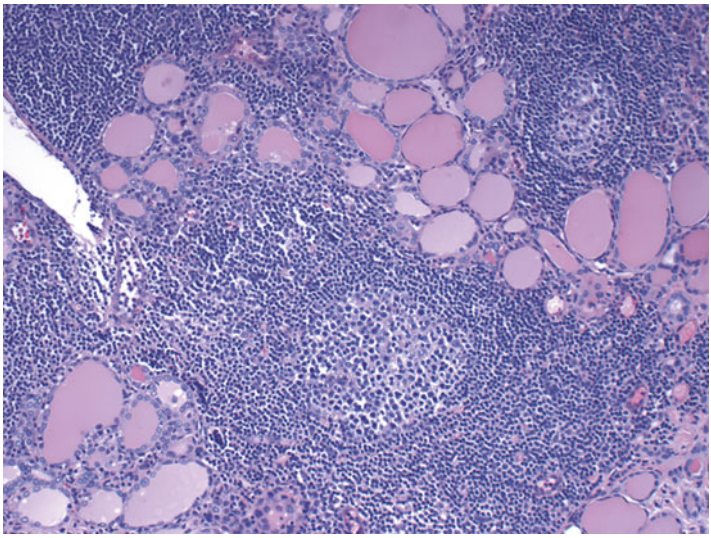

Fig. 5.2 Histologic appearance of Hashimoto thyroiditis. Follicular atrophy and infiltration of the gland by lymphocytes and plasma cells with formation of germinal centers (H&E stain, X100)

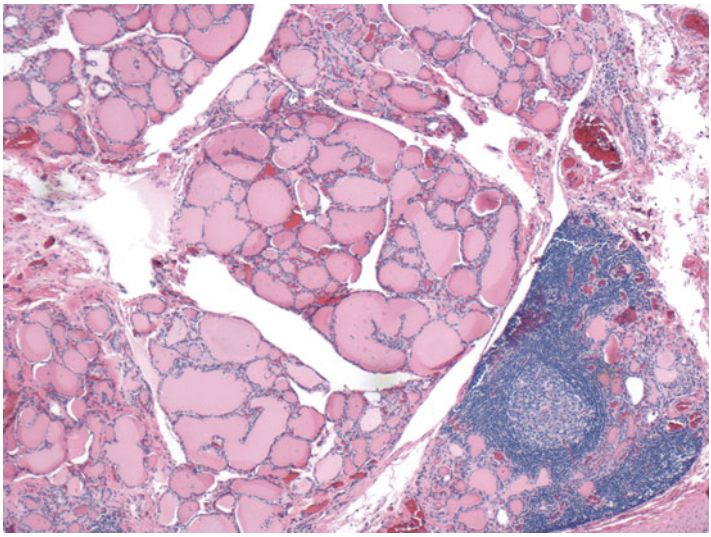

Fig. 5.3 Focal involvement of the thyroid gland by Hashimoto thyroiditis (H&E stain, X40)

formation of nodules (Figs. 5.6 and 5.7). A number of histologic variants of Hashimoto thyroiditis have been described. These include fibrous, fibrous atrophy, hashitoxicosis, and juvenile variants [8]. The fibrous variant is characterized by marked fibrosis, effacement of the follicular architecture, and marked follicular

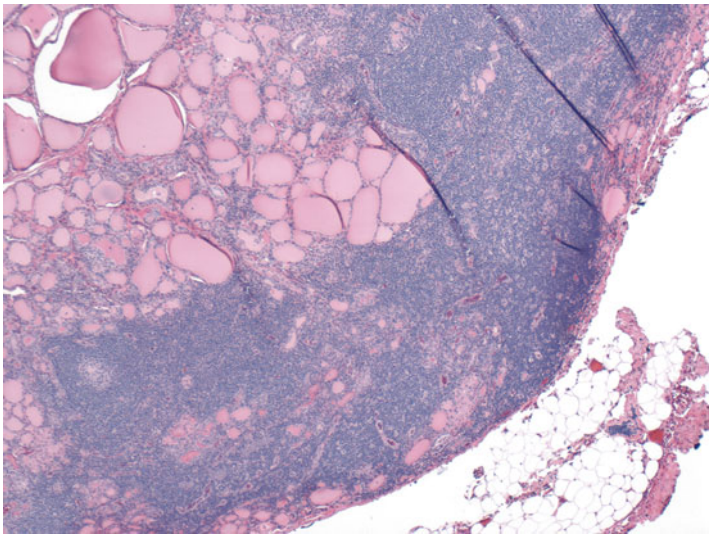

Fig. 5.4 Diffuse involvement of the thyroid gland by Hashimoto thyroiditis (H&E stain, X40)

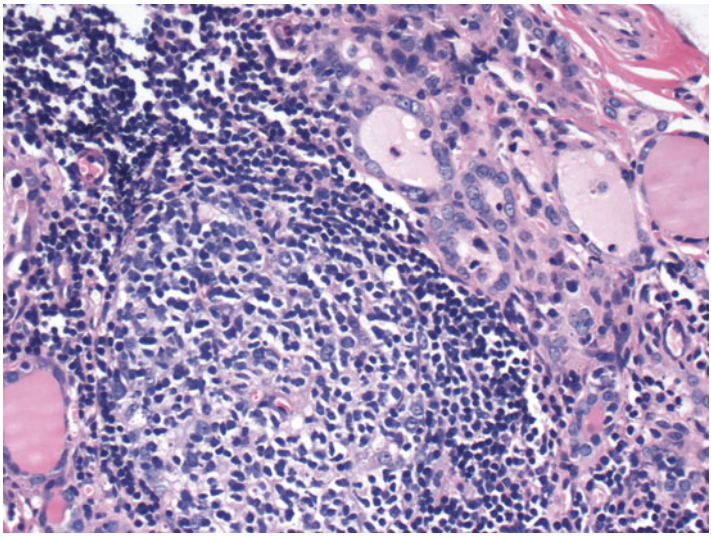

Fig. 5.5 Hashimoto thyroiditis demonstrating an enlarged lymphoid follicle containing large, expanded germinal center (H&E stain, X200)

atrophy. The fibrous atrophy variant is histologically similar to the fibrous variant, but the glands in fibrous atrophy tend to be much smaller. Hashitoxicosis is a variant in which features of Hashimoto thyroiditis coexist with diffuse toxic hyperplasia of Grave's disease. The juvenile variant is an ill-defined form that occurs in younger individuals and shows little or no follicular atrophy on histology.

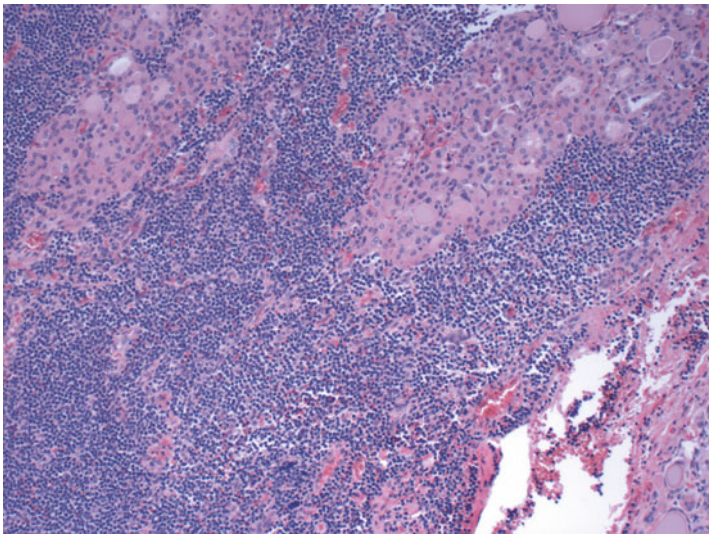

Fig. 5.6 Hashimoto thyroiditis with prominent Hürthle cell metaplasia and lymphoid infiltrate (H&E stain, X100)

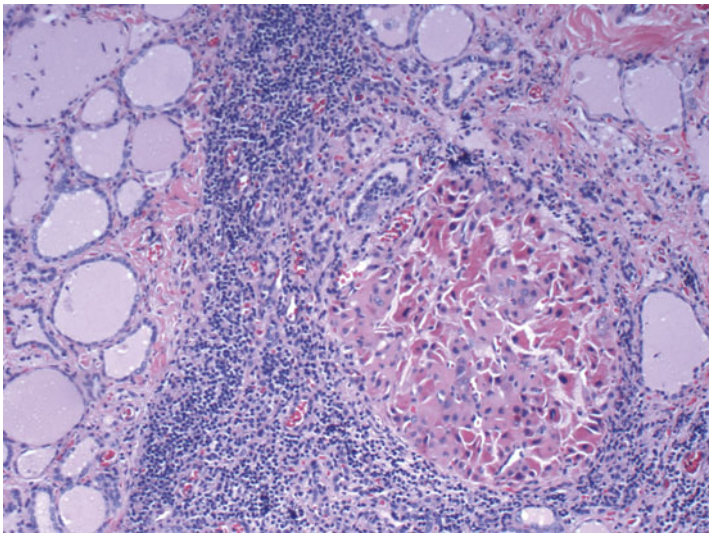

Fig. 5.7 Hashimoto thyroiditis showing a Hürthle cell nodule with background lymphoid aggregates (H&E stain, X100)

In patients with Hashimoto thyroiditis, fine needle aspiration (FNA) is not routinely performed. It is done only when there is a suspicious nodule, which raises the possibility of a coexisting malignancy. The aspirates are usually very cellular and usually characterized by a polymorphous population of lymphocytes, including small lymphocytes, centrocytes, centroblasts, and dendritic cells. Germinal center

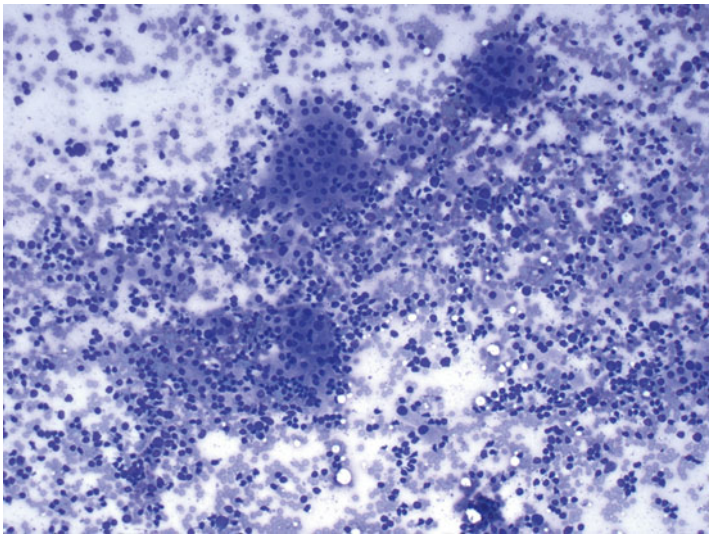

Fig. 5.8 Low-power image of FNA of Hashimoto thyroiditis showing a mixture of epithelial and inflammatory cells (Diff-Quik stain, X100)

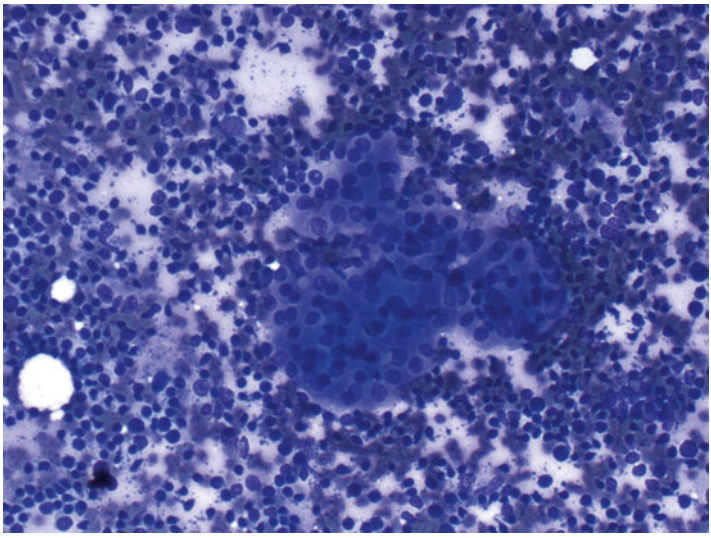

Fig. 5.9 Higher magnification of Hürthle cell fragments in a background of lymphoplasmacytic cells (Diff-Quik stain, X200)

fragments containing dendritic cells as well as tingible body macrophages are also present. Colloid is usually scant to absent. Normal follicular cells are scant or absent and in most cases, only clusters of follicular cells with Hürthle cell metaplasia are seen (Figs. 5.8, 5.9, 5.10, 5.11, 5.12, and 5.13). Because of the intense lymphocytic

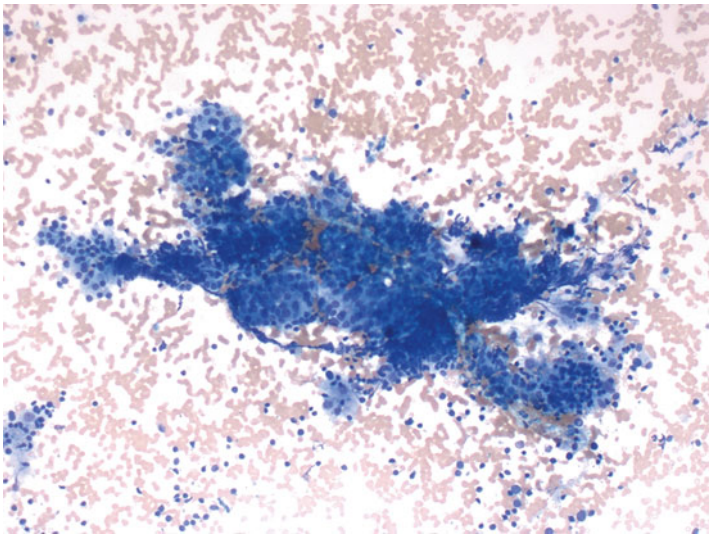

Fig. 5.10 FNA of Hashimoto thyroiditis. Cellular aspirate containing large numbers of epithelial tissue fragments in a background of lymphoid cells (Diff-Quik stain, X100)

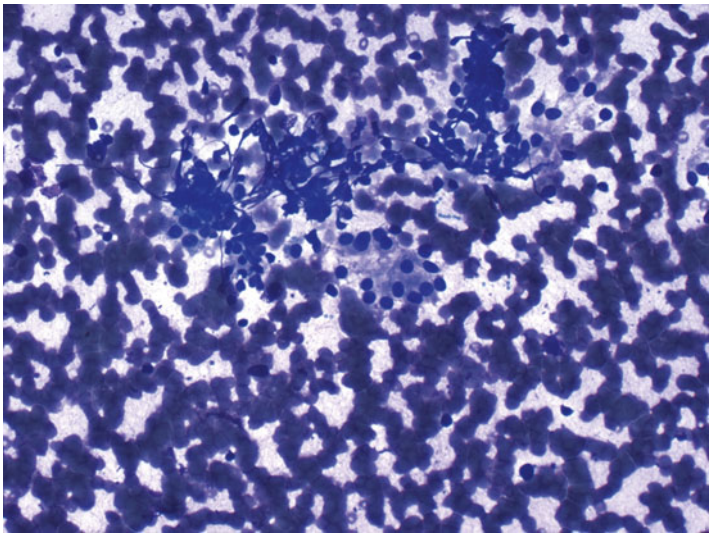

Fig. 5.11 FNA of Hashimoto thyroiditis showing Hürthle cell fragments and crushed, stretched-out lymphocytes (lymphoid tangles) (Diff-Quik stain, X200)

infiltration, these cells have reactive nuclear changes such as chromatin clearing and nuclear enlargement, and these features may lead to a misdiagnosis of papillary thyroid carcinoma. Occasional multinucleated giant cells are seen, and this may lead to confusion with subacute thyroiditis, but the multinucleated giant cells are not as numerous as seen in subacute thyroiditis.

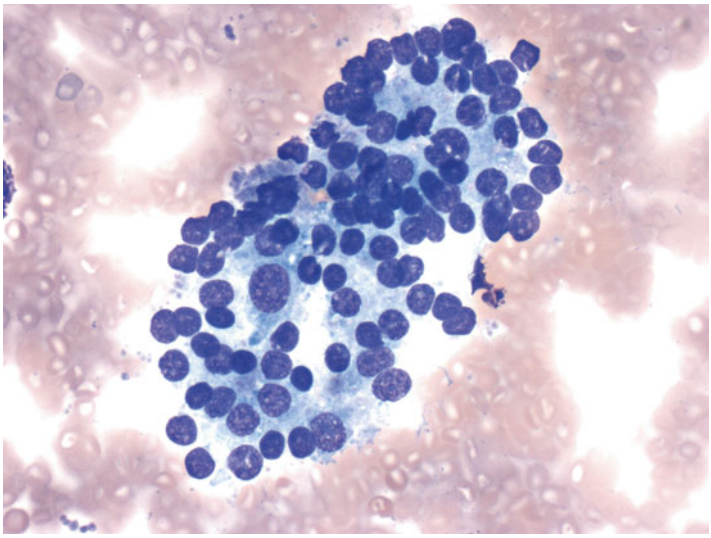

Fig. 5.12 FNA of Hashimoto thyroiditis showing Hürthle cells with some cytologic atypia. Few scattered lymphocytes are present, which favor the diagnosis of lymphocytic thyroiditis (Diff-Quik stain, X400)

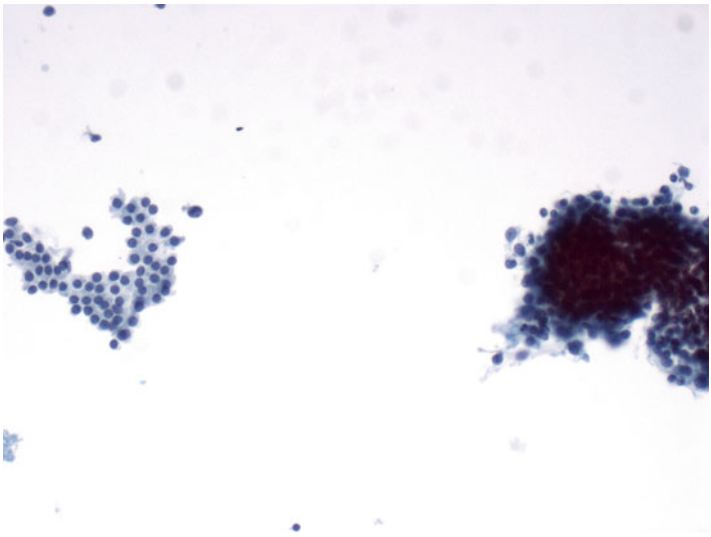

Fig. 5.13 FNA of Hashimoto thyroiditis. Aggregate of tightly packed lymphoid cluster (right) and Hürthle cells (*left*) (Papanicolaou stain, X200)

The proportion of Hürthle cells in Hashimoto thyroiditis varies widely from case to case. In some cases, they are sparse or absent. However, in others, Hürthle cells may proliferate to form nonneoplastic Hürthle cell nodules, and when they are biopsied, Hürthle cells predominate the smears with little or no lymphoid infiltrate

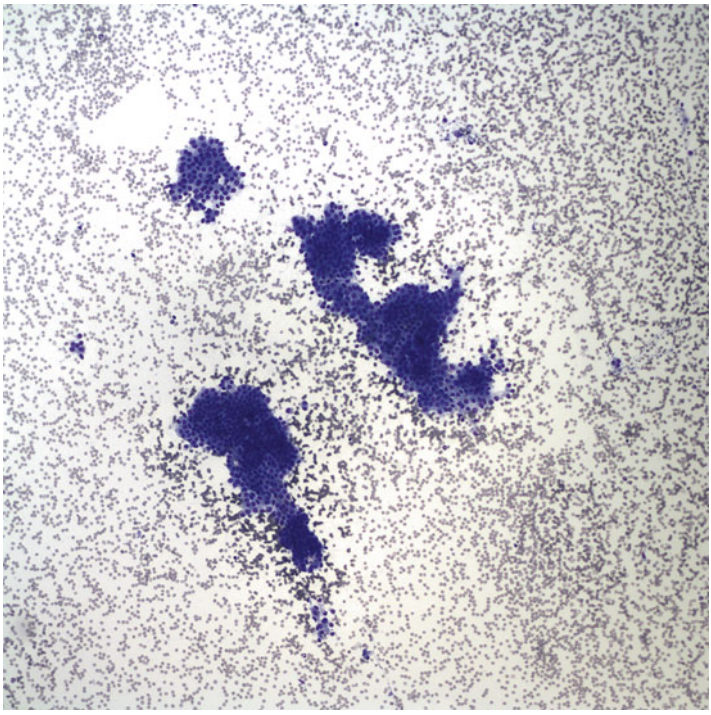

Fig. 5.14 FNA biopsy showing exclusive Hürthle cell population. Biopsy was taken from a Hürthle cell nodule representing Hürthle cell metaplasia in Hashimoto thyroiditis (Diff-Quik stain, X100)

(Figs. 5.14 and 5.15). On cytologic preparations, this can be difficult or impossible to distinguish from a Hürthle cell neoplasm. The cells of Hürthle cell neoplasm, however, usually have more prominent nucleoli than those of Hashimoto thyroiditis, and they usually do not have a prominent lymphoid infiltrate [12]. So, aspiration of exclusive Hürthle cells from a nodule in a background of what is otherwise Hashimoto thyroiditis most likely represents Hürthle cell hyperplasia rather than Hürthle cell neoplasm. However, in a small percentage of cases, the distinction may be difficult, and definite classification may depend on histologic examination. Cases may also be misdiagnosed as follicular neoplasm when the cells have a predominantly microfollicular pattern with paucity of background lymphocytes. The presence of scattered lymphocytes, even when few, should trigger a search for other features of Hashimoto thyroiditis. However, when lymphocytes are absent, it is still necessary to render a diagnosis of follicular neoplasm in order to avoid missing a thyroid follicular neoplasm.

Another common pitfall in the cytologic interpretation of Hashimoto thyroiditis is misdiagnosis as papillary thyroid carcinoma. Epithelial changes such as syncytial tissue fragments of follicular epithelium with papillary-like architecture can often be seen in Hashimoto thyroiditis. The Hürthle cells or residual follicular cells of

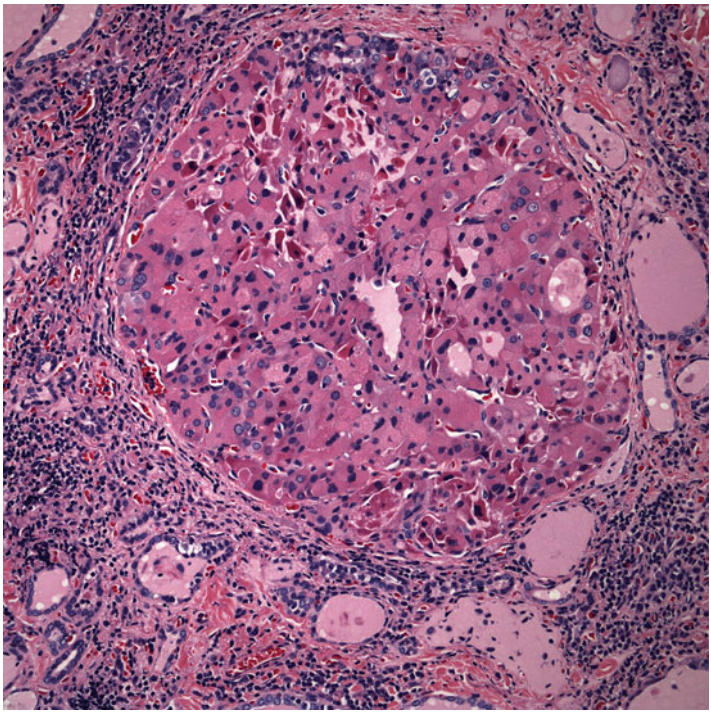

Fig. 5.15 Hashimoto thyroiditis demonstrating prominent nodule with Hürthle cell metaplasia. The surrounding lymphoid infiltrate is sparse. FNA biopsy of such an area is likely to show a predominant or exclusive Hürthle cell population, causing diagnostic difficulties with Hürthle cell neoplasm (H&E stain, X200)

Hashimoto thyroiditis occasionally display chromatin clearing, nuclear enlargement, and rare nuclear grooves. When these are seen especially in the presence of the papillary-like groups, they can lead to misdiagnosis of papillary thyroid carcinoma. If the changes are focal and mild, they may be disregarded (Fig. 5.16). However, a suspicious or malignant interpretation is warranted if the changes are diffuse or associated with other nuclear features of papillary carcinoma (Fig. 5.17).

In the florid lymphoid phase of Hashimoto thyroiditis, fine needle aspiration biopsy can yield an aspirate containing a dense population of lymphocytes that can be easily mistaken for malignant lymphoma [13] (Fig. 5.18). Ancillary tests are needed to differentiate one entity from the other, as cytologic features alone are not sufficient to make this differentiation. Primary lymphomas of the thyroid are mainly of two types: diffuse large B-cell lymphoma (DLBCL) and extranodal marginal zone B-cell lymphoma of mucosa-associated lymphoid tissue (MALT lymphoma) (Figs. 5.19 and 5.20). There may also be secondary involvement of the thyroid by lymphoma from other sites. Please refer to Chap. 6 for a more comprehensive discussion on this.

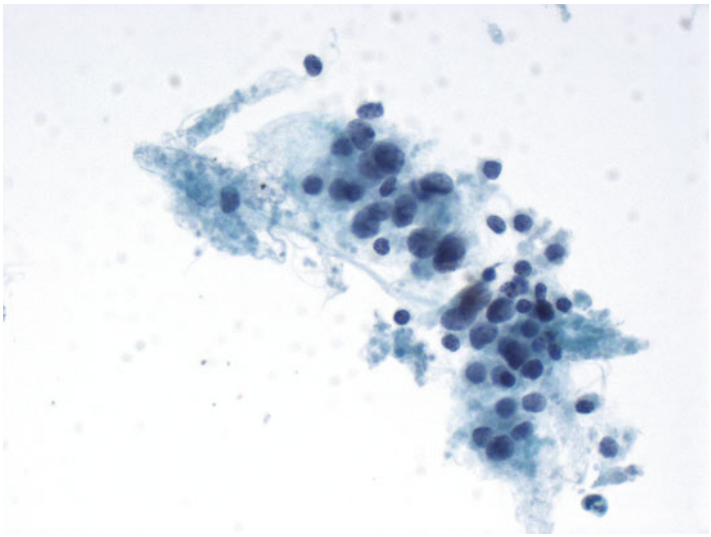

Fig. 5.16 FNA of Hashimoto thyroiditis. Hürthle cells show some nuclear atypia. The nuclei are enlarged, and rare nuclear grooves are seen. There are lymphoid cells in the background. The nuclear atypia is focal, and this is consistent with reactive nuclear changes seen in Hashimoto thyroiditis (Papanicolaou stain, X400)

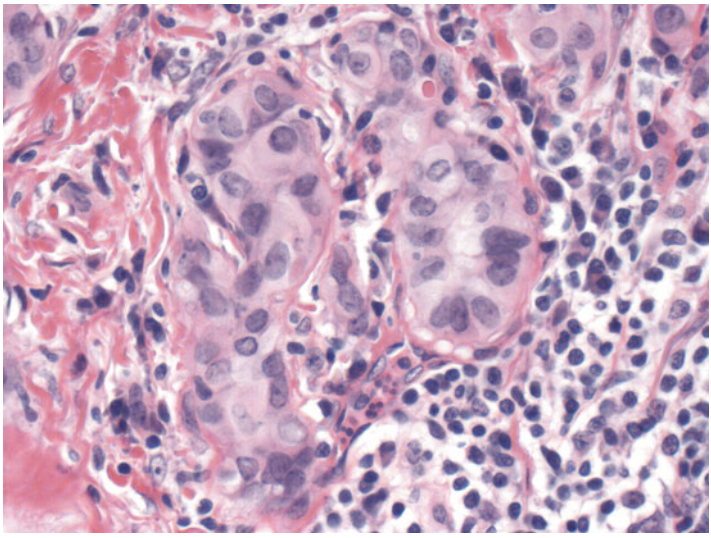

Fig. 5.17 Histologic appearance of Hashimoto thyroiditis showing nuclear atypia. The cells show nuclear enlargement, nuclear grooves, and powdery chromatin. There is some crowding and overlapping. The changes seen here are widespread in this lesion, in which Hashimoto thyroiditis is coexisting with follicular variant of papillary thyroid carcinoma (H&E stain, X400)

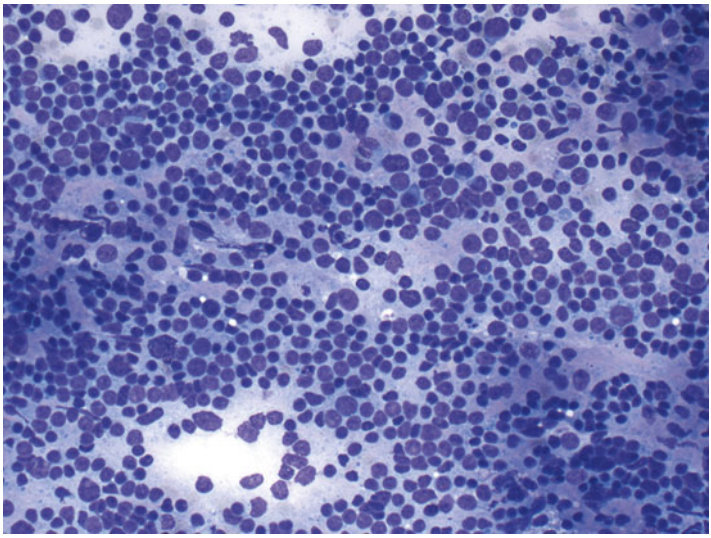

Fig. 5.18 FNA of Hashimoto thyroiditis. The aspirate is cellular, and it contains a dense mixed population of lymphocytes that can be easily mistaken for malignant lymphoma (Diff-Quik stain, X200)

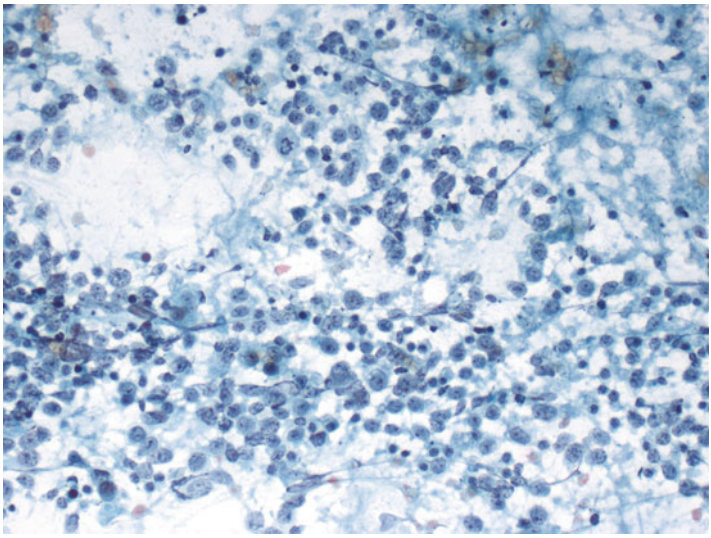

Fig. 5.19 FNA of diffuse large B-cell lymphoma of the thyroid. The aspirate is cellular, and it shows pleomorphic cells with prominent nucleoli, atypical mitosis, and karyorrhectic debris (Papanicolaou stain, X200)

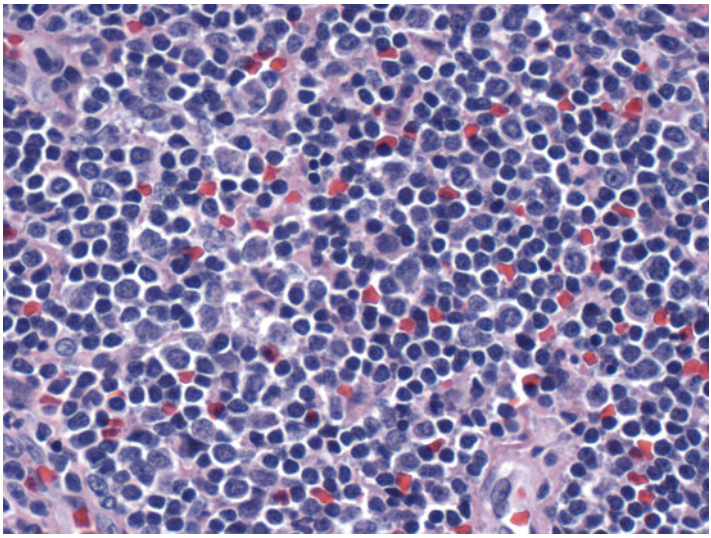

Fig. 5.20 Polymorphous population of lymphoid cells in MALT lymphoma (H&E stain, X400)

Squamous metaplasia has been reported in Hashimoto thyroiditis. When the squamous metaplasia is extensive, it may mimic squamous cell carcinoma or mucoepidermoid carcinoma [14].

References

1. Pearce EN, Farwell AP, Braverman LE. Thyroiditis. N Engl J Med. 2003;348:2646–55.
2. Dayan CM, Daniels GH. Chronic autoimmune thyroiditis. N Engl J Med. 1996;335:99–107.
3. Golden B, Levin L, Ban Y, Concepcion E, Greenberg DA, Tomer Y. Genetic analysis of families with autoimmune diabetes and thyroiditis: evidence for common and unique genes. J Clin Endocrinol Metab. 2005;90:4904–11.
4. Jacobson EM, Tomer Y. The CD40, CTLA-4, thyroglobulin, TSH receptor, and PTPN22 gene quintet and its contribution to thyroid autoimmunity: back to the future. J Autoimmun. 2007;28:85–98.
5. Aozasa K. Hashimoto's thyroiditis as a risk factor of thyroid lymphoma. Acta Pathol Jpn. 1990;40:459–68.
6. Kato I, Tajima K, Suchi T, Aozasa K, Matsuzuka F, Kuma K, Tominaga S. Chronic thyroiditis as a risk factor of B-cell lymphoma in the thyroid gland. Jpn J Cancer Res. 1985;76:1085–90.
7. Vega F, Lin P, Medeiros LJ. Extranodal lymphomas of the head and neck. Ann Diagn Pathol. 2005;9:340–50.
8. Biddinger PW. Thyroiditis. In: Nikiforov YE, Biddinger PW, Thompson LDR, editors. Diagnostic pathology and molecular genetics of the thyroid. Philadelphia, PA: Wolters Kluwer/Lippincott Williams & Wilkins; 2009. p. 39–59.
9. LiVolsi VA. Surgical pathology of the thyroid. Philadelphia, PA: W.B. Saunders; 1990.
10. LiVolsi VA. The pathology of autoimmune thyroid disease: a review. Thyroid. 1994;4:333–9.

11. Mizukami Y, Michigishi T, Kawato M, Sato T, Nonomura A, Hashimoto T, Matsubara F. Chronic thyroiditis: thyroid function and histologic correlations in 601 cases. Hum Pathol. 1992;23:980–8.
12. Cibas ES. Thyroid. In: Cibas ES, Ducatman BS, editors. Cytology: diagnostic principles and clinical correlates. Philadelphia, PA: Saunders Elsevier; 2009. p. 255–84.
13. DeMay RM. The art and science of cytopathology: superficial aspiration cytology. Chicago: ASCP Press; 2012.
14. Ryska A, Ludvíková M, Rydlová M, Cáp J, Zalud R. Massive squamous metaplasia of the thyroid gland—report of three cases. Pathol Res Pract. 2006;202:99–106.

Lymphocyte-Only Aspirates

6

Case Study

A 51-year-old female patient presented with a rapidly growing, painless left thyroid nodule of 2 months duration. There was no history of hoarseness, dysphagia, or dyspnea. Physical examination revealed an enlarged left lobe of the thyroid with a firm, non-tender mass in the left lobe of the thyroid. There were no palpable cervical lymph nodes. There was no family history of thyroid cancer. The patient was not a known smoker and she had no history of excessive alcohol consumption. Thyroid function test showed normal functioning of the thyroid except for high level of thyroid peroxidase antibody (anti-TPO). Ultrasonographic examination showed that the left lobe of the thyroid was enlarged with heterogeneous hypoechoic mass measuring 6.0×4.2×3.9 cm. Numerous diffuse hyperechoic areas were identified in all the lobes. CT scan showed an enlarged thyroid gland, with a 6.0 cm irregularly shaped mass with a poorly defined boundary in the left lobe of the thyroid. The mass showed a lower density than the rest of the thyroid tissue. Fine-needle aspiration biopsy yielded predominantly lymphocytes with rare groups of Hürthle cells and was thought to be atypical lymphoid proliferation in a background of Hashimoto thyroiditis. However, because of the history of rapid enlargement of the mass, a diagnostic thyroid lobectomy was performed. The sections revealed large pleomorphic cells with large nuclei, high N/C ratios and finely granular chromatin, high mitotic activity, and abundant karyorrhectic debris. The background thyroid tissue showed florid Hashimoto thyroiditis. The diagnosis of diffuse large B-cell lymphoma was confirmed by immunohistochemical stains and flow cytometry.

Discussion

Lymphocyte-only aspirates in the setting of a thyroid nodule can pose a significant diagnostic challenge in the interpretation of thyroid fine-needle aspiration specimens. While entities like lymphocytic thyroiditis and lymphoproliferative diseases

A.J. Adeniran, D. Chhieng, *Common Diagnostic Pitfalls in Thyroid Cytopathology*, DOI 10.1007/978-3-319-31602-4_6

(whether primary or secondary) involving the thyroid are well-known conditions that may yield lymphocyte-only aspirates, other entities such as intrathyroidal lymph node, intrathyroidal thymoma, and thyroglossal duct cyst should be included in the differential diagnosis. It is critical that a constellation of clinical and radiologic findings should be taken into consideration before a definitive diagnosis is rendered on thyroid aspirates with lymphocyte-only smears. Also, ancillary studies should be used generously in applicable cases.

Ectopic lymphoid follicles have been described in different conditions and different organs in various locations. This includes thyroid in patients with Hashimoto's thyroiditis, salivary glands in patients with Sjogren's syndrome, and thymus of patients with myasthenia gravis [1–3]. The ectopic lymphoid follicles seen in autoimmune thyroid diseases are regarded as analogs of follicular structures found in secondary lymphoid tissues [4]. The presence of lymph node within the thyroid can be explained as an aberrant heterotopic tissue. Histologically, well-defined lymphoid tissue with a well-defined capsule is seen. This lymphoid tissue is sometimes embedded in mature fat [4] (Fig. 6.1). This aggregate of lymphoid tissue is localized and not diffusely infiltrating and does not destroy the surrounding thyroid tissue. These features favor an intrathyroidal lymph node over Hashimoto's thyroiditis. Cytologic preparations show a polymorphous population of lymphocytes (Fig. 6.2), which can be confirmed by a mixed reactivity of the cells for CD3 and CD20 immunohistochemical stains.

Hashimoto thyroiditis especially in the florid lymphoid phase usually presents as lymphocyte-only aspirates [5]. During this phase, numerous hyperplastic lymphoid follicles are seen throughout the gland, and they often replace the thyroid parenchyma (Fig. 6.3). Fine-needle aspiration biopsy taken during this time shows cells

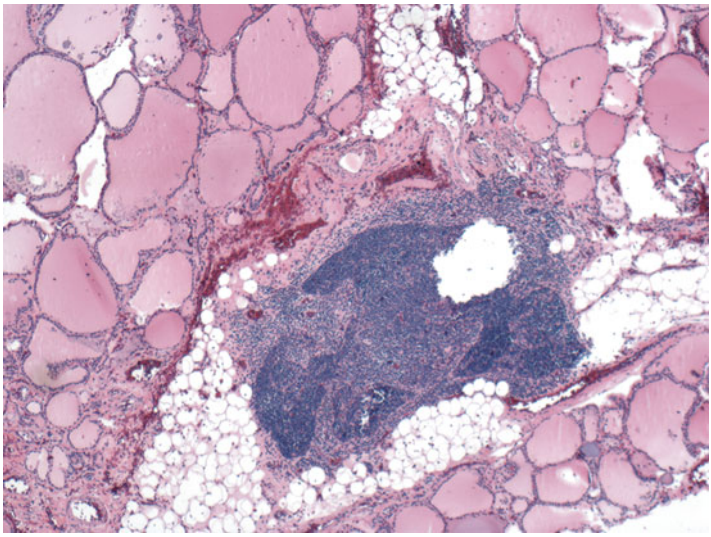

Fig. 6.1 Intrathyroidal lymph node. Well-defined lymphoid tissue with a well-defined capsule is seen. This lymphoid tissue is embedded in mature fat (H&E stain, X40)

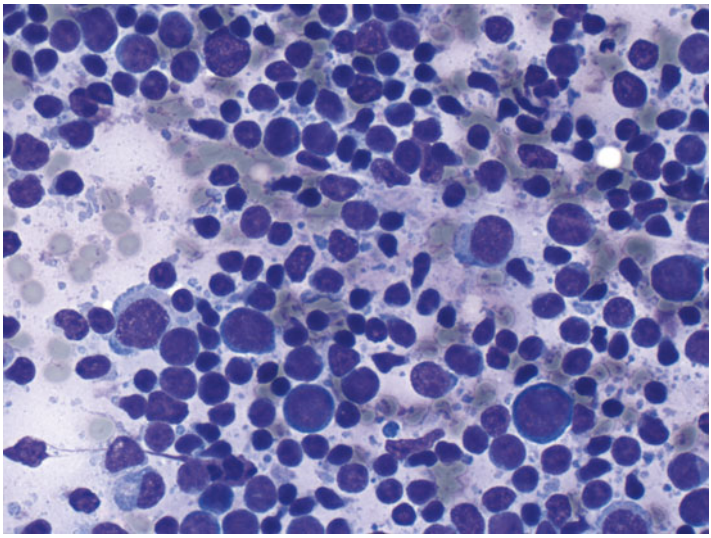

Fig. 6.2 Intrathyroidal lymph node showing polymorphous population of lymphocytes (Diff-Quik stain, X400)

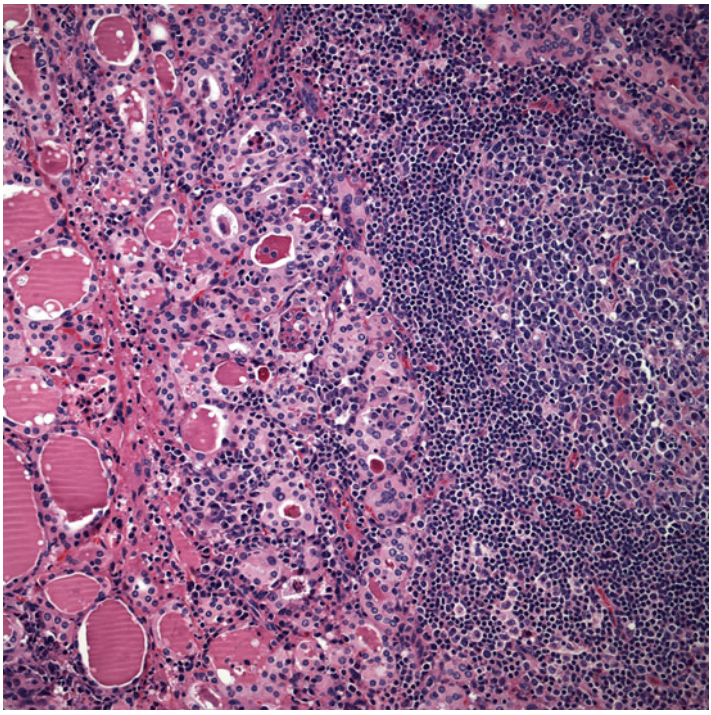

Fig. 6.3 Hashimoto thyroiditis. Hyperplastic lymphoid follicles and Hürthle cells (H&E stain, X40)

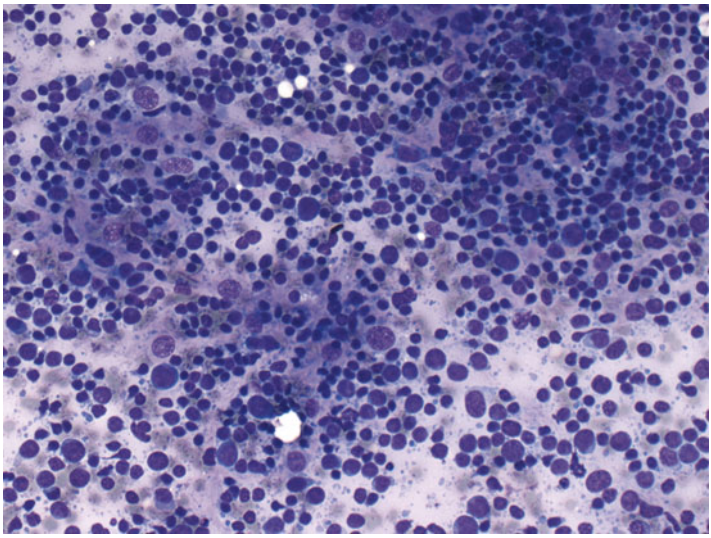

Fig. 6.4 Polymorphous population of lymphocytes in Hashimoto thyroiditis (Diff-Quik stain, X200)

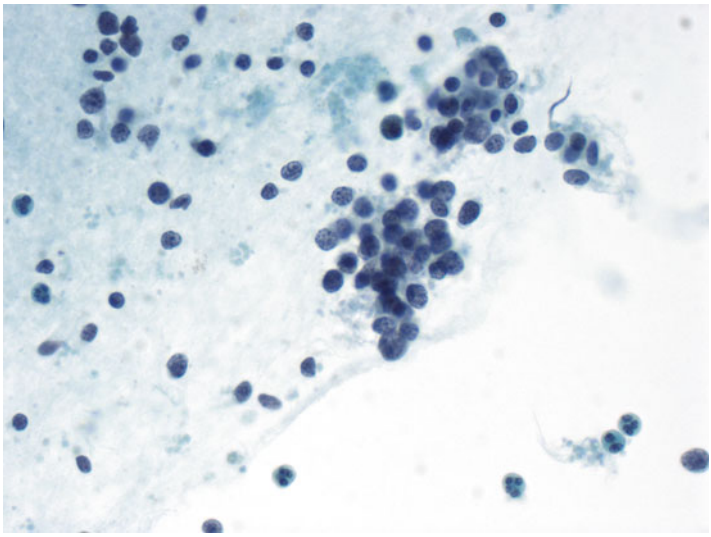

Fig. 6.5 Heterogeneous cell population in Hashimoto thyroiditis (Papanicolaou stain, X400)

with cytology closely resembling an aspirate of a reactive lymph node. These include small lymphocytes and large follicular center lymphocytes (Figs. 6.4, 6.5 and 6.6). Hürthle cells or thyroid follicular cells are sparse and may be absent. The major differential diagnosis is malignant lymphoma, and these two conditions often coexist. The florid lymphoid phase of Hashimoto thyroiditis is more common in

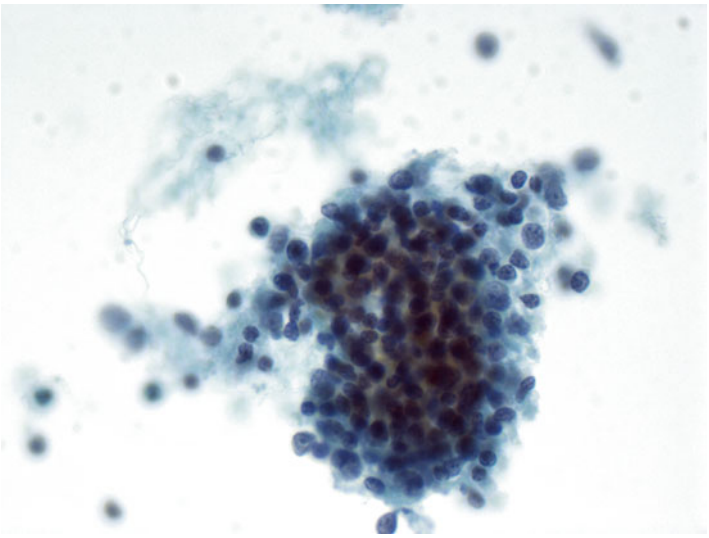

Fig. 6.6 Lymphocyte-only aspirate in Hashimoto thyroiditis. The cells have a polymorphous appearance (Papanicolaou stain, X400)

younger patient, while malignant lymphoma more commonly occurs in older adults. Flow cytometry is an important ancillary study, which helps to make a distinction between benign lymphoid infiltrate and non-Hodgkin lymphoma. The cells in benign lymphoid infiltrate of Hashimoto thyroiditis are polyclonal in origin, and they show mixed population of B and T lymphocytes.

Lymphomas of the thyroid gland constitutes up to 5 % of thyroid neoplasms. They typically occur in middle- to older-aged women, almost always arise in a background of Hashimoto thyroiditis and are of B-cell lineage [6]. The relative risk of developing lymphoma in patients with Hashimoto thyroiditis is 67 to 80 times higher than that in the general population [7]. Primary lymphomas of the thyroid gland are mainly of two types: diffuse large B-cell lymphoma (DLBCL) and extranodal marginal zone B-cell lymphoma of mucosa-associated lymphoid tissue (MALT lymphoma). DLBCL accounts for 50–90 % of lymphomas in the thyroid, while MALT lymphoma accounts for 10–30 % [8–10]. Systemic lymphomas can also involve the thyroid gland [7, 11]. Grossly, they are often large and bulky, may involve one lobe or both lobes of the thyroid, or may present as a solitary nodule. Cut surface is bulging and homogeneous and may have a pearly white to pink appearance (Fig. 6.7). Areas of hemorrhage and necrosis may be seen [12]. Fine-needle aspiration biopsy remains the most efficient method of screening selected patients for lymphoma. It can be suggestive or diagnostic of lymphoma in a large majority of cases. However, the cytologic diagnosis can be challenging especially for low-grade lymphomas arising in the background of Hashimoto thyroiditis. Lymphoma specimens are usually highly cellular.

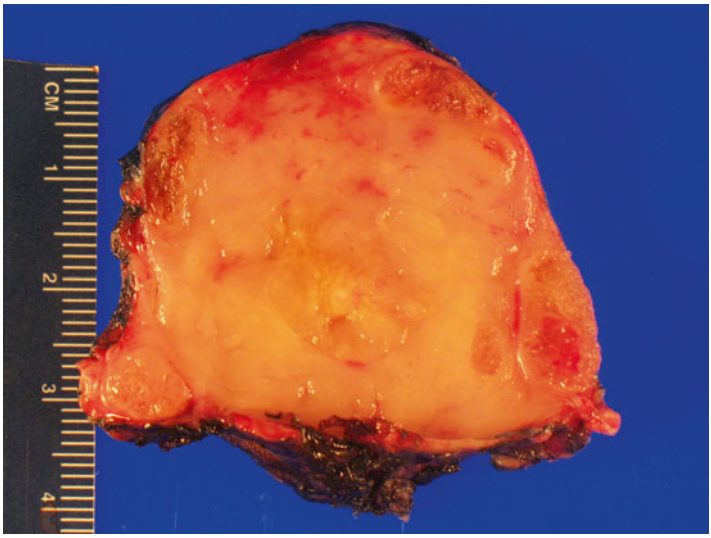

Fig. 6.7 Cut surface of the thyroid showing diffuse involvement of the thyroid lobe by the tumor. Necrosis is present

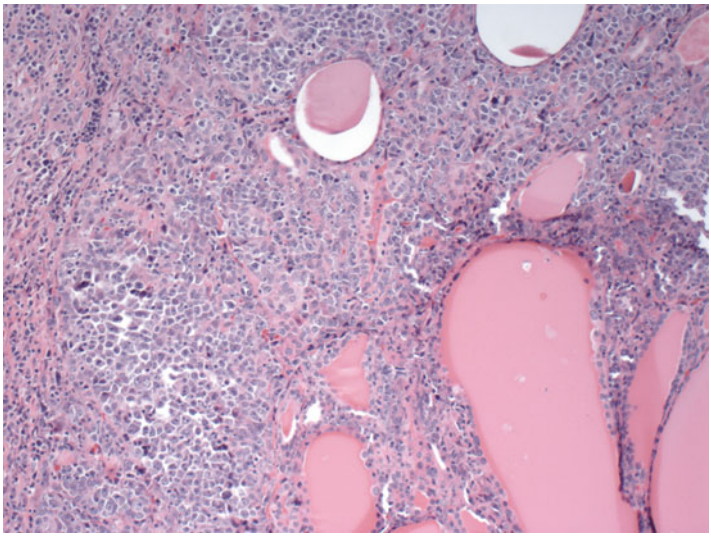

Fig. 6.8 Diffuse large B-cell lymphoma of the thyroid. Massive replacement of thyroid parenchyma by sheets of poorly differentiated lymphoid cells (H&E stain, X100)

Diffuse large B-cell lymphoma is a high-grade neoplasm, which shows massive replacement of thyroid parenchyma by sheets of poorly differentiated lymphoid cells (Fig. 6.8). Aspirates are usually cellular, and they typically show a homogeneous population of poorly differentiated lymphoid cells that are typically larger than normal lymphocytes [12]. The cells are discrete and round, with scant, pale cytoplasm.

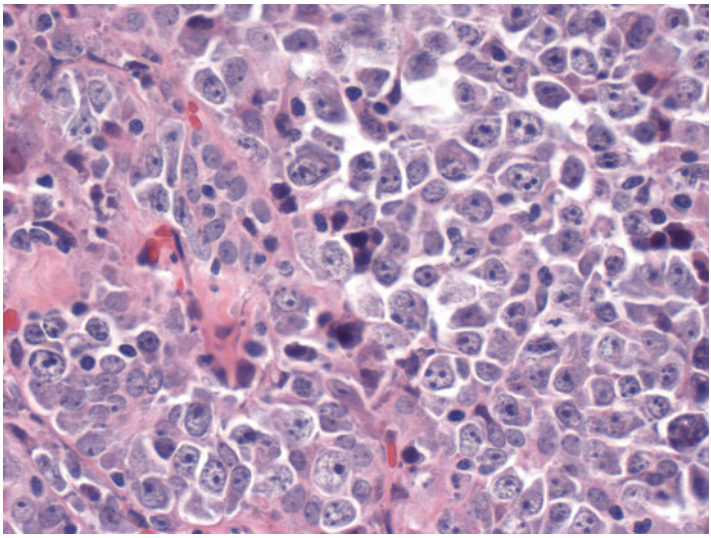

Fig. 6.9 Diffuse large B-cell lymphoma of the thyroid. Monomorphous population of large lymphoma cells. Cells are pleomorphic and they have prominent nucleoli (H&E stain, X400)

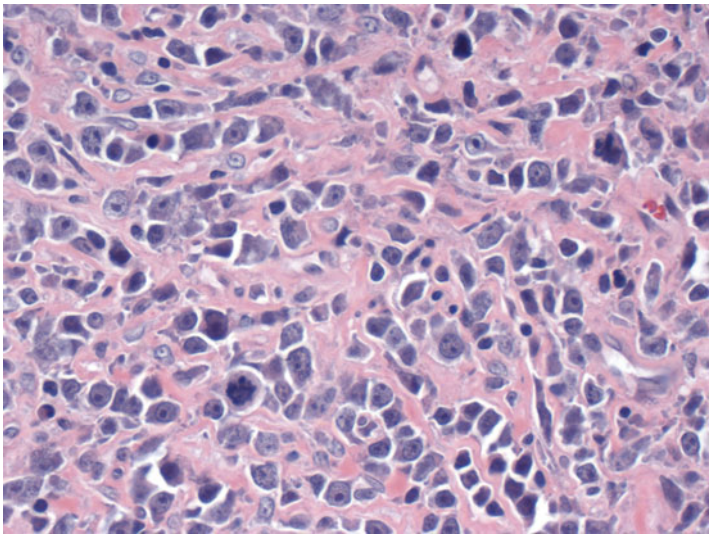

Fig. 6.10 Lymphoma cells are large and monomorphous, with prominent nucleoli and open chromatin pattern. Atypical mitoses and karyorrhectic debris are present. Background is sclerotic (H&E stain, X400)

The nuclei are large, with high N/C ratios and contain finely granular chromatin. Nucleoli are always present and can be either large in a central position or small and multiple in a marginal location. Mitotic activity is frequent. Karyorrhexis is a common feature of high-grade lymphoma (Figs. 6.9, 6.10, 6.11, 6.12, 6.13, and 6.14).

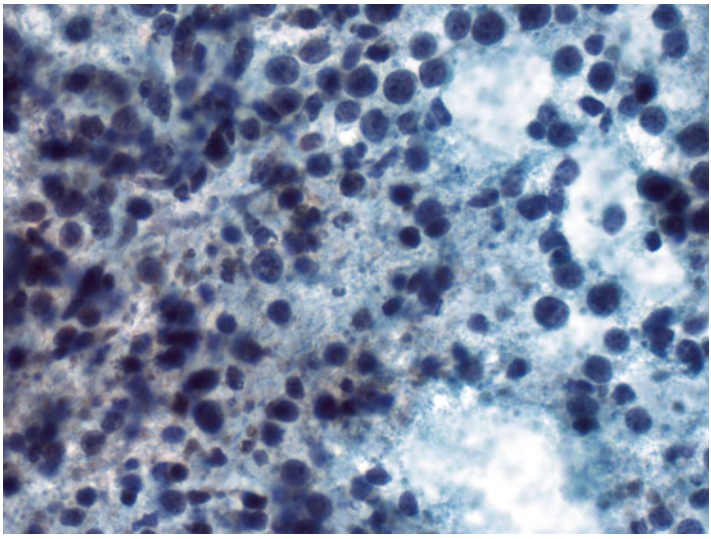

Fig. 6.11 FNA of diffuse large B-cell lymphoma of the thyroid. Monomorphous population of poorly differentiated lymphoid cells (Papanicolaou stain, X400)

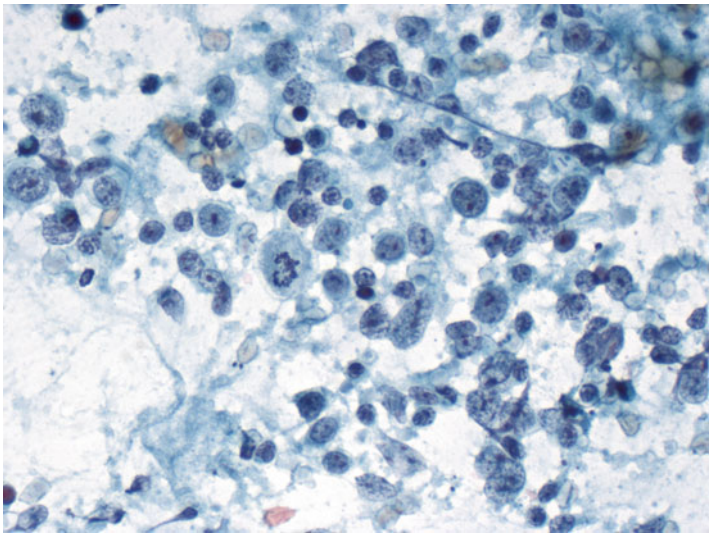

Fig. 6.12 FNA of diffuse large B-cell lymphoma of the thyroid. Cells are pleomorphic and they have prominent nucleoli. Atypical mitosis and karyorrhectic debris are present in the background (Papanicolaou stain, X400)

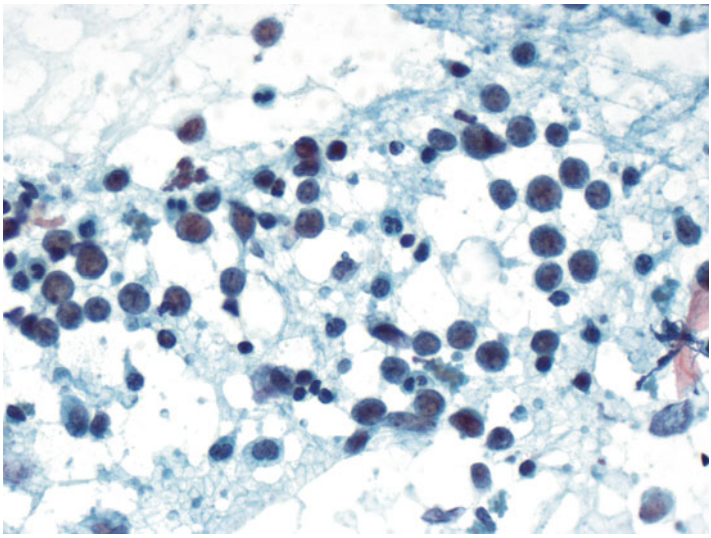

Fig. 6.13 FNA of diffuse large B-cell lymphoma of the thyroid. Monomorphous population of poorly differentiated lymphoid cells (Papanicolaou stain, X400)

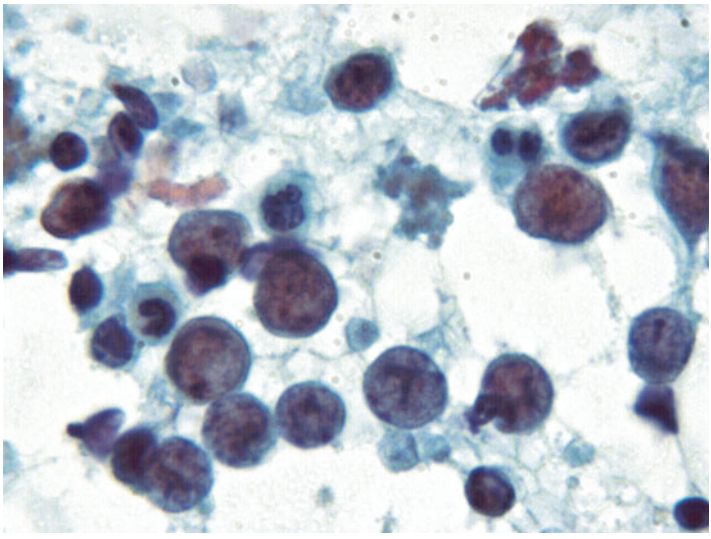

Fig. 6.14 FNA of diffuse large B-cell lymphoma of the thyroid. Pleomorphic cells with highly atypical nuclear features (Papanicolaou stain, X1000)

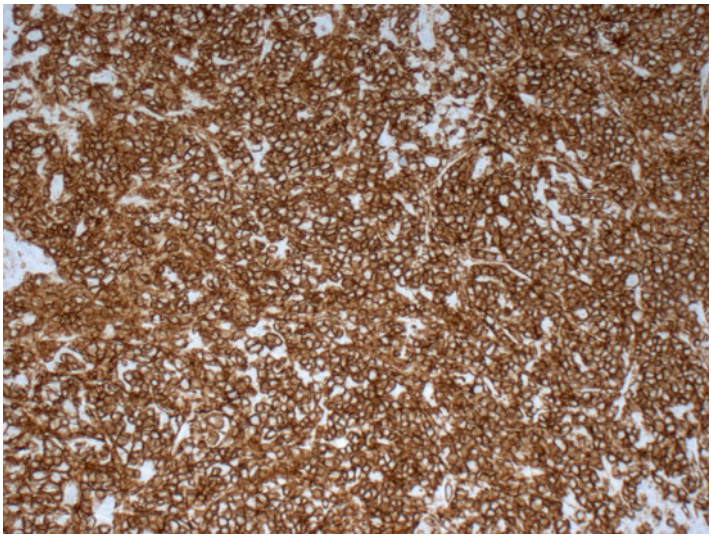

Fig. 6.15 The malignant lymphoid cells show diffuse CD20 expression

This karyorrhectic debris can be mistaken for benign germinal center cells. Lymphoglandular bodies are usually present and theses are only seen on Romanowsky-stained preparations. Depending on the sampling, cytologic features of Hashimoto thyroiditis may be present, either separately from lymphoma cells on the same smear or on different smears representing different areas of the thyroid. Such a diverse pattern is not uncommon and should not prevent one from rendering a diagnosis of lymphoma. The large cells in DLBCL can be mistaken for anaplastic carcinoma or metastatic carcinoma. Cytologic diagnosis can be confirmed by immunohistochemical stains. The cells are positive for CD20 and/or CD79a, but they are not reactive to CD5 and CD23 (Fig. 6.15). A negative cytokeratin stain is also helpful to distinguish the large cells of DLBCL from anaplastic carcinoma or metaplastic carcinoma.

Flow cytometry is an important ancillary study, which confirms the immunohistochemical stains and also demonstrates positive reactivity to light chain immunoglobulins, either kappa or lambda, and establish the clonality. DLBCL can be classified into germinal center B-cell (GCB) or non-GCB immunophenotype. The former is positive for CD10 or BCL6 and has been reported to be associated with better progression-free or overall survival. Distinguishing GCB versus non-GCB DLBCL in the thyroid gland predicts response to therapy; a GCB immunophenotype is associated with a better progression-free and overall survival [13]. The International Prognostic Index and the extent of the DLBCL involvement also affect overall survival [11, 13]. In a recent study [14], it was shown that a subset of DLBCL in the thyroid gland had *BRAF* (24 %) or *NRAS* (8 %) mutations. These mutations were not detected in MALT lymphoma or follicular lymphoma involving the thyroid gland. Translocations of *KMT2A* (formerly known as *MLL*), a gene involved in

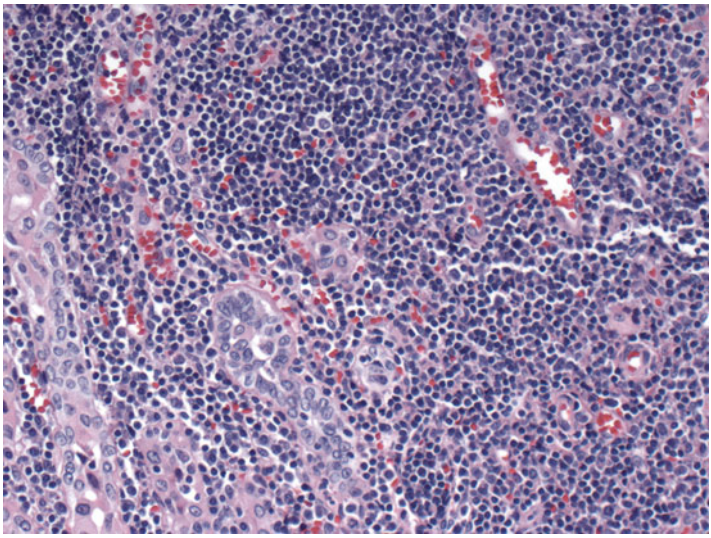

Fig. 6.16 Lymphoepithelial lesions in MALT lymphoma. The thyroid parenchyma is diffusely infiltrated by malignant lymphoid cells, forming lymphoepithelial lesions (H&E stain, X200)

epigenetic modification of DNA, have been described in primary DLBCL of the thyroid gland and are associated with a better prognosis [15].

The cells of MALT lymphoma infiltrate the follicular epithelium, forming "MALT balls" characterized by round aggregates of marginal zone cells filling and expanding the lumina of thyroid follicles [8]. Follicular colonization is more prominent, imparting a nodular architecture that can mimic the pattern of follicular lymphoma. Usually the smears show heterogeneous population of numerous small lymphocytes, centrocyte-like cells, monocytoid B cells, plasma cells, transformed lymphocytes, and prominent lymphoepithelial lesions (Figs. 6.16 and 6.17). This entity can be very difficult to differentiate from the florid lymphoid phase of Hashimoto thyroiditis, and the two diseases can coexist [5]. Hence, a high index of suspicion in cases of severe Hashimoto thyroiditis is needed to avoid missing concurrent MALT lymphoma. Factors favoring MALT lymphoma include obliteration of thyroid parenchyma by a lymphoid infiltrate, interfollicular lymphoma cells with morphology and immunophenotype of marginal zone B cells, follicular colonization by lymphoma cells with marginal zone B cells, and monotypic expression of immunoglobulin light chains. Lymphoepithelial lesions in Hashimoto thyroiditis contain a higher number of T cells compared with those in MALT lymphoma. About half of MALT lymphomas involving the thyroid gland have been reported to be associated with t(3;14)(p14;q32)/*FOXP1-IGH* [8]. MALT lymphoma can mimic plasmacytoma when it presents with extensive plasma cell differentiation. However, the lymphoma cells within the thyroid follicles do not show exuberant plasmacytic differentiation, a clue that helps to differentiate MALT lymphoma from plasmacytoma [8].

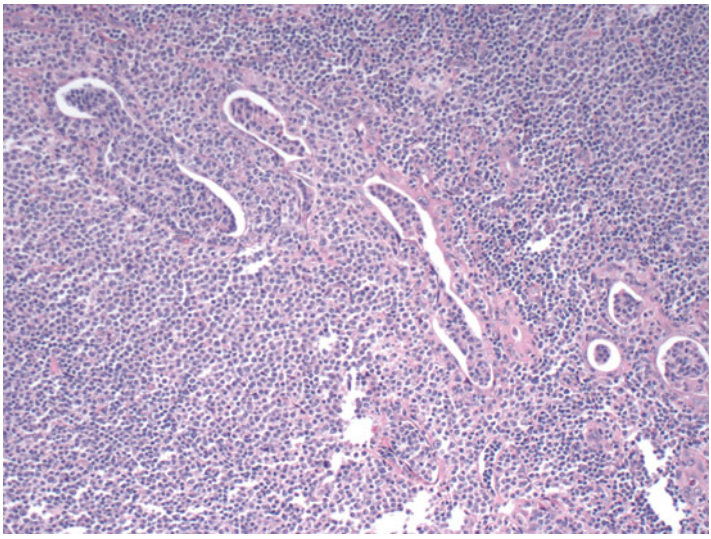

Fig. 6.17 Polymorphous population of cells in MALT lymphoma (H&E stain, X400)

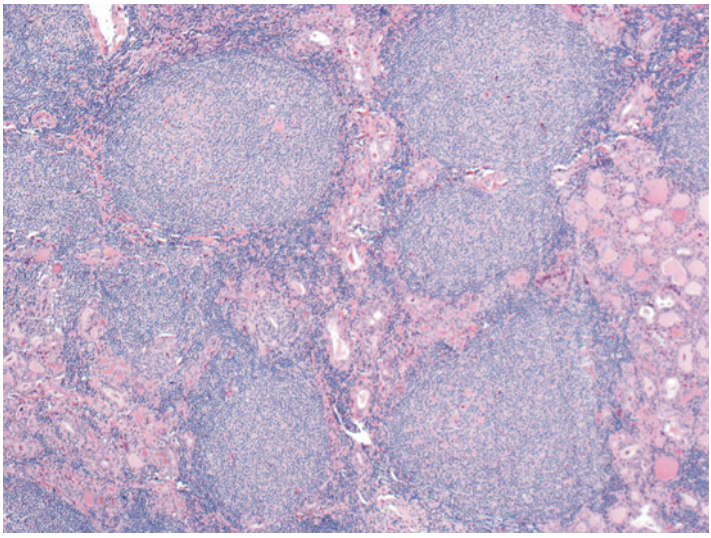

Fig. 6.18 Prominent follicular pattern in follicular lymphoma of the thyroid (H&E stain, X400)

Follicular lymphoma can also involve the thyroid gland, with most patients having evidence of systemic lymphoma or involvement of regional lymph nodes. This is particularly true for patients with low-grade follicular lymphoma [8, 16]. Follicular lymphomas have predominantly follicular pattern (Fig. 6.18). Neoplastic follicles are often poorly defined and often lack mantle zones. Follicular lymphoma

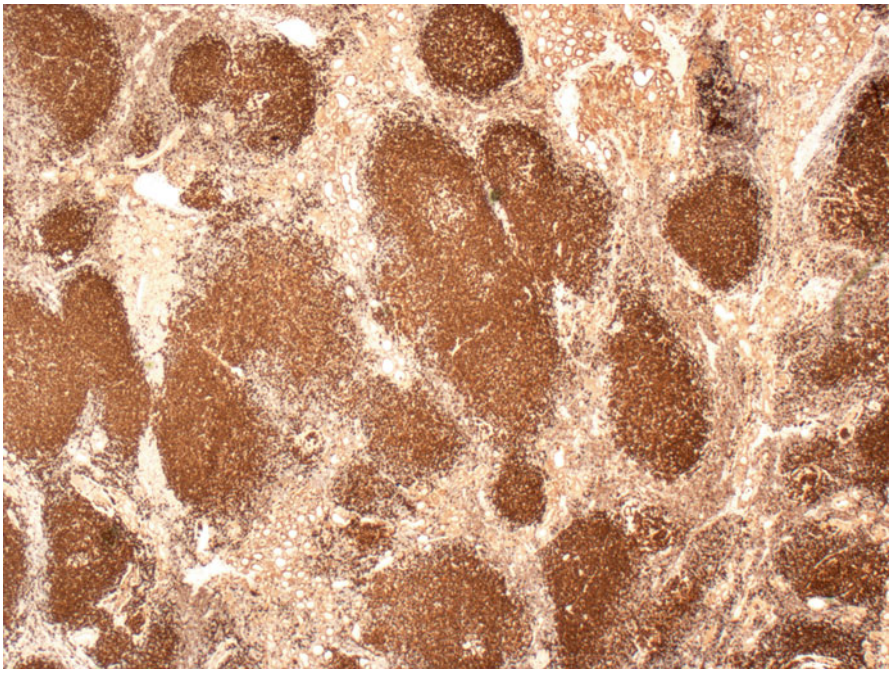

Fig. 6.19 BCL2 expression in follicular lymphoma of the thyroid

involving the thyroid gland can be associated with concurrent Hashimoto thyroiditis and lymphoepithelial lesions. Although follicular lymphomas are generally positive for BCL2 (Fig. 6.19), follicular lymphomas of the thyroid gland, particularly grade 3, can lack expression of CD10 or BCL2, and these tumors also can be negative for t(14;18)(q32;q21)/*IGH-BCL2* [8].

Primary Hodgkin lymphoma is extremely rare, and most cases involving the thyroid have been found to be a secondary involvement [12, 17]. Nodular sclerosing variant is the commonest type. Reed-Sternberg cells or any of its variants are seen on the smears. Cells similar to Reed-Sternberg cells or any of the variants can occur in non-Hodgkin lymphoma as well as in reactive lymphoid proliferations, and this is a common source of diagnostic dilemma. Reed-Sternberg cells are typically positive for CD30 and CD15. The degree of sclerosis can be extensive and this can lead to a misdiagnosis of Riedel thyroiditis or fibrosclerosing variant of Hashimoto thyroiditis. Identification of Reed-Sternberg cells is required for diagnosis [8].

Small lymphocytic lymphoma is one of the rarest subtypes of lymphoma that can involve the thyroid gland. Diagnosis of this entity is difficult, particularly before the recognition of systemic involvement [6]. Cytological examination reveals a predominant cell population of small- to medium-sized cells revealing paracentral to eccentric nuclei with clockface chromatin and abundant sky-blue cytoplasm. Immunohistochemical stains are very helpful in the diagnosis of small lymphocytic lymphoma. The CD20+ neoplastic cells typically co-express CD5 and CD23.

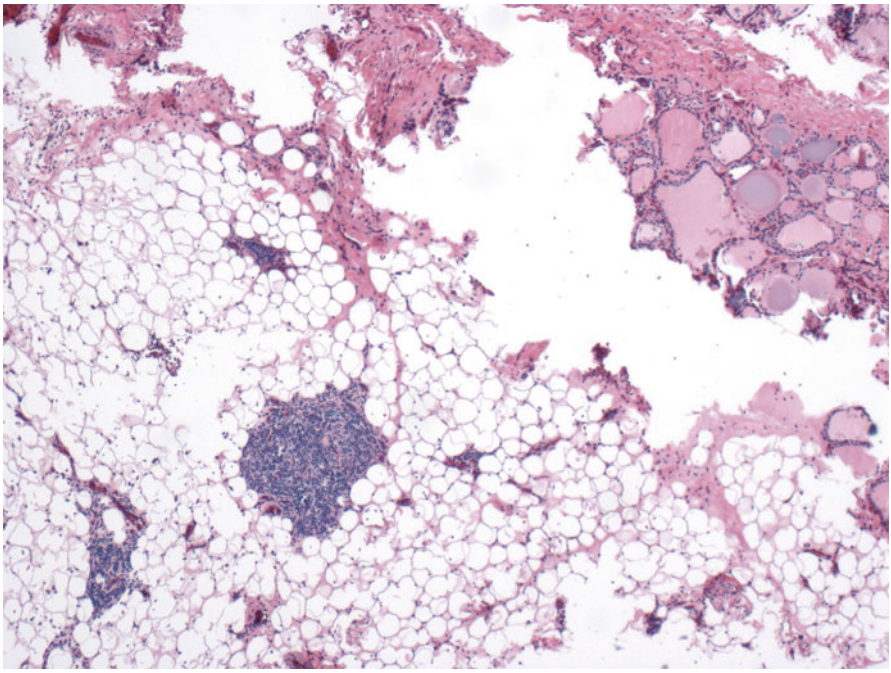

Fig. 6.20 Intrathyroidal thymic tissue (H&E stain, X20)

Given the limitations of establishing a lymphoma diagnosis with only cytomorphology, morphological evaluation is commonly augmented with flow cytometry or immunohistochemistry in the diagnostic workup of lymphocyte-rich or lymphocyte-only fine-needle aspirates from the thyroid showing atypical lymphoid populations. In two studies, morphology in conjunction with flow cytometry or immunohistochemistry had a positive predictive value of 90 % [18, 19].

Ectopic thymic tissue can be found within thyroid parenchyma (Fig. 6.20) and may rarely become hyperplastic or neoplastic. Ectopic thymoma is an unusual finding in the thyroid [20]. Because of the rarity of this lesion, it is often misdiagnosed as Hashimoto's thyroiditis or malignant lymphoma of the thyroid. The histologic appearance is similar to that of mediastinal thymoma. Cytology reveals abundant small lymphocytes with hyperchromatic nuclei and frequent appearance of clumped chromatin. When the epithelial component is sampled, the cells may be interpreted as thyroid follicular cells and may lead to a misdiagnosis of lymphocytic thyroiditis.

Thyroglossal duct cyst can show extensive lymphoid tissue with prominent germinal centers in the wall of the cyst. If the germinal center is sampled, the cells can be mistaken for cells of malignant lymphoma as they show a large population of lymphoid cells with focal aggregates of immature forms. Flow cytometry is helpful in such cases as the cells are typically polyclonal B-cell population.

References

1. Chistiakov DA. Immunogenetics of Hashimoto's thyroiditis. J Autoimmune Dis. 2005;2:1.
2. Harris NL. Lymphoid proliferations of the salivary glands. Am J Clin Pathol. 1999; 111:S94–103.
3. Shiono H, Fujii Y, Okumura M, Takeuchi Y, Inoue M, Matsuda H. Failure to down-regulate Bcl-2 protein in thymic germinal center B cells in myasthenia gravis. Eur J Immunol. 1997; 27:805–9.
4. Abdou AG, Aiad HA. Intrathyroid lymph node tissue in multinodular goiter in an Egyptian female. Saudi Med J. 2009;30:558–60.
5. DeMay RM. The art and science of cytopathology: superficial aspiration cytology. Chicago: ASCP Press; 2012.
6. Gill M, Batra A, Sangwaiya A, Shakya S, Gupta S, Sen R. Small lymphocytic lymphoma of the thyroid mimicking plasmacytoma. Eur Thyroid J. 2014;3:202–5.
7. Vega F, Lin P, Medeiros LJ. Extranodal lymphomas of the head and neck. Ann Diagn Pathol. 2005;9:340–50.
8. Thakral B, Zhou J, Medeiros LJ. Extranodal hematopoietic neoplasms and mimics in the head and neck: an update. Hum Pathol. 2015;46:1079–100.
9. Derringer GA, Thompson LD, Frommelt RA, Bijwaard KE, Heffess CS, Abbondanzo SL. Malignant lymphoma of the thyroid gland: a clinicopathologic study of 108 cases. Am J Surg Pathol. 2000;24:623–39.
10. Thieblemont C, Mayer A, Dumontet C, et al. Primary thyroid lymphoma is a heterogeneous disease. J Clin Endocrinol Metab. 2002;87:105–11.
11. Ha CS, Shadle KM, Medeiros LJ, et al. Localized non-Hodgkin lymphoma involving the thyroid gland. Cancer. 2001;91:629–35.
12. Kini SR. Thyroid cytopathology: an Atlas and text. Philadelphia: Wolters Kluwer/ Lippincott Williams & Wilkins; 2008.
13. Katna R, Shet T, Sengar M, et al. Clinicopathologic study and outcome analysis of thyroid lymphomas: experience from a tertiary cancer center. Head Neck. 2013;35:165–71.
14. Aggarwal N, Swerdlow SH, Kelly LM, et al. Thyroid carcinoma-associated genetic mutations also occur in thyroid lymphomas. Mod Pathol. 2012;25:1203–11.
15. Gindin T, Murty V, Alobeid B, Bhagat G. MLL/KMT2A translocations in diffuse large B-cell lymphomas. Hematol Oncol. 2015;33:239–46.
16. Bacon CM, Diss TC, Ye H, et al. Follicular lymphoma of the thyroid gland. Am J Surg Pathol. 2009;33:22–34.
17. Jayaram G. Hodgkin's disease beginning as a thyroid nodule. Acta Cytol. 1993;37:256–7.
18. Gupta N, Nijhawan R, Srinivasan R, Rajwanshi A, Dutta P, Bhansaliy A, et al. Fine needle aspiration cytology of primary thyroid lymphoma: a report of ten cases. Cytojournal. 2005;2:21.
19. Swart GJ, Wright C, Brundyn K, Mansvelt E, du Plessis M, ten Oever D, et al. Fine needle aspiration biopsy and flow cytometry in the diagnosis of lymphoma. Transfus Apher Sci. 2007;37:71–9.
20. Neill J. Intrathyroid thymoma. Am J Surg Pathol. 1986;10:660–1.

Molecular Testing

7

Case Study

Case 1

The first patient was a 34-year-old female who presented with a 2.5 cm right thyroid nodule detected during a routine physical examination by her family physician. She complained of hoarseness and some difficulty in breathing but no difficulty in swallowing. She had no symptoms of hyperthyroidism and had no history of radiation to the head and neck area. However, there was a family history of thyroid cancer; her maternal first cousin was diagnosed with thyroid cancer at age 17. Physical examination revealed a smooth, mobile right thyroid nodule measuring 2.5 cm; no palpable nodules were noted in the left thyroid lobe. The thyroid function test was within normal limits. Ultrasound examination revealed a 2.5 cm solitary nodule in the right thyroid lobe; the remaining thyroid gland appeared unremarkable. No cervical lymphadenopathy was noted.

Fine needle aspiration biopsy of the right thyroid nodule was performed under ultrasound guidance. The aspirate was of low cellularity and consisted of both micro- and macro-follicles. Hurthle cell changes were noted in some follicular cells (Fig. 7.1). Individual cells showed nuclear enlargement, elongation, powdery chromatin, and rare nuclear groove (Figs. 7.2 and 7.3). Scattered lymphocytes were noted but Colloid was absent (Fig. 7.4). The cytologic diagnosis was follicular lesion of undetermined significance (FLUS) with nuclear atypia. Reflex molecular testing based on the Afirma Gene Expression Classifier platform was performed. The result was suspicious.

The patient underwent a total thyroidectomy. Serial section revealed a solitary, well-circumscribed nodule in the right thyroid lobe, measuring 1.4 cm. The remaining thyroid parenchyma appeared normal grossly. Microscopically, the right nodule appeared partially surrounded with a thin capsule with foci of hemorrhage and fibrosis.

A.J. Adeniran, D. Chhieng, *Common Diagnostic Pitfalls in Thyroid Cytopathology*, DOI 10.1007/978-3-319-31602-4_7

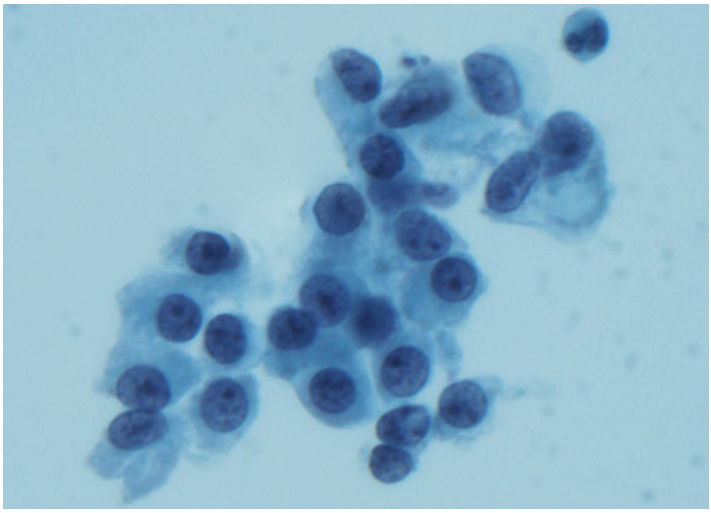

Fig. 7.1 Thyroid FNA-FLUS with nuclear atypia. A small cluster of follicular cells showing Hurthle cell changes (Papanicolaou stain, high power)

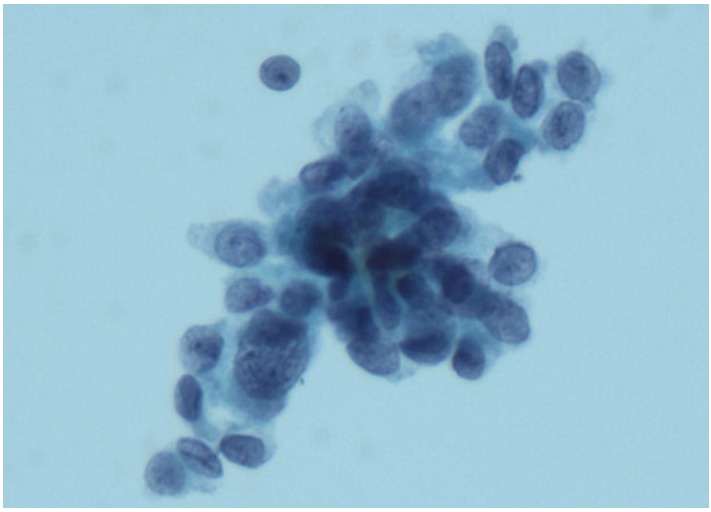

Fig. 7.2 Thyroid FNA-FLUS with nuclear atypia. A small group of follicular cells with nuclear crowding and overlapping. Nuclear enlargement, elongation, and rare nuclear grooves are noted (Papanicolaou stain, high power)

The follicular cells are arranged in both micro- and macro-follicular pattern and appeared flat or cuboidal without any nuclear features of papillary thyroid carcinoma (Figs. 7.5 and 7.6). Scattered lymphoid aggregates were identified.

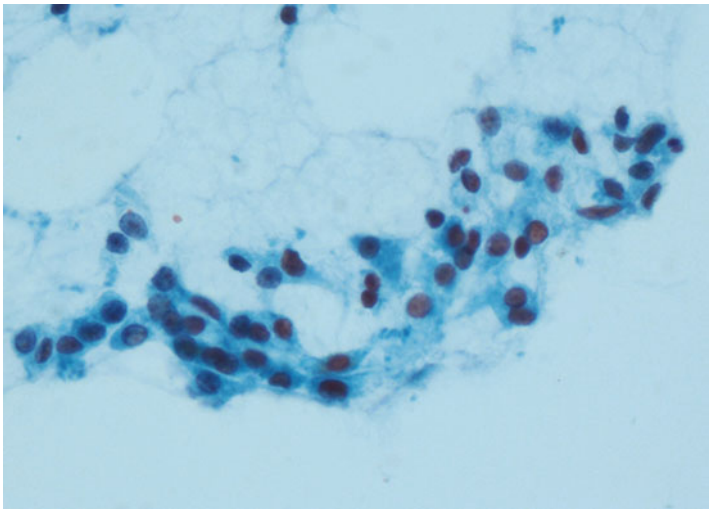

Fig. 7.3 Thyroid FNA-FLUS with nuclear atypia. A loosely cohesive group of follicular cells. Individual cells show moderate amount of granular cytoplasm, nuclear enlargement, elongation, and occasional nuclear grooves (Papanicolaou stain, high power)

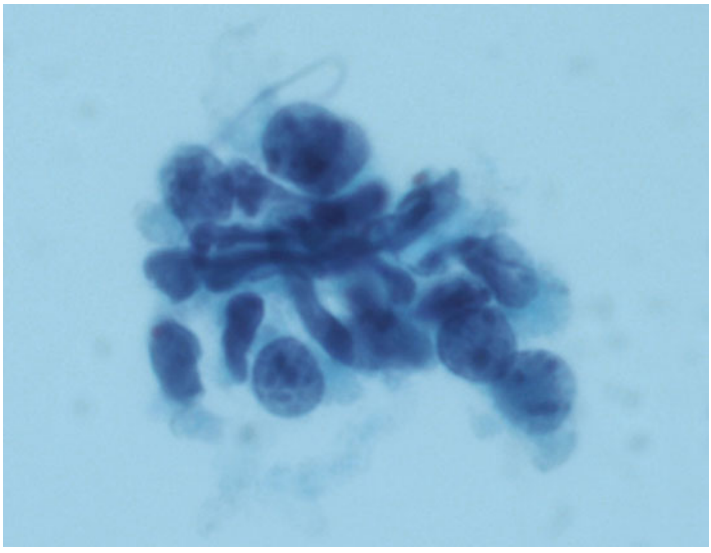

Fig. 7.4 Thyroid FNA-FLUS with nuclear atypia. A small cluster of follicular cells admixed with lymphocytes (direct smear, Papanicolaou stain, high power)

Rare groups of follicular cells showed scattered nuclear grooves (Fig. 7.7). The histologic diagnosis is adenomatous hyperplastic nodule in a background of mild lymphocytic thyroiditis.

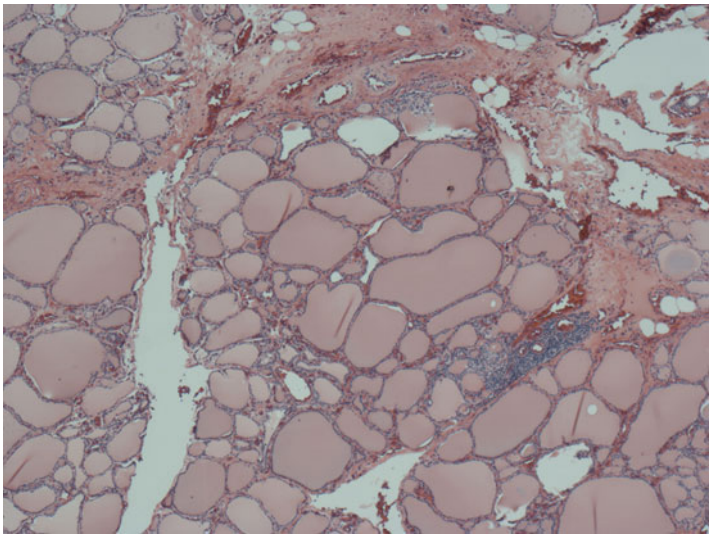

Fig. 7.5 Goiter. Low power showing both micro- and macro-follicular architecture with fibrosis and scattered lymphoid aggregates (H&E, low power)

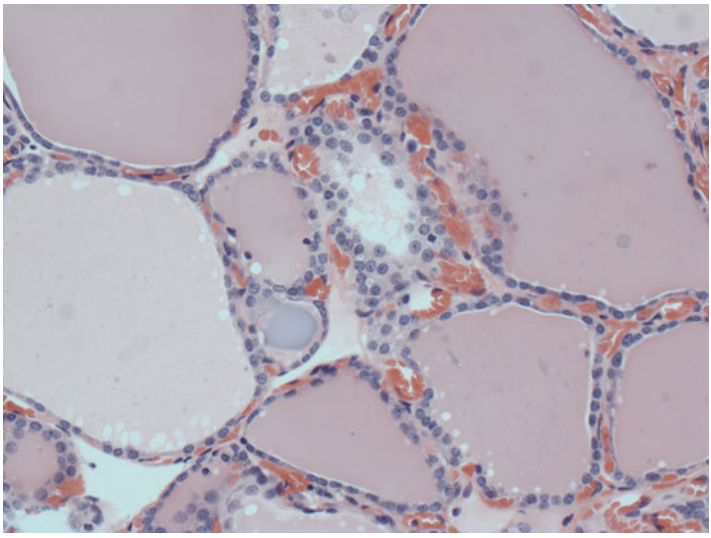

Fig. 7.6 Goiter. Each follicle is lined by flat or cuboidal follicular cells with regular nuclei and no nuclear evidence of papillary thyroid carcinoma (H&E, high power)

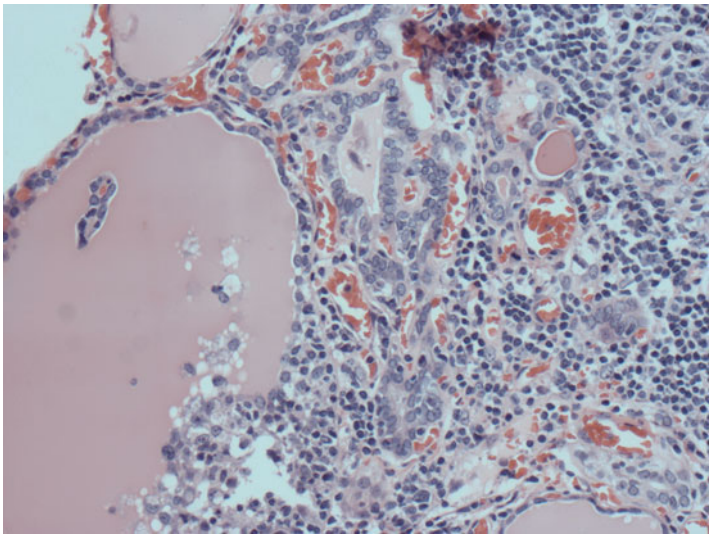

Fig. 7.7 Goiter. A lymphoid aggregate consists of a polymorphous population of lymphocytes. Adjacent follicular cells show mild nuclear enlargement and occasional nuclear grooves (H&E, high power)

Case 2

The second patient was a 62-year-old female with a history of cutaneous T-cell lymphoma. She presented to her endocrinologist for the evaluation of thyroid nodules, which was discovered by imaging and with an "inconclusive" cytologic diagnosis 4 years prior. She did not seek follow-up for her thyroid problem until the time of presentation. She denied any symptoms of hyperthyroidism. She did not complain of any pressure symptoms. Her physical examination was unremarkable without any palpable mass in the cervical region. Her thyroid function was within normal limits.

Ultrasound examination revealed a total of ten nodules within the thyroid gland, which were present 4 years prior. The dominant nodule was located in the right upper lobe, measuring 1.7 cm in greatest dimensions with increased vascularity within the nodule by color Doppler. The remaining nodules ranged from 3 to 5 mm and were distributed throughout both thyroid lobes.

Fine needle aspiration biopsy was performed on the 1.7 cm dominant nodule. The aspirate was scantly cellular and consisted of clusters of follicular cells with mild nuclear crowding (Fig. 7.8). Individual cells showed nuclear enlargement and scattered nuclear inclusion and ill-defined intranuclear inclusion (Figs. 7.9 and 7.10). Abundant macrophages were noted in the background. The cytologic diagnosis was FLUS with nuclear atypia. Reflex molecular testing based on the Afirma Gene Expression Classifier platform was performed. The result was suspicious.

The patient underwent right lobectomy. Serial resection revealed a $1.3 \times 1.0 \times 0.8$ cm well-circumscribed nodule with a tan-yellow cut surface. The remaining thyroid parenchyma was unremarkable. Histologic section of the nodule revealed a partially

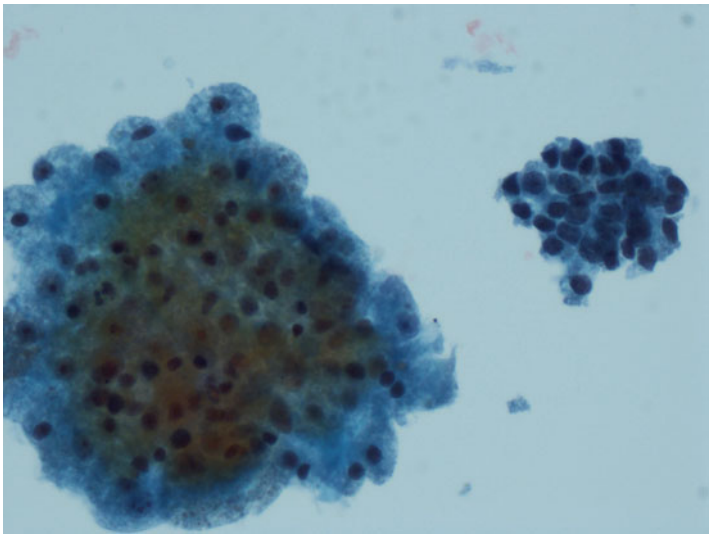

Fig. 7.8 Thyroid FNA-FLUS with nuclear atypia. A small cluster of follicular cells with nuclear overlapping and crowding adjacent to a group of macrophages with abundant foamy/granular cytoplasm (Papanicolaou stain, high power)

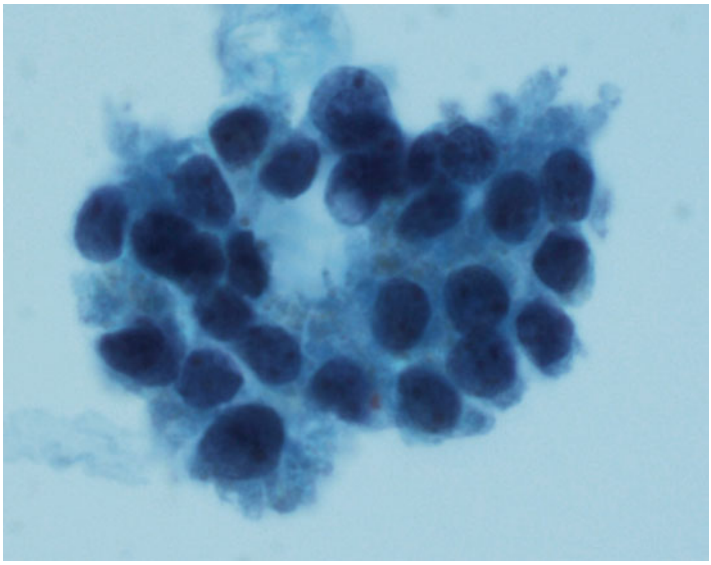

Fig. 7.9 Thyroid FNA-FLUS with nuclear atypia. A small cluster of follicular cells with nuclear crowding and overlapping. A poorly defined intranuclear inclusion is noted (Papanicolaou stain, high power)

encapsulated papillary thyroid carcinoma, classic variant (Figs. 7.11, 7.12, and 7.13). A week later, the patient underwent a completion thyroidectomy which revealed chronic lymphocytic thyroiditis with no evidence of malignancy.

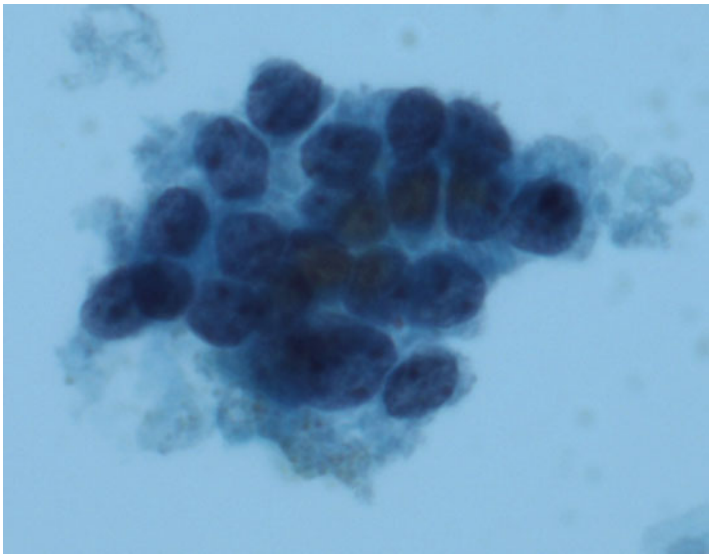

Fig. 7.10 Thyroid FNA-FLUS with nuclear atypia. Another cluster of follicular cells with nuclear crowding and overlapping. The nuclei appear enlarged with occasional nuclear grooves (Papanicolaou stain, high power)

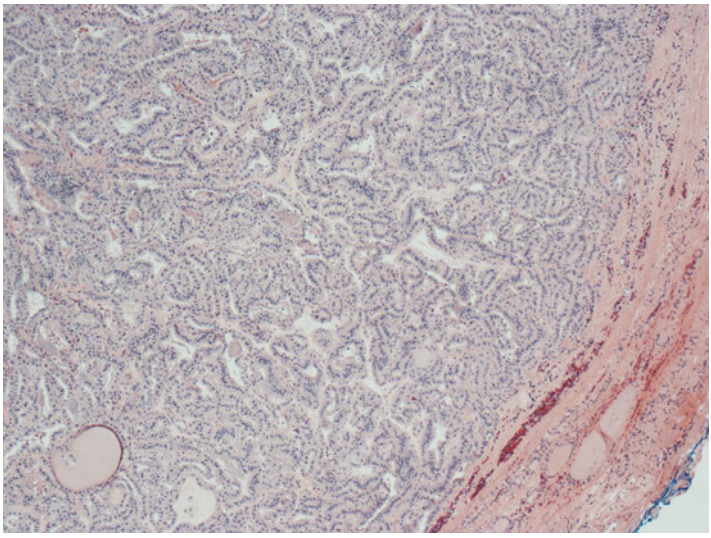

Fig. 7.11 Papillary thyroid carcinoma. A well-circumscribed nodule surrounded by a thin capsule. The neoplastic follicular cells are arranged predominantly in a papillary pattern (H&E, low power)

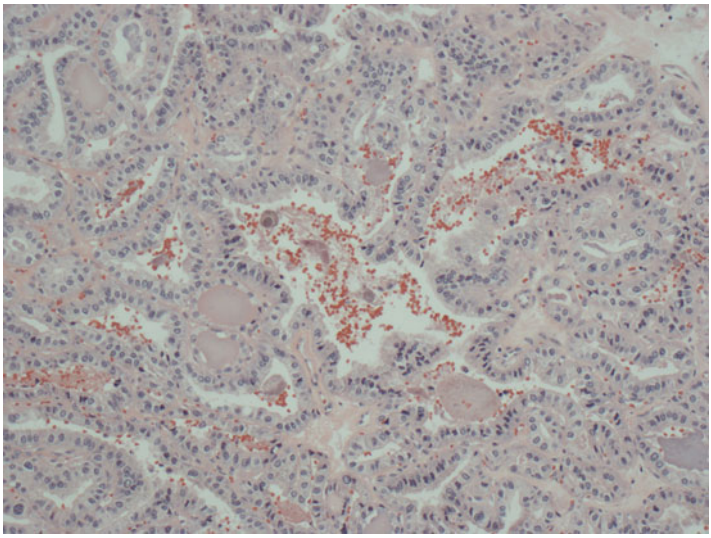

Fig. 7.12 Papillary thyroid carcinoma. Higher magnification showing a complex papillary growth pattern with fibrovascular cores (H&E, high power)

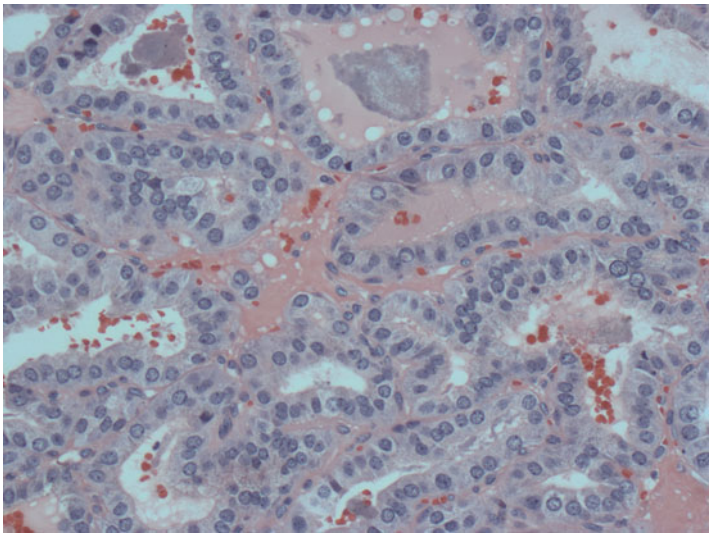

Fig. 7.13 Papillary thyroid carcinoma. Individual follicular cells show moderate amount of eosinophilic cytoplasm, nuclear enlargement, nuclear clearing, powdery chromatin, and frequent nuclear grooves. Intranuclear inclusions are not identified (H&E, high power)

Discussion

Molecular Pathway of Thyroid Carcinogenesis

The rising incidence of thyroid cancer over the past decades is accompanied by a better understanding of the molecular pathways of thyroid carcinogenesis [1]. The pathogenesis of papillary thyroid carcinoma is closely associated with mitogen-activated protein kinase (MAPK) pathway [2]. Point mutations involving *BRAF* and *RAS*, which are loci along the MAPK pathway, account for the majority of PTC [2]. They are followed closely by molecular arrangements such as *RET/PTC* [2]. Approximately, 70–80 % of papillary thyroid cancers harbor one of these molecular alterations, which tend to be mutually exclusive [1, 2]. In addition, three-quarters of follicular cancers demonstrate either *RAS* mutations or the *PAX8/PPARϒ* rearrangement [3, 4]. Mutations involved with the more aggressive variants of thyroid cancers include *PI3K/AKT* pathway or the *TP53* and *CTNNB1* genes [5, 6]. Point mutations in the *RET* gene are found in both familial and sporadic medullary thyroid cancers [7]. Table 7.1 summarizes the common molecular alterations in papillary thyroid carcinomas and follicular-derived neoplasms. Up to 30 % of papillary thyroid carcinomas and up to 30 % of follicular thyroid carcinomas do not demonstrate any of the molecular alterations described above. In addition, *RAS* and, to a lesser extent, *PAX8/PPARϒ*, can be demonstrated in 15–20 % and 2–10 % of follicular adenoma, respectively [8, 9].

Limitations of Cytology

Although thyroid nodules are common findings among adult population, only 5 % are malignant. FNA is the diagnostic choice in the preoperative evaluation of patients with thyroid nodules. FNA, being highly accurate and reliable, is able to

Table 7.1 Molecular alteration in both papillary thyroid carcinomas and follicular-derived neoplasms

Molecular alterations	Type of thyroid tumors	Estimated frequency (%)
BRAF^{V600E}	PTC, NOS	45
	PTC, FV	5
	PTC, Tall cell	80–100
	Anaplastic thyroid carcinoma	25
RAS	Follicular adenoma	20–25
	Follicular carcinoma	30–45
	PTC, FV	30–45
	Poorly differentiated thyroid carcinoma	20–40
	Anaplastic thyroid carcinoma	20–40
RET/PTC	PTC, NOS	25–30
PAX8/PPARϒ	Follicular carcinoma	35
	Follicular adenoma	2–10

classify about 70–80 % of thyroid nodules as definitively benign or malignant. However, FNA cannot reliably rule out a malignancy in about 20–35 % of nodules resulting in an equivocal cytologic diagnosis, i.e., FLUS/AUS, follicular neoplasm, or suspicious for malignancy. According to the Bethesda System of Reporting Thyroid Cytology (TBSRTC), each of these equivocal categories is associated with an estimate risk of malignancy of 10–15 % for FLUS/AUS, 20–30 % for follicular neoplasm, and 60–75 % for suspicious for malignancy [10]. Diagnostic lobectomy to establish a histologic diagnosis is often warranted for patients with a cytologic diagnosis of follicular neoplasm or suspicious for malignancy as well as those with a cytologic diagnosis of FLUS/AUS and clinical and/or ultrasonographic risk factors. However, only 10–40 % of the surgically resected nodules are proven to be malignant, resulting in unnecessary surgery in over 60 % of this subgroup of patients. Furthermore, in those with a malignant outcome, a second surgery is often required to "complete" the thyroidectomy. To minimize both unnecessary surgery and two-step surgeries, a better preoperative diagnostic approach to triage patients with equivocal cytologic diagnoses would be ideal. With a better understanding of the molecular basis of thyroid carcinogenesis, various novel diagnostic tests based on the detection of molecular biomarkers have been developed to improve the diagnostic accuracy of thyroid FNA.

Currently Available Molecular Testing for Routine Clinical Use

The currently available molecular testing available for thyroid FNA can be classified into those involved somatic mutation markers and those involving gene expression classifiers. The latter approach is also referred to as a "rule-out" test because these tests reliably identify nodules that are benign but not malignant nodules. On the other hand, molecular tests detecting one or more somatic mutation markers are referred to as "rule-in" tests because these tests accurately identify malignant nodules but do not predict benignancy.

Detection of Somatic Mutations

BRAF gene mutations have been reported in 50–80 % of papillary thyroid carcinoma, the most prevalent genetic alteration encountered in papillary thyroid carcinoma [11, 12]. The most frequent *BRAF* genetic alteration is a point mutation which results in the production of glutamate instead of valine (V600E) [13]. Although it has been reported in tumors of other organs, [14] *BRAF* mutation involving V600E is highly specific for papillary thyroid carcinoma among other primary thyroid neoplasms and has not been observed in benign thyroid lesions [4, 15, 16]. It is not surprising that this specificity has been evaluated in studies using preoperative FNA samples [17, 18]. According to a meta-analysis based on mostly prospective studies that included more than 5000 thyroid FNA samples tested for $BRAF^{V600E}$, the risk of malignancy is over 99 % when a thyroid FNA is tested positive for this mutation [9].

It has been demonstrated that combining morphologic and *BRAF* mutation analysis improved preoperative identification of PTC by 20–25 % [17, 19, 20]. Patients with nodules that have an equivocal cytologic diagnosis, i.e., FLUS/AUS, or suspicious for malignancy, and are tested positive for *BRAF* mutation would be strong candidates for total thyroidectomy, eliminating the need of a second surgery [17]. Despite high specificity for papillary thyroid carcinoma, molecular testing for BRAF mutation alone has low sensitivity. Furthermore, *BRAF* mutation is not indicated for cases classified as follicular neoplasm or suspicious for follicular neoplasm, since the majority of the malignancies following such a diagnosis are either follicular variant of papillary thyroid carcinoma or, to a lesser extent, follicular carcinoma, both of which rarely demonstrate *BRAF* mutation. One advantage is that *BRAF* testing can be performed using routinely collected cytologic preparations including scrapings of cellular materials from previously stained FNA smears, sections from formalin-fixed, paraffin-embedded cell block, or preferably, residual lavage fluid obtained from washing the needles.

In view of the limited sensitivity of testing for *BRAF* mutation alone, many recommend the use of a panel of molecular mutation markers, which include *BRAF* and *RAS* point mutations as well as *RET/PTC* and *PAX8/PPARγ* rearrangements [6, 21, 22]. Several studies have demonstrated a higher sensitivity for detecting malignant samples when using such a panel of molecular markers [6, 21–24]. The detection of any mutations is highly predictive for malignancy in samples with an equivocal cytologic diagnosis, i.e., FLUS/AUS, follicular neoplasm, or suspicious for malignancy. Overall, the risk of malignancy in mutation-positive cytologic samples is 88 % for FLUS/AUS, 87 % for follicular neoplasm, and 95 % for suspicious for malignancy [25]. When considering individual molecular mutation markers, the detection of *BRAF* mutation, *RET/PTC* or *PAX8/PPARγ* rearrangements, correlates with a malignant outcome in almost 100 % of cases [6, 21, 22] and therefore provides a strong indication for total thyroidectomy (Fig. 7.14). This would avoid the need for repeat FNA and/or a two-step surgery, i.e., a diagnostic lobectomy followed by completion thyroidectomy when the outcome is malignant. On the other hand, the presence of RAS mutations correlates with a malignant outcome only in 74–87 % of cases [6, 21, 22]. Almost all of the remaining nodules that were tested positive for RAS mutations are follicular adenoma. Some have argued that follicular adenoma with RAS mutations may be premalignant and, therefore would be likely to benefit from surgical resection to prevent potential malignant transformation in the future [26, 27].

Although a negative result with this mutational molecular panel significantly decreases the risk of cancer in all equivocal diagnostic categories, it does not eliminate it completely. For example, one study has demonstrated that a negative molecular test result decreases the risk of malignancy from 27 to 14 % in cases diagnosed as follicular neoplasm and from 54 to 28 % in cases diagnosed as suspicious for malignancy [21]. A review of four studies combining all four mutation markers into a single panel demonstrated a sensitivity of 64 %, implying a failure of 36 % to identify thyroid cancers [28]. As a result, diagnostic lobectomy is still warranted in patients with a cytologic diagnosis of follicular neoplasm or suspicious for malignancy but tested negative for the mutational molecular panel [29].

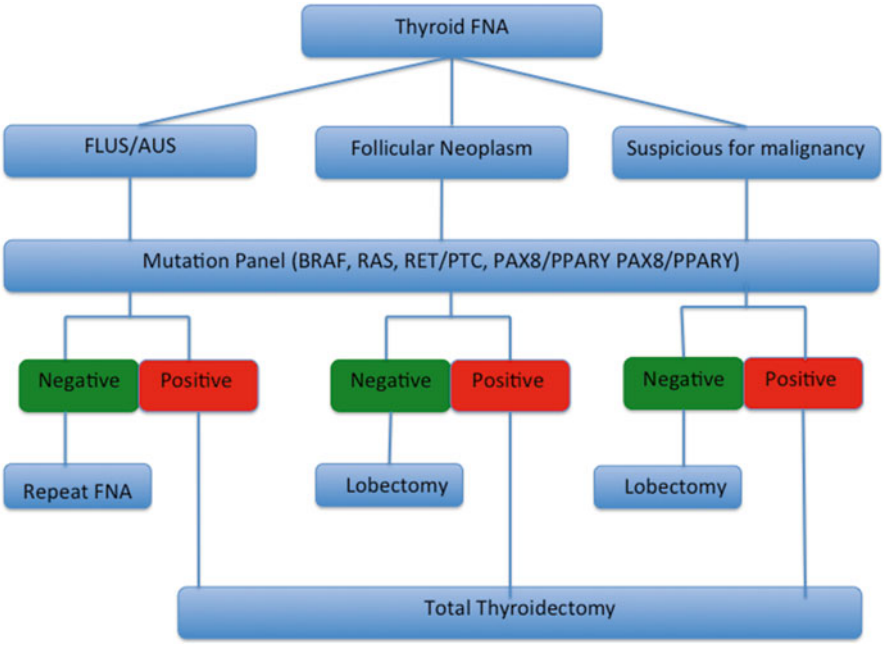

Fig. 7.14 Management algorithm of equivocal thyroid FNA based on a somatic mutation panel

For patients with a cytologic diagnosis of FLUS/AUS, the risk of malignancy ranges from 5 to 15 % and the current recommendation is to undergo repeat FNA within 6 months [10]. According to a study prospectively analyzing over 1000 cytologically indeterminate samples, the authors reported that the risk of malignancy decreases to 6 % for nodules with FLUS/AUS cytologic diagnosis that tested negative for mutation markers [21]. These authors stated that such a low posttest risk of malignancy for these nodules, which is comparable to those with a negative cytology, allows the clinicians the option to follow the patients conservatively with annual ultrasound instead of repeat FNA and/or diagnostic lobectomy [29]. It is important to recognize that the risk of malignancy in mutation negative nodules with equivocal cytologic diagnosis and the test negative predictive value may vary depending on the overall prevalence of cancers in the patient population. For example, with a 14 % prevalence of malignancy in the patient population, the test negative predictive value was 94 %; however, the test negative predictive value would decrease to 89 % when applied to a 24 % prevalence of malignancy seen in a large, multicenter, prospective, and blind study [30]. Furthermore, testing using this panel of molecular mutation markers can only correctly clarify a subgroup of equivocal FNAs [28]. As a result, approximately 80 % of patients with benign nodules and an equivocal cytologic diagnosis would be subjected to unnecessary diagnostic lobectomy and 40 % of patients with malignant but mutation-negative nodules would require a two-step surgery [31].

Somatic mutational testing should not be done on patients with known thyroid malignancy, known nodal and/or distant metastases, malignant or benign FNA results, or functional nodules. Furthermore, it should not be done on patients with clinical indications or strong personal preference for a total thyroidectomy. In addition to collecting samples for cytologic evaluation, two additional passes are required and to be placed in a separate fixative tube for each nodule for molecular testing. Most vendors would advocate routine collection of additional samples for molecular testing on every thyroid nodule biopsied. However, 75–85 % of these efforts would have been wasted since only 15–25 % of the thyroid FNA is classified as equivocal. In addition, multiple passes, especially in patients with more than one nodule, would expose the patients to increased discomforts and risks involved with the procedure.

Gene Expression Classifiers

The approach based on the detection of somatic mutation aims to reliably identify, i.e., rule in, thyroid cancer in patients with equivocal thyroid FNAs. An alternative approach is to reliably identify benign nodules in patients with equivocal thyroid FNAs, i.e., to rule out malignancy with the goal to minimize the number of diagnostic lobectomy. The Afirma GEC, based on the measurement of mRNA expression, was developed to rule out cancers among those with indeterminate cytology. This test is based on the expression analysis of 142 genes and uses a proprietary algorithm to classify the nodules into benign or suspicious groups [30]. The analysis proceeds in a stepwise fashion, first applying 6 cassettes before applying the final benign versus malignant classifier. The first 6 cassettes differentiate specific rare neoplasm subtypes, which include malignant melanoma, renal cell carcinoma, breast carcinoma, parathyroid tissue, and medullary thyroid carcinoma, and act as filters that stop further analysis if any cassette returns a "suspicious" result. If none of these cassettes are triggered, the GEC will proceed to evaluate the expression of 142 genes using a proprietary algorithm to classify indeterminate thyroid nodule FNAs as either "benign" or "suspicious."

According to the initial validation study conducted by the vendor, which was based on the analysis of 256 equivocal thyroid FNAs with subsequent histologic follow up, the negative predictive values of GEC were 95, 94, and 85 % for the nodules with FLUS/AUS, follicular neoplasm/suspicious for follicular neoplasm, and suspicious for malignancy diagnosis, respectively [30]. Subsequent independent, retrospective studies from both academic- and community-based practices also demonstrated that the negative predictive values of GEC ranged between 95 and 100 % [32–34]. Therefore, the risk of malignancy for a nodule with either FLUS/AUS or follicular neoplasm/suspicious for follicular neoplasm diagnosis but a benign GEC result is about 5–6 %, which is comparable to the risk of malignancy (6–8 %) for a thyroid nodule with a benign cytologic diagnosis. Alexander et al. recommended that nodules with an equivocal diagnosis and a benign GEC result

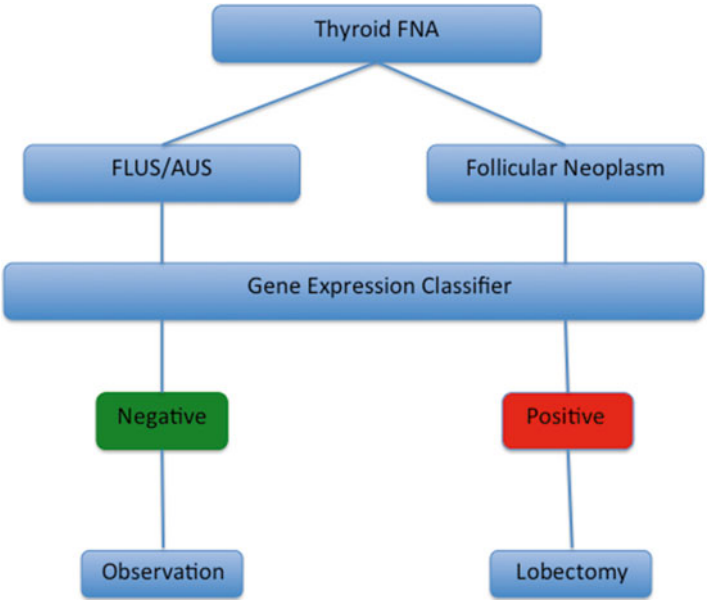

Fig. 7.15 Management algorithm of equivocal thyroid FNA based on a gene expression classifier

could be managed conservatively by observation and periodic ultrasound imaging and thus avoid a diagnostic lobectomy [30] (Fig. 7.15).

It is important to recognize that the pretest risk of malignancy profoundly impacts the test reliability. For Afirma GEC, a pretest risk of malignancy of <23 % is required to achieve a negative predictive value of >95 % and posttest risk of malignancy of <5 % [35]. In the initial validation study of Afirma GEC, the authors reported a pretest risk of malignancy of <23 % for a diagnosis of FLUS/AUS, a negative predictive value of >95 % with Afirma GEC, and a posttest risk of malignancy of <5 %. However, in the literature, the reported risks of malignancy for FLUS/AUS are widely variable, ranging from 6 to 62 % [36, 37]. Thus for a laboratory with a pretest risk of malignancy >23 % for FLUS/AUS, the negative predictive value of the Afirma GEC would drop below 95 % [35]. This illustrates the importance of knowing the pretest risk of malignancy for FLUS/AUS of the laboratory to which the clinicians submit their patients' samples in order to determine whether Afirma GEC can achieve similar performance as those reported by Alexander et al. [30]. Similar calculations could also be made for both follicular neoplasm/suspicious for follicular neoplasm and suspicious for malignant cells category with poorer results for the Afirma GEC, since higher risks of malignancy have been reported for both categories when compared to that of FLUS/AUS [10].

The initial validation data of Afirma GEC reported that 53 % of equivocal FNAs were classified by GEC as benign and a malignancy rate of 39 % for suspicious

Table 7.2 Contraindications for the use of Afirma gene expression classifier (GEC)

1. A concomitant positive FNA diagnosis of papillary thyroid carcinoma in other nodule(s)
2. Known nodal and/or distant metastases
3. Nodules larger than 4–5 cm because of potential sampling errors
4. Nodules with local or compressive symptoms
5. Nodules with suspicious clinical and/or US findings
6. Patients younger than 21 years old—Afirma GEC has not been validated for this subset of patients
7. Patients who prefer surgery regardless of the Afirma GEC results

GEC results [30]. However, subsequent and independent studies observed substantially lower percentages (26–34 %) of equivocal FNAs classified by GEC as benign and a much lower malignancy rate of 13 % of equivocal FNAs classified by GEC as suspicious [32, 33]. This would lower the positive predictive value of the Afirma GEC from 47 to 13 % [30, 32]. Furthermore, the reduction of diagnostic surgeries performed on patients with equivocal cytologic diagnosis would be only 41 %, rather than 75 % as reported in the initial validation study [30]. As a result, it calls into question the results of cost-saving analysis for the Afirma GEC, which claimed that the Afirma GEC modestly improved quality of life while reducing direct healthcare costs by $4653 per 5-year episode of care based on a projected 14 % rate of operation on GEC benign thyroid nodules [38].

Table 7.2 lists the contraindications to Afirma GEC testing. In general, it should not be indicated for nodules that should be managed surgically since Afirma GEC, as a rule-out test, is only beneficial for patients with benign test results and desire to avoid surgery. Similar to mutational testing, the vendor advocates the collection and placement of additional specimens in separate fixative tubes for molecular testing at the time of initial FNA, requiring additional passes. Alternatively, a repeat FNA for molecular testing and cytologic evaluation can be performed after an initial equivocal cytologic diagnosis; Afirma GEC testing may be helpful as a reassurance and avoid surgical intervention. Conservatively, especially in patients who are not suitable surgical candidates.

At present, the decision to perform Afirma GEC testing is based on the in-house cytologic evaluation of the FNAs with the exception of a few selected academic centers, which are allowed to send samples for Afirma testing only. This arrangement may undermine the collaborations between the institutional endocrinologists, endocrine surgeons, and cytopathologists. In addition, there is a small but substantial (14–17 %) percentage of discordant cases in regard to the cytologic classifications between Veracyte and the institutions. As a result, preoperative review of the thyroid FNAs by the institutional cytopathologists is highly recommended.

Beyond the Horizon

MicroRNAs (miRNAS)

MicroRNAs are small RNA sequences (19–25 nucleotides) that function to regulate the expression of genes. Several studies have identified differential expression of several miRNA expressions in thyroid cancers when compared with benign thyroid tissues [39–41]. It has been shown that there are strong differential expressions of miR-221, miR-222, and miR-19 between FNAs of papillary thyroid carcinoma and benign thyroid tissue [41]. However, this approach has yet to be tested on equivocal FNAs in a large, prospective, blinded, multicenter study [42, 43]. In addition, discrepant results are observed in regard to which miRNAs are differentially expressed between follicular carcinomas, follicular adenomas, and adenomatous nodules [43–45].

Next-Generation Sequencing

In the last decade, a new technology called next-generation sequencing (NGS) has emerged. This technology allows the simultaneous sequencing of large panels of genes, i.e., targeted sequencing, using very small amount of nucleic acid, with high sensitivity and in a cost-effective manner compared to traditional Sanger sequencing- and PCR-based methods. In a recent study evaluating 228 thyroid neoplastic and nonneoplastic specimens using NGS, the authors demonstrated 115 mutations, including 110 (75.8 %) mutations in 145 cancer samples and 5 (6.0 %) mutations in 83 benign nodules [46]. In another study, the same group of researchers applied NGS assay to 143 thyroid FNA samples with the cytologic diagnosis of follicular neoplasm/suspicious for follicular neoplasm [47]. Analysis was performed using the target ThyroSeq v2 NGS panel, which simultaneously tests for point mutation in 13 genes and for 42 types of gen fusions that occur in thyroid cancers. With a cancer prevalence of 27 %, the sensitivity and specificity of NGS assay was 90 and 93 % and the positive and negative predictive value was 83 and 96 %, respectively. The authors claimed that despite a significant increase in the negative predictive value as a result of the addition of a large number of additional genetic markers, the positive predictive value of the ThyroSeq v2 NGS panel was comparable to the 86 % reported for the prior 7-oncogene panel assay [47]. Another smaller, retrospective study based on a cohort of 34 indeterminate thyroid FNA samples demonstrated that 5 out of 7 mutation-positive FNA samples had a malignant diagnosis after surgery but only an 8 % cancer risk for nodules with a negative molecular test [48]. These studies highlight the potential benefits of molecular screening by NGS for the management of patients with equivocal thyroid FNA.

Prognostic Assessment

In addition to improving the diagnostic accuracy of thyroid FNA, molecular testing, particularly *BRAF* mutation analysis, may be able to provide significant prognostic and therapeutic information preoperatively. Across several studies, a strong association between the presence of $BRAF^{V600E}$ mutation and negative prognostic clinicopathologic features of papillary thyroid carcinoma such as extrathyroidal extension,

lymph node metastases, advanced tumor stages, tumor recurrence, and tumor-related mortality [12, 49, 50]. However, inconsistent study results have delayed a definitive conclusion on the prognostic role of this particular mutation. One recent study showed that patients tested positive for BRAF mutation demonstrated a significant positive association with extrathyroidal extension and nodal metastases, but the associations were not significant in a multivariate analysis [51]. It appears that additional, preferably prospective, studies would be warranted to determine whether knowledge of *BRAF* mutation status can improve outcomes when incorporated into clinical decision making. Given the costs and the potential for significant psychological and emotional harm related to the anxiety that may accompany *BRAF* mutation testing, it is safe to conclude that there is insufficient evidence to support widespread use of *BRAF* mutation testing for patients with PTC at this time.

References

1. Nikiforov YE. Molecular diagnostics of thyroid tumors. Arch Pathol Lab Med. 2011;135:569–77.
2. Nikiforov YE. Molecular analysis of thyroid tumors. Mod Pathol. 2011;24 Suppl 2:S34–43.
3. Kroll TG, Sarraf P, Pecciarini L, et al. PAX8-PPARgamma1 fusion oncogene in human thyroid carcinoma [corrected]. Science. 2000;289:1357–60.
4. Nikiforova MN, Lynch RA, Biddinger PW, et al. RAS point mutations and PAX8-PPAR gamma rearrangement in thyroid tumors: evidence for distinct molecular pathways in thyroid follicular carcinoma. J Clin Endocrinol Metab. 2003;88:2318–26.
5. Xing M. Genetic alterations in the phosphatidylinositol-3 kinase/Akt pathway in thyroid cancer. Thyroid. 2010;20:697–706.
6. Cantara S, Capezzone M, Marchisotta S, et al. Impact of proto-oncogene mutation detection in cytological specimens from thyroid nodules improves the diagnostic accuracy of cytology. J Clin Endocrinol Metab. 2010;95:1365–9.
7. Elisei R, Cosci B, Romei C, et al. Prognostic significance of somatic RET oncogene mutations in sporadic medullary thyroid cancer: a 10-year follow-up study. J Clin Endocrinol Metab. 2008;93:682–7.
8. Kondo T, Ezzat S, Asa SL. Pathogenetic mechanisms in thyroid follicular-cell neoplasia. Nat Rev Cancer. 2006;6:292–306.
9. Nikiforova MN, Nikiforov YE. Molecular diagnostics and predictors in thyroid cancer. Thyroid. 2009;19:1351–61.
10. Cibas ES, Ali SZ. The Bethesda system for reporting thyroid cytopathology. Thyroid. 2009;19:1159–65.
11. Lee JH, Lee ES, Kim YS. Clinicopathologic significance of BRAF V600E mutation in papillary carcinomas of the thyroid: a meta-analysis. Cancer. 2007;110:38–46.
12. Xing M. BRAF mutation in papillary thyroid cancer: pathogenic role, molecular bases, and clinical implications. Endocr Rev. 2007;28:742–62.
13. Davies H, Bignell GR, Cox C, et al. Mutations of the BRAF gene in human cancer. Nature. 2002;417:949–54.
14. Michaloglou C, Vredeveld LC, Mooi WJ, Peeper DS. BRAF(E600) in benign and malignant human tumours. Oncogene. 2008;27:877–95.
15. Cohen Y, Xing M, Mambo E, et al. BRAF mutation in papillary thyroid carcinoma. J Natl Cancer Inst. 2003;95:625–7.
16. Trovisco V, Soares P, Sobrinho-Simoes M. B-RAF mutations in the etiopathogenesis, diagnosis, and prognosis of thyroid carcinomas. Hum Pathol. 2006;37:781–6.

17. Adeniran AJ, Theoharis C, Hui P, et al. Reflex BRAF testing in thyroid fine-needle aspiration biopsy with equivocal and positive interpretation: a prospective study. Thyroid. 2011;21:717–23.
18. Xing M, Tufano RP, Tufaro AP, et al. Detection of BRAF mutation on fine needle aspiration biopsy specimens: a new diagnostic tool for papillary thyroid cancer. J Clin Endocrinol Metab. 2004;89:2867–72.
19. Nam SY, Han BK, Ko EY, et al. BRAF V600E mutation analysis of thyroid nodules needle aspirates in relation to their ultrasonographic classification: a potential guide for selection of samples for molecular analysis. Thyroid. 2010;20:273–9.
20. Marchetti I, Lessi F, Mazzanti CM, et al. A morpho-molecular diagnosis of papillary thyroid carcinoma: BRAF V600E detection as an important tool in preoperative evaluation of fine-needle aspirates. Thyroid. 2009;19:837–42.
21. Nikiforov YE, Ohori NP, Hodak SP, et al. Impact of mutational testing on the diagnosis and management of patients with cytologically indeterminate thyroid nodules: a prospective analysis of 1056 FNA samples. J Clin Endocrinol Metab. 2011;96:3390–7.
22. Nikiforov YE, Steward DL, Robinson-Smith TM, et al. Molecular testing for mutations in improving the fine-needle aspiration diagnosis of thyroid nodules. J Clin Endocrinol Metab. 2009;94:2092–8.
23. Ferraz C, Rehfeld C, Krogdahl A, et al. Detection of PAX8/PPARG and RET/PTC rearrangements is feasible in routine air-dried fine needle aspiration smears. Thyroid. 2012;22:1025–30.
24. Moses W, Weng J, Kebebew E. Prevalence, clinicopathologic features, and somatic genetic mutation profile in familial versus sporadic nonmedullary thyroid cancer. Thyroid. 2011;21:367–71.
25. Nikiforov YE, Nikiforova MN. Molecular genetics and diagnosis of thyroid cancer. Nat Rev Endocrinol. 2011;7:569–80.
26. Fagin JA. Minireview: branded from the start-distinct oncogenic initiating events may determine tumor fate in the thyroid. Mol Endocrinol. 2002;16:903–11.
27. Zhu Z, Gandhi M, Nikiforova MN, Fischer AH, Nikiforov YE. Molecular profile and clinical-pathologic features of the follicular variant of papillary thyroid carcinoma. An unusually high prevalence of ras mutations. Am J Clin Pathol. 2003;120:71–7.
28. Ferraz C, Eszlinger M, Paschke R. Current state and future perspective of molecular diagnosis of fine-needle aspiration biopsy of thyroid nodules. J Clin Endocrinol Metab. 2011;96:2016–26.
29. Nikiforov YE, Yip L, Nikiforova MN. New strategies in diagnosing cancer in thyroid nodules: impact of molecular markers. Clin Cancer Res. 2013;19:2283–8.
30. Alexander EK, Kennedy GC, Baloch ZW, et al. Preoperative diagnosis of benign thyroid nodules with indeterminate cytology. N Engl J Med. 2012;367:705–15.
31. Eszlinger M, Hegedus L, Paschke R. Ruling in or ruling out thyroid malignancy by molecular diagnostics of thyroid nodules. Best Pract Res Clin Endocrinol Metab. 2014;28:545–57.
32. McIver B, Castro MR, Morris JC, et al. An independent study of a gene expression classifier (afirma) in the evaluation of cytologically indeterminate thyroid nodules. J Clin Endocrinol Metab. 2014;99:4069–77.
33. Harrell RM, Bimston DN. Surgical utility of Afirma: effects of high cancer prevalence and oncocytic cell types in patients with indeterminate thyroid cytology. Endocr Pract. 2014;20:364–9.
34. Alexander EK, Schorr M, Klopper J, et al. Multicenter clinical experience with the Afirma gene expression classifier. J Clin Endocrinol Metab. 2014;99:119–25.
35. McIver B. Evaluation of the thyroid nodule. Oral Oncol. 2013;49:645–53.
36. Vanderlaan PA, Krane JF, Cibas ES. The frequency of "atypia of undetermined significance" interpretations for thyroid fine-needle aspirations is negatively correlated with histologically proven malignant outcomes. Acta Cytol. 2011;55:512–7.

37. Wang CC, Friedman L, Kennedy GC, et al. A large multicenter correlation study of thyroid nodule cytopathology and histopathology. Thyroid. 2011;21:243–51.
38. Li H, Robinson KA, Anton B, Saldanha IJ, Ladenson PW. Cost-effectiveness of a novel molecular test for cytologically indeterminate thyroid nodules. J Clin Endocrinol Metab. 2011;96:E1719–26.
39. He H, Jazdzewski K, Li W, et al. The role of microRNA genes in papillary thyroid carcinoma. Proc Natl Acad Sci U S A. 2005;102:19075–80.
40. Weber F, Teresi RE, Broelsch CE, Frilling A, Eng C. A limited set of human MicroRNA is deregulated in follicular thyroid carcinoma. J Clin Endocrinol Metab. 2006;91:3584–91.
41. Pallante P, Visone R, Ferracin M, et al. MicroRNA deregulation in human thyroid papillary carcinomas. Endocr Relat Cancer. 2006;13:497–508.
42. Kim MI, Alexander EK. Diagnostic use of molecular markers in the evaluation of thyroid nodules. Endocr Pract. 2012;18:796–802.
43. Lodewijk L, Prins AM, Kist JW, et al. The value of miRNA in diagnosing thyroid cancer: a systematic review. Cancer Biomark. 2012;11:229–38.
44. Rossing M. Classification of follicular cell-derived thyroid cancer by global RNA profiling. J Mol Endocrinol. 2013;50:R39–51.
45. Stokowy T, Wojtas B, Fujarewicz K, Jarzab B, Eszlinger M, Paschke R. miRNAs with the potential to distinguish follicular thyroid carcinomas from benign follicular thyroid tumors: results of a meta-analysis. Horm Metab Res. 2014;46:171–80.
46. Nikiforova MN, Wald AI, Roy S, Durso MB, Nikiforov YE. Targeted next-generation sequencing panel (ThyroSeq) for detection of mutations in thyroid cancer. J Clin Endocrinol Metab. 2013;98:E1852–60.
47. Nikiforov YE, Carty SE, Chiosea SI, et al. Highly accurate diagnosis of cancer in thyroid nodules with follicular neoplasm/suspicious for a follicular neoplasm cytology by ThyroSeq v2 next-generation sequencing assay. Cancer. 2014;120:3627–34.
48. Le Mercier M, D'Haene N, De Neve N, et al. Next-generation sequencing improves the diagnosis of thyroid FNA specimens with indeterminate cytology. Histopathology. 2015;66:215–24.
49. Elisei R, Ugolini C, Viola D, et al. BRAF(V600E) mutation and outcome of patients with papillary thyroid carcinoma: a 15-year median follow-up study. J Clin Endocrinol Metab. 2008;93:3943–9.
50. Xing M, Clark D, Guan H, et al. BRAF mutation testing of thyroid fine-needle aspiration biopsy specimens for preoperative risk stratification in papillary thyroid cancer. J Clin Oncol. 2009;27:2977–82.
51. Gouveia C, Can NT, Bostrom A, Grenert JP, van Zante A, Orloff LA. Lack of association of BRAF mutation with negative prognostic indicators in papillary thyroid carcinoma: the University of California, San Francisco, experience. JAMA Otolaryngol Head Neck Surg. 2013;139:1164–70.

Cystic Papillary Thyroid Carcinoma

8

Case Study

A 47-year-old female presented for a workup of possible hyperparathyroidism following repeated bouts of renal calculi. Her calcium levels were found to be high. She had no complaints of hoarseness and no difficulty breathing. Her calcium workup included an ultrasound, which revealed a 2.3 cm complex cystic nodule in the lower pole of the right thyroid lobe. Fine needle aspiration revealed syncytial tissue fragments with cells showing histiocytoid appearance and having the typical nuclear features of papillary thyroid carcinoma. Histological examination revealed 2.1 cm partially ossified cystic papillary carcinoma in the lower pole of the right thyroid lobe. All ten lymph nodes excised from the right central neck compartment were negative for carcinoma. In addition, the patient also had a 1.5 cm right inferior parathyroid adenoma resected. Postoperative course was uneventful.

Discussion

Cystic change/degeneration can be seen in 15–37 % of thyroid nodules [1–6]. In contrast to true simple cysts of the thyroid, most thyroid cysts resulting from degenerative changes lack a complete or well-developed epithelial lining [7]. Most cystic thyroid nodules are benign; however, a good number of them can be malignant. Cystic change is more commonly seen in papillary thyroid carcinoma in comparison to other malignant neoplasms of the thyroid. Up to 10–16 % of PTC can be cystic [3, 7]. The tumor can be purely or partially cystic, unilocular or multilocular, thin walled or thick walled, and may contain residual tumor in the wall. Certain features of the patients' clinical presentation may raise suspicion for malignancy. These features include extremes of age, male sex, family history of thyroid cancer, history of head and neck irradiation, as well as signs of invasiveness such as hoarseness, obstruction, and lymphadenopathy [8].

A.J. Adeniran, D. Chhieng, *Common Diagnostic Pitfalls in Thyroid Cytopathology*, DOI 10.1007/978-3-319-31602-4_8

The histologic appearance of cystic PTC is unique. Typically they show papillary fronds, which project into the cystic cavity (Figs. 8.1, 8.2, 8.3, 8.4, and 8.5). The cystic cavity can be filled with old and new blood, cellular and calcific debris and detached papillary fronds [9]. Macrophages can be seen in variable numbers with or without hemosiderin-laden pigments (Fig. 8.6); the amount of macrophages in a

Fig. 8.1 Gross appearance of a cystic papillary thyroid carcinoma bordered by a thick capsule

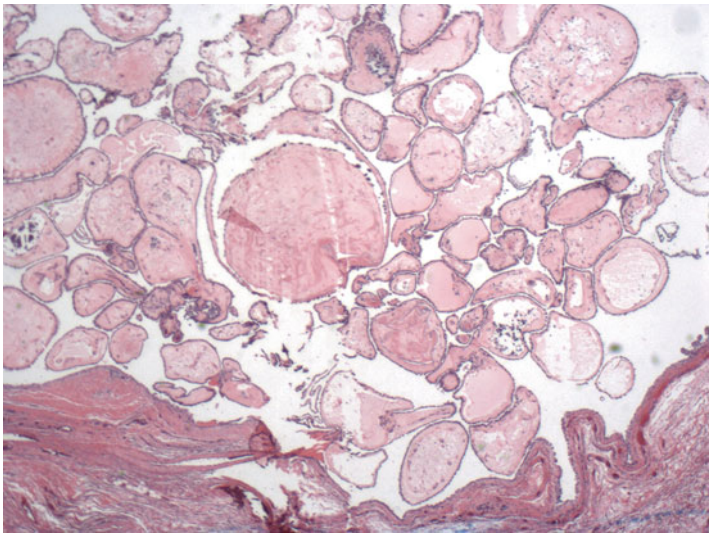

Fig. 8.2 Histologic section of a cystic papillary carcinoma with detached papillae. (H&E stain, 20×)

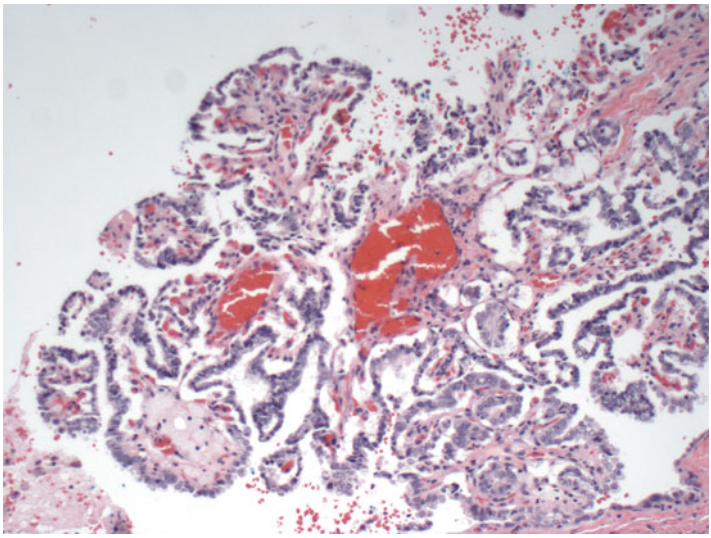

Fig. 8.3 Histologic section of a cystic papillary carcinoma with detached papillae. (H&E stain, 100×)

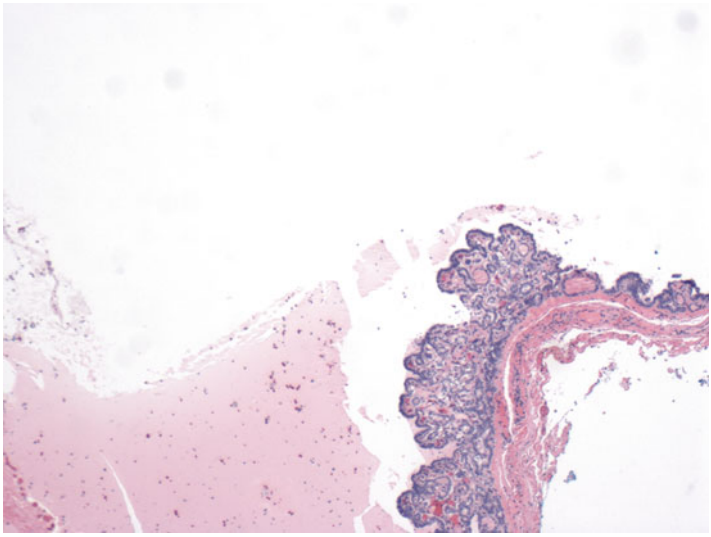

Fig. 8.4 Histologic section of a cystic papillary carcinoma with papillary projections into the lumen. (H&E stain, 40×)

given FNA specimen of PTC is proportional to the cystic component of the tumor. Most patients with cystic PTC have lesions yielding bloody or brown fluid, but clear, yellow fluid can also be aspirated in rare cases [1]. Hemorrhagic or chocolate-colored fluid is usually believed to be more predictive of malignancy, based on the idea that

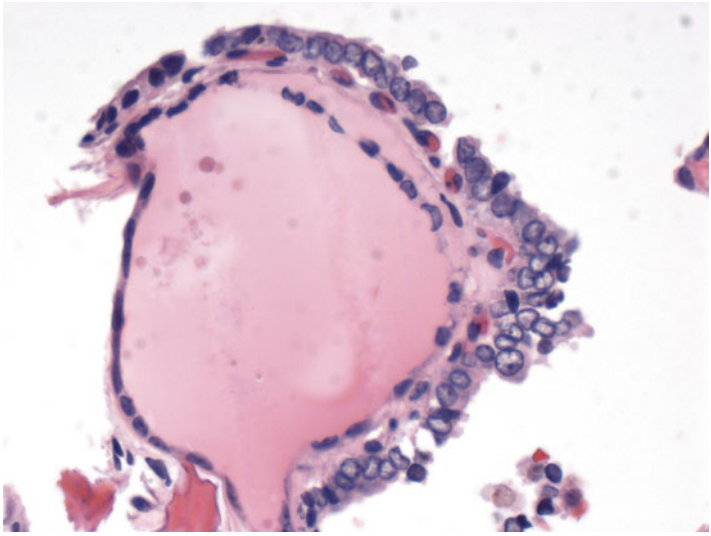

Fig. 8.5 Histologic section of a cystic papillary carcinoma with a detached papilla showing the typical nuclear features of papillary carcinoma. (H&E stain, 400×)

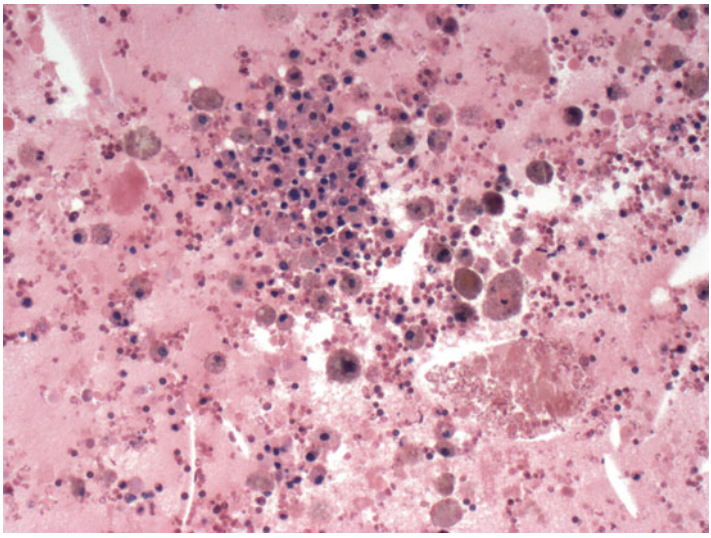

Fig. 8.6 Histologic section of a cystic papillary carcinoma filled with blood, hemosiderin-laden macrophages and cellular debris. (H&E stain, 200×)

a tumor may outgrow its blood supply, undergoing infarction and cavitation, which suggests that the fluid is formed from follicular destruction [4, 5].

There is a high percentage of false-negative result in the evaluation of cystic PTC. This is partly due to sampling error because of the cystic nature of the lesion

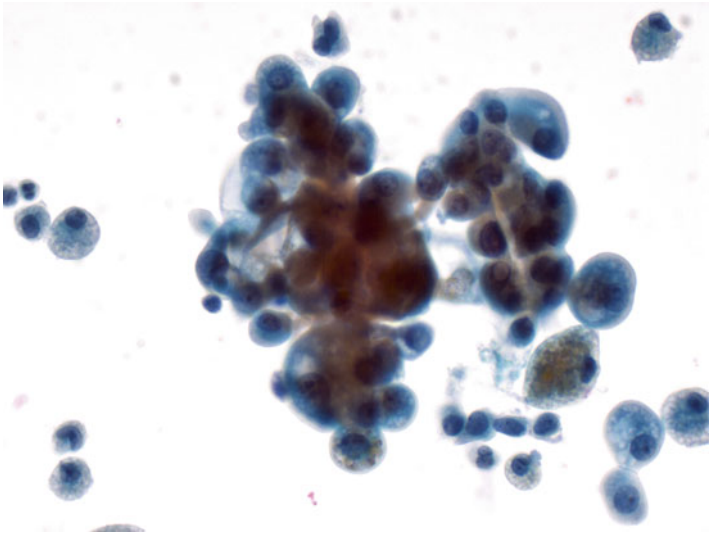

Fig. 8.7 FNA of cystic papillary carcinoma. Syncytial tissue fragments with scalloped borders. There is nuclear enlargement. Rare intranuclear inclusions are present. (Papanicolaou stain, 200×)

and also partly due to cytologic diagnostic errors in the interpretation of the smears due to scant cellularity and degenerative changes in the specimen, which can mask the diagnostic criteria of malignant cells [1, 10]. Systematic examination of cytologic specimens of cystic thyroid nodules is recommended in order to rule out cystic carcinoma and avoid false-negative diagnostic errors [11].

The tissue fragments seen in cystic PTC tend to exhibit scalloped borders (Figs. 8.7 and 8.8), and they arrange themselves in a cartwheel pattern with nuclei at the outside perimeter [9]. Some cytologic features have been found to be useful in the differential diagnosis between cystic PTC and cystic degeneration in a benign hyperplastic nodule (goiter). These cytologic features include three-dimensional fragments, anisonucleosis, nuclear bars, nuclear crowding, nuclear enlargement, intranuclear inclusions, metaplastic cytoplasm, cytoplasmic vacuoles, and autolysis, all of which are more commonly seen in cystic PTC [12–14] (Figs. 8.9 and 8.10). The cytoplasmic vacuoles can be small, multiple, or large, occupying the entire cell and displacing the nucleus to the periphery. The characteristic fine, powdery chromatin of PTC may not be present because the chromatin has a tendency to stain intensely due to degeneration. The repair-like spindled cytomorphologic features present in the majority of benign cysts are not seen [7]. Colloid is absent from aspirates of cystic PTC. The presence of psammoma bodies favors cystic PTC. However, dystrophic calcifications can mimic psammoma bodies, so the presence of naked calcifications without any of the nuclear features of PTC is of no diagnostic significance other than the need for careful examination of all the smears when they are encountered. The combination of macrophages, hemosiderin, cellular debris, and old blood in the background may, however, obscure distinction between PTC and cystic goiters [8].

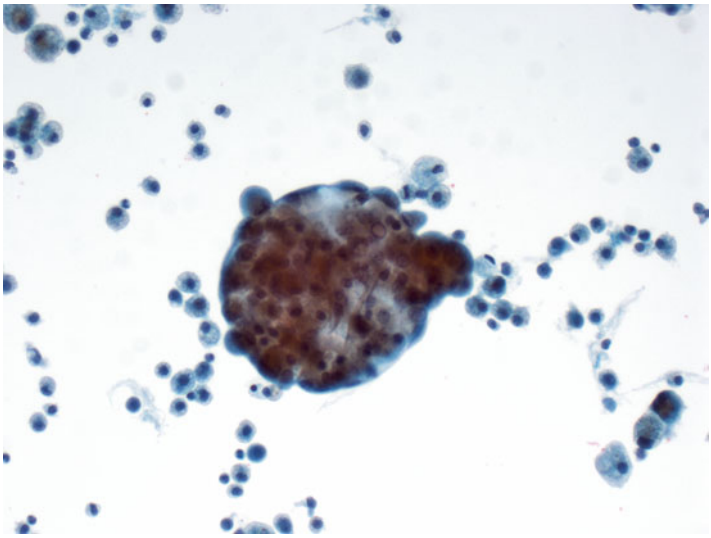

Fig. 8.8 Syncytial tissue fragments of follicular cells with scalloped borders. Rare intranuclear inclusion is present. (Papanicolaou stain, 200×)

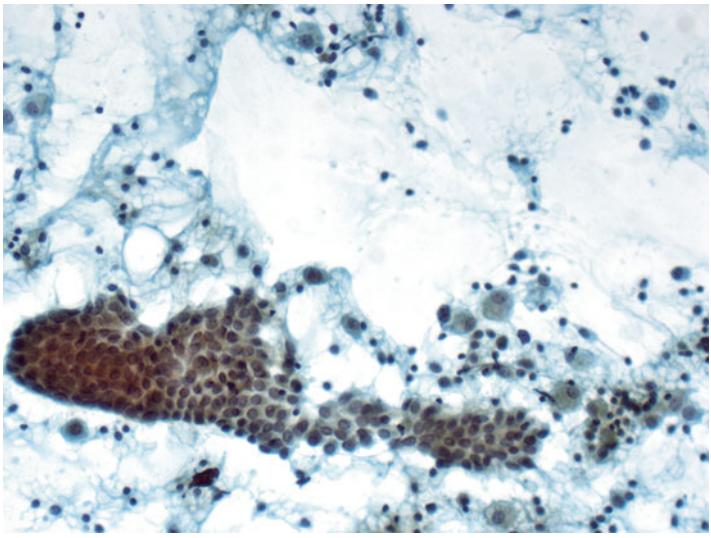

Fig. 8.9 FNA of cystic papillary carcinoma. Papillary cluster of cells in a cystic background. The cells are crowded. Nuclear features of papillary carcinoma such as nuclear enlargement and nuclear grooves are present. (Papanicolaou stain, 200×)

The atypical histiocytoid cells which have been described in smears of cystic PTC [11, 14] have abundant vacuolated cytoplasm, nuclear pleomorphism, and nucleoli. They are larger and more atypical than benign histiocytes. They may also have rare

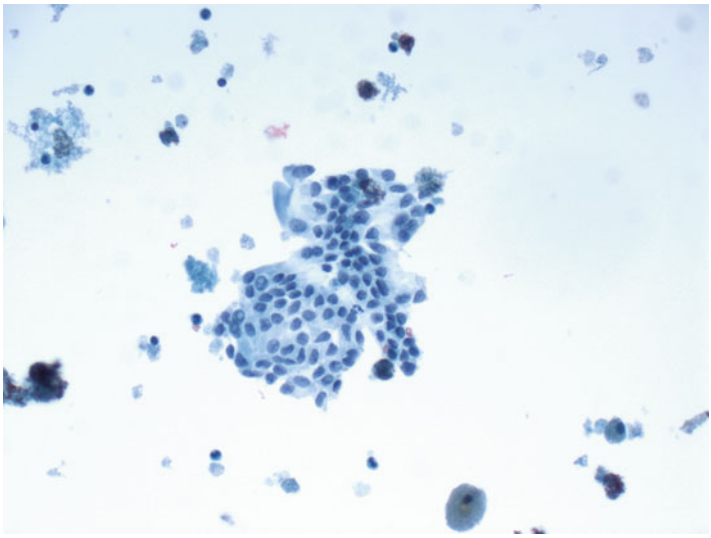

Fig. 8.10 FNA of cystic papillary carcinoma. Papillary cluster of cells in a cystic background. Nuclear features of papillary carcinoma such as nuclear enlargement, nuclear contour irregularity, nuclear grooves and intranuclear inclusions are present. (Papanicolaou stain, 200×)

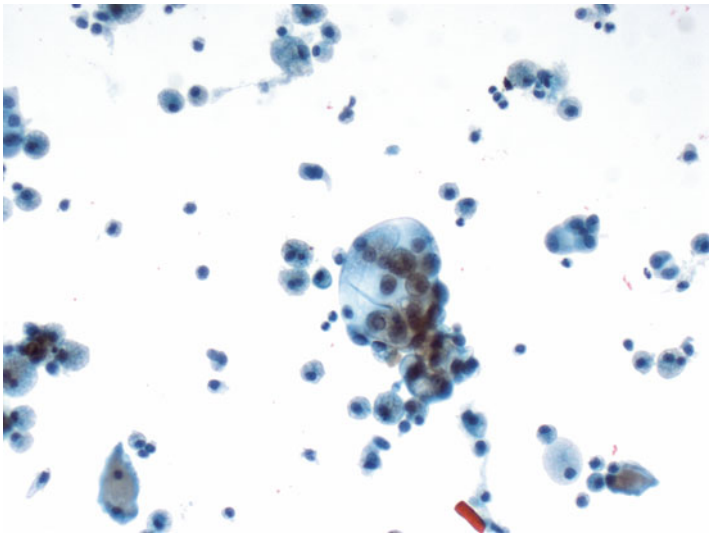

Fig. 8.11 Syncytial tissue fragments with cells showing bubbly vacuolated cytoplasm. The nuclei are larger than those of the surrounding histiocytes. A rare intranuclear inclusion is present. (Papanicolaou stain, 200×)

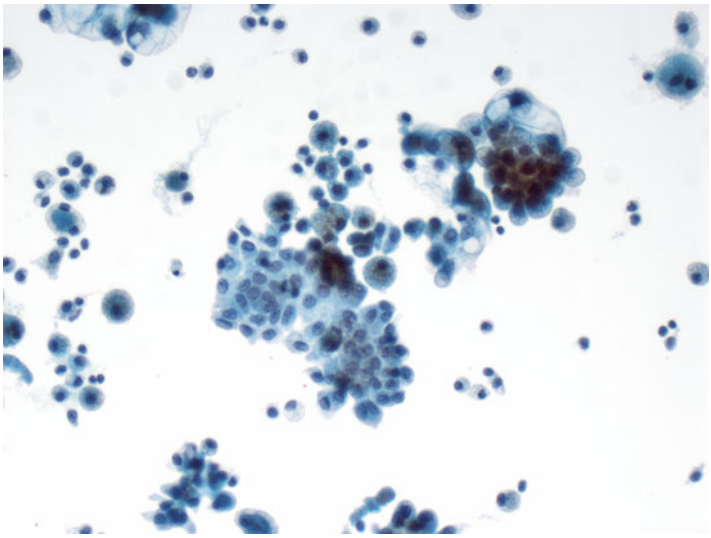

Fig. 8.12 Syncytial tissue fragments with well-defined borders. The cells have nuclei that are larger than those of surrounding histiocytes; and nuclear features of papillary carcinoma are present. The cytoplasm is vacuolated. (Papanicolaou stain, 200×)

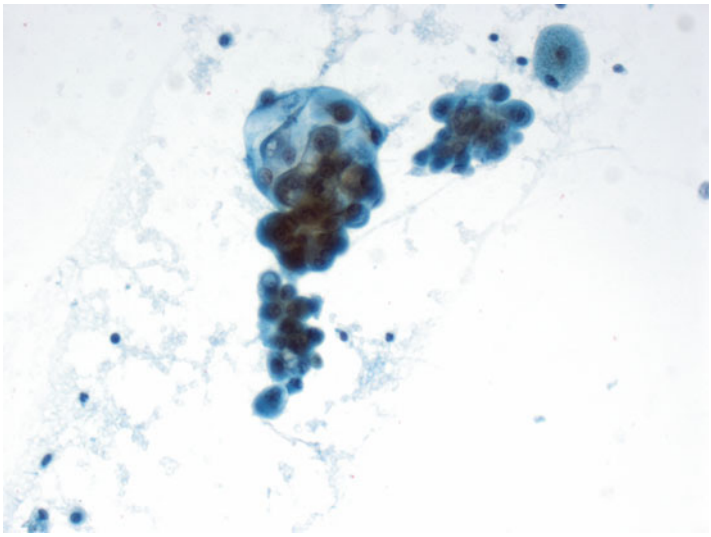

Fig. 8.13 Syncytial tissue fragments with scalloped borders. The cells have bubbly vacuolated cytoplasm. (Papanicolaou stain, 200×)

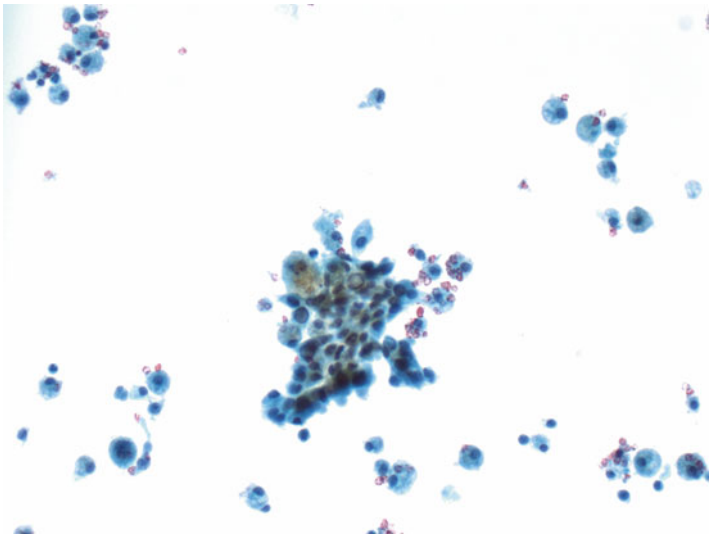

Fig. 8.14 Syncytial tissue fragments with histiocytoid cells. The cells have abundant vacuolated cytoplasm and nuclear features of papillary carcinoma. (Papanicolaou stain, 200×)

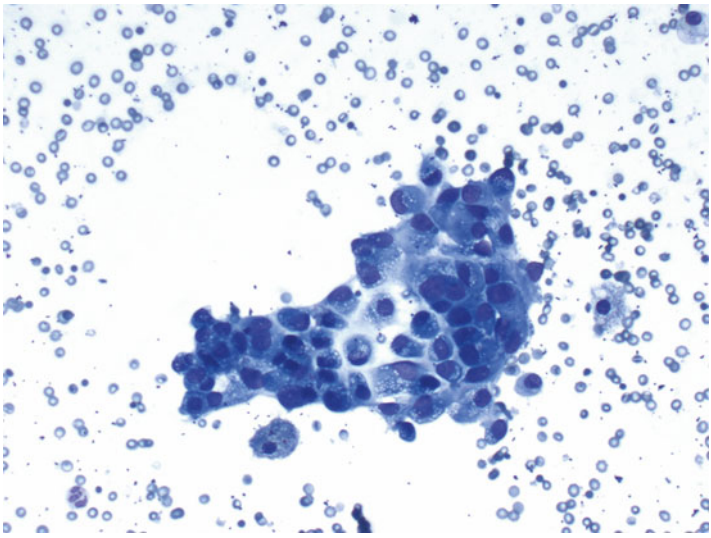

Fig. 8.15 Syncytial tissue fragments with cells showing nuclear pleomorphism and abundant vacuolated cytoplasm. (Diff-Quik stain, 200×)

grooves and rare pseudoinclusions [15] (Figs. 8.11, 8.12, 8.13, 8.14, 8.15, 8.16, and 8.17). Aspirations from cystic degeneration in goiters may show fragments of cells with foamy cytoplasm and enlarged nuclei with nuclear features similar to the histiocytoid cells seen in cystic PTC, and it may be difficult to distinguish one from the

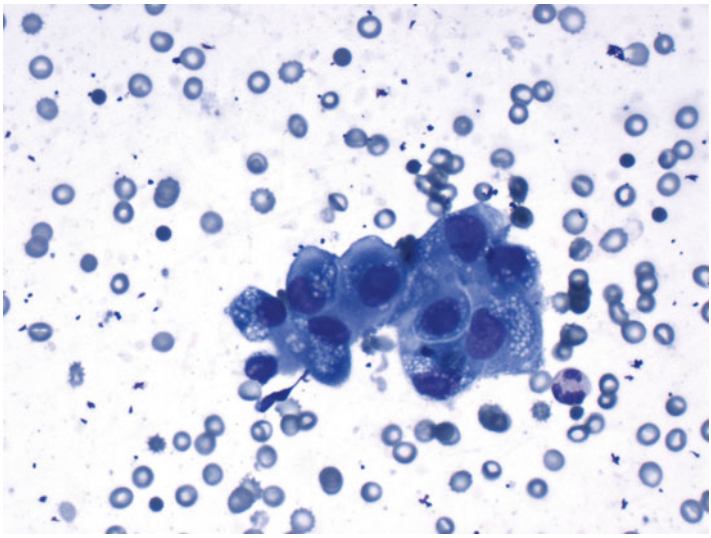

Fig. 8.16 Syncytial tissue fragments with cells showing nuclear pleomorphism and abundant vacuolated cytoplasm. (Diff-Quik stain, 400×)

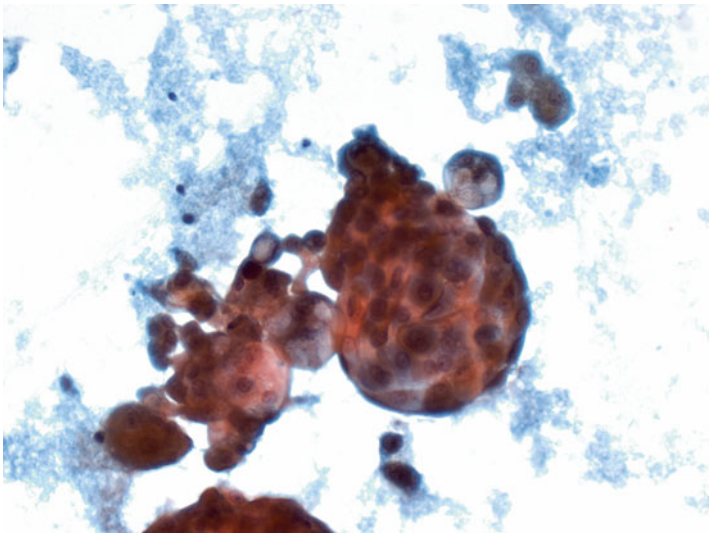

Fig. 8.17 Syncytial tissue fragments with scalloped borders and cells showing abundant vacuolated cytoplasm. Nuclei are larger than those of surrounding histiocytes. (Papanicolaou stain, 200×)

other (Fig. 8.18). Positive immunoreactivity with CD68 and negative with cytokeratin will confirm that these cells are histiocytes/macrophages, which are commonly encountered in FNA specimens of thyroid, and their number is dependent on the cystic component of the thyroid nodule [16]. In order to avoid a false-negative

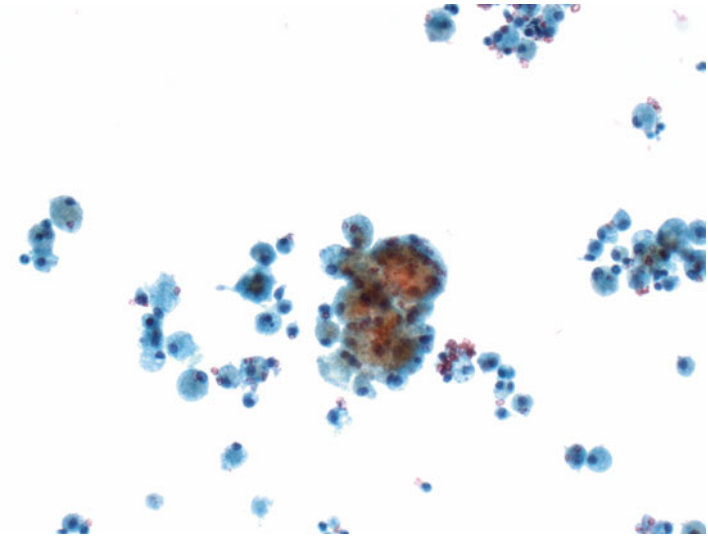

Fig. 8.18 Aggregate of histiocytes in cystic degeneration in a goiter. The nuclei of histiocytes are smaller than in cystic papillary carcinoma. (Diff-Quik stain, 200×)

diagnosis in cystic PTC, a careful search for the nuclear features is essential because degenerating single or clustered malignant cells may appear histiocytic [17]. However, nuclei of degenerating tumor cells appear larger and more plump than those seen in histiocytes, with a moderately high nuclear to cytoplasmic ratio and denser cytoplasm with well-defined or scalloped borders [16].

In the absence of adequate number of follicular cells or when there are overwhelming degenerative changes, a repeat biopsy is recommended [18]. One way to reduce the incidence of re-biopsy is to have adequacy assessment at the time when the FNA biopsy is performed. The instant feedback decreases the rate of insufficient material for diagnosis.

If the lesion is a complex cyst, it is important to note that after the cystic component has been drained, the solid component should be adequately sampled if a residual mass persists after aspiration. In specimens with equivocal diagnosis, one important feature that determines whether or not the nodule should be surgically excised is fluid re-accumulation and the rate of accumulation of the fluid in the cyst. There is hardly ever any re-accumulation of fluid in benign cysts, whereas the fluid in malignant cysts rapidly re-accumulates. Ancillary immunohistochemical markers such as cytokeratin-19 and galectin-3 may be useful in challenging specimens. However, the hypocellularity of most thyroid cyst aspiration specimens would most likely limit or preclude the application of these ancillary tests [7].

We routinely send cystic thyroid nodules with indeterminate diagnosis for BRAF V600E mutation analysis. Given the very high specificity of *BRAF V600E* mutation as a marker for PTC in thyroid nodules with an indeterminate diagnosis and the very high positive predictive value of PTC in thyroid nodules with an indeterminate

diagnosis and with positive *BRAF* mutation, *BRAF* mutation analysis has become a useful adjunct test that helps to stratify these, thus allowing better planning of surgical treatment. Patients with nodules that have an indeterminate diagnosis on FNA and are positive for *BRAF V600E* mutation would be strong candidates for total thyroidectomy. We also sometimes send cases for tests that utilize gene expression or miRNA profiling as well as other genetic tests based on a comprehensive panel of point mutations and gene fusions occurring in thyroid cancers, most notably the ThyroSeq next-generation sequencing panel.

References

1. de los Santos ET, Keyhani-Rofagha S, Cunningham JJ, Mazzaferri EL. Cystic thyroid nodules. The dilemma of malignant lesions. Arch Intern Med. 1990;150:1422–7.
2. Cusick EL, McIntosh CA, Krukowski ZH, et al. Cystic change and neoplasia in isolated thyroid swellings. Br J Surg. 1988;75:982–3.
3. Hsu C, Boey J. Diagnostic pitfalls in the fine needle aspiration of thyroid nodules: a study of 555 cases in Chinese patients. Acta Cytol. 1987;31:699–704.
4. Hammer M, Wortsman J, Folse R. Cancer in cystic lesions of the thyroid. Arch Surg. 1982;117:1020–3.
5. Ashcraft MW, Van Herle AJ. Management of thyroid nodules, I: history and physical examination, blood tests, x-ray tests and ultrasonography. Head Neck Surg. 1981;3:216–27.
6. Clark OH, Okerlund MD, Cavalieri RR, Greenspan F. Diagnosis and treatment of thyroid, parathyroid, and thyroglossal duct cysts. J Clin Endocrinol Metab. 1979;48:983–7.
7. Faquin WC, Cibas ES, Renshaw AA. "Atypical" cells in fine-needle aspiration biopsy specimens of benign thyroid cysts. Cancer. 2005;105:71–9.
8. Goellner JR, Johnson DA. Cytology of cystic papillary carcinoma of the thyroid. Acta Cytol. 1982;26:797–808.
9. Kini SR. Thyroid cytopathology: an Atlas and text. Philadelphia: Wolters Kluwer/Lippincott Williams & Wilkins; 2008.
10. Wolf PL. Biochemical biopsy of thyroid cysts vs cytologic diagnosis—which is preferable? Arch Pathol Lab Med. 1993;117:593–4.
11. Castro-Gómez L, Córdova-Ramírez S, Duarte-Torres R, Alonso de Ruiz P, Hurtado-López LM. Cytologic criteria of cystic papillary carcinoma of the thyroid. Acta Cytol. 2003; 47:590–4.
12. Kini SR, Miller JM, Hamburger JI, Smith MJ. Cytopathology of papillary carcinoma of the thyroid by fine needle aspiration. Acta Cytol. 1980;24:511–21.
13. Kaur A, Jayaram G. Thyroid tumors: cytomorphology of papillary carcinoma. Diagn Cytopathol. 1991;7:462–8.
14. Renshaw AA. "Histiocytoid" cells in fine-needle aspirations of papillary carcinoma of the thyroid: frequency and significance of an under-recognized cytologic pattern. Cancer. 2002; 96:240–3.
15. Harshan M, Crapanzano JP, Aslan DL, Vazquez MF, Saqi A. Papillary thyroid carcinoma with atypical histiocytoid cells on fine-needle aspiration. Diagn Cytopathol. 2009;37:244–50.
16. Nassar A, Gupta P, LiVolsi VA, Baloch Z. Histiocytic aggregates in benign nodular goiters mimicking cytologic features of papillary thyroid carcinoma (PTC). Diagn Cytopathol. 2003;29:243–5.
17. Nayar R, Frost AR. Thyroid aspiration cytology: a "cell pattern" approach to interpretation. Semin Diagn Pathol. 2001;18:81–98.
18. Yang YJ, Haghir S, Wanamaker JR, Powers CN. Diagnosis of papillary carcinoma in a thyroglossal duct cyst by fine-needle aspiration biopsy. Arch Pathol Lab Med. 2000;124:139–42.

Follicular Variant of Papillary Thyroid Carcinoma

9

Case Study

The patient was a 54-year-old female who presented with neck pressure and chronic cough. She had a past history of allergies and angioedema. The patient had no history of dysphagia or hoarseness and no palpitations, tremors, or heat intolerance. On examination, she was found to have a palpable thyroid nodule. Ultrasonographic examination revealed a $2.2 \times 1.7 \times 1.7$ cm nodule in the right lobe of the thyroid with macrocalcifications at the inferior portion. In addition, there were scattered smaller nodules bilaterally. Fine needle aspiration cytology showed a cellular specimen with microfollicles, macrofollicles, and few groups with crowding and overlapping. A small subset showed nuclei with enlargement, elongation, and powdery chromatin. This was signed out as follicular lesion of undetermined significance. *BRAF* gene *V600E* was not detected. A right level 3 lymph node that was biopsied at the same time showed a polymorphous population of lymphocytes with no evidence of metastatic carcinoma. The patient underwent a right thyroid lobectomy, which revealed a 1.8 cm, totally encapsulated follicular variant of papillary thyroid carcinoma. The tumor was limited to the thyroid and the margins were negative. She had a completion thyroidectomy a month after the initial surgery and the postoperative course was uneventful.

Discussion

Several histologic variants of papillary thyroid carcinoma (PTC) have been described, and some are known to have prognostic significance [1]. The follicular variant of PTC (FVPTC) is the most common variant after classic PTC, making up 10–15 % of all PTC [2, 3]. The biologic behavior of FVPTC has been likened to that of classic variant of PTC, as it has been found that local and distant metastases of FVPTC do not occur more often than do those of classic PTC [4]. The tumor is usually circumscribed and encapsulated, which can be complete or partial (Fig. 9.1).

A.J. Adeniran, D. Chhieng, *Common Diagnostic Pitfalls in Thyroid Cytopathology*, DOI 10.1007/978-3-319-31602-4_9

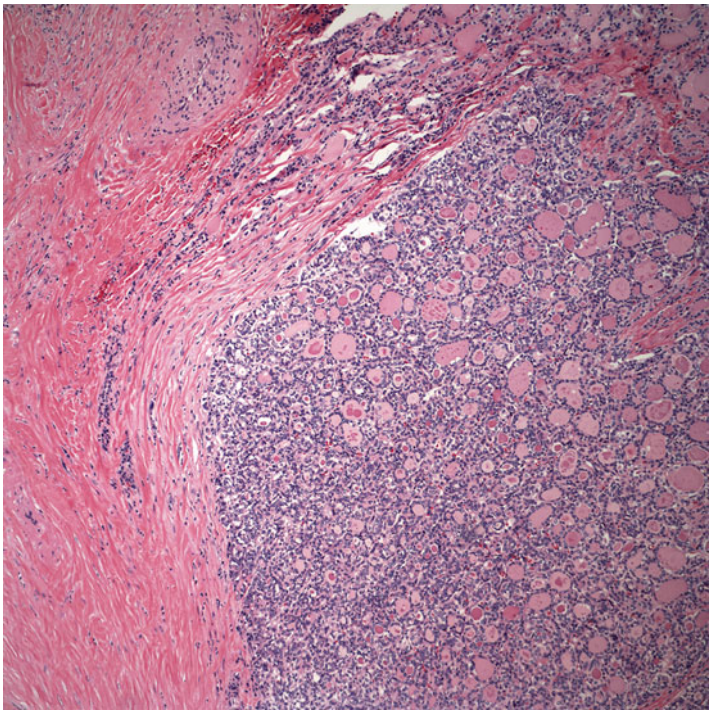

Fig. 9.1 Follicular variant of papillary thyroid carcinoma. Low-power view showing a thickly encapsulated follicular patterned lesion (H&E stain, X100)

However, tumors can also be nonencapsulated and infiltrative. They vary in size and range from microcarcinomas to very large tumors. Histologically, the tumor is characterized by exclusively follicular growth pattern. The follicles vary in size and shape from round to elongated and these follicles are distended with colloid. The lining epithelium may show infolding, but papillae are totally absent or very scanty and poorly developed (Fig. 9.2).

The diagnosis of FVPTC is made by finding the typical nuclear features, which are seen in classic PTC (Fig. 9.3). In theory the rate and ease of diagnosis of FVPTC should be similar to classic PTC since the diagnostic criteria are identical. However cytological diagnosis of FVPTC is challenging and poses a diagnostic problem for the following reasons: (1) nuclear features of PTC are less obvious and focal, (2) absence of papillary groups or large syncytial sheets, and (3) predominance of follicular architecture with rare nuclear alteration and presence of variable colloid component [5–7]. Another important reason for the difficulty on cytomorphology is the overlap in histologic appearance between FVPTC and other lesions in the follicular neoplasm category, namely, follicular adenoma, follicular carcinoma, and benign nonneoplastic follicular lesions [8–10]. For these reasons, it is not uncommon for the diagnosis of FVPTC to be missed on fine needle aspiration. Hence there is a varied interobserver reproducibility even among experienced thyroid pathologists [4, 11–14]. Fine needle aspiration smears are usually cellular (Figs. 9.4 and 9.5) but

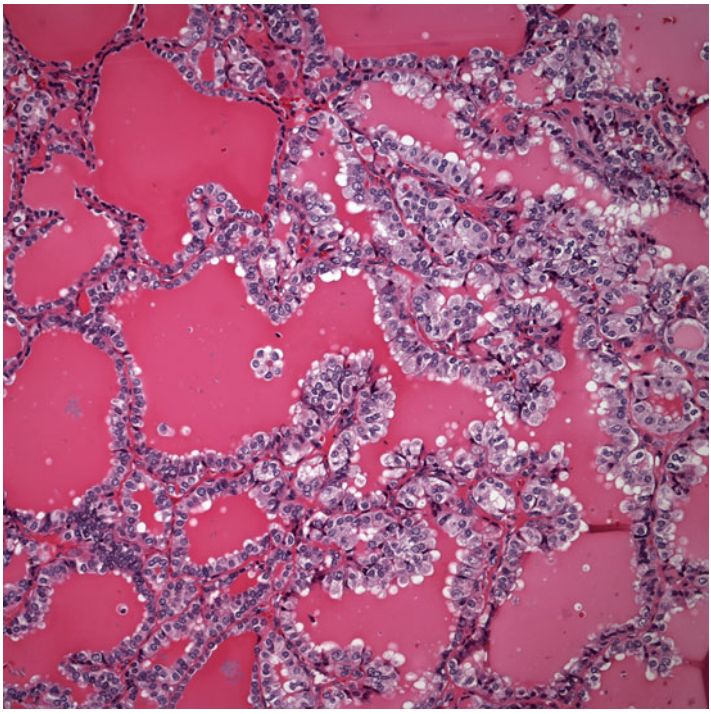

Fig. 9.2 Predominantly follicular growth pattern with focal poorly formed papillae (H&E stain, X200)

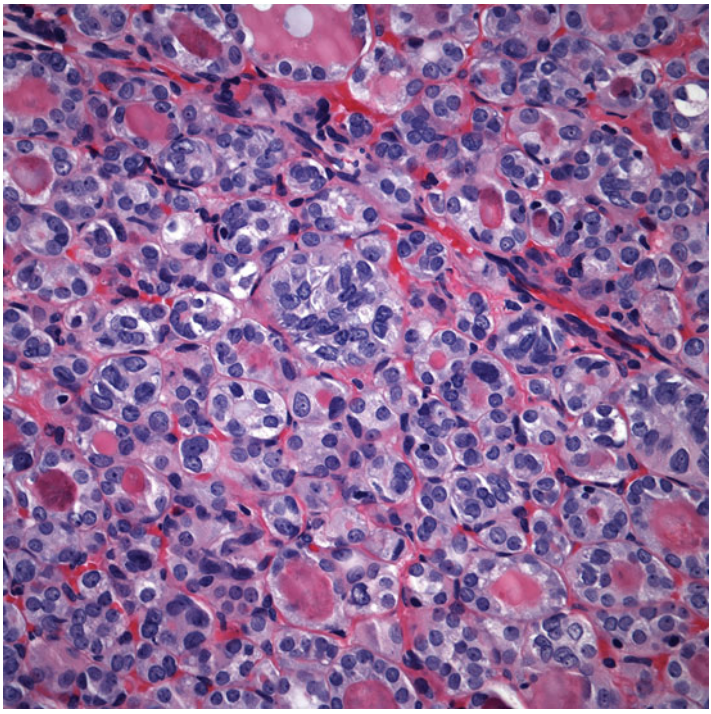

Fig. 9.3 The follicular variant of papillary thyroid carcinoma on histologic section shows follicles lined by nuclei otherwise classic for papillary carcinoma (H&E stain, X200)

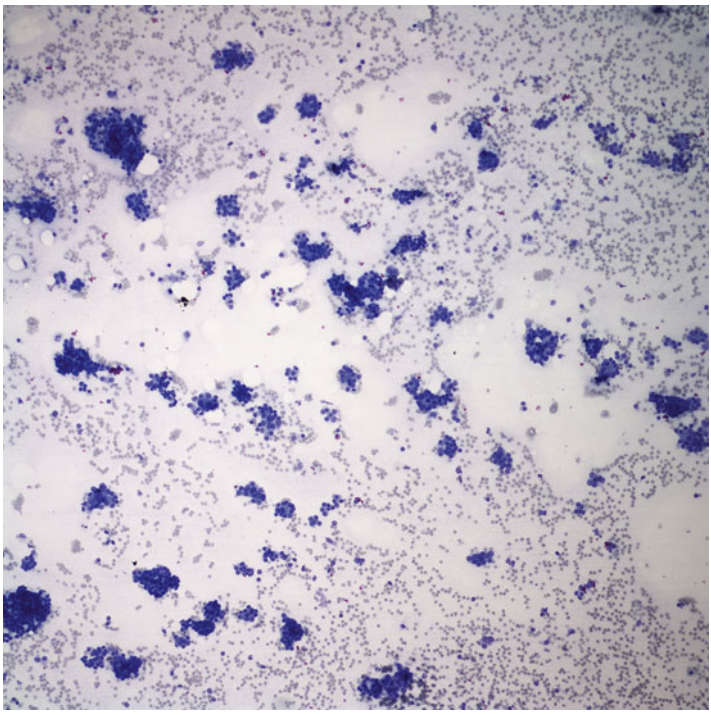

Fig. 9.4 Follicular variant of papillary thyroid carcinoma. There is hypercellularity and the follicular pattern is striking (Diff-Quik stain, X100)

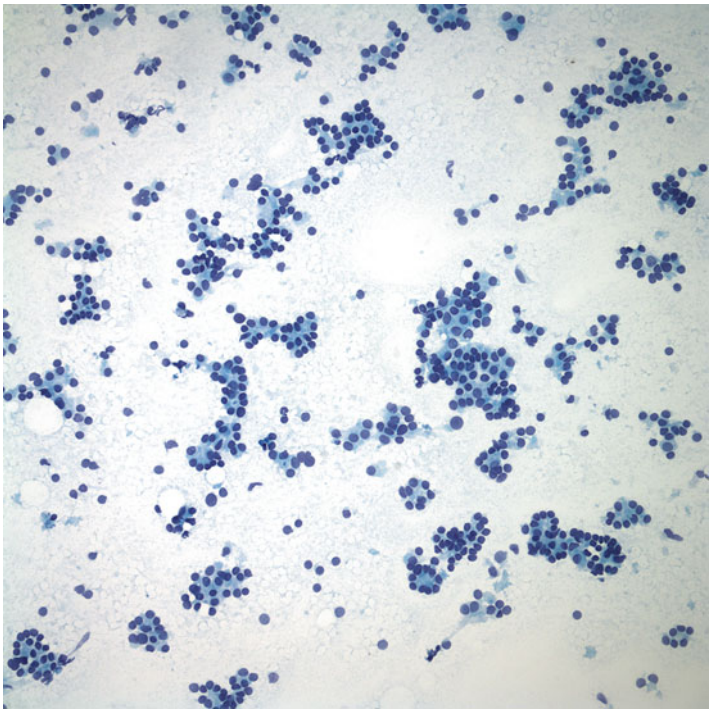

Fig. 9.5 Hypercellularity and striking follicular pattern (Papanicolaou stain, X100)

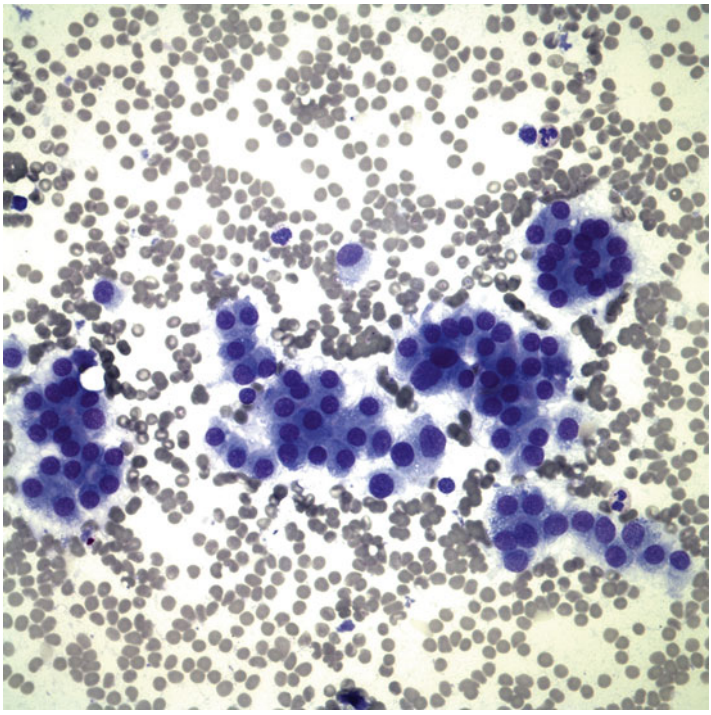

Fig. 9.6 Microfollicles in thyroid FNA smear of follicular variant of papillary carcinoma (Diff-Quik stain, X400)

may be scanty in the presence of desmoplastic stroma. The follicular cells are small to moderately enlarged, arranged in loosely cohesive groups and in syncytial tissue fragments, with and without a follicular pattern (Figs. 9.6, 9.7, 9.8, 9.9, and 9.10). When the predominant architecture is the presence of syncytial tissue fragments, especially in a background of colloid, the lesion can be misdiagnosed as nodular goiter. The cells are usually enlarged, with round to ovoid nuclei, pale powdery chromatin, micronucleoli, grooves, and intranuclear inclusion [15] (Figs. 9.11, 9.12, 9.13, 9.14, 9.15, 9.16, 9.17, and 9.18). It's been determined that these tumors exhibit at least four of six characteristic nuclear features, which should be sufficient for the diagnosis, but these features are less pronounced and typically observed only focally. This is particularly true for chromatin clearing and nuclear grooves, which are significantly less prevalent [16]. Cytoplasm is scant or barely visible and the cell borders are poorly defined. Cells with abundant, finely granular cytoplasm, reminiscent of Hürthle cells, occur in some cases, and these Hürthle cells may provide a clue to the diagnosis of FVPTC [17, 18]. The colloid within the follicle is usually thick and has a bubblegum appearance and may present as balls or blobs and may show peripheral scalloping, which provides a clue to the diagnosis [19, 20]. Background colloid ranges from scant to abundant and the amount correlates with follicle size [21, 22]. When colloid is abundant, the lesion can be mistaken for a

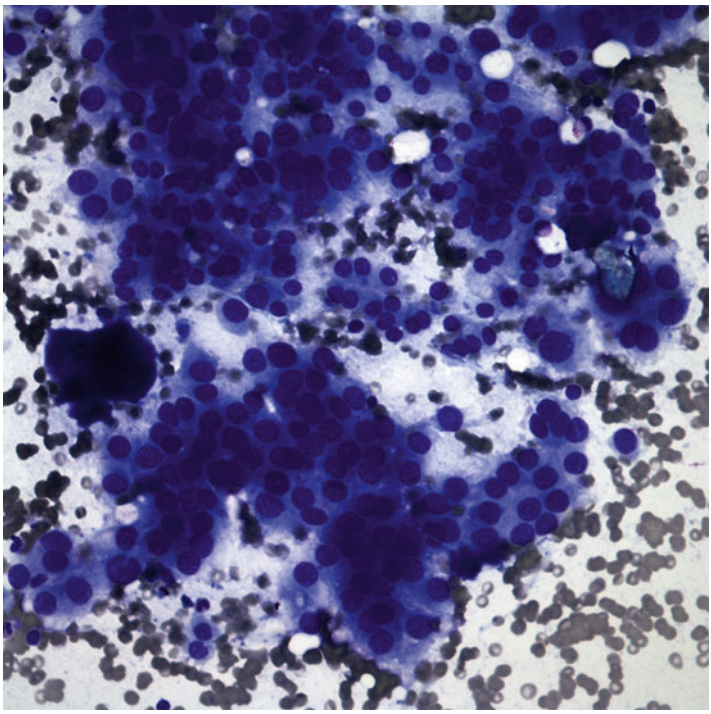

Fig. 9.7 Monolayered sheets of follicular cells and dense colloid globules (Diff-Quik stain, X400)

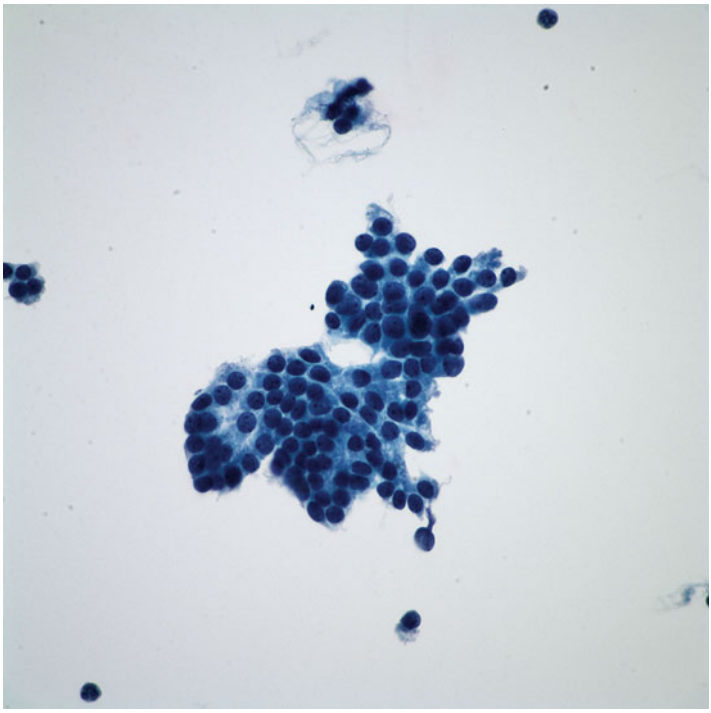

Fig. 9.8 Syncytial tissue fragments with vague follicular pattern. The nuclei have fine, powdery chromatin and micronucleoli (Papanicolaou stain, X600)

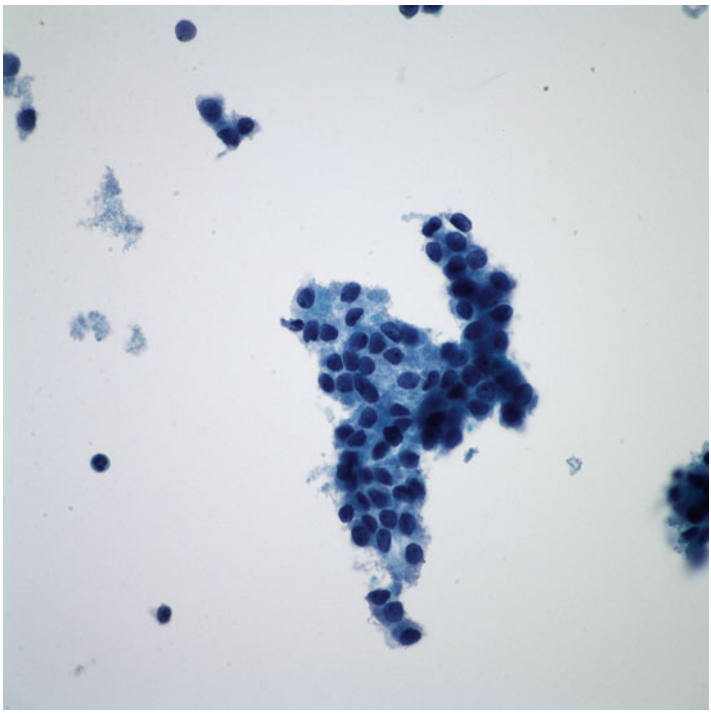

Fig. 9.9 Monolayered sheets of follicular cells. Nuclear grooves are readily appreciated (Papanicolaou stain, X600)

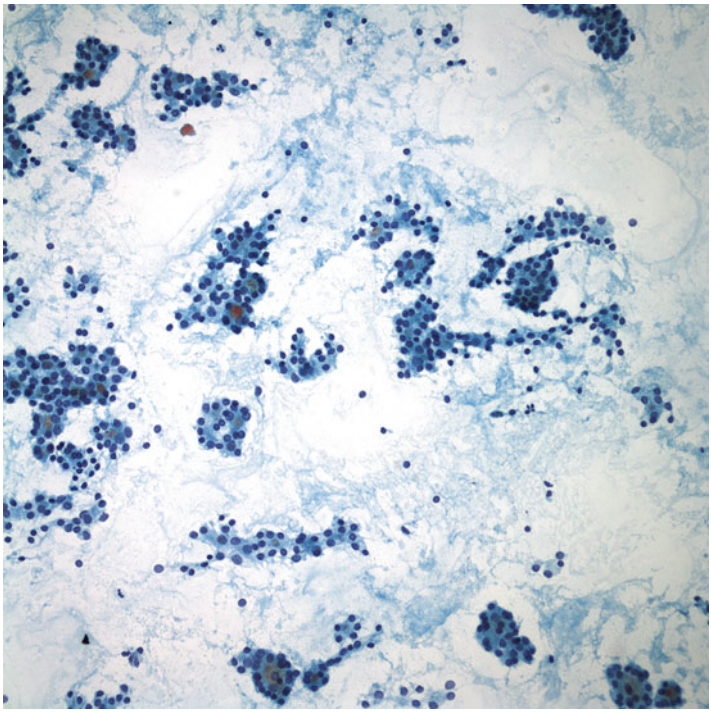

Fig. 9.10 Architectural arrangement of cells in the follicular variant of papillary carcinoma includes microfollicles, macrofollicles, and monolayered epithelial sheets (Papanicolaou stain, X200)

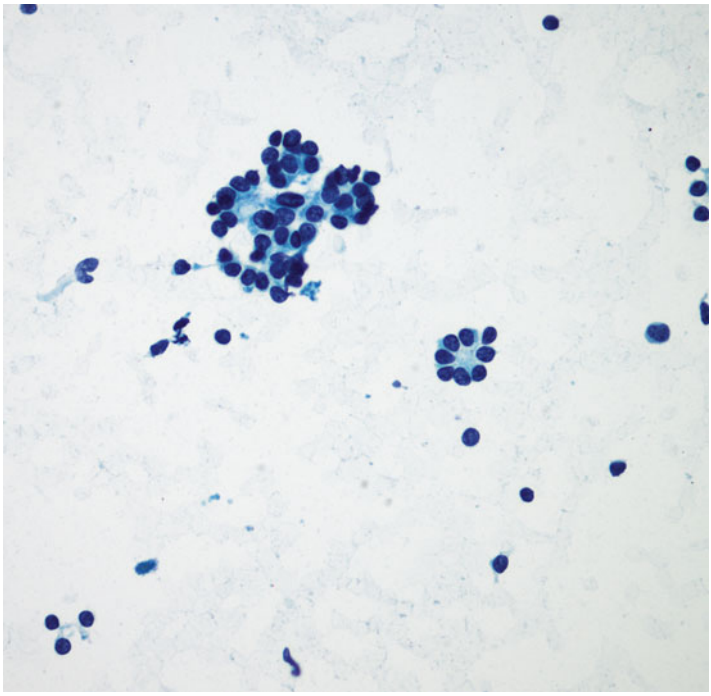

Fig. 9.11 Discrete follicles lined by follicular cells that are enlarged, show nuclear clearing and grooves (Papanicolaou stain, X400)

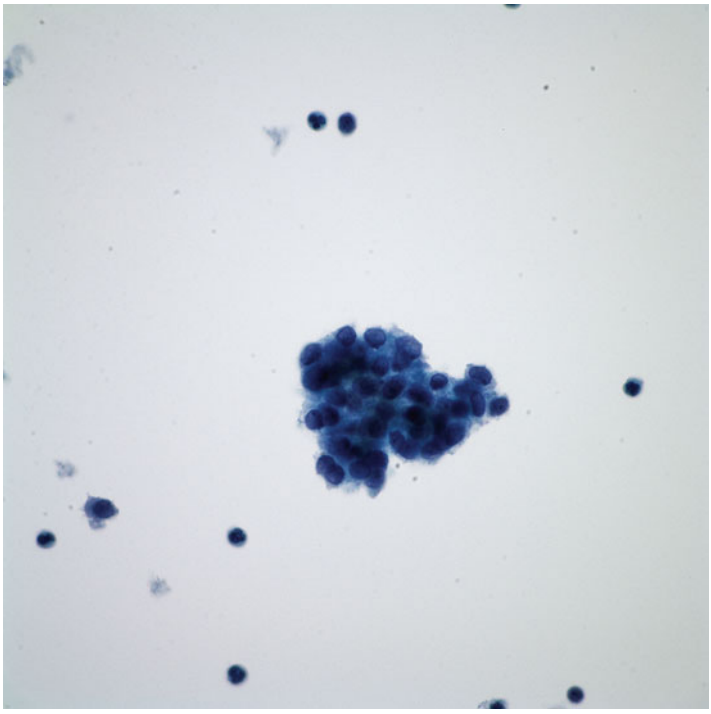

Fig. 9.12 Monotonous population of follicular cells arranged in cohesive follicular groups with nuclear overlapping and crowding (Papanicolaou stain, X600)

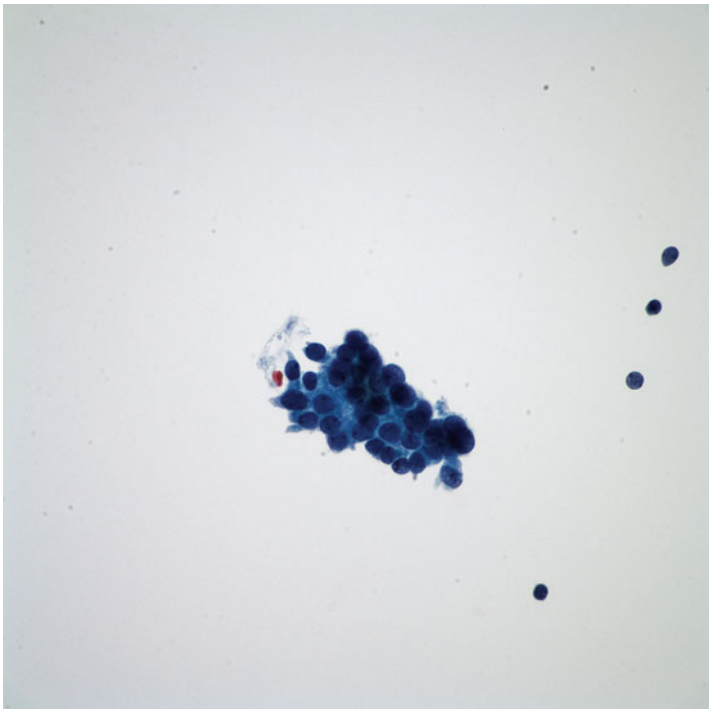

Fig. 9.13 Enlarged follicular cells in a loosely cohesive group (Papanicolaou stain, X600)

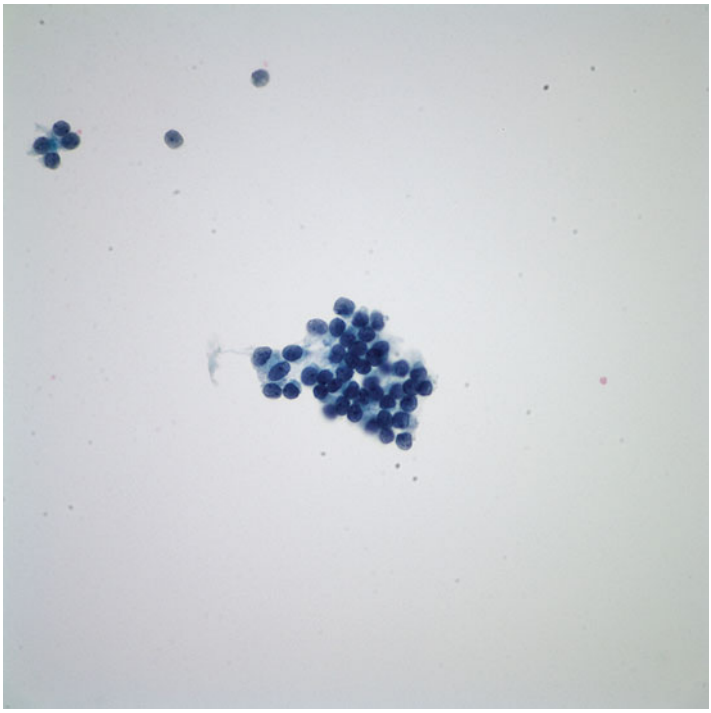

Fig. 9.14 Tumor cells show fine chromatin, irregular nuclear contour, and nuclear grooves (Papanicolaou stain, X600)

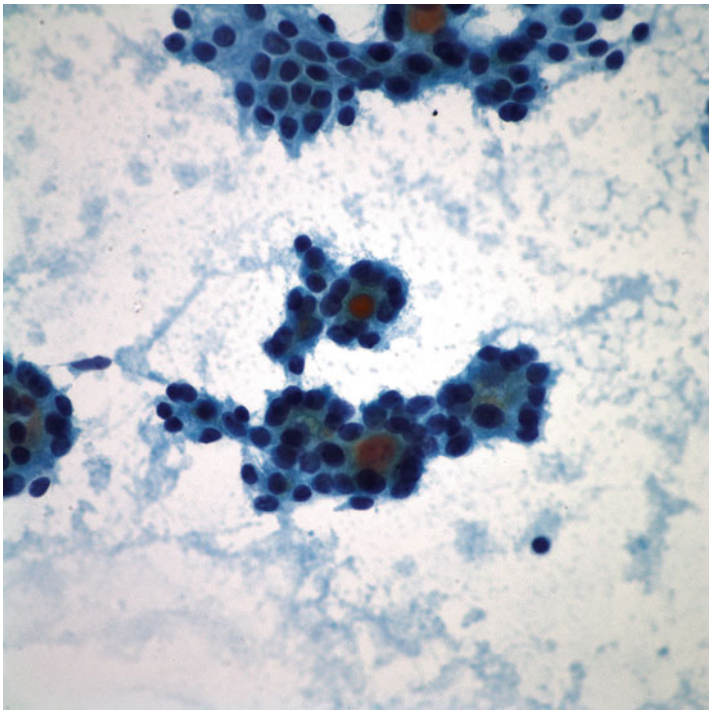

Fig. 9.15 Follicular variant of papillary carcinoma showing microfollicles and enlarged nuclei with pale chromatin and thick colloid. The nuclear changes seen here are very focal (Papanicolaou stain, X600)

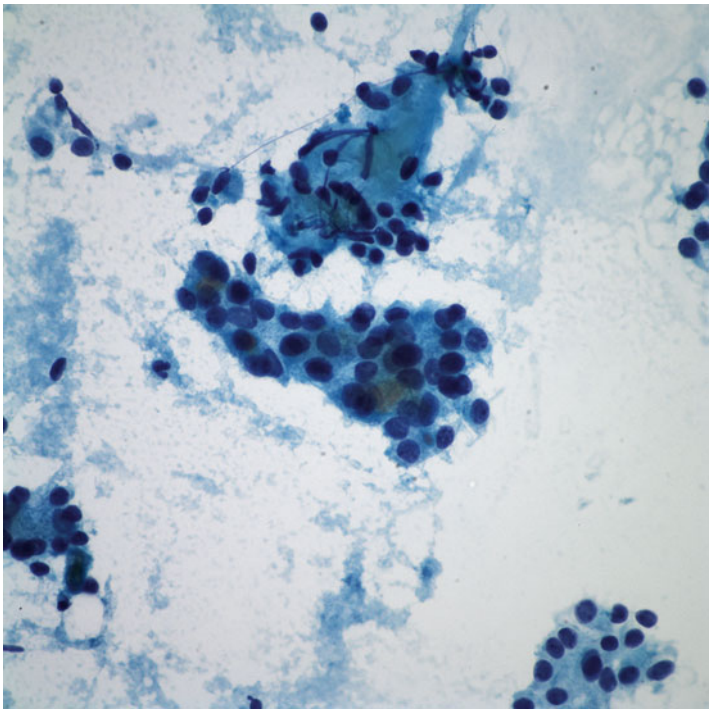

Fig. 9.16 Nuclei of cells in follicular variant of papillary carcinoma showing powdery chromatin (Papanicolaou stain, X600)

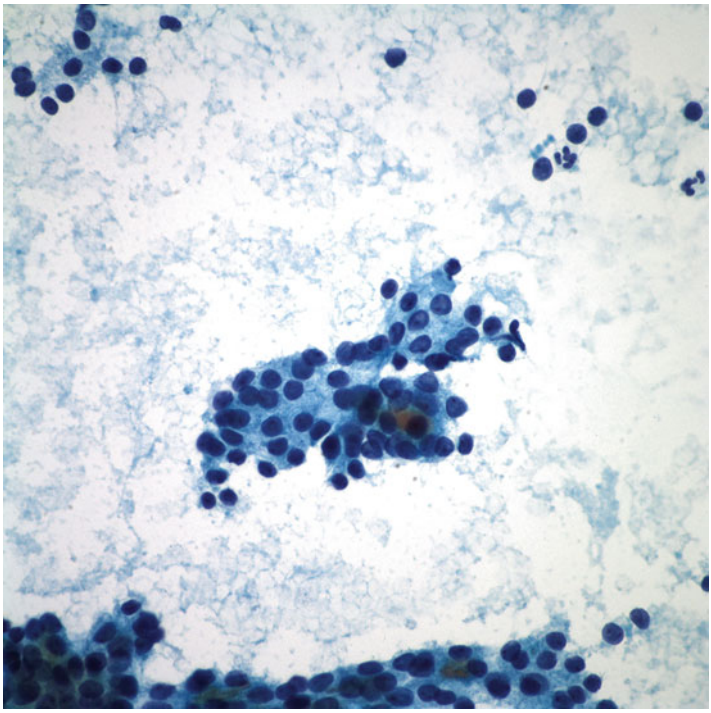

Fig. 9.17 Oval nuclei with nuclear grooves seen in follicular variant of papillary carcinoma (Papanicolaou stain, X600)

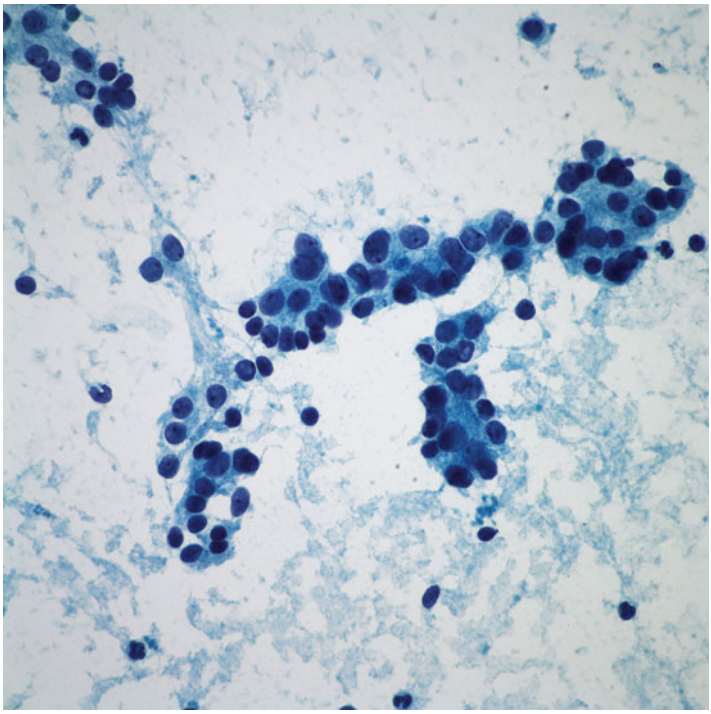

Fig. 9.18 Powdery chromatin, nuclear grooves, and nuclear enlargement are characteristic findings in follicular variant of papillary carcinoma (Papanicolaou stain, X600)

benign colloid nodule. The presence of metachromatic hyaline globules, which are formed from basement membrane-like material, can give the tumor an adenoid cystic pattern [23, 24]. Interfollicular stromal psammoma bodies and multinucleated foreign body-type giant cells are helpful when present, but they are usually scant or absent altogether [15].

The most common diagnostic dilemmas in FVPTC are mistaking it for either goiter or follicular neoplasm. This is due to the fact that there is an overlapping diagnostic criteria for follicular lesions in general and also the paucity of diagnostic features of PTC in this variant, either because they are poorly developed or present only focally. Cases that are highly cellular with microfollicles and scant colloid mimic follicular neoplasm, while those with abundant colloid and few cells mimic goiters. The key to diagnosis is the presence of nuclear features of PTC. These nuclear features are absent in follicular neoplasms, where nuclei tend to be round, with coarser, darker chromatin [25]. Sampling variation can occur in FNA biopsy as the characteristic nuclear features of PTC tend to be more prominent in the subcapsular region of the tumor [26]. Because of the tendency to overdiagnose FVPTC on histology, strict criteria have been proposed for the histologic diagnosis [27]: (1) Nuclei are ovoid rather than round. (2) Nuclei are crowded, often manifesting as lack of polarization in the cells that line a follicle. (3) Nuclei show a clear or pale chromatin pattern, or they exhibit prominent grooving. (4) Psammoma bodies are present. If one or more of these four features are lacking, four or more of the following secondary features have to be present for a diagnosis of FVPTC to be made: (1) the presence of abortive papillae, (2) predominantly elongated or irregularly shaped follicles, (3) dark-staining colloid, (4) the presence of rare nuclear pseudoinclusions, and (5) multinucleated histiocytes in the lumina of follicles.

Some immunohistochemical markers have been reported to be more commonly expressed in PTC than in benign thyroid lesions. These include high molecular weight cytokeratin, cytokeratin 19 (CK19), vimentin, HBME1, galectin-3, CD57, CD15, and CD44. However, these markers are not sufficiently discriminatory to aid in the diagnosis of problematic cases [28]. CK19 is usually positive in PTC (including FVPTC) and is usually negative or focally positive in goiter and other benign lesions; however inflamed tissue may stain intensely [29, 30]. HBME1 marks PTC (Fig. 9.19) but can also be positive in some nodular goiters and follicular adenomas. Galectin-3 is usually positive in PTC (Fig. 9.20) but also marks many benign lesions [31].

Follicular variant of papillary carcinoma has a high prevalence of RAS mutations and a low prevalence of *BRAF* mutations and RET/PTC rearrangements. This genotype is closer to the follicular thyroid tumors rather than to classic PTCs, suggesting that this variant of PTC may occupy, at least biologically, an intermediate position between thyroid follicular neoplasms and classic PTCs. This possibility is further supported by demonstrations that both the global pattern of chromosomal aberrations and gene expression profile of FVPTC have substantial differences from the classic PTC and in some instances are more similar to thyroid follicular tumors [16, 32, 33]. Tumors with *RAS* mutations also demonstrate the lowest prevalence of lymph node metastases and extrathyroidal extension. Their stage at presentation is intermediate between more advanced in BRAF-positive tumors and mostly early stages of tumors harboring *RET/PTC* [16].

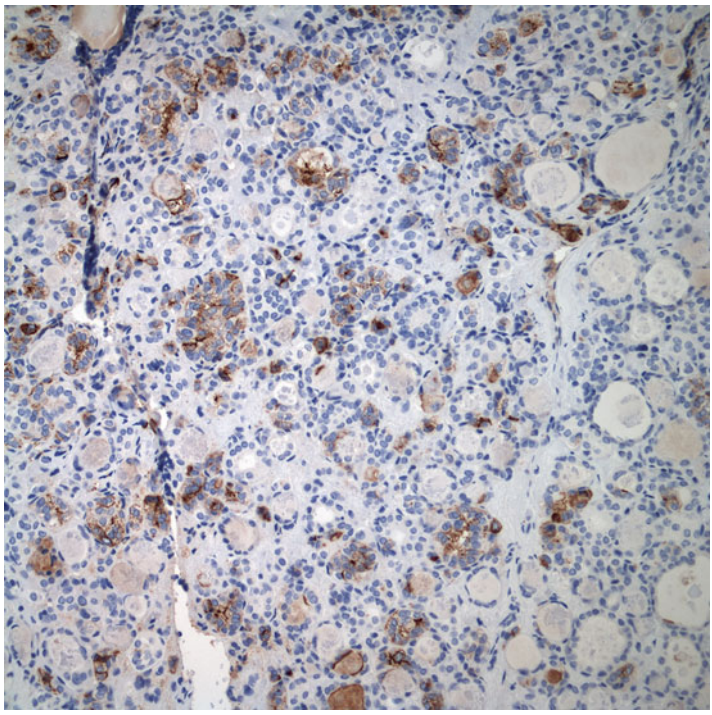

Fig. 9.19 The neoplastic cells are immunoreactive with HBME1

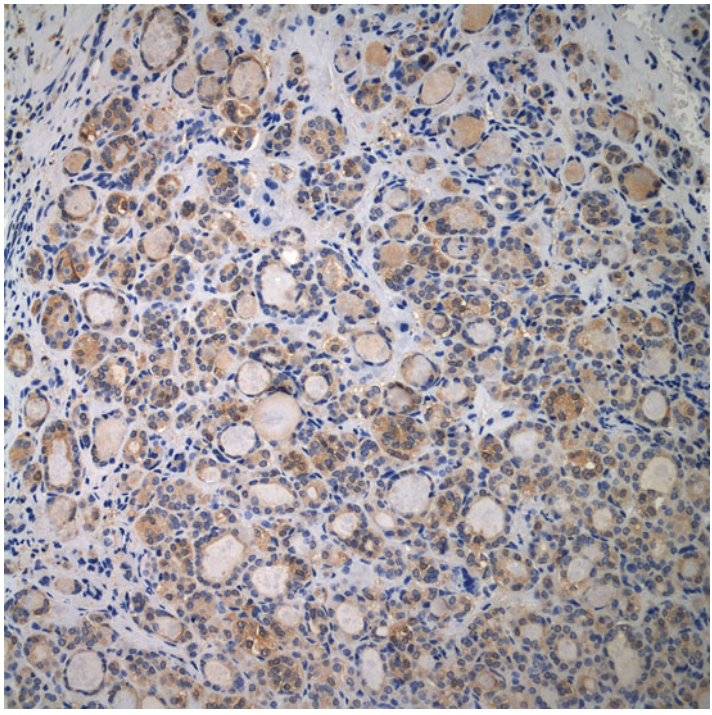

Fig. 9.20 The neoplastic cells are immunoreactive with galectin-3

Fine needle aspiration biopsy is very sensitive for the diagnosis of the conventional PTC. On the contrary, reported sensitivity of FNA in FVPTC is significantly low [34–37]. Most of the studies have reported sensitivities ranging from 9 to 37 % [2, 9, 34–37]. Given this low sensitivity, FVPTC poses a significant diagnostic challenge. The diagnostic dilemma in the preoperative detection of FVPTC is not only in enhancing the specificity of preoperative diagnosis but also to simultaneously increase the sensitivity of detection so that patients with malignancy are discovered soon enough to allow effective therapy.

In a recent study, the definitive preoperative diagnosis was 27 % with a diagnostic accuracy of 38 % [38]. The diagnostic accuracy rate included both diagnostic categories of positive for PTC and suspicious for PTC. Diagnostic accuracy as used in the study was to point out the exact nature of the nodule that required immediate attention. Many studies have shown that precise recognition of FVPTC is low due to the rarity of the nuclear features, which are necessary to making a definitive diagnosis. Separate studies have concluded that majority of the cytology specimens from patients with FVPTC were interpreted as suspicious for malignant lesion or follicular neoplasm [18, 39].

Up to 23 % of FVPTC are usually diagnosed as follicular neoplasm on thyroid FNA, which should trigger immediate surgical intervention (lobectomy) according to the thyroid cancer guidelines [38, 40]. For follicular neoplasms, most investigators believe that intraoperative evaluation does not provide accurate definitive diagnosis, and a thyroid lobectomy is the standard initial surgical intervention [2]. One way to ensure that FVPTC cases which have been diagnosed as follicular neoplasm on FNA get proper attention is to further subclassify the follicular neoplasm category into three subcategories: (1) microfollicular patterned neoplasm, (2) follicular lesion with some features suggestive of but not diagnostic of FVPTC, and (3) Hürthle cell neoplasm. The second subcategory of follicular neoplasm consists of cases that exhibit enough atypical nuclear features which are beyond the AUS/FLUS diagnostic category but not enough to place them in the suspicious for PTC category. In our experience there are a number of cases in which some nuclear features of PTC (most commonly nuclear clearing and rare grooves) are present. The frequency of these nuclear features varies from case to case but generally not enough nuclear changes to place them in the suspicious for PTC category. Our experience has been that the subcategory of follicular lesion with some features suggestive of but not diagnostic for FVPTC allows the pathologist to characterize follicular lesion one step further and gives more information to the clinician as to the level of concern that the lesions in this subcategory elicit. It is to ensure that patients with lesions in this subcategory of follicular neoplasm are ultimately referred for surgical consultation.

References

1. Lam AK, Lo CY, Lam KS. Papillary carcinoma of thyroid: a 30-yr clinicopathological review of the histological variants. Endocrine Pathol. 2005;16:323–30.
2. Kesmodel SB, Terhune KP, Canter RJ, et al. The diagnostic dilemma of follicular variant of papillary thyroid carcinoma. Surgery. 2003;134:1005–12.

3. Shih SR, Shun CT, Su DH, et al. Follicular variant of papillary thyroid carcinoma: diagnostic limitations of fine needle aspiration cytology. Acta Cytol. 2005;49:383–6.
4. Tielens ET, Sherman SI, Hruban RH, Ladenson PW. Follicular variant of papillary thyroid carcinoma. A clinicopathologic study. Cancer. 1994;73:424–31.
5. El Hag IA, Kollur SM. Benign follicular thyroid lesions versus follicular variant of papillary carcinoma: differentiation by architectural pattern. Cytopathology. 2004;15:200–5.
6. Zacks JF, de las Morenas A, Beazley RM, O'Brien MJ. Fine-needle aspiration cytology diagnosis of colloid nodule versus follicular variant of papillary carcinoma of the thyroid. Diagn Cytopathol. 1998;18:87–90.
7. Wu HH, Jones JN, Grzybicki DM, Elsheikh TM. Sensitive cytologic criteria for the identification of follicular variant of papillary thyroid carcinoma in fine-needle aspiration biopsy. Diagn Cytopathol. 2003;29:262–6.
8. Williams MD, Suliburk JW, Staerkel GA, et al. Clinical significance of distinguishing between follicular lesion and follicular neoplasm in thyroid fine-needle aspiration biopsy. Ann Surg Oncol. 2009;16:3146–53.
9. Jogai S, Adesina AO, Temmim L, et al. Follicular variant of papillary thyroid carcinoma—a cytological study. Cytopathology. 2004;15:212–6.
10. Dobrinja C, Trevisan G, Liguori G, et al. Sensitivity evaluation of fine-needle aspiration cytology in thyroid lesions. Diagn Cytopathol. 2009;37:230–5.
11. DeMay RM. Follicular lesions of the thyroid. W(h)ither follicular carcinoma? Am J Clin Pathol. 2000;114:681–3.
12. Elsheikh TM, Asa SL, Chan JK, DeLellis RA, Heffess CS, LiVolsi VA, Wenig BM. Interobserver and intraobserver variation among experts in the diagnosis of thyroid follicular lesions with borderline nuclear features of papillary carcinoma. Am J Clin Pathol. 2008;130:736–44.
13. Ghossein R. Problems and controversies in the histopathology of thyroid carcinomas of follicular cell origin. Arch Pathol Lab Med. 2009;133:683–91.
14. Lloyd RV, Erickson LA, Casey MB, Lam KY, Lohse CM, Asa SL, Chan JK, DeLellis RA, Harach HR, Kakudo K, LiVolsi VA, Rosai J, Sebo TJ, Sobrinho-Simoes M, Wenig BM, Lae ME. Observer variation in the diagnosis of follicular variant of papillary thyroid carcinoma. Am J Surg Pathol. 2004;28:1336–40.
15. Kini SR. Thyroid cytopathology: an Atlas and text. Philadelphia: Wolters Kluwer/ Lippincott Williams & Wilkins; 2008.
16. Adeniran AJ, Zhu Z, Gandhi M, et al. Correlation between genetic alterations and microscopic features, clinical manifestations, and prognostic characteristics of thyroid papillary carcinomas. Am J Surg Pathol. 2006;30:216–22.
17. Baloch ZW, Gupta PK, Yu GH, Sack MJ, LiVolsi VA. Follicular variant of papillary carcinoma. Cytologic and histologic correlation. Am J Clin Pathol. 1999;111:216–22.
18. Logani S, Gupta PK, LiVolsi VA, et al. Thyroid nodules with FNA cytology suspicious for follicular variant of papillary thyroid carcinoma: follow-up and management. Diagn Cytopathol. 2000;23:380–5.
19. Fulciniti F, Benincasa G, Vetrani A, Palombini L. Follicular variant of papillary carcinoma: cytologic findings on FNAB samples-experience with 16 cases. Diagn Cytopathol. 2001;25:86–93.
20. Nair M, Kapila K, Karak AK, Verma K. Papillary carcinoma of the thyroid and its variants: a cytohistological correlation. Diagn Cytopathol. 2001;24:167–73.
21. Baloch ZW, Sack MJ, Yu GH, Livolsi VA, Gupta PK. Fine-needle aspiration of thyroid: an institutional experience. Thyroid. 1998;8:565–9.
22. Oertel YC, Oertel JE. Diagnosis of malignant epithelial thyroid lesions: fine needle aspiration and histopathologic correlation. Ann Diagn Pathol. 1998;2:377–400.
23. Mandal S, Jain S. Adenoid cystic pattern in follicular variant of papillary thyroid carcinoma: a report of four cases. Cytopathology. 2010;21:93–6.
24. Haji BE, Ahmed MS, Prasad A, Omar MS, Das DK. Papillary thyroid carcinoma with an adenoid cystic pattern: report of a case with fine-needle aspiration cytology and immunocytochemistry. Diagn Cytopathol. 2004;30:418–21.

25. DeMay RM. The art and science of cytopathology: superficial aspiration cytology. Chicago: ASCP Press; 2012.
26. Baloch ZW, Shafique K, Flannagan M, Livolsi VA. Encapsulated classic and follicular variants of papillary thyroid carcinoma: comparative clinicopathologic study. Endocr Pract. 2010;16:952–9.
27. Chan J. Strict criteria should be applied in the diagnosis of encapsulated follicular variant of papillary thyroid carcinoma. Am J Clin Pathol. 2002;117:16–8.
28. Chan JKC. Tumors of the thyroid and parathyroid glands. In: Fletcher CDM, editor. Diagnostic histopathology of tumors. 2nd ed. Edinburgh, Scotland: Churchill Livingstone; 2000. p. 959–1056.
29. Cheung CC, Ezzat S, Freeman JL, Rosen IB, Asa SL. Immunohistochemical diagnosis of papillary thyroid carcinoma. Mod Pathol. 2001;14:338–42.
30. Nasser SM, Pitman MB, Pilch BZ, Faquin WC. Fine-needle aspiration biopsy of papillary thyroid carcinoma: diagnostic utility of cytokeratin 19 immunostaining. Cancer. 2000;90:307–11.
31. Mehrotra P, Okpokam A, Bouhaidar R, Johnson SJ, Wilson JA, Davies BR, Lennard TW. Galectin-3 does not reliably distinguish benign from malignant thyroid neoplasms. Histopathology. 2004;45:493–500.
32. Chevillard S, Ugolin N, Vielh P, et al. Gene expression profiling of differentiated thyroid neoplasms: diagnostic and clinical implications. Clin Cancer Res. 2004;10:6586–97.
33. Wreesmann VB, Ghossein RA, Hezel M, et al. Follicular variant of papillary thyroid carcinoma: genome-wide appraisal of a controversial entity. Genes Chromosomes Cancer. 2004;40:355–64.
34. Lin HS, Komisar A, Opher E, Blaugrund SM. Follicular variant of papillary carcinoma: the diagnostic limitations of preoperative fine-needle aspiration and intraoperative frozen section evaluation. Laryngoscope. 2000;110:1431–6.
35. Caraway NP, Sneige N, Samaan NA. Diagnostic pitfalls in thyroid fine-needle aspiration: a review of 394 cases. Diagn Cytopathol. 1993;9:345–50.
36. Powari M, Dey P, Saikia UN. Fine needle aspiration cytology of follicular variant of papillary carcinoma of thyroid. Cytopathology. 2003;14:212–5.
37. Yang J, Schnadig V, Logrono R, Wasserman PG. Fine-needle aspiration of thyroid nodules: a study of 4703 patients with histologic and clinical correlations. Cancer. 2007;111:306–15.
38. Ustun B, Chhieng D, Prasad ML, Holt E, Hammers L, Carling T, Udelsman R, Adeniran AJ. Follicular variant of papillary thyroid carcinoma: accuracy of FNA diagnosis and implications for patient management. Endocr Pathol. 2014;25:257–64.
39. Jain M, Khan A, Patwardhan N, et al. Follicular variant of papillary thyroid carcinoma: a comparative study of histopathologic features and cytology results in 141 patients. Endocr Pract. 2001;7:79–84.
40. Cooper DS, Doherty GM, Haugen BR, et al. Management guidelines for patients with thyroid nodules and differentiated thyroid cancer. Thyroid. 2006;16:109–42.

Variants of Papillary Thyroid Carcinoma 10

Case Study

A 33-year-old woman was found to have bilateral thyroid nodules by CT scan during the workup after a motor vehicle accident. Otherwise, she was asymptomatic and had no complaints of hoarseness, difficulty in breathing, and swallowing. She was euthyroid. She had no history of radiation to the head and neck and no family history of thyroid cancer. Physical examination was negative. Ultrasound examination revealed multiple thyroid nodules in both lobes. The two right nodules measured 2 and 1.3 cm, respectively. The left nodule measured 1 cm in greatest dimension.

Fine needle aspiration biopsy was performed on all three nodules. The aspirate from the left nodule consisted of cohesive groups of follicular cells with considerable crowding and overlapping (Fig. 10.1). Individual tumor cells appeared oval to columnar with variable amount of cytoplasm (Fig. 10.2). Nuclear clearing and grooves as well as nuclear inclusions were readily apparent (Figs. 10.3 and 10.4). The cytologic diagnosis was papillary thyroid carcinoma. Both nodules in the right lobes demonstrated cytologic findings of hyperplastic nodule with cystic degeneration.

The patient underwent total thyroidectomy and left central lymph node dissection. Serial sectioning revealed a single, well-circumscribed, 1 cm nodule in the left thyroid lobe with a solid, tan cut surface. Two well-circumscribed, homogenous nodules were noted in the right thyroid lobe, measuring 1.2 and 1 cm, respectively. Histology of the left thyroid nodule showed a predominantly papillary pattern (Fig. 10.5). The papillae contained fibrovascular cores and were lined by tall columnar follicular cells (Fig. 10.6). The latter demonstrated moderate amount of eosinophilic cytoplasm, and oval to elongated nuclei with nuclear grooves, irregular nuclear membranes, nuclear clearing, and intranuclear inclusions were identified. The neoplastic follicular cells demonstrated diffuse and intense nuclear staining pattern with β-catenin (Fig. 10.7), estrogen receptor, and PAX 8. They were negative for thyroglobulin. Based on the histologic and immunophenotypic findings, a

A.J. Adeniran, D. Chhieng, *Common Diagnostic Pitfalls in Thyroid Cytopathology*, DOI 10.1007/978-3-319-31602-4_10

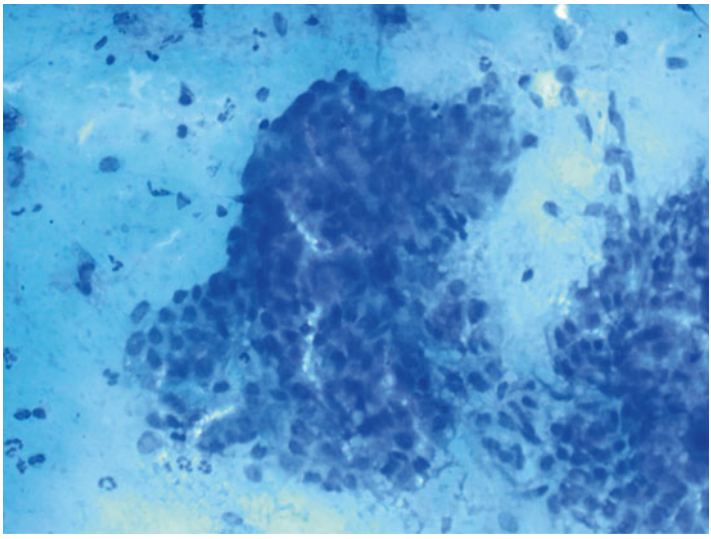

Fig. 10.1 Thyroid FNA-cribriform-morular variant of PTC. Large tissue fragment with considerable crowding and overlapping. Slit-like spaces are noted within the cluster (Diff-Quik stain, low power)

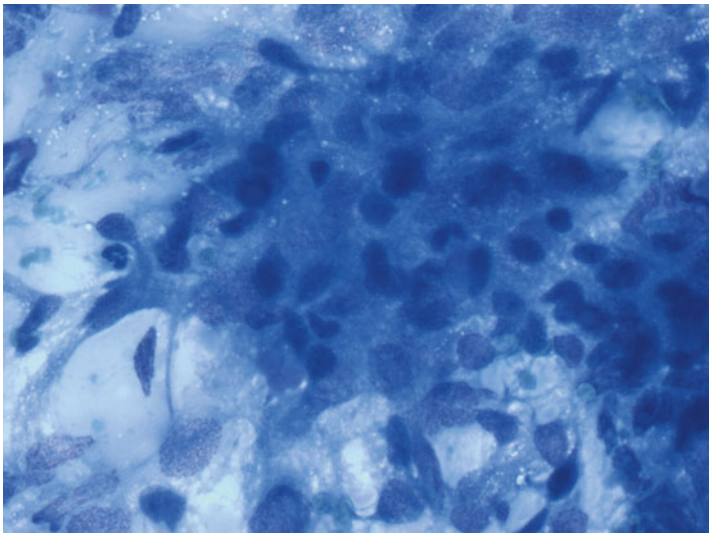

Fig. 10.2 Thyroid FNA-cribriform-morular variant of PTC. Individual tumor cells appear oval to columnar with variable amount of cytoplasm (Diff-Quik stain, high power)

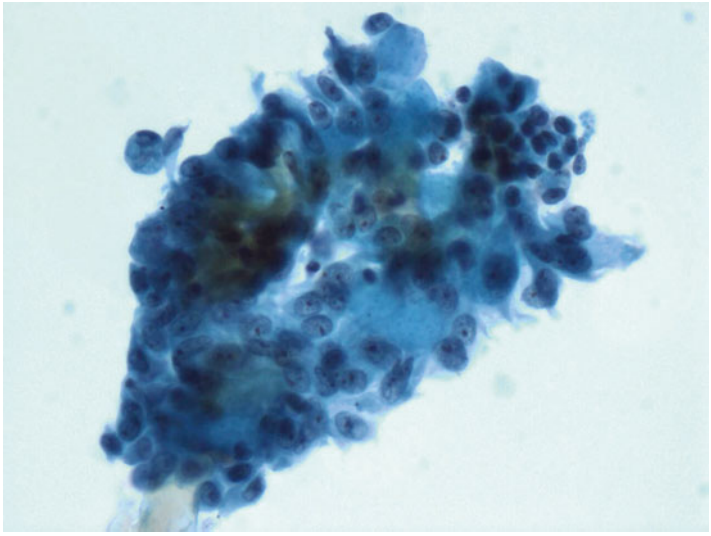

Fig. 10.3 Thyroid FNA-cribriform-morular variant of PTC. A crowded group of follicular cells with slit-like spaces. The follicular cells have powdery chromatin and small nucleoli (Papanicolaou stain, high power)

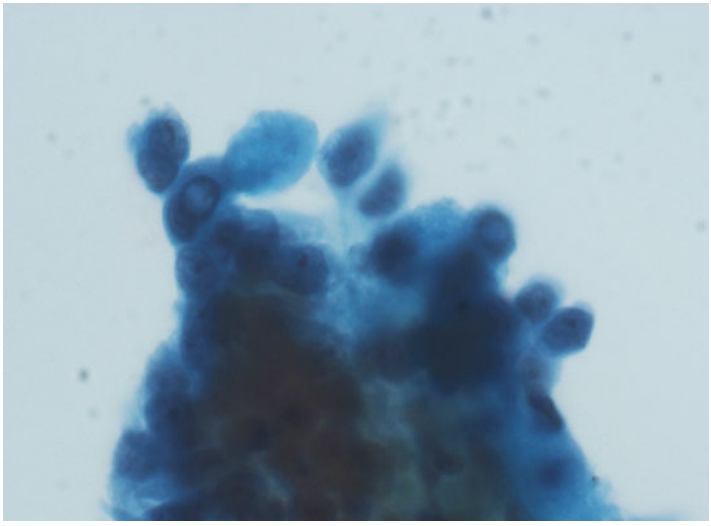

Fig. 10.4 Thyroid FNA-cribriform-morular variant of PTC. Nuclear clearing is a characteristic feature of this variant (Papanicolaou stain, high power)

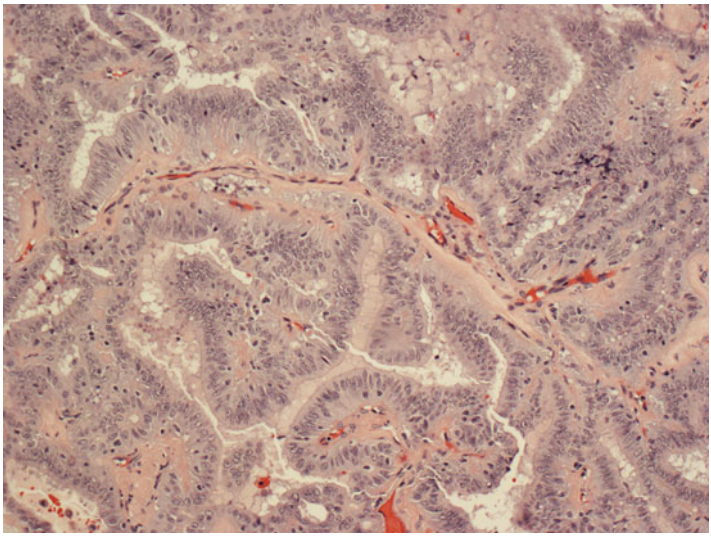

Fig. 10.5 Cribriform-morular variant of PTC. The tumor demonstrates a predominantly papillary architecture with fibrovascular cores (H&E stain, low power)

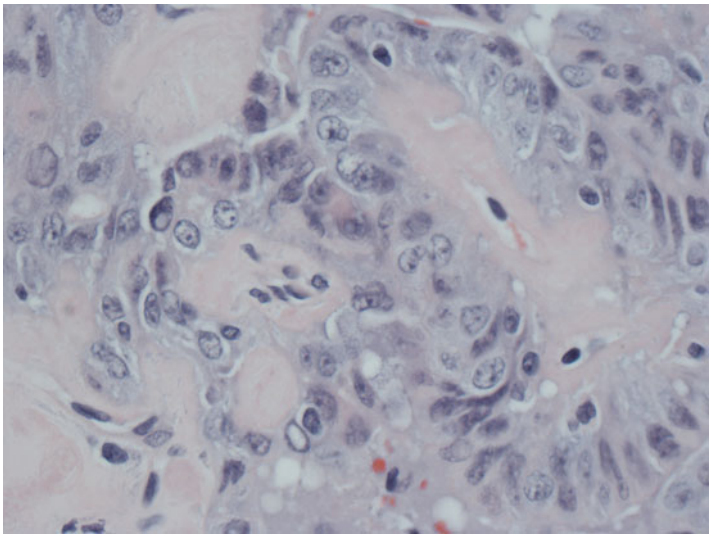

Fig. 10.6 Cribriform-morular variant of PTC. The papillae are lined by tall columnar follicular cells. The nuclei appear oval to elongated with nuclear grooves, nuclear clearing, and intranuclear inclusions (H&E stain, high power)

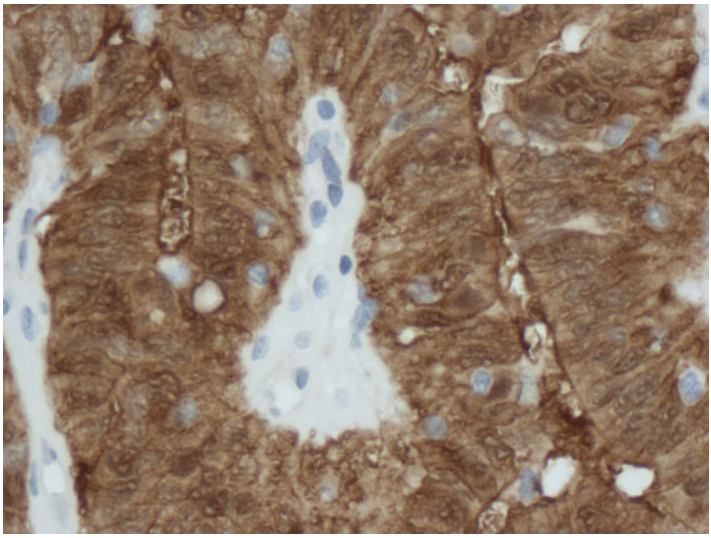

Fig. 10.7 Cribriform-morular variant of PTC. The tumor cells demonstrate intense and diffuse nuclear and cytoplasmic staining with β-catenin (H&E stain, high power)

diagnosis of papillary thyroid carcinoma, cribriform-morular variant was rendered despite the absence of morular (squamous) metaplasia. Both right thyroid nodules were found to be hyperplastic adenomatous nodules.

Discussion

A number of histologic variants of papillary thyroid carcinoma (PTC) have been recognized (Table 10.1). Variants of PTC account for approximately 15–25 % of all cases of papillary carcinoma. The classification of these variants is based on the architectural (growth) patterns, the cell types, and the stromal reaction. Some variants, such as the follicular and cystic variants, have little implications on prognosis, but may present diagnostic challenges. On the other hand, certain variants, such as tall cell and diffuse sclerosing variants, are known to behave more aggressively and carry worse prognosis than the conventional variant of PTC.

The common denominator for all the variants is the presence of nuclear features of PTC, characterized by nuclear crowding/overlapping, nuclear enlargement, powdery chromatin, nuclear clearing, nuclear grooves, and intranuclear cytoplasmic inclusions. These nuclear features allow the correct identification of PTC both histologically and cytologically. Some of the architectural patterns such as encapsulation and tumor size are readily recognized histologically; however, their cytologic identification is generally not possible. In addition, it is quite common to see multiple growth patterns and/or cell types as well as varying degrees of nuclear atypia within a given PTC. Depending on the areas sampled, the cytology may not be

Table 10.1 Histologic variants of papillary thyroid carcinoma

• Conventional
• Follicular
• Macrofollicular
• Oncocytic
• Clear cell
• Papillary thyroid carcinoma with nodular fasciitis-like stroma
• Warthin-like
• Diffuse sclerosing
• Columnar cell
• Tall cell
• Cribriform morular
• Solid
• Encapsulated
• Papillary micro-carcinoma

representative of the major morphologic pattern. More importantly, a definitive cytologic diagnosis of PTC may not be always possible if the typical nuclear changes of PTC were subtle or not readily apparent. The potential benefit of recognizing certain variants, namely, those with more aggressive clinical course, may help the clinicians to plan for more aggressive treatment, such as initial radical surgery with systematic central neck dissection. In this chapter, we would discuss selected variants of PTC that may pose diagnostic challenges and/or prognostic implications. Both follicular and cystic variants of PTC will be discussed in separate chapters.

Oncocytic Variant and Clear Cell Changes

Oncocytic variant of PTC accounts for 3.5–11 % of all PTC and behaves clinically and biologically similar to conventional PTC [1, 2] (Fig. 10.8). Aspirates from oncocytic variant of PTC are cellular and composed of predominantly polygonal cells with abundant granular eosinophilic cytoplasm [3]. The neoplastic cells can be arranged in papillary clusters, loosely cohesive tissue fragments, microfollicles, or single-cell pattern (Figs. 10.9 and 10.10). The nuclei demonstrate conventional PTC nuclear features, which distinguish it from Hurthle cell neoplasms and other oncocytic neoplasms (Fig. 10.11). However, there exist a small number of tumors in which the distinction between oncocytic variant of PTC and Hurthle cell lesions is not possible [4]. The presence of pale chromatin and nuclear grooves is well recognized in Hurthle cells in the absence of PTC [5] (Fig. 10.12). On the other hand, aspirates from oncocytic PTC with cystic changes may contain neoplastic cells that may be mistaken as repair or cyst-lining cells, resulting in a false-negative interpretation [4] (Fig. 10.13).

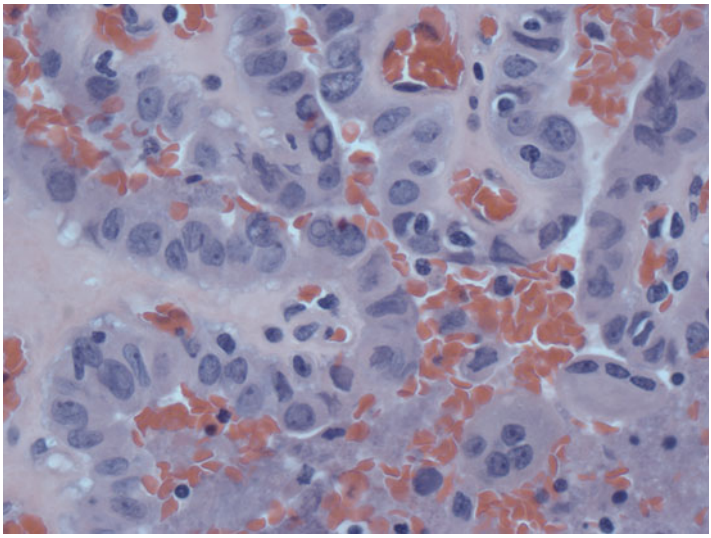

Fig. 10.8 Oncocytic variant of PTC. The tumor is composed of predominantly oncocytic cells with abundant eosinophilic, granular cytoplasm. Nuclear features such as powdery chromatin, nuclear grooves, and intranuclear inclusions are noted (H&E stain, high power)

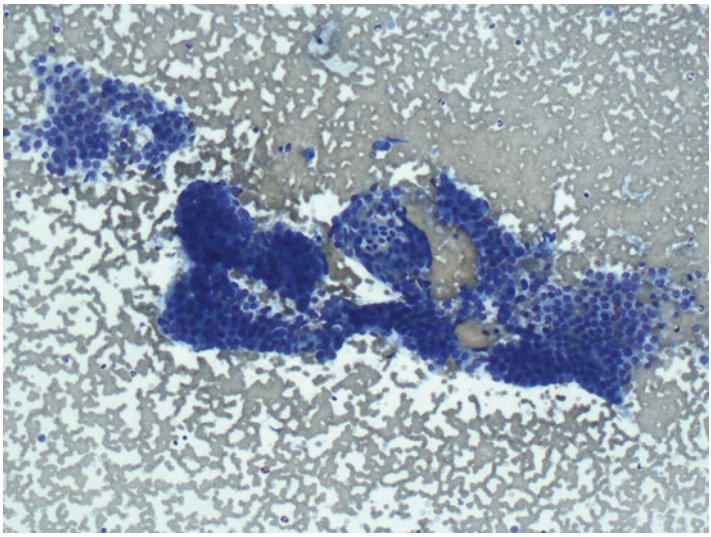

Fig. 10.9 Thyroid FNA-oncocytic variant of PTC. Large tissue fragments composed entirely Hurthle cells (Diff-Quik stain, low power)

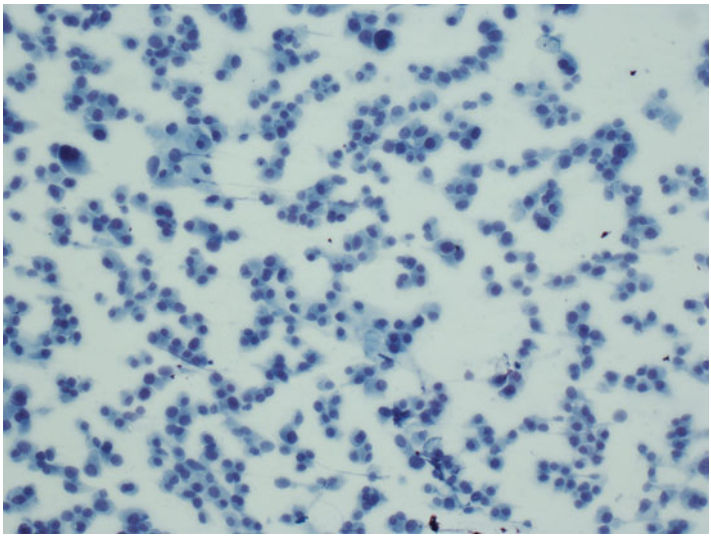

Fig. 10.10 Thyroid FNA-oncocytic variant of PTC. Predominantly loosely cohesive groups and single Hurthle cells are noted in this example (Diff-Quik stain, low power)

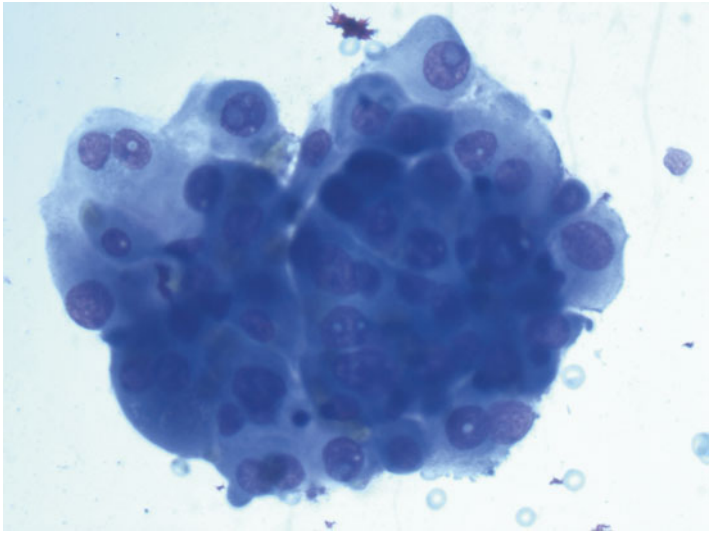

Fig. 10.11 Thyroid FNA-oncocytic variant of PTC. Individual Hurthle cells show abundant granular cytoplasm. Nuclear inclusions are frequently noted (Diff-Quik stain, high power)

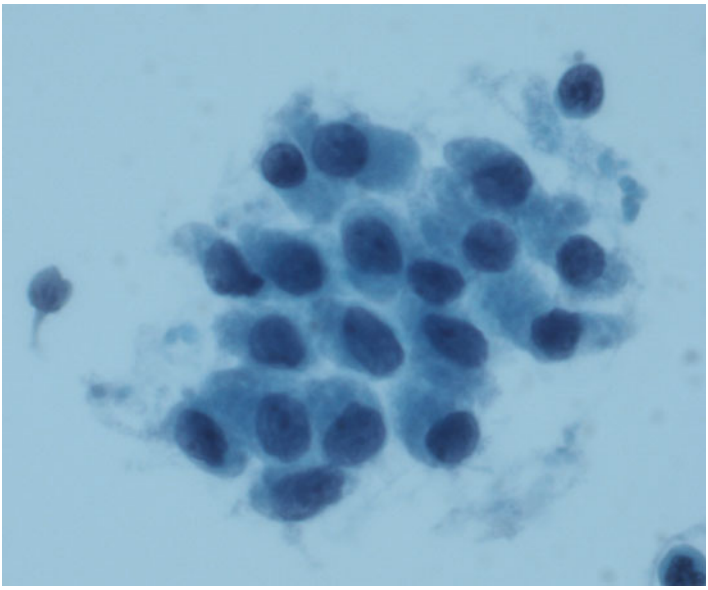

Fig. 10.12 Thyroid FNA-Hurthle cell neoplasm. The lack of nuclear features of papillary thyroid carcinoma would favor a Hurthle cell neoplasm. Subsequent follow-up reveals a hyperplastic adenomatous nodule of Hurthle cells (Diff-Quik stain, high power)

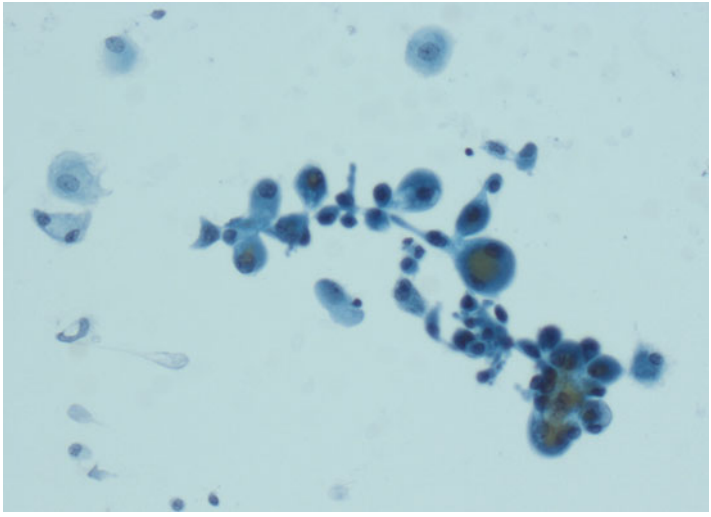

Fig. 10.13 Thyroid FNA-oncocytic variant of PTC with cystic degeneration. Neoplastic Hurthle cells can be mistaken for cyst-lining cells, especially when the nuclear features of papillary thyroid carcinoma are not readily apparent. This may result in a false-negative diagnosis (Papanicolaou stain, high power)

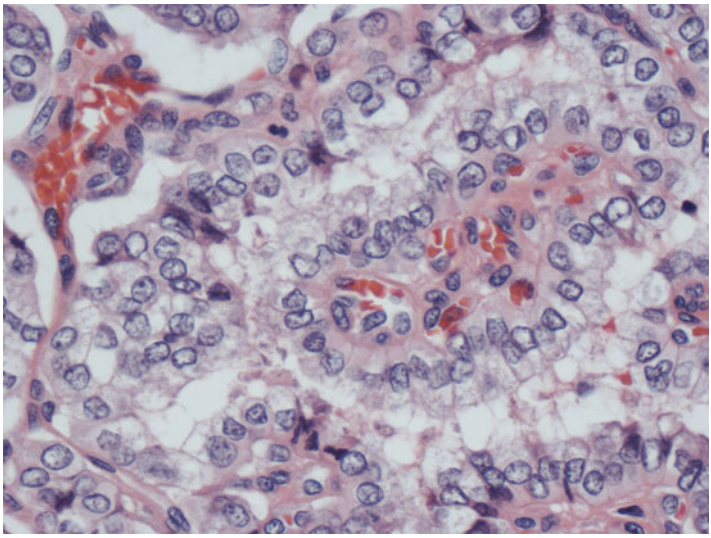

Fig. 10.14 Papillary thyroid carcinoma with clear cell changes. The neoplastic follicular cells lining the papillae show marked clear cell changes (H&E stain, high power)

Clear cell changes have been described in conventional, oncocytic, and other variants of PTC [6–8]. In some of these tumors, both oncocytic and clear cell changes are noted. The clear cytoplasm is a result of either glycogen accumulation of vesicular formation [8] (Fig. 10.14). Cytologically, neoplastic cells with clear cell changes demonstrate pale or vacuolated cytoplasm (Fig. 10.15). Not infrequently, they can appear as naked nuclei devoid of cytoplasm. The differential diagnosis would include medullary carcinoma and metastatic renal cell carcinoma (Fig. 10.16).

Warthin-Like Variant

This uncommon variant is characterized by oncocytic neoplastic cells arranged in papillary formation with a striking lymphoplasmacytic infiltration of the fibrovascular stalks and stroma, resembling a Warthin's tumor of the salivary gland [9] (Figs. 10.17 and 10.18). The tumors often arise in a background of florid lymphocytic thyroiditis. On low magnification, the aspirates demonstrate clusters of Hurthle cells in a lymphoid background, resembling that of a Hashimoto's thyroiditis [10–13] (Figs. 10.19 and 10.20). Papillary structures containing lymphocytes and plasma cells can be occasionally seen. Prominent cystic changes have been described in some of these tumors [13]. In addition to the finding of readily recognizable nuclear features of conventional PTC (Fig. 10.21), prominent nucleoli are also evident in the neoplastic Hurthle cells (Fig. 10.22).

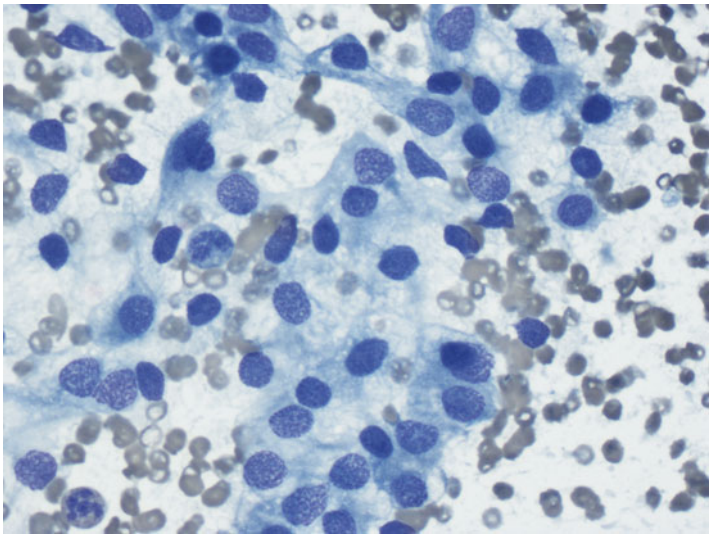

Fig. 10.15 Thyroid FNA-papillary thyroid carcinoma with clear cell changes. The follicular cells demonstrate abundant pale or vacuolated cytoplasm (Diff-Quik stain, high power)

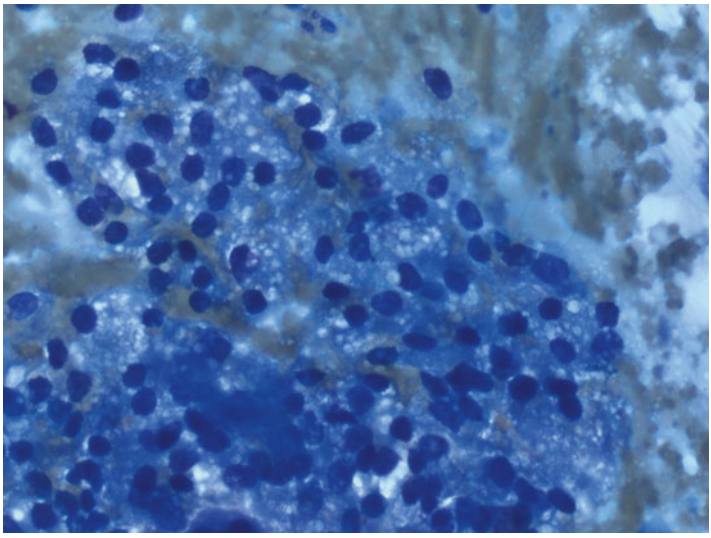

Fig. 10.16 Thyroid FNA-metastatic renal cell carcinoma. A cohesive cluster of neoplastic cells with vacuolated/clear cytoplasm. The nuclei usually demonstrate substantial pleomorphism (Diff-Quik stain, high power)

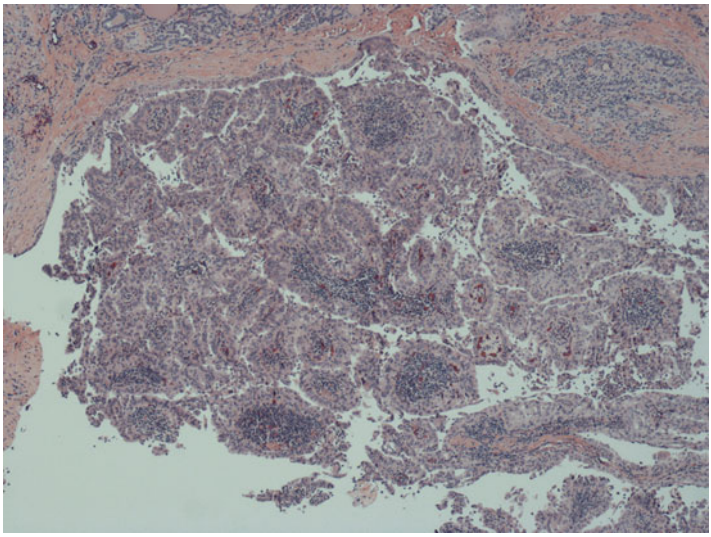

Fig. 10.17 Warthin-like variant of PTC. A cystic tumor consisting of numerous papillae with a striking lymphoid stroma (H&E stain, low power)

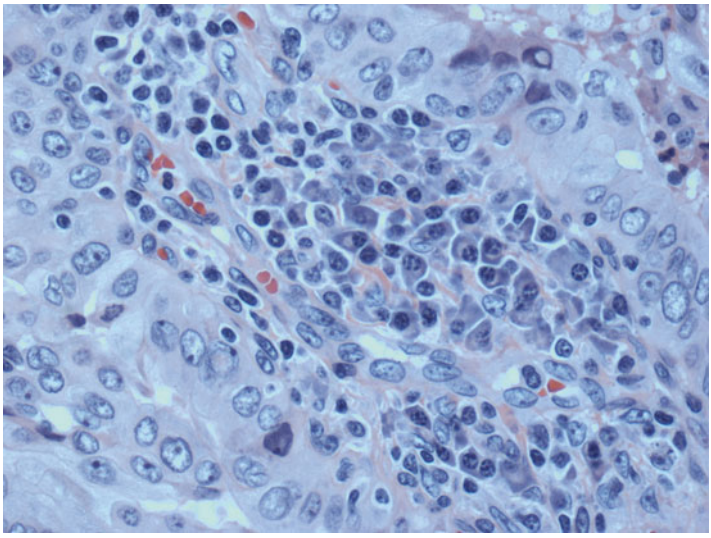

Fig. 10.18 Warthin-like variant of PTC. The tumor cells are Hurthle cells with nuclear features of PTC. The stroma consists of an intense lymphoplasmacytic infiltrate (H&E stain, high power)

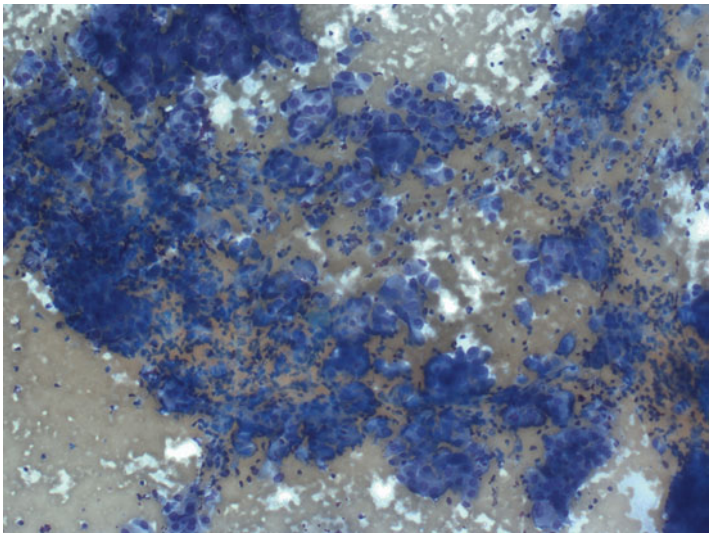

Fig. 10.19 Thyroid FNA-Warthin-like variant of PTC. The cellular aspirate demonstrates abundant Hurthle cells in a polymorphous lymphoid background (Diff-Quik stain, low power)

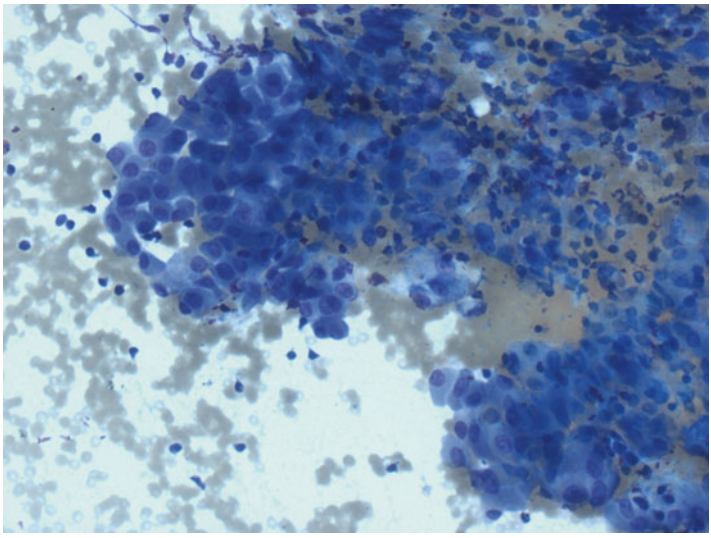

Fig. 10.20 Thyroid FNA-Warthin-like variant of PTC. Higher magnification showing clusters of Hurthle cells infiltrated by lymphocytes, resembling Hashimoto's thyroiditis (Diff-Quik stain, high power)

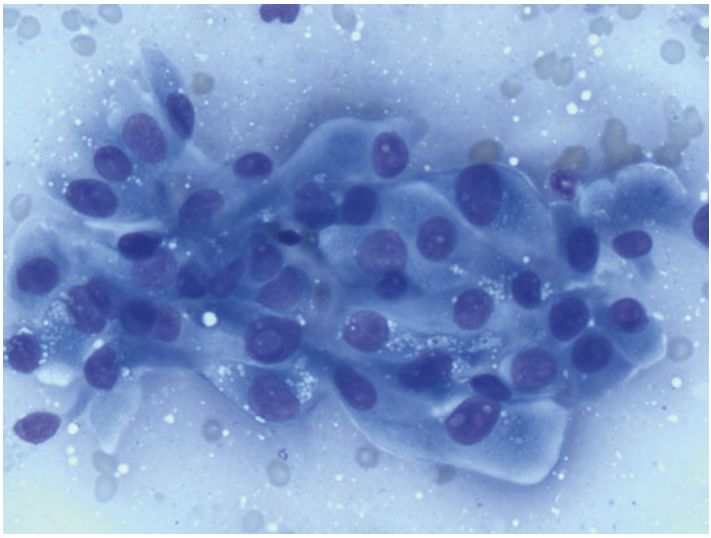

Fig. 10.21 Thyroid FNA-Warthin-like variant of PTC. Individual Hurthle cells have abundant granular cytoplasm and round to oval nuclei. An intranuclear inclusion is noted (Diff-Quik stain, high power)

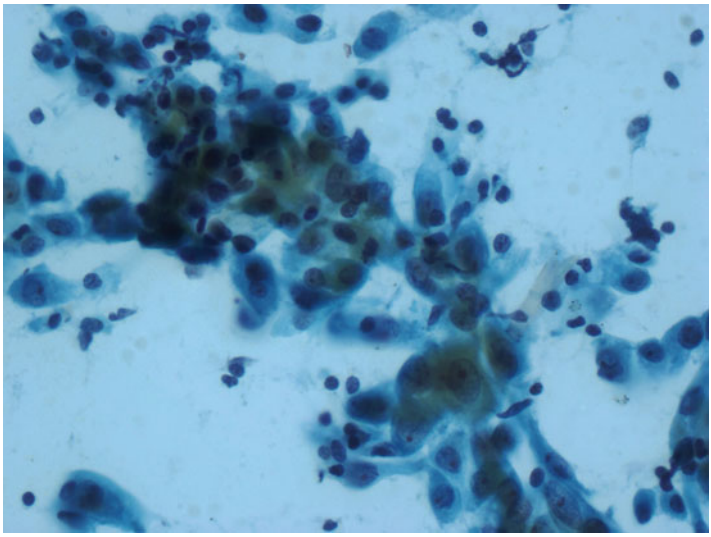

Fig. 10.22 Thyroid FNA-Warthin-like variant of PTC. Loosely cohesive group of Hurthle cells admixed with lymphocytes. The Hurthle cells show powdery chromatin, small nucleoli, and occasional intranuclear inclusion (Papanicolaou stain, high power)

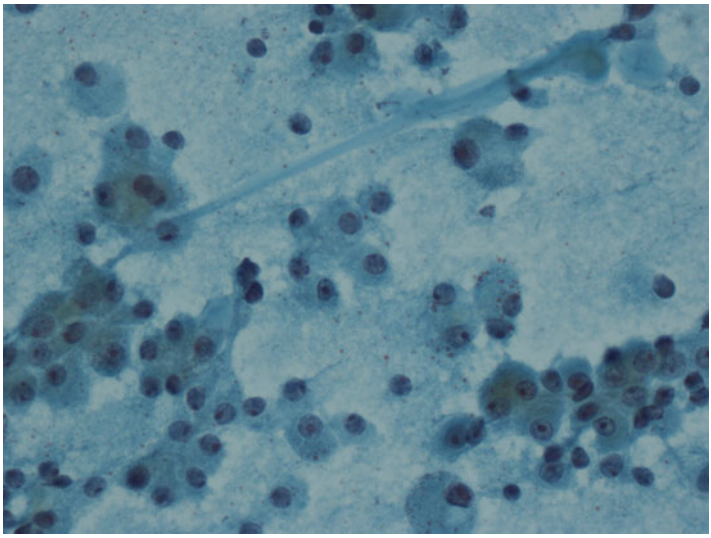

Fig. 10.23 Thyroid FNA-Hurthle cell neoplasm. The aspirate is composed of predominantly Hurthle cells without any nuclear features of PTC. No lymphocytes are noted in the background (Papanicolaou stain, high power)

The differential diagnosis includes other thyroid malignancies with different degrees of oncocytic metaplasia such as oncocytic and tall cell variants of PTC and Hurthle cell carcinoma. The latter usually lack lymphoplasmacytic infiltrate (Fig. 10.23). In addition, the presence of tall columnar cells would favor tall cell variant (Fig. 10.24). The differential diagnosis should also include conventional PTC arising in the background of lymphocytic thyroiditis. The finding of two cell populations, namely, neoplastic "non-Hurthle" follicular cells with nuclear features of PTC and a background population of Hurthle cells, would favor a conventional PTC with background Hashimoto's thyroiditis (Fig. 10.25). False-negative cases have also been reported; cases of Warthin-like variant PTC were underdiagnosed as "lymphocytic thyroiditis" on FNA [13] (Fig. 10.26). The combination of prominent cystic changes and lymphoid infiltrates can be mistaken for a benign lymphoepithelial cyst, which is lined by flattened squamous or bronchial-type epithelium and lacks a papillary growth pattern.

Papillary Thyroid Carcinoma with Nodular Fasciitis-Like Stroma

This variant of PTC is characterized by a prominent stromal proliferation with spindle cells arranged in fascicles, vascular proliferation, and a lymphohistiocytic infiltrate, resembling granulation tissue or nodular fasciitis [14]. Individual stromal spindle cells have plump nuclei with finely granular chromatin and distinct nucleoli. Because of the prominence of the stromal proliferation within the tumors, some

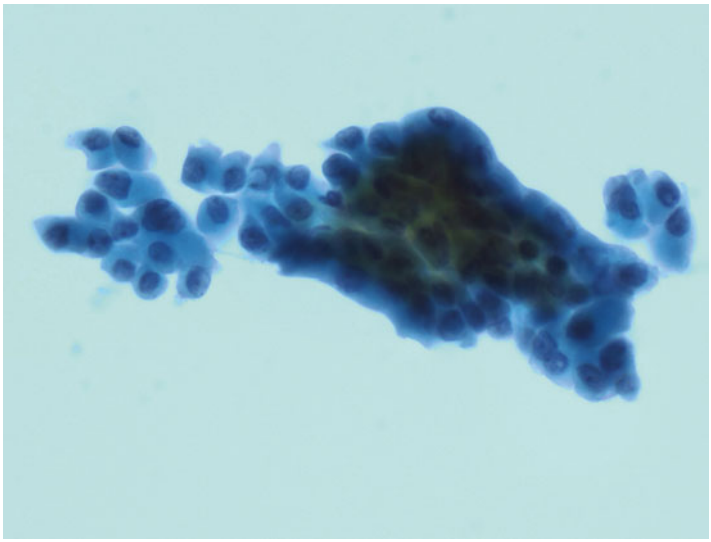

Fig. 10.24 Thyroid FNA-tall cell variant of PTC. The finding of tall columnar follicular cells and a lack of lymphoid background would favor a PTC of tall cell variant rather than Warthin-like variant (Papanicolaou stain, high power)

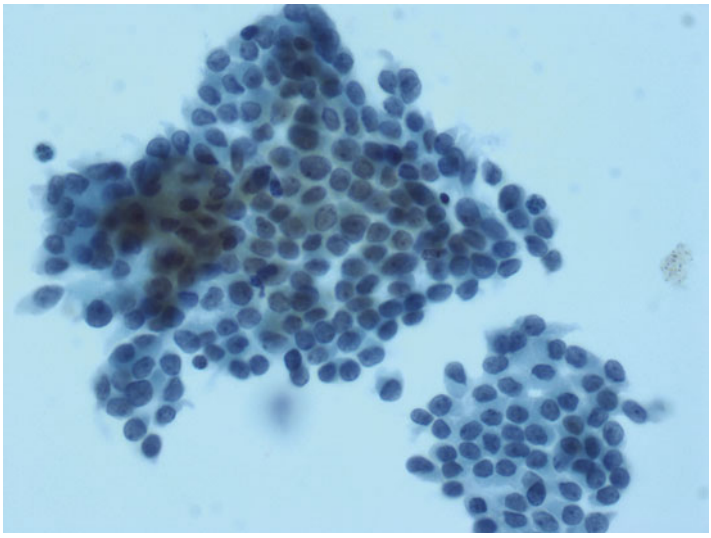

Fig. 10.25 Thyroid FNA-classic variant of PTC with or without a background of thyroiditis. Two different types of follicular cells are noted: clusters of non-oncocytic follicular cells and Hurthle cells with nuclear features of PTC (Papanicolaou stain, high power)

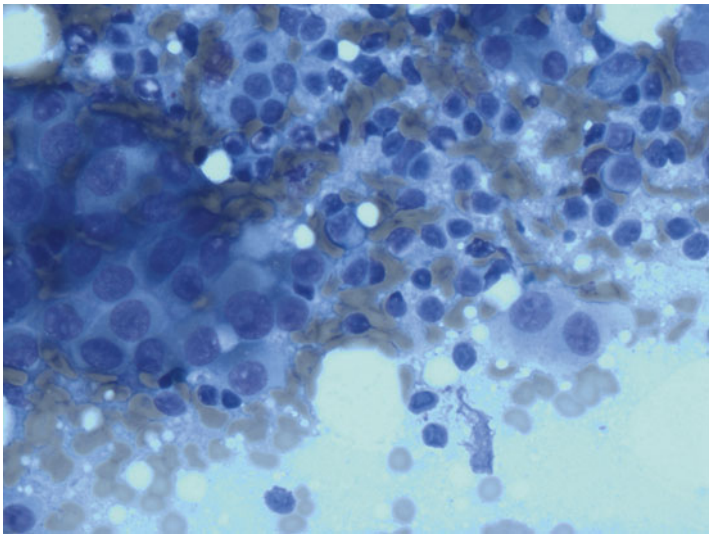

Fig. 10.26 Thyroid FNA-Warthin-like variant of PTC. Hurthle cells admixed with a polymorphous population of lymphocytes. This finding may be mistaken for a Hashimoto's thyroiditis when the nuclear features of PTC are not readily apparent (Papanicolaou stain, high power)

authors experienced difficulties in aspirating the tumor, resulting in paucicellular specimen with minimal epithelial component [15, 16]. On the other hand, some authors have misinterpreted the entity as spindle cell neoplasms, such as sarcoma, because of the prominence of the spindle cell component [17].

Macrofollicular Variant

It is a very uncommon histologic subtype of PTC and thought to have a better prognosis than conventional PTC due to its lower incidence of nodal metastases [18]. It is usually encapsulated and characterized histologically by a predominant macrofollicular growth pattern (over 50 % of the tumor) [18]. These macrofollicles, measuring more than 250 μm across, are lined by large cuboidal cells with ground-glass chromatin pattern, cuboidal cells with more stippled chromatin, and/or small hyperchromatic cells; nuclear grooves are only noted in cells with ground-glass chromatin pattern.

The cytologic presentation of macrofollicular variant can be quite heterogeneous [19–24]. For example, the cellularity can range from scant to moderate to marked. Similarly, the amount and texture of colloid is quite variable, ranging from abundant to small amount and from watery to dense with more than three-quarters of the case showing moderate to abundant thin watery colloid (Fig. 10.27). The follicular cells often arrange in monolayer sheets with minimal overlapping and crowding (Fig. 10.28). One feature that was frequently described in the literature is the absence

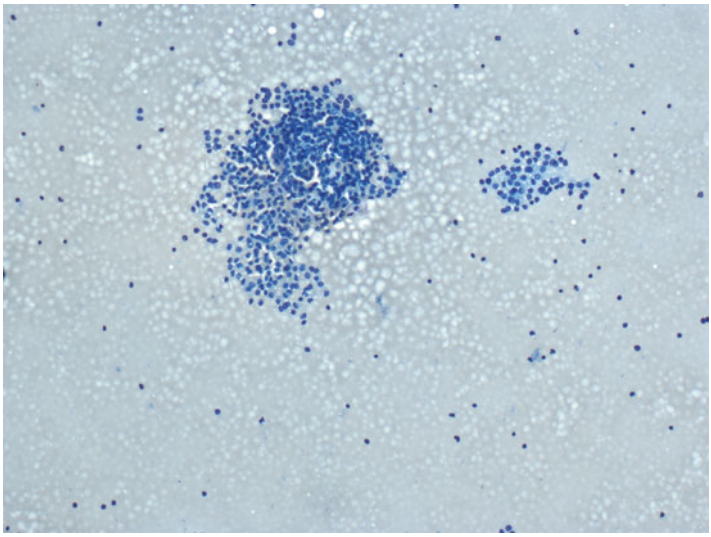

Fig. 10.27 Thyroid FNA-macrofollicular variant of PTC. The aspirate is of low cellularity with abundant watery colloid and occasional sheet of follicular cells (Diff-Quik stain, low power)

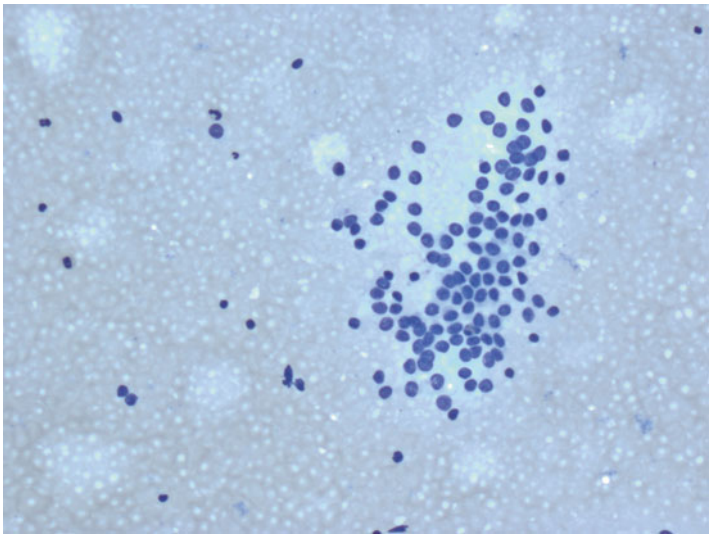

Fig. 10.28 Thyroid FNA-macrofollicular variant of PTC. The follicular cells arrange in monolayer sheets with minimal overlapping and crowding. Individual cells have round to oval nuclei. Nuclear features of PTC are not readily apparent (Diff-Quik stain, high power)

of widespread characteristic features of conventional PTC. The common nuclear findings are presence of round/oval nuclei, small indistinct to conspicuous nucleoli, chromatin clearing, mild nuclear overlapping, and infrequent nuclear grooves [24]. Moreover, less than half of the cases demonstrate intranuclear inclusions, which range from rare to few. Given the variability in the cellularity, the abundance of colloid, and the subtlety of the nuclear features, it is not surprising that a definitive diagnosis of PTC may be difficult to achieve with this variant of PTC and contribute to the occasional false-negative diagnosis on FNA. Therefore, it may be prudent to render a diagnosis of FLUS/AUS when subtle nuclear atypia is noted in a background of abundant colloid so that appropriate patient management may be done.

Diffuse Sclerosing Variant

This variant accounts for between 0.1 and 5 % of all PTCs and is more frequently seen in young women with mean age ranged from 20 to 35 years [25–27]. It is considered to have an unfavorable prognosis with higher incidence of extrathyroidal extension and cervical nodal as well as pulmonary metastases in comparison with conventional PTC [27, 28]. Histologically, this variant is characterized by diffuse involvement of one or both lobes rather than a dominant nodule, dense sclerosis with broad bands of collagenous tissue, extensive squamous metaplasia, numerous psammoma bodies, and marked lymphocytic infiltrates in addition to the typical features of PTC (Figs. 10.29, 10.30, and 10.31). Because of the diffuse and often

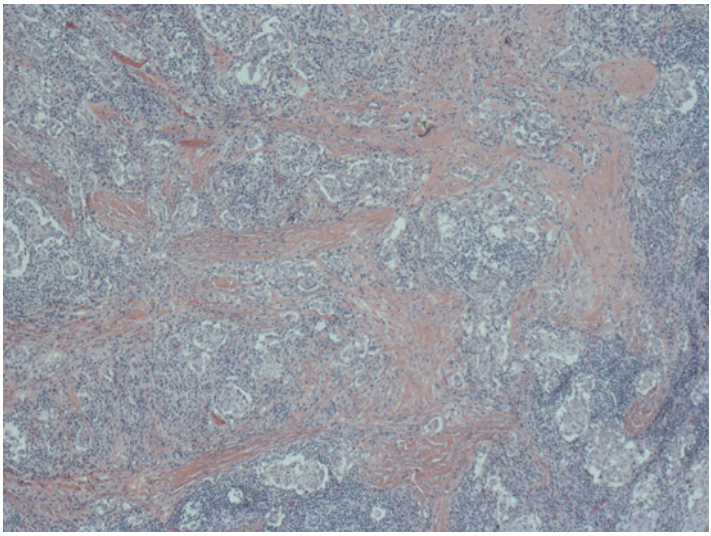

Fig. 10.29 Diffuse sclerosing variant of PTC. Low magnification showing irregular nests of tumor cells separated by broad collagenous fibrous stroma (H&E stain, low power)

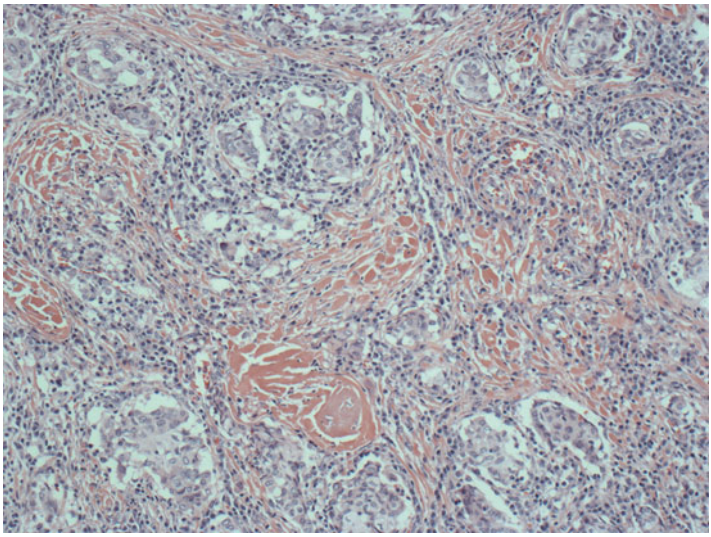

Fig. 10.30 Diffuse sclerosing variant of PTC. The follicular cells have abundant dense eosinophilic cytoplasm, resembling squamous cells. There is also a lymphocytic infiltrate within the nest of tumor cells and the collagenous stroma (H&E stain, high power)

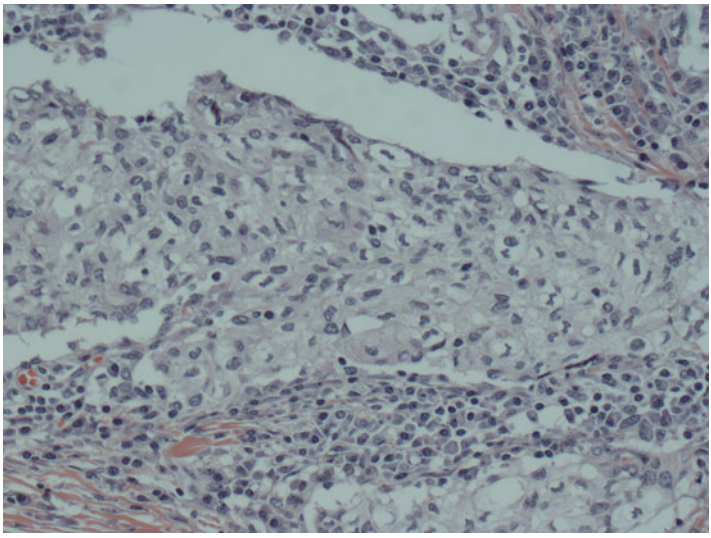

Fig. 10.31 Diffuse sclerosing variant of PTC. The nuclei of the follicular cells are oval to elongated with irregular nuclear borders, powdery chromatin, and nuclear grooves. There is an intense lymphoplasmacytic infiltrate adjacent to the follicular cells (H&E stain, high power)

bilateral involvement of the thyroid gland and the presence of marked lymphocytic infiltrates, diagnosis is often delayed because it shares similar clinical and ultrasonographic findings to lymphocytic thyroiditis [27, 29, 30].

All reported cases of diffuse sclerosing variant of PTC evaluated by FNA presented the classical nuclear features of PTC; therefore, allowing a definitive diagnosis of PTC [31–35] (Fig. 10.32). Certain histologic feature, namely, dense sclerosis with broad bands of fibrous tissue, is seldom observed in FNA from diffuse sclerosing variant of PTC (Fig. 10.33). Other histologic features, such as the presence of numerous psammoma bodies (Fig. 10.34), metaplastic squamous epithelium (Fig. 10.35), and marked lymphocytic infiltrates (Fig. 10.36), have been described in most of the reported cases. However, these findings are not entirely specific for the diffuse sclerosing variant of PTC but can be seen in conventional and other variants of PTC singly or in various combinations. Therefore, it may not be possible to recognize this variant based on cytology alone. However, the finding of quantity and the wide distribution of these features and the clinical setting of diffuse thyroid enlargement in young women would suggest the diagnosis of a diffuse sclerosing variant. Recently, Takagi et al. described the findings of three-dimensional cell balls, frequently admixed with lymphocytes, in over 90 % of the 20 aspirates of diffuse sclerosing variant [35] (Fig. 10.37). The authors asserted that a diagnosis of diffuse sclerosing variant of PTC should be suspected when these balls, which are rare findings in FNA cytology of thyroid, are noted in combination with other findings. Occasionally, the marked lymphocytic infiltrates can obscure the neoplastic follicular cells, mimicking a lymphocytic thyroiditis and resulting in a false-negative diagnosis.

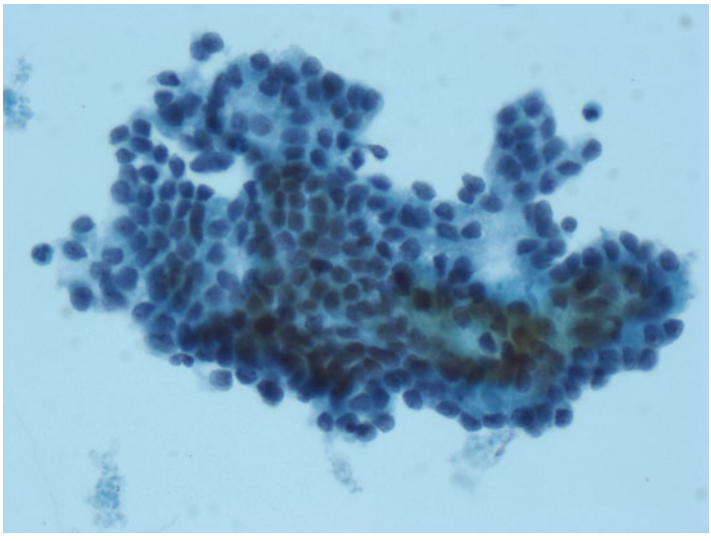

Fig. 10.32 Thyroid FNA-diffuse sclerosing variant of PTC. The group demonstrates considerable nuclear crowding and overlapping. The nuclei are enlarged with irregular nuclear borders, powdery chromatin, and nuclear grooves (Papanicolaou stain, low power)

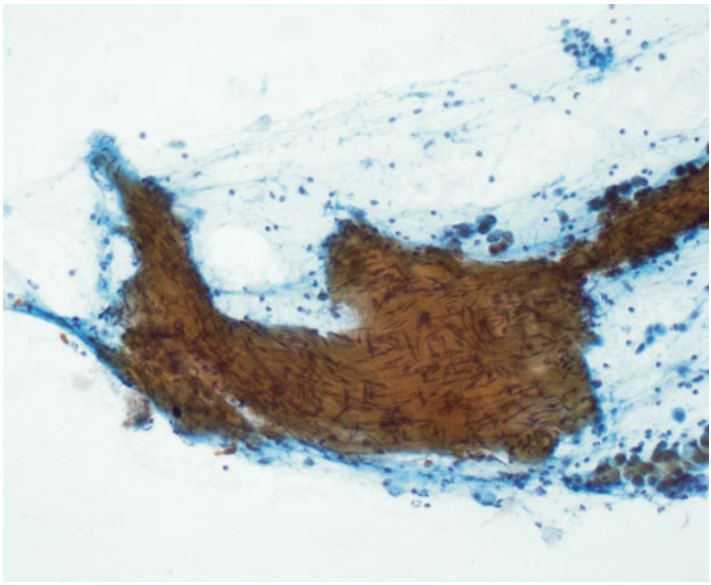

Fig. 10.33 Thyroid FNA-diffuse sclerosing variant of PTC. A dense fibrous stromal fragment is noted. However, it is not a common finding (Papanicolaou stain, low power)

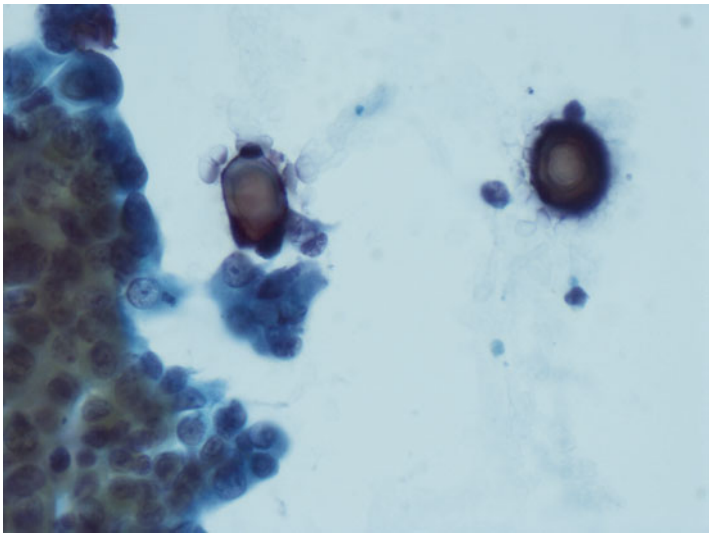

Fig. 10.34 Thyroid FNA-diffuse sclerosing variant of PTC. Calcified debris with concentric lamina, i.e., psammoma bodies, are identified adjacent to crowded clusters of follicular cells (Papanicolaou stain, high power)

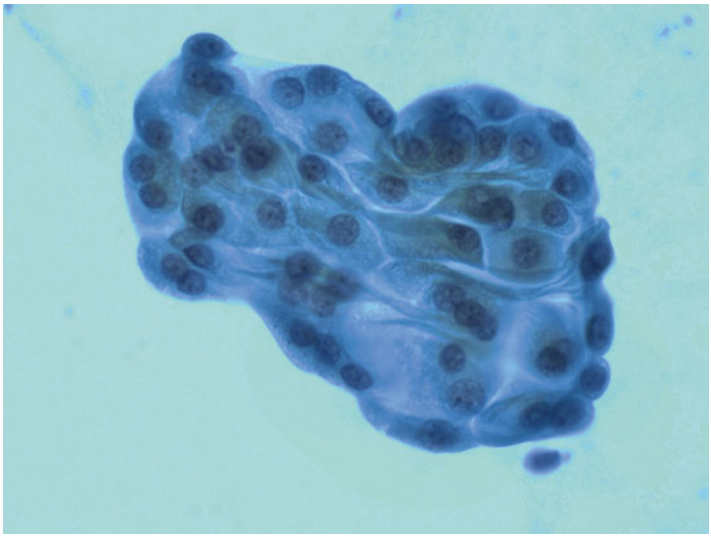

Fig. 10.35 Thyroid FNA-diffuse sclerosing variant of PTC. Balls of follicular cells with abundant dense opaque cytoplasm most likely represent squamous metaplasia (Papanicolaou stain, high power)

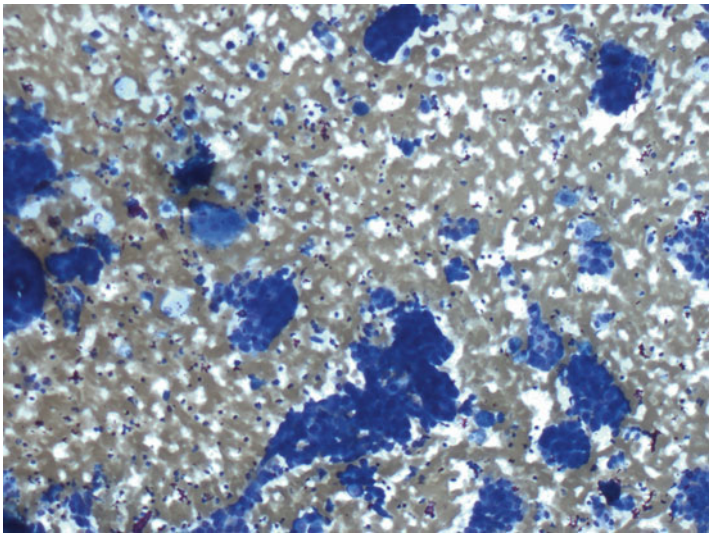

Fig. 10.36 Thyroid FNA-diffuse sclerosing variant of PTC. A conspicuous lymphoid background is noted among clusters and syncytial fragments of follicular cells (Diff-Quik stain, low power)

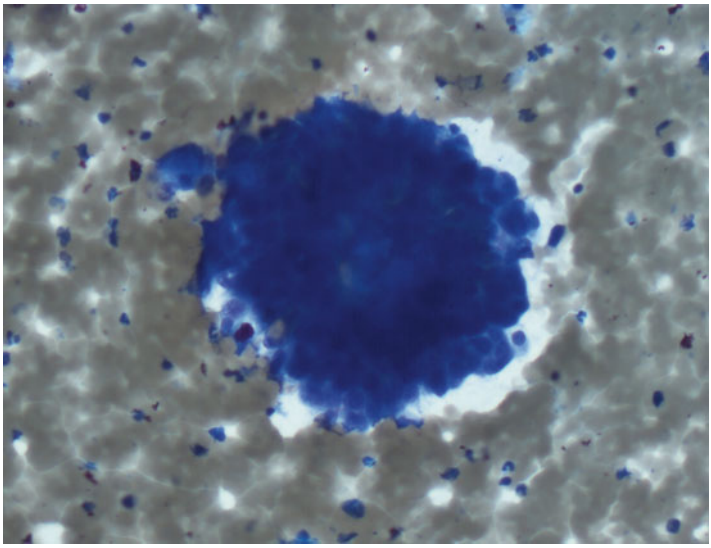

Fig. 10.37 Thyroid FNA-diffuse sclerosing variant of PTC. Three-dimensional cell balls consisting of follicular cells admixed with lymphocytes (Diff-Quik stain, high power)

Solid Variant

The solid variant comprises about 3 % of all PTCs [36, 37]. Patients with solid variant of PTC have a less favorable prognosis with a higher incidence of distant metastases than those with conventional PTC but much better prognosis than those with poorly differentiated thyroid carcinoma [38]. It affects most commonly adolescents and young adults as well as individuals with a history of radiation exposure. The histologic criteria for classifying a PTC solid variant include predominantly (>70 %) solid growth pattern of primary tumor, presence of typical cytologic and nuclear features of typical PTC, and absence of tumor necrosis [38] (Figs. 10.38 and 10.39).

The cytologic presentation of solid variant of PTC consists of three different patterns: cohesive syncytial-type tissue fragments, a microfollicular/trabecular pattern, and a dyshesive single-cell pattern [26, 39, 40] (Fig. 10.40). The nuclear features of the neoplastic cells are quite variable, ranging from cases demonstrating typical nuclear features of conventional PTC to cases with absence of PTC nuclear features. As a result, rendering a definitive diagnosis of PTC preoperatively may be challenging in some cases of solid variant of PTC (Fig. 10.41). Attempts to correlate the cytologic pattern with surgical pathology revealed that the single-cell pattern tended to be associated with infiltrative growth pattern, whereas the other two patterns were more likely to be associated with encapsulated tumors or those with pushing borders [40].

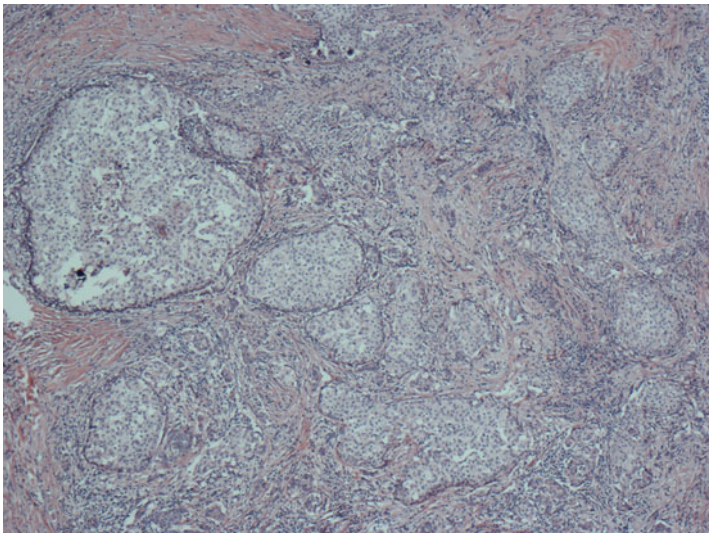

Fig. 10.38 Solid variant of PTC. Irregular islands of follicular cells in a solid growth pattern. No papillary or follicular structures are present (H&E stain, low power)

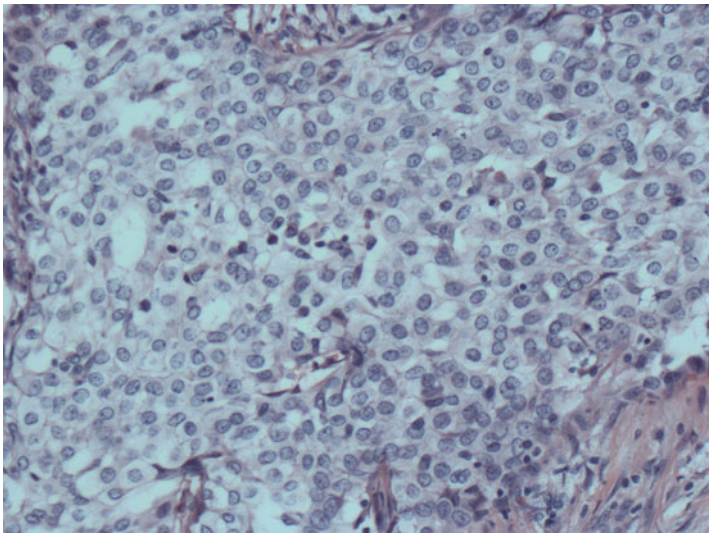

Fig. 10.39 Solid variant of PTC. The tumor cells have abundant pale cytoplasm and well-defined cytoplasmic borders. Individual nuclei demonstrate powdery chromatin and nuclear grooves (H&E stain, high power)

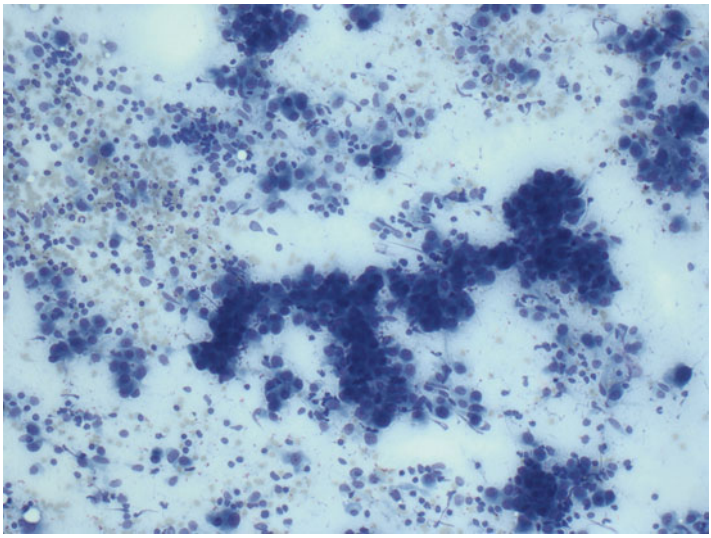

Fig. 10.40 Thyroid FNA-solid variant of PTC. The aspirate is cellular and consists of large tissue fragments, small clusters, and single cells (Diff-Quik stain, low power)

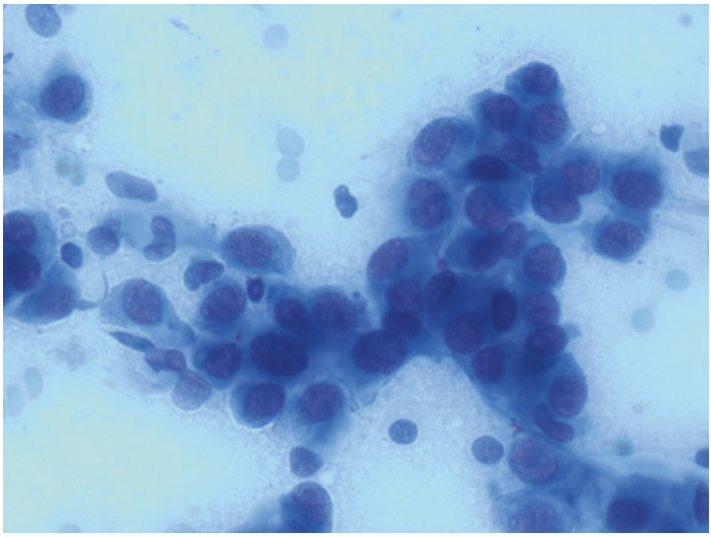

Fig. 10.41 Thyroid FNA-solid variant of PTC. Individual cells show considerable nuclear enlargement, scant to moderate amount of cytoplasm, and increased nuclear to cytoplasmic ratio. There is considerable nuclear crowding and overlapping (Diff-Quik stain, high power)

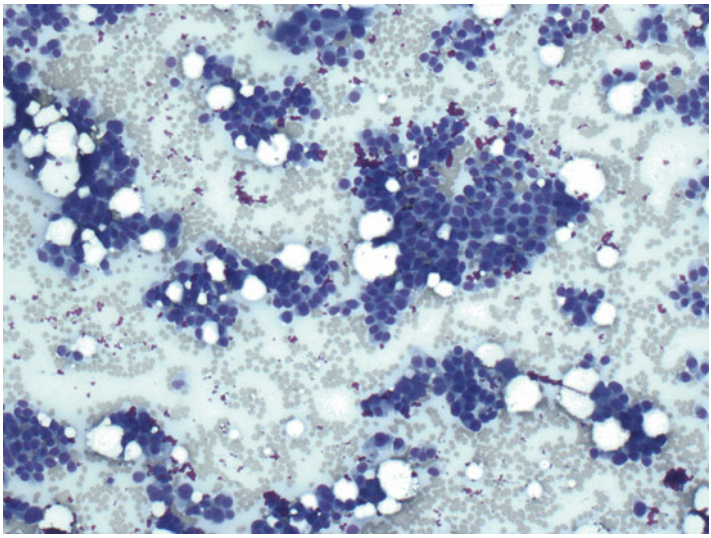

Fig. 10.42 Thyroid FNA-poorly differentiated thyroid carcinoma. The aspirate is cellular and demonstrates large tissue fragments and small loosely cohesive clusters of cells with increased nuclear to cytoplasmic ratio (Diff-Quik stain, low power)

Because of the absence of papillary structures and less developed nuclear features of PTC, the differential diagnosis would include a wide variety of thyroid malignancies. For aspirates with follicular pattern, the differential diagnosis would be follicular neoplasm and follicular variant of PTC. When presented with a cohesive, syncytial tissue pattern, solid variant of PTC should be differentiated from poorly differentiated thyroid carcinoma (Fig. 10.42). The finding of nuclear features of PTC and the absence of tumor necrosis favor the former. The differential diagnosis of medullary thyroid carcinoma should be considered when presented with a loosely cohesive/single-cell pattern (Fig. 10.43). The distinction lies in the nuclear features. Although pseudonuclear inclusions may be observed in medullary thyroid carcinoma, nuclear chromatin clearing and nuclear grooves are infrequent, and the nuclei of medullary thyroid carcinoma usually demonstrate a "salt-and-pepper" chromatin pattern (Fig. 10.44). Furthermore, the tumor cells of medullary thyroid carcinoma react positively with calcitonin but negatively with thyroglobulin.

Tall Cell Variant

This variant is the most common form of PTC with aggressive clinical behavior; patients with tall cell variant of PTC have a higher incidence of extrathyroidal extension, vascular invasion, local recurrence, and distant metastases when compared to those with conventional PTC [41, 42]. The incidence of tall cell variant of PTC ranges from 4 to 17% [41, 43]. Histologically, it is characterized by tall

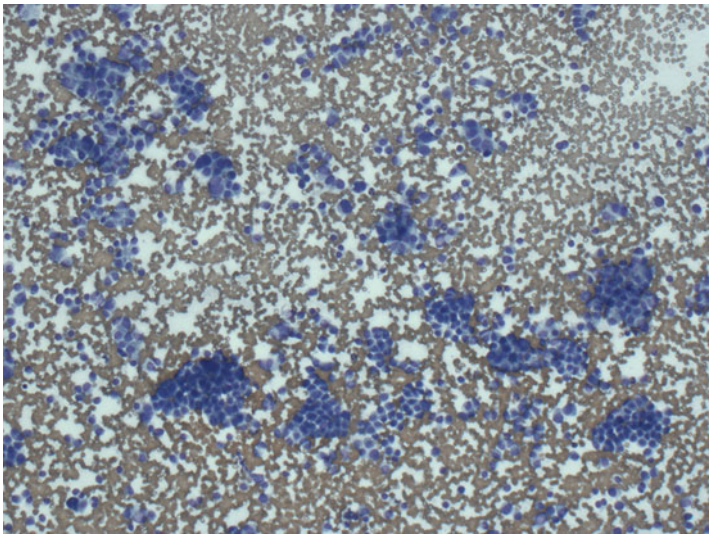

Fig. 10.43 Thyroid FNA-medullary thyroid carcinoma. The aspirate demonstrates loosely cohesive clusters with abundant single cells in the background (Diff-Quik stain, low power)

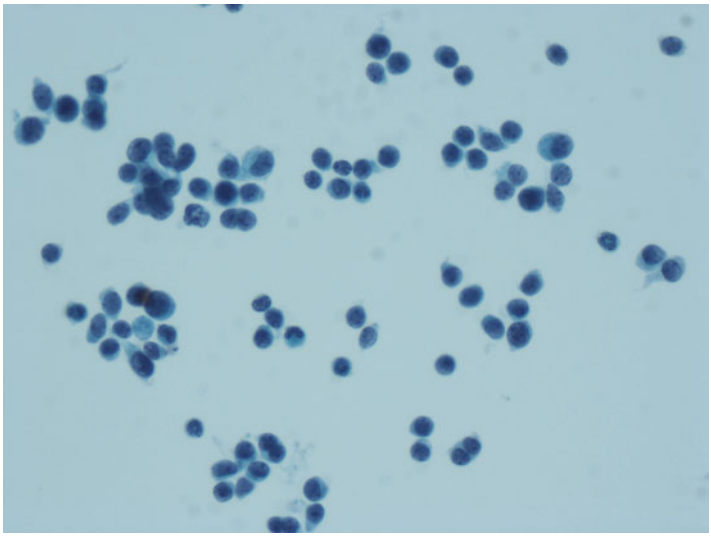

Fig. 10.44 Thyroid FNA-medullary thyroid carcinoma. The neoplastic cells are relatively small and uniform with finely granular cytoplasm (Diff-Quik stain, low power)

neoplastic cells whose height is at least twice their width; in addition, the tall cell components comprise at least 30 % of the tumor cell population [41, 44] (Fig. 10.45). Individual neoplastic cells demonstrate abundant eosinophilic cytoplasm and nuclear features similar to those of conventional PTC (Fig. 10.46).

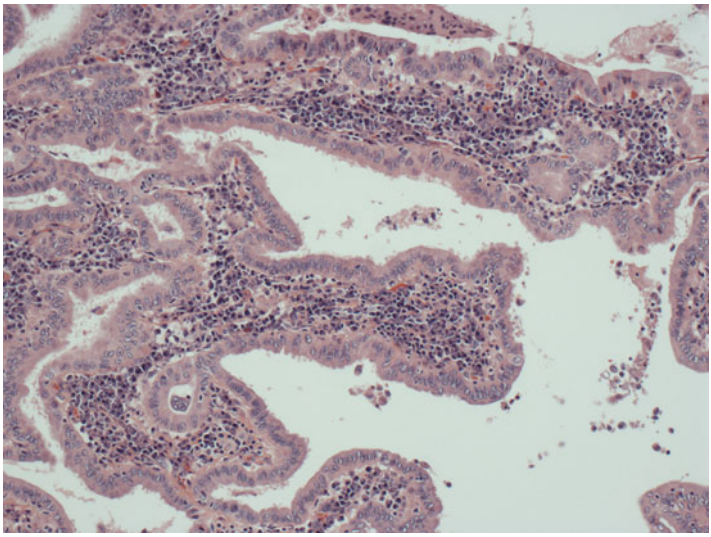

Fig. 10.45 Tall cell variant of PTC. Tumor with a predominantly papillary architecture lined by tall columnar cells and lymphoid background (H&E, low power)

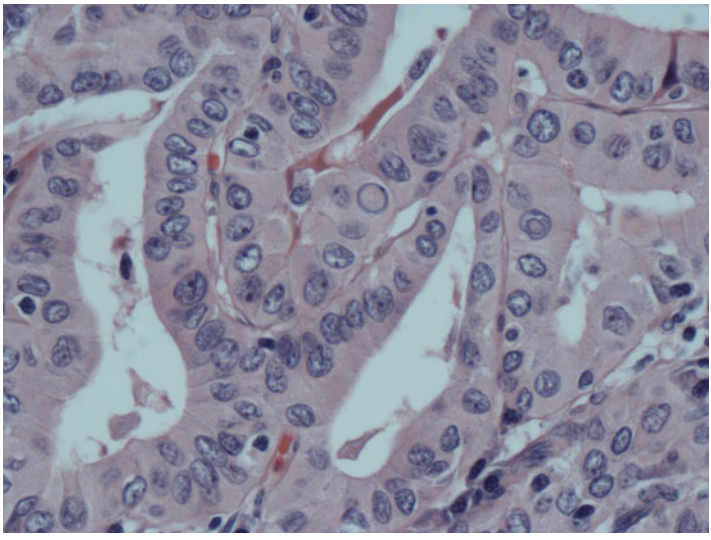

Fig. 10.46 Tall cell variant of PTC. High magnification shows the follicular cells are tall columnar whose height is at least twice their width. Nuclear features of PTC are readily apparent (H&E, x400)

Cytologic features of tall cell variant include large elongated/tall cells with a large amount of eosinophilic or cyanophilic cytoplasm, indistinct cell borders, basally located nuclei, and readily recognized nuclear features of PTC [43, 45–47]

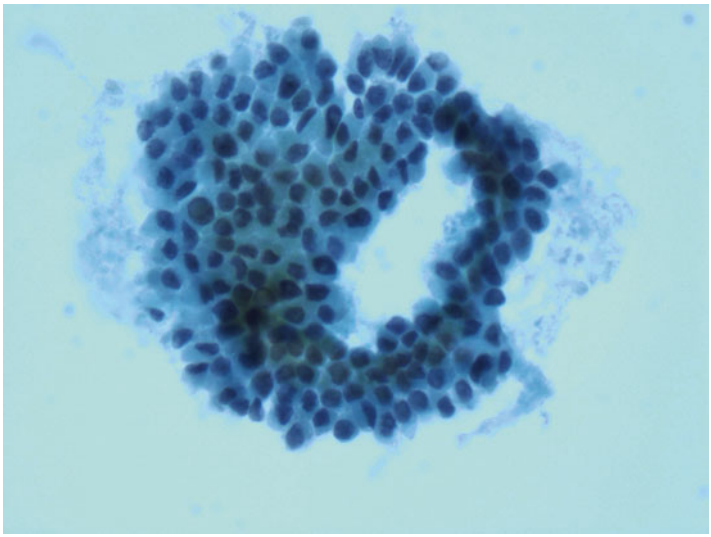

Fig. 10.47 Thyroid FNA-tall cell variant of PTC. A sheet of follicular cells composed of both polygonal and tall columnar follicular cells. Nuclear crowding and irregular nuclear contours are noted (Papanicolaou stain, high power)

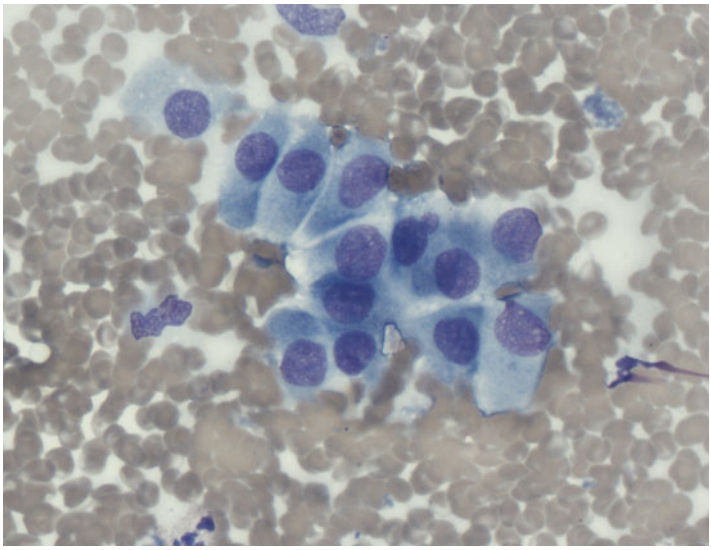

Fig. 10.48 Thyroid FNA-tall cell variant of PTC. A small group of tall columnar follicular cells whose height is at least twice their width (Diff-Quik stain, high power)

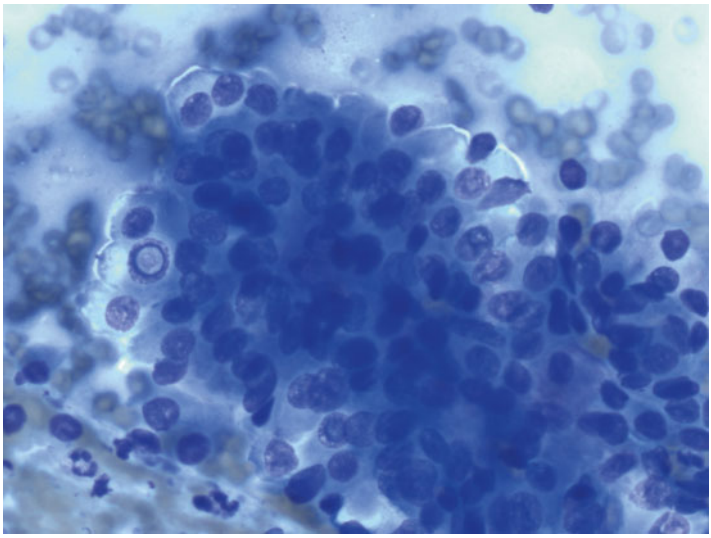

Fig. 10.49 Thyroid FNA-tall cell variant of PTC. Nuclear features in form of nuclear enlargement and nuclear inclusions are readily apparent (Diff-Quik stain, high power)

(Figs. 10.47, 10.48, and 10.49). Because of the latter, a cytologic diagnosis of PTC is usually quite straightforward for tall cell variant of PTC. However, the tall cell features may not be as prominent in cytologic preparations as they are in histologic sections. Instead, the neoplastic "tall" cells frequently appear as large polygonal cells with abundant granular eosinophilic cytoplasm and indistinct cell borders, resembling Hurthle cells [46] (Figs. 10.50 and 10.51). According to one study, six reviewers were only able to correctly diagnose 30–40 % of tall cell variant of PTC in a randomized study of ten cases of tall cell variant and ten cases of conventional PTC [46]. Other cytologic findings that suggest the presence of tall cell feature includes small and multiple "soap-bubble"-type intranuclear pseudoinclusions and the presence of tall, columnar cells with cytoplasmic tail (tadpole-like) [46, 47] (Fig. 10.52).

The differential diagnosis of tall cell variant includes lesions with abundant eosinophilic cytoplasm such as Hurthle cell neoplasm, oncocytic variant of PTC, and Warthin-like variant of PTC. The lack of typical nuclear features of PTC and the presence of prominent central nucleoli would favor a diagnosis of Hurthle cell neoplasm (Fig. 10.53). The presence of marked lymphoid infiltrate would favor a diagnosis of Warthin-like variant of PTC (Fig. 10.54); however, rare cases of tall cell variant of PTC with extensive lymphocyte infiltration have been reported [48]. It may be difficult if not impossible to distinguish from oncocytic variant and conventional PTC if the tall, columnar neoplastic cells are not apparent (Fig. 10.55). Given the potential sampling error and overlapping cytologic finding with other thyroid lesions, taking a conservative approach by including a qualifier "papillary thyroid carcinoma with features suggestive of tall cell variant" when less than 50 % of the neoplastic cells demonstrate unequivocal cytology features of tall cell variant of

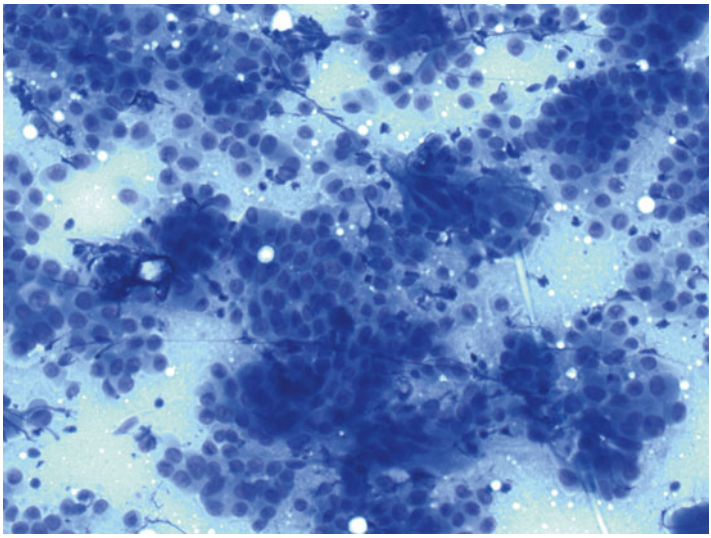

Fig. 10.50 Thyroid FNA-tall cell variant of PTC. In many instances, the neoplastic follicular cells appear as large polygonal cells with abundant granular cytoplasm and indistinct cell borders, resembling Hurthle cells (Diff-Quik stain, high power)

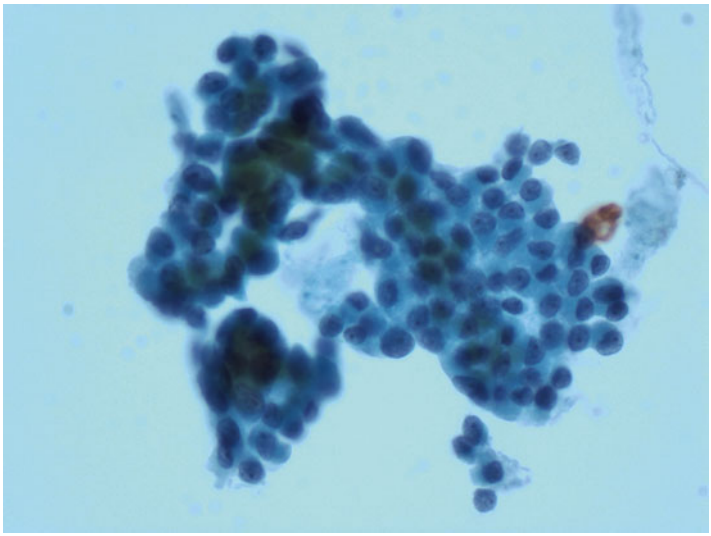

Fig. 10.51 Thyroid FNA-tall cell variant of PTC. The neoplastic follicular cells often appear as large polygonal cells with abundant granular cytoplasm, resembling Hurthle cells. Tall columnar cells may not be noted (Papanicolaou stain, high power)

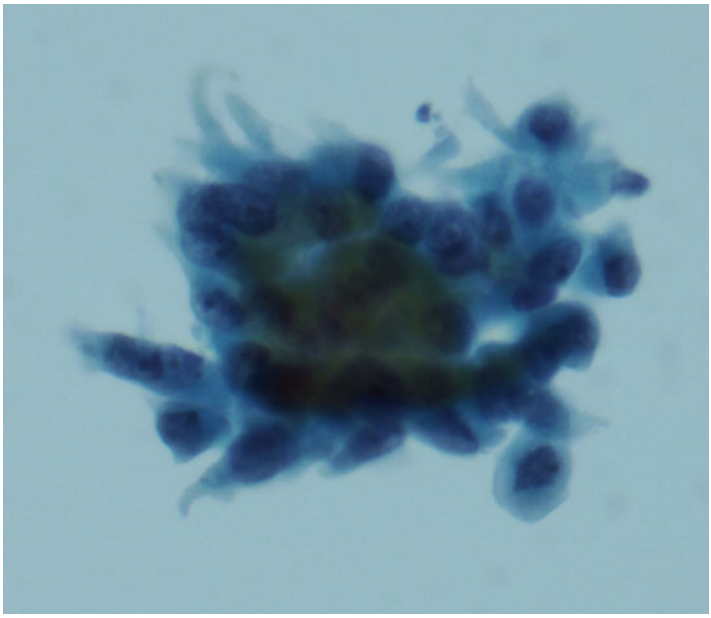

Fig. 10.52 Thyroid FNA-tall cell variant of PTC. These tall columnar neoplastic follicular cells show moderate amount of cytoplasm with a taper end, resembling a tadpole (Papanicolaou stain, high power)

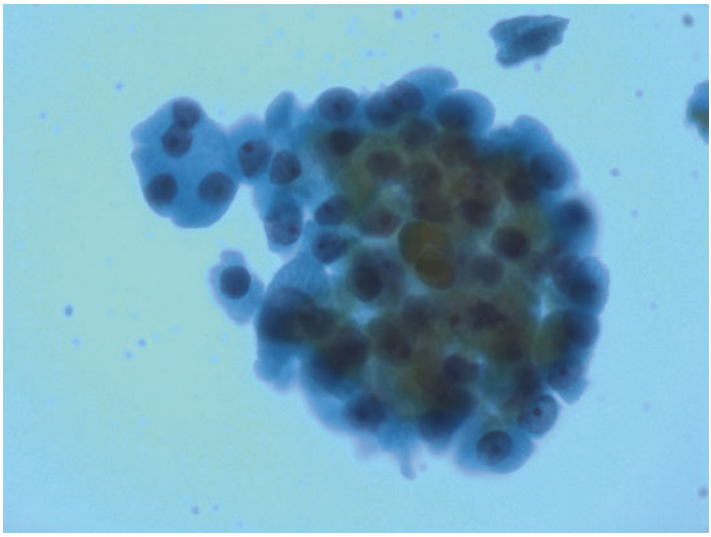

Fig. 10.53 Thyroid FNA-Hurthle cell neoplasm. The presence of abundant Hurthle cells without any nuclear features of PTC should be diagnosed as Hurthle cell neoplasm. This lesion was found to be a Hurthle cell carcinoma on subsequent follow-up (Papanicolaou stain, high power)

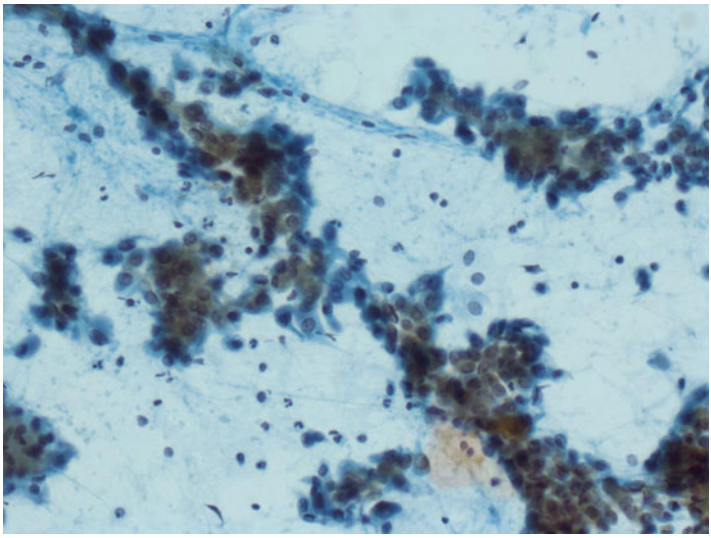

Fig. 10.54 Thyroid FNA-Warthin-like variant of PTC. Oncocytic cells admixed with a lymphoid background. The distinction between Warthin-like variant of PTC and tall cell variant of PTC with a lymphoid background may be difficult (Papanicolaou stain, high power)

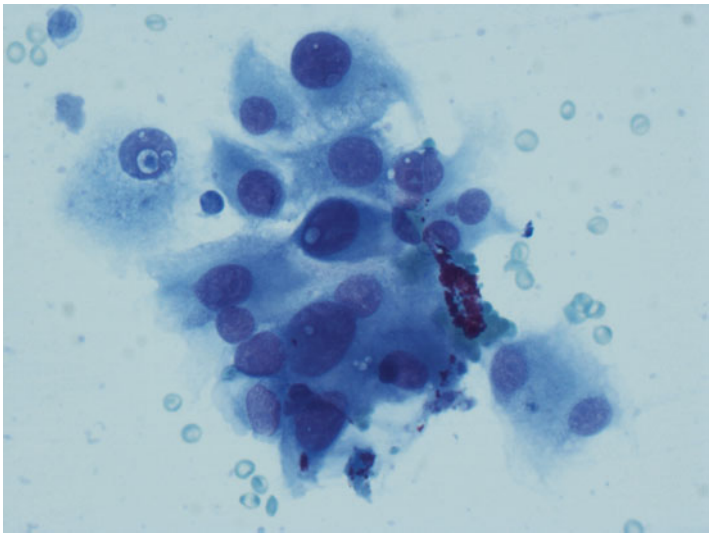

Fig. 10.55 Thyroid FNA-oncocytic variant of PTC. Aspirate of tall cell variant of PTC with predominance of polygonal cells may resemble that of an oncocytic variant of PTC (Diff-Quik stain, high power)

PTC is recommended [46]. A definitive diagnosis of tall cell variant of PTC should be deferred to surgically resected specimens.

Columnar Cell Variant

This variant is rare and exhibits aggressive behavior with frequent invasion of surrounding soft tissue and even distant metastasis [49]. Histology reveals papillary fronds and follicles lined by pseudostratified columnar cells with hyperchromatic nuclei and pale cytoplasm with or without vacuolation [49] (Fig. 10.56). The neoplastic cells are columnar in shape but lack abundant eosinophilic cytoplasm; furthermore, the nuclei do not necessarily demonstrate the typical nuclear features of PTC (Fig. 10.57). Pseudostratification of nuclei is a prominent cytologic feature, resembling cells from a colonic adenoma, and has been described in all the published cases of FNA-columnar cell variant of PTC [28, 50–53] (Fig. 10.58). The columnar cells can arrange in large tissue fragments, papillary structures, microfollicles, monolayer sheets, and singly in various combinations (Fig. 10.59). Hyperchromatic nuclei are frequently noted, but typical nuclear features of PTC are only focally present or altogether absent (Fig. 10.60). As a result, a definitive diagnosis of PTC was not rendered in more than half of the reported cases of FNA [50, 52, 53]. The main differential diagnosis is tall cell variant, which lacks the feature of pseudostratification and demonstrates columnar and polygonal cells with abundant eosinophilic cytoplasm and

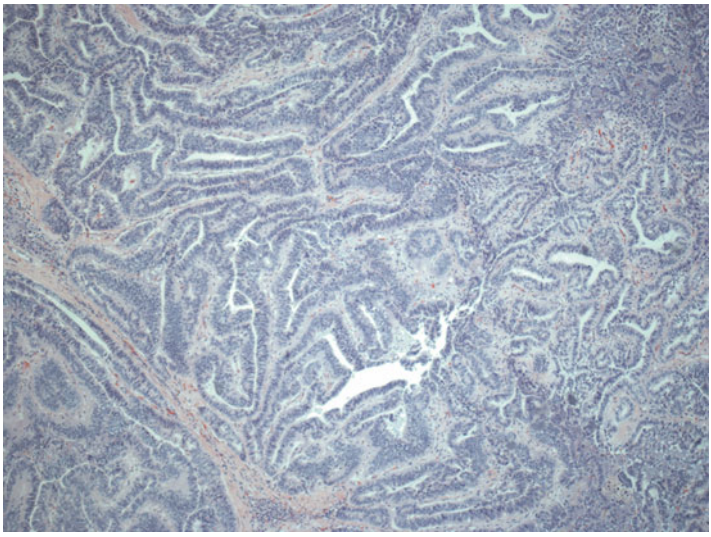

Fig. 10.56 Columnar cell variant of PTC. The tumor consists of predominantly papillary fronds lined by columnar cells with hyperchromatic nuclei and scant pale cytoplasm. No colloid is noted in the background (H&E stain, low power)

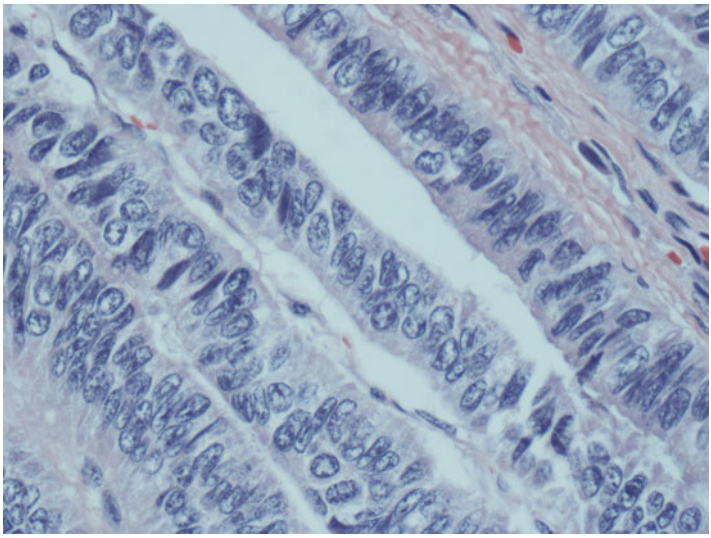

Fig. 10.57 Columnar cell variant of PTC. Higher magnification shows the lining cells are tall columnar with scant amount of pale cytoplasm. The nuclei are elongated and hyperchromatic with chromatin clearing. Nuclear grooves and inclusions are not identified (H&E stain, high power)

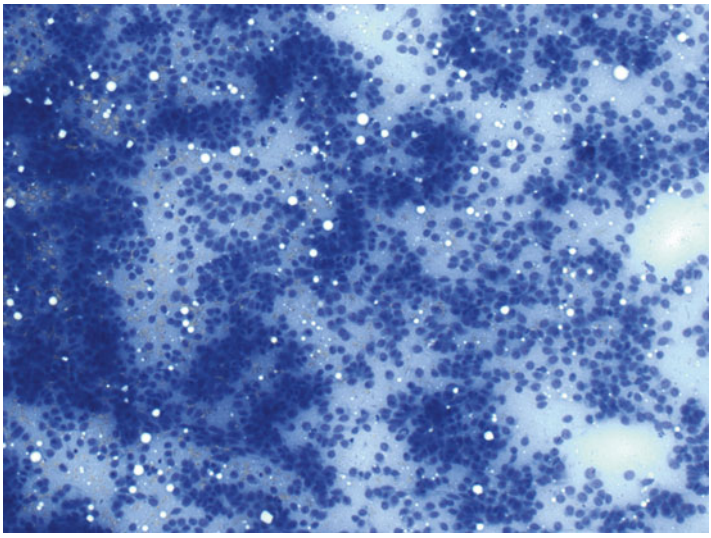

Fig. 10.58 Thyroid FNA-columnar variant of PTC. The aspirate is highly cellular and consists of large tissue fragments, loosely cohesive groups, and single cells (Diff-Quik stain, low power)

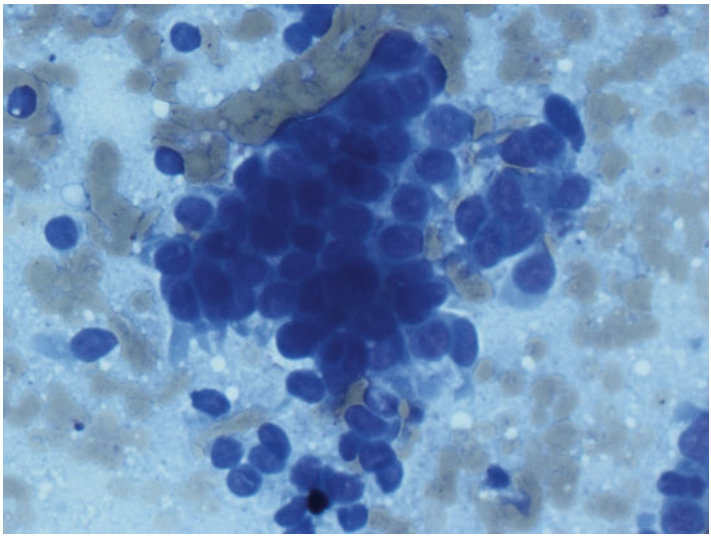

Fig. 10.59 Thyroid FNA-columnar cell variant of PTC. A strip of follicular cells with pseudostratification. Individual cells demonstrate scant amount of cytoplasm, resulting in high nuclear to cytoplasmic ratio. Majority of the cells have round to oval nuclei; the remaining cells have elongated nuclei (Diff-Quik stain, high power)

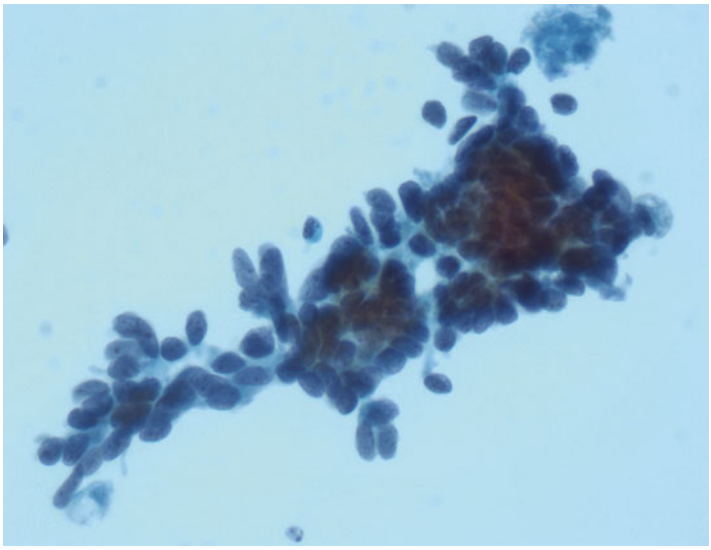

Fig. 10.60 Thyroid FNA-columnar cell variant of PTC. A hyperchromatic, crowded group of follicular cells with scant cytoplasm and high nuclear to cytoplasmic ratio. Individual nuclei range from round to oval to elongated with powdery chromatin. Nuclear grooves and inclusions are not identified (Papanicolaou stain, high power)

readily recognizable nuclear features of PTC. The neoplastic cells of columnar cell variant of PTC have also been mistaken as bronchial epithelial cells inadvertently aspirated from the larynx while performing a thyroid FNA [52]. The presence of terminal bars/cilia would favor bronchial epithelial cells.

Cribriform-Morular Variant

This rare variant typically occurs in patients with familial adenomatous polyposis (FAP) [54]. In this setting, the patients are usually young females and present with multifocal disease. However, sporadic cases with single tumor focus have also been reported [55, 56]. It is characterized by papillary structures lined by tall columnar cells; cribriform pattern without colloid, solid and spindle cell areas; and squamous morules (Fig. 10.61). Focally, individual tumor cells demonstrate nuclear clearing and grooves (Fig. 10.62). The cytology more or less recapitulates the histology. The cribriform structures are represented by slit-like empty spaces among cell clusters and bars anastomosing cell clusters (Fig. 10.63). Morules are composed of spindle and oval tumor cells with abundant dense cytoplasm, mimicking squamous metaplasia (Fig. 10.64). Individual neoplastic follicular cells often appear as tall columnar and spindle-shaped cells. Nuclear clearing is usually less apparent on cytologic

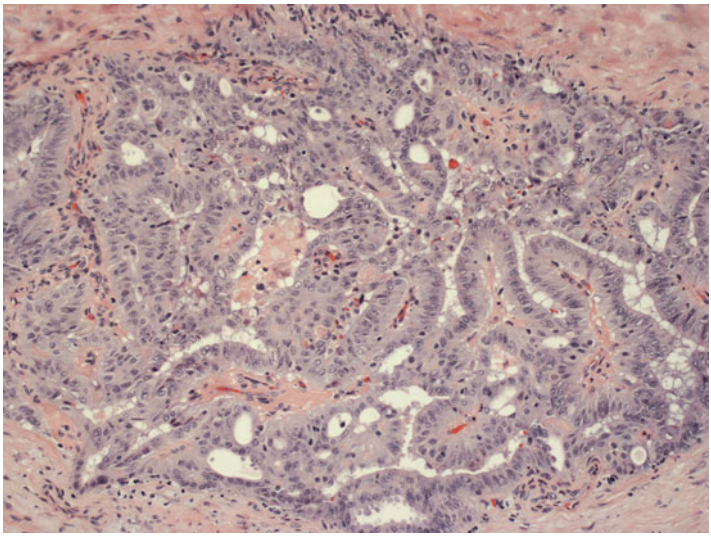

Fig. 10.61 Cribriform-morular variant of PTC. A tumor with both papillary and cribriform growth pattern (H&E stain, low power)

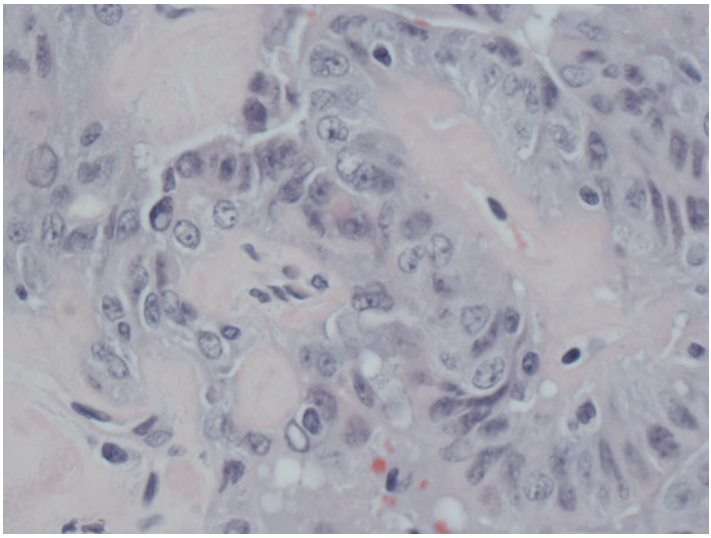

Fig. 10.62 Cribriform-morular variant of PTC. The tumor cells are columnar shaped with abundant eosinophilic cytoplasm. The nuclei demonstrate characteristic nuclear clearing and inclusions (H&E stain, high power)

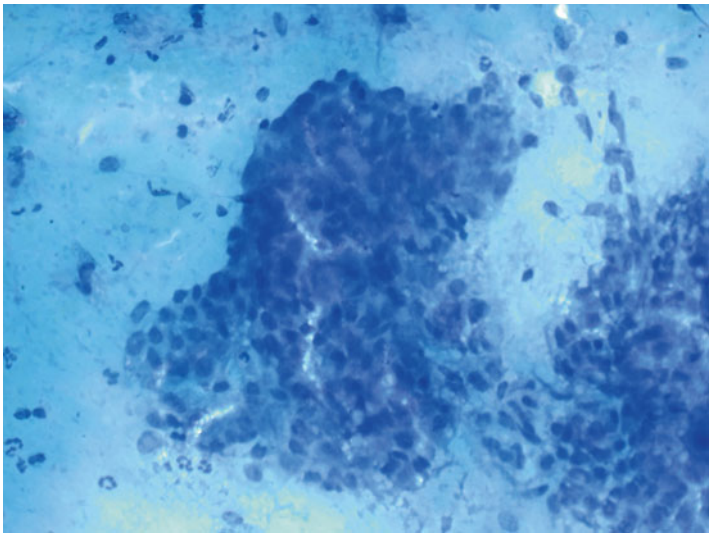

Fig. 10.63 Thyroid FNA-cribriform-morular variant of PTC. Large tissue fragment with considerable crowding and overlapping. Slit-like spaces are noted within the cluster (Diff-Quik stain, low power)

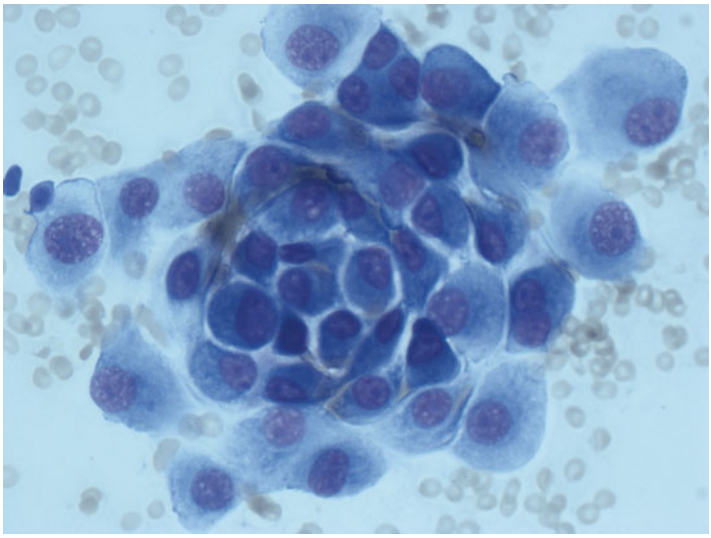

Fig. 10.64 Thyroid FNA-cribriform-morular variant of PTC. A tight group of oval cells with abundant dense opaque cytoplasm, most likely derived from a squamous morule (Diff-Quik stain, high power)

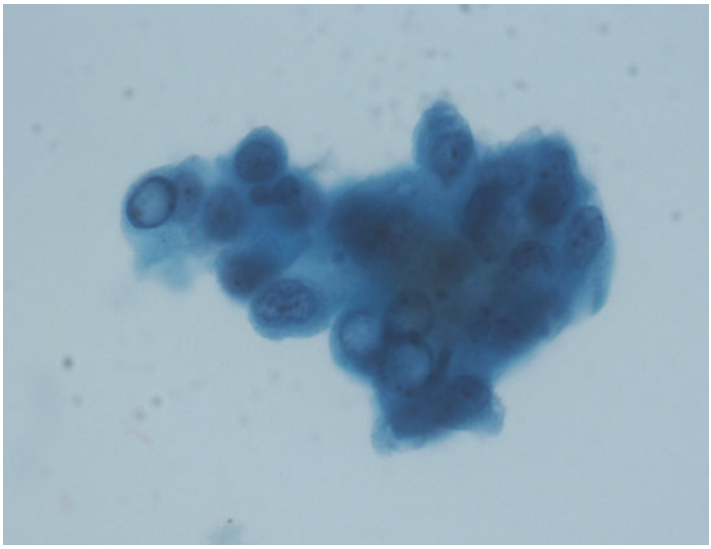

Fig. 10.65 Thyroid FNA-cribriform-morular variant of PTC. The nuclei of the follicular cells often demonstrate prominent nuclear clearing with peripheral nuclear membrane thickening (Papanicolaou stain, high power)

preparation and appears as pale-staining area occupying most of nuclei with peripheral condensed chromatin (Fig. 10.65). It differs from intranuclear inclusions by a lack of cytoplasmic staining and the sharp circumscription of the nuclear membrane. Intranuclear inclusions can also be seen but are less frequent. The demonstration of positive nuclear staining with antibody against β-catenin is useful in confirming the diagnosis of cribriform-morular variant.

About one-third of cribriform-morular variant of PTC are diagnosed simultaneously with FAP; and the thyroid carcinoma is diagnosed first in one-third of the cases and later in about one-third of the cases. Over 95 % of the thyroid carcinomas associated with FAP are papillary carcinoma, particularly the cribriform-morular type. FAP is an autosomal dominant disease and caused by a germ line mutation of the *APC* gene, which is located on the long arm of chromosome 5 (5q21-22) and is known to be a tumor suppressor gene. FAP is characterized by the development of multicentric colorectal adenomatous polyps, which can undergo malignant transformation. Because of these findings, the finding of cribriform-morular variant PTC raises the possibility of an accompanying FAP, and the patients should undergo a comprehensive investigation including a colonoscopy and genetic testing.

References

1. Berho M, Suster S. The oncocytic variant of papillary carcinoma of the thyroid: a clinicopathologic study of 15 cases. Hum Pathol. 1997;28:47–53.
2. Beckner ME, Heffess CS, Oertel JE. Oxyphilic papillary thyroid carcinomas. Am J Clin Pathol. 1995;103:280–7.
3. Chen KT. Fine-needle aspiration cytology of papillary Hurthle-cell tumors of thyroid: a report of three cases. Diagn Cytopathol. 1991;7:53–6.
4. Renshaw AA. Fine-needle aspirations of papillary carcinoma with oncocytic features: an expanded cytologic and histologic profile. Cancer Cytopathol. 2011;119:247–53.
5. Ali SZ, Cibas ES. The Bethesda system for reporting thyroid cytopathology. New York, NY: Springer; 2010.
6. Carcangiu ML, Sibley RK, Rosai J. Clear cell change in primary thyroid tumors. A study of 38 cases. Am J Surg Pathol. 1985;9:705–22.
7. Schroder S, Bocker W. Clear-cell carcinomas of thyroid gland: a clinicopathological study of 13 cases. Histopathology. 1986;10:75–89.
8. Civantos F, Albores-Saavedra J, Nadji M, Morales AR. Clear cell variant of thyroid carcinoma. Am J Surg Pathol. 1984;8:187–92.
9. Apel RL, Asa SL, LiVolsi VA. Papillary Hurthle cell carcinoma with lymphocytic stroma. "Warthin-like tumor" of the thyroid. Am J Surg Pathol. 1995;19:810–4.
10. Baloch ZW, LiVolsi VA. Fine-needle aspiration cytology of papillary Hurthle cell carcinoma with lymphocytic stroma "Warthin-like tumor" of the thyroid. Endocr Pathol. 1998;9:317–23.
11. Fadda G, Mule A, Zannoni GF, Vincenzoni C, Ardito G, Capelli A. Fine needle aspiration of a warthin-like thyroid tumor. Report of a case with differential diagnostic criteria vs. other lymphocyte-rich thyroid lesions. Acta Cytol. 1998;42:998–1002.
12. Yousef O, Dichard A, Bocklage T. Aspiration cytology features of the warthin tumor-like variant of papillary thyroid carcinoma. A report of two cases. Acta Cytol. 1997;41:1361–8.
13. Baloch ZW, LiVolsi VA. Warthin-like papillary carcinoma of the thyroid. Arch Pathol Lab Med. 2000;124:1192–5.

14. Chan JK, Carcangiu ML, Rosai J. Papillary carcinoma of thyroid with exuberant nodular fasciitis-like stroma. Report of three cases. Am J Clin Pathol. 1991;95:309–14.
15. Lee YS, Nam KH, Hong SW, Yun JS, Chung WY, Park CS. Papillary thyroid carcinoma with nodular fasciitis-like stroma. Thyroid. 2008;18:577–8.
16. Leal II, Carneiro FP, Basilio-de-Oliveira CA, et al. Papillary carcinoma with nodular fasciitis-like stroma—a case report in pregnancy. Diagn Cytopathol. 2008;36:139–41.
17. Yang YJ, LiVolsi VA, Khurana KK. Papillary thyroid carcinoma with nodular fasciitis-like stroma. Pitfalls in fine-needle aspiration cytology. Arch Pathol Lab Med. 1999;123:838–41.
18. Albores-Saavedra J, Gould E, Vardaman C, Vuitch F. The macrofollicular variant of papillary thyroid carcinoma: a study of 17 cases. Hum Pathol. 1991;22:1195–205.
19. Bongiovanni M, Gremaud M, Moulin CS, Scheidegger C, Biton C, Clement S. Macrofollicular variant of follicular thyroid carcinoma: a clinical, cytologic, morphologic, and image analysis study of a unique case. Ann Diagn Pathol. 2009;13:101–5.
20. Chung D, Ghossein RA, Lin O. Macrofollicular variant of papillary carcinoma: a potential thyroid FNA pitfall. Diagn Cytopathol. 2007;35:560–4.
21. Fadda G, Fiorino MC, Mule A, LiVolsi VA. Macrofollicular encapsulated variant of papillary thyroid carcinoma as a potential pitfall in histologic and cytologic diagnosis. A report of three cases. Acta Cytol. 2002;46:555–9.
22. Lugli A, Terracciano LM, Oberholzer M, Bubendorf L, Tornillo L. Macrofollicular variant of papillary carcinoma of the thyroid: a histologic, cytologic, and immunohistochemical study of 3 cases and review of the literature. Arch Pathol Lab Med. 2004;128:54–8.
23. Mesonero CE, Jugle JE, Wilbur DC, Nayar R. Fine-needle aspiration of the macrofollicular and microfollicular subtypes of the follicular variant of papillary carcinoma of the thyroid. Cancer. 1998;84:235–44.
24. Policarpio-Nicolas ML, Sirohi D. Macrofollicular variant of papillary carcinoma, a potential diagnostic pitfall: a report of two cases including a review of literature. Cytojournal. 2013;10:16.
25. Lam AK, Lo CY. Diffuse sclerosing variant of papillary carcinoma of the thyroid: a 35-year comparative study at a single institution. Ann Surg Oncol. 2006;13:176–81.
26. Thompson LD, Wieneke JA, Heffess CS. Diffuse sclerosing variant of papillary thyroid carcinoma: a clinicopathologic and immunophenotypic analysis of 22 cases. Endocr Pathol. 2005;16:331–48.
27. Carcangiu ML, Bianchi S. Diffuse sclerosing variant of papillary thyroid carcinoma. Clinicopathologic study of 15 cases. Am J Surg Pathol. 1989;13:1041–9.
28. Sen A, Nalwa A, Mathur SR, Jain D, Iyer VK. Cytomorphology of columnar cell variant of papillary carcinoma thyroid: a case report and review of the literature. Cytojournal. 2014;11:27.
29. Martin-Perez E, Larranaga E, Serrano P. Diffuse sclerosing variant of papillary carcinoma of the thyroid. Eur J Surg. 1998;164:713–5.
30. Soares J, Limbert E, Sobrinho-Simoes M. Diffuse sclerosing variant of papillary thyroid carcinoma. A clinicopathologic study of 10 cases. Pathol Res Pract. 1989;185:200–6.
31. Bongiovanni M, Triponez F, McKee TA, Kumar N, Matthes T, Meyer P. Fine-needle aspiration of the diffuse sclerosing variant of papillary thyroid carcinoma masked by florid lymphocytic thyroiditis; a potential pitfall: a case report and review of the literature. Diagn Cytopathol. 2009;37:671–5.
32. Lee JY, Shin JH, Han BK, et al. Diffuse sclerosing variant of papillary carcinoma of the thyroid: imaging and cytologic findings. Thyroid. 2007;17:567–73.
33. Odashiro DN, Nguyen GK. Diffuse sclerosing variant papillary carcinoma of the thyroid: report of four cases with fine-needle aspirations. Diagn Cytopathol. 2006;34:247–9.
34. Kumarasinghe MP. Cytomorphologic features of diffuse sclerosing variant of papillary carcinoma of the thyroid. A report of two cases in children. Acta Cytol. 1998;42:983–6.
35. Takagi N, Hirokawa M, Nobuoka Y, Higuchi M, Kuma S, Miyauchi A. Diffuse sclerosing variant of papillary thyroid carcinoma: a study of fine needle aspiration cytology in 20 patients. Cytopathology. 2014;25:199–204.
36. Akslen LA, LiVolsi VA. Prognostic significance of histologic grading compared with subclassification of papillary thyroid carcinoma. Cancer. 2000;88:1902–8.

37. Carcangiu ML, Zampi G, Pupi A, Castagnoli A, Rosai J. Papillary carcinoma of the thyroid. A clinicopathologic study of 241 cases treated at the University of Florence, Italy. Cancer. 1985;55:805–28.
38. Nikiforov YE, Erickson LA, Nikiforova MN, Caudill CM, Lloyd RV. Solid variant of papillary thyroid carcinoma: incidence, clinical-pathologic characteristics, molecular analysis, and biologic behavior. Am J Surg Pathol. 2001;25:1478–84.
39. Nguyen GK, Lee MW. Solid/trabecular variant papillary carcinoma of the thyroid: report of three cases with fine-needle aspiration. Diagn Cytopathol. 2006;34:712–4.
40. Giorgadze TA, Scognamiglio T, Yang GC. Fine-needle aspiration cytology of the solid variant of papillary thyroid carcinoma: a study of 13 cases with clinical, histologic, and ultrasound correlations. Cancer Cytopathol. 2015;123(2):71–81.
41. Ghossein R, Livolsi VA. Papillary thyroid carcinoma tall cell variant. Thyroid. 2008;18: 1179–81.
42. Kazaure HS, Roman SA, Sosa JA. Aggressive variants of papillary thyroid cancer: incidence, characteristics and predictors of survival among 43,738 patients. Ann Surg Oncol. 2012;19: 1874–80.
43. Urano M, Kiriyama Y, Takakuwa Y, Kuroda M. Tall cell variant of papillary thyroid carcinoma: its characteristic features demonstrated by fine-needle aspiration cytology and immunohistochemical study. Diagn Cytopathol. 2009;37:732–7.
44. LiVolsi VA. Papillary carcinoma tall cell variant (TCV): a review. Endocr Pathol. 2010;21:12–5.
45. Lee SH, Jung CK, Bae JS, Jung SL, Choi YJ, Kang CS. Liquid-based cytology improves preoperative diagnostic accuracy of the tall cell variant of papillary thyroid carcinoma. Diagn Cytopathol. 2014;42:11–7.
46. Guan H, Vandenbussche CJ, Erozan YS, et al. Can the tall cell variant of papillary thyroid carcinoma be distinguished from the conventional type in fine needle aspirates? A cytomorphologic study with assessment of diagnostic accuracy. Acta Cytol. 2013;57:534–42.
47. Solomon A, Gupta PK, LiVolsi VA, Baloch ZW. Distinguishing tall cell variant of papillary thyroid carcinoma from usual variant of papillary thyroid carcinoma in cytologic specimens. Diagn Cytopathol. 2002;27:143–8.
48. Ozaki O, Ito K, Mimura T, Sugino K, Hosoda Y. Papillary carcinoma of the thyroid. Tall-cell variant with extensive lymphocyte infiltration. Am J Surg Pathol. 1996;20:695–8.
49. Wenig BM, Thompson LD, Adair CF, Shmookler B, Heffess CS. Thyroid papillary carcinoma of columnar cell type: a clinicopathologic study of 16 cases. Cancer. 1998;82:740–53.
50. Ylagan LR, Dehner LP, Huettner PC, Lu D. Columnar cell variant of papillary thyroid carcinoma. Report of a case with cytologic findings. Acta Cytol. 2004;48:73–7.
51. Perez F, Llobet M, Garijo G, Barcelo C, Castro P, Bernado L. Fine-needle aspiration cytology of columnar-cell carcinoma of the thyroid: report of two cases with cytohistologic correlation. Diagn Cytopathol. 1998;18:352–6.
52. Jayaram G. Cytology of columnar-cell variant of papillary thyroid carcinoma. Diagn Cytopathol. 2000;22:227–9.
53. Hui PK, Chan JK, Cheung PS, Gwi E. Columnar cell carcinoma of the thyroid. Fine needle aspiration findings in a case. Acta Cytol. 1990;34:355–8.
54. Harach HR, Williams GT, Williams ED. Familial adenomatous polyposis associated thyroid carcinoma: a distinct type of follicular cell neoplasm. Histopathology. 1994;25:549–61.
55. Ng SB, Sittampalam K, Goh YH, Eu KW. Cribriform-morular variant of papillary carcinoma: the sporadic counterpart of familial adenomatous polyposis-associated thyroid carcinoma. A case report with clinical and molecular genetic correlation. Pathology. 2003;35:42–6.

56. Cameselle-Teijeiro J, Chan JK. Cribriform-morular variant of papillary carcinoma: a distinctive variant representing the sporadic counterpart of familial adenomatous polyposis-associated thyroid carcinoma? Mod Pathol. 1999;12:400–11.

Medullary Carcinoma

11

Case Study

A 50-year-old female who presented to her primary care physician and was found to have a thyroid nodule on routine screening examination. She had no complaints of hoarseness, difficulty swallowing, or difficulty breathing. She had no symptoms of hyperthyroidism, no history of radiation to the neck or face, and no previous history of neck surgery. Patient reported that she had never smoked, never used smokeless tobacco, was not a drinker, and never used illicit drugs. There was no family history of thyroid cancer or adrenal problems.

Ultrasonographic examination revealed a $3.5 \times 2.5 \times 2.5$ cm nodule in the right lobe. The nodule had internal hyperechoic foci and a hypoechoic halo and vascularity. Multiple prominent abnormal appearing lymph nodes with loss of fatty hilum and some calcifications were noted within the right neck. Fine-needle aspiration biopsy of the thyroid performed at the time of ultrasonographic examination yielded a highly cellular specimen showing clusters of cells and single cells in the absence of colloid. Individual cells showed plasmacytoid appearance with high nuclear-to-cytoplasmic ratio. Nuclear changes were present that included nuclear enlargement and "salt and pepper" chromatin. Lymph nodes from right level 4 showed cells with a similar appearance. Immunohistochemical stains were performed on both specimens with appropriate controls, and the cells were positive for calcitonin while negative for thyroglobulin. The immunohistochemical profile was consistent with medullary carcinoma. Serum calcitonin level was 3655 pg/mL, and the serum CEA level was 79.80 ng/mL. Calcium was normal. Patient underwent total thyroidectomy with bilateral central neck dissection and right modified radical neck dissection. There was a 5.0-cm encapsulated, tan-yellow mass, with focal hemorrhagic areas and evidence of microcystic changes. The histology was confirmed to be medullary carcinoma, with evidence of lymphovascular invasion, and 17 of 42 lymph nodes were positive for metastatic carcinoma. She was screened for *RET* mutation and was negative. She was also screened for pheochromocytoma by 24-h urine and had a negative result. Her 2 weeks postoperative calcitonin level was down to

A.J. Adeniran, D. Chhieng, *Common Diagnostic Pitfalls in Thyroid Cytopathology*, DOI 10.1007/978-3-319-31602-4_11

122 pg/mL and CEA down to 12.40 ng/mL. By 2 months, calcitonin was down to 74 pg/mL and CEA was 5.09 ng/mL. Neck mapping ultrasound scan done 6 months after surgery was negative. The patient was put on lifelong surveillance with calcitonin levels as well as lifelong thyroid replacement therapy.

Discussion

Medullary carcinoma comprises 5–10 % of all thyroid malignancies [1, 2], and it arises from the calcitonin-producing parafollicular C cells. It is caused by mutations in the RET proto-oncogene. Clinically, it occurs in two forms—familial and sporadic. The familial form is transmitted as an autosomal dominant trait, and it includes three types: multiple endocrine neoplasia type 2A (MEN 2A), MEN 2B, and non-MEN familial type. MEN 2A and MEN 2B types are more common in males, and they occur at a younger age, while the non-MEN familial type is slightly more common in women. The non-MEN familial form of medullary carcinoma accounts for about 35 % of hereditary cases [3]. The sporadic form of medullary carcinoma occurs more commonly in women, with a mean age of 50 years [4]. Medullary carcinoma demonstrates variable behavior from indolent disease to highly aggressive, progressive disease [5]. It mostly progresses in an indolent fashion and has a 15-year survival rate of 85 %, but it has a tendency to spread to locoregional lymph nodes early, making surgical cure difficult [6]. Total thyroidectomy and lymphadenectomy result in biochemical cure only 40 % of the time [6, 7]. Even when a biochemical cure is achieved, approximately 9 % of patients will later develop recurrent disease [7].

The main secretory product of the C cells is the hormone calcitonin, which serves as a useful sensitive marker for the presence of medullary carcinoma [8, 9], although a rare case of medullary carcinoma with undetectable preoperative serum calcitonin has been reported [10]. The secretion of calcitonin can be used to confirm the diagnosis [11], indicate treatment efficacy, [12], and monitor for disease progression or recurrence [13]. Medullary carcinomas typically present as hypofunctioning cold nodules. Plain X-rays of the neck may show dense calcifications. Ultrasonographic examination shows hypoechoic mass [14]. Tumor is usually located in the lateral thyroid, near the upper pole, where C cell concentration is highest. Sporadic forms of medullary carcinoma are typically unilateral, while heritable forms are most often bilateral and multicentric [15]. Tumor is usually well-defined, non-encapsulated nodule with size variability, which may range from less than 1 cm to several centimeters and may replace the entire lobe (Figs. 11.1 and 11.2). Its cut surface is tan-white to gray or pink, usually flat. The consistency varies from soft to firm to gritty and without areas of hemorrhage and necrosis. Calcification may be present [14]. Medullary carcinoma is most commonly diagnosed by fine-needle aspiration (FNA) of a new thyroid nodule, with a sensitivity of 60–90 % [8, 16, 17]. FNA cannot always distinguish medullary carcinoma based on cytology alone, so immunohistochemical staining for calcitonin, chromogranin A, or carcinoembryonic antigen can increase accuracy [18]. Recent small studies have shown improved sensitivity with calcitonin measurement in FNA washout fluid with as high as 100 % accuracy [19, 20].

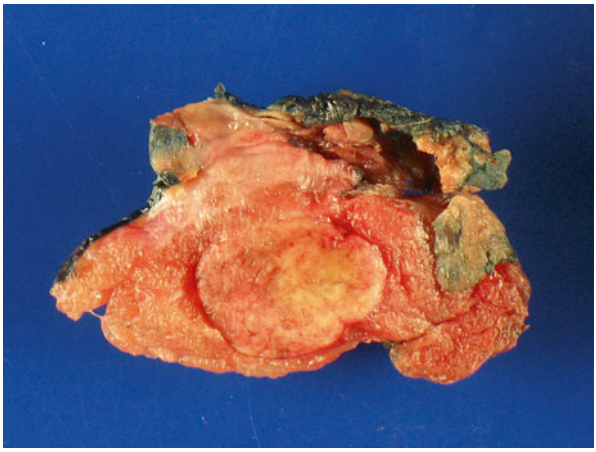

Fig. 11.1 A gross photograph of medullary thyroid carcinoma showing a well-circumscribed tumor

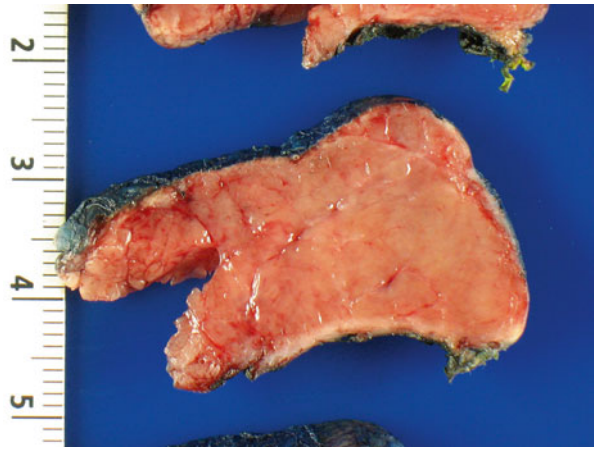

Fig. 11.2 A gross photograph of medullary thyroid carcinoma showing diffuse infiltration of the thyroid tissue and replacing the entire lobe

The histologic spectrum of medullary carcinoma is extremely wide and varies from tumor to tumor and within the same tumor, often mimicking other types of follicular-derived tumors such as papillary, follicular, insular, Hürthle cell, or anaplastic carcinomas [4, 14, 21–23]. Tumor cells are arranged in sheets, nests, or ribbons and can be polygonal, round, spindle shaped, or plasmacytoid (Figs. 11.3, 11.4, 11.5, 11.6, and 11.7). Nuclei are round or oval, and nucleoli are usually not prominent. Intranuclear pseudoinclusions, which are indistinguishable from those seen in papillary carcinomas, are seen. In rare cases, cells can be markedly enlarged and pleomorphic. Amyloid deposits are seen in 80 % of cases and can be confirmed with the Congo red stain [14] (Figs. 11.8 and 11.9).

There is a broad spectrum of cytopathologic features in medullary carcinoma, depending on the histomorphology. It is monomorphic if only one pattern is evident and polymorphic if a combination of different morphologic patterns is seen [14].

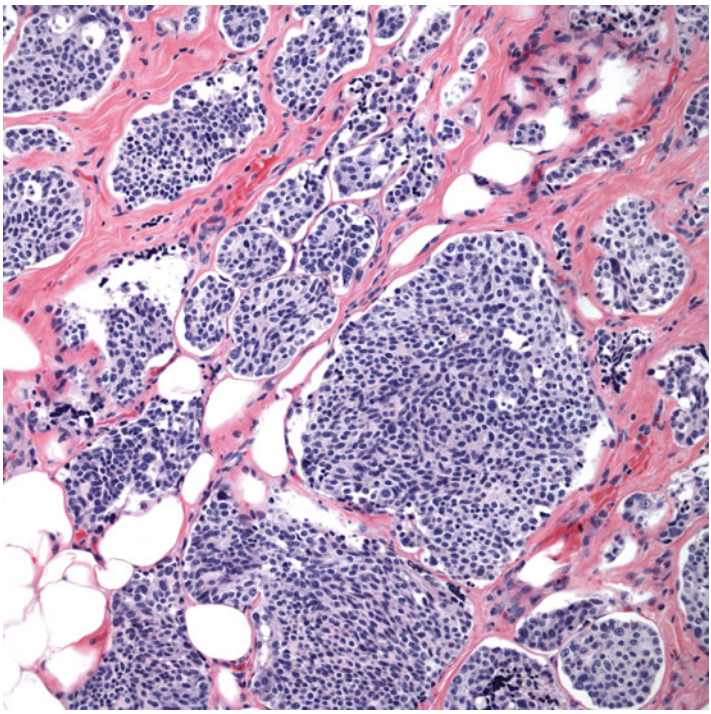

Fig. 11.3 Medullary carcinoma showing a lobular pattern. The lobules vary in size, separated by bands of fibrous tissue (H&E stain, X200)

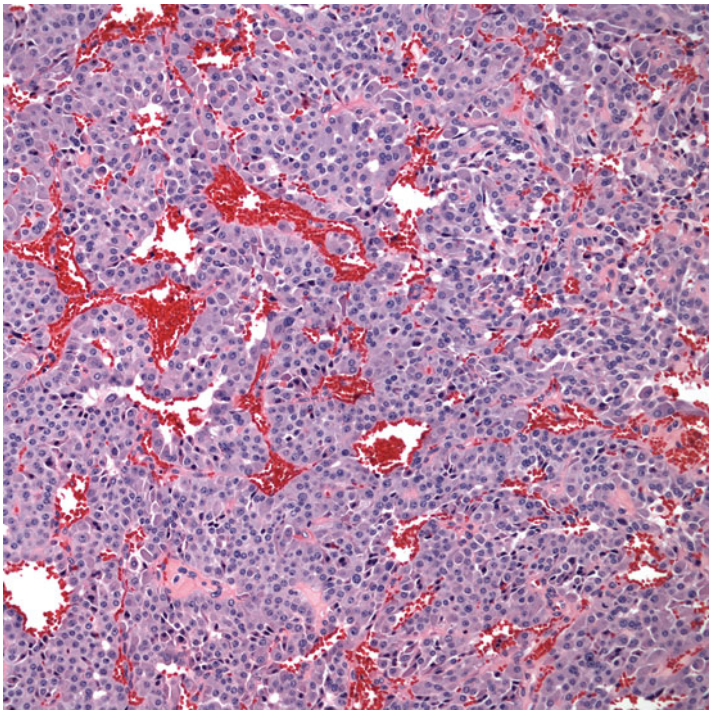

Fig. 11.4 Solid growth pattern of medullary carcinoma (H&E stain, X200)

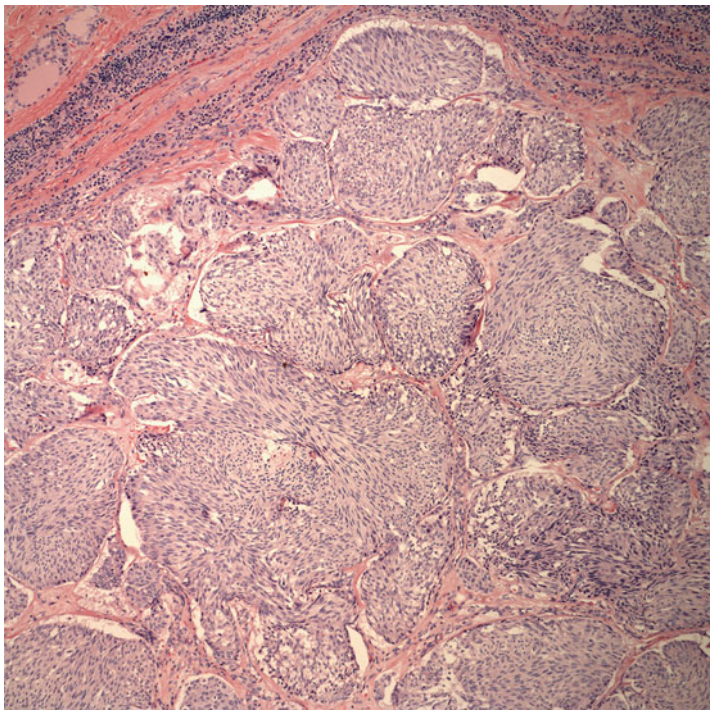

Fig. 11.5 Medullary carcinoma with a spindle cell pattern. The spindle cells from large nests, separated by fibrous tissue septa (H&E stain, X100)

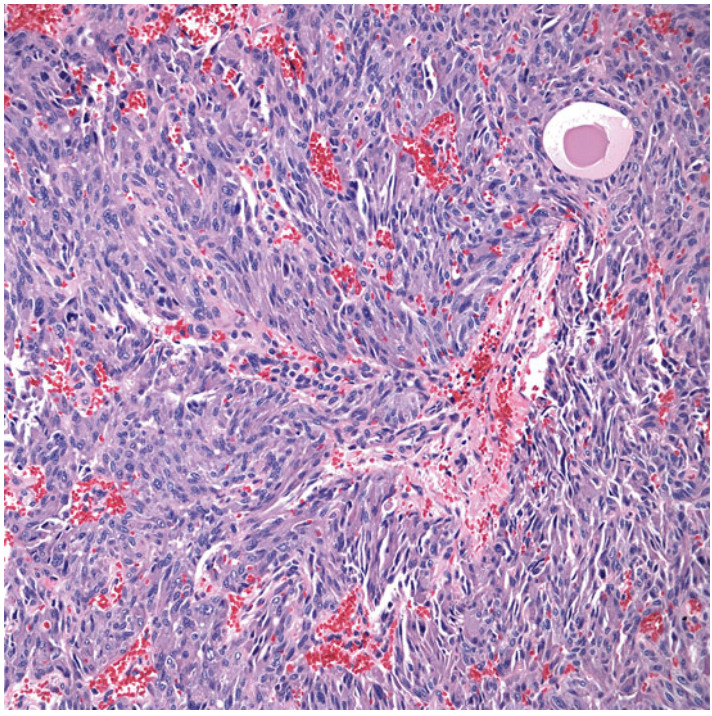

Fig. 11.6 Medullary carcinoma with a spindle cell pattern (H&E stain, X200)

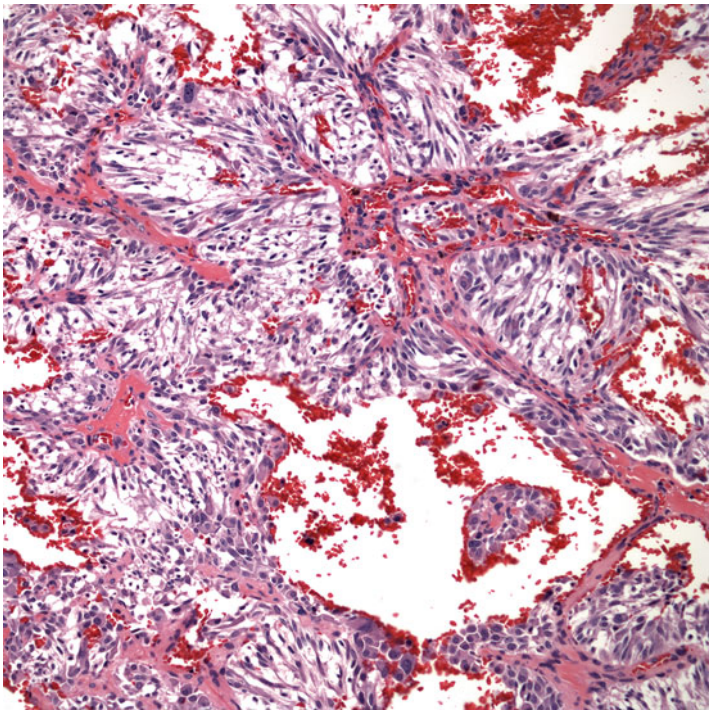

Fig. 11.7 Medullary carcinoma with spindle cell appearance and cytoplasmic clearing (H&E stain, X200)

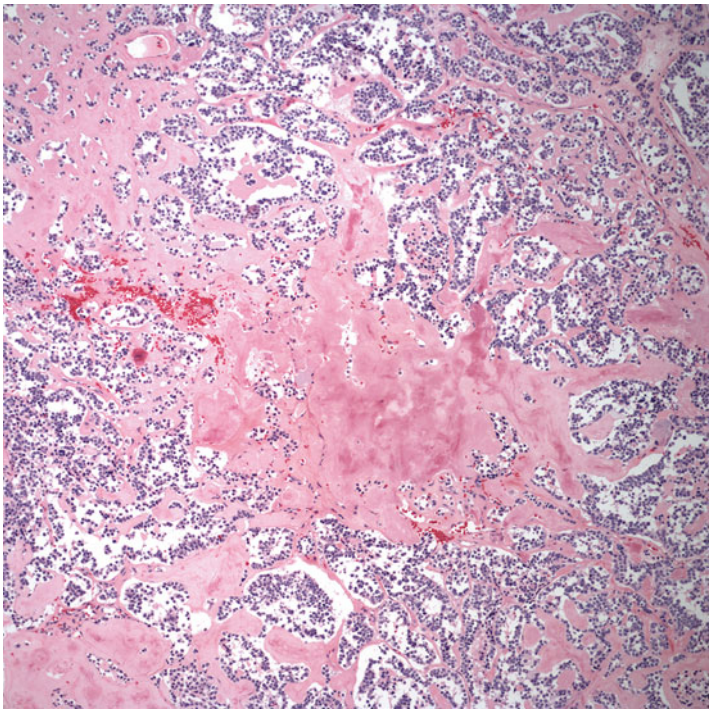

Fig. 11.8 Medullary carcinoma with amyloid in the stroma (H&E stain, X200)

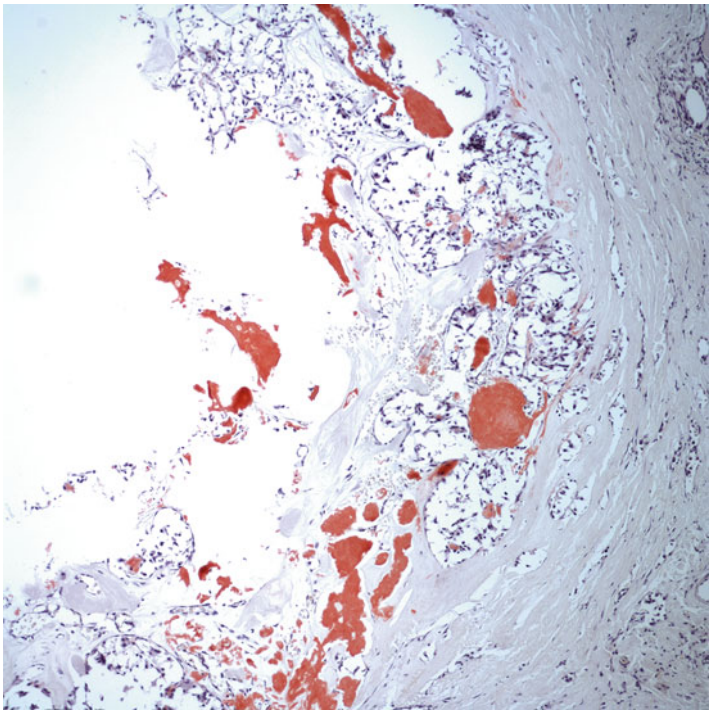

Fig. 11.9 Congo red stain highlights amyloid deposition

The aspirates are usually highly cellular; however, scant cellularity is encountered with carcinomas containing extensive amyloid deposits and calcification. Because of its diverse cytologic presentations with different cellular morphologies, medullary carcinoma can simulate other neoplastic processes including anaplastic carcinoma, malignant lymphoma, carcinoid tumor, plasmacytoma, malignant melanoma, and soft tissue neoplasms. Tumor cells are predominantly single cells but can also be seen as sheets, loose clusters, syncytia, rosettes, cords, and papillae [17, 24–26] (Figs. 11.10, 11.11, 11.12, 11.13, and 11.14). The cells are usually uniform in size and shape but occasionally can present as large pleomorphic cells. Cytoplasm is moderate to abundant and finely granular. Nuclei are eccentrically placed, giving the cells a plasmacytoid appearance, and binucleation and multinucleation are common (Figs. 11.15, 11.16, and 11.17). Nuclei have a coarsely granular chromatin texture and inconspicuous nucleoli, thereby giving the so-called "salt and pepper" appearance (Fig. 11.18). Intranuclear inclusions may be found in up to half of cases [27]. Ultrastructurally, the tumor cells contain membrane-bound secretory granules, the sites of storage of calcitonin, and other peptides [28]. One cell-type appearance may predominate, but cells can occur in any combination. Amyloid is present in most cases and can be very similar in appearance to colloid (Fig. 11.19). However, it can be distinguished with the aid of Congo red stain, which shows apple-green birefringence on polarized light.

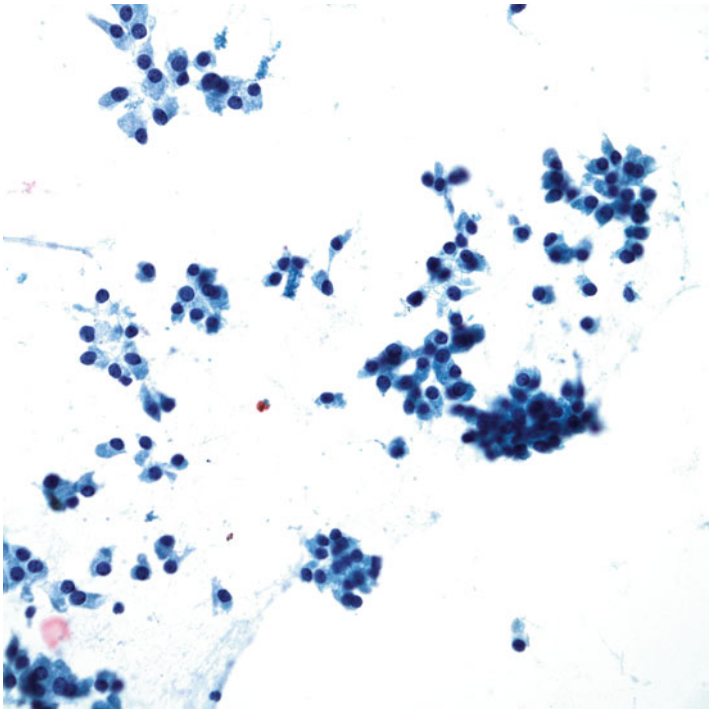

Fig. 11.10 FNA of medullary carcinoma showing loosely cohesive cells and single cells. The cells are round and cuboidal. There is moderate amount of cytoplasm. Individual cells have eccentrically placed nuclei (Papanicolaou stain, X400)

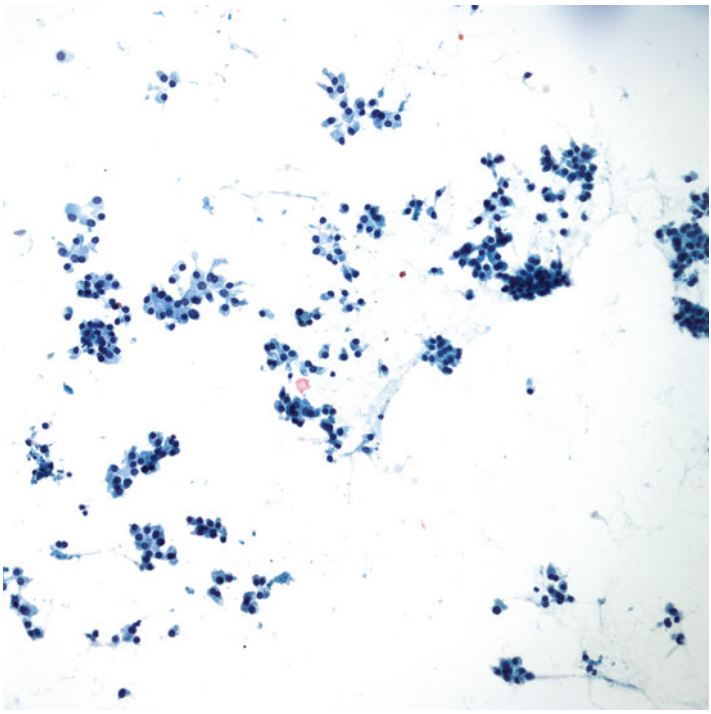

Fig. 11.11 Medullary carcinoma showing loosely cohesive tissue fragments. The cells are round and monomorphic with eccentric bland nuclei (Papanicolaou stain, X200)

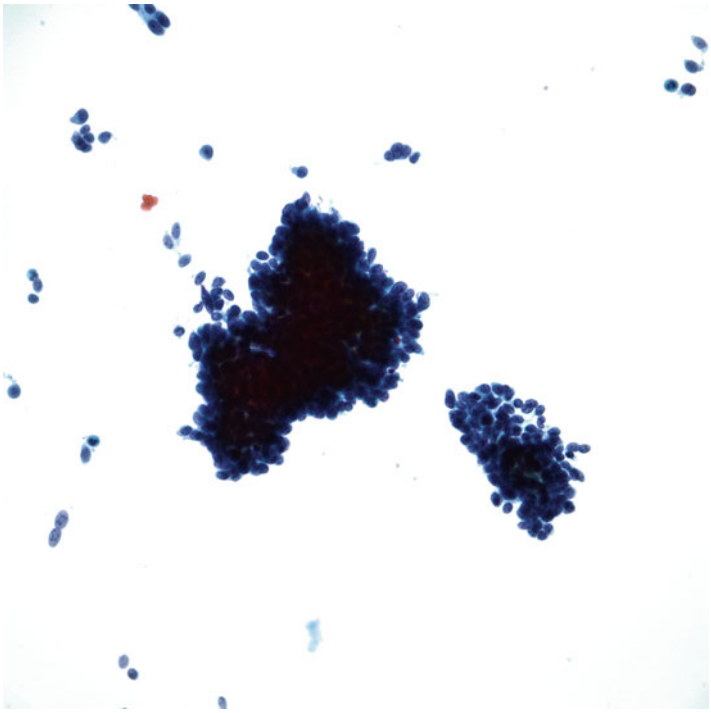

Fig. 11.12 The medullary carcinoma cells in this aspirate are compactly arranged in tissue fragments (Papanicolaou stain, X400)

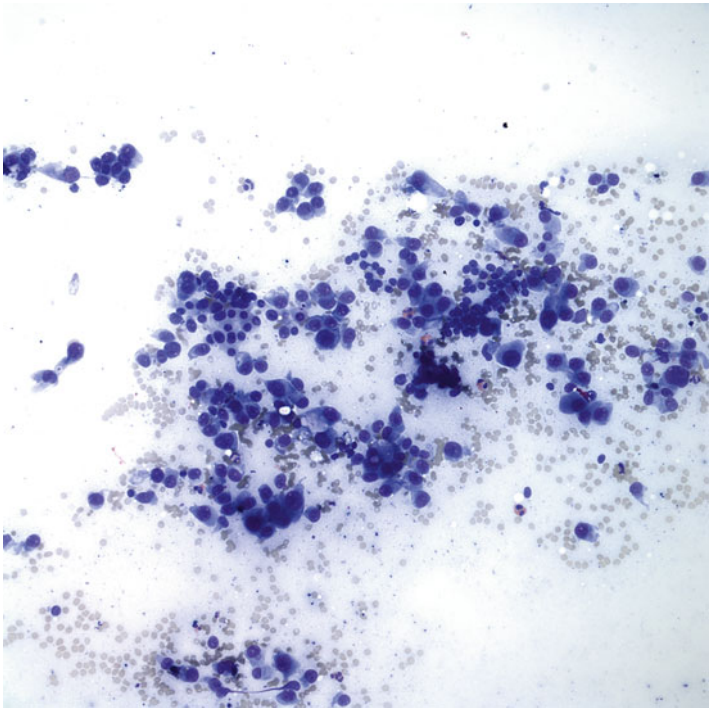

Fig. 11.13 Medullary carcinoma showing dispersed single cells with plasmacytoid appearance (Papanicolaou stain, X200)

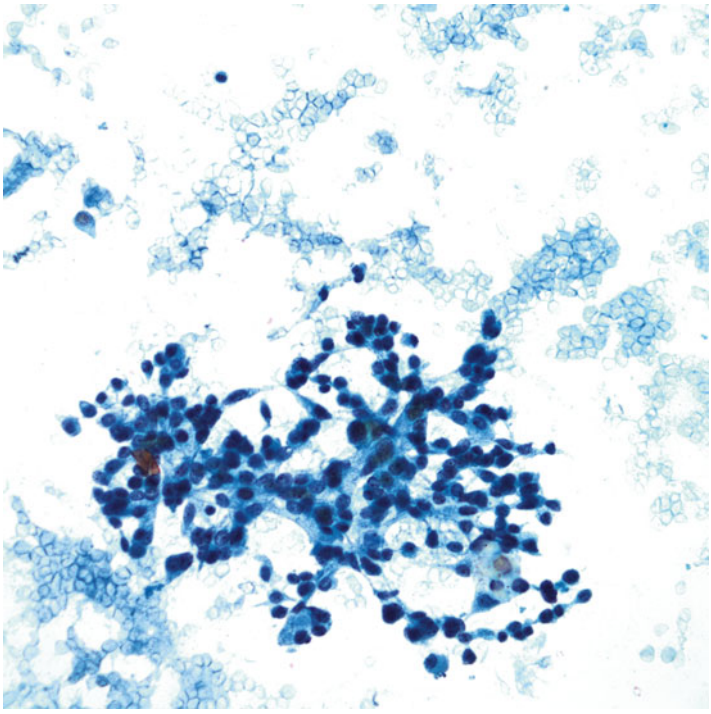

Fig. 11.14 The presence of syncytial tissue fragment in medullary carcinoma (Papanicolaou stain, X400)

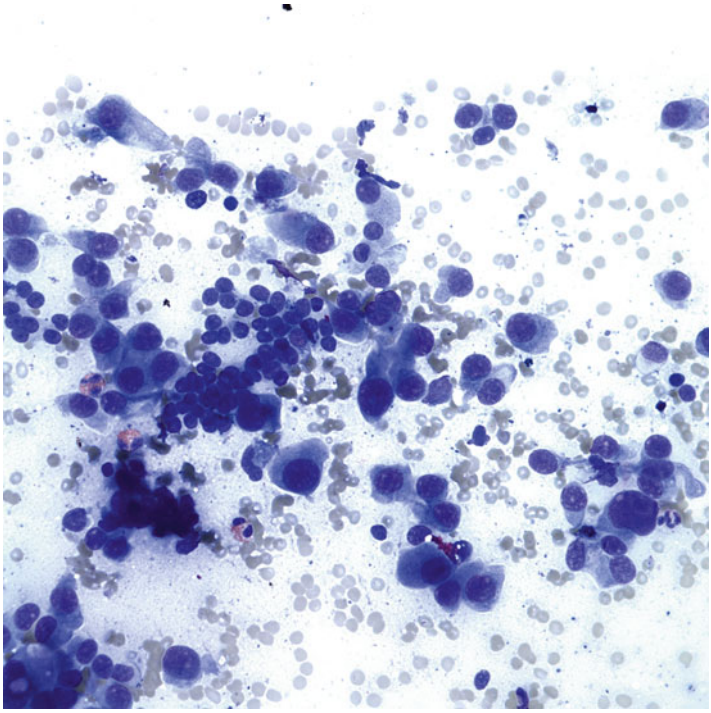

Fig. 11.15 Medullary carcinoma with eccentrically placed nuclei, giving the cells a plasmacytoid appearance. Intranuclear pseudoinclusion is often present (Papanicolaou stain, X400)

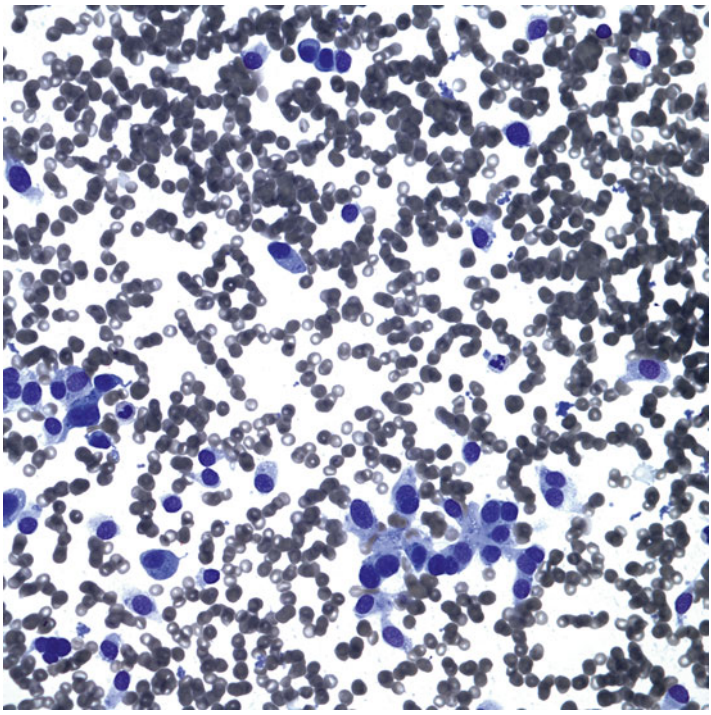

Fig. 11.16 Medullary carcinoma with dispersed single cells showing a plasmacytoid appearance (Papanicolaou stain, X400)

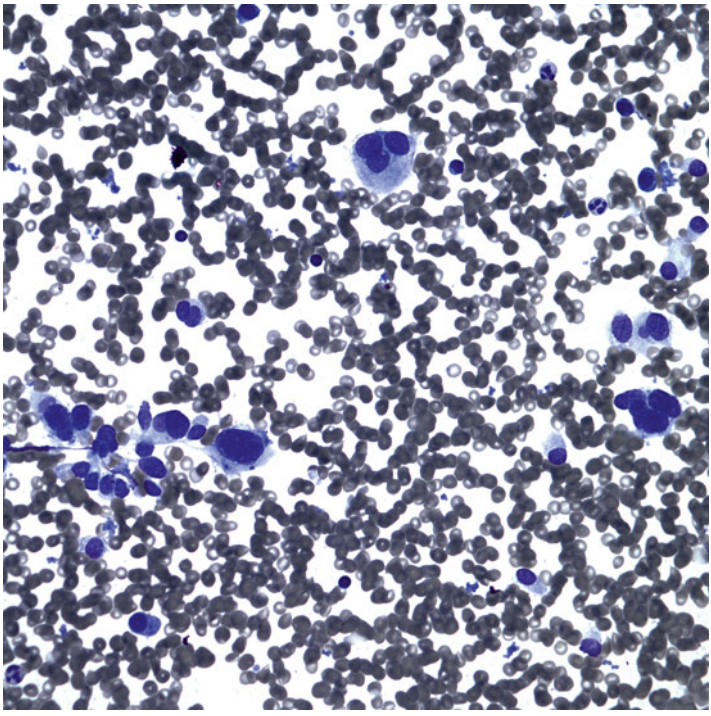

Fig. 11.17 Binucleation and multinucleation are common features in medullary carcinoma (Papanicolaou stain, X400)

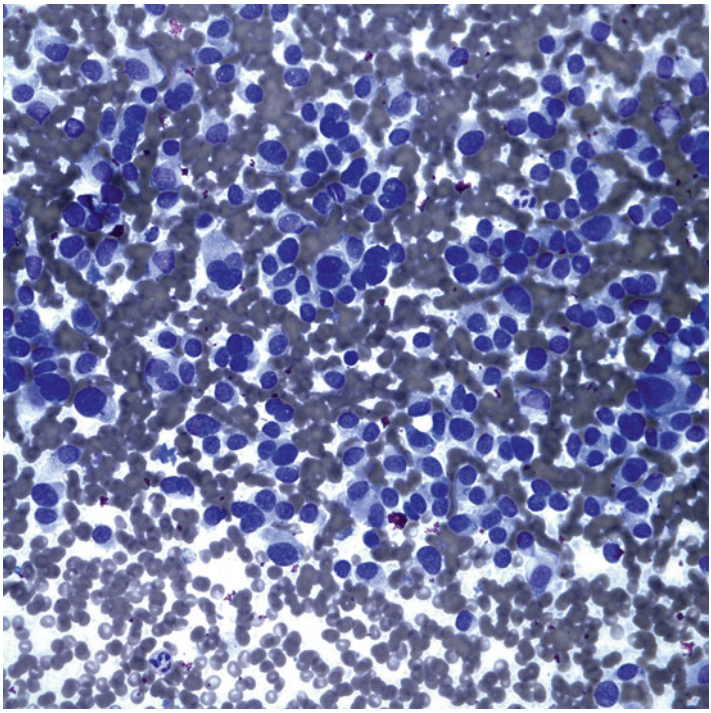

Fig. 11.18 Nuclei have a coarsely granular chromatin texture and inconspicuous nucleoli, thereby giving the so-called "salt and pepper" appearance (Papanicolaou stain, X400)

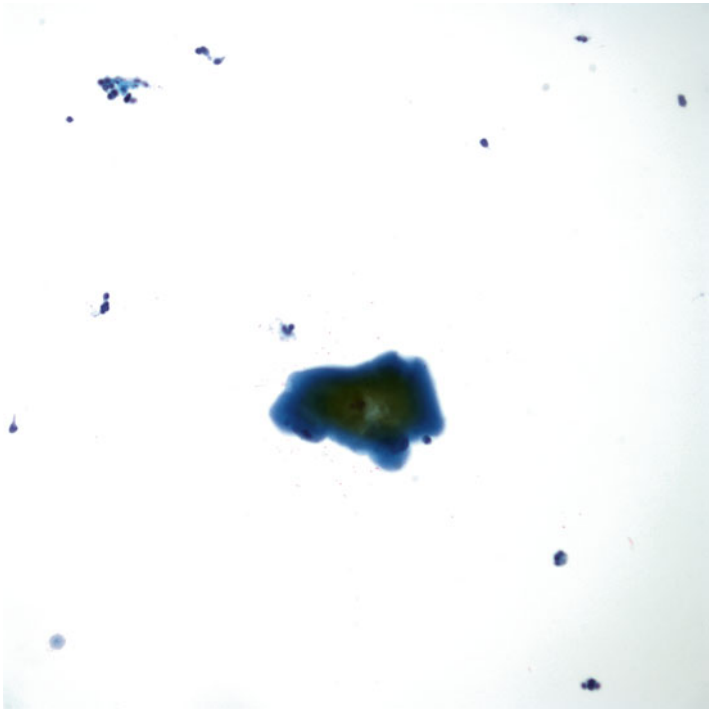

Fig. 11.19 Dense acellular material in FNA of medullary carcinoma, representing amyloid (Papanicolaou stain, X200)

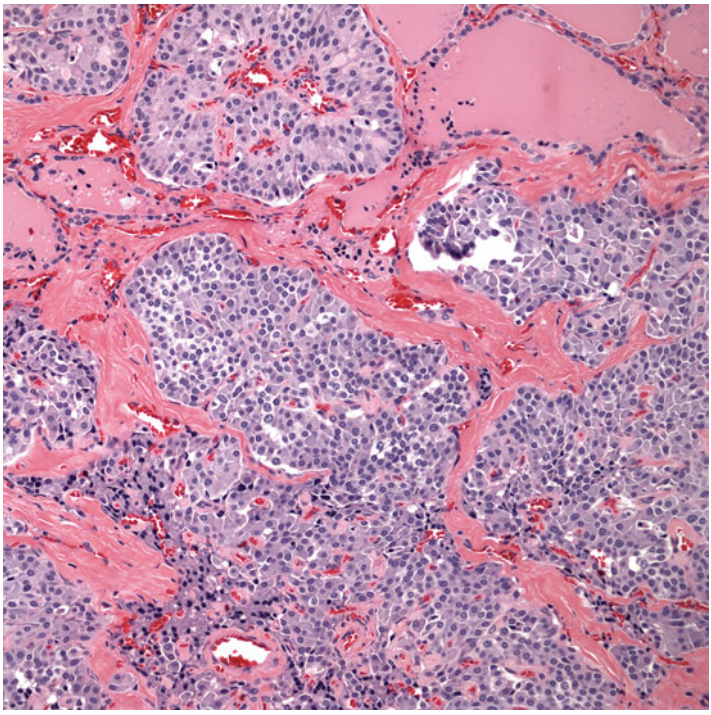

Fig. 11.20 Medullary carcinoma showing nests with a predominantly, uniform cuboidal cell pattern (H&E stain, X200)

Numerous cytoarchitectural variants of medullary carcinoma are now well recognized [21, 23, 29–32], although most tumors have admixtures of them (Figs. 11.20, 11.21, 11.22 and 11.23). The different subtypes do not have an important impact on prognosis, but their recognition is important to avoid confusion with other tumor types. The presence of papillary structures in medullary carcinoma can mimic papillary carcinoma (PTC) especially when intranuclear inclusions and psammoma bodies are present [33, 34] (Fig. 11.24). Amyloid may also be confused with the thick "chewing-gum-like" colloid of PTC [33]. Some variants of PTC such as the columnar or the oncocytic variant, in which the typical nuclear features of PTC are not well developed, may also enter into the differential diagnosis. The presence of papillary structures or even of true papillae with fibrovascular cores is not specific for PTC as it may also be found in the papillary or pseudopapillary variant of medullary carcinoma [17, 33, 35]. On rare occasion, PTC and medullary carcinoma may coexist in the same gland [36].

Tumor cell arrangement as rosettes and microfollicles can mimic a follicular neoplasm [17, 37] (Figs. 11.25, 11.26, and 11.27). In a study by Bose et al. [38], a microfollicular pattern was present in 13 of 38 cases (34.2 %) of medullary carcinoma. This pattern may even be prominent in some cases [17]. Conversely, in some follicular neoplasms, cell dissociation and the presence of polymorphic cells may occur, resembling medullary carcinoma.

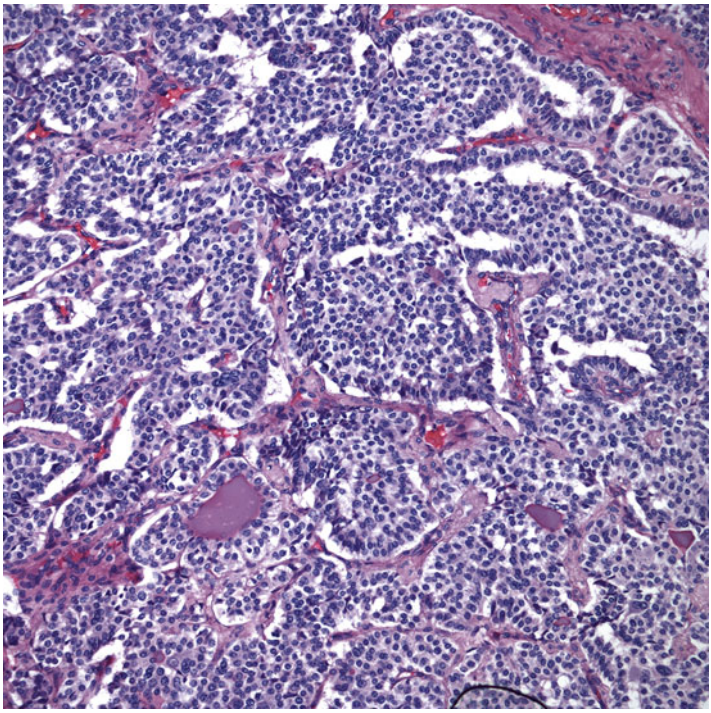

Fig. 11.21 Medullary carcinoma showing a mixture of solid and pseudo-glandular growth patterns. The cells are small and round. This appearance is reminiscent of carcinoid tumors (Papanicolaou stain, X200)

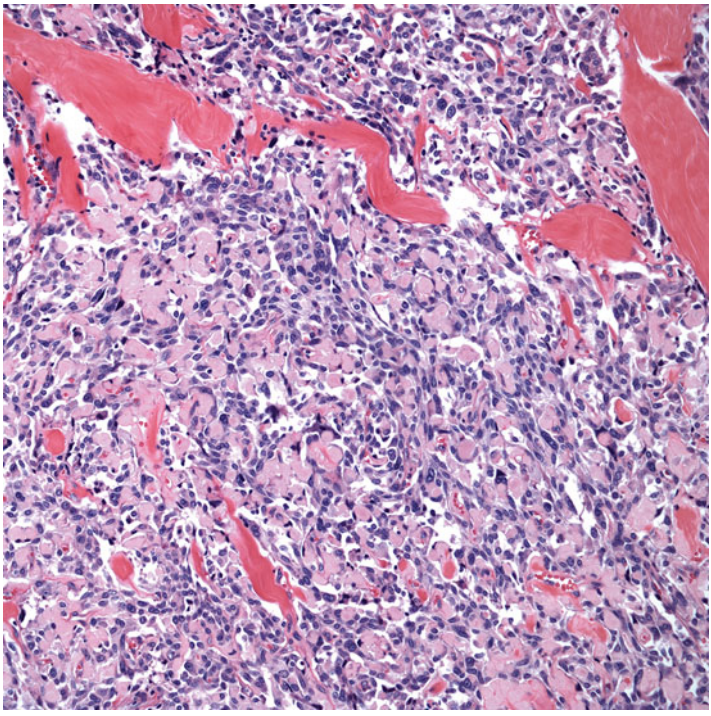

Fig. 11.22 The presence of prominent basement membrane-like material in medullary carcinoma (Papanicolaou stain, X200)

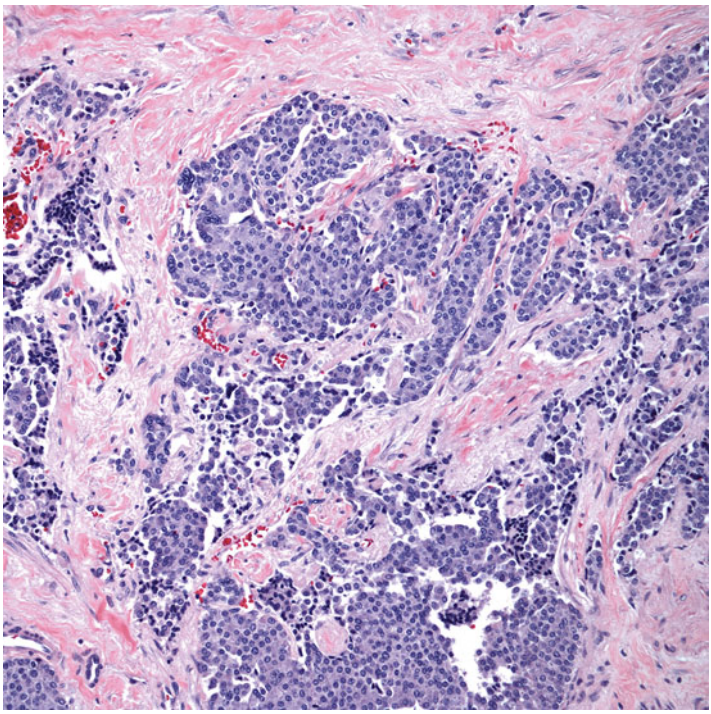

Fig. 11.23 Small nests, cords, and ribbon-like growth patterns in medullary carcinoma (Papanicolaou stain, X200)

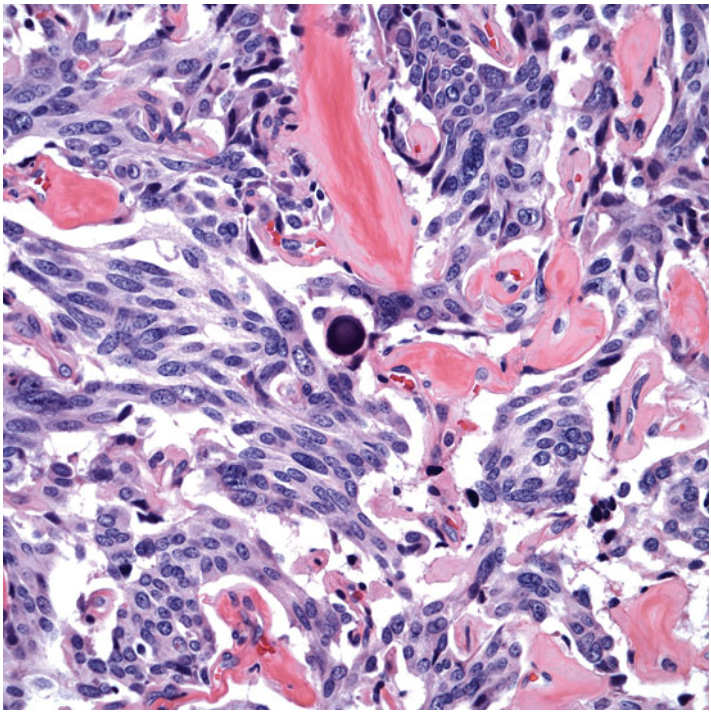

Fig. 11.24 The presence of Psammoma bodies is a common finding in medullary carcinoma (Papanicolaou stain, X200)

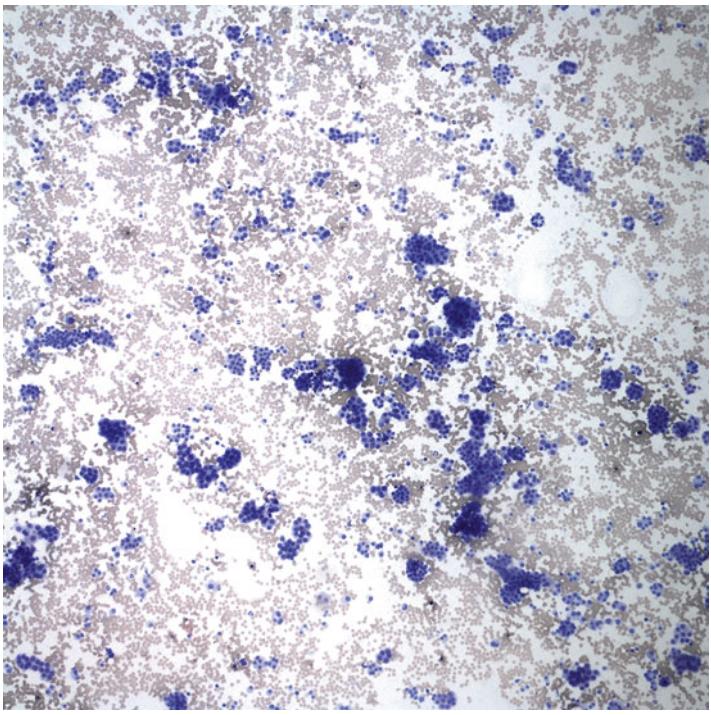

Fig. 11.25 Hypercellular specimen with numerous rosettes and small follicles in the absence of colloid. This pattern may be mistaken for a follicular neoplasm (Papanicolaou stain, X100)

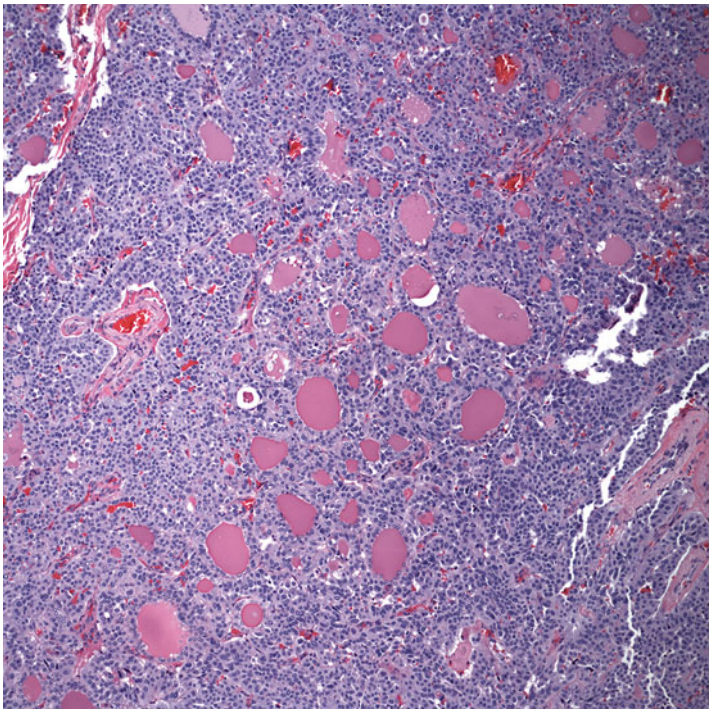

Fig. 11.26 Tumor cell arrangement as prominent follicles can mimic a follicular neoplasm (H&E stain, X100)

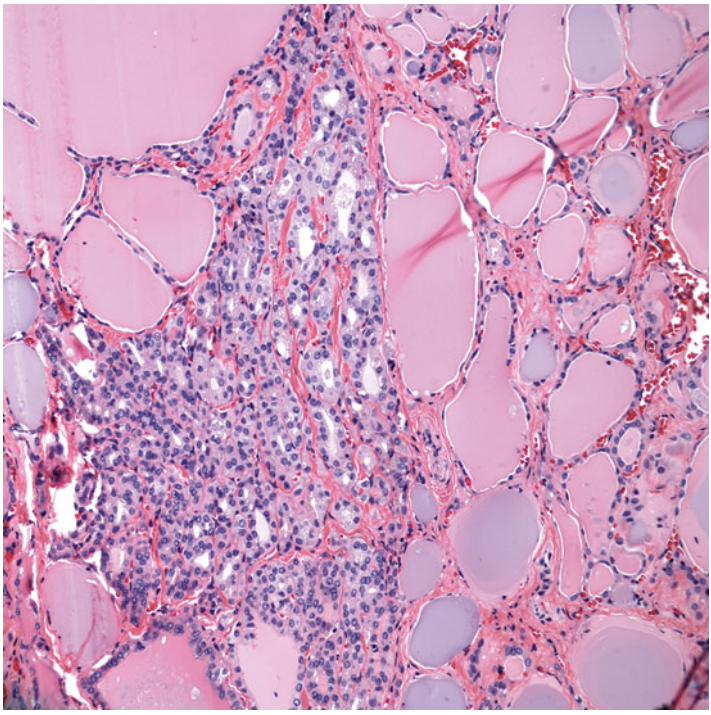

Fig. 11.27 Another image showing prominent follicular growth pattern in medullary carcinoma (H&E stain, X200)

Dispersed single cell pattern can mimic a lymphoma and can also mimic a plasmacytoma when the dispersed single cells have prominent plasmacytoid appearance. In primary thyroid plasmacytoma, discohesive plasmacytoid cells and amyloid/amyloid-like materials, which are major features of medullary carcinoma, may all be seen. However, the tumor cells of medullary carcinoma are generally larger than plasma cells [39] (Figs. 11.28 and 11.29).

Medullary carcinoma with a pure or predominant spindle cell component can mimic spindle cell sarcoma, melanoma, or sarcomatoid carcinoma [40]. Spindle or bizarre cells can mimic a sarcoma or anaplastic carcinoma. The spindle-type cells in medullary carcinoma when present singly and in loose clusters can also be misinterpreted in FNA samples as anaplastic carcinoma; however, it lacks the nuclear pleomorphism, mitotic activity, and necrosis of the latter.

Dispersed single polygonal cells with abundant granular cytoplasm are commonly seen in regular medullary carcinoma. However, oncocytic medullary carcinoma is dominated by tumor cells that look like Hürthle cells and can be confused with Hürthle cell neoplasm [41] (Figs. 11.30, 11.31, 11.32, and 11.33). As such, medullary carcinoma should be considered in the differential diagnosis of any thyroid Hürthle cell neoplasm. Cytologic features favoring medullary carcinoma include the paucity of macronucleoli and the presence of amyloid. Similar to

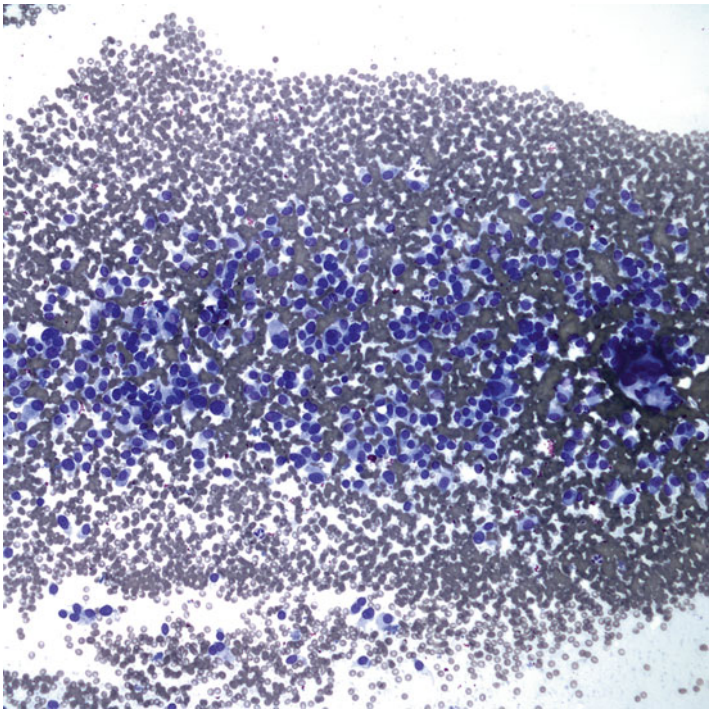

Fig. 11.28 Plasmacytoma is a major differential diagnosis. However, as seen here, cells of medullary carcinoma are generally larger than plasma cells (Diff-Quik stain, X200)

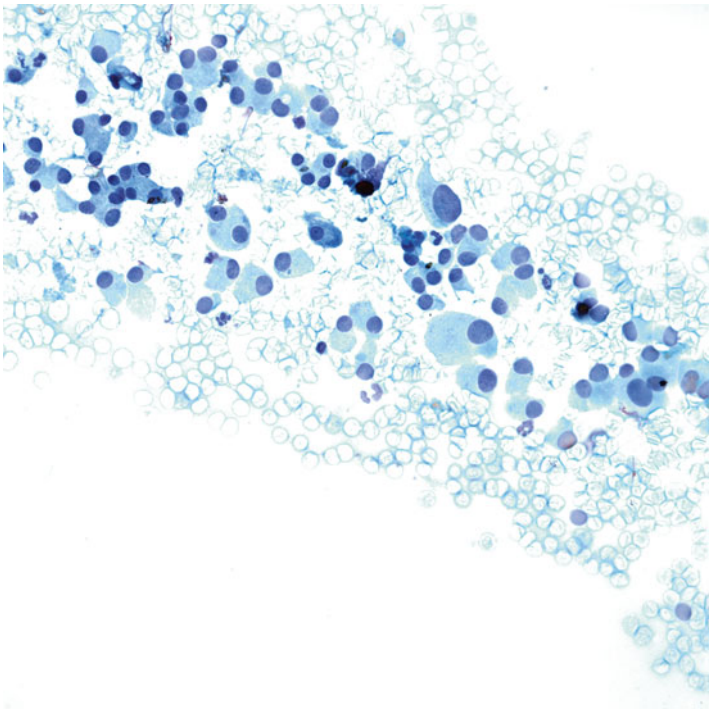

Fig. 11.29 Tumor cells in medullary carcinoma are generally larger than plasma cells (Papanicolaou stain, X400)

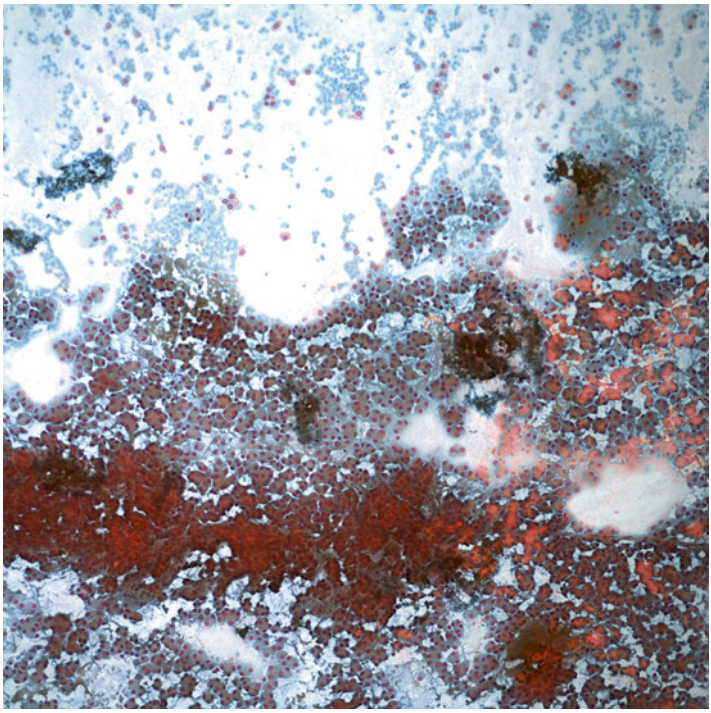

Fig. 11.30 Tumor cells that look like Hürthle cells and arranged as microfollicles dominate oncocytic medullary carcinoma. This can be confused with Hürthle cell neoplasm (Papanicolaou stain, X100)

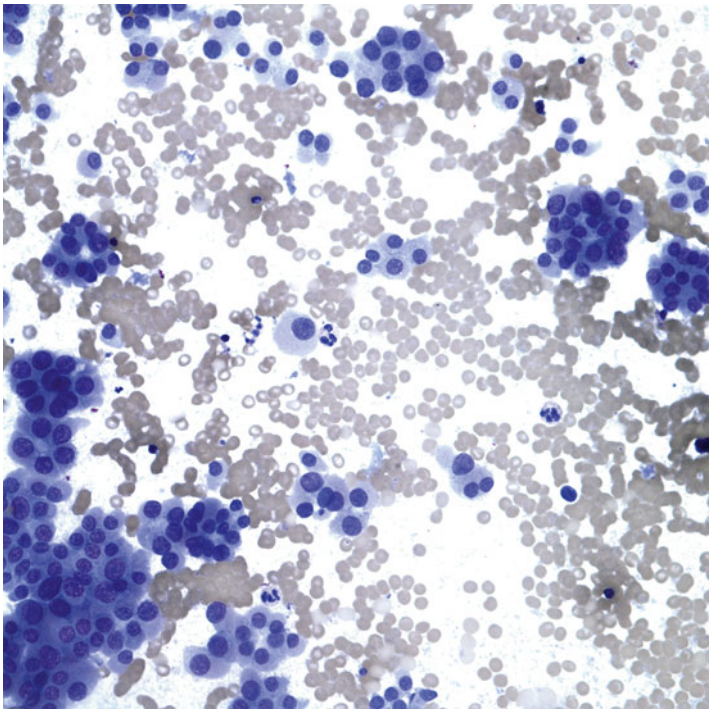

Fig. 11.31 Oncocytic cells arranged as small follicles may be confused with Hürthle cell neoplasm (Diff-Quik stain, X400)

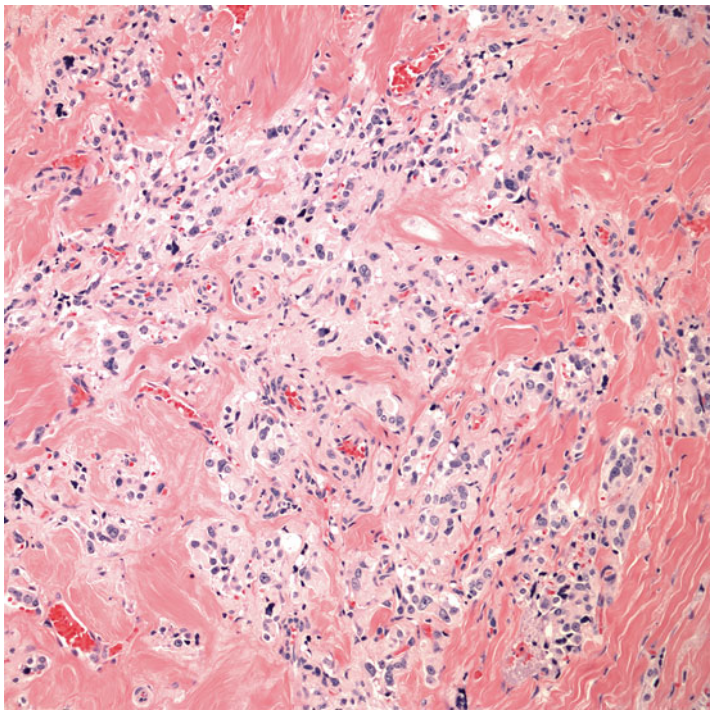

Fig. 11.32 Large polygonal cells with abundant oncocytic cytoplasm bear a morphologic resemblance to Hürthle cell neoplasm (H&E stain, X200)

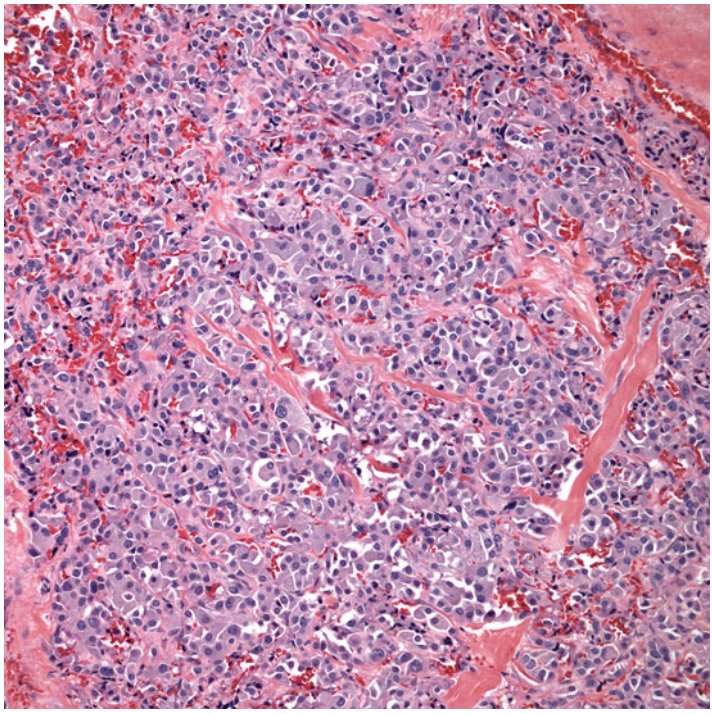

Fig. 11.33 Solid growth pattern with oncocytic neoplasm in oncocytic medullary carcinoma (H&E stain, X200)

medullary carcinoma, Hürthle cell neoplasms often present as hypercellular, discohesive single cells with eccentric nuclei (plasmacytoid cells), and granular cytoplasm [26, 42]. However, rather than a salt-and-pepper chromatin, most cells of a Hürthle cell neoplasm have a prominent red macronucleolus. In contrast, macronucleoli are identified only in a minority of cells in typical medullary carcinoma [17, 40]. However, as mentioned previously, an oncocytic variant of medullary carcinoma has been recognized where most tumor cells may be of the oncocytic type [33, 41]. Therefore, in difficult cases, immunocytochemistry with calcitonin, CEA, and thyroglobulin will solve the diagnostic dilemma (Figs. 11.34, 11.35, and 11.36).

The small cell variant of medullary carcinoma is a very unusual tumor, which behaves more aggressively than typical medullary carcinoma [4]. It may be impossible on morphologic examination to distinguish this variant from metastatic small cell carcinoma of the lung or of another site (e.g., bladder). Other small cell tumors such as lymphoma, neuroblastoma, and primitive neuroectodermal tumor also enter into the differential diagnosis [43, 44]. Moreover, amyloid may be absent, and immunoreactivity for calcitonin can be negative in this variant [4, 45], which is why some authors may arguably consider it as a primary small cell carcinoma of the thyroid or as an undifferentiated form of medullary carcinoma [46, 47]. However,

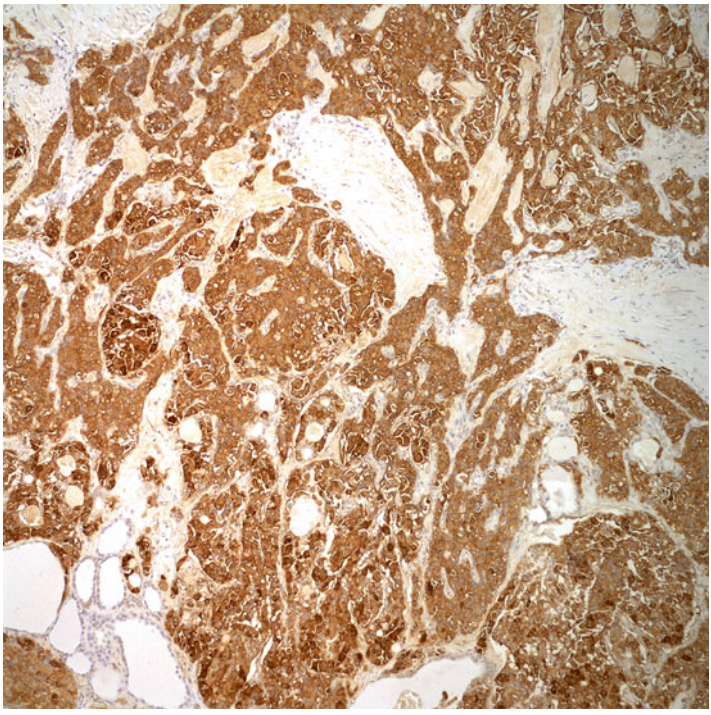

Fig. 11.34 Medullary carcinoma demonstrating strong and diffuse positive reactivity with calcitonin stain

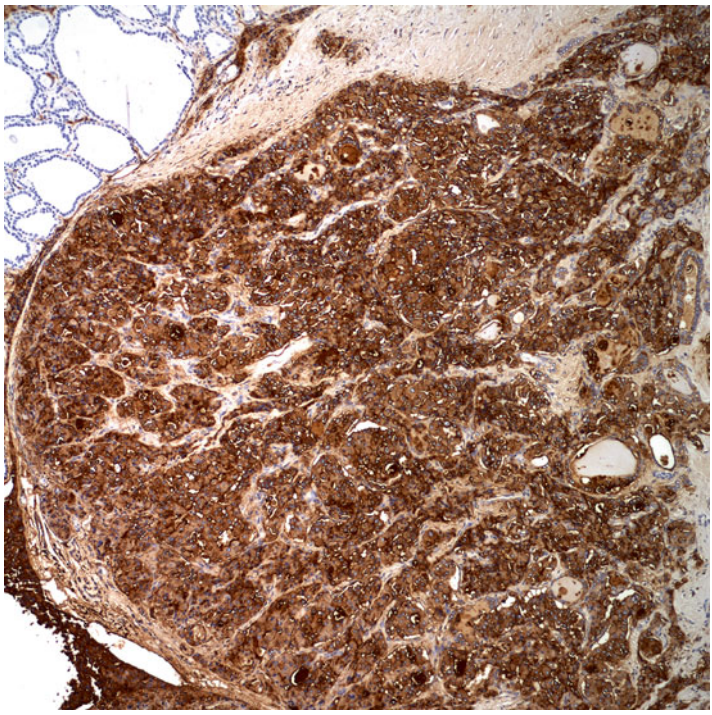

Fig. 11.35 Medullary carcinoma demonstrating strong and diffuse positive reactivity with polyclonal CEA stain

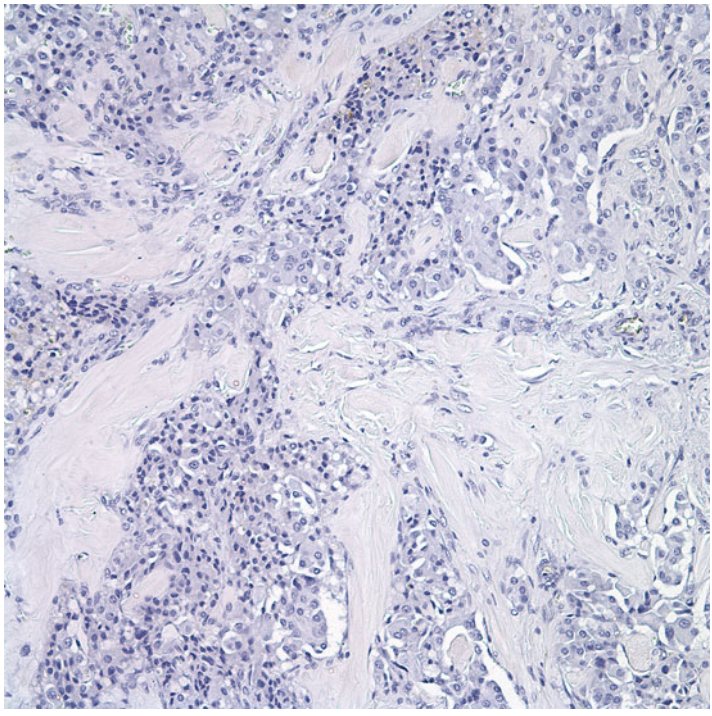

Fig. 11.36 Medullary carcinoma demonstrating negative reactivity with thyroglobulin stain

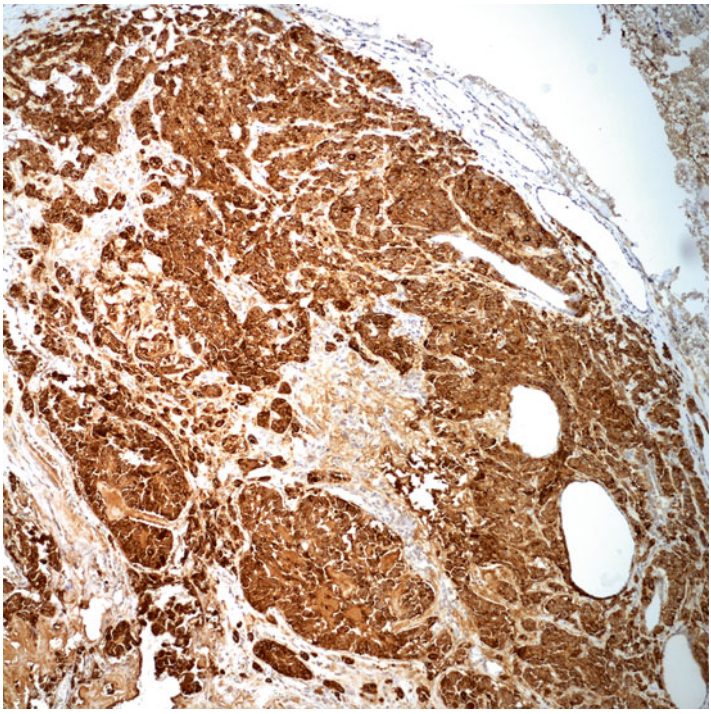

Fig. 11.37 Medullary carcinoma demonstrating strong and diffuse positive reactivity with chromogranin stain

CEA will often be positive as in other types of medullary carcinoma (88–100 % of cases) [4]. Positivity for CEA supports a diagnosis of medullary carcinoma even in the absence of calcitonin and other neuroendocrine marker immunoreactivity in the setting of MEN2. Consequently, a panel of antibodies consisting of calcitonin, CEA, PAX-8, chromogranin (Fig. 11.37), cytokeratin, and leukocyte common antigen is useful for the correct diagnosis. Thyroid transcription factor 1 (TTF-1) is not helpful as it will often also be positive in metastatic small cell carcinoma from the lung or from other sites. Diagnosis of the small cell variant of medullary carcinoma should be made with caution, particularly when tumor cells do not express calcitonin [46]. Some tumors initially interpreted as small cell variants of medullary carcinoma proved to be examples of metastatic neuroendocrine carcinomas to the thyroid, after follow-up [47, 48]. In difficult cases, the distinction may rely only on the clinical history.

Poorly differentiated carcinoma, especially the insular type, may be extremely difficult to distinguish from medullary carcinoma. Sometimes, a more differentiated component with microfollicles and colloid will also be present. Immunocytochemistry will also be very helpful in this differential diagnosis. The pigmented variant of medullary carcinoma and the clear cell variant of medullary carcinoma can mimic melanoma or renal clear cell carcinoma (Fig. 11.38), respectively. Clinical correlation and immunocytochemistry are crucial in avoiding pitfalls in these situations.

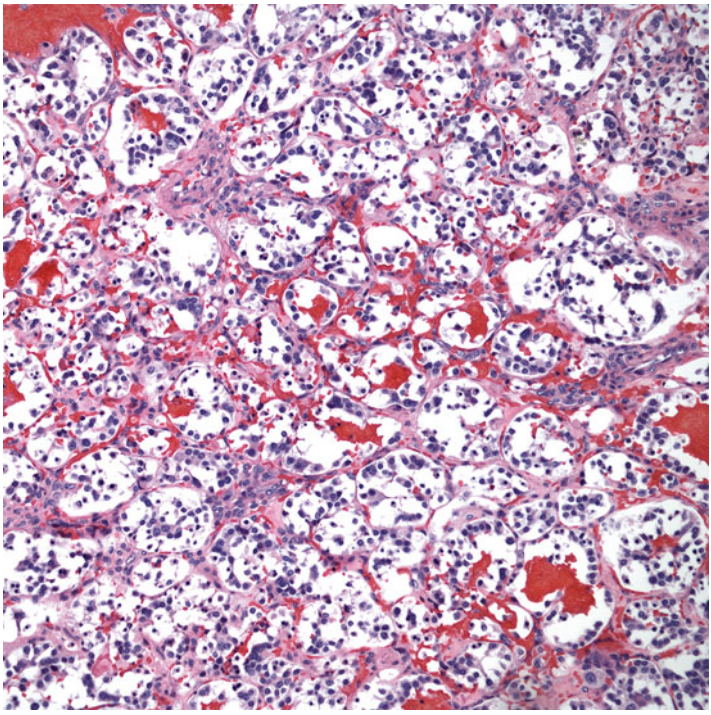

Fig. 11.38 Medullary carcinoma with cells showing prominent clearing of the cytoplasm. This can mimic clear cell renal cell carcinoma and other tumors with clear cell features (H&E, X200)

The most useful marker for the diagnosis of medullary carcinoma is calcitonin, with a reported sensitivity of 74–100 % on cytology [17, 49]. Sporadic cases of medullary carcinoma may be less frequently immunoreactive (74–79 %) than familial cases (100 %) [38, 50]. Although calcitonin is also the most specific marker for medullary carcinoma, a nonspecific reaction of the antibodies can occur with oncocytic neoplasms, possibly leading to a misdiagnosis of medullary carcinoma. However, if immunochemistry for thyroglobulin is performed, medullary carcinoma cells should be negative in contrast to follicular cell-derived oncocytic neoplasms. CEA is also very sensitive (80–100 %) for medullary carcinoma but is less specific than calcitonin. Multiple immunohistochemical stains can usually be performed whenever there is enough cell block material following an FNA. However, more often than not, cell block is infrequently made, and most centers rely on direct smears and thin prep material for the interpretation of thyroid FNA. When medullary carcinoma is suspected in such cases, it is usually prudent to make additional thin prep slides, and limited immunohistochemical stains (most importantly, calcitonin) can be performed on such (Fig. 11.39). Very rarely, original smears may have to be destained for calcitonin stain to be performed. When none of these is possible, it is expedient to suspect medullary carcinoma and append a note in the diagnosis to state that the patient will benefit from serum calcitonin assay.

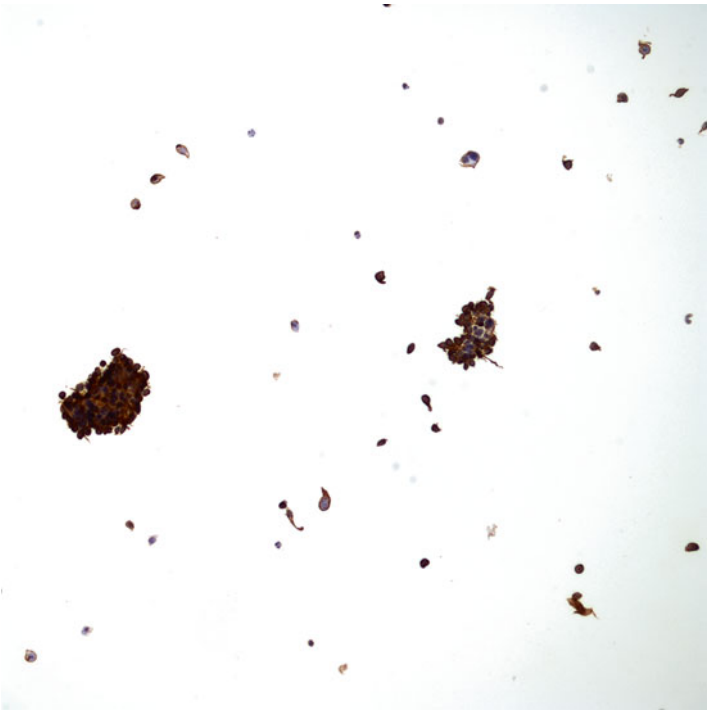

Fig. 11.39 The cells show strong reactivity with calcitonin stain performed on ThinPrep material

References

1. Baloch ZW, LiVolsi VA. Neuroendocrine tumors of the thyroid gland. Am J Clin Pathol. 2001;115(Suppl):S56–67.
2. DeLellis R. In: DeLellis RA, Lloyd RV, Heitz PU, et al., editors. Pathology and genetics of tumors of endocrine organs, World Health Organization classification of tumors. Lyon: IARC Press; 2004. p. 122–3.
3. You YN, Lakhani V, Wells Jr SA, Moley JF. Medullary thyroid cancer. Surg Oncol Clin N Am. 2006;15:639–60.
4. Rosai J, DeLellis RA, Cargangiu ML, Frable WJ, Tallini G. Tumors of the thyroid and parathyroid glands. Atlas of tumor pathology. Fascicle 21, series 4. Washington, DC: Armed Forces Institute of Pathology; 2014.
5. Hu MI, Ying AK, Jimenez C. Update on medullary thyroid cancer. Endocrinol Metab Clin North Am. 2014;43:423–42.
6. Rendl G, Manzl M, Hitzl W, Sungler P, Pirich C. Long-term prognosis of medullary thyroid carcinoma. Clin Endocrinol (Oxf). 2008;69:497–505.
7. Modigliani E, Cohen R, Campos JM, Conte-Devolx B, Maes B, Boneu A, Schlumberger M, Bigorgne JC, Dumontier P, Leclerc L, Corcuff B, Guilhem I. Prognostic factors for survival and for biochemical cure in medullary thyroid carcinoma: results in 899 patients. The GETC Study Group. Groupe d'étude des tumeurs à calcitonine. Clin Endocrinol (Oxf). 1998;48:265–73.

8. Bugalho MJ, Santos JR, Sobrinho L. Preoperative diagnosis of medullary thyroid carcinoma: fine needle aspiration cytology as compared with serum calcitonin measurement. J Surg Oncol. 2005;91:56–60.
9. Clark JR, Fridman TR, Odell MJ, Brierley J, Walfish PG, Freeman JL. Prognostic variables and calcitonin in medullary thyroid cancer. Laryngoscope. 2005;115:1445–50.
10. Brutsaert EF, Gersten AJ, Tassler AB, Surks MI. Medullary thyroid cancer with undetectable serum calcitonin. J Clin Endocrinol Metab. 2015;100:337–41.
11. Pelizzo MR, Boschin IM, Bernante P, Toniato A, Piotto A, Pagetta C, Nibale O, Rampin L, Muzzio PC, Rubello D. Natural history, diagnosis, treatment and outcome of medullary thyroid cancer: 37 years experience on 157 patients. Eur J Surg Oncol. 2007;33:493–7.
12. Fugazzola L, Pinchera A, Luchetti F, Iacconi P, Miccoli P, Romei C, Puccini M, Pacini F. Disappearance rate of serum calcitonin after total thyroidectomy for medullary thyroid carcinoma. Int J Biol Markers. 1994;9:21–4.
13. Meijer JA, Le Cessie S, van den Hout WB, Kievit J, Schoones JW, Romijn JA, Smit JW. Calcitonin and carcinoembryonic antigen doubling times as prognostic factors in medullary thyroid carcinoma: a structured meta-analysis. Clin Endocrinol (Oxf). 2010;72:534–42.
14. Kini S. Thyroid cytopathology: an Atlas and text. Philadelphia: Wolters Kluwer/Lippincott Williams & Wilkins; 2008.
15. Matias-Guiu X, De Lellis R. Medullary thyroid carcinoma: a 25-year perspective. Endocr Pathol. 2014;25:21–9.
16. Chang TC, Wu SL, Hsiao YL. Medullary thyroid carcinoma: pitfalls in diagnosis by fine needle aspiration cytology and relationship of cytomorphology to RET proto-oncogene mutations. Acta Cytol. 2005;49:477–82.
17. Papaparaskeva K, Nagel H, Droese M. Cytologic diagnosis of medullary carcinoma of the thyroid gland. Diagn Cytopathol. 2000;22:351–8.
18. Chen H, Sippel RS, O'Dorisio MS, Vinik AI, Lloyd RV, Pacak K, North American Neuroendocrine Tumor Society (NANETS). The North American Neuroendocrine Tumor Society consensus guideline for the diagnosis and management of neuroendocrine tumors: pheochromocytoma, paraganglioma, and medullary thyroid cancer. Pancreas. 2010;39:775–83.
19. Boi F, Maurelli I, Pinna G, Atzeni F, Piga M, Lai ML, Mariotti S. Calcitonin measurement in wash-out fluid from fine needle aspiration of neck masses in patients with primary and metastatic medullary thyroid carcinoma. J Clin Endocrinol Metab. 2007;92:2115–8.
20. Kudo T, Miyauchi A, Ito Y, Takamura Y, Amino N, Hirokawa M. Diagnosis of medullary thyroid carcinoma by calcitonin measurement in fine-needle aspiration biopsy specimens. Thyroid. 2007;17:635–8.
21. Papotti M, Sambataro D, Pecchioni C, Bussolati G. The pathology of medullary carcinoma of the thyroid: review of the literature and personal experience on 62 cases. Endocr Pathol. 1996;7:1–20.
22. Colson YL, Carty SE. Medullary thyroid carcinoma. Am J Otolaryngol. 1993;14:73–81.
23. Uribe M, Fenoglio-Preiser CM, Grimes M, Feind C. Medullary carcinoma of the thyroid gland. Clinical, pathological, and immunohistochemical features with review of the literature. Am J Surg Pathol. 1985;9:577–94.
24. Schreiner AM, Yang GC. Medullary thyroid carcinoma presenting as rectangular cell type on fine-needle aspiration. Diagn Cytopathol. 2009;37:213–6.
25. Us-Krasovec M, Flezar M, Kloboves-Prevodnik V. Rare cytologic findings in medullary thyroid carcinoma. Acta Cytol. 2002;46:434–6.
26. Forrest CH, Frost FA, de Boer WB, Spagnolo DV, Whitaker D, Sterrett BF. Medullary carcinoma of the thyroid: accuracy of diagnosis of fine-needle aspiration cytology. Cancer. 1998;84:295–302.
27. Us-Krasovec M, Auersperg M, Bergant D, Golouh R, Kloboves-Prevodnik V. Medullary carcinoma of the thyroid glad: diagnostic cytopathological characteristics. Pathologica. 1998;90:5–13.
28. DeLellis RA, May L, Tashjian Jr AH, Wolfe HJ. C-cell granule heterogeneity in man. An ultrastructural immunocytochemical study. Lab Invest. 1978;38:263–9.

29. Albores-Saavedra J, LiVolsi VA, Williams ED. Medullary carcinoma. Semin Diagn Pathol. 1985;2:137–46.
30. Harach HR, Bergholm U. Medullary carcinoma of the thyroid with carcinoid-like features. J Clin Pathol. 1993;46:113–7.
31. Sambade C, Baldaque-Faria A, Cardoso-Oliveira M, Sobrinho-Simões M. Follicular and papillary variants of medullary carcinoma of the thyroid. Pathol Res Pract. 1988;184:98–107.
32. Mendelsohn G, Baylin SB, Bigner SH, Wells Jr SA, Eggleston JC. Anaplastic variants of medullary thyroid carcinoma: a light-microscopic and immunohistochemical study. Am J Surg Pathol. 1980;4:333–41.
33. Kulacoglu S, Ashton-Key M, Buley I. Pitfalls in the diagnosis of papillary carcinoma of the thyroid. Cytopathology. 1998;9:193–200.
34. Wirth LJ, Ross DS, Randolph GW, et al. Case records of the Massachusetts General Hospital. Case 5-2013. A 52-year-old woman with a mass in the thyroid. N Engl J Med. 2013;368: 664–73.
35. Das A, Gupta SK, Banerjee AK, et al. Atypical cytologic features of medullary carcinoma of the thyroid. A review of 12 cases. Acta Cytol. 1992;36:137–41.
36. Adnan Z, Arad E, Dana J, et al. Simultaneous occurrence of medullary and papillary thyroid microcarcinomas: a case series and review of the literature. J Med Case Rep. 2013;7:26.
37. Suster S. Thyroid tumors with a follicular growth pattern: problems in differential diagnosis. Arch Pathol Lab Med. 2006;130:984–8.
38. Bose S, Kapila K, Verma K. Medullary carcinoma of the thyroid: a cytological, immunocytochemical, and ultrastructural study. Diagn Cytopathol. 1992;8:28–32.
39. Pusztaszeri MP, Bongiovanni M, Faquin WC. Update on the cytologic and molecular features of medullary thyroid carcinoma. Adv Anat Pathol. 2014;21:26–35.
40. Bhanot P, Yang J, Schnadig VJ, et al. Role of FNA cytology and immunochemistry in the diagnosis and management of medullary thyroid carcinoma: report of six cases and review of the literature. Diagn Cytopathol. 2007;35:285–92.
41. Dominguez-Malagon H, Delgado-Chavez R, Torres-Najera M, Gould E, Albores-Saavedra J. Oxyphil and squamous variants of medullary thyroid carcinoma. Cancer. 1989;63:1183–8.
42. Green I, Ali SZ, Allen EA, et al. A spectrum of cytopathologic variations in medullary thyroid carcinoma. Fine needle aspiration findings in 19 cases. Cancer. 1997;81:40–4.
43. Harach HR, Bergholm U. Small cell variant of medullary carcinoma of the thyroid with neuroblastoma-like features. Histopathology. 1992;21:378–80.
44. Kumar M, Gupta P, Chaubey A. The thyroid: an extremely rare primary site of neuroblastoma. Hum Pathol. 2006;37:1357–60.
45. Yerly S, Triponez F, Meyer P, et al. Medullary thyroid carcinoma, small cell variant, as a diagnostic challenge on fine needle aspiration: a case report. Acta Cytol. 2010;54 Suppl 5:911–7.
46. Eusebi V, Damiani S, Riva C, et al. Calcitonin free oat-cell carcinoma of the thyroid gland. Virchows Arch A Pathol Anat Histopathol. 1990;417:267–71.
47. Matias-Guiu X, LaGuette J, Puras-Gil AM, et al. Metastatic neuroendocrine tumors to the thyroid gland mimicking medullary carcinoma: a pathologic and immunohistochemical study of six cases. Am J Surg Pathol. 1997;21:754–62.
48. Puente S, Velasco A, Gallel P, Pallares J, Perez-Ruiz L, Ros S, Maravall J, Matias-Guiu X. Metastatic small cell carcinoma to the thyroid gland: a pathologic and molecular study demonstrating the origin in the urinary bladder. Endocr Pathol. 2008;19:190–6.
49. Das DK, Mallik MK, George SS, et al. Secretory activity in medullary thyroid carcinoma: a cytomorphological and immunocytochemical study. Diagn Cytopathol. 2007;35:329–37.
50. Takami H, Bessho T, Kameya T, et al. Immunohistochemical study of medullary thyroid carcinoma: relationship of clinical features to prognostic factors in 36 patients. World J Surg. 1988;12:572–9.

Hyalinizing Trabecular Tumor

12

Case Study

An 85-year-old white female was noted to have a right thyroid nodule on routine medical examination. She had no history of hoarseness, difficulty in swallowing, or difficulty in breathing and no symptoms of hyperthyroidism. She had no history of radiation to the neck or face and no history of neck surgery. Patient had a past medical history of hypertension and stage 3 kidney failure with hyperkalemia. Patient had never smoked and had no family history of thyroid cancer. Physical examination revealed a low thyroid, with a smooth, mobile nodule in the right lobe. There was no palpable cervical lymphadenopathy. Thyroid ultrasonographic evaluation showed a $2.7 \times 2.0 \times 1.9$ cm hypoechoic nodule in the right lobe. The nodule was well defined and had grade III intranodular vascularity, and there were some calcifications within the nodule. Fine needle aspiration cytology of the right thyroid showed scant follicular cells with nuclear enlargement and rare intranuclear inclusions and was read as suspicious for papillary thyroid carcinoma. Patient subsequently had a right thyroid lobectomy. The lobe showed a 3.0 cm well-circumscribed nodule. Tumor cells had oval, enlarged nuclei with abundant nuclear grooves and were arranged in nests and trabeculae surrounded by hyalinized stroma. The tumor showed numerous intranuclear inclusions and intracytoplasmic yellow bodies and showed strong membranous staining for MIB-1. Features were characteristic of hyalinizing trabecular tumor. Postoperative course was unremarkable.

Discussion

Hyalinizing trabecular tumor of the thyroid gland is a rare neoplasm of follicular origin that is characterized by an encapsulated nodule, a prominent trabecular growth pattern, and stromal hyalinization [1]. It is thought to be a rare variant of follicular adenoma, and it is also known as paraganglioma-like adenoma of the thyroid. The tumor has a predilection for women and the average age is in the 4th decade, but a wide age range has been reported [1, 2]. In previous reports,

A.J. Adeniran, D. Chhieng, *Common Diagnostic Pitfalls in Thyroid Cytopathology*, DOI 10.1007/978-3-319-31602-4_12

hyalinizing trabecular tumor was frequently associated with other abnormalities in the thyroid gland, most commonly lymphocytic thyroiditis, but was also seen together with papillary and follicular neoplasms as well as multinodular goiter [3, 4]. This tumor typically behaves in a benign fashion but malignant cases have been reported [5, 6]. There is a suggestion that there is a possibility that these malignant cases represent misdiagnosis of thyroid carcinoma with a focal hyalinized or trabecular growth pattern [7]. There has been significant debate on the most appropriate terminology for these tumors since their original description as hyalinizing trabecular adenomas in 1987 [1]. Due to the concern of a possible relationship with papillary thyroid carcinoma and case reports of malignant variants, the term "hyalinizing trabecular tumors" was proposed and is currently the classification accepted by the World Health Organization [8]. The possibility that hyalinizing trabecular tumors represent a variant of papillary thyroid carcinoma has been considered given that the tumors frequently coexist, and they share similar morphologic and nuclear features such as clearing, enlargement, elongation, grooves and inclusions, and the presence of occasional psammoma bodies. The fact that RET/PTC rearrangements have been detected in some tumors [9] and some show variable expression of galectin-3 [10] also adds credence to the suggestion that this tumor may represent a variant of papillary thyroid carcinoma. It has been previously reported [11] that the RET/PTC gene rearrangements found in hyalinizing trabecular tumors confirmed the "long-standing suspicion" that these tumors are in fact a variant of papillary thyroid carcinoma. However, on further genetic analysis, hyalinizing trabecular tumors have since been shown to be a discrete entity from papillary thyroid carcinoma with an absence of BRAF mutations [9], differential expression of miRNAs [12], and unique staining patterns for molecular markers including CD56 and MIB-1 [13, 14].

On gross examination, hyalinizing trabecular tumors are usually well circumscribed or encapsulated. Their color typically ranges from yellow to tan to gray pink, with a granular texture [15, 16] (Fig. 12.1). In comparison, papillary thyroid carcinomas are typically gray-white and lack a capsule. The histological sections show encapsulated tumor and the neoplastic cells are oval and polygonal to elongated, and spindle cells are arranged as solid nests or in a trabecular or alveolar growth pattern separated by variable dense hyaline stroma [4] (Figs. 12.2, 12.3, 12.4, and 12.5). The trabeculae are two- to three-cell-layer thick. The neoplastic cells adjacent to the stroma are often mummified, and those within the trabeculae form a pseudofollicular pattern, with or without colloid [2]. Elongated neoplastic cells may also align with their bases inserted vertically into the capillaries of the delicate fibrovascular stroma [17]. The cell nuclei often have perinuclear clearing, nuclear grooves, and nuclear inclusions similar to papillary thyroid carcinoma (Fig. 12.6). Cytoplasm is usually abundant and homogeneous, although it can be granular or vacuolar. Cytoplasmic hyaline bodies are characteristic, but these can also be seen in other thyroid neoplasms. Yellow cytoplasmic inclusions called "yellow bodies" are a distinctive feature unique from papillary thyroid carcinomas and represent lysosomes [18] (Fig. 12.7). Calcifications and psammoma bodies can be seen interspersed throughout the stroma [15]. Hyaline material is present

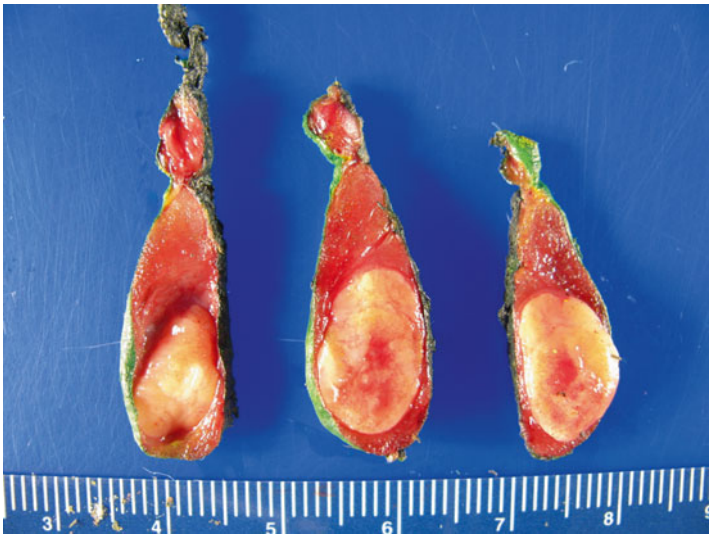

Fig. 12.1 Hyalinizing trabecular tumor. Thyroidectomy showing a large, discrete, encapsulated, well-circumscribed tan-yellow nodule

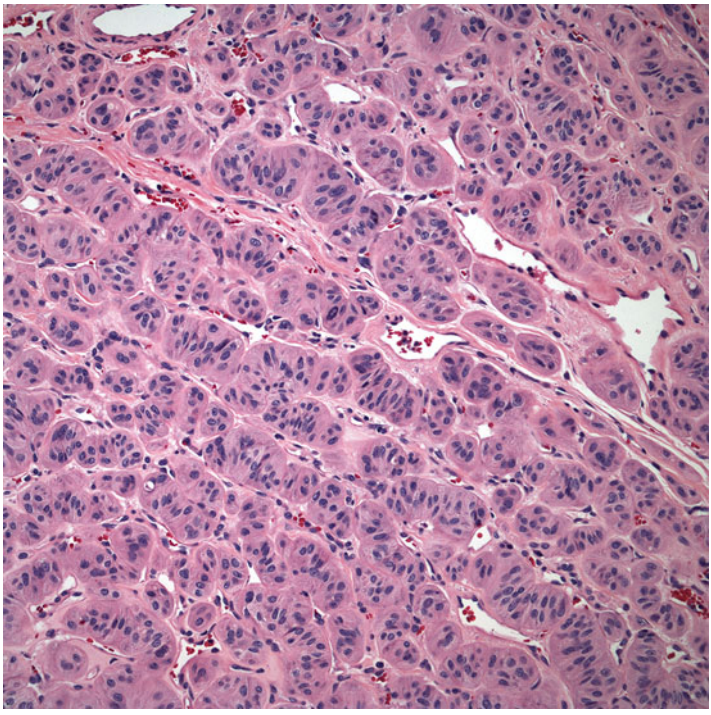

Fig. 12.2 Hyalinizing trabecular tumor. Histologic section showing trabecular growth pattern (H&E stain, X200)

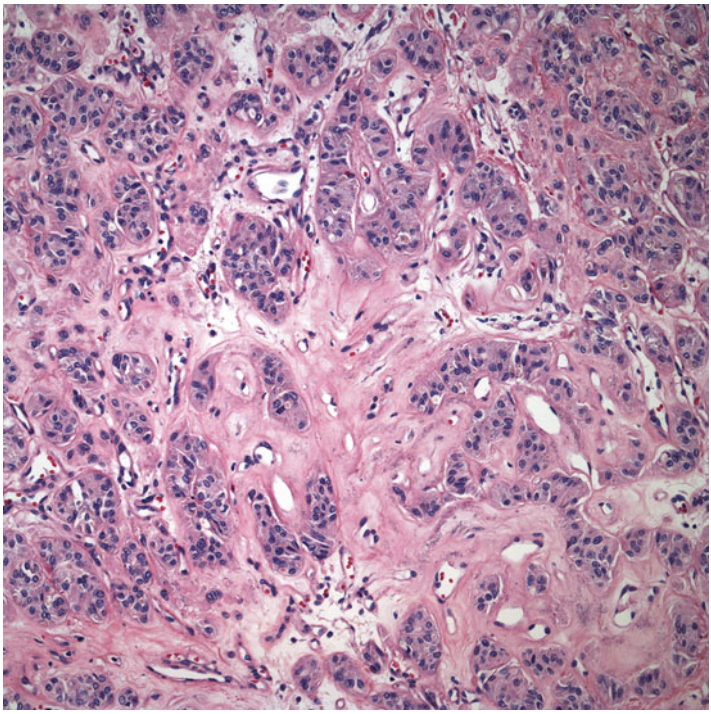

Fig. 12.3 Dense hyalinizing stroma separating the nests and trabeculae of neoplastic follicular cells (H&E stain, X200)

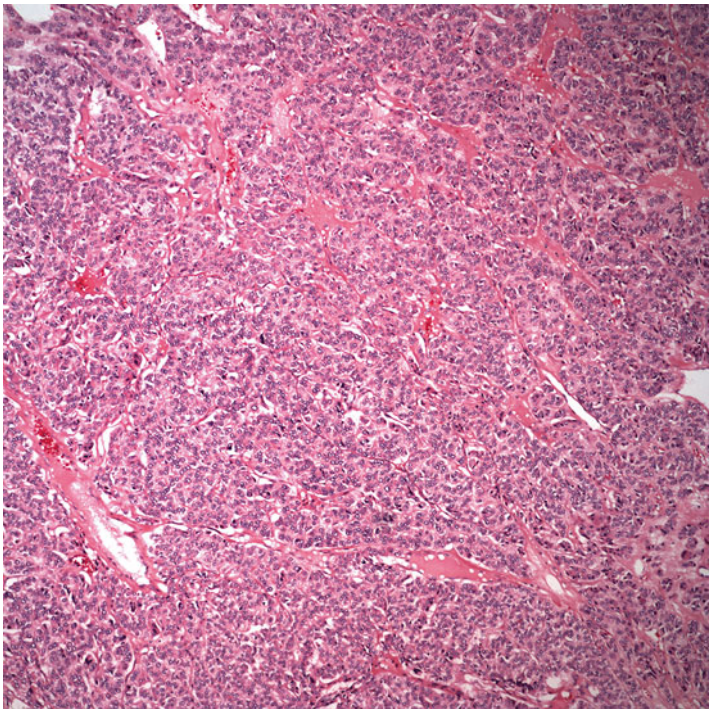

Fig. 12.4 Solid nests of tumor cells (H&E stain, X100)

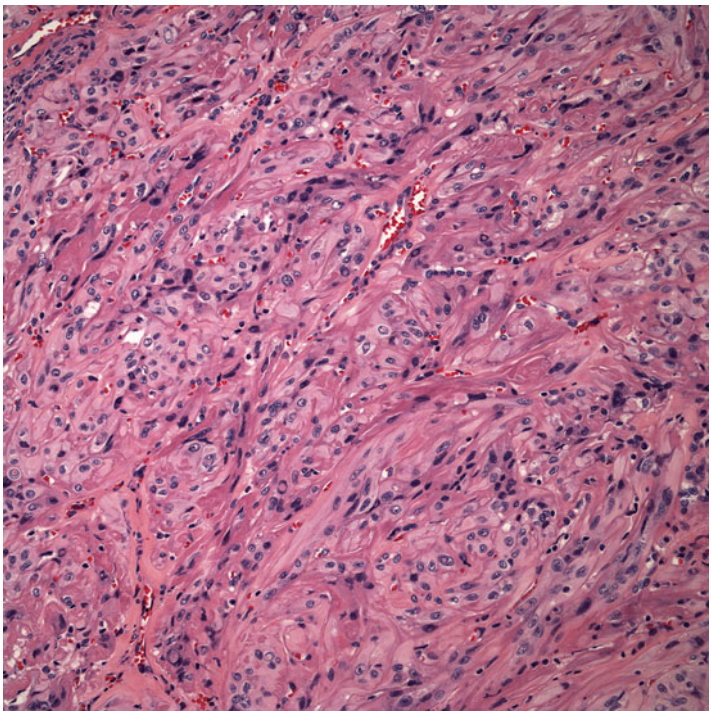

Fig. 12.5 Spindle cells arranged as solid nests (H&E stain, X200)

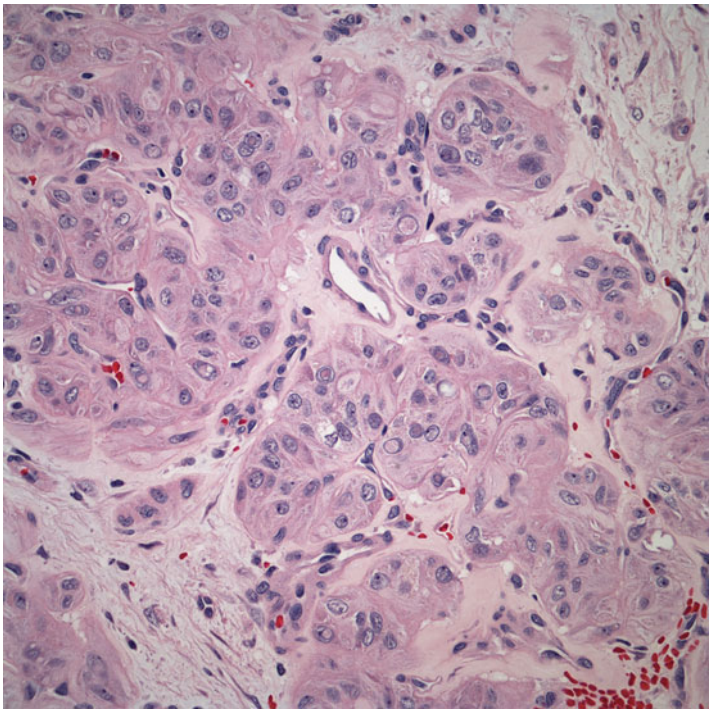

Fig. 12.6 Nuclear features in hyalinizing trabecular tumor—perinuclear clearing, nuclear grooves, and numerous intranuclear inclusions (H&E stain, 400)

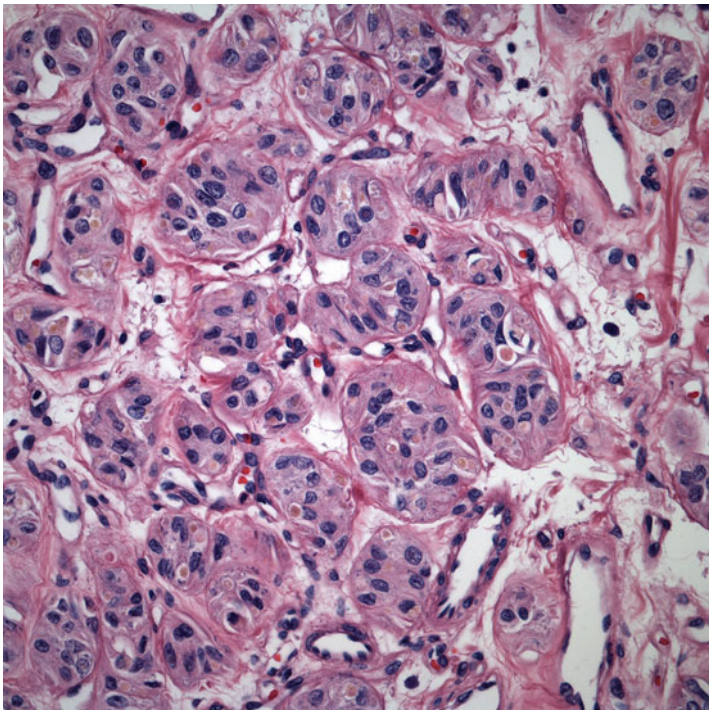

Fig. 12.7 The cytoplasm of many of the cells contains a *pale yellow*, spherical, refractile inclusion (*yellow* bodies) (H&E stain, X400)

extensively in both intracellular and extracellular locations. The hyaline material is finely fibrillar with fringed edges and forms irregular lumpy deposits. It can be mistaken for dense colloid or amyloid.

The characteristic FNA cytological findings of hyalinizing trabecular tumor are cellular arrangement of syncytial tissue fragments and cohesive aggregates oriented radially around hyaline material, in a bloody background (Figs. 12.8, 12.9, and 12.10). Cells are oval to spindled, with low nuclear-cytoplasmic ratio, fine chromatin, perinuclear clearing, abundant intranuclear inclusions, nuclear grooves, and occasional cytoplasmic yellow bodies [14, 19, 20] (Figs. 12.11, 12.12, 12.13, 12.14, and 12.15). There is a background of hyaline material (Figs. 12.16 and 12.17). Nuclear crowding and overlapping, papillary architecture, and microfollicular pattern are not typically seen. Of the two stains commonly used in cytology, the Papanicolaou stain is the more useful in cytodiagnosis of hyalinizing trabecular tumor because it reveals superior nuclear detail. The hyaline material, however, is more easily visualized with the Diff-Quik method because it is stained pink (metachromatic) against a blue background. The cytoplasmic yellow bodies are also more easily identified with the Diff-Quik stain. The Papanicolaou stain is superior in displaying the nuclear grooves, cytoplasmic invaginations, and nuclear overlapping. Thus, the two stains reveal different features of the tumor and are complementary. Ideally, both should be performed on all thyroid FNA biopsies [14].

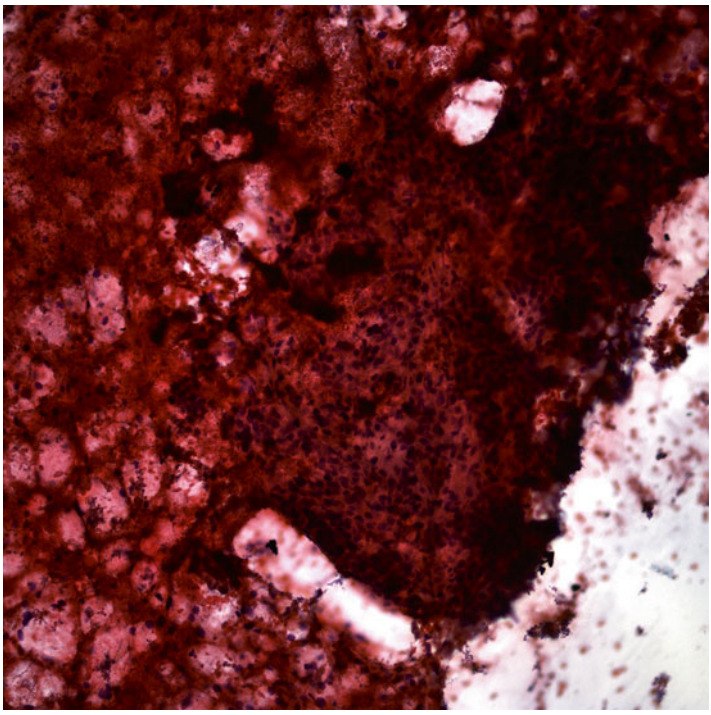

Fig. 12.8 Cohesive tissue fragments in a bloody background (Papanicolaou stain, X200)

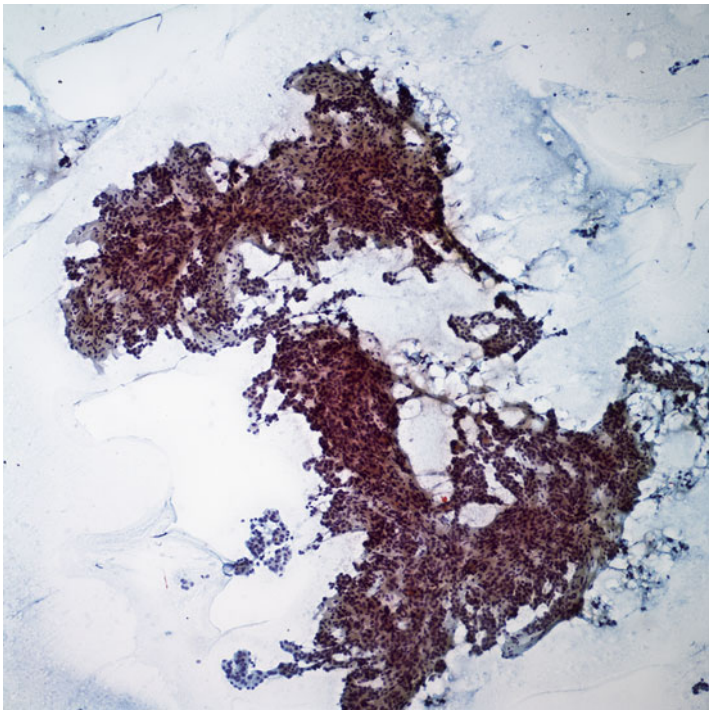

Fig. 12.9 Low-power view showing anastomosing trabeculae. Hyaline stroma is seen between the follicular cells (Papanicolaou stain, X100)

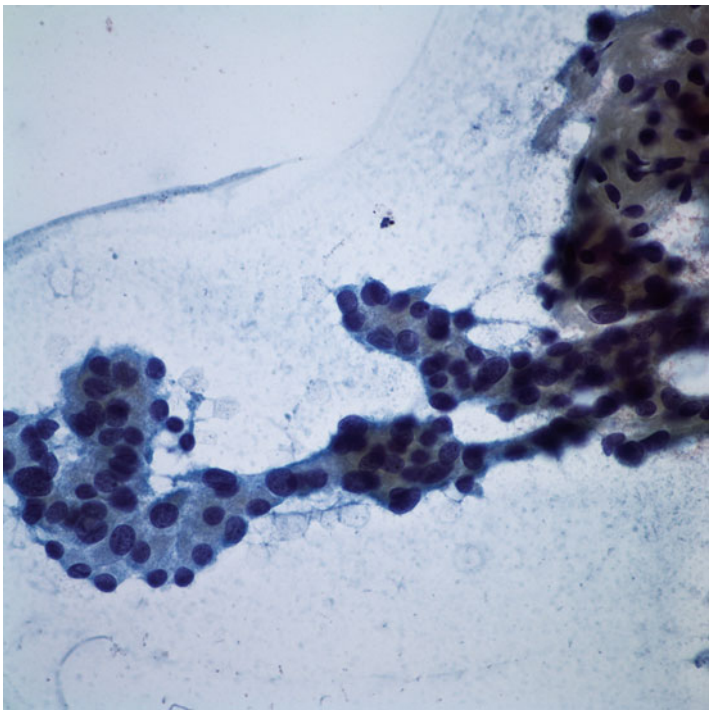

Fig. 12.10 Syncytial fragments of follicular cells with trabecular pattern (Papanicolaou stain, X400)

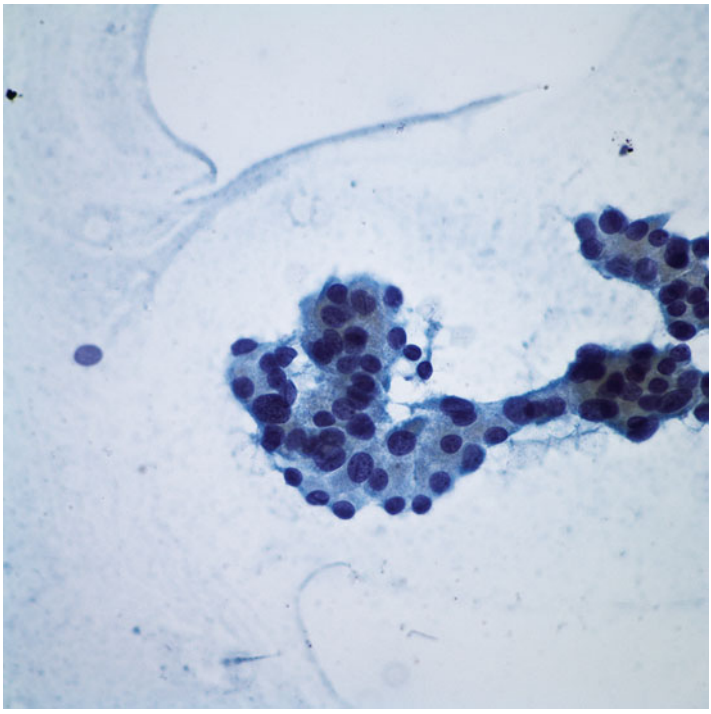

Fig. 12.11 Syncytial fragments of follicular cells with trabecular pattern. Scattered nuclear grooves are present. The cytoplasm is abundant and granular (Papanicolaou stain, X600)

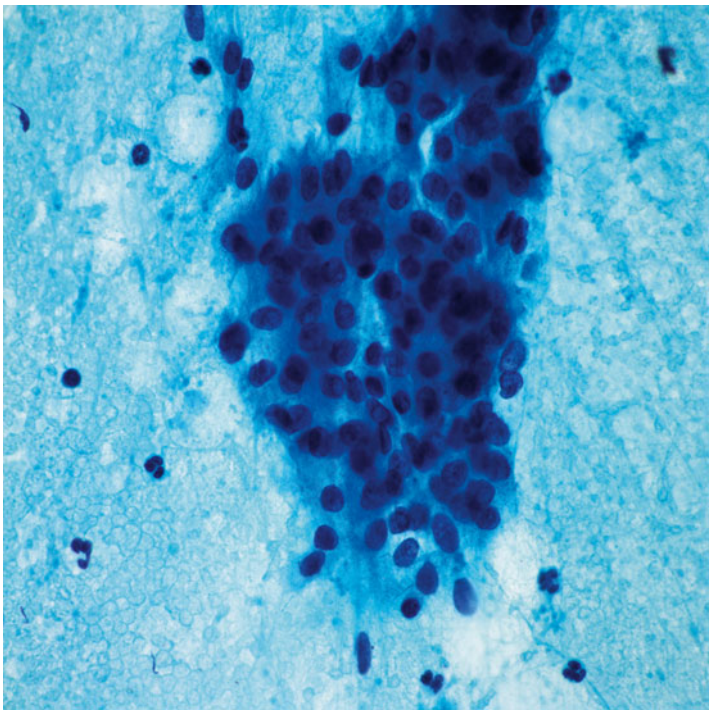

Fig. 12.12 Syncytial fragments of follicular cells. Cells with fine chromatin, nuclear grooves, and intranuclear inclusions (Papanicolaou stain, X600)

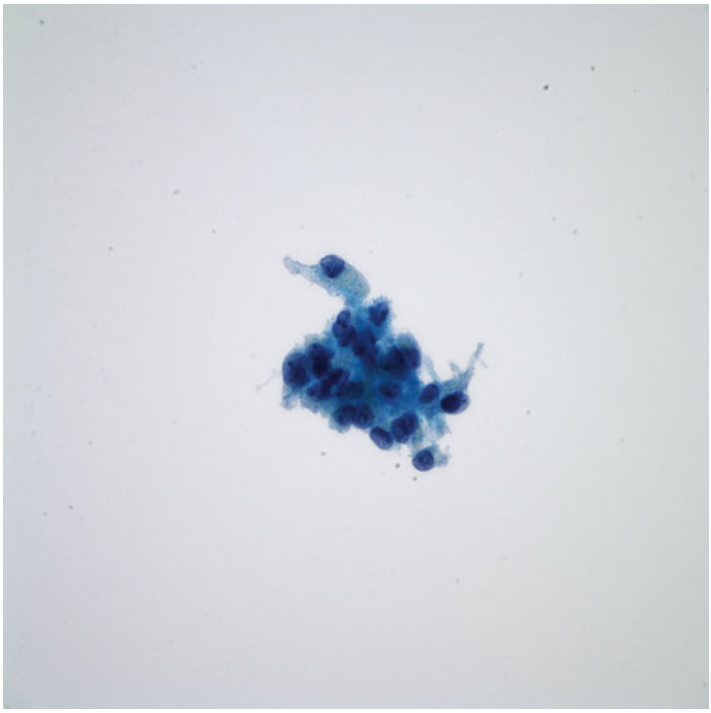

Fig. 12.13 Cells showing nuclei with powdery chromatin and nuclear grooves. The cytoplasm is abundant and granular (Papanicolaou stain, X600)

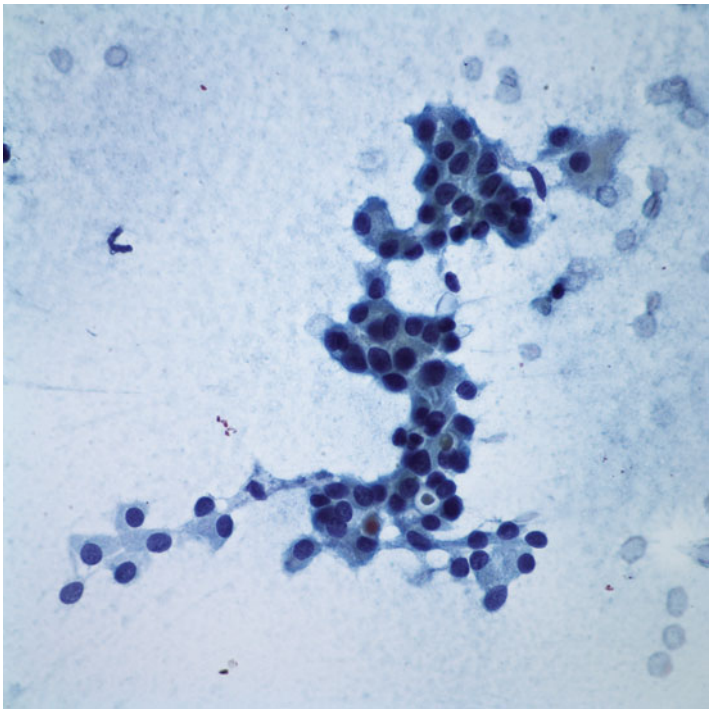

Fig. 12.14 Syncytial fragments of follicular cells with trabecular pattern. The cells show intracytoplasmic "yellow bodies" (Papanicolaou stain, X600)

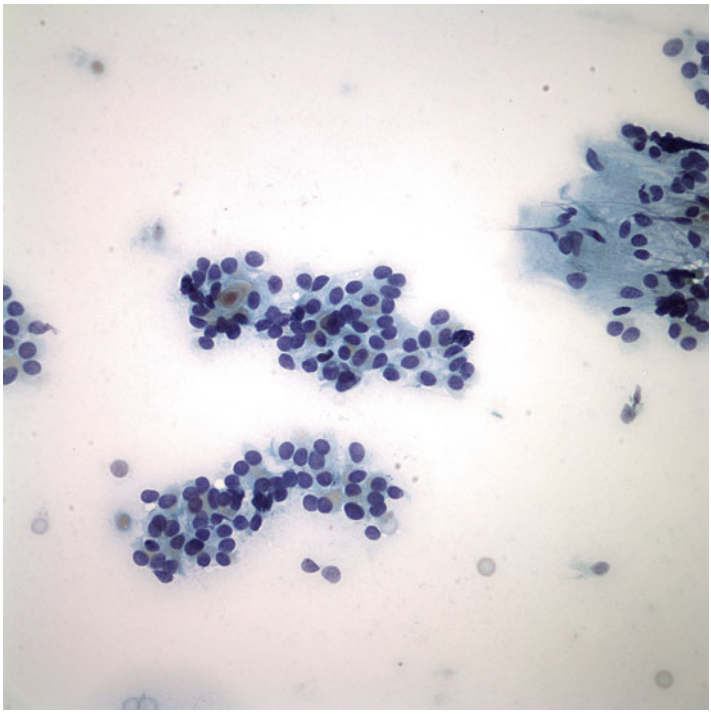

Fig. 12.15 Syncytial fragments of follicular cells with trabecular pattern. The cells show intracytoplasmic "yellow bodies." Hyaline stroma is seen in the right upper corner of the image (Papanicolaou stain, X400)

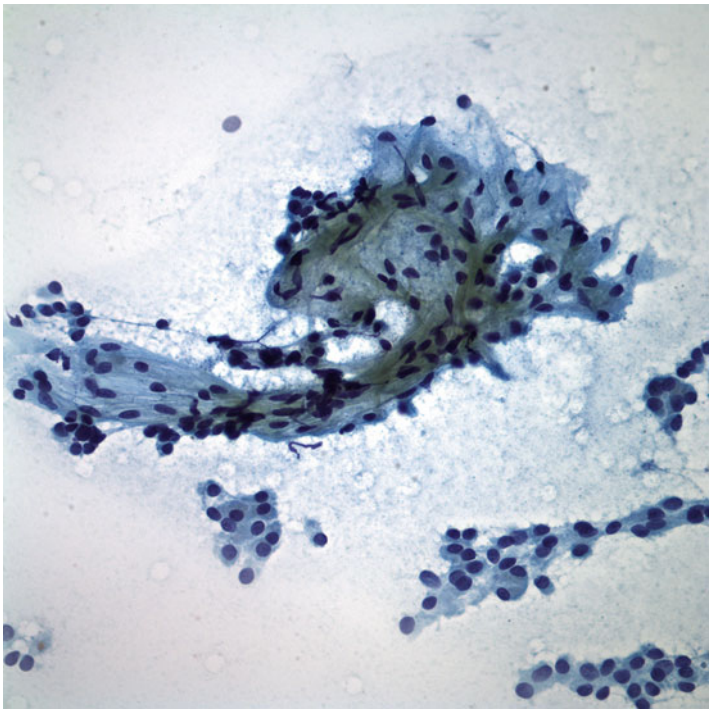

Fig. 12.16 Hyaline stroma is seen between the follicular cells (Papanicolaou stain, X400)

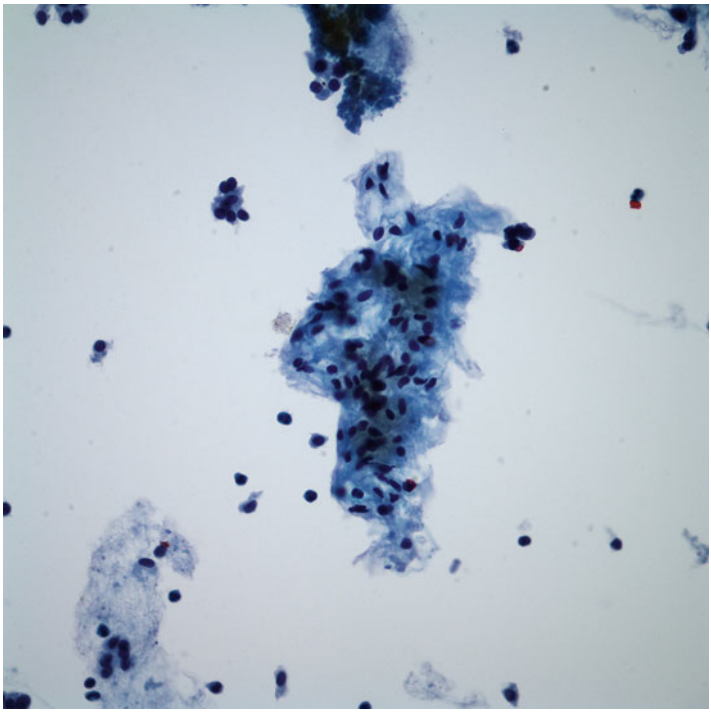

Fig. 12.17 Hyaline stroma (Papanicolaou stain, X400)

Hyalinizing trabecular tumors are frequently mistaken for papillary carcinoma, medullary carcinoma, or paraganglioma. Shared nuclear features between papillary carcinoma and hyalinizing trabecular tumor include nuclear groove and intranuclear inclusion. Of these features, intranuclear inclusion is mainly responsible for misdiagnosis, but true papillae, multinucleated giant cells, and bubblegum colloid are not present in hyalinizing trabecular tumor. Changes that have been reported to be more prevalent in hyalinizing trabecular tumor than in papillary cancer, and therefore can be helpful in establishing the diagnosis, include pronounced accumulation of basement membrane material giving rise to characteristic stromal deposits seen in fine needle aspirates [21, 22] and the presence of cytoplasmic yellow bodies [18]. Indeed, because of similar nuclear features and the presence of psammoma bodies, hyalinizing trabecular tumor is considered a subtype of papillary carcinoma, which is supported by the presence of the RET/PTC oncogene translocation (commonly found in papillary carcinoma) in some cases of hyalinizing trabecular tumor [9, 11]. However, the *RET/PTC* translocation is not specific for papillary carcinoma and has been found in several thyroid conditions, including Hashimoto's thyroiditis [23]. Furthermore, hyalinizing trabecular tumor is not associated with the *BRAF* mutation that frequently occurs in papillary carcinoma [9, 24, 25].

Immunohistochemically, like papillary carcinoma, hyalinizing trabecular tumor expresses thyroglobulin and TTF-1 (Fig. 12.18). Hyalinizing trabecular tumor can

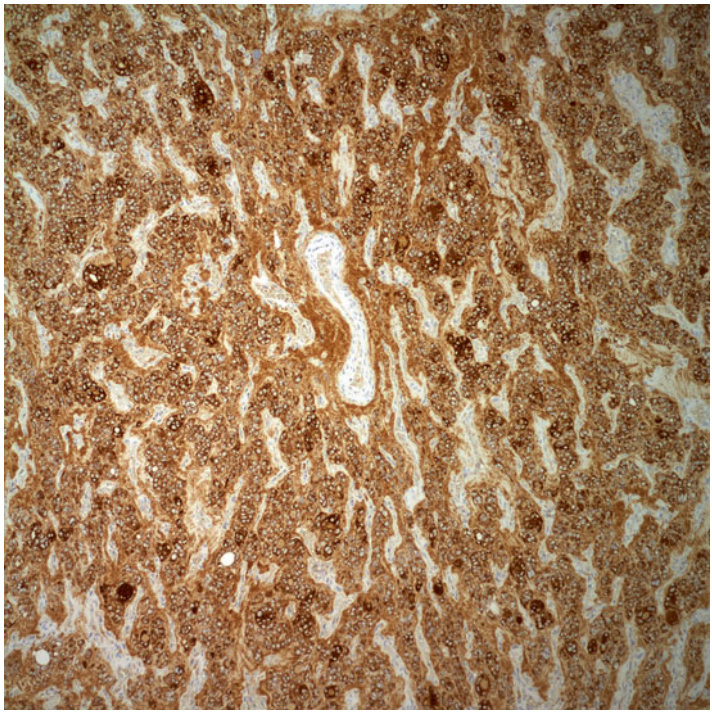

Fig. 12.18 Thyroglobulin immunoreactivity in hyalinizing trabecular tumor

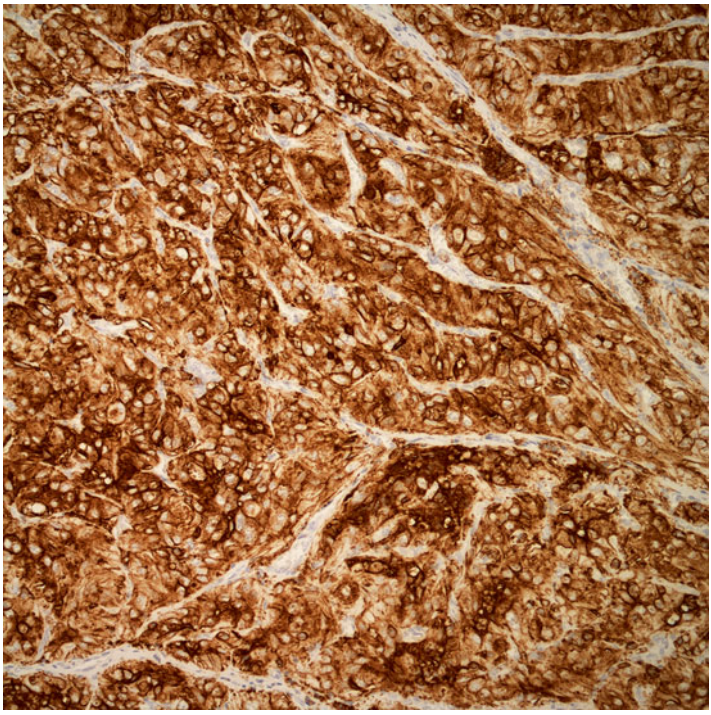

Fig. 12.19 Hyalinizing trabecular tumor characteristically shows strong membranous staining for MIB-1

be distinguished reliably from other thyroid neoplasms by MIB-1 staining. Hyalinizing trabecular tumor characteristically shows strong membranous staining for MIB-1, which is not observed in any other thyroid neoplasm [14, 26, 27] (Fig. 12.19). Other immunohistochemical markers, such as chromogranin A and galectin-3, are known to be useful diagnostic markers in medullary carcinoma or papillary carcinoma and have been reported to be positive in some hyalinizing trabecular tumor cases, which raises the possibility of diagnostic confusion [10, 28]. Therefore, preoperative MIB-1 staining in cell block material may be useful in cases suspicious for hyalinizing trabecular tumor. In a recent and detailed analysis of the expression of different cytokeratins in hyalinizing trabecular tumors and papillary carcinomas, evidence was found that the two lesions express distinct and different cytokeratin patterns [29]. For example, high molecular weight cytokeratin is expressed in papillary carcinoma but not in hyalinizing trabecular tumor. In addition, cytokeratin 19 is strongly expressed in papillary carcinoma, whereas it is weakly or not expressed in hyalinizing trabecular tumor [29]. Also, hyalinizing trabecular tumor is mostly negative or only weakly positive for galectin-3 and HBME-1, whereas most papillary thyroid cancers show strong staining for these markers [10, 30, 31].

Hyalinizing trabecular tumor can also pose diagnostic difficulties in the differentiation from medullary carcinoma. The presence of elongated and spindled cell forms, dispersed cellularity, and hyaline acellular material in the aspirates of some of these lesions can lead to the misdiagnosis of medullary carcinoma [32]. The presence of amorphous hyaline material in the aspirate may suggest amyloid. Because the histological changes seen in hyalinizing trabecular tumors can be misinterpreted as medullary carcinoma, additional diagnostic features that differentiate the lesions are important [4]. The confusion with medullary carcinoma has arisen because of two findings in hyalinizing trabecular tumor: the shape of the nucleus (oval or spindle in both) and the presence of the hyaline material. Cytologically, medullary carcinoma can be distinguished from hyalinizing trabecular tumor by background, architectural arrangement of the cells, and nuclear chromatin pattern. Amyloid, hyaline, and colloid may closely resemble each other in FNA preparations. Medullary carcinoma is excluded if the lesion is positive for thyroglobulin and negative for calcitonin and other neuroendocrine markers on immunohistochemistry. Both hyalinizing trabecular tumor and medullary carcinoma are often positive for Congo red and other amyloid markers, illustrating why the differential diagnosis between the two lesions is sometimes difficult [4].

Intrathyroidal paraganglioma may be considered in the diagnosis but it is very rare. This occurs when a small, solid, alveolar pattern of tumor growth and vascularity coincide and dominate. The alveolar groupings of the cells simulate the "zellballen" pattern, and the vascular component completes a picture mimicking paraganglioma. However, in paraganglioma, the cell clusters do not have lumens, colloid is not present, and the nuclei are not spindle shaped [1]. Neuroendocrine differentiation has been reported in some cases of hyalinizing trabecular tumor, and it is this expression of markers such as chromogranin and neuron-specific enolase that makes the distinction from paraganglioma difficult [31]. Immunoreactivity for thyroglobulin and TTF-1 excludes paraganglioma.

Hürthle cell neoplasm is in the differential diagnosis of hyalinizing trabecular tumor because both neoplasms have polygonal, large cells with abundant granular cytoplasm and eccentric nuclei, although in the former, the cytoplasmic granularity and eosinophilia are striking. Detection of hyaline material in hyalinizing trabecular tumor helps in the diagnosis [14].

References

1. Carney JA, Ryan J, Goellner JR. Hyalinizing trabecular adenoma of the thyroid gland. Am J Surg Pathol. 1987;11:583–91.
2. Hicks MJ, Batsakis JG. Hyalinizing trabecular adenoma of the thyroid gland. Ann Otol Rhinol Laryngol. 1993;102:239–40.
3. Chan JK, Tse CC, Chiu HS. Hyalinizing trabecular adenoma-like lesion in multinodular goitre. Histopathology. 1990;16:611–4.
4. Evenson A, Mowschenson P, Wang H, Connolly J, Mendrinos S, Parangi S, Hasselgren PO. Hyalinizing trabecular adenoma—an uncommon thyroid tumor frequently misdiagnosed as papillary or medullary thyroid carcinoma. Am J Surg. 2007;193:707–12.

5. Molberg K, Albores-Saavedra J. Hyalinizing trabecular carcinoma of the thyroid gland. Hum Pathol. 1994;25:192–7.
6. McCluggage WG, Sloan JM. Hyalinizing trabecular carcinoma of thyroid gland. Histopathology. 1996;28:357–62.
7. Galgano MT, Mills SE, Stelow EB. Hyalinizing trabecular adenoma of the thyroid revisited: a histologic and immunohistochemical study of thyroid lesions with prominent trabecular architecture and sclerosis. Am J Surg Pathol. 2006;30:1269–73.
8. DeLellis RA, Lloyd RV, Heitz PU, Eng C. World Health Organization classification of tumours. Pathology and genetics of tumours of endocrine organs. Lyon: IARC Press; 2004.
9. Salvatore G, Chiappetta G, Nikiforov YE, Decaussin-Petrucci M, Fusco A, Carney JA, Santoro M. Molecular profile of hyalinizing trabecular tumours of the thyroid: high prevalence of RET/PTC rearrangements and absence of B-raf and N-ras point mutations. Eur J Cancer. 2005;41:816–21.
10. Gaffney RL, Carney JA, Sebo TJ, Erickson LA, Volante M, Papotti M, Lloyd RV. Galectin-3 expression in hyalinizing trabecular tumors of the thyroid gland. Am J Surg Pathol. 2003;27:494–8.
11. Cheung CC, Boerner SL, MacMillan CM, Ramyar L, Asa SL. Hyalinizing trabecular tumor of the thyroid: a variant of papillary carcinoma proved by molecular genetics. Am J Surg Pathol. 2000;24:1622–6.
12. Sheu S, Vogel E, Worm K, Grabellus F, Schwertheim S, Schmid KW. Hyalinizing trabecular tumor of the thyroid—differential expression of distinct miRNAs compared with papillary thyroid carcinoma. Histopathology. 2010;56:632–40.
13. Lee S, Hong S, Koo JS. Immunohistochemical subclassification of thyroid tumors with prominent hyalinizing trabecular pattern. APMIS. 2011;119:529–36.
14. Casey MB, Sebo TJ, Carney JA. Hyalinizing trabecular adenoma of the thyroid gland identification through MIB-1 staining of fine-needle aspiration biopsy smears. Am J Clin Pathol. 2004;122:506–10.
15. Howard BE, Gnagi SH, Ocal IT, Hinni ML. Hyalinizing trabecular tumor masquerading as papillary thyroid carcinoma on fine-needle aspiration. ORL J Otorhinolaryngol Relat Spec. 2013;75:309–13.
16. Carney JA, Hirokawa M, Lloyd RV, Papottie M, Sebo TJ. Hyalinizing trabecular tumors of the thyroid gland are almost all benign. Am J Surg Pathol. 2008;32:1877–89.
17. Kini SR. Thyroid cytopathology: an Atlas and text. Philadelphia: Wolters Kluwer/Lippincott Williams & Wilkins; 2008.
18. Rothenberg HJ, Goellner JR, Carney JA. Prevalence and incidence of cytoplasmic yellow bodies in thyroid neoplasms. Arch Pathol Lab Med. 2003;127:715–7.
19. Kuma S, Hirokawa M, Miyauchi A, Kakudo K, Katayama S. Cytologic features of hyalinizing trabecular adenoma of the thyroid. Acta Cytol. 2003;47:399–404.
20. Boccato P, Mannara GM, LaRosa F, Rinaldo A, Ferlito A. Hyalinizing trabecular adenoma of the thyroid diagnosed by fine-needle aspiration biopsy. Ann Otol Rhinol Laryngol. 2000;109:235–8.
21. Bondeson L, Bondeson AG. Clue helping to distinguish hyalinizing trabecular adenoma from carcinoma of the thyroid in fine-needle aspirates. Diagn Cytopathol. 1994;10:25–9.
22. Katoh R, Kakudo K, Kawaoi A. Accumulated basement membrane material in hyalinizing trabecular tumors of the thyroid. Mod Pathol. 1999;12:1057–61.
23. Rhoden KJ, Unger K, Salvatore G, et al. RET/papillary thyroid cancer rearrangement in nonneoplastic thyrocytes: follicular cells of Hashimoto's thyroiditis share low-level recombination events with a subset of papillary carcinoma. J Clin Endocrinol Metab. 2006;91:2414–23.
24. Trovisco V, Vieira deCastro I, Soares P, et al. BRAF mutations are associated with some histological types of papillary thyroid carcinoma. J Pathol. 2004;202:247–51.
25. Baloch ZW, Puttaswamy K, Brose M, LiVolsi VA. Lack of BRAF mutations in hyalinizing trabecular neoplasm. Cytojournal. 2006;3:17.
26. Hirokawa M, Shimizu M, Manabe T, Kuroda M, Mizoguchi Y. Hyalinizing trabecular adenoma of the thyroid: its unusual cytoplasmic immunopositivity for MIB1. Pathol Int. 1995;45:399–401.

27. Hirokawa M, Carney JA. Cell membrane and cytoplasmic staining for MIB-1 in hyalinizing trabecular adenoma of the thyroid gland. Am J Surg Pathol. 2000;24:575–8.
28. Shikama Y, Osawa T, Yagihashi N, Kurotaki H, Yagihashi S. Neuroendocrine differentiation in hyalinizing trabecular tumor of the thyroid. Virchows Arch. 2003;443:792–6.
29. Hirokawa M, Carney JA, Ohtsuki Y. Hyalinizing trabecular adenoma and papillary carcinoma of the thyroid gland express different cytokeratin patterns. Am J Surg Pathol. 2000;24: 877–81.
30. Cerasoli S, Tabarri B, Farabegoli P, Vascotto L, Lanzanova G, Pasquinelli GA, Tison V. Hyalinizing trabecular adenoma of the thyroid. Report of two cases, with cytologic, immunohistochemical and ultrastructural studies. Tumori. 1992;78:274–9.
31. Katoh R, Jasani B, Williams ED. Hyalinizing trabecular adenoma of the thyroid. A report of three cases with immunohistochemical and ultrastructural studies. Histopathology. 1989;15: 211–24.
32. Huss LJ, Mendelsohn G. Medullary carcinoma of the thyroid gland: an encapsulated variant resembling the hyalinizing trabecular (paraganglioma-like) adenoma of the thyroid. Mod Pathol. 1990;3:581–5.

Poorly Differentiated Thyroid Carcinoma 13

Case Study

A 60-year-old woman presented with symptoms of hoarseness and discomfort in swallowing. She had a history of hyperthyroidism, which was treated with radioactive iodine 20+ years ago. She did not have any history of radiation to the head and neck area or family history of thyroid cancer. Physical examination revealed an enlarged palpable left thyroid lobe. There were no signs of hyperthyroidism. Ultrasound examination revealed a left nodule, measuring 5 cm and occupying almost the entire left thyroid lobe. A smaller, heterogeneous nodule, measuring 1.1 cm was also noted in right thyroid lobe.

A fine-needle aspiration was performed on the left thyroid nodule. The aspirate was cellular and consisted of follicular cells arranged as numerous microfollicular structures (Figs. 13.1 and 13.2). Individual follicular cells were of small to medium size with scant to moderate amount of cytoplasm (Fig. 13.3). No nuclear features of papillary thyroid carcinoma were noted. Rare mitotic figures were identified (Fig. 13.4). No colloid or macrophages were identified in the background. The cytologic diagnosis was follicular neoplasm.

The patient underwent a total thyroidectomy. Serial resection revealed a 4.5 cm thyroid nodule with a hemorrhagic center in the left thyroid lobe. The tumor consisted of follicular cells arranged in both trabecular and insular patterns separated by thin fibrovascular stroma (Fig. 13.5). Follicular structures were noted within the nests of tumor cells (Fig. 13.6). Individual tumor cells appeared small and relatively uniform with hyperchromatic, convoluted nuclei and indistinct nucleoli (Fig. 13.7). Nuclear features typical of papillary thyroid carcinoma were not apparent. Increased mitotic figures (more than 3 per 10 high-power field) were noted. No necrosis was found. A small focus of extrathyroidal extension was identified. The non-neoplastic thyroid showed florid Hashimoto's thyroiditis. The histologic diagnosis was poorly differentiated thyroid carcinoma.

A.J. Adeniran, D. Chhieng, *Common Diagnostic Pitfalls in Thyroid Cytopathology*, DOI 10.1007/978-3-319-31602-4_13

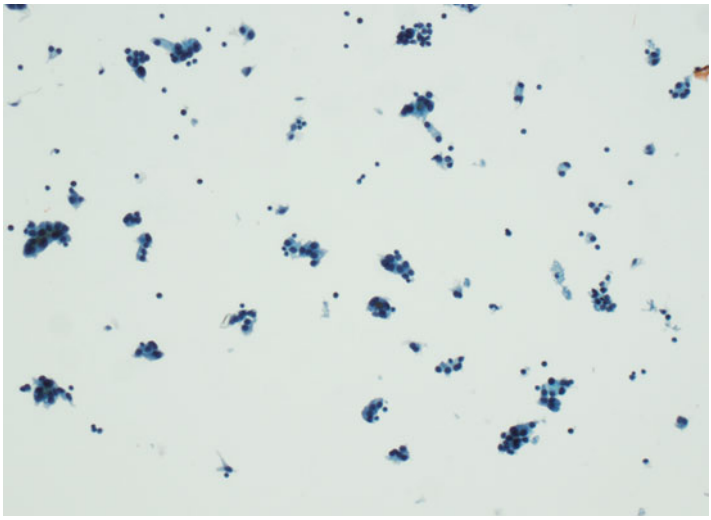

Fig. 13.1 Thyroid FNA-poorly differentiated thyroid carcinoma. The aspirate is cellular and consists of numerous small clusters and scattered single cells. There is no colloid in the background (Papanicolaou stain, low power)

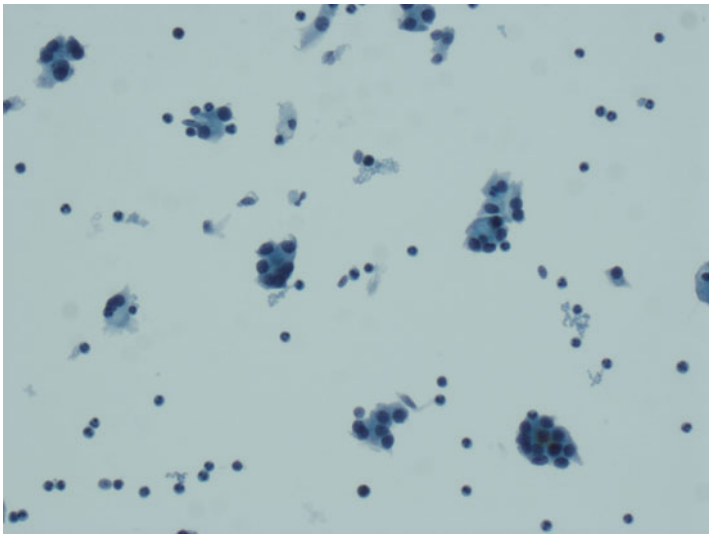

Fig. 13.2 Thyroid FNA-poorly differentiated thyroid carcinoma. High magnification reveals that the clusters are mostly microfollicles without luminal formation (Papanicolaou stain, high power)

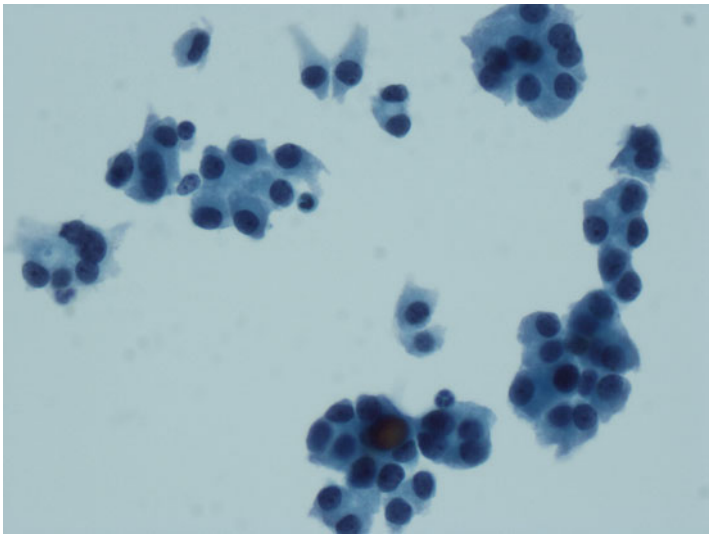

Fig. 13.3 Thyroid FNA-poorly differentiated thyroid carcinoma. The microfollicles consist of small- to medium-sized follicular cells with scant to moderate amount of cytoplasm (Papanicolaou stain, high power)

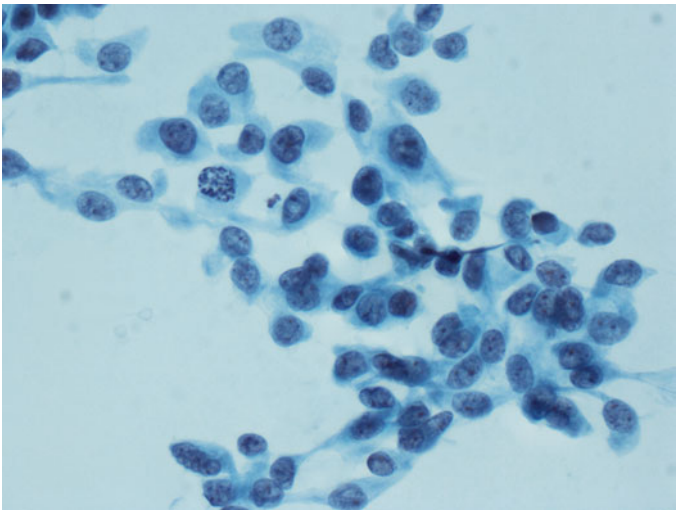

Fig. 13.4 Thyroid FNA-poorly differentiated thyroid carcinoma. The nuclei of the follicular cells vary from oval to angulated. The chromatin appears coarsely granular with small indistinct nucleoli. Rare mitotic figure is present. Nuclear features of papillary thyroid carcinoma are not identified (Papanicolaou stain, high power)

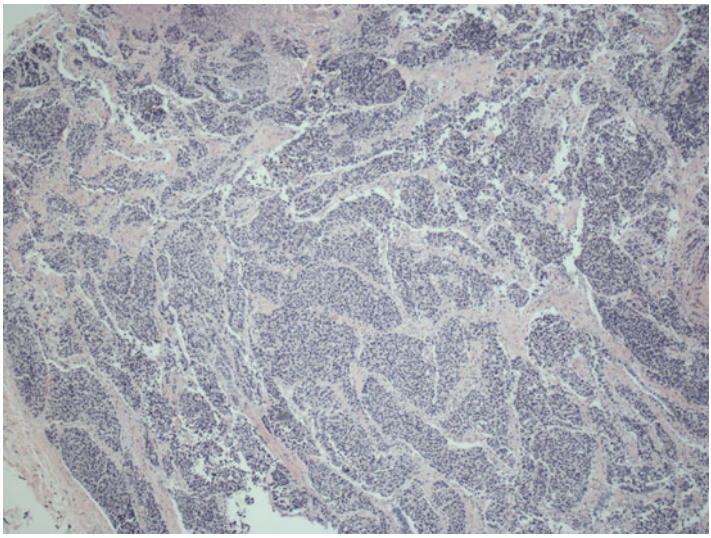

Fig. 13.5 Poorly differentiated thyroid carcinoma. A partially encapsulated tumor consists of follicular cells arranged in both trabecular and insular growth pattern separated by stroma (H&E stain, low power)

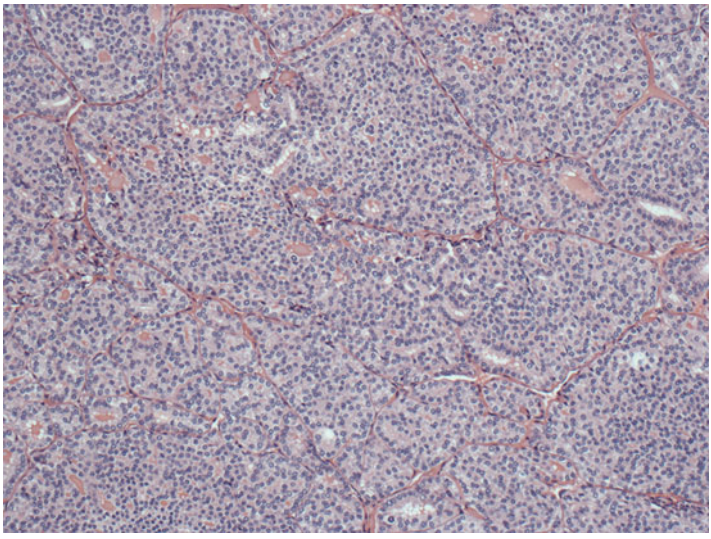

Fig. 13.6 Poorly differentiated thyroid carcinoma. Higher magnification reveals irregular nests of follicular cells separated by fibrovascular stroma. Microfollicular structures are noted within the nests (H&E stain, high power)

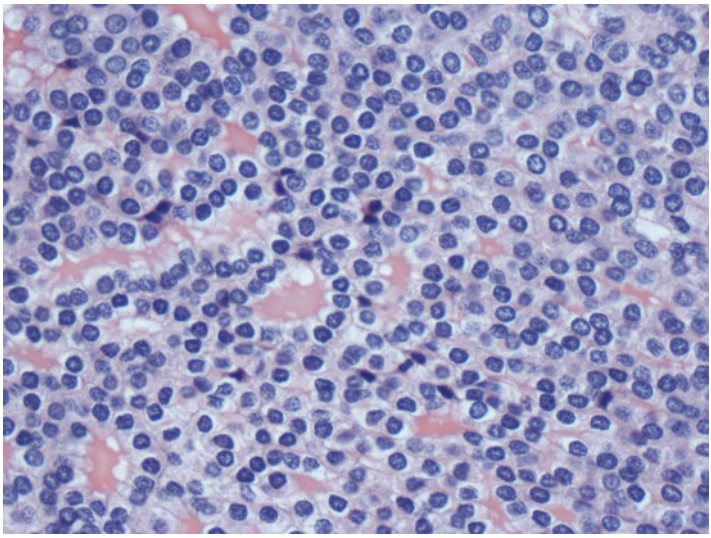

Fig. 13.7 Poorly differentiated thyroid carcinoma. Individual follicular cells demonstrate moderate amount of pale cytoplasm and well-defined cytoplasmic borders. The nuclei appear round to oval to slightly angulated and contain coarsely granular chromatin. Nuclear grooves and nuclear inclusions are not present (H&E stain, high power)

Discussion

Poorly differentiated thyroid carcinoma, a follicular cell-derived malignancy, accounts for 4–7 % of all thyroid cancers [1]. It occupies an intermediate position between well-differentiated and anaplastic thyroid carcinoma in regard to morphology and biologic behavior. It is also known as "insular" carcinoma because of its growth pattern of solid clusters or nests of cells reminiscent of a carcinoid tumor. It may arise de novo or be associated with a well-differentiated thyroid carcinoma. Clinically, it usually occurs in older individuals and frequently presents at an advanced stage with extra-thyroidal extension as well as metastases to regional lymph nodes, lung, and bones.

Histologically, the insular growth pattern is readily recognized at low magnification and is characterized by well-defined nests of tumor cells surrounded by fibrovascular septa of variable thickness (Fig. 13.8). Follicular structures are sometimes noted within the tumor nests (Fig. 13.9). Individual tumor cells appear small and relatively uniform with hyperchromatic, convoluted nuclei, and indistinct nucleoli (Fig. 13.10). Nuclear features typical of papillary thyroid carcinoma are usually not apparent. Mitotic figures and necrosis are common findings (Fig. 13.11). Other growth patterns, including trabecular and solid patterns, are also recognized and often coexist with the insular growth pattern [2].

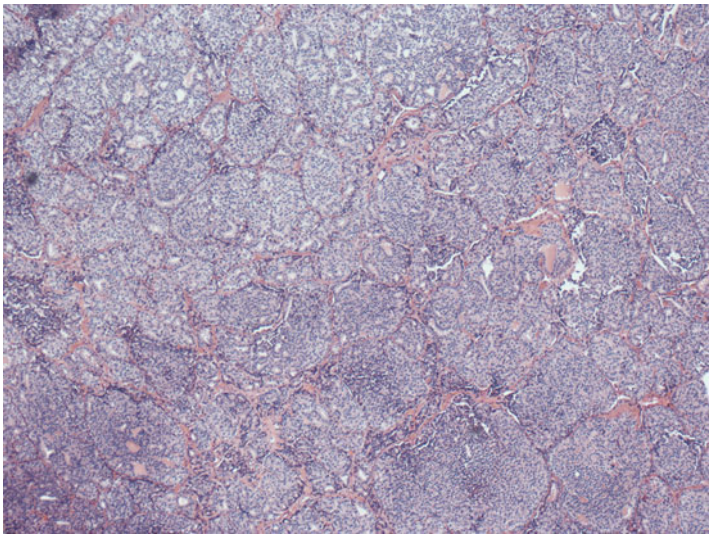

Fig. 13.8 Poorly differentiated thyroid carcinoma. A solid proliferation of neoplastic follicular cells in an insular pattern separated by very thin fibrovascular stroma (H&E stain, low power)

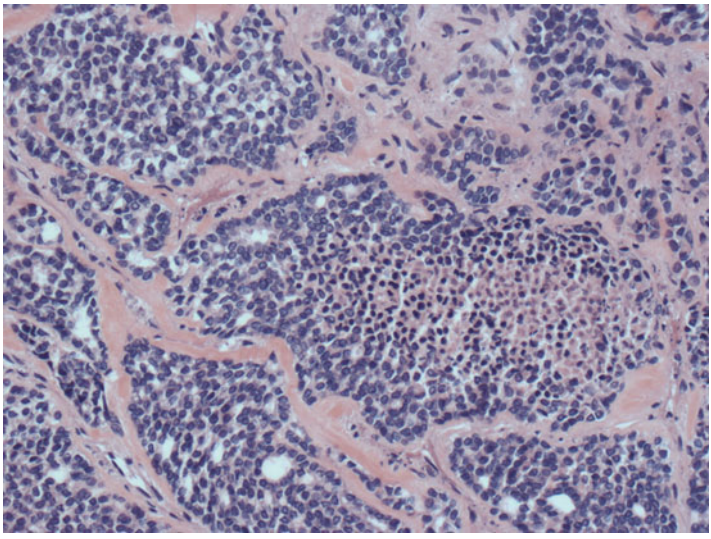

Fig. 13.9 Poorly differentiated thyroid carcinoma. Higher magnification reveals irregular nests of follicular cells separated by very thin fibrovascular stroma. Microfollicular structures with or without colloid are noted within the nests (H&E stain, high power)

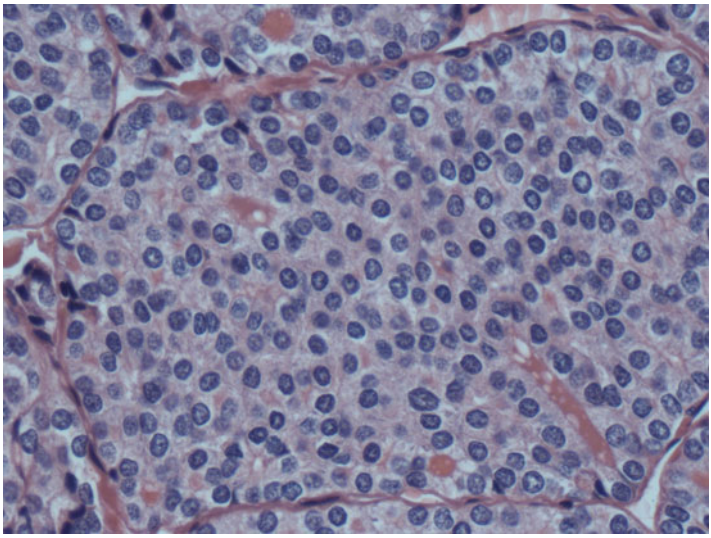

Fig. 13.10 Poorly differentiated thyroid carcinoma. Individual follicular cells demonstrate moderate amount of granular cytoplasm. The nuclei appear round to oval to slightly angulated and contain coarsely granular chromatin. Nuclear features of papillary thyroid carcinoma such as nuclear grooves and nuclear inclusions are not present (H&E stain, high power)

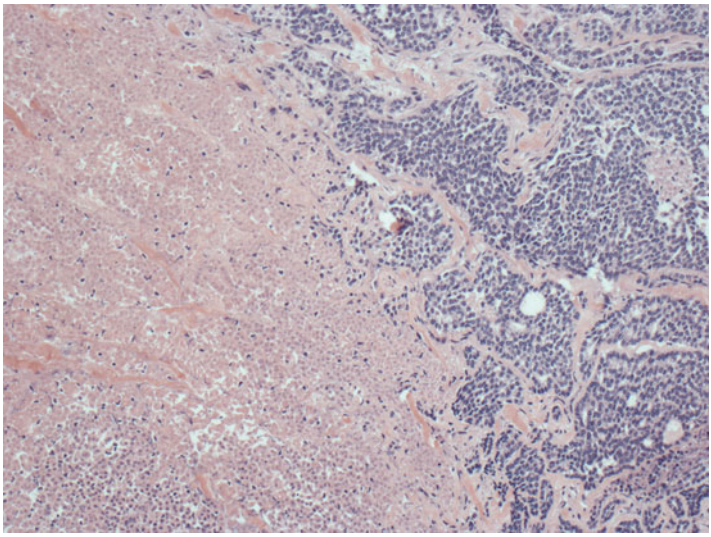

Fig. 13.11 Poorly differentiated thyroid carcinoma. Large area of tumor necrosis can be seen in about one-third of the tumors (H&E stain, low power)

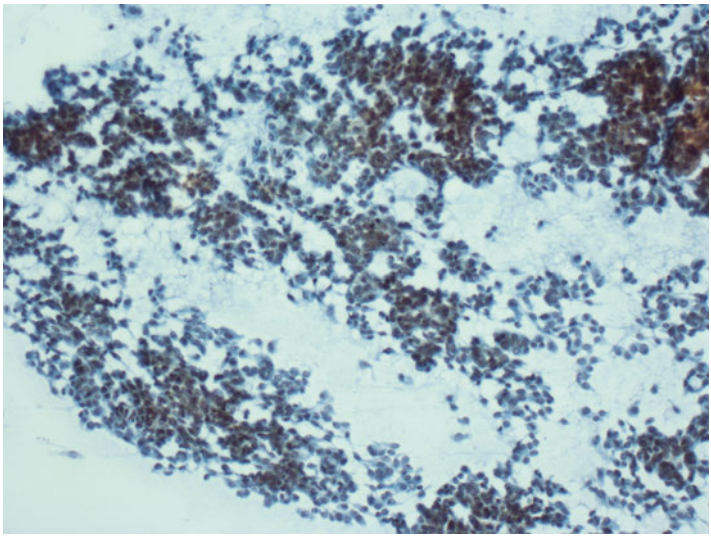

Fig. 13.12 Thyroid FNA-poorly differentiated thyroid carcinoma. Cellular aspirate with no colloid in the background. The follicular cells are arranged in loosely cohesive irregular clusters (Papanicolaou stain, low power)

Few studies have described the cytology of poorly differentiated thyroid carcinoma [2–5]. The aspirates are usually highly cellular with scant colloid (Fig. 13.12). The tumor cells arrange in loosely cohesive clusters with overlapping and crowding (Fig. 13.13). Variable number of single isolated cells is often noted in the background. Microfollicular structures with or without intraluminal colloid have been described (Fig. 13.14). The tumor cells consist of small- to medium-sized cells with scant cytoplasm, round nuclei, granular chromatin, indistinct nucleoli, and high nuclear-to-cytoplasmic ratio; resulting in a relatively monomorphic appearance (Fig. 13.15). Nuclear grooves and inclusions are infrequent and limited to a small proportion of the tumor cells [4]. Occasional bi/multinucleation, nucleomegaly, and mitotic figures have been noted but marked pleomorphism is not present (Fig. 13.16). Necrosis is observed in less than one-third of the reported cases [2, 4]. The latter may be explained by the fact that the necrotic areas are small in poorly differentiated thyroid carcinoma and may not be present in cytology due to sampling error. The identification of mitotic figures and/or necrosis facilitates the diagnosis of poorly differential thyroid carcinoma.

Cytologically, the differential diagnosis of poorly differentiated thyroid carcinoma includes follicular neoplasm, follicular variant of papillary thyroid carcinoma, and neoplasms composed of small malignant cells such as medullary thyroid carcinoma and metastases such as small-cell carcinoma. Both reactive and neoplastic lymphoid lesions should also be considered in the differential diagnosis. It has been reported that a significant number of poorly differentiated thyroid carcinoma with and without nuclear grooving and overlapping have been misclassified as follicular variant of papillary thyroid carcinoma and follicular neoplasm on FNA, respectively,

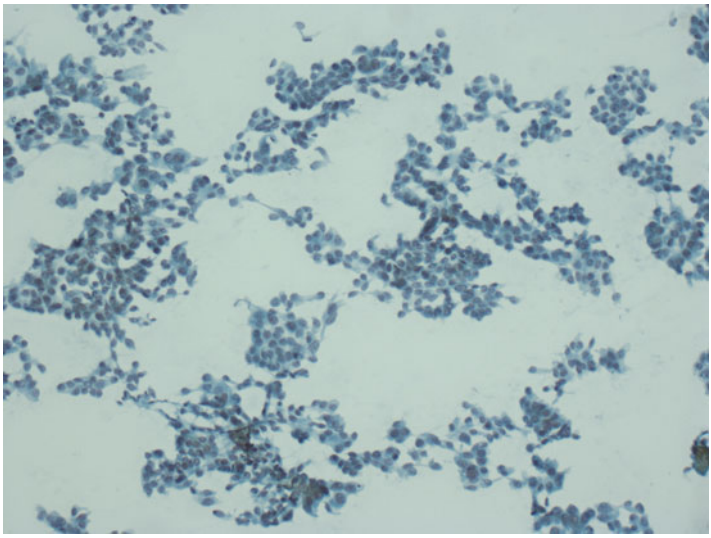

Fig. 13.13 Thyroid FNA-poorly differentiated thyroid carcinoma. The follicular cells are arranged haphazardly with mild nuclear crowding and overlapping. Microfollicular formation is also noted (Papanicolaou stain, high power)

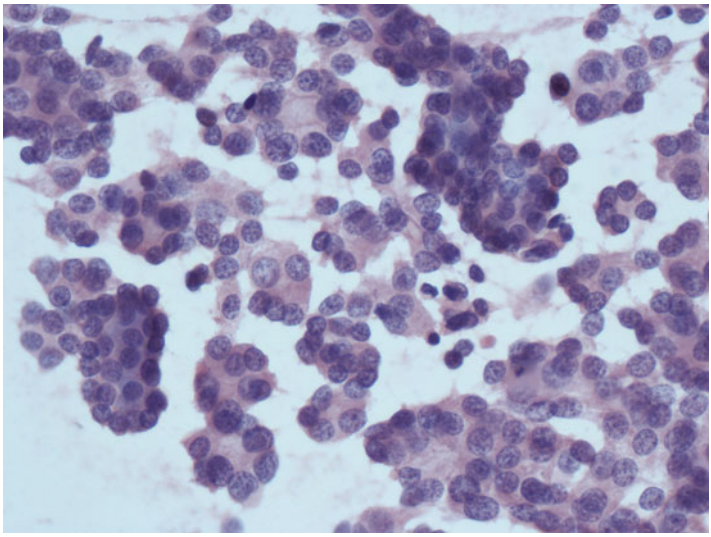

Fig. 13.14 Thyroid FNA-poorly differentiated thyroid carcinoma. In this example, the microfollicular structure is prominent (H&E stain, high power)

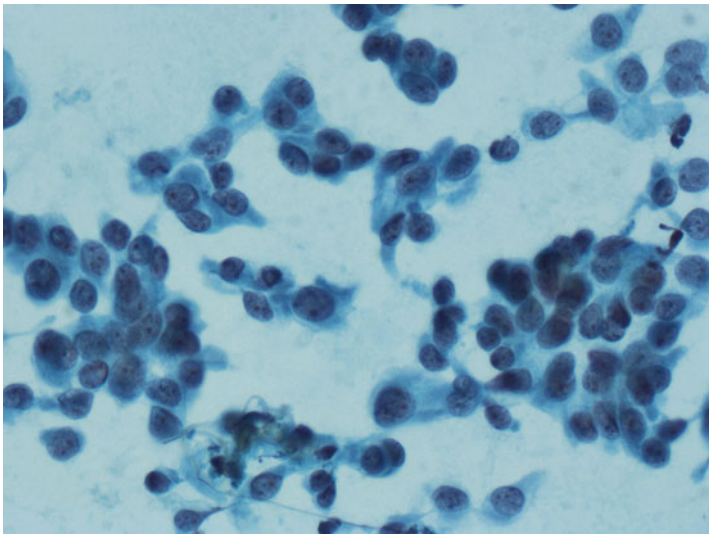

Fig. 13.15 Thyroid FNA-poorly differentiated thyroid carcinoma. The cytoplasm is scant to moderate. The nuclei vary from oval to angulated. The chromatin appears coarsely granular with small nucleoli. Nuclear features of papillary thyroid carcinoma are not identified (Papanicolaou stain, high power)

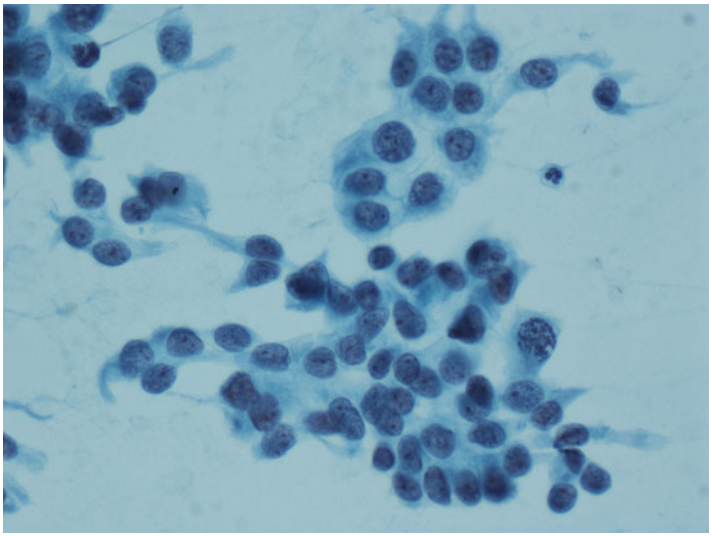

Fig. 13.16 Thyroid FNA-poorly differentiated thyroid carcinoma. The follicular cells demonstrate mild-to-moderate nuclear anisonucleosis. Rare mitotic figure is present (Papanicolaou stain, high power)

because of the presence of microfollicular structures (Figs. 13.17 and 13.18) [2, 4]. Helpful features that favor a poorly differentiated thyroid carcinoma over the other

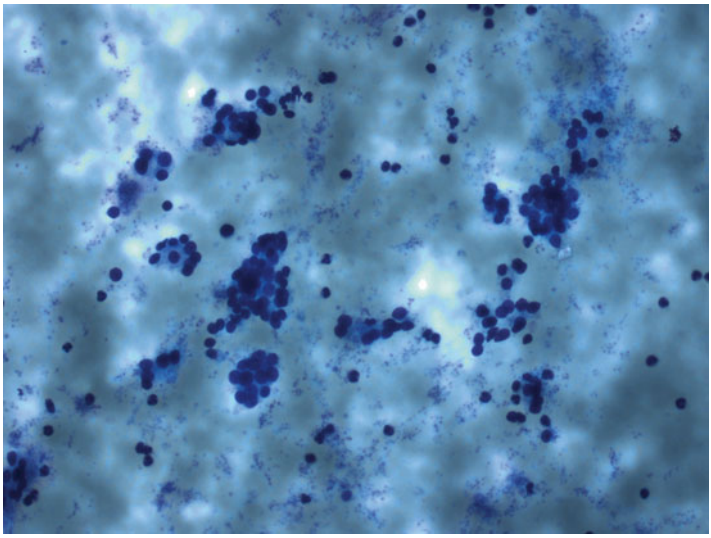

Fig. 13.17 Thyroid FNA-follicular neoplasm. Numerous microfollicles are noted with no colloid in the background. The follicular cells are uniform without any significant cytologic atypia. Subsequent follow-up reveals a follicular adenoma (Diff-Quik stain, low power)

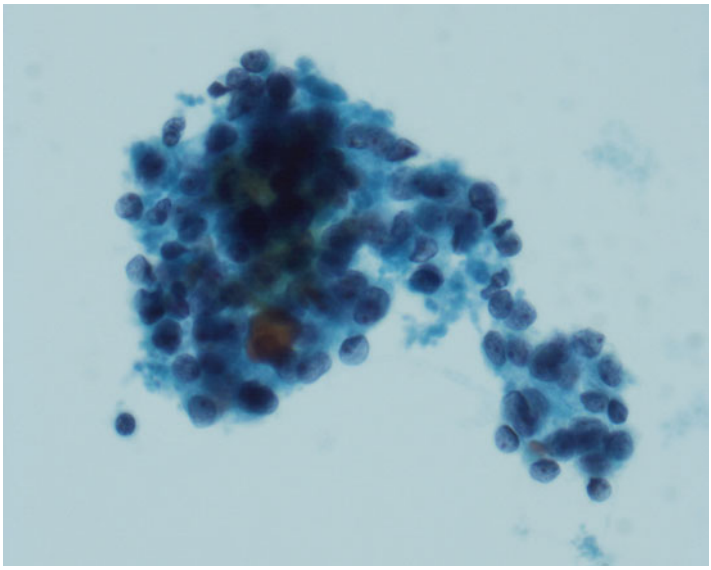

Fig. 13.18 Thyroid FNA-follicular variant of papillary thyroid carcinoma. Crowded clusters of follicular with ill-defined microfollicular structures. Individual cells show powdery chromatin and infrequent nuclear grooves (Papanicolaou stain, high power)

two entities are the presence of marked nuclear overlapping and crowding, mitotic figures, and necrosis [4].

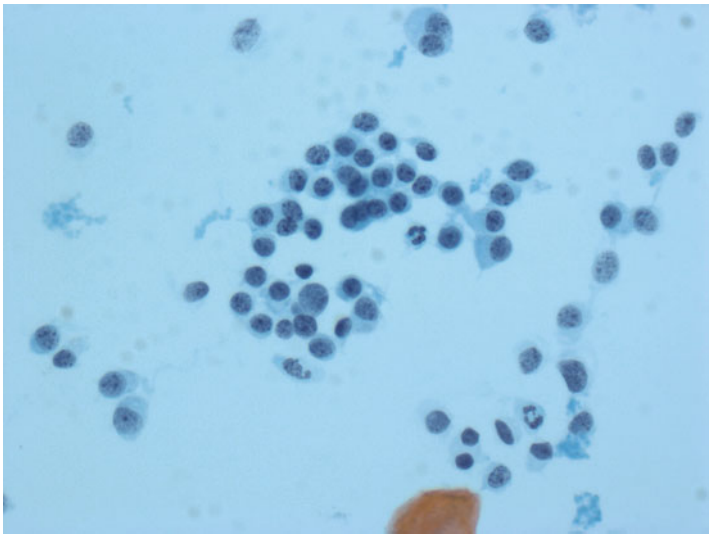

Fig. 13.19 Thyroid FNA-medullary thyroid carcinoma. The predominantly small-cell pattern of medullary carcinoma should be considered in the differentiated diagnosis. The loosely cohesive pattern and the finding of "salt-and-pepper" chromatin would favor a medullary thyroid carcinoma (Papanicolaou stain, high power)

Cases of poorly differentiated thyroid carcinoma with a conspicuous single-cell pattern may be difficult to differentiate from medullary thyroid carcinoma, especially the small-cell variant, on morphology alone. Both bi/multinucleated tumor cells and nucleomegaly can be found in both entities (Fig. 13.19). The finding of colloid in poorly differentiated thyroid carcinoma can be mistaken for amyloid in medullary thyroid carcinoma on Diff-Quik stain. However, the chromatin pattern of medullary thyroid carcinoma is typically described as "salt and pepper" rather than coarsely granular. Mitotic figures and/or necrosis are generally not observed with medullary thyroid carcinoma. Positive immunocytochemical staining with calcitonin and elevated serum calcitonin level will be noted with medullary thyroid carcinoma but not poorly differentiated thyroid carcinoma.

The common features shared between poorly differentiated thyroid carcinomas and metastatic small-cell carcinomas include small cell size, frequent mitoses, and necrosis (Fig. 13.20). Furthermore, both entities are TTF-1 and cytokeratin positive. However, small-cell carcinomas usually demonstrate marked nuclear pleomorphism with nuclear molding while the tumor cells of poorly differentiated thyroid carcinomas appear monomorphic with round and relatively uniform nuclei. In addition, thyroglobulin is strongly expressed by poorly differentiated thyroid carcinoma but not metastatic small-cell carcinoma. Without immunostains such as thyroglobulin and lymphoid markers, poorly differentiated thyroid carcinoma can also be mistaken for a low-grade lymphoproliferative process because of the loosely cohesive small-cell pattern (Fig. 13.21). The finding of lymphoglandular bodies would favor the latter.

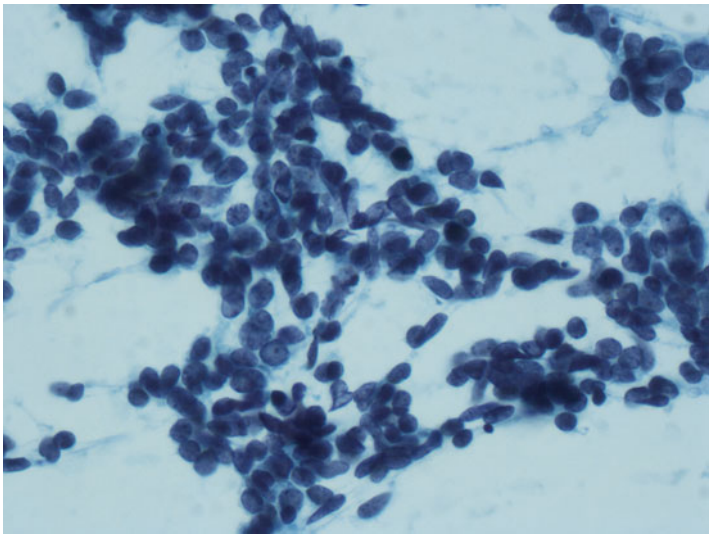

Fig. 13.20 Thyroid FNA-metastatic small-cell lung carcinoma. Crowded cohesive group of relatively small neoplastic cells with high nuclear-to-cytoplasmic ratio. Compared to poorly differentiated thyroid carcinoma, the neoplastic cells of small-cell carcinoma demonstrate more significant nuclear atypia with nuclear molding as well as frequent apoptotic and mitotic figures (Papanicolaou stain, high power)

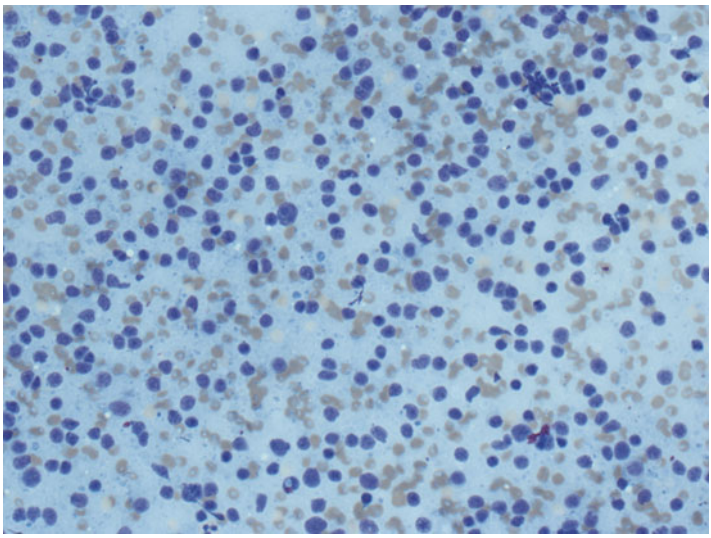

Fig. 13.21 Thyroid FNA-follicular center cell lymphoma, Grade I. The small-cell pattern of a low-grade B-cell lymphoma should be considered in the differential diagnosis. The presence of lymphoglandular bodies should favor a lymphoid lesion. Immunophenotyping would demonstrate a monoclonal B-cell population (Diff-Quik stain, high power)

References

1. Sobrinho-Simoes M, Albores-Saavedra J, Tallini G, et al. Poorly differentiated carcinoma. In: DeLellis R, Lloyd R, Heitz P, editors. Pathology and genetics of tumours of endocrine organs (IARC WHO classification of tumours). Lyon: IARC Press; 2004. p. 73–6.
2. Bongiovanni M, Sadow PM, Faquin WC. Poorly differentiated thyroid carcinoma: a cytologic-histologic review. Adv Anat Pathol. 2009;16:283–9.
3. Barwad A, Dey P, Nahar Saikia U, et al. Fine needle aspiration cytology of insular carcinoma of thyroid. Diagn Cytopathol. 2012;40 Suppl 1:E43–7.
4. Kane SV, Sharma TP. Cytologic diagnostic approach to poorly differentiated thyroid carcinoma: a single-institution study. Cancer Cytopathol. 2015;123:82–91.
5. Guiter GE, Auger M, Ali SZ, Allen EA, Zakowski MF. Cytopathology of insular carcinoma of the thyroid. Cancer. 1999;87:196–202.

Anaplastic Thyroid Carcinoma

14

Case Study

A 34-year-old male presented with a 2-month history of left neck pain and fullness, which worsened with lying supine. The patient also complained of voice fatigue and mild difficulty in swallowing but there was no hoarseness. There was no history of radiation to the head and neck region. He was a nonsmoker and social drinker. Family history included possible thyroid cancer in his mother. Physical examination revealed a well-developed male in no apparent distress. Significant findings included enlarged thyroid gland with bilateral tenderness upon palpation. There was no palpable cervical adenopathy.

Ultrasonographic examination revealed an enlarged left thyroid gland, which consisted of a left thyroid nodule, measuring at least 4 cm in greatest dimension. No enlarged lymph nodes were identified. Thyroid function test and serum calcitonin level were within normal limits. Fiber-optic laryngoscopy revealed bilateral mobile vocal cords and patent airway.

A fine-needle aspiration biopsy of the left thyroid nodule was preformed. The aspirate was moderately cellular (Fig. 14.1) and demonstrated two cellular components (Fig. 14.2). The first component consisted of three-dimensional cohesive groups of follicular cells with scant to moderate amount of cytoplasm and high nuclear-to-cytoplasmic ratio. Ill-defined follicular structures were noted. The nuclei were oval/round and relatively uniform with inconspicuous nucleoli (Figs. 14.3 and 14.4). The second cellular component consisted of predominantly single- or three-dimensional crowded groups of large, pleomorphic neoplastic cells (Figs. 14.5 and 14.6). Individual cells demonstrated moderate to abundant amount of cytoplasm, oval- to spindle-shaped nuclei, and irregular nuclear contours. Bi- or multi-nucleated forms were common. Other findings included osteoclastic-like multinucleated giant cells (Fig. 14.7) and conspicuous metachromatic extracellular material intermixed with loosely cohesive groups of large, pleomorphic neoplastic cells (Fig. 14.8). The cytologic impression was that of a poorly differentiated malignant neoplasm;

A.J. Adeniran, D. Chhieng, *Common Diagnostic Pitfalls in Thyroid Cytopathology*, DOI 10.1007/978-3-319-31602-4_14

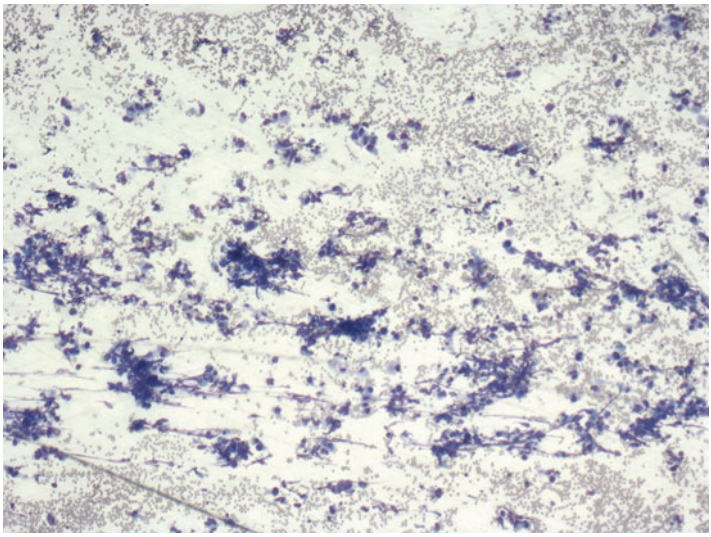

Fig. 14.1 Thyroid FNA-anaplastic thyroid carcinoma. The aspirate is markedly cellular and consists of tissue fragments, loosely cohesive groups, and single cells (Diff-Quik stain, low power)

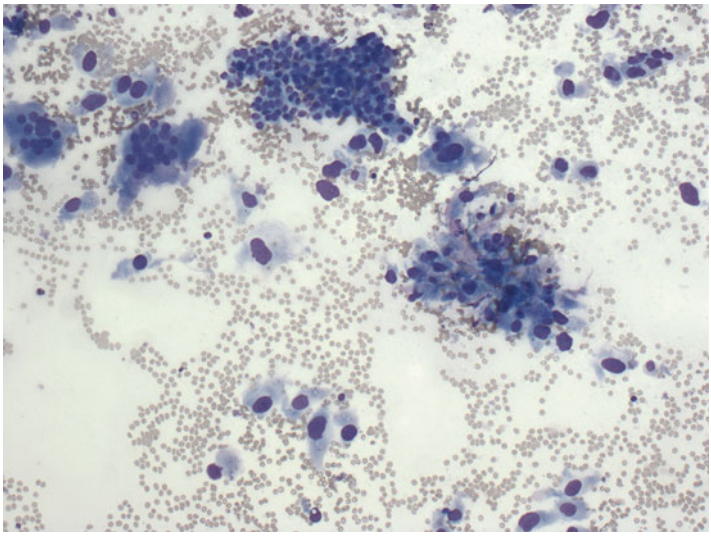

Fig. 14.2 Thyroid FNA-anaplastic thyroid carcinoma. The aspirate consists of two cellular components: large, pleomorphic neoplastic cells and smaller, relatively uniform follicular cells (Diff-Quik stain, high power)

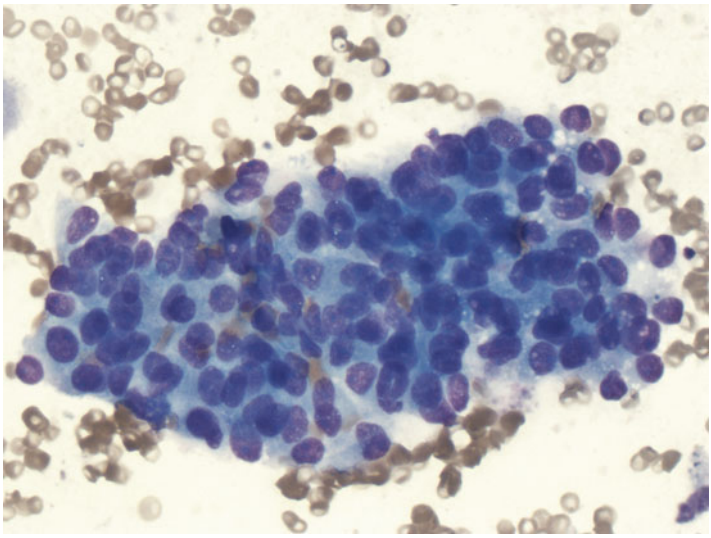

Fig. 14.3 Thyroid FNA-anaplastic thyroid carcinoma. Three-dimensional cohesive groups of follicular cells with scant to moderate amount of cytoplasm, high nuclear-to-cytoplasmic ratio, oval/round nuclei, and inconspicuous nucleoli (Diff-Quik stain, high power)

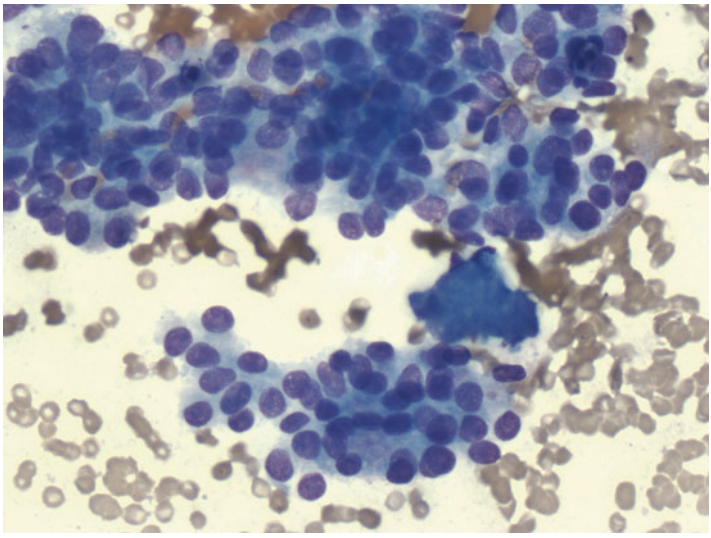

Fig. 14.4 Thyroid FNA-anaplastic thyroid carcinoma. Ill-defined follicular structures are also noted (Diff-Quik stain, high power)

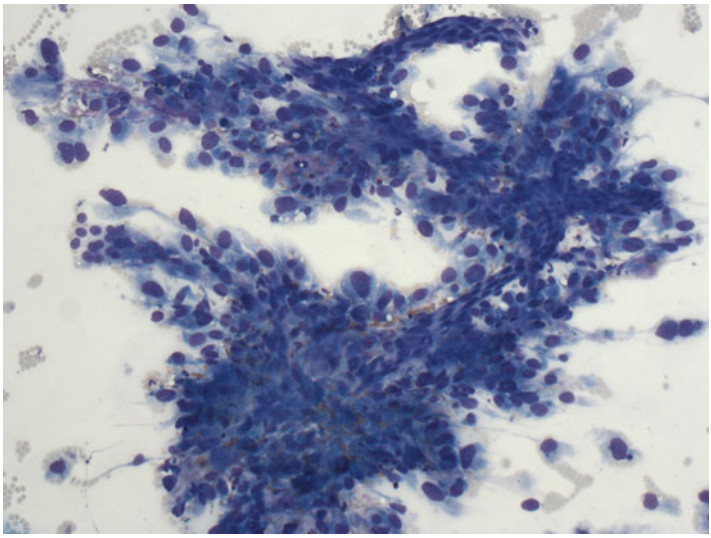

Fig. 14.5 Thyroid FNA-anaplastic thyroid carcinoma. Large, irregular tissue fragments consisting of pleomorphic epithelioid and spindle neoplastic cells (Diff-Quik stain, high power)

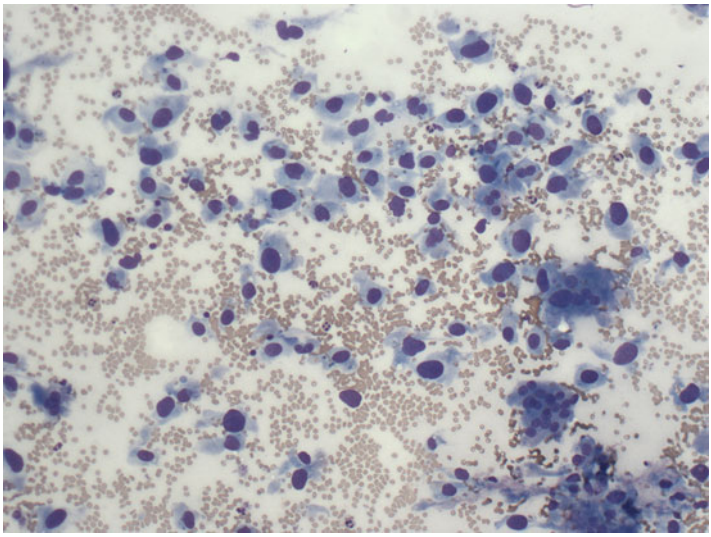

Fig. 14.6 Thyroid FNA-anaplastic thyroid carcinoma. Single, loosely cohesive, large, pleomorphic epithelioid and spindle neoplastic cells with moderate to abundant amount of cytoplasm and irregular nuclei (Diff-Quik stain, high power)

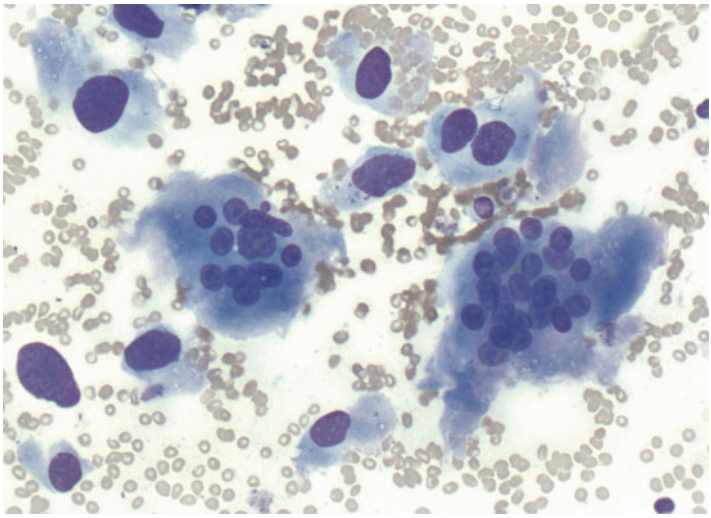

Fig. 14.7 Thyroid FNA-anaplastic thyroid carcinoma. Osteoclast-like multinucleated giant cells are frequently noted (Diff-Quik stain, high power)

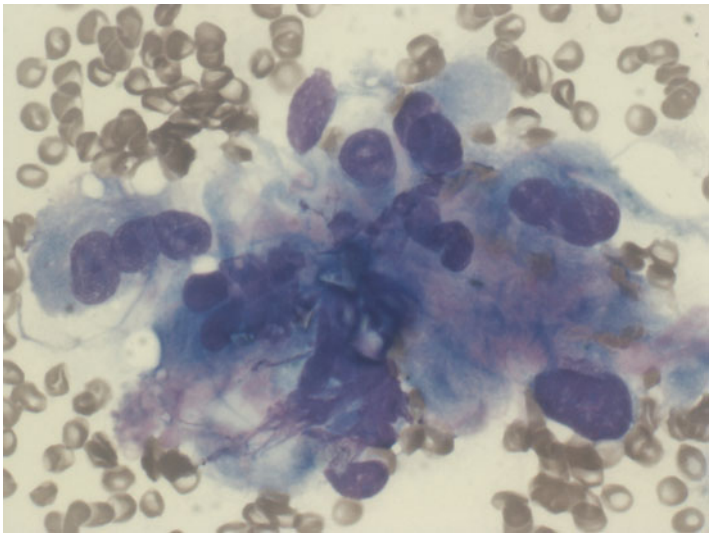

Fig. 14.8 Thyroid FNA-anaplastic thyroid carcinoma. Metachromatic extracellular material admixed with pleomorphic epithelioid and spindle neoplastic cells (Diff-Quik stain, high power)

the differential diagnosis included anaplastic thyroid carcinoma, metastatic carcinoma, melanoma, and sarcoma. No additional material was available for ancillary study.

The patient underwent total thyroidectomy and left central neck dissection. Grossly, the left thyroid lobe was markedly enlarged, measuring 9×8×5 cm. The thyroid capsule was grossly intact. Serial sectioning revealed a multi-lobulated encapsulated mass in the left lobe, measuring 8×8×5 cm and replacing almost the entire left lobe. The cut surface appeared variegated with tan-grey areas admixed with pale yellow and hemorrhagic areas. The right thyroid lobe appeared grossly normal. Microscopic sections of the left thyroid mass revealed an encapsulated tumor with extensive capsular invasion. The majority of tumor (>90 %) consisted of large, pleomorphic epithelioid and spindle neoplastic cells in solid growth pattern (Fig. 14.9). Individual neoplastic cells demonstrated moderate to abundant amount of eosinophilic cytoplasm, oval/round to spindle-shaped nuclei, and prominent nucleoli (Figs. 14.10 and 14.11). Bi- or multi-nucleated forms as well as osteoclastic-like giant cells were frequently noted (Fig. 14.12). Osteoid production was noted in some area as well as areas of necrosis (Fig. 14.13). In addition to the anaplastic component, a small portion of the tumor (<10 %) consisted of smaller, relatively uniform neoplastic cells in a predominantly microfollicular pattern. No nuclear features of papillary thyroid carcinoma were identified. These findings were consistent with the remnant of a follicular carcinoma (Figs. 14.14 and 14.15). The tumor cells of the anaplastic component were negative for pan-cytokeratin, TTF-1, and PAX8; on the contrary, the tumor cells of the follicular carcinoma reacted strongly with pan-cytokeratin, TTF-1, and PAX8. Extensive vascular invasion was noted. However, all five lymph nodes were negative for metastatic disease. The final diagnosis was anaplastic thyroid carcinoma arising from a follicular thyroid carcinoma.

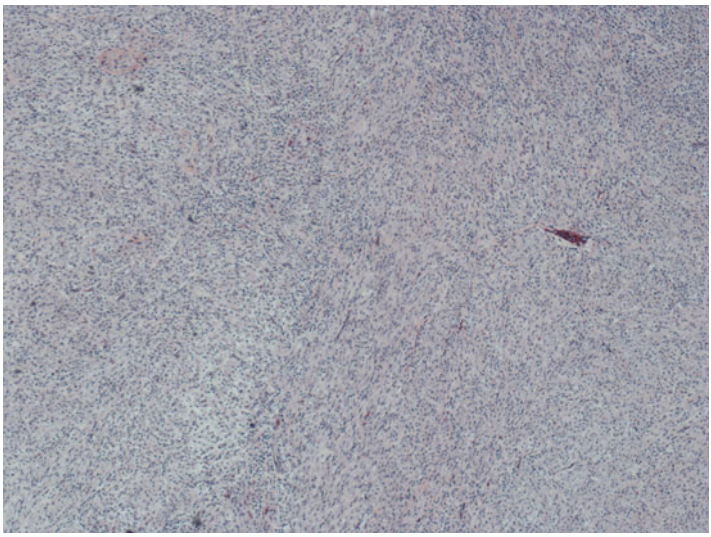

Fig. 14.9 Anaplastic thyroid carcinoma arising from a follicular carcinoma. The larger portion of the tumor consists of neoplastic cells in solid growth pattern (H&E, low power)

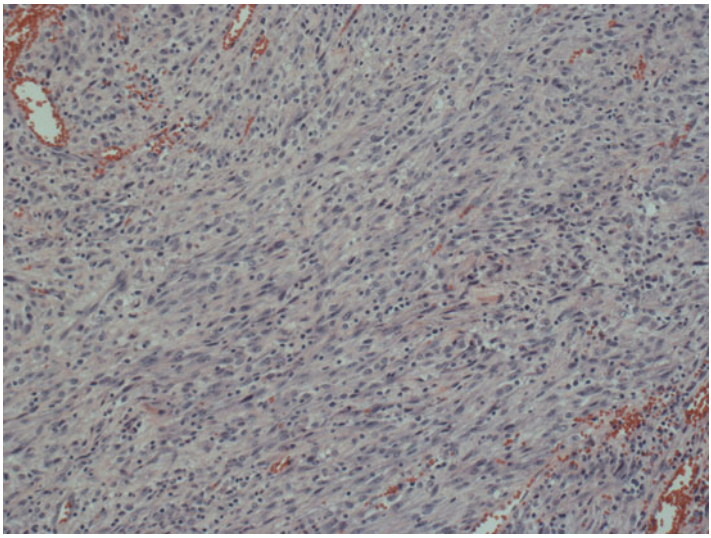

Fig. 14.10 Anaplastic thyroid carcinoma arising from a follicular carcinoma. The neoplastic cells consist of a mixture of large, pleomorphic spindle and epithelioid forms with little intervening stroma (H&E, low power)

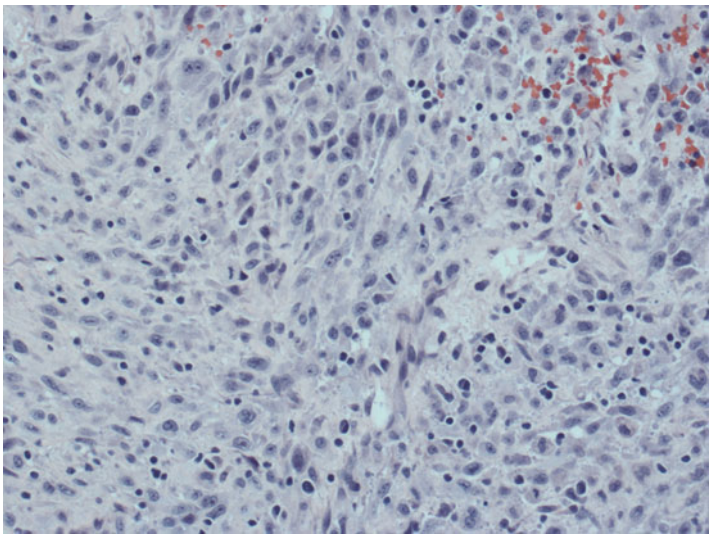

Fig. 14.11 Anaplastic thyroid carcinoma arising from a follicular carcinoma. Individual neoplastic cells demonstrate moderate amount of eosinophilic cytoplasm and oval to elongated nuclei with vesicular chromatin, prominent nucleoli, and thick, irregular nuclear membranes (H&E, low power)

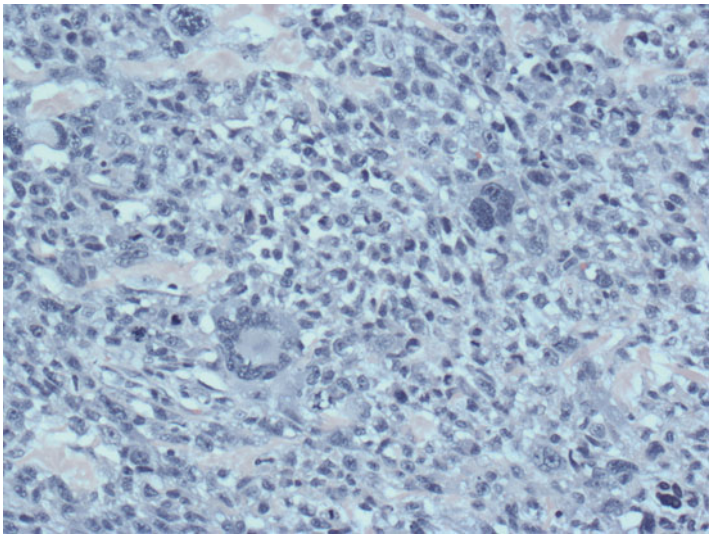

Fig. 14.12 Anaplastic thyroid carcinoma arising from a follicular carcinoma. Pleomorphic multinucleated and osteoclastic-like giant cells are frequently noted. In addition, abnormal mitotic figures are readily apparent (H&E, low power)

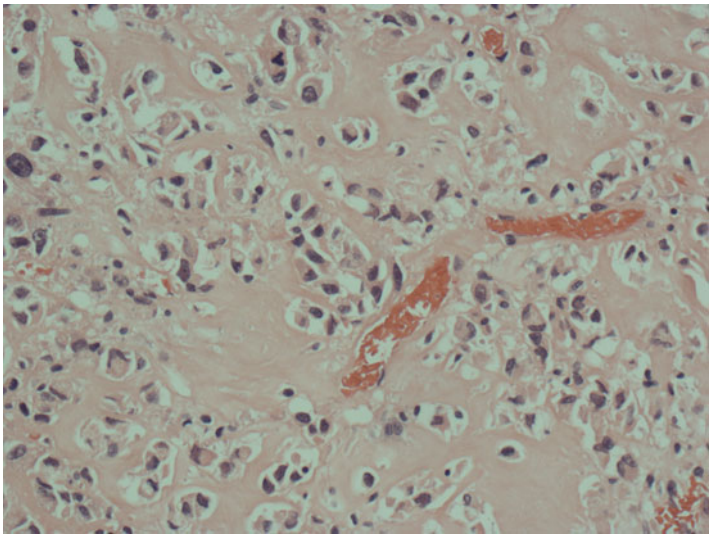

Fig. 14.13 Anaplastic thyroid carcinoma arising from a follicular carcinoma. Abundant eosinophilic, extracellular material consistent with osteoid is admixed with neoplastic cells (H&E, high power)

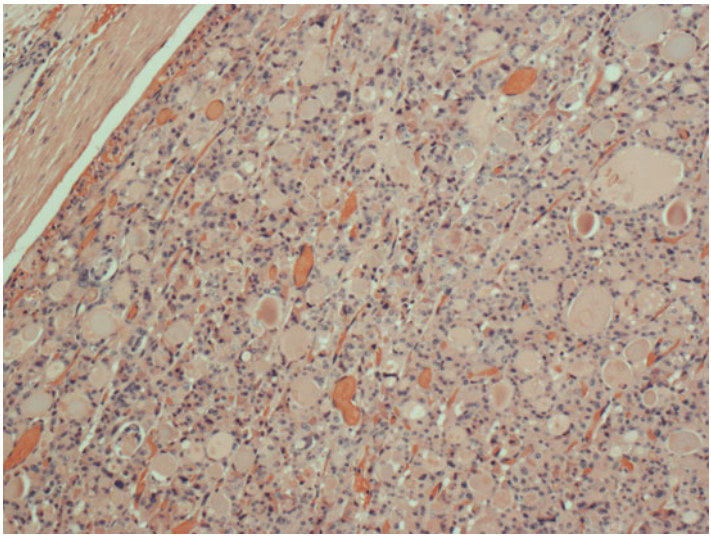

Fig. 14.14 Anaplastic thyroid carcinoma arising from a follicular carcinoma. A small portion of tumor demonstrates predominantly a follicular growth pattern (H&E, low power)

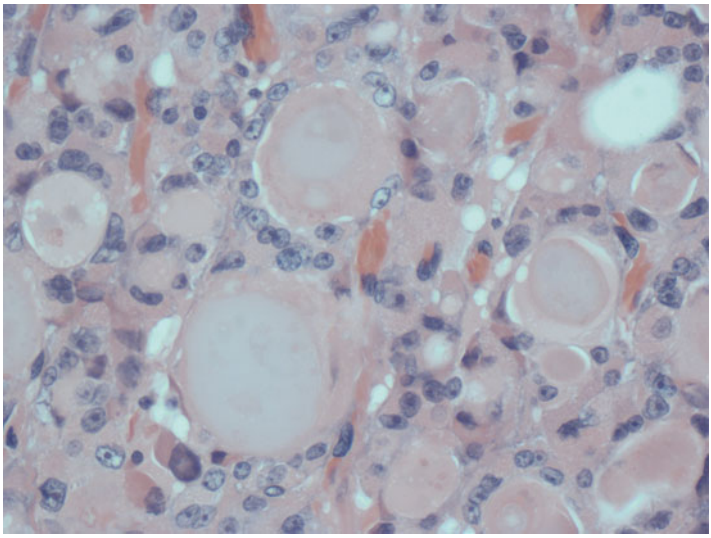

Fig. 14.15 Anaplastic thyroid carcinoma arising from a follicular carcinoma. The follicles are lined by cuboidal follicular cells with smaller, relatively uniform nuclei. Evidences of nuclear features of papillary thyroid carcinoma are not identified (H&E, high power)

Discussion

Anaplastic thyroid carcinoma is the most aggressive form of primary thyroid malignancy, with a median survival of less than 6 months following the initial diagnosis [1]. It is uncommon and accounts for less than 3 % of all thyroid malignancies; however, it contributes up to 50 % of the annual mortality secondary to thyroid cancer [2]. Unlike patients with other primary thyroid malignancies, who often benefit from complete surgical resection, the best survival results are observed in inoperable patients who received primary chemotherapy and radiation therapy rather than primary surgical resection [3, 4]. Therefore, an accurate preoperative diagnosis of anaplastic thyroid carcinoma would be helpful to avoid unnecessary surgery and allow the patients proceed directly to more optimal nonsurgical therapy [5].

Clinically, almost all patients with anaplastic thyroid carcinoma are elderly and present with a rapidly enlarging, painful neck mass with or without pressure symptoms such as hoarseness, dysphagia, and dyspnea. Physical examination reveals a fixed and hard thyroid gland. Cervical nodal and/or distant metastases are noted in at least 40 % of patients at the time of presentation. The frequent ultrasonographic findings of anaplastic thyroid carcinoma include a solitary mass, marked hypoechogenicity, irregular margins, and internal calcification; these findings are nonspecific and can be seen in other aggressive forms of thyroid cancers [6]. When an anaplastic thyroid carcinoma is suspected clinically and/or ultrasonographically, tissue confirmation by FNA is often required to establish a definitive diagnosis and to guide subsequent clinical management.

Histologically, anaplastic thyroid carcinomas are composed of a mixture of markedly atypical/pleomorphic spindle, epithelioid, and giant cells with considerable variations in both the proportions and distributions of these cellular components from tumors to tumors (Fig. 14.16). The epithelioid component often exhibits squamoid features, resembling the cells of non-keratinizing, poorly differentiated squamous cell carcinomas. The giant cells may contain single or multiple, pleomorphic nuclei; occasional osteoclast-like giant cells are also noted (Fig. 14.17). Spindle cells can be arranged in fascicles or a storiform pattern and can result in a sarcomatoid appearance when it is the predominant or exclusive component (Fig. 14.18). Hemorrhage, necrosis, and inflammatory infiltrate may be seen with all cell patterns (Fig. 14.19). In up to 70 % of anaplastic thyroid carcinomas, there is evidence of a pre-existing well-differentiated thyroid carcinoma, either papillary or follicular [7].

The cellularity and the cytologic presentations of anaplastic thyroid carcinoma are variable depending on the histologic type and the extent of tumor necrosis [8–10]. For example, tumors with a predominant spindle cell pattern with sclerosis tend to be paucicellular (Fig. 14.20) whereas tumors with giant and epithelioid cells often yield highly cellular aspirates (Fig. 14.21). Tumors with extensive hemorrhage, inflammatory infiltrate, or necrosis may obscure the malignant cells and yield unsatisfactory samples (Fig. 14.22). The malignant cells are often present singly, as loosely cohesive groups, or infrequently as syncytial tissue fragments. Individual cells vary in size and shape from small to giant forms and from round/oval to polygonal, to spindle, to various bizarre shapes (Figs. 14.23 and 14.24). The nuclei are

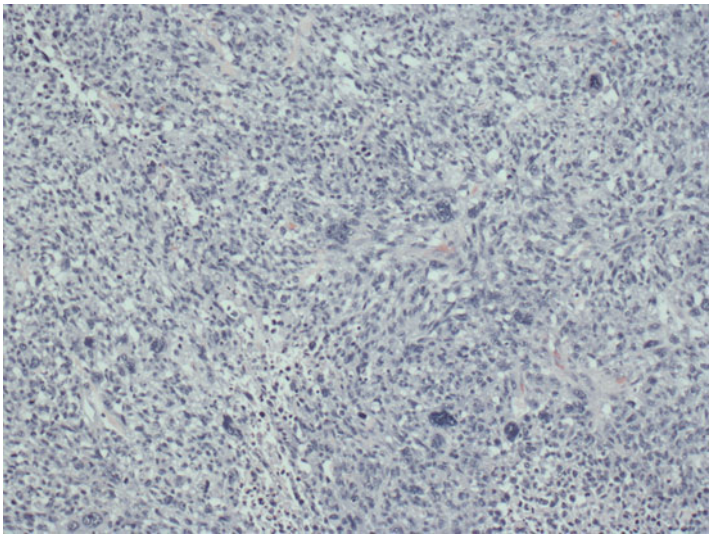

Fig. 14.16 Anaplastic thyroid carcinoma. It is typically characterized by a mixture of markedly atypical/pleomorphic spindle, epithelioid, and giant cells with considerable variation in both proportions and distributions (H&E, low power)

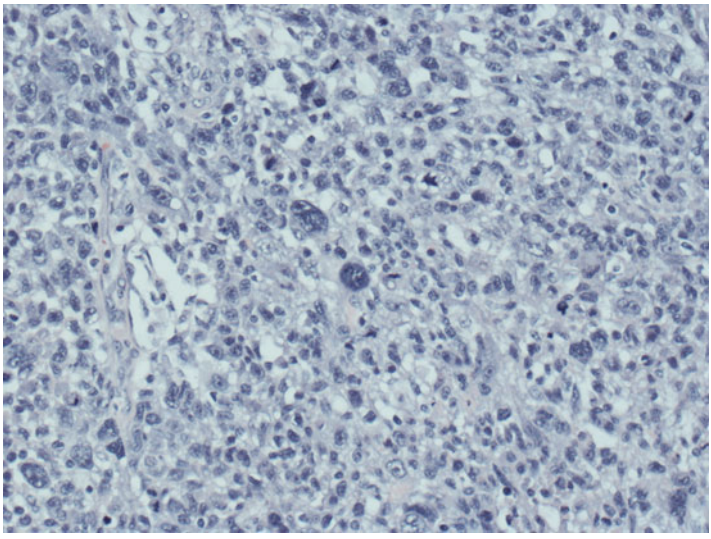

Fig. 14.17 Anaplastic thyroid carcinoma. Individual neoplastic cells show marked pleomorphism with nuclear enlargement, anisonucleosis, prominent nucleoli, multinucleation, and increased nuclear/cytoplasmic ratio (H&E, high power)

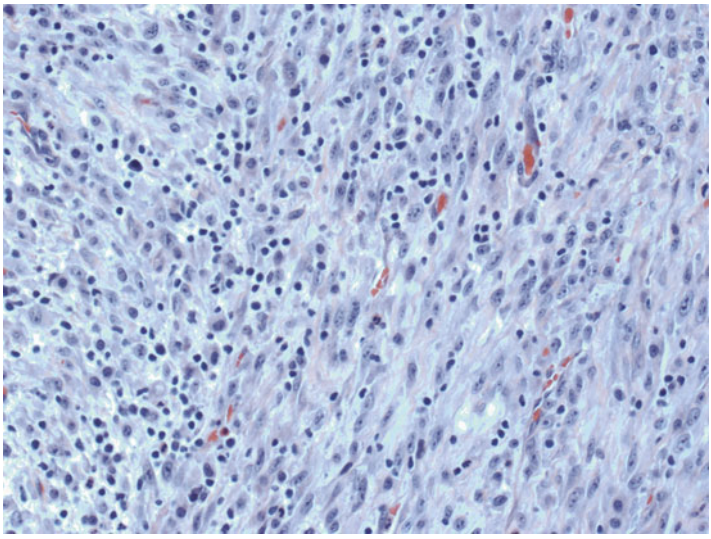

Fig. 14.18 Anaplastic thyroid carcinoma. This tumor consists of predominantly neoplastic spindle cells arranged in fascicles, resembling a high-grade sarcoma. Individual tumor cells have abundant eosinophilic cytoplasm, elongated nuclei with vesicular chromatin, prominent, sometimes multiple, nucleoli (H&E, high power)

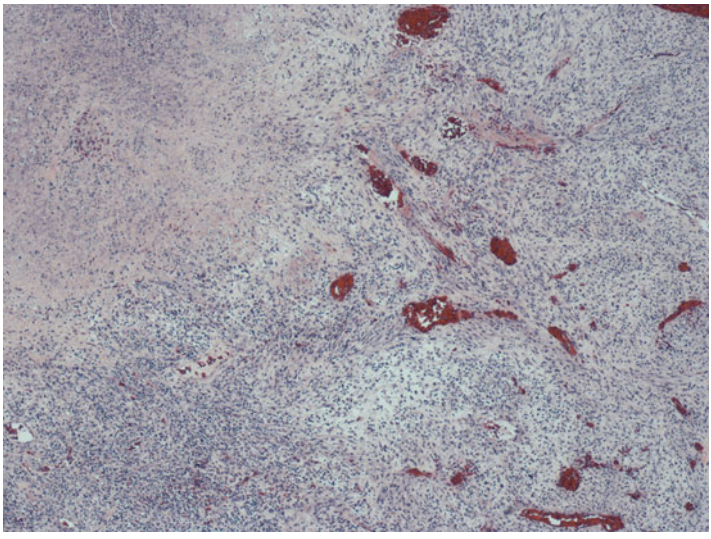

Fig. 14.19 Anaplastic thyroid carcinoma. Areas of necrosis are frequently noted (H&E, low power)

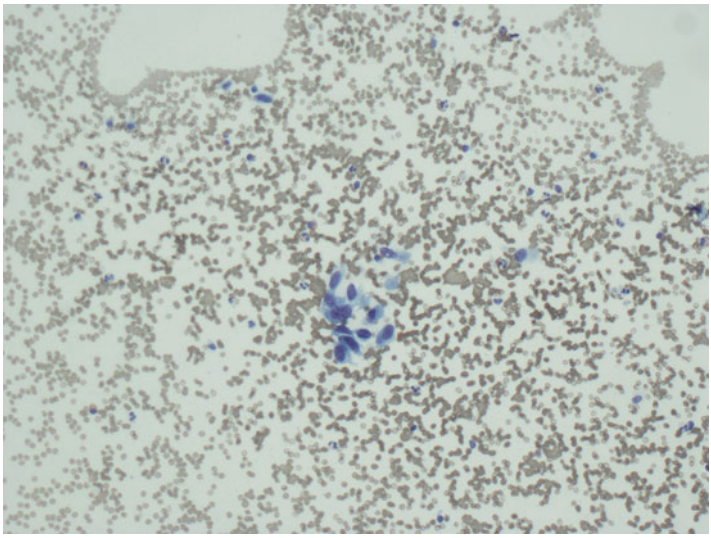

Fig. 14.20 Thyroid FNA-anaplastic thyroid carcinoma. Paucicellular specimen with scattered atypical spindle-shaped neoplastic cells (Diff Quik stain, low power)

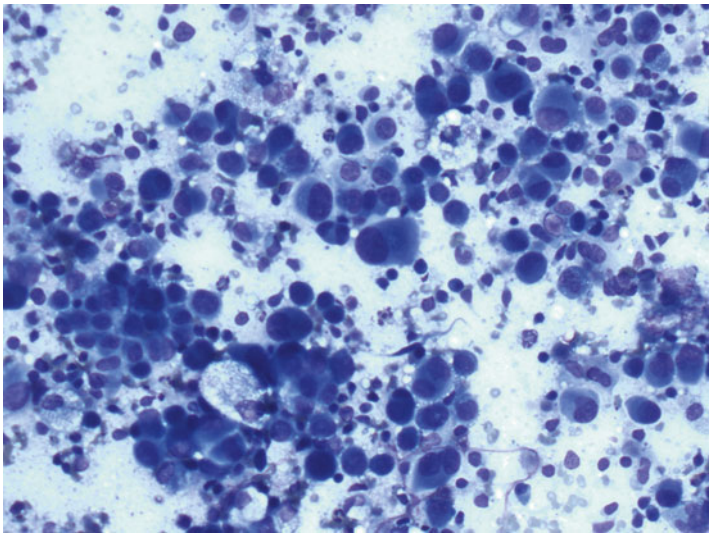

Fig. 14.21 Thyroid FNA-anaplastic thyroid carcinoma. Markedly cellular specimen with predominantly epithelioid neoplastic cells (Diff Quik stain, high power)

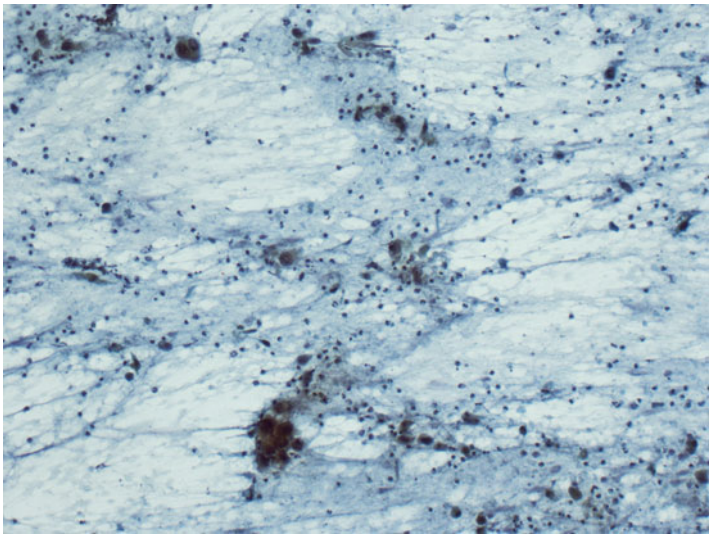

Fig. 14.22 Thyroid FNA-anaplastic thyroid carcinoma. Extensive necrosis with inflammatory and cellular debris. Neoplastic cells are not readily apparent (Papanicolaou stain, low power)

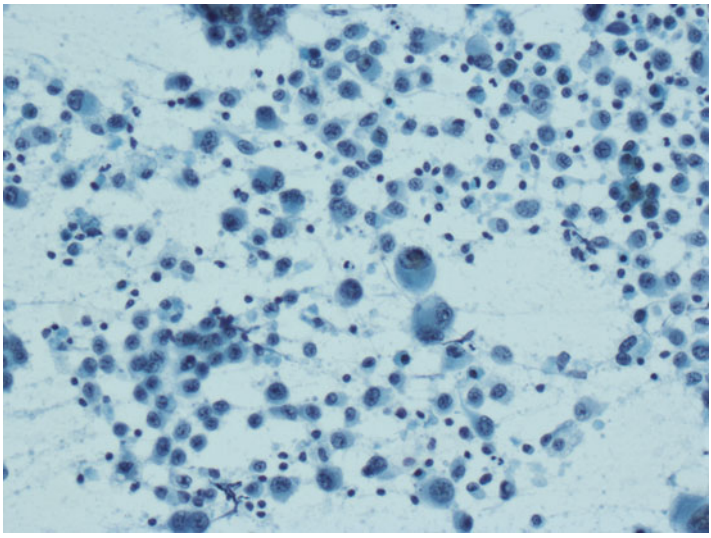

Fig. 14.23 Thyroid FNA-anaplastic thyroid carcinoma. Predominantly loosely cohesive epithelioid cells. Marked anisonucleosis is apparent (Papanicolaou stain, high power)

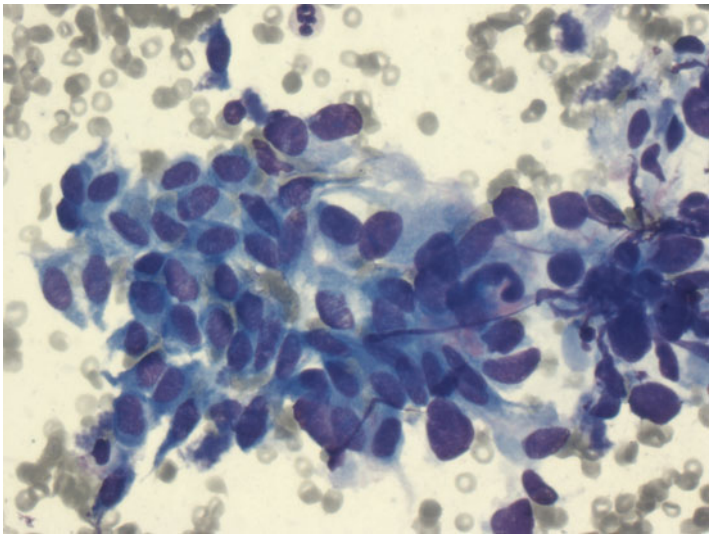

Fig. 14.24 Thyroid FNA-anaplastic thyroid carcinoma. Crowded cluster of spindle-shaped neoplastic cells with moderate amount of cytoplasm and elongated nuclei (Diff-Quik stain, high power)

large with irregular nuclear membranes, coarsely granular chromatin, prominent nucleoli, and frequent intranuclear inclusions. Binucleated or multinucleated forms as well as normal and abnormal mitotic figures are common findings (Fig. 14.25). The cytoplasm appears pale to dense, and sometime clear. Emperipolesis may be seen in neoplastic giant cells. Keratinization may be focally evident in squamous-type neoplastic cells. In well-sampled cases, cytologic evidence of a well-differentiated thyroid carcinoma (papillary or follicular) may be found (Fig. 14.26).

Given the cytologic presentation along with adequate cellularity, the cytologic diagnosis of anaplastic carcinoma is usually quite straightforward with a diagnostic accuracy in the range of 85–90 % [8]. False-negative diagnoses have been reported and are attributed to one of the following factors: (1) paucicellular samples from spindle cell variant containing excessive collagenous stroma; (2) obscuring inflammatory and cellular debris from tumors with extensive necrosis (Fig. 14.27); or (3) predominantly neutrophilic infiltrate masquerading as abscess (Fig. 14.28) [6, 8, 9]. In addition, cases of anaplastic thyroid carcinoma have been underdiagnosed as well-differentiated thyroid carcinoma or even follicular neoplasm due to sampling error since a substantial percentage of anaplastic thyroid carcinomas consists of foci of well-differentiated thyroid carcinoma. Some benign conditions such as abscess, Riedel's and subacute thyroiditis with granulomatous inflammation (Fig. 14.29), cyst-lining cells from cystic degeneration in nodular goiters (Fig. 14.30), or radiation-induced changes (Fig. 14.31) may present with markedly atypical non-neoplastic histiocytic and/or stromal cells that can be misinterpreted as anaplastic thyroid carcinoma. In these conditions, the atypical cells are often sparse. Furthermore, a diagnosis of anaplastic thyroid carcinoma should be made cautiously if the patient's demographics and/or clinical presentation do not fit those of anaplastic thyroid carcinoma.

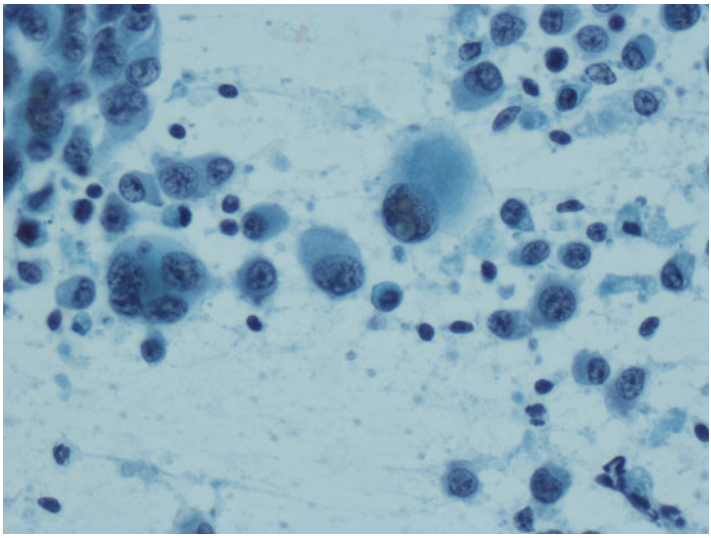

Fig. 14.25 Thyroid FNA-anaplastic thyroid carcinoma. Binucleated and multinucleated giant cells are present. Some tumor cells possess abundant dense cytoplasm and eccentrically located nuclei, resulting in a plasmacytoid/rhabdoid appearance (Papanicolaou stain, high power)

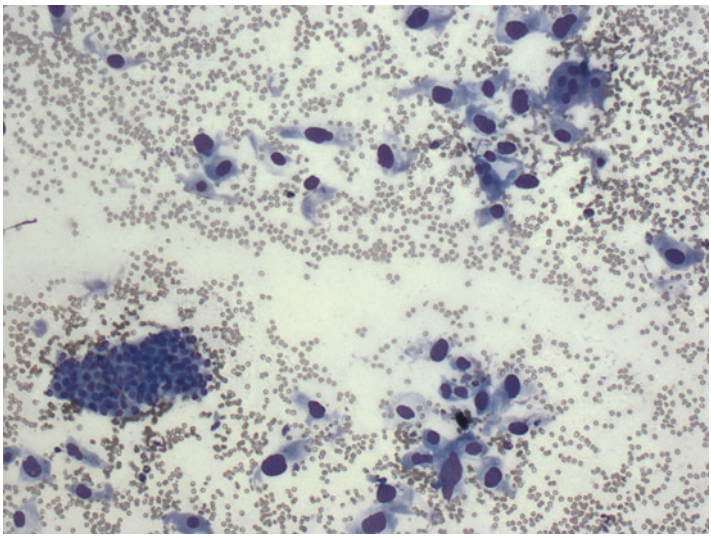

Fig. 14.26 Thyroid FNA-anaplastic thyroid carcinoma. Two cellular components are noted. In addition to the loosely cohesive pleomorphic spindle-shaped cells, a cluster of smaller, relatively uniform neoplastic follicular cells are also noted. The latter denote remnant of a well-differentiated thyroid carcinoma (Diff-Quik stain, high power)

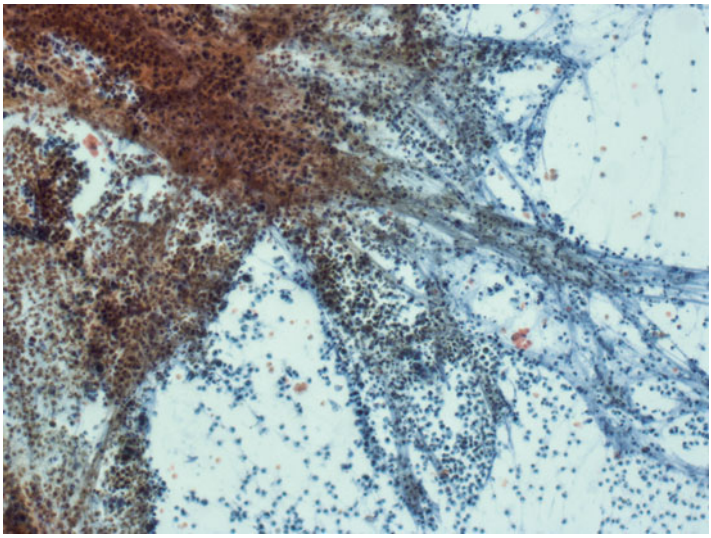

Fig. 14.27 Thyroid FNA-anaplastic thyroid carcinoma. Some aspirates consist of extensive necrosis with inflammatory and cellular debris, obscuring the underlying neoplastic cells (Papanicolaou stain, low power)

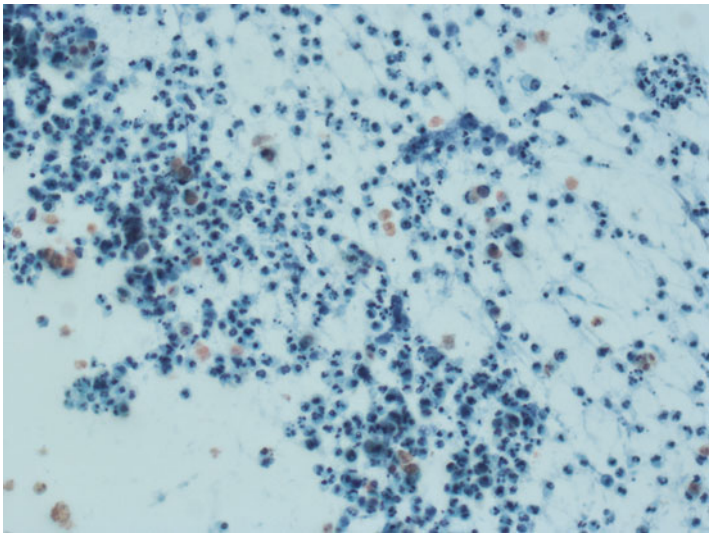

Fig. 14.28 Thyroid FNA-anaplastic thyroid carcinoma. Some aspirates consist of predominantly neutrophilc infiltrate, which can be confused with abscess (Papanicolaou stain, high power)

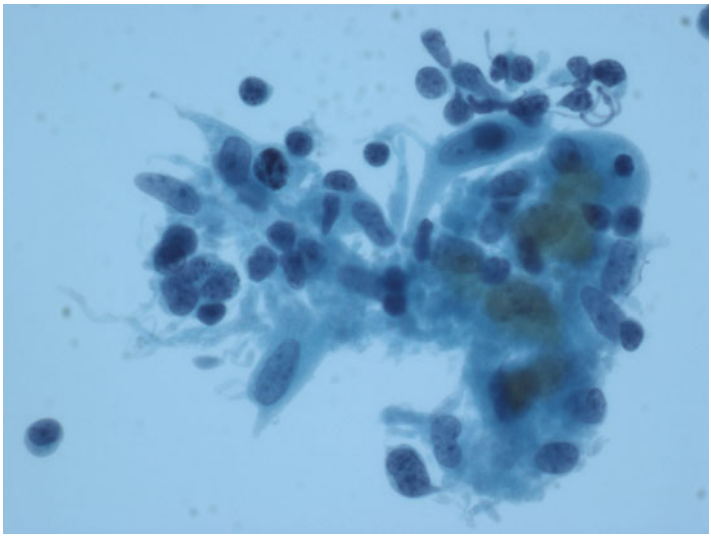

Fig. 14.29 Thyroid FNA-subacute thyroiditis. The finding of aggregate of epithelioid histiocytes consistent with non-necrotizing granuloma is characteristic of subacute thyroiditis. Epithelioid histiocytes can display considerable atypia, which can be mistaken for a malignancy. The presence of abundant cytoplasm, "carrot-shaped" nuclei, and mature lymphocytes favor a benign process (Papanicolaou stain, high power)

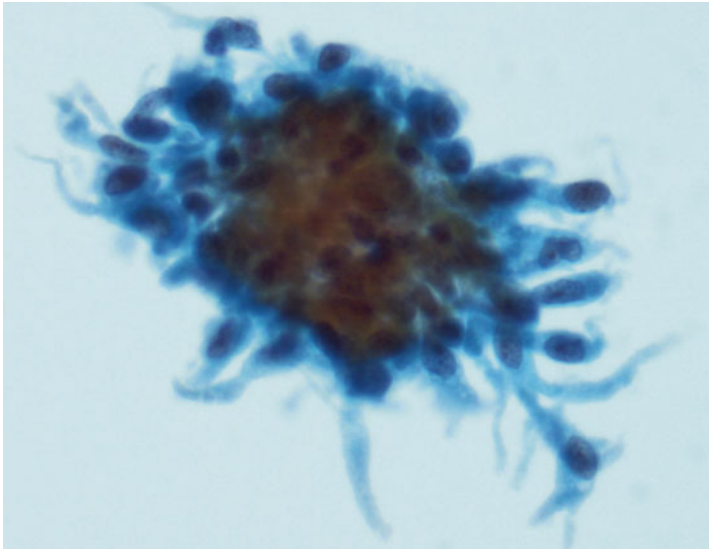

Fig. 14.30 Thyroid FNA-cystic degeneration in nodular goiter. Aggregates of mildly atypical spindle-shaped cells derived from cyst-lining cells. Nuclear enlargement and prominent nucleoli can be noted and be mistaken for a neoplasm (Papanicolaou stain, high power)

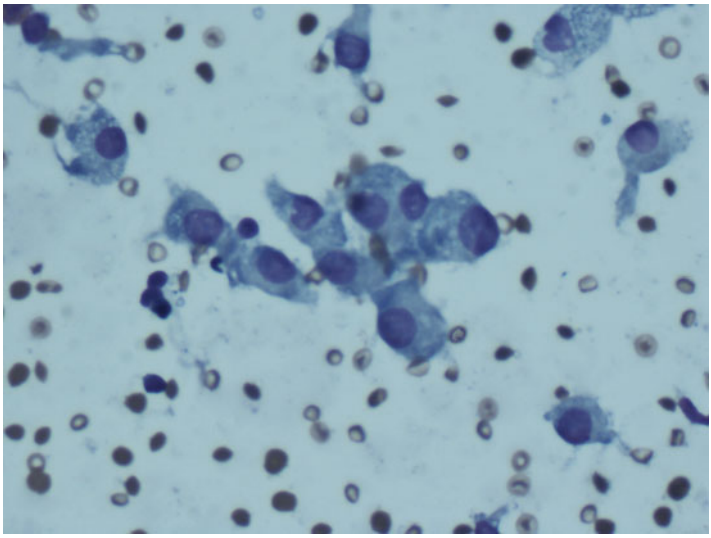

Fig. 14.31 Thyroid FNA-atypia in patient with Graves' disease status posttreatment with radioactive iodine. Scattered follicular cells with cytoplasmic and nuclear enlargement, resulting in normal nuclear-to-cytoplasmic ratio (Diff Quik stain, high power)

Because of its diverse cytologic presentations with different cellular morphologies, anaplastic thyroid carcinoma can simulate other neoplastic processes including medullary carcinoma, metastatic tumors, lymphoma, and sarcoma. Cytologic features that are shared by both medullary carcinoma and anaplastic thyroid carcinoma include hypercellularity, a dispersed single-cell pattern, spindle cell morphology, and nuclear pleomorphism (Figs. 14.32 and 14.33). The finding of the typical "salt-and-pepper" chromatin and relative uniformity of the majority of the neoplastic cells would favor a medullary carcinoma (Fig. 14.34). Metastatic tumors should always be considered in the differential diagnosis, especially in patients with a clinical history of non-thyroid cancer. For example, metastatic melanomas often present with single, pleomorphic cells with or without cytoplasmic melanin pigments (Fig. 14.35). Metastatic poorly differentiated squamous cell carcinoma from the head and neck region and upper aerodigestive tract can be difficult to distinguish from anaplastic thyroid carcinoma with a predominant squamous component (Fig. 14.36). Metastatic carcinoma from other sites should be considered especially in patients with a prior history of non-thyroidal malignancy (Fig. 14.37). Anaplastic thyroid carcinoma can also be confused with high-grade large lymphoma such as diffuse large cell non-Hodgkin's lymphoma, anaplastic large-cell lymphoma, and Hodgkin's lymphoma because of the dispersed, single-cell pattern and the finding of occasional pleomorphic giant cells (Fig. 14.38). Anaplastic thyroid carcinomas with a spindle cell pattern can simulate a mesenchymal malignancy, both primary and secondary.

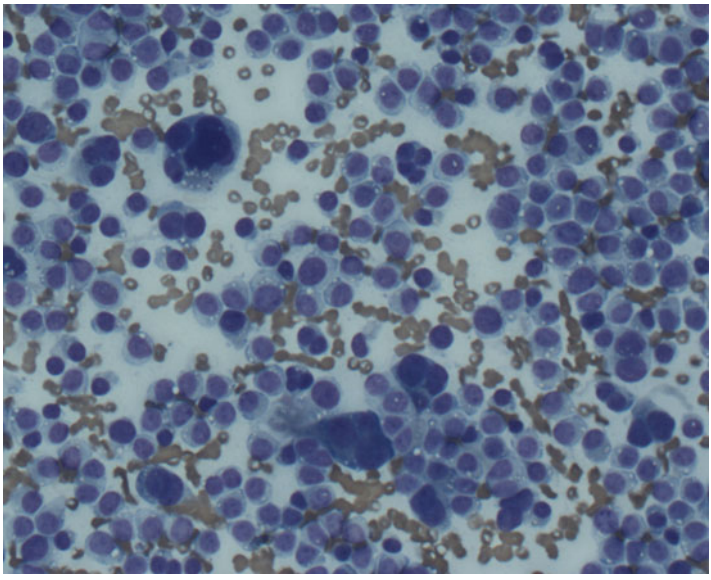

Fig. 14.32 Thyroid FNA-medullary carcinoma. Loosely cohesive epithelioid cells with eccentrically located, round to oval nuclei. Binucleated and multinucleated giant cells can be present (Diff-Quik stain, high power)

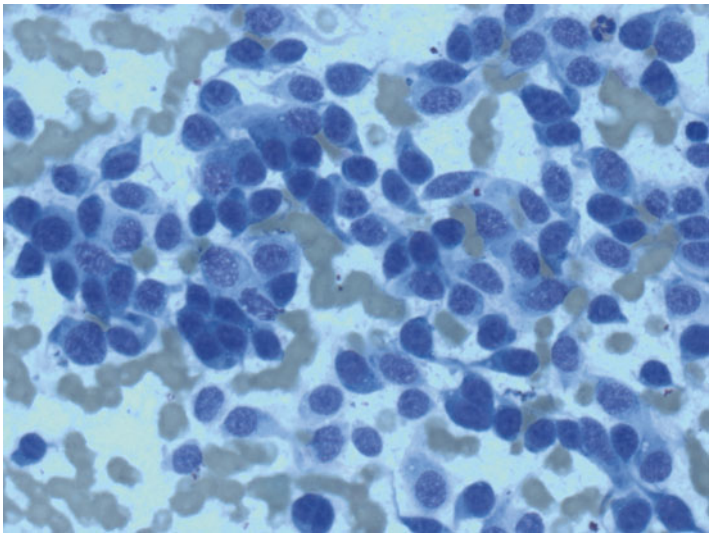

Fig. 14.33 Thyroid FNA-medullary carcinoma. Loosely cohesive spindle-shaped and epithelioid cells are typical finding of medullary carcinoma (Diff-Quik stain, high power)

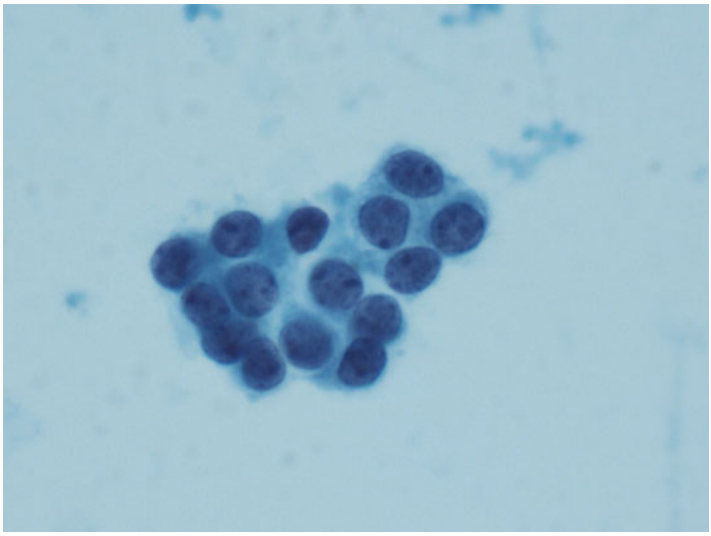

Fig. 14.34 Thyroid FNA-medullary carcinoma. The finding of "salt-pepper" chromatin favors a diagnosis of medullary carcinoma (Papanicolaou stain, high power)

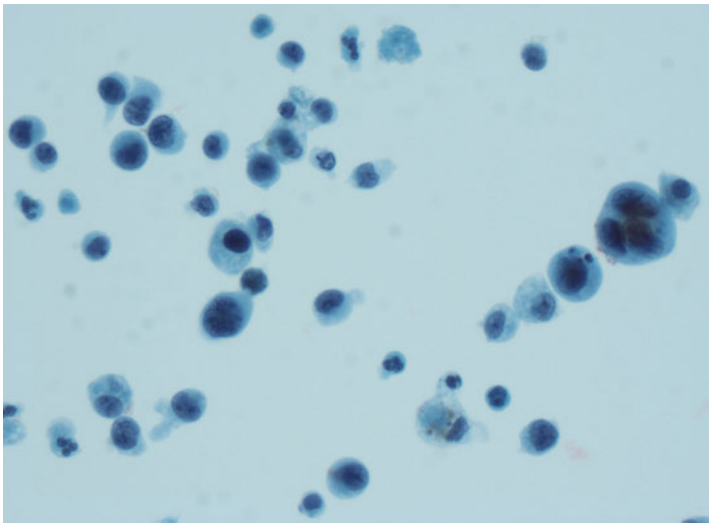

Fig. 14.35 Thyroid FNA-metastatic melanoma. Predominantly single epithelioid cells with plasmacytoid appearance. Prominent nucleoli and multinucleation are frequent findings. Cytoplasmic pigment is noted in occasional neoplastic cells (Papanicolaou stain, high power)

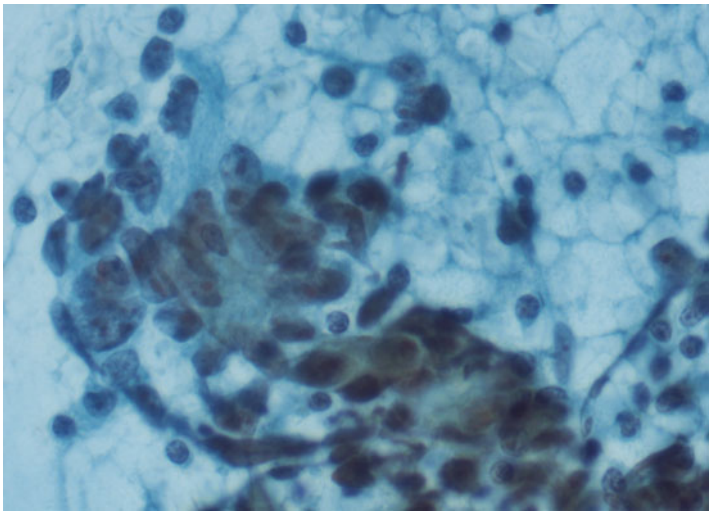

Fig. 14.36 Thyroid FNA-metastatic squamous cell carcinoma. Cohesive crowded group of atypical, non-keratinizing squamous cells with spindle-shaped cells. The patient had a history of laryngeal squamous cell carcinoma status post-laryngectomy (Papanicolaou stain, high power)

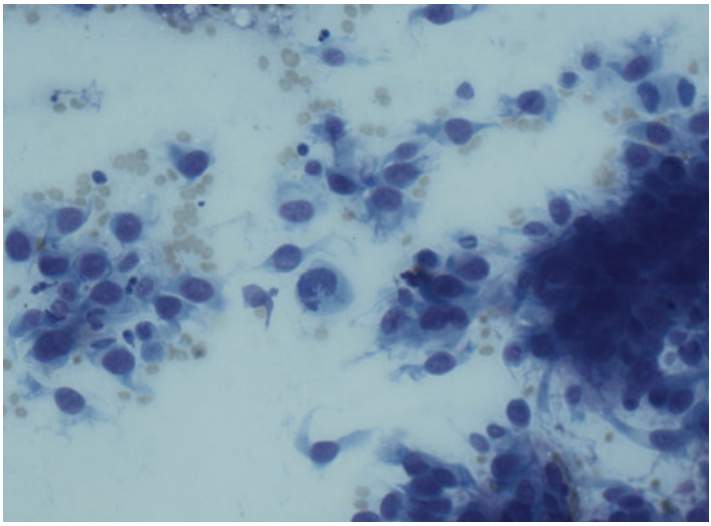

Fig. 14.37 Thyroid FNA-metastatic adenocarcinoma from breast. Single and cohesive groups of markedly atypical epithelioid and spindle-shaped neoplastic cells. The patient had a stage IV breast carcinoma with widespread metastases (Diff-Quik stain, high power)

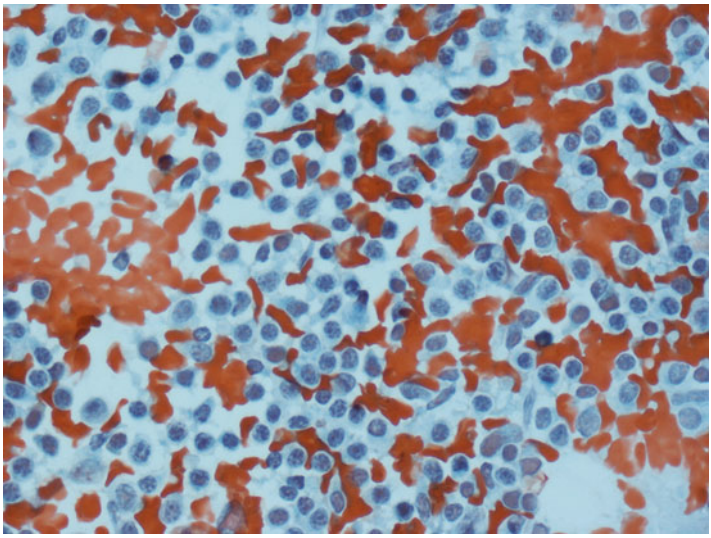

Fig. 14.38 Thyroid FNA-large B-cell non-Hodgkin's lymphoma. Predominantly single cells with scant amount of non-descript cytoplasm, round-to-oval nuclei, and coarse chromatin. Corresponding flow cytometry revealed a monoclonal B-cell population with kappa light chain restriction (Papanicolaou stain, high power)

Immunocytochemistry can be helpful in the differential diagnosis of anaplastic thyroid carcinoma. Cytokeratin is the most useful marker in establishing the epithelial nature of the neoplasm since it is consistently positive in anaplastic thyroid carcinomas. Anaplastic thyroid carcinomas are nonreactive to calcitonin, Melan-A, and leukocyte common antigen (LCA), thus excluding medullary carcinoma, melanoma, and lymphoma. Differential diagnosis from metastatic carcinoma can be challenging since the majority of anaplastic thyroid carcinomas are negative for thyroglobulin (up to 60 %) and thyroid transcription factor-1 (TTF-1; up to 80 %) [8, 11]. More recently, it has been demonstrated that PAX8, which is associated with thyroid organogenesis, was found to be consistently expressed in 80 % of anaplastic thyroid carcinoma in tissue sections [11]. Unfortunately, the results with cytology preparations were mixed. Rivera et al. did not observe any reactivity to PAX8 in their five cases of anaplastic thyroid carcinoma [12] whereas Bellevicine et al. reported PAX8 positivity in their three cases of anaplastic thyroid carcinoma including one with a spindle cell pattern [13]. Thus, the jury is still out in regard to the usefulness of PAX8 in the cytologic differential diagnosis of anaplastic thyroid carcinoma. It is important to note that all three markers, thyroglobulin, TTF-1, and PAX8, are positive with well-differentiated primary thyroid carcinomas, both papillary and follicular.

References

1. Nagaiah G, Hossain A, Mooney CJ, Parmentier J, Remick SC. Anaplastic thyroid cancer: a review of epidemiology, pathogenesis, and treatment. J Oncol. 2011;2011:542358.
2. Kebebew E, Greenspan FS, Clark OH, Woeber KA, McMillan A. Anaplastic thyroid carcinoma. Treatment outcome and prognostic factors. Cancer. 2005;103:1330–5.
3. Pudney D, Lau H, Ruether JD, Falck V. Clinical experience of the multimodality management of anaplastic thyroid cancer and literature review. Thyroid. 2007;17:1243–50.
4. Besic N, Auersperg M, Us-Krasovec M, Golouh R, Frkovic-Grazio S, Vodnik A. Effect of primary treatment on survival in anaplastic thyroid carcinoma. Eur J Surg Oncol. 2001;27:260–4.
5. Greenblatt DY, Woltman T, Harter J, Starling J, Mack E, Chen H. Fine-needle aspiration optimizes surgical management in patients with thyroid cancer. Ann Surg Oncol. 2006;13:859–63.
6. Suh HJ, Moon HJ, Kwak JY, Choi JS, Kim EK. Anaplastic thyroid cancer: ultrasonographic findings and the role of ultrasonography-guided fine needle aspiration biopsy. Yonsei Med J. 2013;54:1400–6.
7. Venkatesh YS, Ordonez NG, Schultz PN, Hickey RC, Goepfert H, Samaan NA. Anaplastic carcinoma of the thyroid. A clinicopathologic study of 121 cases. Cancer. 1990;66:321–30.
8. Us-Krasovec M, Golouh R, Auersperg M, Besic N, Ruparcic-Oblak L. Anaplastic thyroid carcinoma in fine needle aspirates. Acta Cytol. 1996;40:953–8.
9. Luze T, Totsch M, Bangerl I, et al. Fine needle aspiration cytodiagnosis of anaplastic carcinoma and malignant haemangioendothelioma of the thyroid in an endemic goitre area. Cytopathology. 1990;1:305–10.
10. Guarda LA, Peterson CE, Hall W, Baskin HJ. Anaplastic thyroid carcinoma: cytomorphology and clinical implications of fine-needle aspiration. Diagn Cytopathol. 1991;7:63–7.
11. Nonaka D, Tang Y, Chiriboga L, Rivera M, Ghossein R. Diagnostic utility of thyroid transcription factors Pax8 and TTF-2 (FoxE1) in thyroid epithelial neoplasms. Mod Pathol. 2008;21:192–200.
12. Rivera M, Sang C, Gerhard R, Ghossein R, Lin O. Anaplastic thyroid carcinoma: morphologic findings and PAX-8 expression in cytology specimens. Acta Cytol. 2010;54:668–72.
13. Bellevicine C, Iaccarino A, Malapelle U, Sasso FC, Biondi B, Troncone G. PAX8 is expressed in anaplastic thyroid carcinoma diagnosed by fine-needle aspiration: a study of three cases with histological correlates. Eur J Endocrinol. 2013;169:307–11.

Metastatic Neoplasms to the Thyroid

15

Case Study

A 65-year-old female with a history significant for morbid obesity, hypertension, and ductal breast carcinoma presented with 1-year history of swelling in the neck, voice fatigue, and mild difficulty in swallowing. There was no history of radiation to the head and neck region. She reported that she had never smoked, never used smokeless tobacco, never used illicit drugs and was not a drinker. Her family history included breast and ovarian cancer in her mother, and diabetes in her father. There was no history of thyroid disease. Physical examination revealed a well-developed female who was not in any obvious distress. Examination of the neck revealed diffusely enlarged thyroid gland. There was no cervical adenopathy. Ultrasonographic examination revealed that the right lobe of the thyroid gland was enlarged and replaced by an isoechoic nodule that measured approximately $4.1 \times 3.7 \times 3.5$ cm. However, the exact measurement was more as some aspect of this nodule was substernal and not accessible via ultrasound. The nodule was complex, cystic without internal calcifications. The left lobe of the thyroid gland was also significantly enlarged and substernal. Approximate measurement of the left lobe was $3.9 \times 3.6 \times 3.5$ cm. This lobe was heterogeneous in appearance, and contained a $3.0 \times 3.0 \times 1.5$ cm iso/hyperechoic nodule in the mid-pole. There were no internal calcifications. An assessment of multinodular goiter was made. Fine-needle aspiration biopsy of both thyroid lobes yielded a moderately cellular specimen showing mixed micro- and macrofollicular hyperplasia in a background of abundant colloid, consistent with multinodular goiter. Over the next several months, the neck swelling increased in size and her difficulty in swallowing and other compressive symptoms worsened. Computed tomography scan showed that the thyroid gland was enlarged and heterogeneous, measuring $9.9 \times 7.1 \times 5.4$ cm on the left and $9.5 \times 6.7 \times 3.7$ cm on the right. The thyroid gland was well marginated and mildly displaced the esophagus and trachea posteriorly and to the right with greater than 50 % reduction in the cross-sectional area of the trachea. There was mild splaying of the common carotid

A.J. Adeniran, D. Chhieng, *Common Diagnostic Pitfalls in Thyroid Cytopathology*, DOI 10.1007/978-3-319-31602-4_15

arteries and internal jugular veins. She was scheduled to undergo resection of her goiter when she developed a seizure the night before her operation, prompting work-up which revealed brain metastasis from her known breast cancer. A repeat FNA on the right lobe of the thyroid done around the same time showed hypercellular specimen with cohesive sheets of malignant cells. The nuclei were enlarged and variably hyperchromatic, and also varied in size and shape. Nucleoli were large and prominent, and irregularly shaped. After she was stabilized, she underwent total thyroidectomy to relieve the compressive symptoms and metastatic breast carcinoma was confirmed by histology. She also underwent radiation therapy to treat her brain metastasis.

Discussion

Secondary neoplasms of the thyroid gland, are uncommon. The incidence has been reported to be between 0.1 and 3 % [1–3], but they have been reported as incidental findings in autopsy studies with a frequency of 4.4–24 % in patients with a known primary cancer or widespread malignancy [4, 5]. This incidence may actually be increasing as a result of increased surveillance over the last few decades by imaging studies, including ultrasound and ultrasound-guided FNA biopsy [2, 6]. In contrast to primary tumors of the thyroid, metastatic tumors occur in a nearly equal sex distribution and are significantly older than the average population that presents with a thyroid nodule [1, 2, 5, 7]. Therefore, the increased likelihood of a possible secondary tumor should be considered when interpreting FNA biopsy of thyroid lesions in patients above the age of 50 years. Clinically, they can be indistinguishable from primary thyroid tumors [8–10]. Metastatic neoplasms can present as a solitary "cold" nodule, and sometimes as a functioning nodule [11], and may also present as numerous, small, discrete nodules, or diffuse involvement, which may be variably symptomatic [12]. They can present with features of hyperthyroidism, and they can also simulate acute or chronic thyroiditis, including elevated antithyroid antibody titers [13–15]. A thyroid nodule may be the first sign of metastasis in a patient with known cancer and rarely is the presenting finding of an unknown primary tumor [2, 16, 17]. The possibility of metastasis should always be considered whenever a patient presents with a thyroid nodule and they have a history of malignancy elsewhere in the body or when the cytologic picture is not consistent with or suggestive of common thyroid neoplasms. However, in 25–50 % of cases, there is no previous history of malignancy, and the thyroid metastasis is the first manifestation of an occult malignancy [17, 18]. The most common primary sites of metastasis to the thyroid are kidney, lung, breast, gastrointestinal tract, especially colon, melanoma, and malignant lymphoma [1, 7, 19]. However, other sites such as soft tissue, genital, and urothelial malignancies have also been reported [20, 21]. The thyroid gland may also be involved by direct extension from malignancies of the head and neck region, including laryngeal, oro-pharyngeal, and esophageal carcinomas [12, 22]. Very rarely, an extrathyroidal tumor can metastasize to a primary thyroid tumor [1, 23, 24].

Over the past few decades, fine-needle aspiration biopsy has emerged as the leading test for the evaluation of thyroid nodules [25–27]. The FNA biopsy is sensitive, but may not be specific for secondary malignancy, because metastatic tumors can mimic primary thyroid tumors cytologically [28, 29]. The accuracy of FNA biopsy in the diagnosis of metastatic tumors to the thyroid has been reported to be between 74 and 87 % [7]. The high accuracy may be attributed to the obvious malignant features especially in patients with prior diagnosis of malignancy in other sites [1]. It is important to distinguish secondary thyroid tumors from the primary tumors because patients who have metastasis to the thyroid have a poor prognosis in general, and most die shortly after the confirmation of distant metastasis [2–4, 28].

The cytologic pattern of a metastatic tumor depends upon the manner of thyroid involvement by the secondary neoplasm, and on the histologic type of the tumor as well as their stage of differentiation [30]. Although the cytological features of metastasis are distinct and clearly different from what is otherwise expected in primary tumors, there can be an admixture of atypical follicular cells, which can be misinterpreted as primary follicular neoplasm [1].

Renal cell carcinomas (RCCs) are the most common secondary malignant tumors involving the thyroid. The neoplastic cells are polygonal or elongated with clear cytoplasm, distinct cytoplasmic membranes, and small compact eccentric nuclei (Figs. 15.1–15.4). Nuclear pleomorphism is minimal to nonexistent. Although clear cell features are the dominant findings, cells with slightly eosinophilic cytoplasm can be present [31]. The cytologic features of thyroid papillary carcinoma such as nuclear enlargement, nuclear contour irregularity, dispersed to optically clear-appearing nuclear chromatin, crowding or overlapping nuclei, nuclear grooves, and nuclear

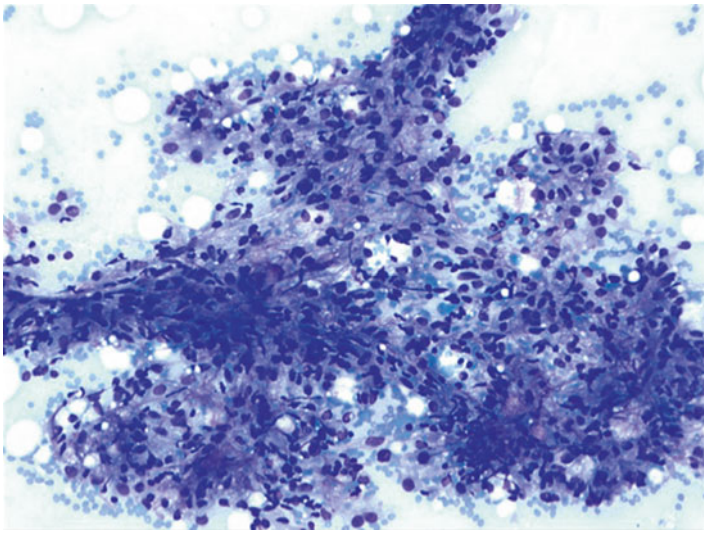

Fig. 15.1 FNA of metastatic clear cell renal cell carcinoma (RCC) to the thyroid. The clear cells of RCC have abundant, fragile, finely vacuolated cytoplasm (Diff-Quik stain, X200)

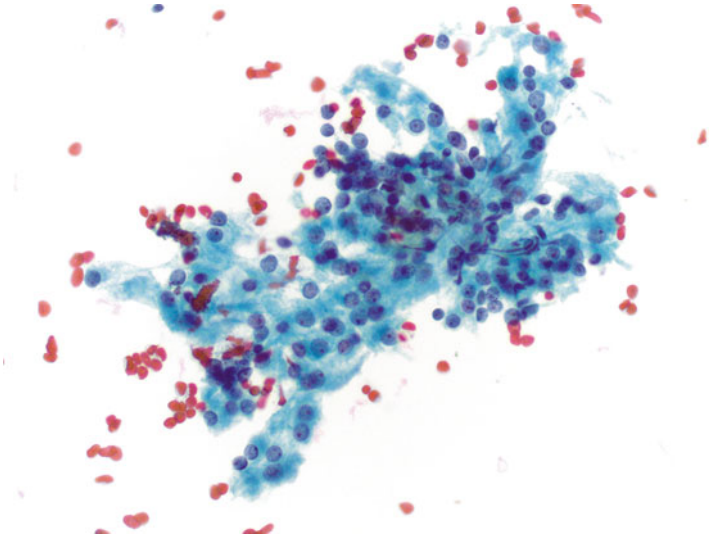

Fig. 15.2 FNA of metastatic clear cell RCC to the thyroid. The neoplastic cells are polygonal with clear cytoplasm, distinct cytoplasmic membranes, and small compact eccentric nuclei (Papanicolaou stain, X400)

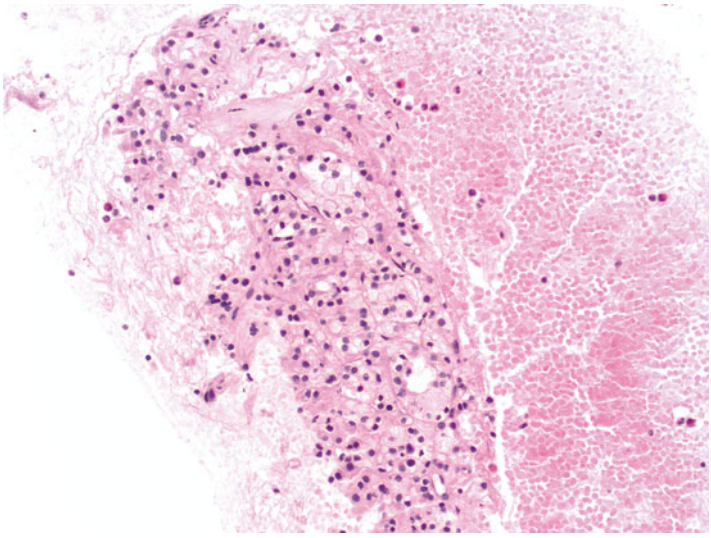

Fig. 15.3 Cell block material from the FNA of clear cell RCC (H&E stain, X200)

inclusions are not identified. A common pitfall is differentiating between metastatic clear cell RCC and dominant clear cell component within a primary thyroid follicular neoplasm (Fig. 15.5). Ancillary markers can be used effectively, as RCCs typically are immunoreactive for RCC, CAIX (Fig. 15.6), and CD10 (Fig. 15.7), while

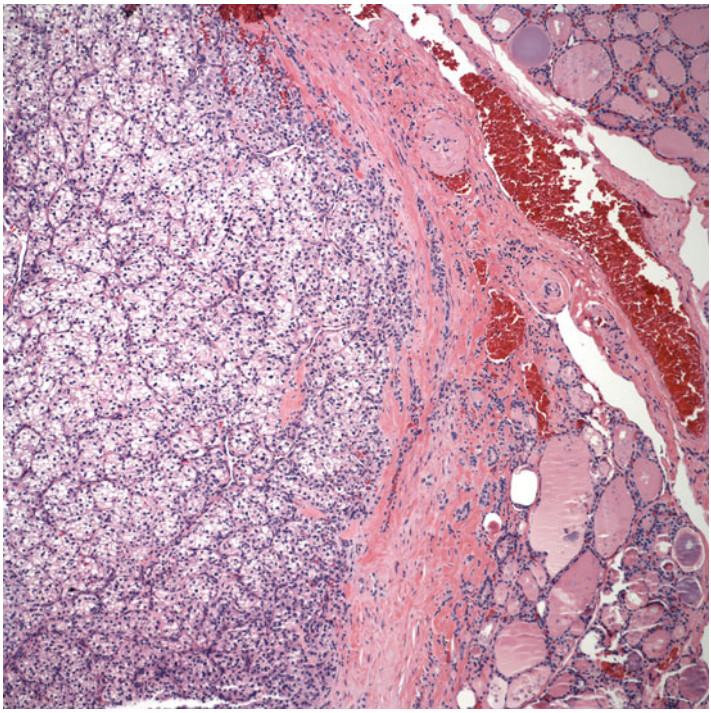

Fig. 15.4 Compact nests of neoplastic cells in metastatic clear cell RCC with adjacent normal thyroid follicles (H&E stain, X100)

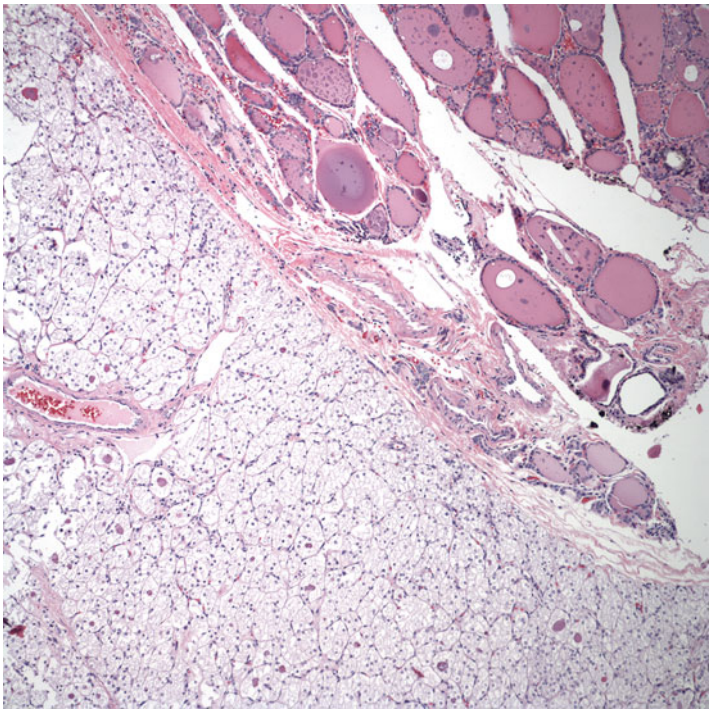

Fig. 15.5 Clear cell change in follicular adenoma of the thyroid with adjacent normal thyroid follicles (H&E stain, X100)

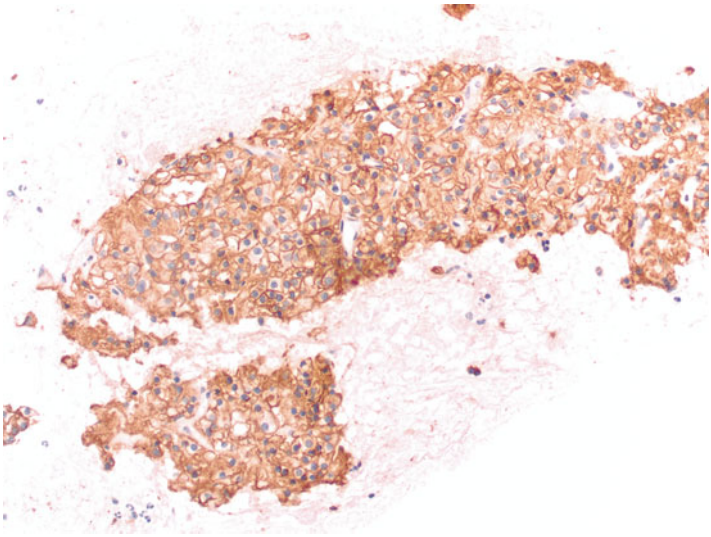

Fig. 15.6 Metastatic clear cell RCC to the thyroid. CAIX stain showing a membranous staining pattern

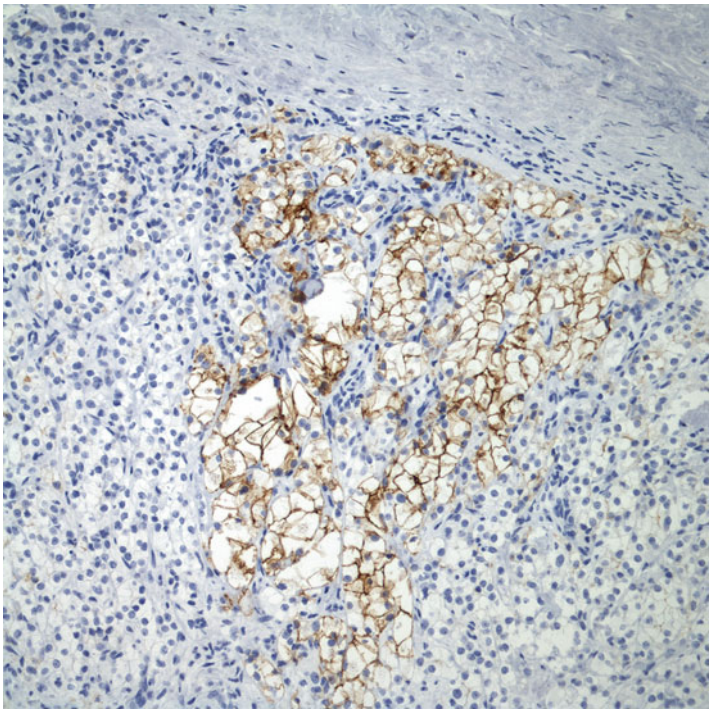

Fig. 15.7 Metastatic clear cell RCC to the thyroid. CD10 stain showing a membranous staining pattern

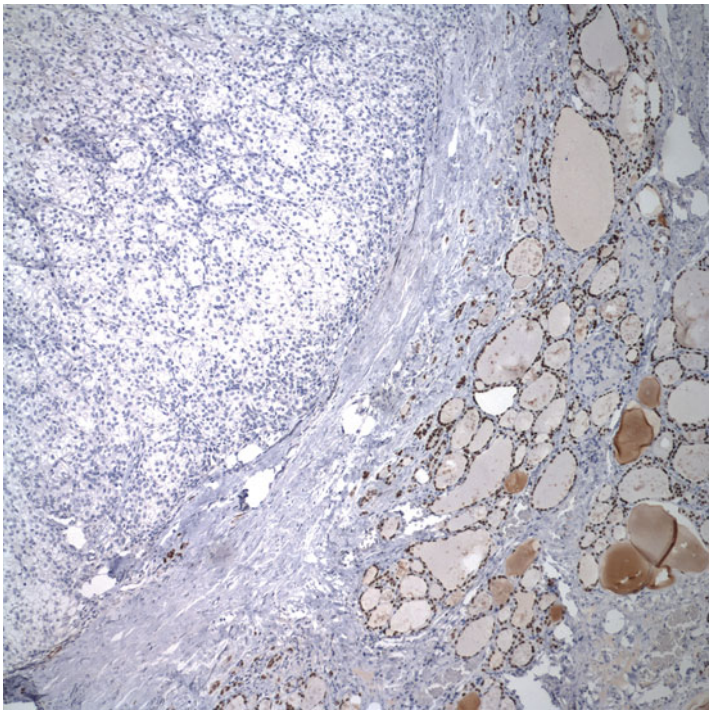

Fig. 15.8 TTF-1 stain is negative in the cells of clear cell RCC while positive in adjacent normal thyroid follicles

negative for thyroglobulin and TTF-1 (Figs. 15.8 and 15.9) [1, 32, 33]. Metastatic clear cell RCC with granular cell features can be difficult to distinguish from primary Hürthle cell tumor. PAX-8 is not a useful marker for distinguishing between them because it is expressed in both [34].

Metastases from breast or lung carcinomas may be very difficult to distinguish from primary thyroid neoplasms. Single-file pattern of cells and intracytoplasmic lumina suggest breast origin (Figs. 15.10–15.15) [17]. Ancillary studies are helpful in making a diagnosis of metastatic breast carcinoma. Positive markers in breast carcinoma include GATA-3 (Fig. 15.16), GCDFP-15, and mammaglobin (Fig. 15.17) and these markers are usually negative in the thyroid. TTF-1 and thyroglobulin are usually positive in primary thyroid tumors of follicular origin while they are negative in breast tumors (Fig. 15.18). For metastatic lung adenocarcinoma, the atypical cells are usually arranged in three-dimensional clusters, gland-forming clusters, or as single atypical glands. Scant colloid and few benign-looking follicular epithelial cells may be present in the background (Figs. 15.19 and 15.20). Intranuclear cytoplasmic inclusions may be identified and this may lead to erroneous diagnosis of papillary thyroid carcinoma (PTC) [35]. The interpretation of malignancy is usually straightforward, but these morphological features may be insufficient to establish the primary site, given the microscopic overlap between well-differentiated lung

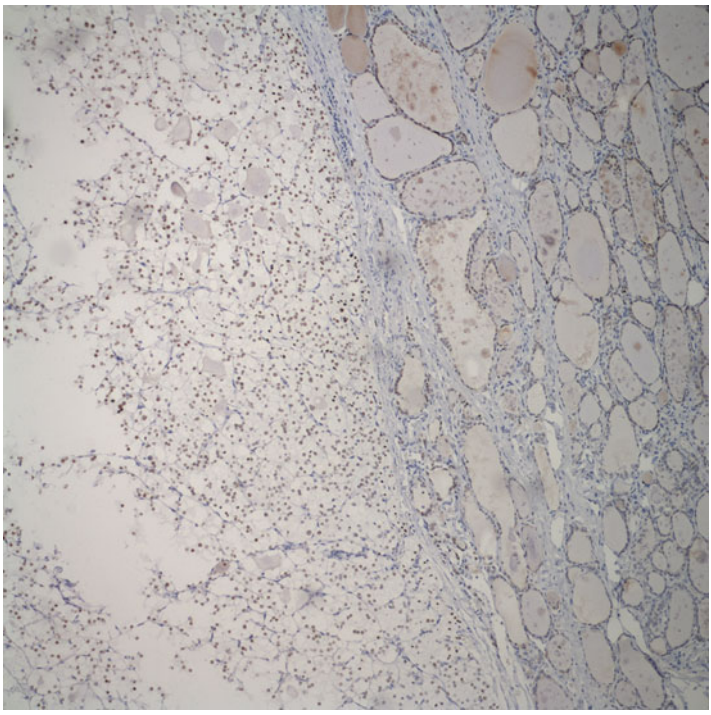

Fig. 15.9 Positive TTF-1 stain in follicular adenoma with clear cell change. This confirms the primary thyroid origin of the cells in this neoplasm

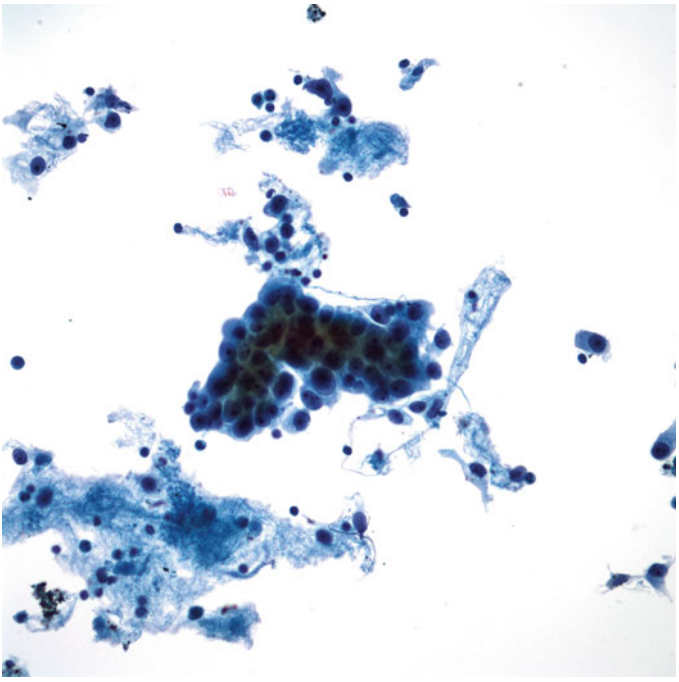

Fig. 15.10 Metastatic ductal carcinoma of the breast to the thyroid. Cluster of malignant ductal cells with scattered single cells in the background (Papanicolaou stain, X400)

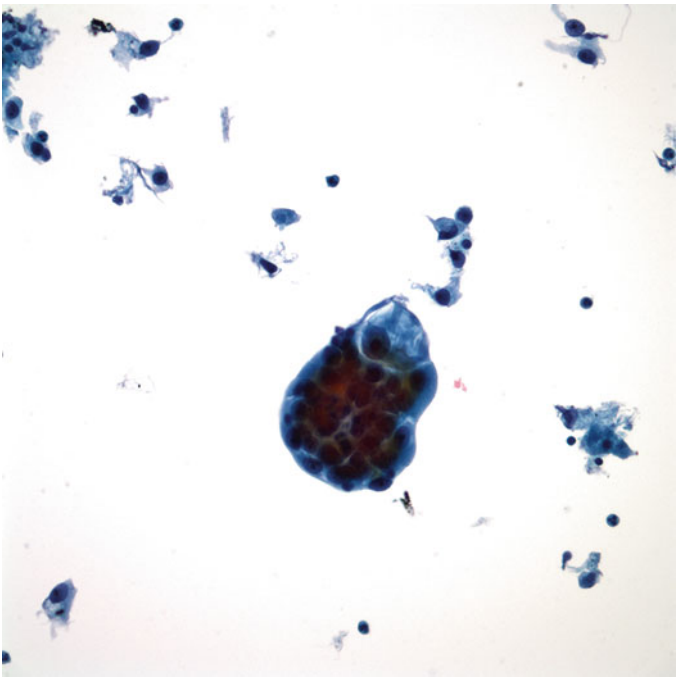

Fig. 15.11 Metastatic ductal carcinoma of the breast to the thyroid. Cluster of malignant ductal cells with rare intracytoplasmic vacuole (Papanicolaou stain, X400)

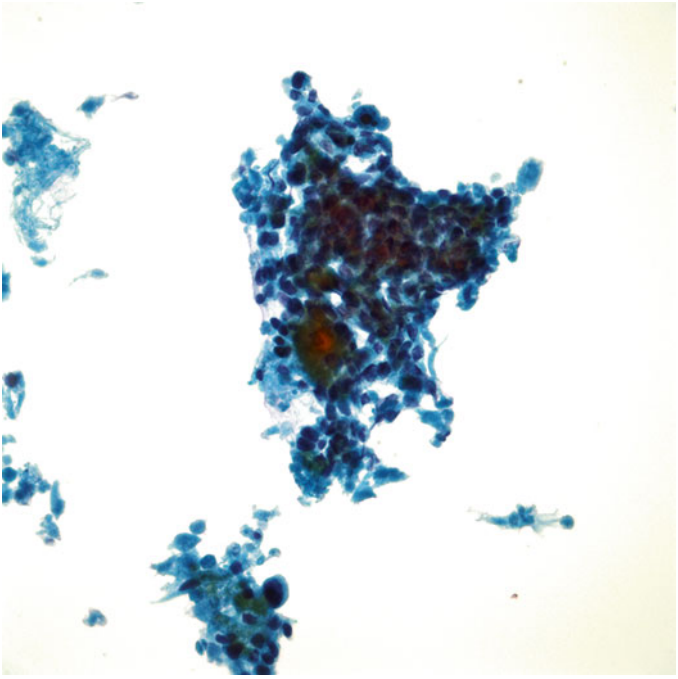

Fig. 15.12 Metastatic ductal carcinoma of the breast to the thyroid. Cluster of malignant ductal cells with focal calcification. This calcification may be confused with psammoma body that is typically seen in papillary thyroid carcinoma (Papanicolaou stain, X400)

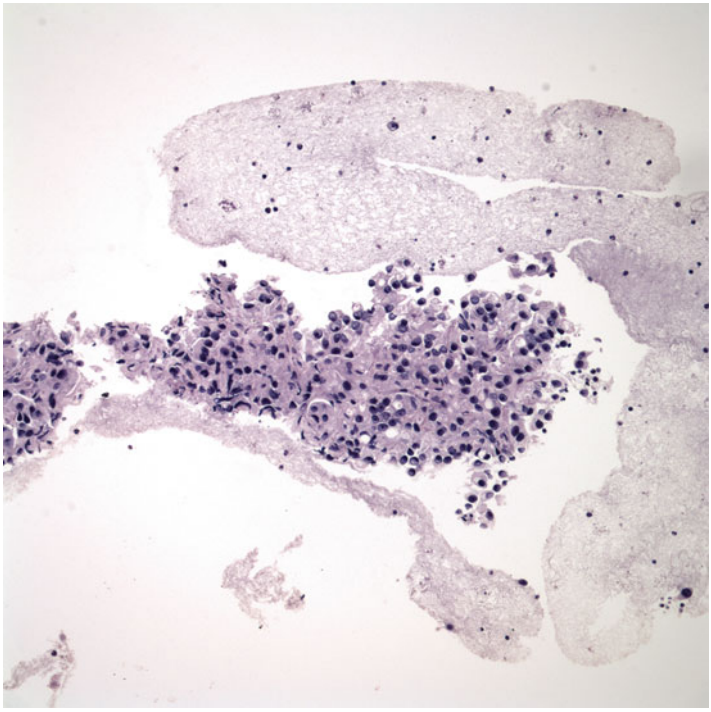

Fig. 15.13 Cell block material from metastatic breast ductal carcinoma to the thyroid. Cells show apocrine change (H&E stain, X200)

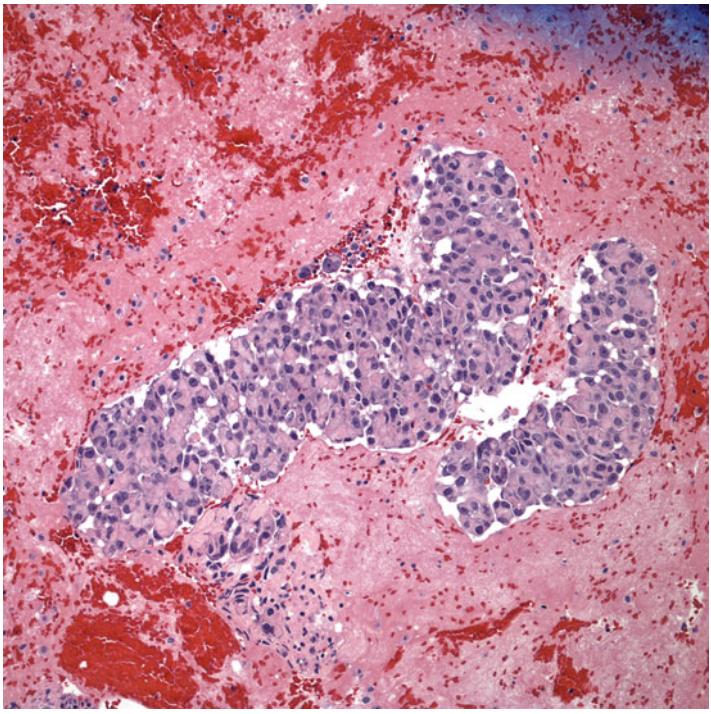

Fig. 15.14 Cell block material from metastatic breast ductal carcinoma to the thyroid. Individual cells show plasmacytoid features (H&E stain, X200)

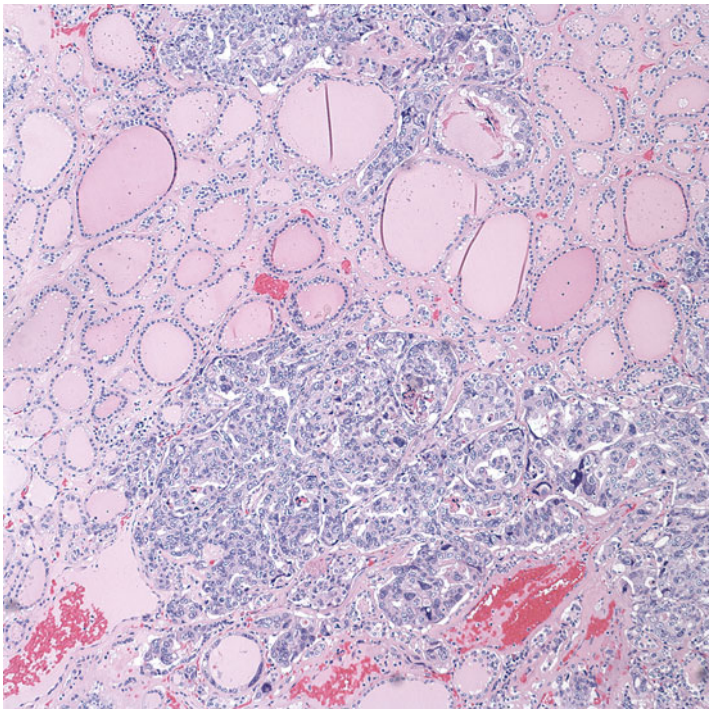

Fig. 15.15 Metastatic ductal carcinoma of the breast to the thyroid. Infiltrating ductal cells with adjacent normal thyroid follicles (H&E stain, X100)

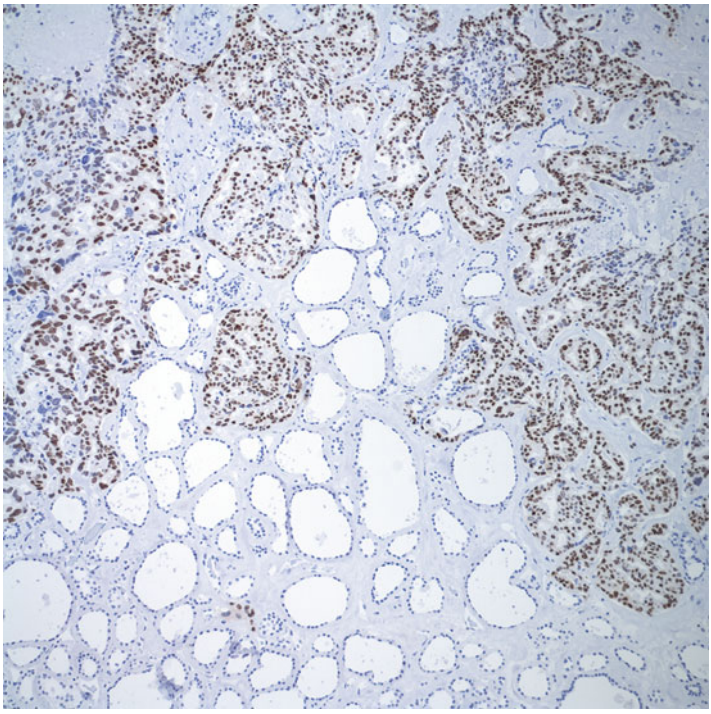

Fig. 15.16 Neoplastic cells showing strong and diffuse nuclear positivity for GATA-3 stain in metastatic ductal carcinoma of the breast to the thyroid

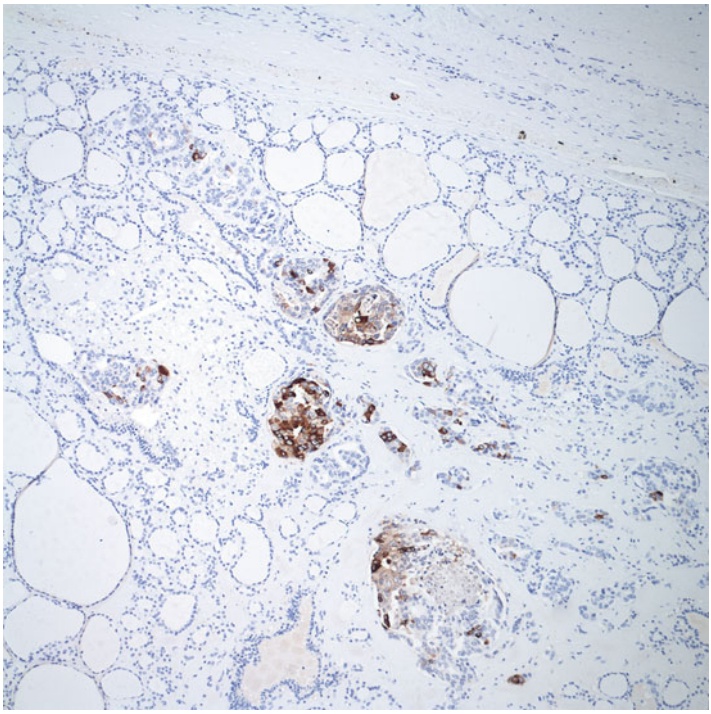

Fig. 15.17 Neoplastic cells showing cytoplasmic staining for mammaglobin, consistent with breast origin

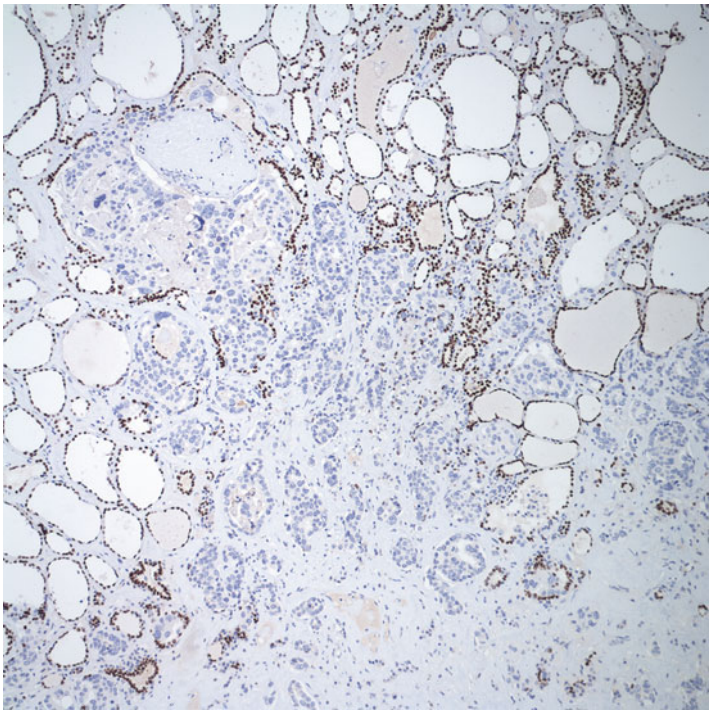

Fig. 15.18 TTF-1 stain is negative in the cells of metastatic breast carcinoma while positive in adjacent normal thyroid follicles

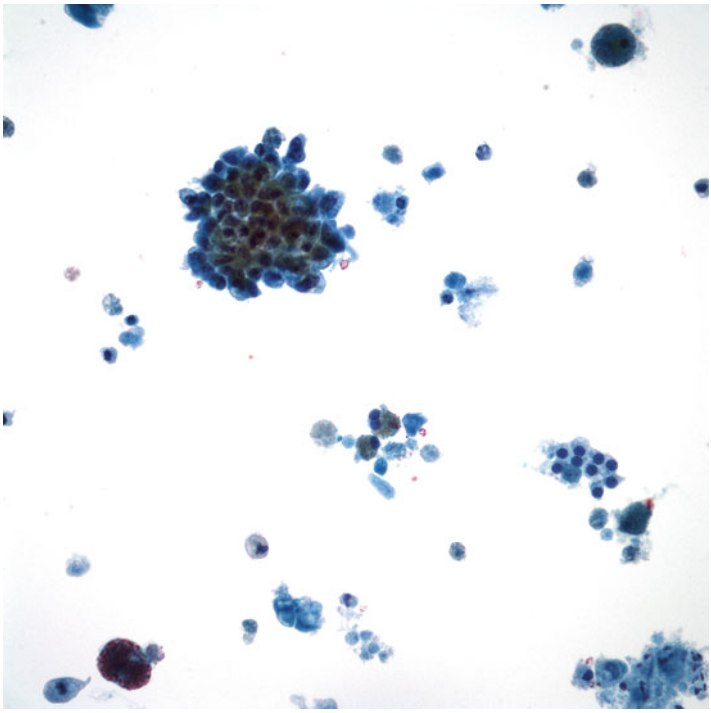

Fig. 15.19 Metastatic lung adenocarcinoma to the thyroid. Three-dimensional cluster of neoplastic cells in a background of goiter. There is a second population of cells with the appearance of normal follicular cells and a cystic background (Papanicolaou stain, X400)

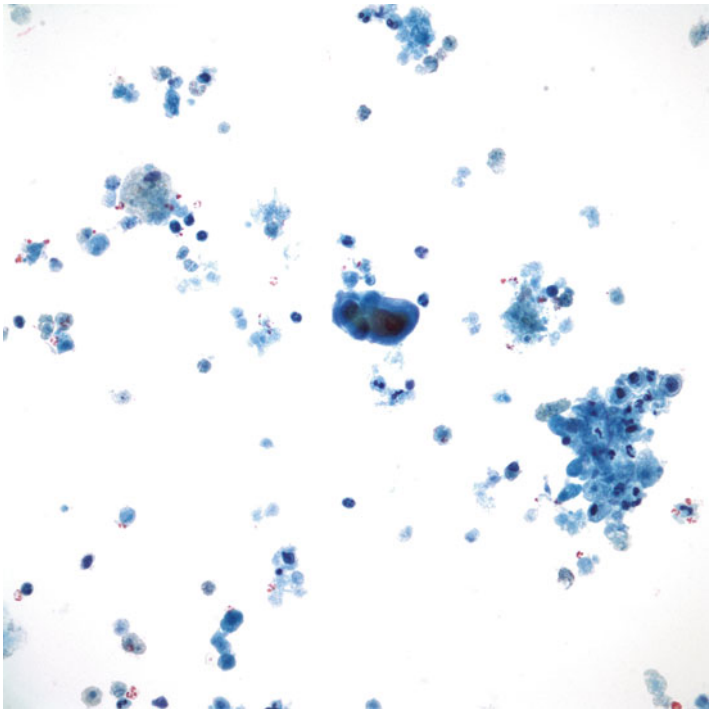

Fig. 15.20 Metastatic lung adenocarcinoma to the thyroid. Cluster of neoplastic cells in a necrotic background (Papanicolaou stain, X400)

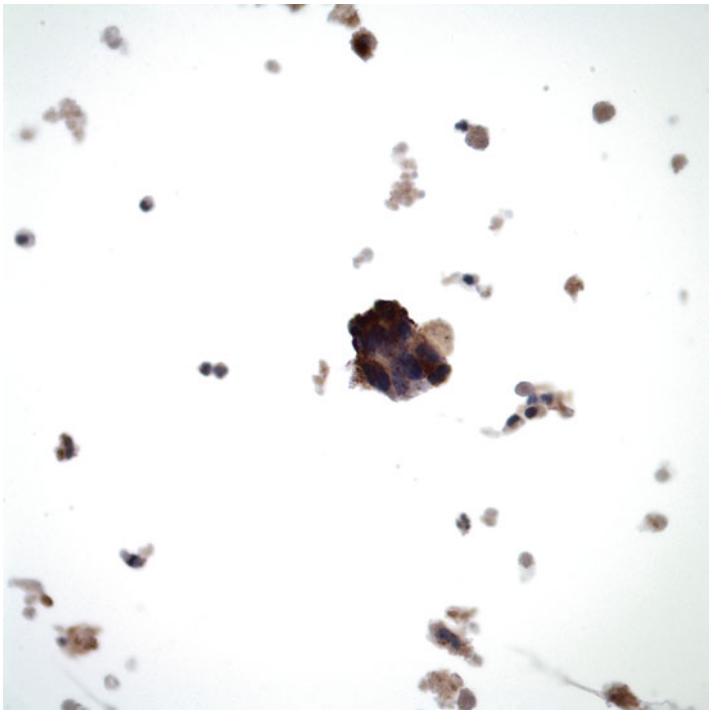

Fig. 15.21 Metastatic lung adenocarcinoma to the thyroid. These neoplastic cells are positive for napsin A

adenocarcinoma with mixed papillary and acinar features and follicular patterned PTC. Ancillary studies should help in arriving at the diagnosis. TTF-1 is of no use in differentiating between primary thyroid neoplasms and metastasis from the lung since TTF-1 is expressed in both. Thyroglobulin and PAX-8 are more useful as markers of thyroid differentiation while napsin A is typically positive in lung adenocarcinomas (Fig. 15.21).

Squamous cell carcinoma of the thyroid usually represents direct extension from esophageal or laryngeal primary tumors. While keratinization is a feature of squamous cell carcinoma (Figs. 15.22 and 15.23), it is worthy of note that keratinization may be seen in papillary thyroid carcinoma. Benign squamous metaplasia is also commonly seen in the thyroid; hence keratinization is not an absolute proof against primary thyroid tumors [36].

In malignant melanoma, the individual tumor cells display ill-defined cytoplasm and oval nuclei, with finely granular, optically clear chromatin. Poorly formed nuclear grooves and intranuclear cytoplasmic inclusions may be present in a few cells (Fig. 15.24) [37] and this may be a major pitfall in misdiagnosis as PTC. Often, intracytoplasmic brownish pigment granules are identified (Fig. 15.25). While this is pathognomonic of metastatic melanoma especially when a prior diagnosis of melanoma is available, one must be careful not to dismiss this as hemosiderin pigment within macrophages. Melanoma is typically positive for melan-A and HMB-45 stains.

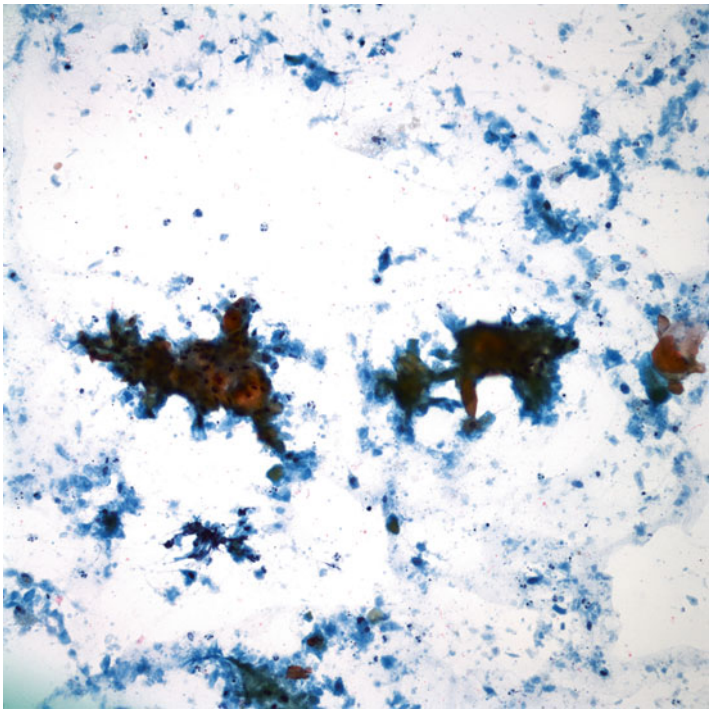

Fig. 15.22 Metastatic squamous cell carcinoma to the thyroid. Sheets of keratinized squamous cells in a necrotic background (Papanicolaou stain, X200)

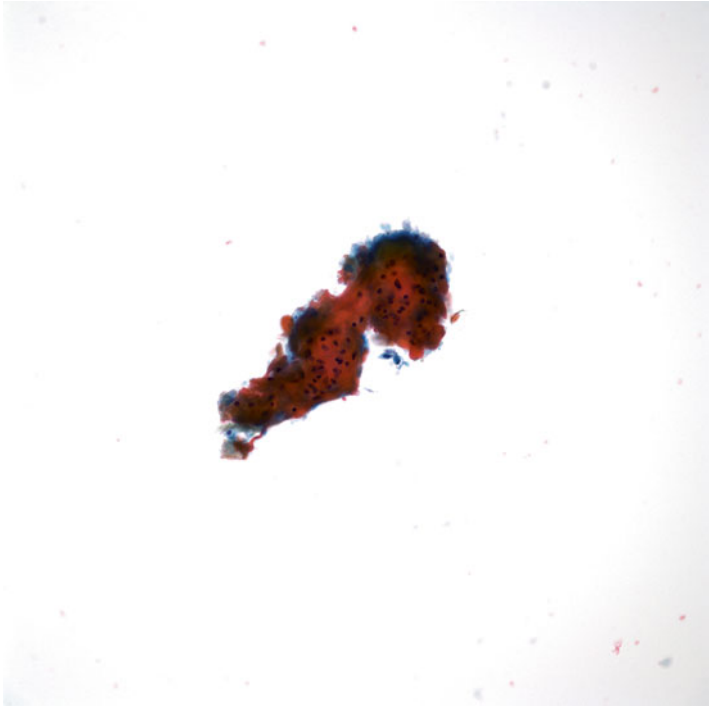

Fig. 15.23 Metastatic squamous cell carcinoma to the thyroid. The neoplastic squamous cells often appear very bland (Papanicolaou stain, X200)

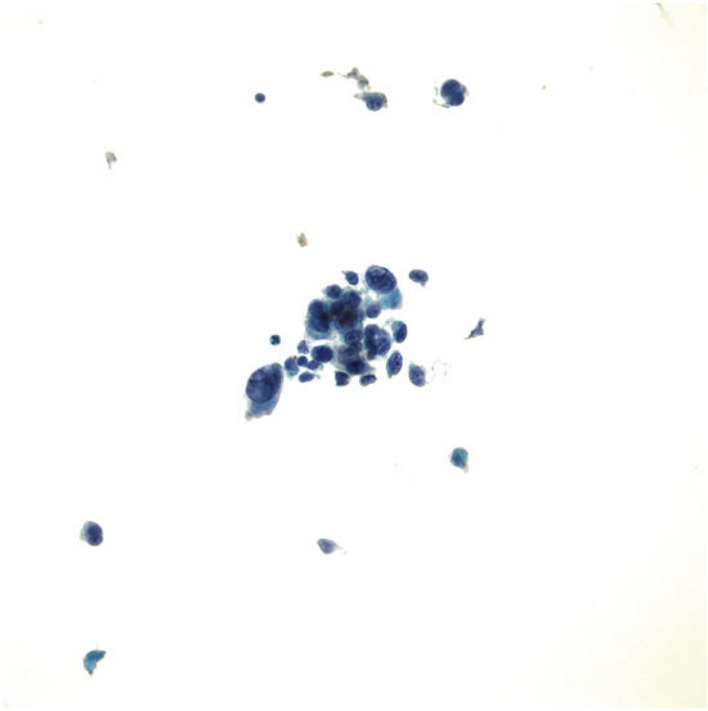

Fig. 15.24 Metastatic melanoma to the thyroid. Cells with poorly formed nuclear grooves and intranuclear cytoplasmic inclusions. This is a potential pitfall in misdiagnosis as PTC (Papanicolaou stain, X400)

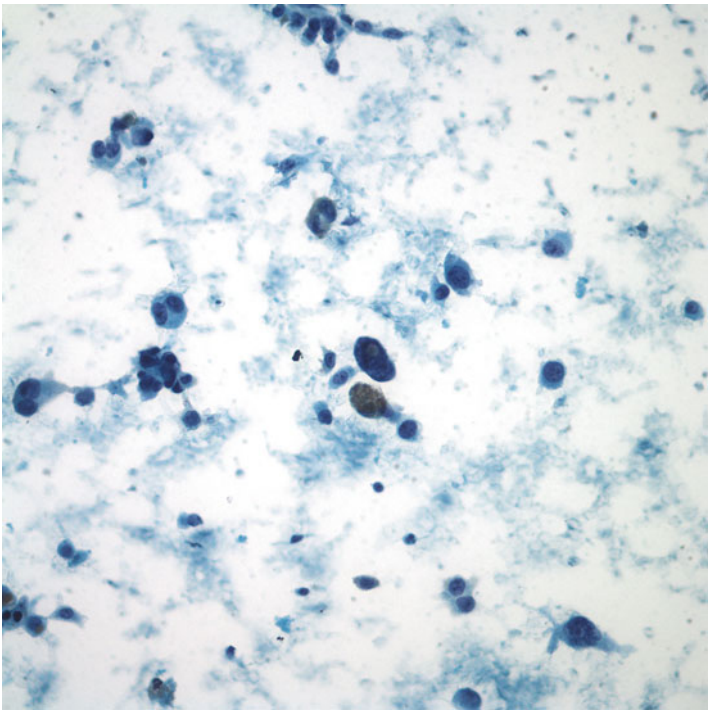

Fig. 15.25 Metastatic melanoma to the thyroid. Cells showing intracytoplasmic brownish pigment granules, consistent with melanin (Papanicolaou stain, X400)

Soft-tissue sarcomas involving the thyroid are very rare; hence a primary spindle cell-type anaplastic carcinoma and other entities such as spindle epithelial tumors with thymus-like differentiation must be ruled out.

References

1. Pusztaszeri M, Wang H, Cibas ES, Powers CN, Bongiovanni M, Ali S, Khurana KK, Michaels PJ, Faquin WC. Fine-needle aspiration biopsy of secondary neoplasms of the thyroid gland: a multi-institutional study of 62 cases. Cancer Cytopathol. 2015;123:19–29.
2. Nakhjavani MK, Gharib H, Goellner JR, van Heerden JA. Metastasis to the thyroid gland. A report of 43 cases. Cancer. 1997;79:574–8.
3. Cichoń S, Anielski R, Konturek A, Barczyński M, Cichoń W. Metastases to the thyroid gland: seventeen cases operated on in a single clinical center. Langenbecks Arch Surg. 2006;391: 581–7.
4. Papi G, Fadda G, Corsello SM, Corrado S, Rossi ED, Radighieri E, Miraglia A, Carani C, Pontecorvi A. Metastases to the thyroid gland: prevalence, clinicopathological aspects and prognosis: a 10-year experience. Clin Endocrinol (Oxf). 2007;66:565–71.
5. Wood K, Vini L, Harmer C. Metastases to the thyroid gland: the Royal Marsden experience. Eur J Surg Oncol. 2004;30:583–8.
6. Chen AY, Jemal A, Ward EM. Increasing incidence of differentiated thyroid cancer in the United States, 1988-2005. Cancer. 2009;115:3801–7.
7. Chung AY, Tran TB, Brumund KT, Weisman RA, Bouvet M. Metastases to the thyroid: a review of the literature from the last decade. Thyroid. 2012;22:258–68.
8. Chung CH, Wang CH, Wang TY, Huang JK, Leu YS. Extraskeletal Ewing sarcoma mimicking a thyroid nodule. Thyroid. 2006;16:1065–6.
9. Michelow PM, Leiman G. Metastases to the thyroid gland: diagnosis by aspiration cytology. Diagn Cytopathol. 1995;13:209–13.
10. Treadwell T, Alexander BB, Owen M, McConnell TH, Ashworth CT. Clear cell renal carcinoma masquerading as a thyroid nodule. South Med J. 1981;74:878–9.
11. Watts NB. Carcinoma metastatic to the thyroid: prevalence and diagnosis by fine-needle aspiration cytology. Am J Med Sci. 1987;293:13–7.
12. Rosai J, DeLellis RA, Cargangiu ML, Frable WJ, Tallini G. Tumors of the thyroid and parathyroid glands. Atlas of Tumor Pathology. Fascicle 21, Series 4. Washington, DC: Armed Forces Institute of Pathology; 2014.
13. Farwell AP, Braverman LE. Inflammatory thyroid disorders. Otolaryngol Clin North Am. 1996;29:541–56.
14. Ferrara G, Ianniello GP, Nappi O. Thyroid metastases from a ductal carcinoma of the breast. A case report. Tumori. 1997;83:783–7.
15. Watts NB, Sewell CW. Carcinomatous involvement of the thyroid presenting as subacute thyroiditis. Am J Med Sci. 1988;296:126–8.
16. Lee MW, Batoroev YK, Odashiro AN, Nguyen GK. Solitary metastatic cancer to the thyroid: a report of five cases with fine-needle aspiration cytology. Cytojournal. 2007;4:5.
17. Schmid KW, Hittmair A, Ofner C, Tötsch M, Ladurner D. Metastatic tumors in fine needle aspiration biopsy of the thyroid. Acta Cytol. 1991;35:722–4.
18. Smith SA, Gharib H, Goellner JR. Fine-needle aspiration. Usefulness for diagnosis and management of metastatic carcinoma to the thyroid. Arch Intern Med. 1987;147:311–2.
19. Montero PH, Ibrahimpasic T, Nixon IJ, Shaha AR. Thyroid metastasectomy. J Surg Oncol. 2014;109:36–41.
20. Gattuso P, Castelli MJ, Reyes CV. Fine needle aspiration cytology of metastatic sarcoma involving the thyroid. South Med J. 1989;82:1158–60.
21. Tuncer M, Faydaci G, Altin G, Erdogan BA, Kibar S, Sanli A, Bilgici D. Metastasis of non-muscle-invasive bladder cancer into the thyroid gland: a literature review accompanied by a rare case. Korean J Urol. 2014;55:222–5.

22. DeLellis R. In: DeLellis RA, Lloyd RV, Heitz PU, et al., editors. Pathology and genetics of tumors of endocrine organs, World Health Organization classification of tumors. Lyon: IARC Press; 2004. p. 122–3.
23. Chacho MS, Greenebaum E, Moussouris HF, Schreiber K, Koss LG. Value of aspiration cytology of the thyroid in metastatic disease. Acta Cytol. 1987;31:705–12.
24. Medas F, Calò PG, Lai ML, Tuveri M, Pisano G, Nicolosi A. Renal cell carcinoma metastasis to thyroid tumor: a case report and review of the literature. J Med Case Rep. 2013;7:265.
25. Baloch ZW, LiVolsi VA, Asa SL, Rosai J, Merino MJ, Randolph G, Vielh P, DeMay RM, Sidawy MK, Frable WJ. Diagnostic terminology and morphologic criteria for cytologic diagnosis of thyroid lesions: a synopsis of the National Cancer Institute Thyroid Fine-Needle Aspiration State of the Science Conference. Diagn Cytopathol. 2008;36:425–37.
26. American Thyroid Association (ATA) Guidelines Taskforce on Thyroid Nodules and Differentiated Thyroid Cancer, Cooper DS, Doherty GM, Haugen BR, Kloos RT, Lee SL, Mandel SJ, Mazzaferri EL, McIver B, Pacini F, Schlumberger M, Sherman SI, Steward DL, Tuttle RM. Revised American Thyroid Association management guidelines for patients with thyroid nodules and differentiated thyroid cancer. Thyroid. 2009;19:1167–214.
27. Faquin WC, Bongiovanni M, Sadow PM. Update in thyroid fine needle aspiration. Endocr Pathol. 2011;22:178–83.
28. Lam KY, Lo CY. Metastatic tumors of the thyroid gland: a study of 79 cases in Chinese patients. Arch Pathol Lab Med. 1998;122:37–41.
29. Lin JD, Weng HF, Ho YS. Clinical and pathological characteristics of secondary thyroid cancer. Thyroid. 1998;8:149–53.
30. Kini S. Thyroid cytopathology: an atlas and text. Philadelphia: Wolters Kluwer/Lippincott Williams & Wilkins; 2008.
31. Heffess CS, Wenig BM, Thompson LD. Metastatic renal cell carcinoma to the thyroid gland: a clinicopathologic study of 36 cases. Cancer. 2002;95:1869–78.
32. Rizzo M, Rossi RT, Bonaffini O, Scisca C, Sindoni A, Altavilla G, Benvenga S. Thyroid metastasis of clear cell renal carcinoma: report of a case. Diagn Cytopathol. 2009;37:759–62.
33. Al-Ahmadie HA, Alden D, Qin LX, Olgac S, Fine SW, Gopalan A, Russo P, Motzer RJ, Reuter VE, Tickoo SK. Carbonic anhydrase IX expression in clear cell renal cell carcinoma: an immunohistochemical study comparing 2 antibodies. Am J Surg Pathol. 2008;32:377–82.
34. Ordóñez NG. Value of PAX 8 immunostaining in tumor diagnosis: a review and update. Adv Anat Pathol. 2012;19:140–51.
35. Bellevicine C, Vigliar E, Malapelle U, Carelli E, Fiorelli A, Vicidomini G, Cappabianca S, Santini M, Troncone G. Lung adenocarcinoma and its thyroid metastasis characterized on fine-needle aspirates by cytomorphology, immunocytochemistry, and next-generation sequencing. Diagn Cytopathol. 2015;43:585–9.
36. DeMay RM. The art and science of cytopathology: superficial aspiration cytology. Chicago: American Society for Clinical Pathology Press; 2012.
37. Miiji LO, Nguyen GK. Metastatic melanoma of the thyroid mimicking a papillary carcinoma in fine-needle aspiration. Diagn Cytopathol. 2005;32:374–6.

Thyroglobulin Detection in Fine-Needle Aspiration of Nodal Metastases from Differentiated Thyroid Cancers

16

Case Study

Patient was a 41-year-old woman status post-total thyroidectomy and central lymph node dissection for a 2.1 cm conventional papillary thyroid carcinoma 1 year prior. There was no evidence of lymphovascular invasion. Three lymph nodes were sampled and were negative for metastases. After achieving a TSH level of 33, a thyroglobulin level of 0.6 ng/ml, and an anti-thyroglobulin antibody level at 64 IU/ml with TSH suppression therapy, she received 32 mCi of I-31. Her post-therapy scan showed 2 foci of uptake in the thyroid bed consistent with residual thyroid tissue. She continued her TSH suppression therapy.

At her 1-year follow-up post-surgery (or 4 months after post-therapy scan), her work-up showed a thyroglobulin level of 1.4 ng/ml and an anti-thyroglobulin antibody level of 2.6 IU/ml. Physical examination did not reveal any palpable cervical or supraclavicular adenopathies. Ultrasound examination showed a suspicious-appearing sub-centimeter lymph node in left level 4. FNA and thyroglobulin assay of the L4 lymph node were performed under ultrasound guidance.

Cytology of the L4 lymph node showed abundant hemosiderin laden macrophages in a background of scattered lymphocytes (Fig. 16.1). No follicular cells were present for evaluation (Fig. 16.2). The cytologic impression was cystic lesion with the comment that a metastatic lesion could not be ruled out in view of the patient's prior history of papillary thyroid carcinoma. The thyroglobulin level of the aspirate was reported to be over 30,000 ng/ml (normal level < 1 ng/ml) using chemiluminescent method. Based on the thyroglobulin level and the cytologic findings, the patient was presumed to have metastatic papillary thyroid carcinoma involving the left level 4 lymph node.

The patient underwent left central neck dissection and modified radical neck dissection of levels II, III, IV, and V. Histologic section of the level IV lymph node showed a cystic structure with a thick fibrous wall (Fig. 16.3). The cyst was lined by neoplastic cells with abundant eosinophilic cytoplasm and enlarged, nuclei (Fig. 16.4). Nuclei showed powdery chromatin, nuclear clearing, and nuclear grooves (Fig. 16.5).

A.J. Adeniran, D. Chhieng, *Common Diagnostic Pitfalls in Thyroid Cytopathology*, DOI 10.1007/978-3-319-31602-4_16

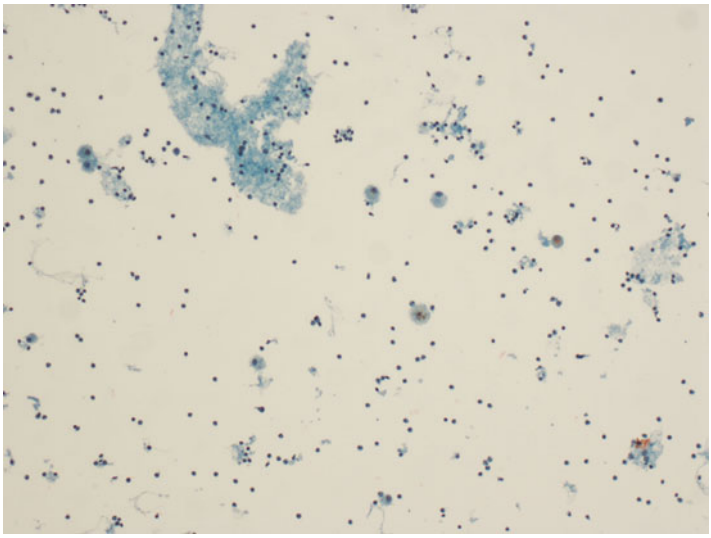

Fig. 16.1 L4 lymph node FNA-cystic lesion. The aspirate is of low cellular and consists of scattered macrophages and scattered lymphocytes (Papanicolaou stain, low power)

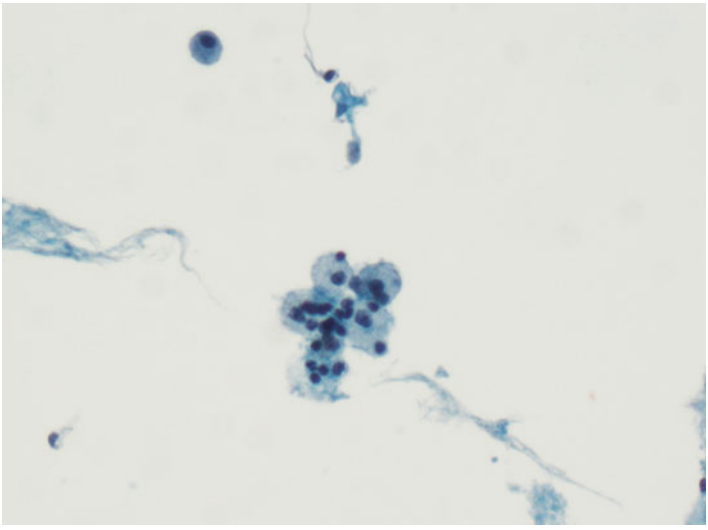

Fig. 16.2 L4 lymph node FNA-cystic lesion. Macrophages with abundant foamy cytoplasm arranged in small groups or singly. Lymphocytes are also noted (Papanicolaou stain, low power)

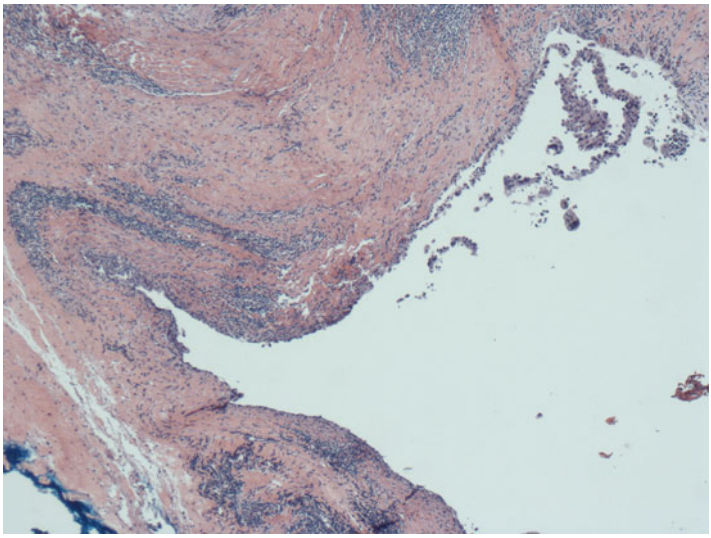

Fig. 16.3 Metastatic PTC, level 4 lymph node. The lymph node is replaced by a cystic structure composed of thick fibrous wall and scattered lymphoid aggregates (H&E, low power)

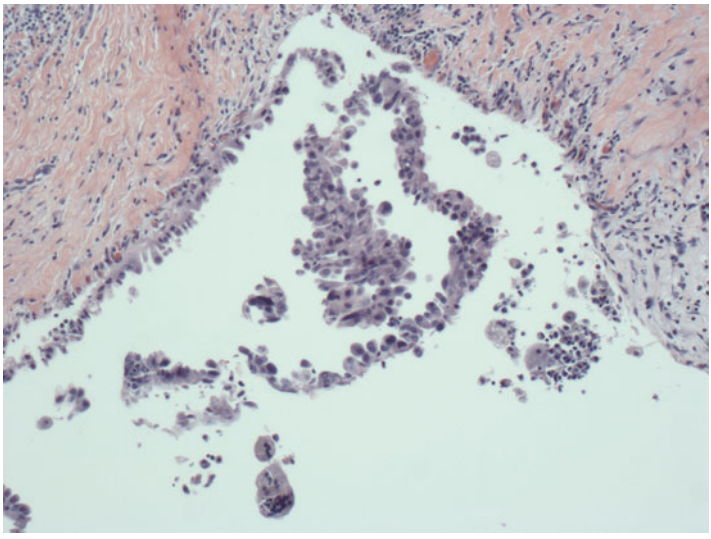

Fig. 16.4 Metastatic PTC, level 4 lymph node. The lining of the cystic structure consists of neoplastic follicular cells with abundant granular eosinophilic cytoplasm and enlarged nuclei. Multinucleated giant cells are also noted (H&E, high power)

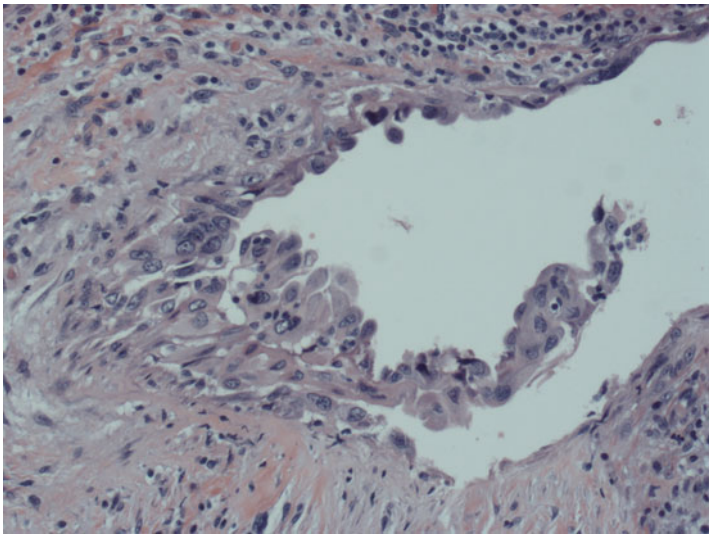

Fig. 16.5 Metastatic PTC, level 4 lymph node. The nuclei of neoplastic cells show powdery chromatin, nuclear clearing, and nuclear grooves (H&E, high power)

Eight out of 42 lymph nodes were found to have metastatic papillary thyroid carcinoma involving other levels except level V. The largest lymph node measured 2 cm. No extranodal extension was noted. She was given I-131 therapy at a dose of 152 mCi along with thyrogen stimulation postoperatively.

Discussion

Involvement of cervical lymph nodes by metastatic disease is reported in 20–50 % of patients with differentiated thyroid cancer, especially in those with papillary thyroid carcinoma (PTC) [1, 2]. Ultrasound is superior to CT scan in identifying the presence of abnormal cervical lymph nodes. It allows for the preoperative detection of non-palpable cervical lymph node metastasis in patients with FNA-proven or -suspected thyroid cancer and may potentially alter the extent and approach of surgery in these patients [3–5]. Hypoechogenicity, loss of fatty hilum, cystic change, calcification, round shape, and abnormal vascular pattern are typical ultrasonographic features associated with metastatic lymph nodes [6, 7]. Although ultrasound examination is very accurate in identifying suspicious lymph nodes, these ultrasonographic features, such as loss of fatty hilum, are not pathognomonic and can also be seen in reactive lymphadenopathy.

Fine-needle aspiration biopsy (FNA) is usually required to confirm or rule out metastasis because reactive lymphadenopathy is common in the neck region. According to American Thyroid Association (ATA) guidelines, ultrasound-guided FNA is the most accurate and cost-effective method for evaluating enlarged cervical

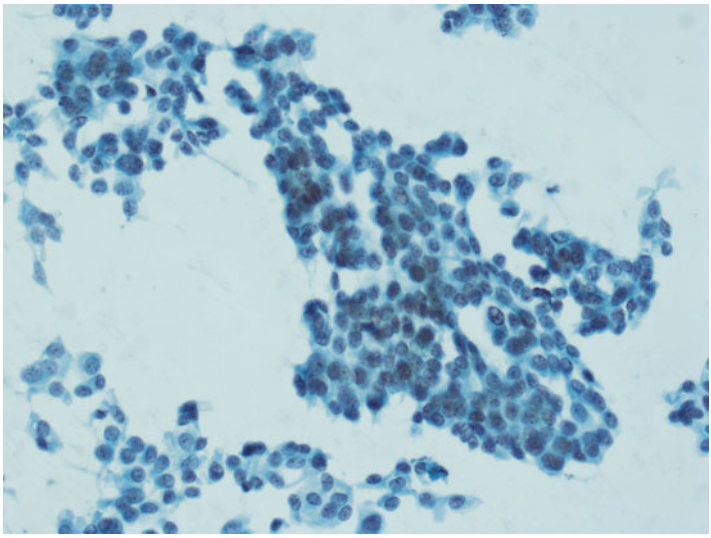

Fig. 16.6 Lymph node FNA-metastatic PTC. This aspirate consists predominantly of sheets of neoplastic follicular cells with indistinct cell borders, nuclear enlargement, powdery chromatin, nuclear grooves, and infrequent nuclear inclusions (Papanicolaou stain, high power)

lymph nodes in patients with FNA-proven or -suspected thyroid cancer [8]. Cytologic features of metastatic PTC in cervical lymph nodes are similar to those of primary PTC. Some authors have observed a significantly higher percentage of cell sheets with indistinct cell borders [9] (Fig. 16.6). In addition, there is a higher frequency of cystic change due to degeneration in nodal metastases when compared to primary tumors [9, 10]. For example, one study reported that the incidences of cystic change were 52.5 % (9.1 % with marked cystic change) and 74.5 % (24.5 % with marked cystic changed) in primary PTC and nodal metastases [10]. The presence of foamy macrophages was also significantly more frequent in the metastatic nodes than in the primary tumor (51.1 % vs. 26.3 %) [9]. Grossly, aspiration of PTC metastatic nodes with cystic change usually produces chocolate-brown fluid.

Although ultrasound-guided FNA is highly accurate in diagnosing nodal metastases of differentiated thyroid cancers, it is operator dependent; therefore, the diagnostic accuracy can vary according to the ability of the operator or pathologist. False-positive rate in diagnosing nodal metastasis by FNA is uncommon, ranging from 0.09 to 1.7 % [11, 12]. On the other hand, small lymph nodes are technically difficult to biopsy and poor epithelial cellularity may be encountered in larger lymph nodes with cystic changes. These contribute to the relatively high false-negative rate of 6–8 % [13, 14]; in one study, the authors reported a false-negative rate of 44.6 % [15].

Thyroglobulin (Tg) assay in the needle rinse has been reported to increase the sensitivity of FNA in diagnosing nodal metastases from a differentiated thyroid carcinoma [13, 16–20]. The rationale is that Tg is produced only by follicular cells, and its detection in non-thyroidal tissues, such as lymph nodes, allows the diagnosis

of metastases of differentiated thyroid carcinoma [21]. Tg assay is recommended by the revised American Thyroid Association (ATA) guidelines for the follow-up of patients with differentiated thyroid carcinoma [8] and is cited by ATA consensus review regarding the anatomy, terminology, and rationale for lateral neck dissection in differentiated thyroid carcinoma [22].

Tg assay of lymph node aspirates has been shown to be a fairly accurate tool to detect cervical nodal metastases from differentiated thyroid carcinoma. According to a meta-analysis of 24 studies and 2865 suspicious lymph nodes from patients during diagnostic work-up of thyroid nodules or follow-up of thyroid cancer, both the sensitivity and specificity of Tg assay were 95.0 % with a positive and negative likelihood ratio of 16 and 0.1, respectively [18]. One advantage of Tg assay of FNA is the ability to use the same needle and syringe for collecting samples for Tg assay after preparation of cytology smears; that is, no separate dedicated needle pass is needed. Tg assay of lymph node aspirates can be performed preoperatively or postoperatively, i.e., with or without the presence of thyroid gland. Tg levels of the lymph node aspirates may be higher in patients with thyroid gland when compared to those without; this may be a source of bias [18]. The sensitivity and specificity of Tg assay in patients without a thyroid gland are 97 and 94 %, which are higher than those with a thyroid gland (sensitivity 86 % and specificity 90 %) [18].

Despite its accuracy, some areas of uncertainty persist such as the collecting protocol and the cutoff values. Although various solutions such as Hanks' balance solution, PBS, and Tg-free solution shipped with measurement kit have been used for rinsing the needles, the most practical and widely employed solution for the needle wash is normal saline solution, which has been shown to have no matrix effect [23].

The volumes of solution used ranged from 0.125 to 3 ml with the majority of studies reported using 1 ml [18]. It should be kept in mind that Tg assay of FNA is not a concentration measure, but reflects the dilution of the Tg left in the needles in the arbitrarily selected volume of washout fluid. Although most laboratories have chosen to express Tg in aspirate in nanograms per milliliter (ng/mL), the most correct way to express is to use nanograms per FNA unit [24].

There is no established consensus on the cutoff value for Tg assay in FNA. The largest published study reported an optimal cutoff of 1 ng/ml with a sensitivity and specificity of 95 % and 91 %, respectively [25]. However, various studies have used cutoff values ranging from 0.2 to 50 ng/ml. Some authors set the threshold to the mean value +2 SD for the negative patients, and others used the highest Tg levels detected in patients with reactive lymph node. Some studies advocated the use of cutoff values equal to serum Tg concentration; the potential benefit of this approach is improved diagnostic accuracy (sensitivity 97 % and specificity 95 %) in the presence of detectable serum Tg, such as before thyroidectomy or in the presence of distant metastasis. However, it requires the collection of a serum sample at the time of FNA.

Anti-Tg antibodies can be detected in 15–30 % of patients with thyroid cancer. Although the presence of anti-Tg antibodies affects the detection of serum Tg by immunometric assays, it did not appear that the Tg assay of FNA would be significantly affected by the presence of serum anti-Tg antibodies [26, 27]. One likely plausible explanation is that the exceedingly elevated thyroglobulin concentration in positive nodal aspirates is able to saturate all Tg antibody-binding sites.

Rare false-positive and -negative cases have been reported [18]. The majority of these false-positive cases were from FNA of level VI lymph nodes, which are located in the central lower neck area. In this area, it may be difficult to distinguish aspirates from nodal aspirates from those with inadvertently aspirated thyroid tissue [28]. Another possible cause of false positives may be the matrix effects as a result of the presence of components in the solution for rinsing the needles [23, 29]. False-negative cases are usually due to aspirates from nodal metastases of poorly differentiated thyroid carcinoma or medullary carcinoma [27, 30].

Tg assay of FNA from cervical lymph nodes has high sensitivity and specificity in the detection of nodal metastases from differentiated thyroid carcinoma. However, Tg assay of FNA should not replace cytologic evaluation because of the possibility of both false-positive and -negative results. In addition, standardization in terms of sample collection and analysis is still lacking.

References

1. Chow SM, Law SC, Chan JK, Au SK, Yau S, Lau WH. Papillary microcarcinoma of the thyroid-Prognostic significance of lymph node metastasis and multifocality. Cancer. 2003;98:31–40.
2. Scheumann GF, Gimm O, Wegener G, Hundeshagen H, Dralle H. Prognostic significance and surgical management of locoregional lymph node metastases in papillary thyroid cancer. World J Surg. 1994;18:559–67. discussion 567–558.
3. Kouvaraki MA, Shapiro SE, Fornage BD, et al. Role of preoperative ultrasonography in the surgical management of patients with thyroid cancer. Surgery. 2003;134:946–54. discussion 954–945.
4. Solorzano CC, Carneiro DM, Ramirez M, Lee TM, Irvin III GL. Surgeon-performed ultrasound in the management of thyroid malignancy. Am Surg. 2004;70:576–80. discussion 580–572.
5. Stulak JM, Grant CS, Farley DR, et al. Value of preoperative ultrasonography in the surgical management of initial and reoperative papillary thyroid cancer. Arch Surg. 2006;141:489–94. discussion 494–486.
6. Kim DW, Choo HJ, Lee YJ, Jung SJ, Eom JW, Ha TK. Sonographic features of cervical lymph nodes after thyroidectomy for papillary thyroid carcinoma. J Ultrasound Med. 2013;32:1173–80.
7. Leboulleux S, Girard E, Rose M, et al. Ultrasound criteria of malignancy for cervical lymph nodes in patients followed up for differentiated thyroid cancer. J Clin Endocrinol Metab. 2007;92:3590–4.
8. Cooper DS, Doherty GM, Haugen BR, et al. Management guidelines for patients with thyroid nodules and differentiated thyroid cancer. Thyroid. 2006;16:109–42.
9. Tseng FY, Hsiao YL, Chang TC. Cytologic features of metastatic papillary thyroid carcinoma in cervical lymph nodes. Acta Cytol. 2002;46:1043–8.
10. Carcangiu ML, Zampi G, Pupi A, Castagnoli A, Rosai J. Papillary carcinoma of the thyroid. A clinicopathologic study of 241 cases treated at the University of Florence, Italy. Cancer. 1985;55:805–28.
11. Hsu C, Leung BS, Lau SK, Sham JS, Choy D, Engzell U. Efficacy of fine-needle aspiration and sampling of lymph nodes in 1,484 Chinese patients. Diagn Cytopathol. 1990;6:154–9.
12. Steel BL, Schwartz MR, Ramzy I. Fine needle aspiration biopsy in the diagnosis of lymphadenopathy in 1,103 patients. Role, limitations and analysis of diagnostic pitfalls. Acta Cytol. 1995;39:76–81.
13. Frasoldati A, Toschi E, Zini M, et al. Role of thyroglobulin measurement in fine-needle aspiration biopsies of cervical lymph nodes in patients with differentiated thyroid cancer. Thyroid. 1999;9:105–11.

14. Frasoldati A, Valcavi R. Challenges in neck ultrasonography: lymphadenopathy and parathyroid glands. Endocr Pract. 2004;10:261–8.
15. Jun HH, Kim SM, Kim BW, Lee YS, Chang HS, Park CS. Overcoming the limitations of fine needle aspiration biopsy: detection of lateral neck node metastasis in papillary thyroid carcinoma. Yonsei Med J. 2015;56:182–8.
16. Cignarelli M, Ambrosi A, Marino A, et al. Diagnostic utility of thyroglobulin detection in fine-needle aspiration of cervical cystic metastatic lymph nodes from papillary thyroid cancer with negative cytology. Thyroid. 2003;13:1163–7.
17. Cunha N, Rodrigues F, Curado F, et al. Thyroglobulin detection in fine-needle aspirates of cervical lymph nodes: a technique for the diagnosis of metastatic differentiated thyroid cancer. Eur J Endocrinol. 2007;157:101–7.
18. Grani G, Fumarola A. Thyroglobulin in lymph node fine-needle aspiration washout: a systematic review and meta-analysis of diagnostic accuracy. J Clin Endocrinol Metab. 2014;99: 1970–82.
19. Kim MJ, Kim EK, Kim BM, et al. Thyroglobulin measurement in fine-needle aspirate washouts: the criteria for neck node dissection for patients with thyroid cancer. Clin Endocrinol (Oxf). 2009;70:145–51.
20. Uruno T, Miyauchi A, Shimizu K, et al. Usefulness of thyroglobulin measurement in fine-needle aspiration biopsy specimens for diagnosing cervical lymph node metastasis in patients with papillary thyroid cancer. World J Surg. 2005;29:483–5.
21. Johnson NA, Tublin ME. Postoperative surveillance of differentiated thyroid carcinoma: rationale, techniques, and controversies. Radiology. 2008;249:429–44.
22. Stack Jr BC, Ferris RL, Goldenberg D, et al. American Thyroid Association consensus review and statement regarding the anatomy, terminology, and rationale for lateral neck dissection in differentiated thyroid cancer. Thyroid. 2012;22:501–8.
23. Borel AL, Boizel R, Faure P, et al. Significance of low levels of thyroglobulin in fine needle aspirates from cervical lymph nodes of patients with a history of differentiated thyroid cancer. Eur J Endocrinol. 2008;158:691–8.
24. Pacini F, Fugazzola L, Lippi F, et al. Detection of thyroglobulin in fine needle aspirates of nonthyroidal neck masses: a clue to the diagnosis of metastatic differentiated thyroid cancer. J Clin Endocrinol Metab. 1992;74:1401–4.
25. Salmaslioglu A, Erbil Y, Citlak G, et al. Diagnostic value of thyroglobulin measurement in fine-needle aspiration biopsy for detecting metastatic lymph nodes in patients with papillary thyroid carcinoma. Langenbecks Arch Surg. 2011;396:77–81.
26. Baskin HJ. Detection of recurrent papillary thyroid carcinoma by thyroglobulin assessment in the needle washout after fine-needle aspiration of suspicious lymph nodes. Thyroid. 2004;14: 959–63.
27. Boi F, Baghino G, Atzeni F, Lai ML, Faa G, Mariotti S. The diagnostic value for differentiated thyroid carcinoma metastases of thyroglobulin (Tg) measurement in washout fluid from fine-needle aspiration biopsy of neck lymph nodes is maintained in the presence of circulating anti-Tg antibodies. J Clin Endocrinol Metab. 2006;91:1364–9.
28. Li QK, Nugent SL, Straseski J, et al. Thyroglobulin measurements in fine-needle aspiration cytology of lymph nodes for the detection of metastatic papillary thyroid carcinoma. Cancer Cytopathol. 2013;121:440–8.
29. Giovanella L, Ceriani L, Suriano S, Crippa S. Thyroglobulin measurement on fine-needle washout fluids: influence of sample collection methods. Diagn Cytopathol. 2009;37:42–4.
30. Baldini E, Sorrenti S, Di Gioia C, et al. Cervical lymph node metastases from thyroid cancer: does thyroglobulin and calcitonin measurement in fine needle aspirates improve the diagnostic value of cytology? BMC Clin Pathol. 2013;13:7.

Pediatric Thyroid FNA

17

Case Study

A 19-year-old Caucasian male presented to an outside institution with 1-year history of a palpable left supraclavicular mass. He noticed that the mass had been increasing in size for the past 6 months before presentation. He also complained of dysphagia but had no complaints of hoarseness and difficulty in breathing. An FNA of the supraclavicular mass was preformed and revealed metastatic papillary thyroid carcinoma which was confirmed by positive reactivity with CK7, thyroglobulin, and TTF-1 but negative for CK20. The patient was then referred to our institution for further management.

He had no symptoms of hyperthyroidism. He had a history of intrauterine radiation exposure since his mother worked at a nuclear plant when she was pregnant with the patient. He had no family history of thyroid cancer. Physical examination was within normal limit except for palpable left cervical lymph nodes in the anterior and supraclavicular regions. The thyroid gland was smooth, mobile, and devoid of any palpable nodules. The thyroid function test was within normal limits.

Ultrasound of the neck showed a questionable 1 cm left thyroid nodule with an area of calcification. In addition, there were also enlarged abnormal lymph nodes in left level IV and right level II. Fine needle aspiration biopsy was performed on the left thyroid nodule, left level IV, and right level II lymph nodes. The FNA of the left thyroid nodule demonstrated marked cellularity with tumor cells arranged in papillae and crowded groups (Figs. 17.1 and 17.2). Individual cells demonstrate nuclear enlargement, nuclear grooves, and intranuclear inclusions (Fig. 17.3). The diagnosis was papillary thyroid carcinoma. Not surprisingly, the FNAs from both left and right lymph nodes were positive for metastatic papillary thyroid carcinoma (Figs. 17.4 and 17.5).

The patient then underwent total thyroidectomy and central and bilateral modified radical neck dissection. Histologically, the thyroid gland revealed a multifocal papillary thyroid carcinoma (Figs. 17.6 and 17.7) involving the left lobe with extensive extrathyroidal extension (Fig. 17.8) and vascular invasion (Fig. 17.9) involving both lobes. A total of 18 out of 56 lymph nodes were positive for metastatic carcinoma.

A.J. Adeniran, D. Chhieng, *Common Diagnostic Pitfalls in Thyroid Cytopathology*, DOI 10.1007/978-3-319-31602-4_17

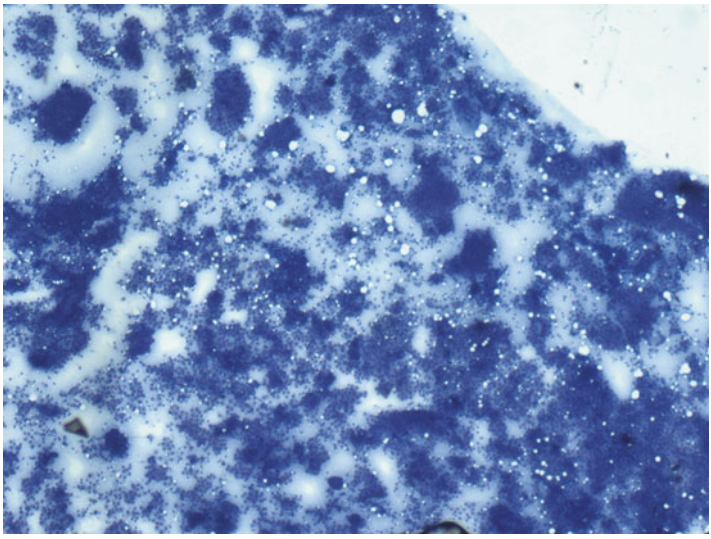

Fig. 17.1 Left thyroid FNA-positive for PTC. The aspirate is markedly cellular and consists of numerous large and small sheets and clusters of follicular cells. No colloid is noted in the background (Diff Quik stain, low power)

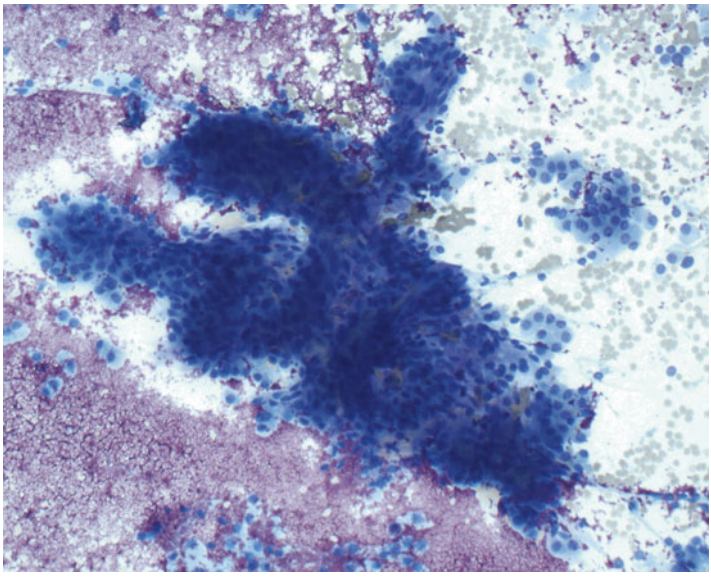

Fig. 17.2 Left thyroid FNA-positive for PTC. A large cluster of follicular cells arranged in complex papillary architecture (Diff Quik stain, high power)

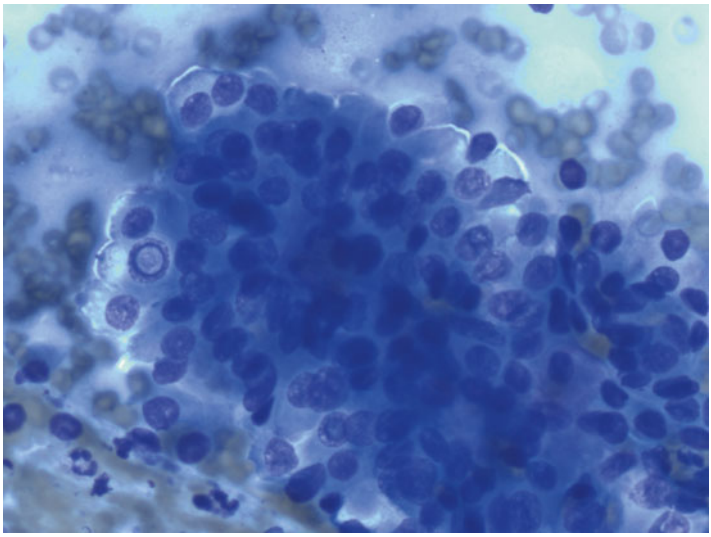

Fig. 17.3 Left thyroid FNA-positive for PTC. Individual cells show nuclear overlapping and crowding, nuclear enlargement, nuclear grooves, and occasional nuclear inclusions. There is also moderate amount of dense cytoplasm (Diff Quik stain, high power)

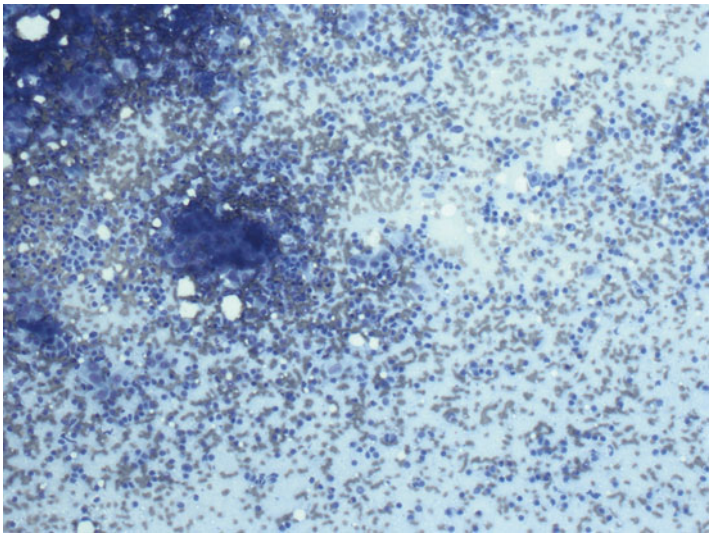

Fig. 17.4 L4 lymph node FNA-positive for metastatic PTC. Rare cohesive clusters of follicular cells in a background of mixed lymphoid population (Diff Quik stain, low power)

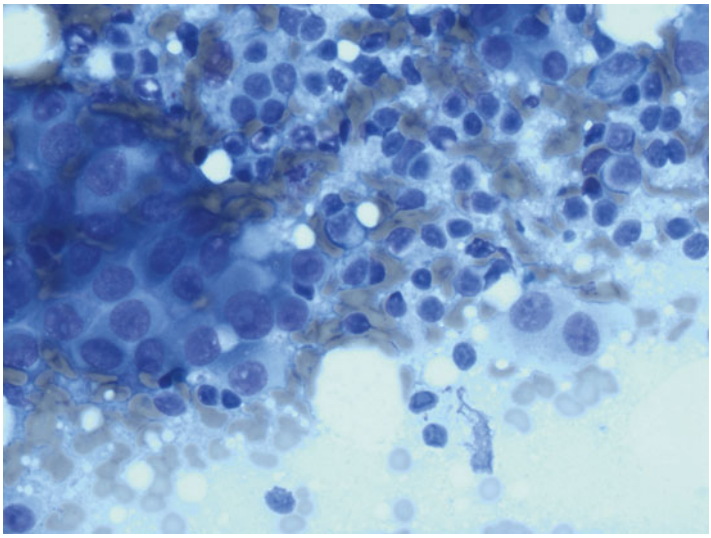

Fig. 17.5 L4 lymph node FNA-positive for metastatic PTC. Rare cohesive clusters of follicular cells in a background of mixed lymphoid population (Diff Quik stain, low power)

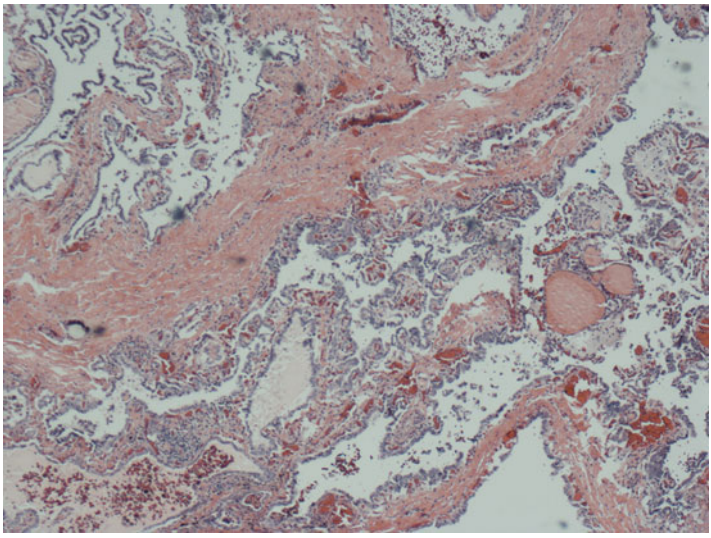

Fig. 17.6 Papillary thyroid carcinoma, left thyroid lobe. The tumor is composed of complex papillary fronds separated by thick fibrous stroma (H&E, low power)

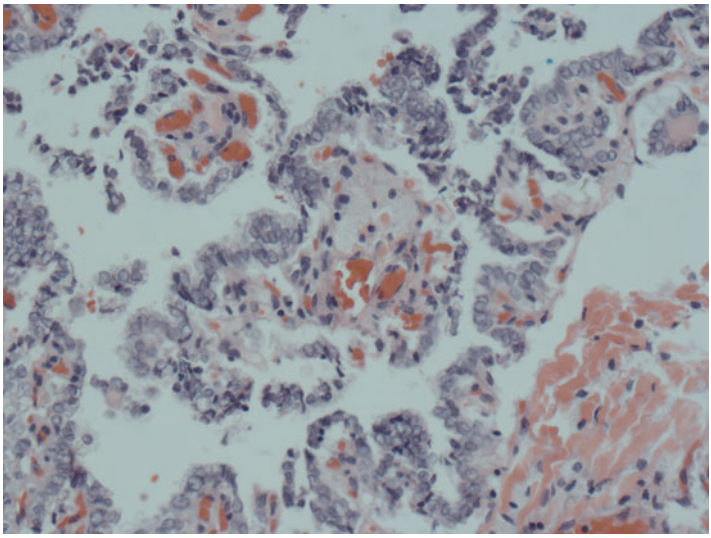

Fig. 17.7 Papillary thyroid carcinoma, left thyroid lobe. The papillae are lined by cuboidal to low columnar follicular cells with nuclear clearing, powdery chromatin, and nuclear grooves. Nuclear overlapping and crowding are apparent (H&E, high power)

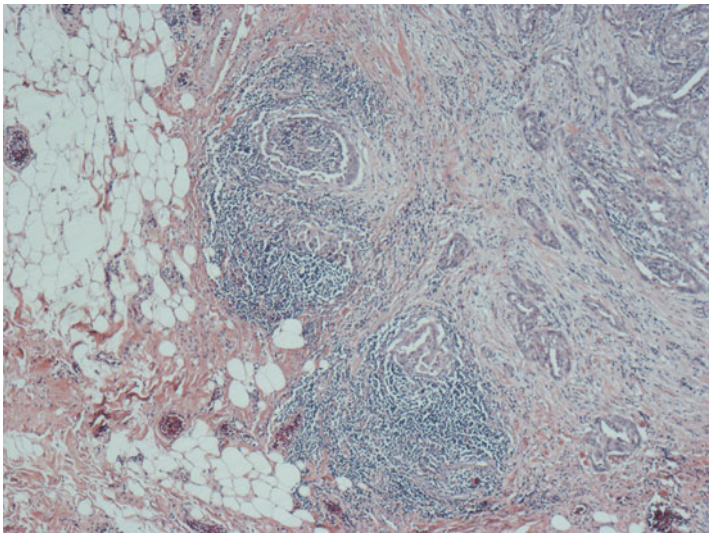

Fig. 17.8 Papillary thyroid carcinoma with extrathyroidal extension, left thyroid lobe. Islands of neoplastic follicular cells arranged in follicles and papillae infiltrating the perithyroidal adipose tissue. Intense lymphoid infiltrate and desmoplastic reaction are noted (H&E, low power)

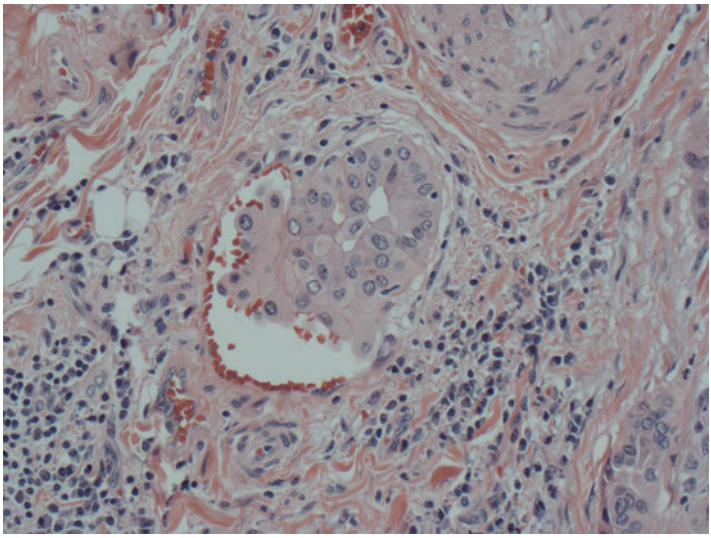

Fig. 17.9 Papillary thyroid carcinoma with vascular invasion, left thyroid lobe. A small vessel contains a cluster of follicular cells with abundant eosinophilic cytoplasm. Nuclei show powdery chromatin, nuclear clearing, and nuclear grooves (H&E, high power)

Discussion

Among the pediatric and adolescent population, thyroid nodules are infrequent with an incidence of 1–2 % [1–3]. However, the risk of malignancy of thyroid nodules in this subgroup of patients is much higher, ranging from 14 to 40 %, when compared to that of adult population [3–5]. Until recently, many have advocated surgical resection, rather than triaging by FNA, as the initial management of choice in view of the high malignancy risk in pediatric and adolescent population [6]. One plausible explanation is the rarity of literature on pediatric thyroid FNA. In addition, these reports are often in disagreement with each other. On one hand, many authors have reported high sensitivity and specificity of FNA in differentiating between benign and malignant thyroid nodules in pediatric population, recommending the avoidance of surgery for those with benign cytologic interpretations [7–11]. On the other hand, other studies have shown that the performance of thyroid FNA was inferior in pediatric population when compared to that of adult population; as a result, surgery would still be required to rule out a malignancy even with a benign cytologic interpretation [12, 13].

The cytology of various thyroid lesions is similar to that of adults. Hence, many challenges encountered in pediatric population are similar to those in the adult populations. Some of these challenges have been addressed in other chapters.

The recent introduction of the Bethesda System for Reporting Thyroid Cytopathology (TBSRTC) has provided a standardized reporting scheme for reporting thyroid FNA cytology as well as the estimated risk of malignancy for

Table 17.1 Frequency of distribution of various diagnostic categories based on data from the institution of one of the coauthors (unpublished data)

Cytologic diagnostic category	Patients 21 years or younger (%)	General population (%)	Ranges reported in the literature
Nondiagnostic	5.4	8.7	1.8–23.6 % (12.9 %)
Negative for malignancy	65.1	73.6	54.0–73.8 % (63.1 %)
FLUS/AUS	6.3	5.6	3.0–18.0 % (9.9 %)
Follicular neoplasm	4.2	4.5	1.2–9.7 % (4.9 %)
Suspicious for malignancy	5.4	2.0	1.3–6.2 % (2.3 %)
Positive for malignancy	13.6	5.6	2.0–7.0 % (5.0 %)

Table 17.2 Histologic outcomes of various diagnostic categories based on data from the institution of one of the coauthors (unpublished data)

	Histologic outcomes		
Cytologic diagnostic categories	Malignant (%)	Neoplastic (%)	Non-neoplastic (%)
Nondiagnostic	33.3	0.0	66.7
Negative for malignancy	8.3	8.3	83.4
FLUS/AUS	45.5	18.2	36.4
Follicular neoplasm	35.7	42.9	21.4
Suspicious for malignancy	94.1	0.0	5.9
Positive for malignancy	100.0	0.0	0.0

each diagnostic category [14]. Table 17.1 shows the frequency of distribution of each diagnostic category among patients 21 years old or younger at the institution of one of the coauthors based on a cohort of 332 thyroid FNA between 2008 and 2013 using TBSRTC (unpublished data). The percentage of thyroid FNA classified as "positive" and "suspicious" for malignancy are significantly much higher in the pediatric population when compared to the general population. Interestingly, there are no statistically significant differences in the percentages of thyroid FNA classified as "FLUS" or "follicular neoplasm" between the pediatric and general populations.

There is little literature on the performance of TBSTRC in the pediatric population. Table 17.2 summarizes the cytologic-histologic correlation based on 109 thyroid FNA in the pediatric population between 2008 and 2013 (unpublished data). Based on the data from the institution of one of the authors, the sensitivity and specificity of thyroid FNA using the TBSTRC were 97 % and 96 %, respectively, whereas a diagnosis of either "suspicious" or "positive" for malignancy was considered positive and cases classified as "FLUS" and "follicular neoplasm" were excluded from the calculation. According to a meta-analysis of 12 articles on pediatrics thyroid FNA, the sensitivities and the specificities ranged from 64 to 100 % and from 57 to 97 %, respectively, with the pooled estimate sensitivity of 94 % and specificity of 81 % [6].

The majority of the malignancies encountered in the pediatric population are papillary thyroid carcinoma [7, 10, 15]. Cases of medullary carcinoma are also observed occasionally. However, the incidence of follicular or Hurthle cell carcinoma is extremely rare.

About one third of patients with a cytologic diagnosis of "follicular neoplasm" are found to harbor a malignant thyroid nodule; all are papillary thyroid carcinoma, follicular variant. Even on retrospective review, nuclear features that characterize papillary thyroid carcinoma are either nondetectable or very subtle.

Based on the data from the institution of one of the authors, the percentage of equivocal thyroid FNAs, i.e., cases with the cytologic diagnosis of FLUS/AUS and follicular neoplasm, is about 10.5 %, which is comparable to that observed in the general population (unpublished data). However, other authors in the literature have reported a much higher percentage of equivocal thyroid FNAs (35 %) in their pediatric population [4]. These authors have attributed their higher frequency of the FLUS/AUS category partly to the reluctance to diagnose malignancy in a young patient and partly to the low cellularity secondary to difficulty in sampling of these lesions.

According to TBSRTC, the estimated malignancy rate for FLUS/AUS category and follicular neoplasm is about 10–15 % and 25–45 %, respectively, for the general population [14]. Some have reported higher malignancy rates for both categories in pediatric population [15]. Regardless, a diagnostic thyroid lobectomy may be warranted to rule out a malignancy when other clinical and/or ultrasonographic risk factors are also present. However, this approach is invasive and has a high risk of complications including recurrent laryngeal nerve injury and anesthesia complications. Furthermore, if lobectomy is found to harbor a malignancy, the patient would have to undergo a completion thyroidectomy, in turn, placing the patient under the same risks a second time.

Although there is plenty of literature on the use of molecular testing in triaging adult patients with equivocal thyroid FNA, there are only a few studies examining this subject in the pediatric population. Using mutational analysis that is known to be associated with papillary thyroid carcinomas (*BRAF, RAS, RET/PTC, PAX8/PPARγ*), Buryk et al. have demonstrated that molecular testing can improve positive predictive value of FNA to nearly 100 % and minimize unnecessary second procedures [16]. One major limitation of this approach is that a malignancy cannot be ruled out based on a negative molecular testing since not all malignant thyroid lesions, including a substantial number of papillary thyroid carcinomas, would demonstrate any of these mutations. Currently, there is no data on the use of Afirma for the triaging of equivocal thyroid FNA in pediatric patients; as a result the use of Afirma as a triaging tool is not indicated in pediatric patients.

References

1. Hung W. Nodular thyroid disease and thyroid carcinoma. Pediatr Ann. 1992;21:50–7.
2. Hung W, August GP, Randolph JG, Schisgall RM, Chandra R. Solitary thyroid nodules in children and adolescents. J Pediatr Surg. 1982;17:225–9.

3. Telander RL, Zimmerman D, Kaufman BH, van Heerden JA. Pediatric endocrine surgery. Surg Clin North Am. 1985;65:1551–87.
4. Monaco SE, Pantanowitz L, Khalbuss WE, et al. Cytomorphological and molecular genetic findings in pediatric thyroid fine-needle aspiration. Cancer Cytopathol. 2012;120:342–50.
5. Scott MD, Crawford JD. Solitary thyroid nodules in childhood: is the incidence of thyroid carcinoma declining? Pediatrics. 1976;58:521–5.
6. Stevens C, Lee JK, Sadatsafavi M, Blair GK. Pediatric thyroid fine-needle aspiration cytology: a meta-analysis. J Pediatr Surg. 2009;44:2184–91.
7. Amrikachi M, Ponder TB, Wheeler TM, Smith D, Ramzy I. Thyroid fine-needle aspiration biopsy in children and adolescents: experience with 218 aspirates. Diagn Cytopathol. 2005;32:189–92.
8. Arda IS, Yildirim S, Demirhan B, Firat S. Fine needle aspiration biopsy of thyroid nodules. Arch Dis Child. 2001;85:313–7.
9. Corrias A, Einaudi S, Chiorboli E, et al. Accuracy of fine needle aspiration biopsy of thyroid nodules in detecting malignancy in childhood: comparison with conventional clinical, laboratory, and imaging approaches. J Clin Endocrinol Metab. 2001;86:4644–8.
10. Hosler GA, Clark I, Zakowski MF, Westra WH, Ali SZ. Cytopathologic analysis of thyroid lesions in the pediatric population. Diagn Cytopathol. 2006;34:101–5.
11. Khurana KK, Labrador E, Izquierdo R, Mesonero CE, Pisharodi LR. The role of fine-needle aspiration biopsy in the management of thyroid nodules in children, adolescents, and young adults: a multi-institutional study. Thyroid. 1999;9:383–6.
12. Lugo-Vicente H, Ortiz VN, Irizarry H, Camps JI, Pagan V. Pediatric thyroid nodules: management in the era of fine needle aspiration. J Pediatr Surg. 1998;33:1302–5.
13. Willgerodt H, Keller E, Bennek J, Emmrich P. Diagnostic value of fine-needle aspiration biopsy of thyroid nodules in children and adolescents. J Pediatr Endocrinol Metab. 2006;19:507–15.
14. Cibas ES, Ali SZ. The Bethesda system for reporting thyroid cytopathology. Thyroid. 2009;19:1159–65.
15. Smith M, Pantanowitz L, Khalbuss WE, Benkovich VA, Monaco SE. Indeterminate pediatric thyroid fine needle aspirations: a study of 68 cases. Acta Cytol. 2013;57:341–8.
16. Buryk MA, Monaco SE, Witchel SF, et al. Preoperative cytology with molecular analysis to help guide surgery for pediatric thyroid nodules. Int J Pediatr Otorhinolaryngol. 2013;77:1697–700.

Ectopic Thyroid Tissue Versus Nodal Metastasis

18

Case Study

A 44-year-old woman was initially noted to have several thyroid nodules detected by ultrasound 7 year ago during her workup for infertility. No biopsy was performed at that time because of the small size of the nodules. Her latest follow-up ultrasound revealed an ill-defined 6 mm left thyroid nodule, which had grown in size, as well as a left inferior cervical mass at level IV measuring 1 cm. She had no complaints of hoarseness or difficulty in swallowing and breathing. She had no symptoms of hyperthyroidism. She had no history of radiation to the head and neck area and no family history of thyroid cancer. Physical examination was unremarkable. No other cervical lymphadenopathy was identified on imaging.

Fine needle aspiration biopsy was performed for the left thyroid nodule and the left inferior cervical mass. The cytology of the left thyroid nodule was consistent with that of a papillary thyroid carcinoma (Figs. 18.1 and 18.2). On the other hand, the aspirate from left inferior cervical mass was of low cellularity and consisted of abundant colloid and a few small clusters of benign-appearing follicular cells (Figs. 18.3 and 18.4). Nuclear features of papillary thyroid carcinoma were not identified. The cytologic findings of the left inferior cervical mass resembled that of a goiter, suggestive of ectopic thyroid tissue.

The patient subsequently underwent total thyroidectomy, left central neck dissection, and excisional biopsy of left inferior cervical mass. The total thyroidectomy revealed a conventional papillary thyroid carcinoma, measuring 0.4 cm (Figs. 18.5 and 18.6). Twelve lymph nodes were identified which were all negative for malignancy. The histology of the left inferior neck mass demonstrated both macro- and micro-follicles of varying sizes, which were lined by flattened or cuboidal follicular cells (Figs. 18.7 and 18.8). Fibrosis with lymphocytic infiltrates was noted. The findings were that of a benign goiter, consistent with ectopic thyroid tissue.

A.J. Adeniran, D. Chhieng, *Common Diagnostic Pitfalls in Thyroid Cytopathology*, DOI 10.1007/978-3-319-31602-4_18

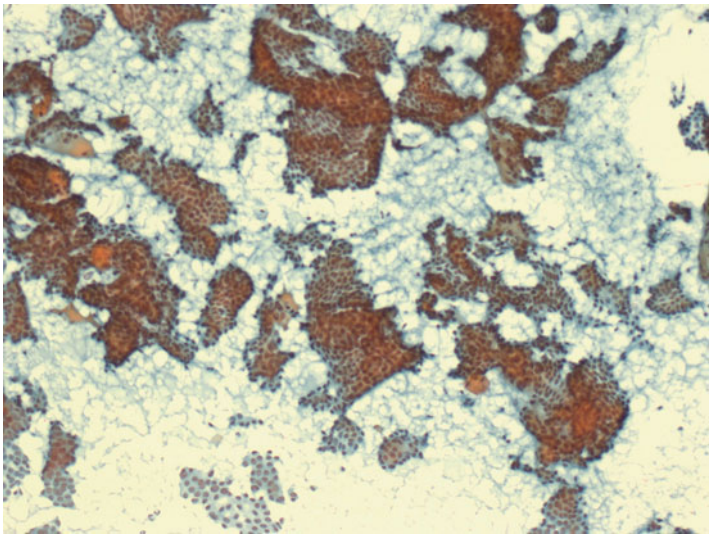

Fig 18.1 Thyroid FNA-papillary thyroid carcinoma. The aspirate is markedly cellular and consists of numerous large tissue fragments. Colloid is scant (Papanicolaou stain, low power)

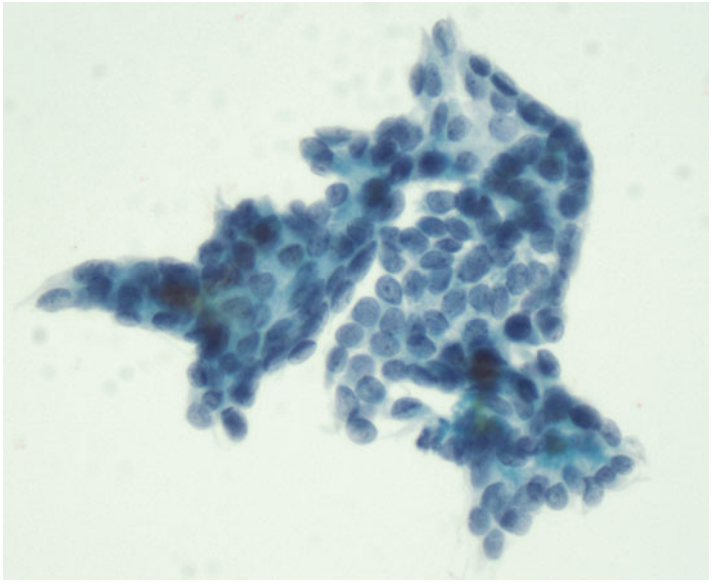

Fig 18.2 Papillary thyroid carcinoma, thyroid FNA. Irregular tissue fragments with nuclear crowding and overlapping. Individual cells appear oval to elongate with nuclear enlargement, powdery chromatin, and nuclear grooves (Papanicolaou stain, high power)

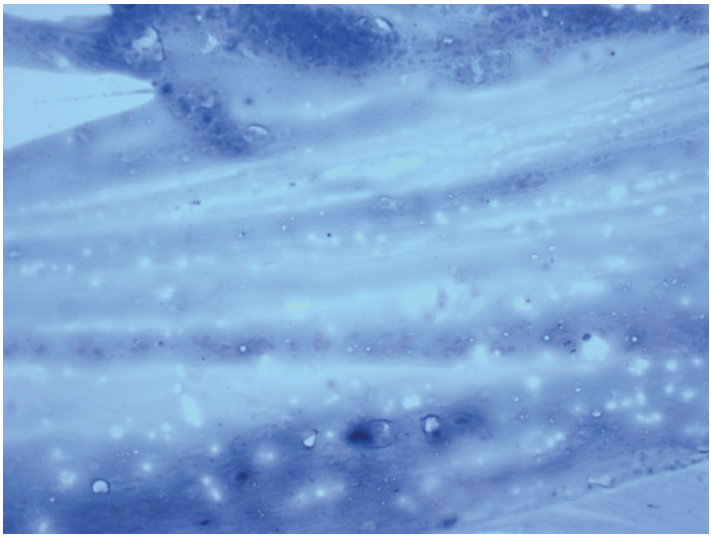

Fig 18.3 Left level IV mass FNA-benign thyroid tissue. The specimen is of low cellularity and consists of abundant colloid. Follicular cells are scant (Diff-Quik stain, low power)

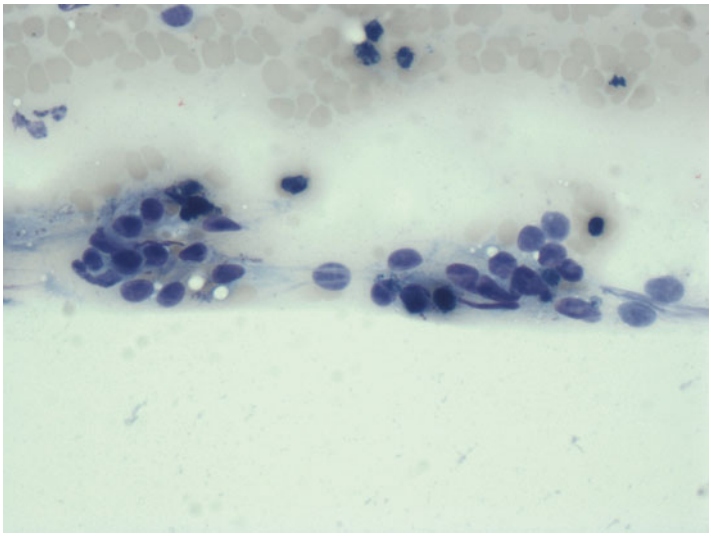

Fig 18.4 Left level IV mass FNA-benign thyroid tissue. High magnification shows several small clusters of benign-appearing follicular cells. Nuclear features characteristic of papillary thyroid carcinoma are absent (Diff-Quik stain, low power)

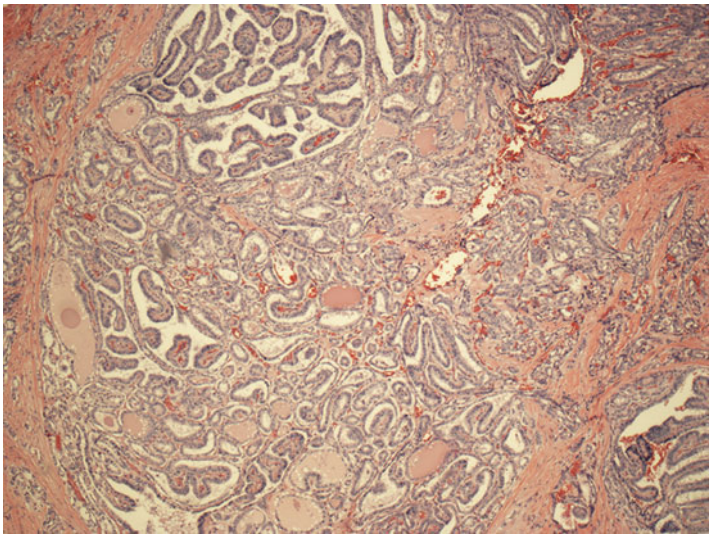

Fig 18.5 Papillary thyroid carcinoma. Partially encapsulated thyroid nodule with a predominant papillary growth pattern. Fibrovascular cores are noted in some of the papillae (H&E, x40)

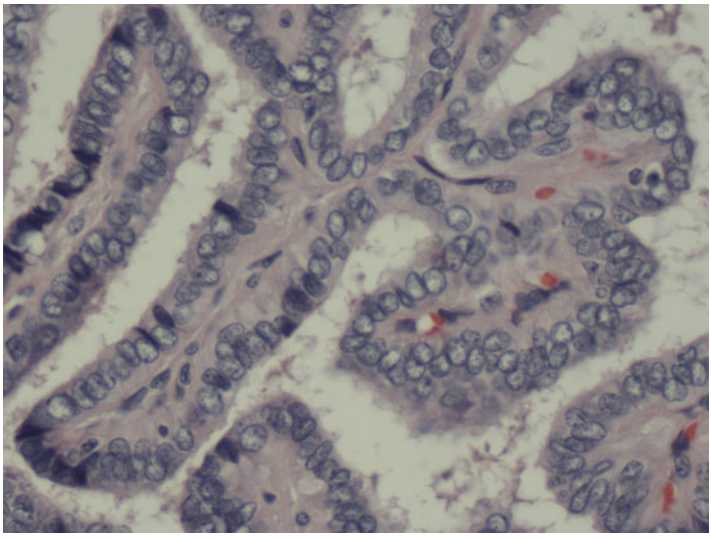

Fig 18.6 Papillary thyroid carcinoma. Papillae with fibrovascular cores are lined by follicular cells with nuclear considerable crowding. The follicular cells show nuclear clearing, powdery chromatin, and nuclear grooves (H&E, x400)

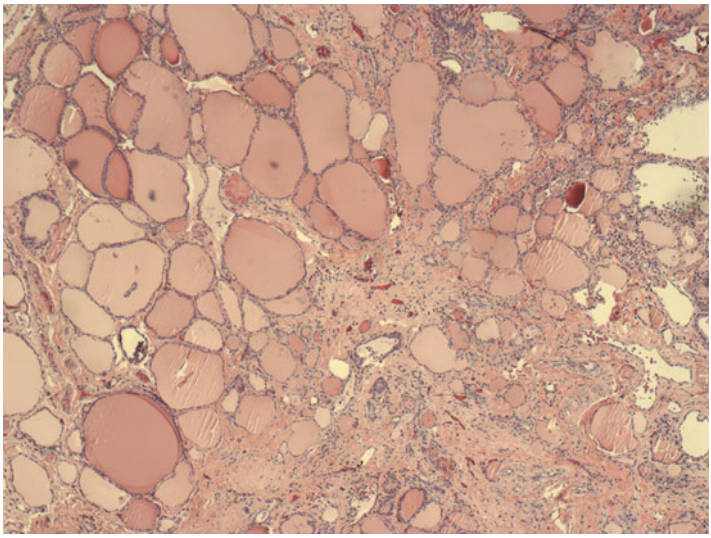

Fig 18.7 Ectopic thyroid tissue with goiter. Thyroid follicles of varying sizes are noted with fibrosis and scattered lymphocytic infiltrate (H&E, x400)

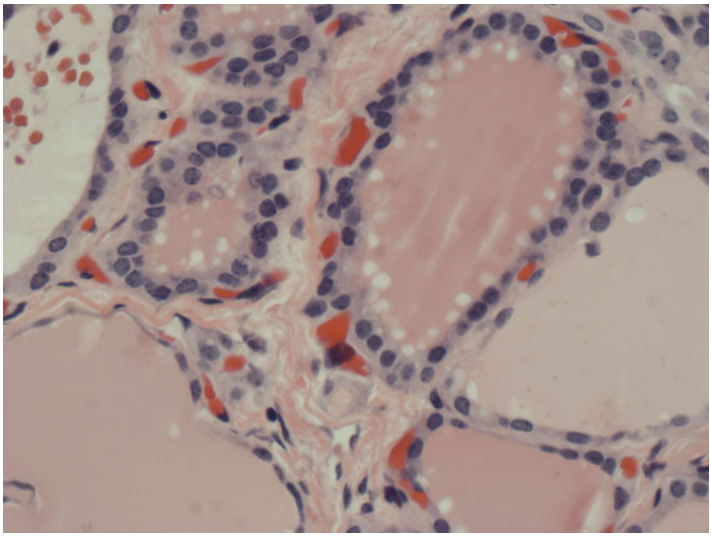

Fig 18.8 Ectopic thyroid tissue with goiter. The thyroid follicles are lined by cuboidal and flat follicular cells with round to oval nuclei and fine granular chromatin. The follicles are separated by fibrous stroma (H&E, x400)

Discussion

The finding of thyroid tissue in the aspirates of a neck mass unconnected to the thyroid gland would, in no doubt, create a diagnostic challenge from a cytologic point of view. The cytologist is faced with two options: whether the aspirate represents a metastatic thyroid malignancy to the cervical node or ectopic thyroid tissue/benign thyroid inclusions in cervical lymph nodes. This diagnostic dilemma would be further complicated when the patient also has a known history of thyroid malignancy.

Ectopic thyroid tissue, a well-known developmental abnormality, refers to the presence of thyroid tissue in the neck, which is distinct from and without any connection to the thyroid gland. It is often attributed to the abnormal migration of the thyroid gland during embryogenesis, and therefore, is generally located in the midline region. The occurrence of ectopic thyroid tissue occurring in the lateral and submandibular area is rare [1]. The histology of the ectopic thyroid tissue ranges from normal to various non-neoplastic processes such as atrophy, adenomatous hyperplasia, lymphocytic thyroiditis, and rarely, malignant transformation.

Benign thyroid inclusions may rarely be found in the lateral neck nodes. Some authors have considered that all thyroid tissues found in the lateral cervical nodes represent nodal metastases from a primary thyroid carcinoma, irrespective of its histological aspect [2, 3]. Others have accepted the existence of benign thyroid tissue inclusions in cervical lymph nodes [4, 5]. However, the criteria for defining "benign thyroid inclusions" are very stringent; Table 18.1 lists the clinicopathologic features of benign thyroid inclusions in cervical lymph nodes [6].

If the histologic distinction between a metastatic thyroid malignancy to the cervical node and ectopic thyroid tissue/benign thyroid inclusion in lateral neck nodes

Table 18.1 Clinicopathologic features of benign thyroid inclusion in cervical lymph node

• Microscopic focus: occupying one-third or less of the node
• Limited to one lymph node
• Lymph node located medial to jugular vein
• Intracapsular or immediately subcapsular
• Uncrowded, normal appearing follicles
• Normal nuclei size
• Lack nuclear features of papillary carcinoma
• Absence of psammoma bodies
• Absence of stromal reaction
• Absence of staining for galectin-3 or HBME-1
• Absence of BRAF, RET/PTC, or RAS mutations

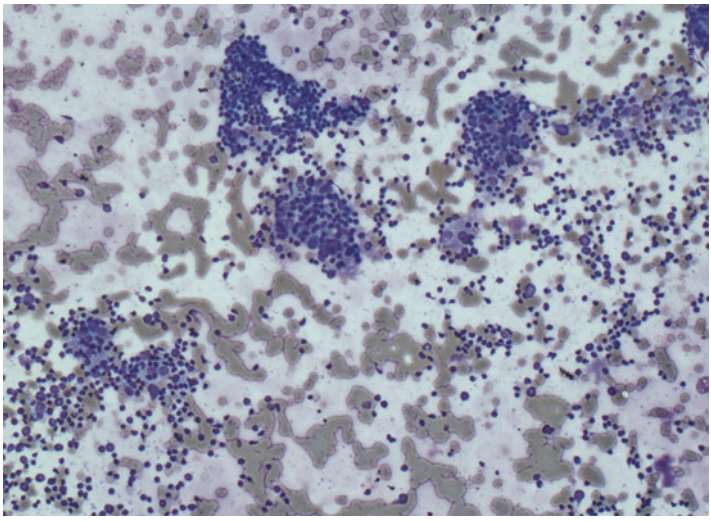

Fig 18.9 Ectopic thyroid FNA-lymphocytic thyroiditis. The aspirate is cellular and composed of a polymorphous population of lymphocytes (Diff-Quik stain, low power)

can be difficult, attempts to differentiate these entities cytologically would be even more challenging. The finding of cytologically benign-appearing follicular cells with or without colloid does not necessarily imply a benign process since the pattern of growth of certain thyroid carcinomas can be so well differentiated as to simulate non-neoplastic thyroid tissue. On the other hand, the presence of cytologic and/or architectural atypia in follicular cells, even if accompanied by a lymphoid background, does not always indicate a metastatic thyroid carcinoma [7]. Similarly, the presence or absence of a lymphoid background would not provide any helpful clues as to whether the target is a lymph node or not since ectopic thyroid tissue can be involved by lymphocytic or Hashimoto's thyroiditis [8] (Figs. 18.9 and 18.10) whereas the entire lymph node can be replaced by metastatic disease (Fig. 18.11). In these instances, it is best to avoid making a definitive diagnosis of "metastatic thyroid carcinoma." A sounder, more conservative approach would be to include ectopic thyroid tissue or nodal benign thyroid inclusion in the list of differential diagnosis and to propose surgical excision for further histologic correlation. However, there are a few cytologic features, when present, that are diagnostic of metastases; they include psammoma bodies and unequivocal nuclear features characteristic of papillary thyroid carcinoma.

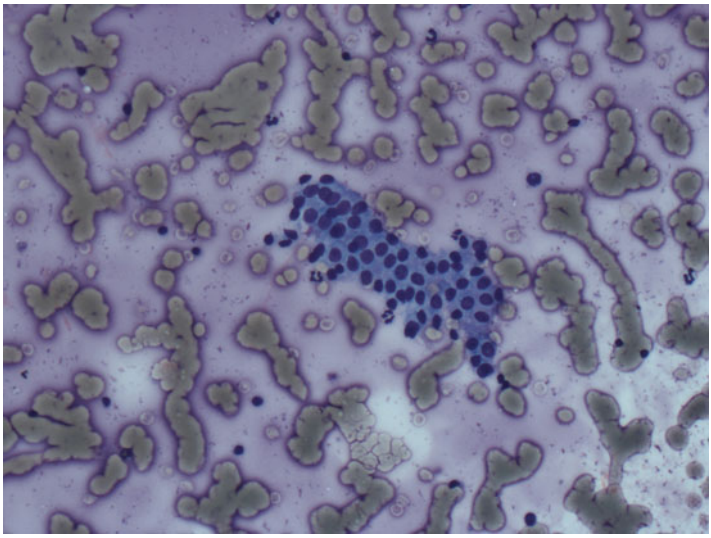

Fig 18.10 Ectopic thyroid FNA-lymphocytic thyroiditis. High magnification shows scattered follicular cells with Hurthle cell changes are noted. Subsequent follow-up shows ectopic thyroid tissue with florid lymphocytic thyroiditis (Diff-Quik stain, high power)

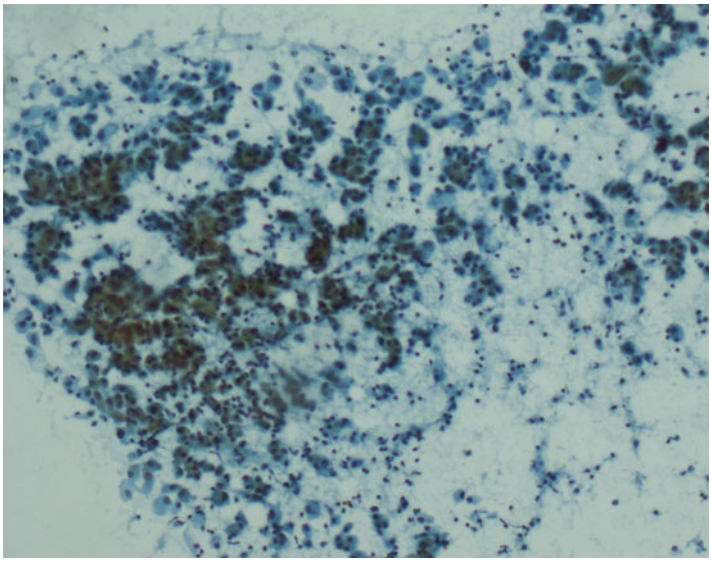

Fig 18.11 Left level IV lymph node-metastatic papillary thyroid carcinoma. The aspirate shows predominantly neoplastic follicular cells in numerous tissue fragments admixed with scattered lymphocytes. Histologic follow-up reveals metastatic PTC completely replacing the lymph node (Diff-Quik stain, low power)

References

1. Kumar R, Sharma S, Marwah A, Moorthy D, Dhanwal D, Malhotra A. Ectopic goiter masquerading as submandibular gland swelling: a case report and review of the literature. Clin Nucl Med. 2001;26:306–9.
2. Kozol RA, Geelhoed GW, Flynn SD, Kinder B. Management of ectopic thyroid nodules. Surgery. 1993;114:1103–6. discussion 1106–1107.
3. Butler JJ, Tulinius H, Ibanez ML, Ballantyne AJ, Clark RL. Significance of thyroid tissue in lymph nodes associated with carcinoma of the head, neck or lung. Cancer. 1967;20:103–12.
4. Ansari-Lari MA, Westra WH. The prevalence and significance of clinically unsuspected neoplasms in cervical lymph nodes. Head Neck. 2003;25:841–7.
5. Fliegelman LJ, Genden EM, Brandwein M, Mechanick J, Urken ML. Significance and management of thyroid lesions in lymph nodes as an incidental finding during neck dissection. Head Neck. 2001;23:885–91.
6. Biddinger PW. Embryology and developmental lesions. In: Nikiforov YE, Biddinger PW, Thompson LDR, editors. Diagnostic pathology and molecular genetics of the thyroid: a comprehensive guide for practicing thyroid pathology. Philadelphia PA: Lippincott Williams & Wilkins; 2012. p. 11–32.
7. Paksoy N. Ectopic lesions as potential pitfalls in fine needle aspiration cytology: a report of 3 cases derived from the thyroid, endometrium and breast. Acta Cytol. 2007;51:222–6.
8. Singh M, Jha R, Jain S, Bansal R. Fine needle aspiration of a lingual thyroid with Hashimoto's thyroiditis. Cytopathology. 2013;24:275–7.

Parathyroid Tissue Versus Thyroid Tissue 19

Case Study

A 72-year-old male who presented with sudden onset severe right flank pain, which was colicky in nature and radiated to the inner right thigh. The patient has had three previous episodes of kidney stones. He also had a history of gastroesophageal reflux disease, but no pancreatitis or ulcers. His memory and concentration were poor. Although he was in a good mood at the time of presentation, he had a history of depression. The patient had no bone pain or recent fractures and no complaint of hoarseness, difficulty swallowing, or difficulty breathing. He had a 26-pack year smoking history but quit smoking about 13 years ago. The patient's father had a history of kidney stones but no history of hypercalcemia or parathyroid surgery in the family. Examination of the neck revealed a normal thyroid gland without palpable masses. There was no cervical or supraclavicular lymphadenopathy. He had a calcium level of 11.3 mg/dL and a parathyroid hormone (PTH) value of 132 pg/mL. 24 h urinary calcium was 232 mg. Ultrasonographic examination showed a normal thyroid gland. There was a 1.5 cm hypoechoic density posterior-inferior to the right thyroid lobe and a 2.9 cm hypoechoic density posterior-inferior to the left thyroid lobe. Sestamibi scan showed bilateral uptake consistent with bilateral enlarged parathyroid glands. Fine needle aspiration was done and it revealed clusters of bland epithelial cells with oncocytic features. PTH stain was positive on cells in additional ThinPrep material. The patient underwent bilateral neck exploration and subtotal parathyroidectomy with intraoperative PTH measurements. Double parathyroid adenomas were removed. Baseline PTH measurement prior to surgical manipulation was 128 pg/mL while it was 45 pg/mL at 45 min following resection. The right inferior parathyroid gland weighed 341 mg, very cellular, and was composed predominantly of oxyphil cells with clusters of chief cells. The left inferior gland weighed 1779 mg and was similar in morphologic appearance to the right gland. The patient did well postoperatively. He had no symptoms of hypocalcemia.

A.J. Adeniran, D. Chhieng, *Common Diagnostic Pitfalls in Thyroid Cytopathology*, DOI 10.1007/978-3-319-31602-4_19

Discussion

Fine needle aspiration biopsy is not routinely performed in the assessment of parathyroid gland lesions; hence, information on the cytopathologic findings is limited. A common pitfall in the diagnosis of thyroid nodules is the inadvertent sampling of parathyroid tissue, which may be difficult to distinguish from thyroid tissue on FNA due to similar cytologic features [1, 2]. Parathyroid cells are usually loosely clustered into small groups, often with a syncytial arrangement forming branching, loose, two-dimensional clusters (Figs. 19.1, 19.2, and 19.3). Microfollicular architecture is prevalent on ThinPrep preparations and this may contribute to overinterpretation of parathyroid tissue as follicular neoplasm of the thyroid [3] (Figs. 19.4 and 19.5). They may also be present as single cells. Naked nuclei are usually present, especially in smears (Fig. 19.6). Hemosiderin-laden macrophages may be present. Parathyroid cells on ThinPrep preparations show round, centrally placed nuclei with stippled nuclear chromatin. The nuclei often appear smaller and darker on ThinPrep preparations than on corresponding FNA smears. The cytoplasm is scant to moderate (Figs. 19.7, 19.8, 19.9, 19.10, 19.11, 19.12, and 19.13). In cases with oncocytic differentiation, the cytoplasm has a granular appearance with increased density [3]. Absence of colloid is a helpful hint in parathyroid aspirates; however colloid-like material can be produced by hyperplastic parathyroid glands and can be confused with true colloid [3, 4]. Also, true colloid can be accidentally picked up as the needle crosses thyroid tissue on its way to parathyroid tissue sampling.

Aspirate of parathyroid adenoma may be misdiagnosed as papillary thyroid carcinoma. This is because parathyroid adenoma can present a wide spectrum of cytologic features with several characteristics that are not seen in normal parathyroid

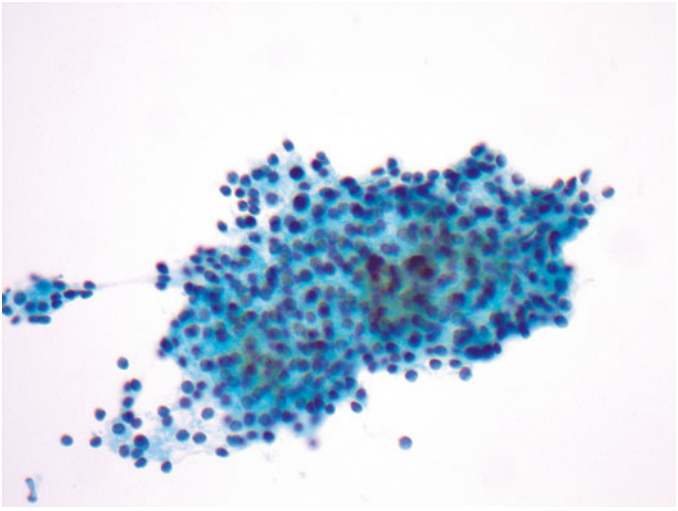

Fig. 19.1 Cellular parathyroid aspirate showing a flat sheet of cells with small, round nuclei (Papanicolaou stain, X400)

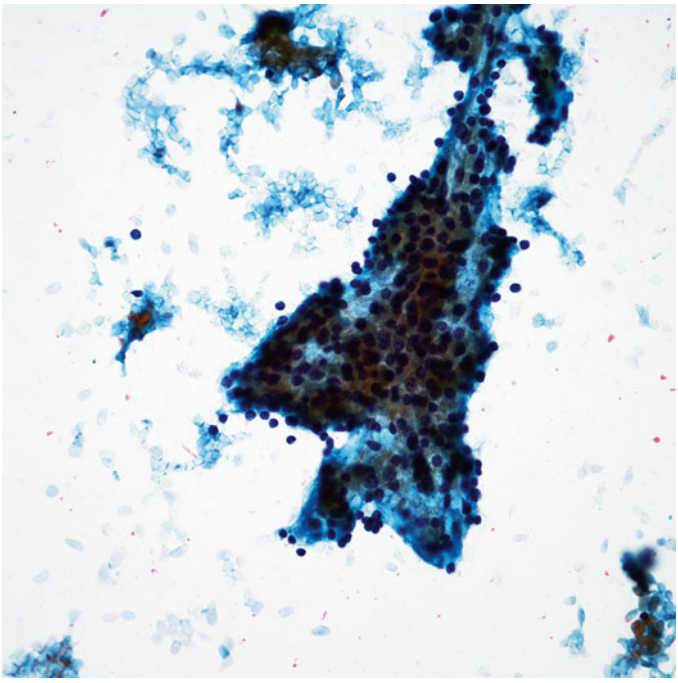

Fig. 19.2 Syncytial tissue fragment. Nuclei are small, dark, round, and uniform. Cytoplasm is lacy in appearance (Papanicolaou stain, X400)

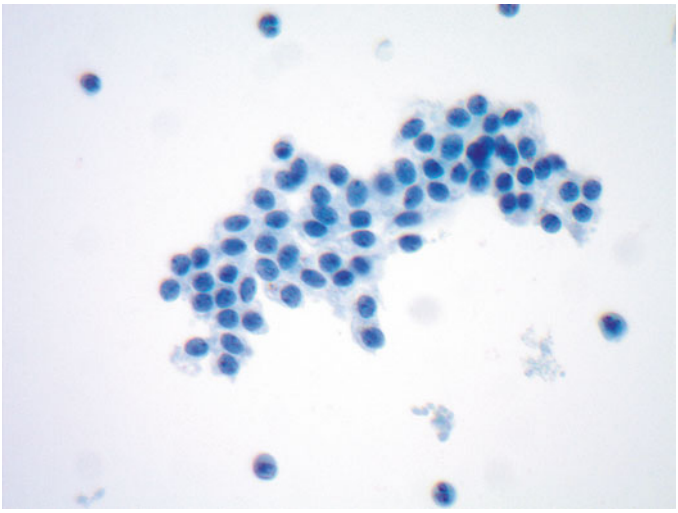

Fig. 19.3 Flat sheet of parathyroid cells demonstrating small, round nuclei with lacy cytoplasm (Papanicolaou stain, X600)

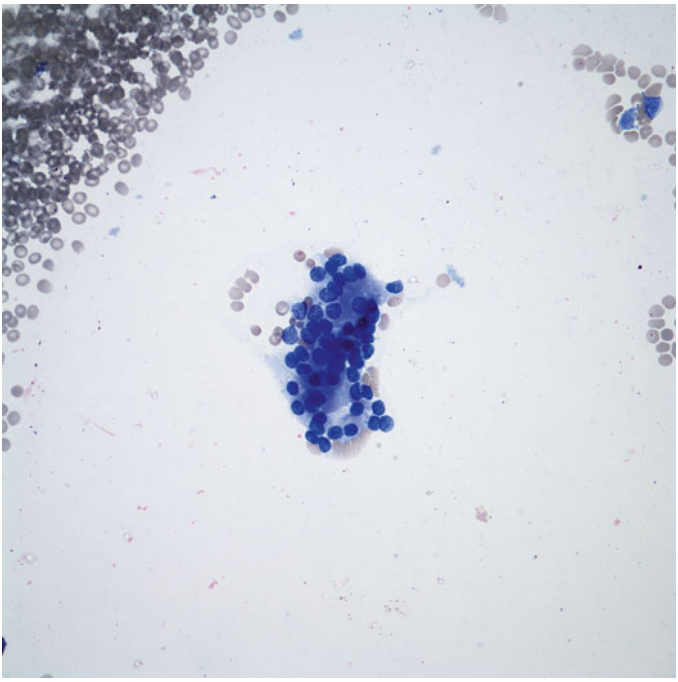

Fig. 19.4 Microfollicular arrangement of parathyroid cells (Diff-Quik stain, X400)

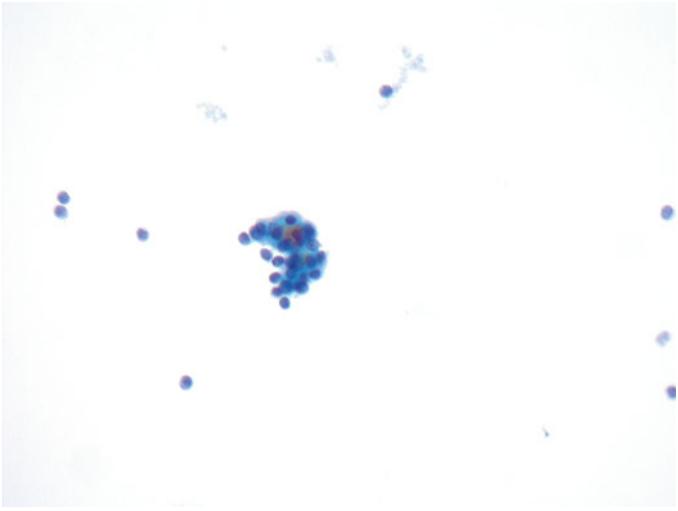

Fig. 19.5 Small follicle-like formations showing cells with small, uniform, round to oval nuclei (Papanicolaou stain, X400)

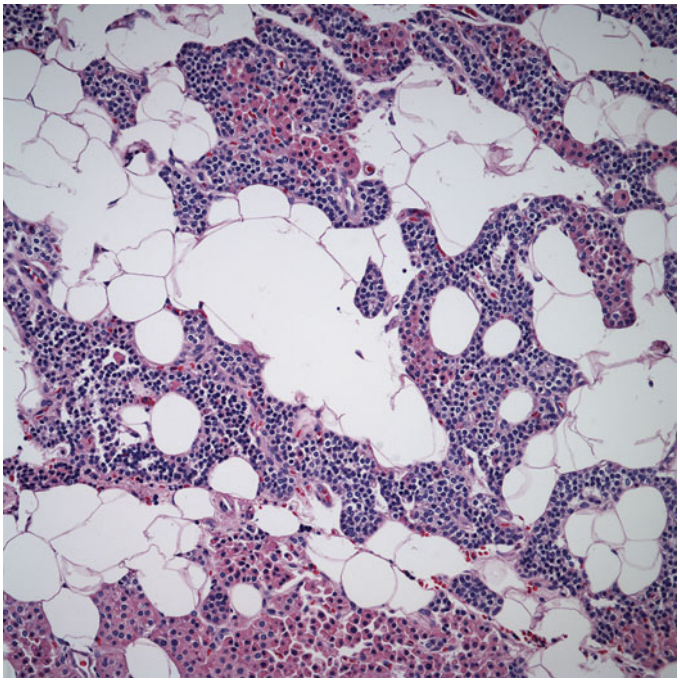

Fig. 19.6 Normal parathyroid gland showing predominantly chief cells and few clusters of oxyphil cells (H&E stain, X200)

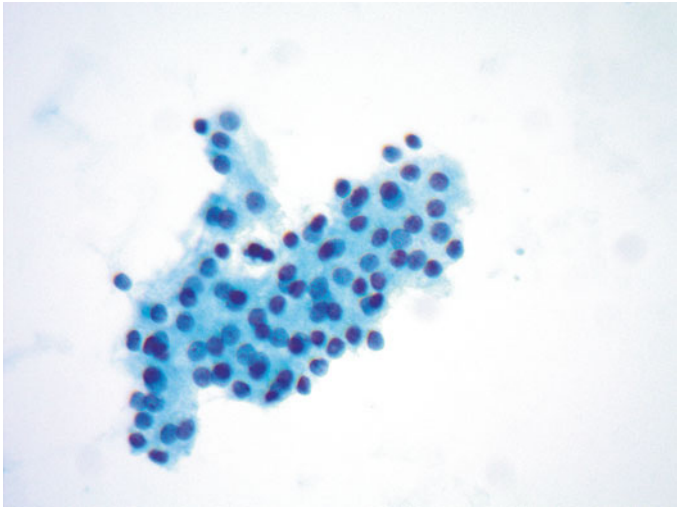

Fig. 19.7 Flat sheet of parathyroid cells. Scattered naked nuclei are also present on the smear (Papanicolaou stain, X600)

Fig. 19.8 Parathyroid cells demonstrating small, round nuclei with lacy cytoplasm (Papanicolaou stain, X600)

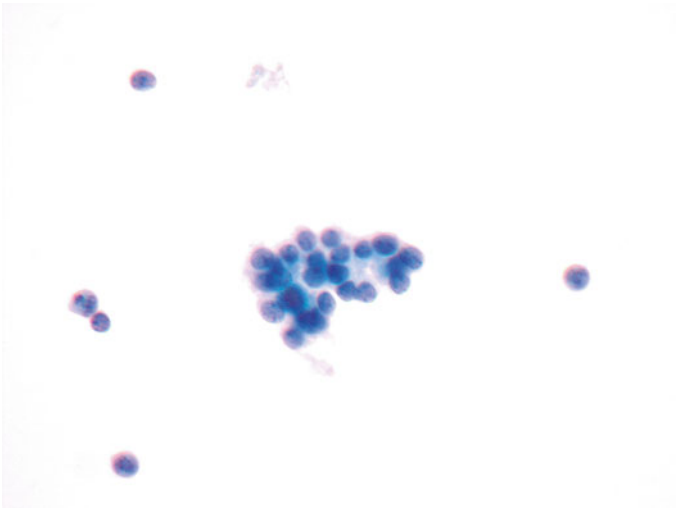

Fig. 19.9 Small, round nuclei with stippled nuclear chromatin (Papanicolaou stain, X600)

tissue, notably branching tissue fragments of epithelial cells with a papillary-like architecture (Fig. 19.14). The presence of this papillary-like architecture alone is not a diagnostic feature of PTC unless it is accompanied by the typical nuclear features such as nuclear enlargement, nuclear crowding/overlapping, nuclear contour irregularity, powdery chromatin, nuclear grooves, and intranuclear inclusions. When the diagnosis is in doubt, parathyroid hormone immunostain should be performed and positive PTH stain will confirm parathyroid origin [5] (Fig. 19.15).

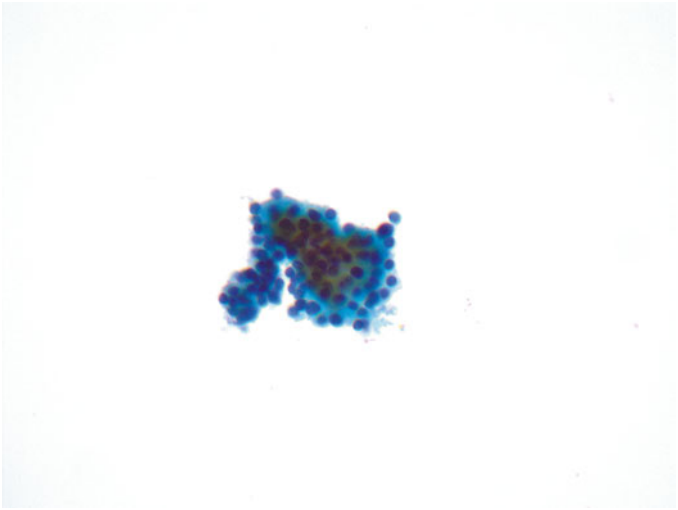

Fig. 19.10 Cluster of parathyroid cells showing small, round, dark nuclei (Papanicolaou stain, X400)

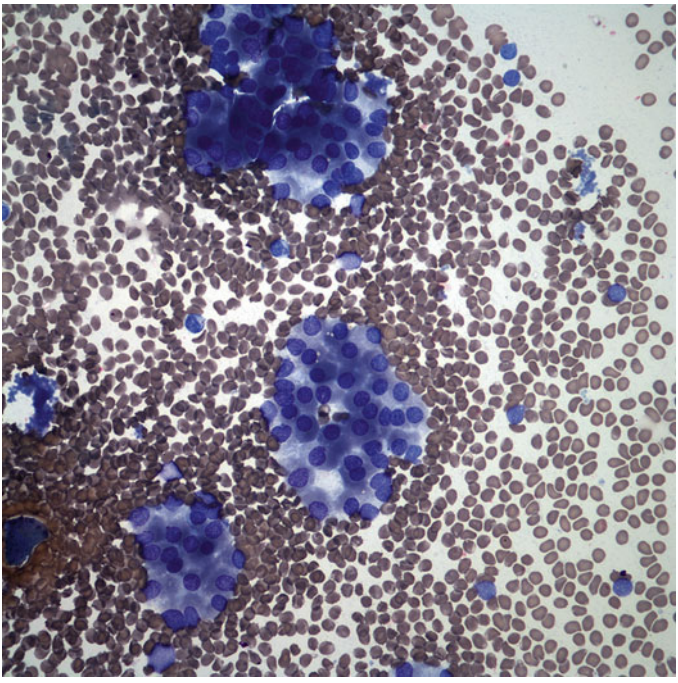

Fig. 19.11 Small follicle-like formations with parathyroid cells showing stippled nuclear chromatin (Diff-Quik stain, X400)

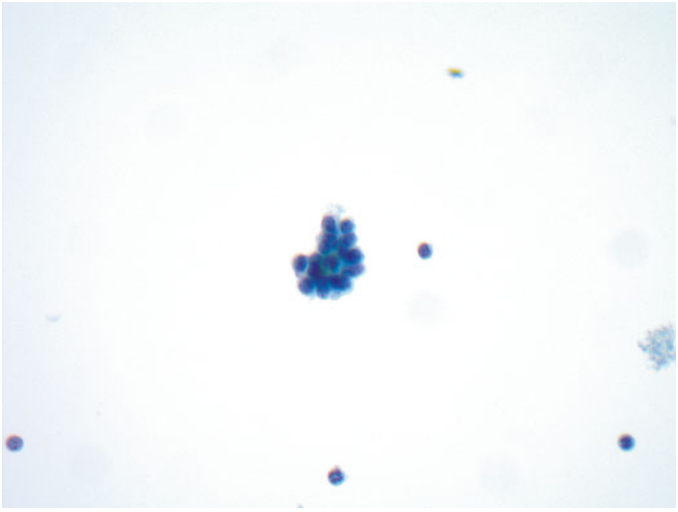

Fig. 19.12 Microfollicular pattern. Cells with stippled nuclear chromatin (Papanicolaou stain, X400)

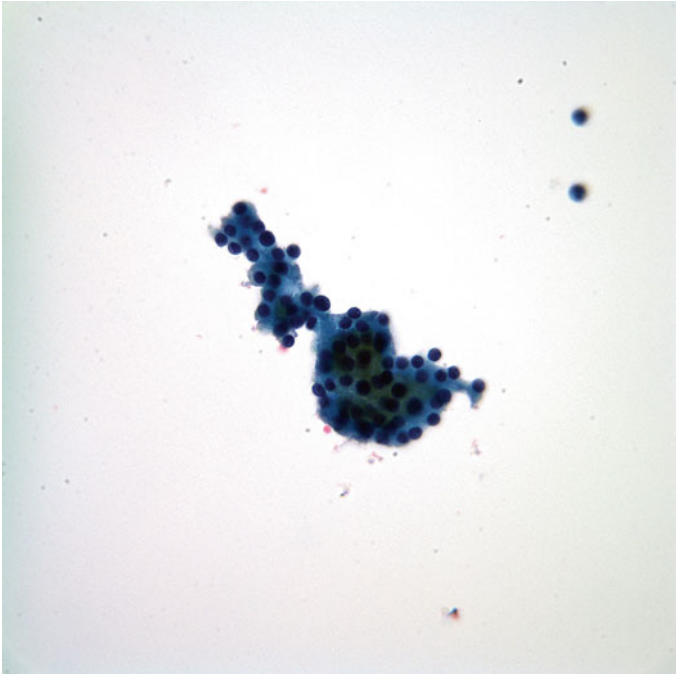

Fig. 19.13 Loose tissue fragments and microfollicles, showing small, round, dark nuclei (Papanicolaou stain, X400)

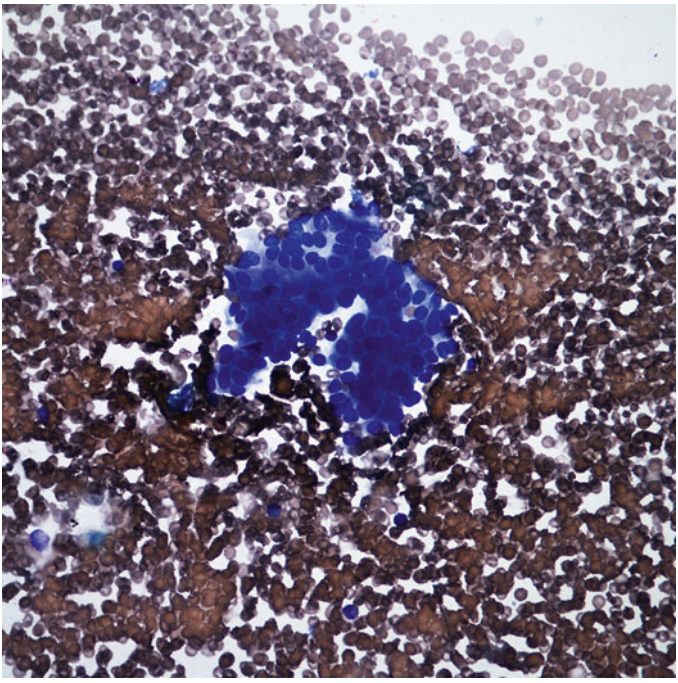

Fig. 19.14 Parathyroid cells arranged in small papillary clusters. The cells are small and the nuclei are round and uniform. There are no nuclear features of papillary thyroid carcinoma (Diff-Quik stain, X400)

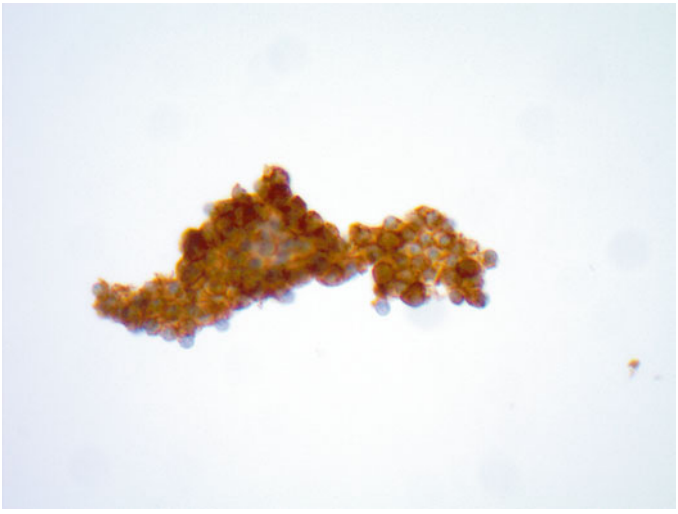

Fig. 19.15 Immunohistochemistry stain for parathyroid hormone is positive

Because colloid is usually scant to absent in follicular neoplasms of the thyroid, the differentiation between follicular neoplasm and cellular parathyroid tissue is extremely difficult. This diagnostic dilemma may be solved by PTH and/or thyroglobulin immunostains. The small size of parathyroid cells and their presentation in tight, three-dimensional clusters resembles the cytologic pattern of insular carcinoma of the thyroid and is a potential diagnostic pitfall. Immunoreactivity to parathyroid hormone will confirm the origin of the cells. Parathyroid cells also contain glycogen and argyrophil granules that can be demonstrated by PAS and silver stain, respectively.

In oncocytic parathyroid adenoma, the cells can be confused with Hürthle cell associated lesions of the thyroid such as Hürthle cell neoplasm, adenomatous hyperplasia with Hürthle cell changes, or chronic lymphocytic thyroiditis [6, 7] (Fig. 19.16). This is partly because oncocytic parathyroid adenoma may have follicular structures and can also have colloid-like material in the background. The presence of oncocytic cells and naked nuclei of chief cells in parathyroid cytologic specimens can mimic Hürthle cells and lymphocytes, respectively, and may lead to a misdiagnosis of lymphocytic thyroiditis [8, 9]. There are some cytomorphologic features that are helpful to differentiate between oncocytic parathyroid and Hürthle cell neoplasm. Parathyroid cells are smaller and have pale scant cytoplasm in combination with the highly eosinophilic cytoplasm. The cell borders are poorly defined. The nuclei of the parathyroid cells are usually round to oval with stippled chromatin or salt and pepper appearance and may sometimes have small nucleoli (Figs. 19.17 and 19.18). Numerous naked

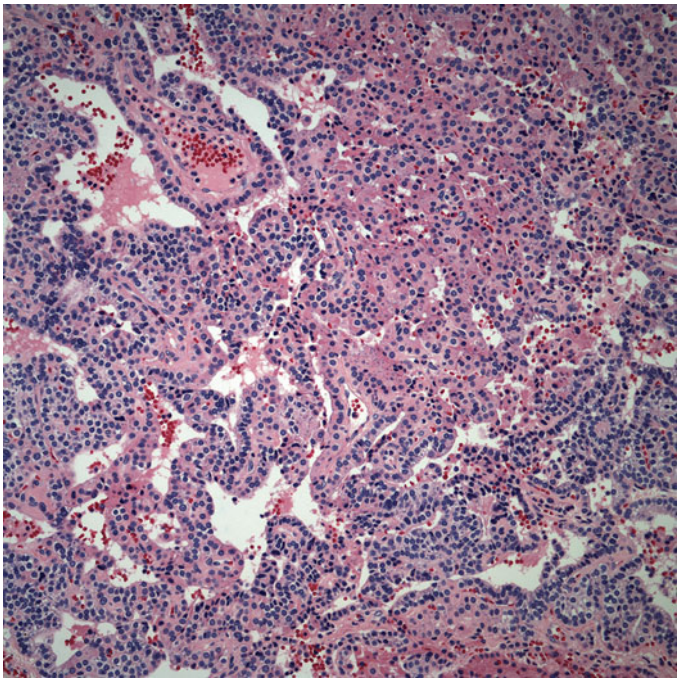

Fig. 19.16 Parathyroid adenoma with oxyphil cells (H&E stain, X200)

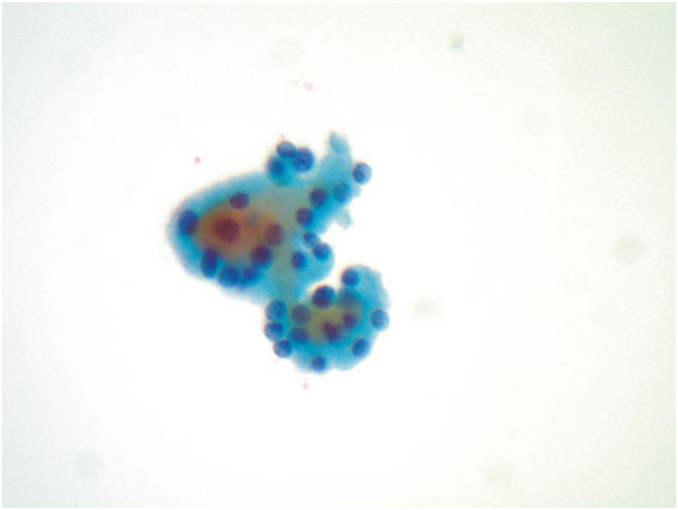

Fig. 19.17 Oncocytic parathyroid adenoma cells may mimic Hürthle cell neoplasm in the thyroid. Parathyroid cells are smaller and the cell borders are poorly defined. The nuclei are usually round to oval with stippled chromatin or salt and pepper appearance and may sometimes have small nucleoli (Papanicolaou stain, X600)

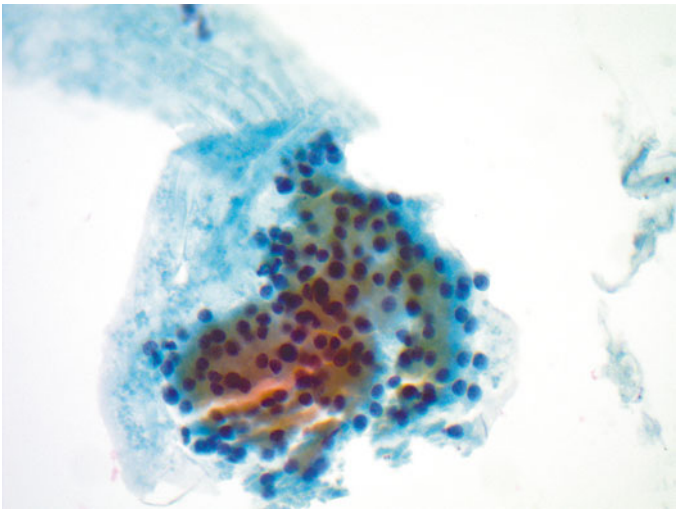

Fig. 19.18 Sheets of oncocytic cells in oncocytic parathyroid adenoma. The nuclei are smaller than thyroid follicular cell nuclei, and they are round to oval. Cytoplasm is abundant and granular (Papanicolaou stain, X400)

nuclei, approximately the size of erythrocytes, in the background of the smear favor a parathyroid lesion [6]. Hürthle cell neoplasms of the thyroid have much larger and more prominent nucleoli, and the cells tend to be more discohesive [10].

Although some studies have suggested that there are subtle differences in the cytology of parathyroid hyperplasia and adenoma [11], others have found no difference between the cytologic features [3, 12]. Cytologic features can be helpful in identifying a parathyroid origin of cells, but it is difficult to make a distinction between normal parathyroid gland and hyperplasia, adenoma, or carcinoma [1].

In addition to pathologic features, clinical features and radiologic appearance of the lesion are also helpful to differentiate between thyroid and parathyroid tissue. In parathyroid adenomas, clinical information of hyperparathyroidism and the associated features is important and will alert one to the possibility of a parathyroid lesion. A clinical history of hyperparathyroidism and/or an elevated FNA PTH level will help in guiding the cytopathologist to making the correct diagnosis. However, knowledge of the cytomorphologic features is useful in confirming the clinical impression and may be very critical to making the correct diagnosis in cases where the clinical history is not provided. Normal parathyroid glands are seldom seen during ultrasonographic examination of patients with thyroid nodules. Enlarged parathyroid glands appear as ovoid mass with homogeneously hypoechoic echogenicity in relation to the thyroid gland [6, 13]. Doppler images help to distinguish parathyroid glands from thyroid nodules. Parathyroid glands typically have a peripheral rim of vascularity and asymmetrically increased blood flow compared to the thyroid [14].

A panel of immunohistochemical studies, which include parathyroid hormone (PTH), thyroglobulin, thyroid transcription factor (TTF-1), and neuroendocrine markers, notably chromogranin, is usually employed in the diagnosis of difficult cases. Typically, parathyroid cells stain positive for PTH and chromogranin, and negative for thyroglobulin and TTF-1 while thyroid follicular cells are positive for thyroglobulin and TTF-1 and negative for PTH and chromogranin. In cases with a hypocellular cell block or when there is inability to perform immunohistochemistry on cytology slides, the diagnosis has to be made on cytologic features alone. Analyses of the PTH level of the washouts of FNA might also be helpful [15, 16]. FNA PTH levels are highly sensitive and specific in the identification of parathyroid tissue sampling on FNA [17].

In addition to thyroid follicular cells, medullary thyroid carcinoma is also included in the differential diagnosis of parathyroid cells [18]. Medullary thyroid carcinoma and parathyroid lesions share the same features of stippled nuclear chromatin, round to oval cells, loose clusters, and single cells. The concurrent presence of spindle and oval cells with a granular cytoplasm and an absence of naked nuclei favor medullary thyroid carcinoma. Immunohistochemical stains for PTH and calcitonin are helpful in differentiating between medullary carcinoma and parathyroid lesions.

References

1. Dimashkieh H, Krishnamurthy S. Ultrasound guided fine needle aspiration biopsy of parathyroid gland and lesions. Cytojournal. 2006;3:6.
2. Tseleni-Balafouta S, Gakiopoulou H, Kavantzas N, Agrogiannis G, Givalos N, Patsouris E. Parathyroid proliferations: a source of diagnostic pitfalls in FNA of thyroid. Cancer. 2007;111:130–6.

3. Odronic SI, Reynolds JP, Chute DJ. Cytologic features of parathyroid fine-needle aspiration on ThinPrep preparations. Cancer Cytopathol. 2014;122:678–84.
4. Kini U, Shariff S, Thomas JA. Ultrasonically guided fine needle aspiration of the parathyroid. A report of 2 cases. Acta Cytol. 1993;37:747–51.
5. Kini S. Thyroid cytopathology: an atlas and text. Philadelphia: Wolters Kluwer/Lippincott Williams & Wilkins; 2008.
6. Sriphrapradang C, Sornmayura P, Chanplakorn N, Trachoo O, Sae-Chew P, Aroonroch R. Fine-needle aspiration cytology of parathyroid carcinoma mimic hürthle cell thyroid neoplasm. Case Rep Endocrinol. 2014;2014:680876.
7. Paker I, Yilmazer D, Yandakci K, Arikok AT, Alper M. Intrathyroidal oncocytic parathyroid adenoma: a diagnostic pitfall on fine-needle aspiration. Diagn Cytopathol. 2010;38:833–6.
8. Bondeson L, Bondeson AG, Nissborg A, Thompson NW. Cytopathological variables in parathyroid lesions: a study based on 1,600 cases of hyperparathyroidism. Diagn Cytopathol. 1997;16:476–82.
9. Abati A, Skarulis MC, Shawker T, Solomon D. Ultrasound-guided fine-needle aspiration of parathyroid lesions: a morphological and immunocytochemical approach. Hum Pathol. 1995;26:338–43.
10. Giorgadze T, Stratton B, Baloch ZW, LiVolsi VA. Oncocytic parathyroid adenoma: problem in cytological diagnosis. Diagn Cytopathol. 2004;31:276–80.
11. Liu F, Gnepp DR, Pisharodi LR. Fine needle aspiration of parathyroid lesions. Acta Cytol. 2004;48:133–6.
12. Tseng FY, Hsiao YL, Chang TC. Ultrasound-guided fine needle aspiration cytology of parathyroid lesions. A review of 72 cases. Acta Cytol. 2002;46:1029–36.
13. Yabuta T, Tsushima Y, Masuoka H, et al. Ultrasonographic features of intrathyroidal parathyroid adenoma causing primary hyperparathyroidism. Endocr J. 2011;58:989–94.
14. Lane MJ, Desser TS, Weigel RJ, Jeffrey Jr RB. Use of color and power doppler sonography to identify feeding arteries associated with parathyroid adenomas. Am J Roentgenol. 1998;171:819–23.
15. Owens CL, Rekhtman N, Sokoll L, Ali SZ. Parathyroid hormone assay in fine-needle aspirate is useful in differentiating inadvertently sampled parathyroid tissue from thyroid lesions. Diagn Cytopathol. 2008;36:227–31.
16. Kwak JY, Kim E, Moon HJ, et al. Parathyroid incidentalomas detected on routine ultrasound-directed fine-needle aspiration biopsy in patients referred for thyroid nodules and the role of parathyroid hormone analysis in the samples. Thyroid. 2009;19:743–8.
17. Abdelghani R, Noureldine S, Abbas A, Moroz K, Kandil E. The diagnostic value of parathyroid hormone washout after fine-needle aspiration of suspicious cervical lesions in patients with hyperparathyroidism. Laryngoscope. 2013;123:1310–3.
18. Kruljac I, Pavić I, Mateša N, et al. Intrathyroid parathyroid carcinoma with intrathyroidal metastasis to the contralateral lobe: source of diagnostic and treatment pitfalls. Jpn J Clin Oncol. 2011;41:1142–6.

Evaluation of Thyroid Bed Sampling

20

Case Study

A 75-year-old patient with a history of papillary thyroid carcinoma (PTC), status post total thyroidectomy, and central lymph node dissection. Postoperatively she received radioactive iodine. She has had regular follow-up ultrasound examination of the neck region. Her baseline thyroglobulin level on levothyroxine suppression was initially normal but slowly increased over the past 2 years to a level of 4.2 ng/mL. Six years after the initial surgery, she had a thyrogen-stimulated whole body scan, which demonstrated no significant iodine avid neoplasia. However, her thyroglobulin level was 11.47 ng/mL, suggesting some residual disease. The patient had some discomfort in the right paratracheal region, but had no hoarseness or difficulty swallowing. On examination the neck was supple without any palpable masses. Ultrasound revealed a 1.2 cm nodule in the thyroid bed and FNA of the nodule showed recurrent PTC. The patient underwent reoperative right central neck dissection and right modified central neck dissection with intraoperative ultrasound. Recurrent PTC was confirmed in the soft tissue from the thyroid bed. Lymph nodes were negative for metastatic carcinoma. Her postoperative course was uneventful.

Discussion

Differentiated thyroid carcinomas are usually treated with total thyroidectomy, followed by cervical lymph node dissection when there is either evidence of tumor involving the lymph nodes at the time of initial diagnosis or a high likelihood of lymph node metastasis. After the initial surgery, radioactive iodine therapy is often given to ablate any residual thyroid tissue in cases of papillary and follicular carcinomas [1]. Up to 15–30 % of patients treated surgically have recurrent and/or persistent tumor in the postsurgical thyroid bed [2, 3]. Postsurgical surveillance for persistent and recurrent disease is a major component in the long-term management of these patients. Iodine-131 whole body scan, serial serum thyroglobulin testing,

A.J. Adeniran, D. Chhieng, *Common Diagnostic Pitfalls in Thyroid Cytopathology*, DOI 10.1007/978-3-319-31602-4_20

and measurement of stimulated thyroglobulin levels have all been used as surveillance tools for the detection of recurrent thyroid carcinoma [4]. Although thyroglobulin is a sensitive marker for the detection of recurrent and metastatic differentiated thyroid carcinoma of follicular origin, thyroglobulin levels may not be elevated in patients with recurrent or metastatic papillary and follicular carcinomas because of the following reasons: (1) The tumor may produce anomalous thyroglobulin that is not recognized by the antibody used in the detection system [5]; (2) The patient may develop antithyroglobulin antibodies [6]; (3) The tumor cells may dedifferentiate and lose the ability to produce thyroglobulin [6]; (4) Small recurrent or metastatic tumors may produce undetectable amounts of thyroglobulin [1].

Following total thyroidectomy in patients with thyroid cancer, the current standard of care is for new lesions within the thyroid bed to be evaluated by ultrasound-guided FNA to determine if the new lesion is due to either residual hyperplastic thyroid tissue or recurrent thyroid cancer [7–10]. Disease free, postoperative thyroid bed should have a uniform echogenic texture on ultrasound examination. Any hypoechoic mass is suspicious for recurrence [11]; however, a distinction between recurrent tumor and its benign mimics is not always possible with imaging techniques [12]. Although thyroid bed recurrences can occur in isolation, they are more likely to be associated with metastases to the lymph nodes in the neck, elevation of thyroglobulin or calcitonin levels, or positive radioactive iodine scan of the thyroid region [1]. The sensitivity of ultrasound-guided FNA for detecting recurrent carcinoma in the thyroid bed of sonographically indeterminate lesions after thyroidectomy is 100 % and the overall specificity is 85.7 % [1]. Based on information from the aspirate sample, decisions are made to either treat the patient with definitive therapy for recurrent cancer or manage conservatively otherwise [7, 10]. It has been shown that the likelihood of a positive FNA from the thyroid bed is directly correlated with serum thyroglobulin, multifocal disease, extrathyroidal extension, and number of positive lymph nodes or metastasis to any site while factors such as patient age, gender, and margin status at the time of initial thyroidectomy have been found to have no impact on tumor recurrence [7]. A nondiagnostic reading is an infrequent occurrence in the FNA of thyroid bed and the rate is similar to the nondiagnostic rate reported with FNAs from native thyroid nodules [13]. In these cases, the lesion most likely represents previous surgical scarring or granulation tissue [1, 14]. The FNA sampling issue also affects interpretation of thyroid bed lesions. Low specimen cellularity with scant characteristic tumor cells may prevent an accuracy interpretation [15]. The risk of a nondiagnostic FNA is inversely proportional to the size of the nodule [7]. The negative predictive value of FNA in thyroid bed evaluation following thyroidectomy is in the order of 88.4 % [7]. However, considering the fact that most patients do not have tissue follow-up following a negative FNA diagnosis, the actual value might be much lower.

Treatment of patients with recurrent thyroid carcinoma is diverse, with some recommending neck dissection as a possible treatment option [10], whereas others recommend close clinical observation based on the clinical picture of tumor size and burden [8]. Percutaneous ethanol injection is a newer procedure, which is gaining popularity as it has a very favorable risk-benefit ratio. However, the average time between thyroidectomy and tumor bed recurrence is usually long, which reiterates the indolent course of thyroid neoplasms and perhaps reinforces the need for an

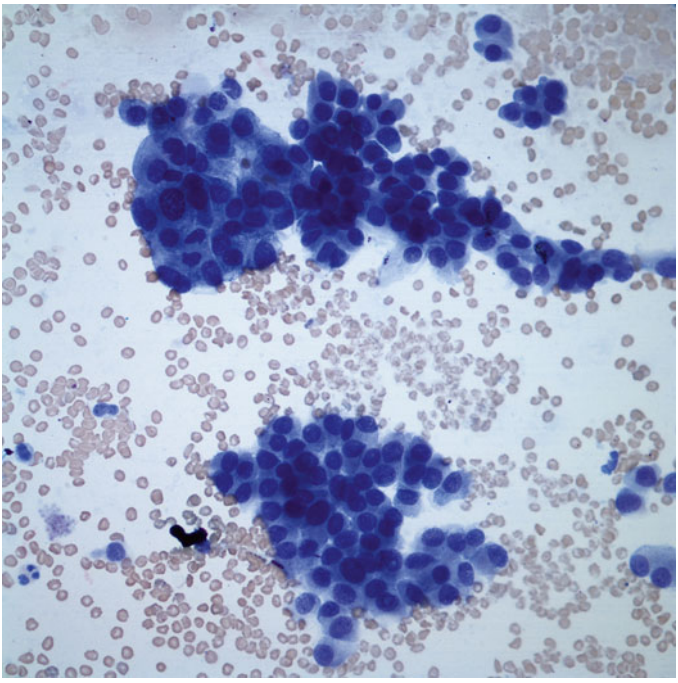

Fig. 20.1 Smear of the thyroid bed lesion fine needle aspirate from a patient with a history of papillary thyroid carcinoma shows groups of atypical follicular cells with elongated nuclei, fine chromatin, nuclear grooves, and intranuclear inclusions (Diff-Quik stain, X400)

individualized treatment, in which the risks and benefits of various options are considered and potential treatment-related comorbidities are minimized.

The cytologic smears of recurrent papillary carcinoma are usually cellular and the typical nuclear features of papillary carcinoma are frequently present (Figs. 20.1, 20.2, and 20.3). In medullary carcinoma, the cytologic features may be heterogeneous. Cells can be dispersed singly with plasmacytoid appearance and occasional binucleation of individual cells and they typically have the so-called salt and pepper chromatin appearance (Figs. 20.4 and 20.5). Tumor cells can also have spindled appearance (Fig. 20.6). Immunohistochemical staining for calcitonin and neuroendocrine markers such as chromogranin are helpful in establishing the diagnosis of recurrent medullary carcinoma (Fig. 20.7).

In recurrent follicular carcinoma, the aspirates are cellular with uniform follicular cells forming microfollicles [15]. In recurrent Hürthle cell carcinoma, the aspirates show tumor cells with granular, eosinophilic cytoplasm and a large nucleus with prominent nucleolus in single cells or loosely arranged follicular patterns. These features are usually similar to those seen in the tumor cells from the patients' prior thyroidectomy specimens [1].

Direct extension of squamous cell carcinoma of the head and neck region to the thyroid bed is common, and this diagnosis should be entertained when the thyroid bed FNA shows a malignant neoplasm with squamous features (Figs. 20.8 and 20.9).

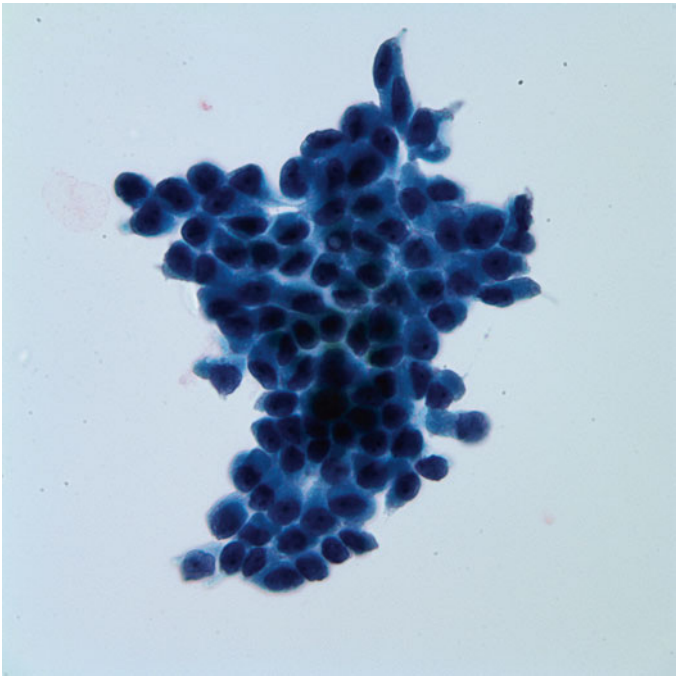

Fig. 20.2 High power image showing the typical nuclear features of papillary thyroid carcinoma (Papanicolaou stain, X1000)

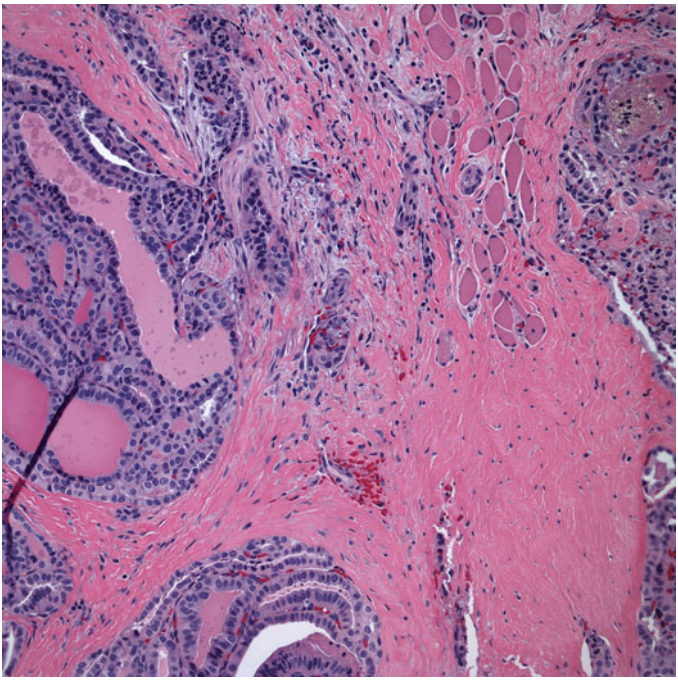

Fig. 20.3 Papillary thyroid carcinoma invading the soft tissue of the thyroid bed (H&E stain, X200)

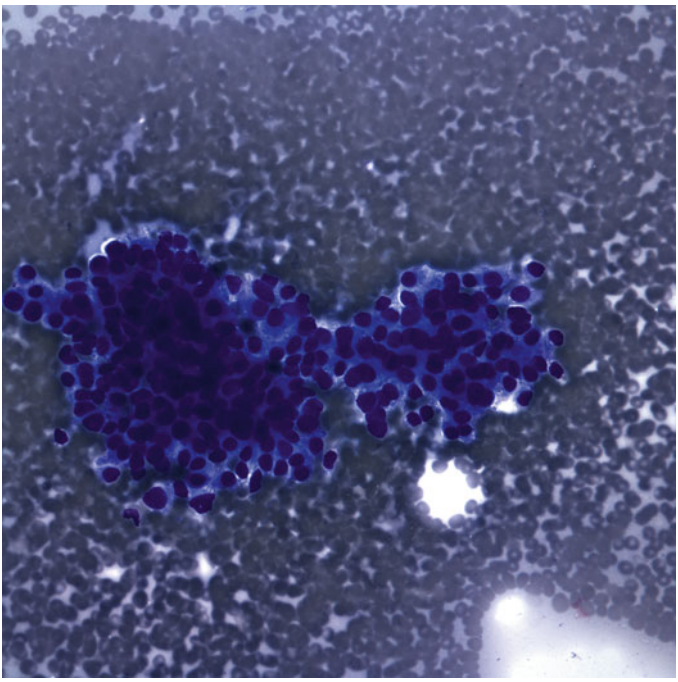

Fig. 20.4 Tumor cells from recurrent medullary carcinoma (Diff-Quik stain, X400)

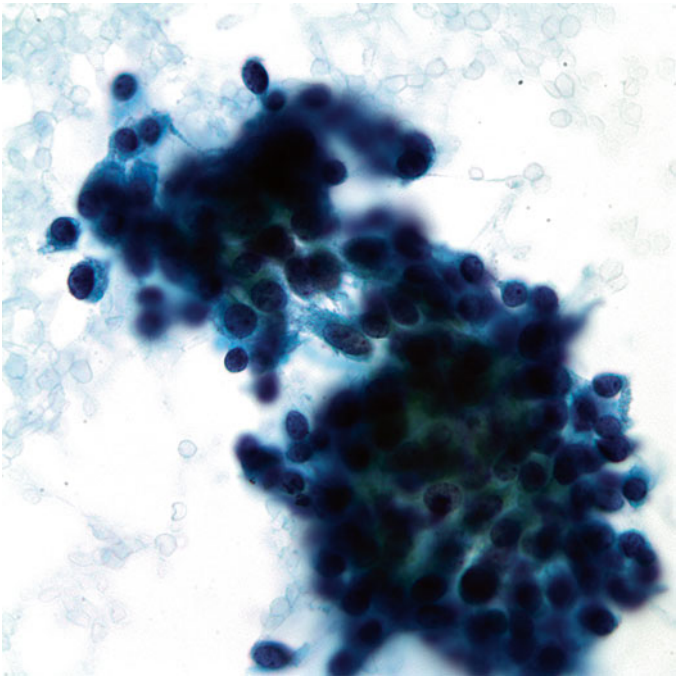

Fig. 20.5 Individual cells show typical neuroendocrine nuclear features (Papanicolaou stain, X1000)

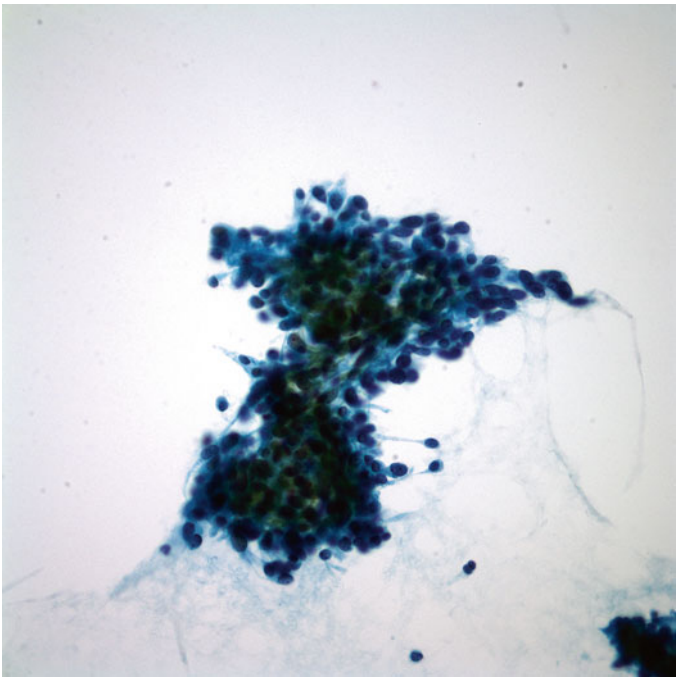

Fig. 20.6 Spindle cell features in medullary carcinoma (Papanicolaou stain, X400)

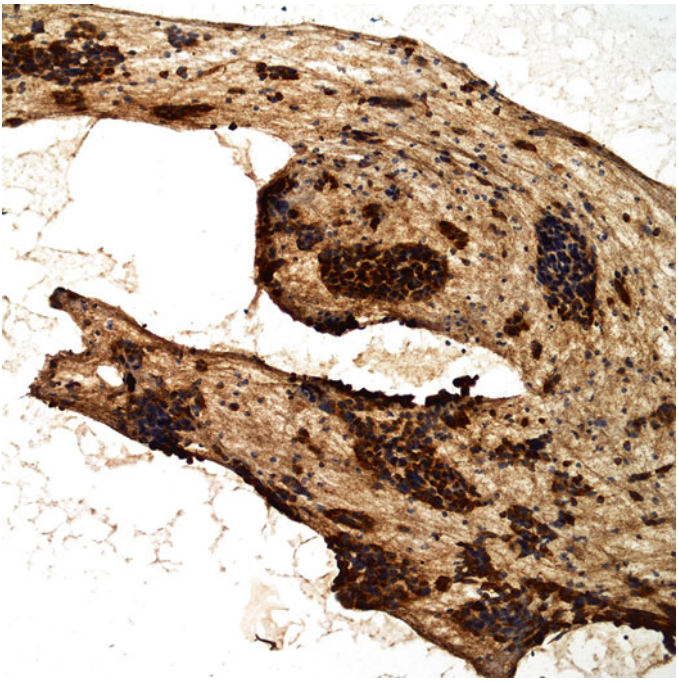

Fig. 20.7 Calcitonin stain performed on a de-stained Papanicolaou-stained slide showing a positive staining pattern

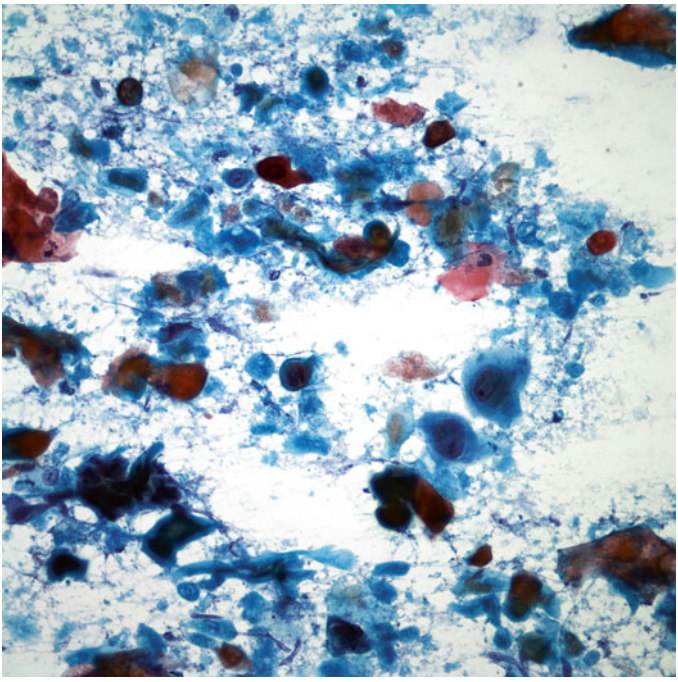

Fig. 20.8 Direct extension of squamous cell carcinoma into the thyroid bed. Highly atypical squamous cells in a necrotic background (Papanicolaou stain, X400)

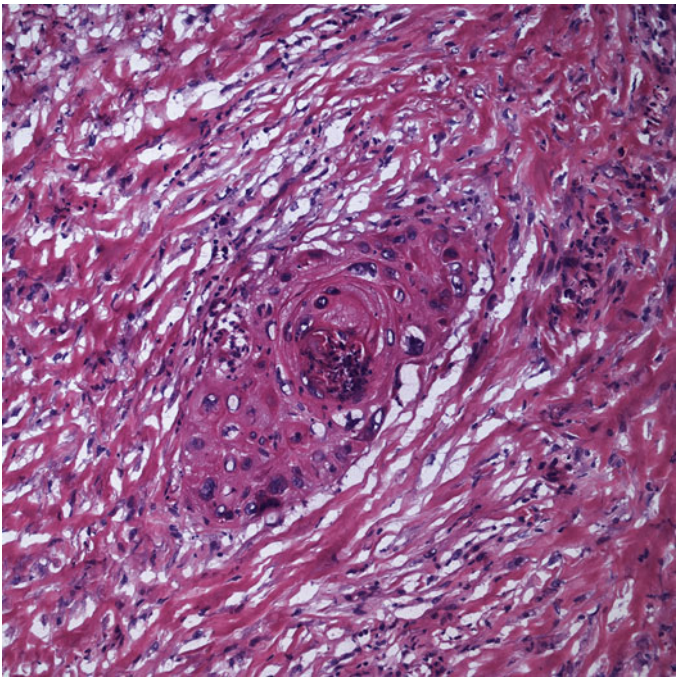

Fig. 20.9 Infiltrating squamous cell carcinoma in the soft tissue of the thyroid bed (H&E stain, X200)

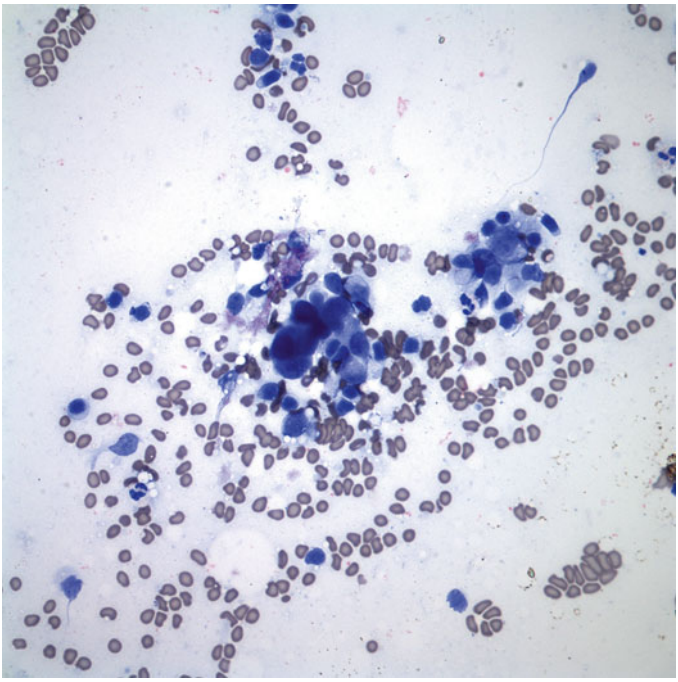

Fig. 20.10 Metastatic adenocarcinoma from the upper gastrointestinal tract to the thyroid bed. The malignant cells are glandular in appearance (Diff-Quik stain, X400)

Metastatic malignant neoplasms from distant sites to the thyroid bed should also be considered, and immunohistochemical stains are helpful to determine the site of origin (Figs. 20.10, 20.11 and 20.12).

It should be noted that not all masses in the thyroid bed are neoplastic. Benign entities may include hyperplasia of residual normal thyroid, normal parathyroid gland, benign lymph nodes, and benign reparative changes such as fibrosis and suture granulomas. Smears of residual hyperplastic thyroid tissue usually show thyroid follicular cells in a micro- and macrofollicular pattern with varying amounts of colloid in the background without the nuclear features of papillary carcinoma (Figs. 20.13, 20.14, and 20.15). The presence of Hürthle cells and lymphocytes in the thyroid bed can be problematic as it is often difficult to determine if this is Hashimoto's thyroiditis or tumor within a lymph node in the central neck compartment. In such scenarios, history of background Hashimoto's thyroiditis in the prior thyroidectomy specimen is helpful. Also, a comparison should be made between the Hürthle cells and the prior tumor cells. Another diagnostic pitfall is interpretation of therapy-induced atypical cellular changes as a neoplastic process. Benign enlarged lymph nodes can also be seen in the thyroid bed and this is characterized by a mixed population of lymphocytes (Figs. 20.16, 20.17, and 20.18).

Aspiration of benign parathyroid tissue in the thyroid bed may yield highly cellular smears with cells arranged in a microfollicular pattern that may be interpreted as recurrent follicular carcinoma [1, 16]. The cells of the parathyroid gland are usually smaller compared to follicular epithelial cells (Figs. 20.19 and 20.20).

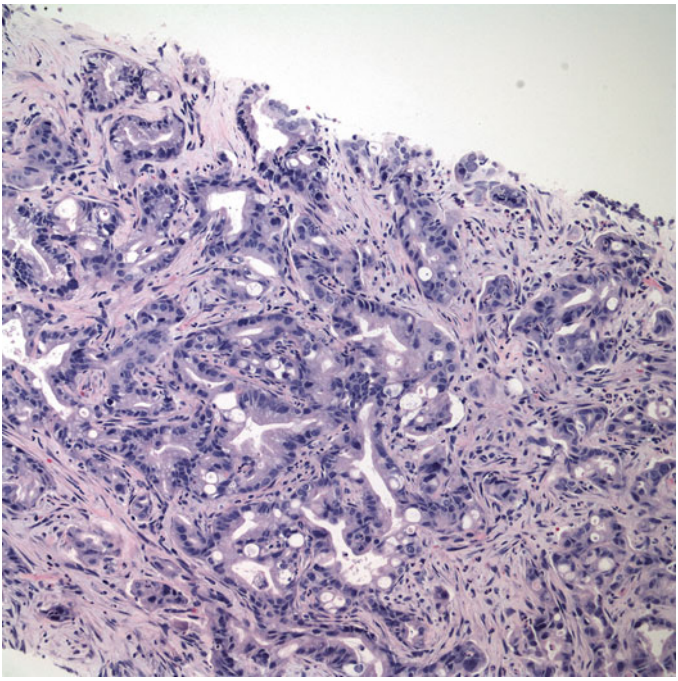

Fig. 20.11 Metastatic intestinal-type adenocarcinoma in the soft tissue of the thyroid bed (H&E stain, X200)

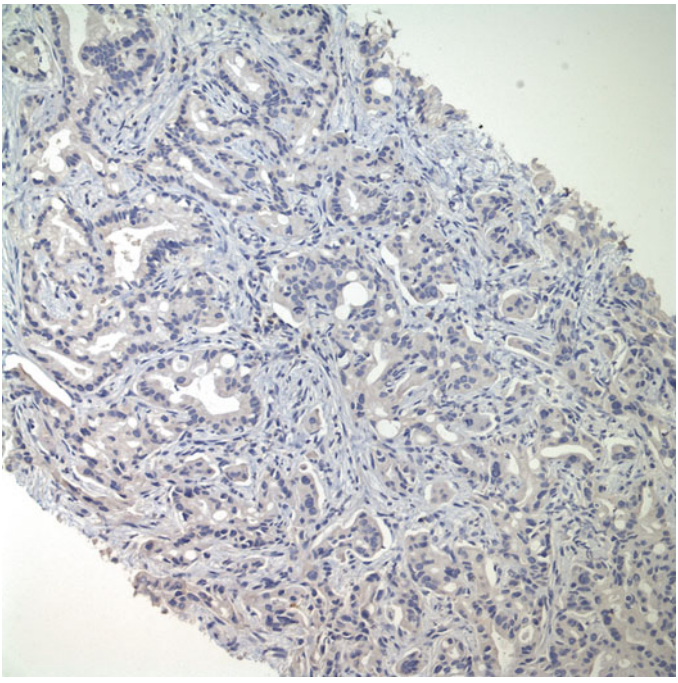

Fig. 20.12 TTF-1 stain is negative in the cells of metastatic adenocarcinoma, confirming that the tumor is not of thyroid origin

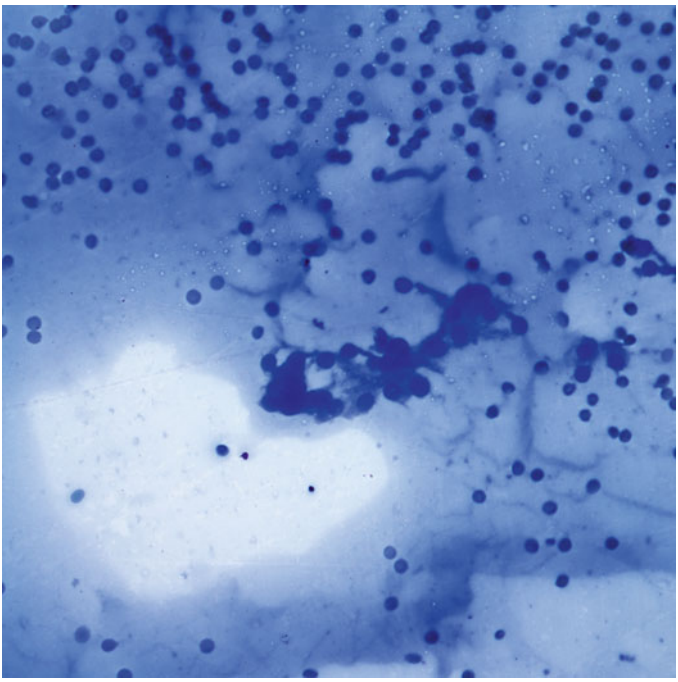

Fig. 20.13 Residual hyperplastic thyroid tissue in the thyroid bed showing thyroid follicular cells in a background of abundant colloid (Papanicolaou stain, X400)

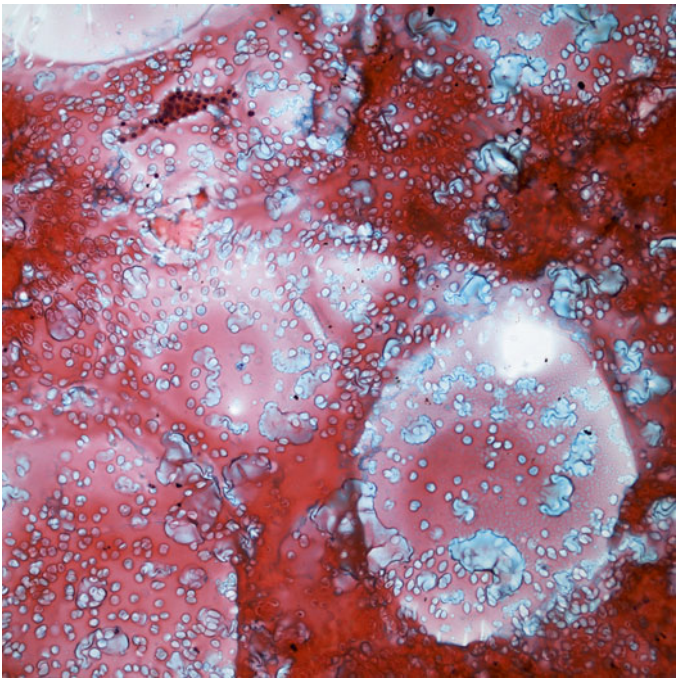

Fig. 20.14 Residual hyperplastic thyroid tissue showing rare group of Hürthle cells in a background of abundant colloid (Papanicolaou stain, X200)

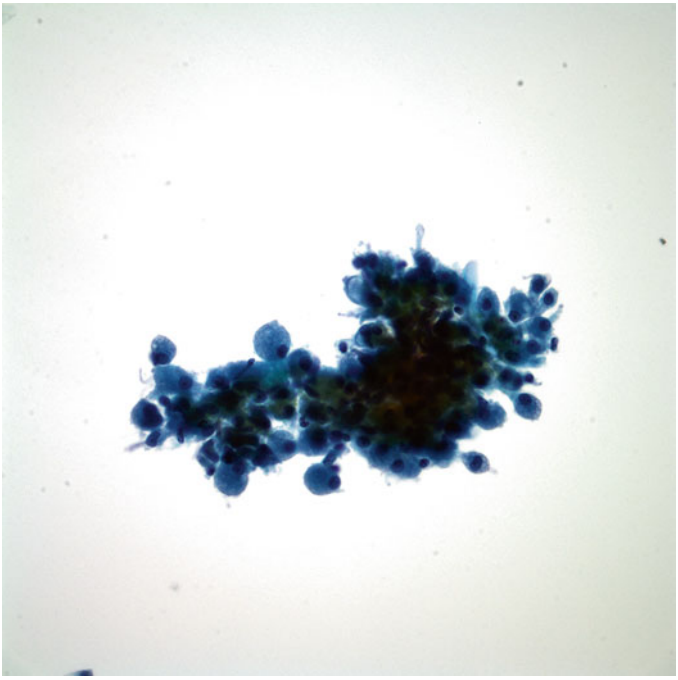

Fig. 20.15 Cystic degeneration with abundant macrophages is a common finding in residual hyperplastic thyroid tissue (Papanicolaou stain, X400)

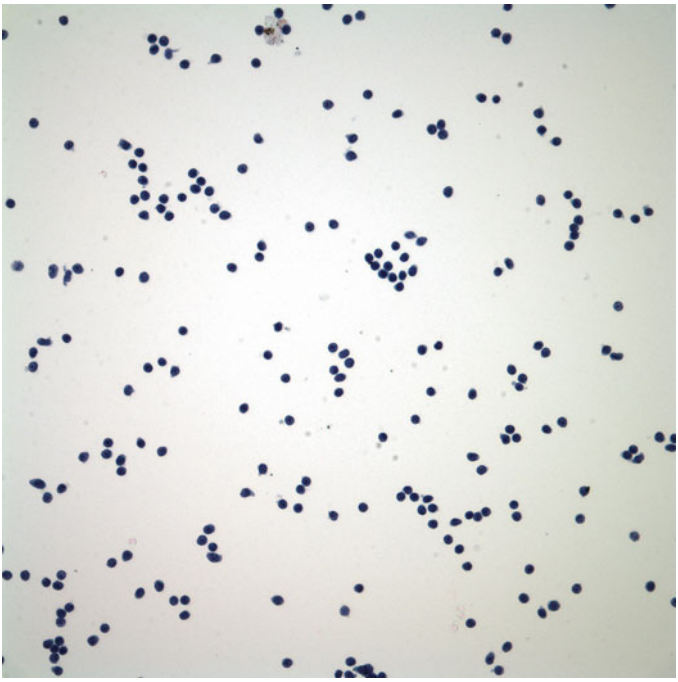

Fig. 20.16 Lymph node sampling in the thyroid bed showing a polymorphous population of small lymphocytes (Papanicolaou stain, X400)

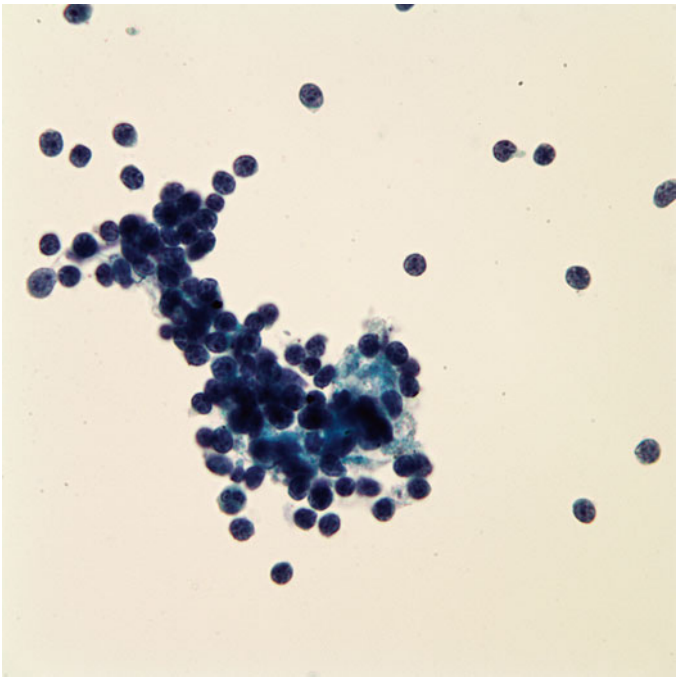

Fig. 20.17 Mixed population of lymphocytes consistent with reactive lymph node sampling (Papanicolaou stain, X1000)

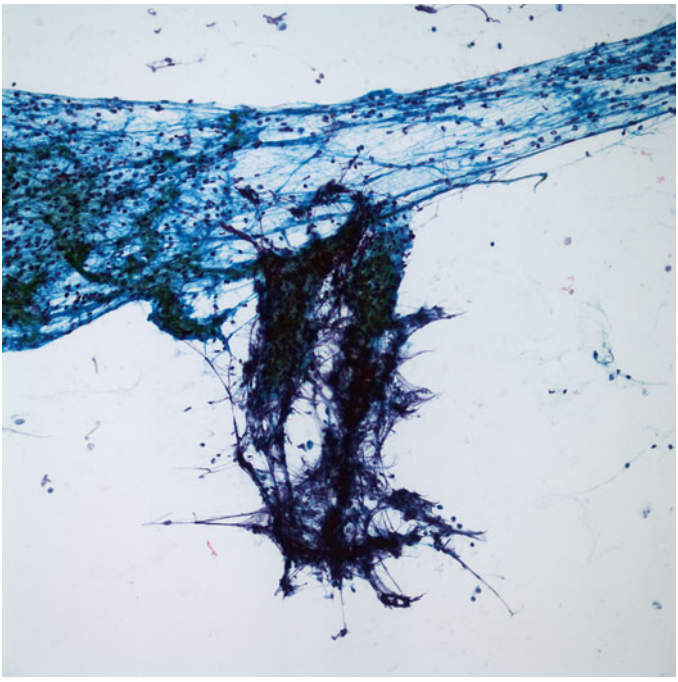

Fig. 20.18 The presence of lymphoid tangles may be the only indication of lymph node sampling (Papanicolaou stain, X200)

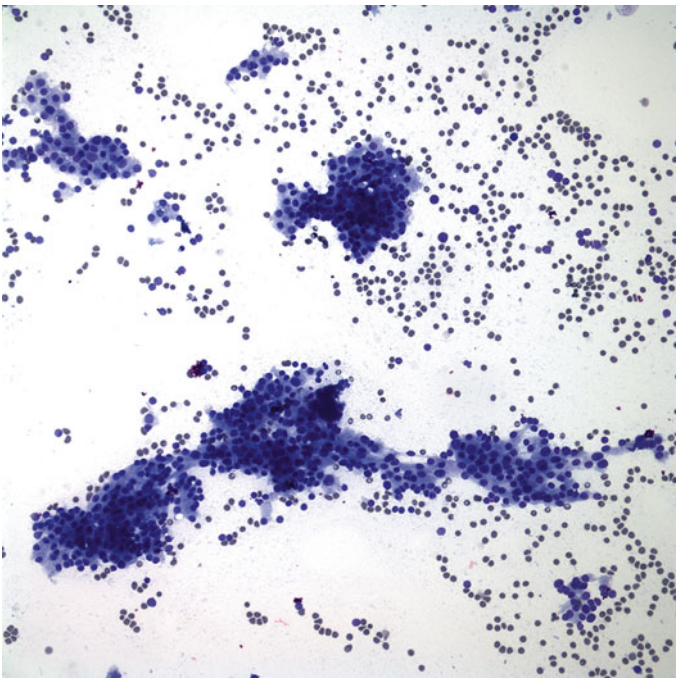

Fig. 20.19 Hypercellular parathyroid tissue in the thyroid bed (Papanicolaou stain, X200)

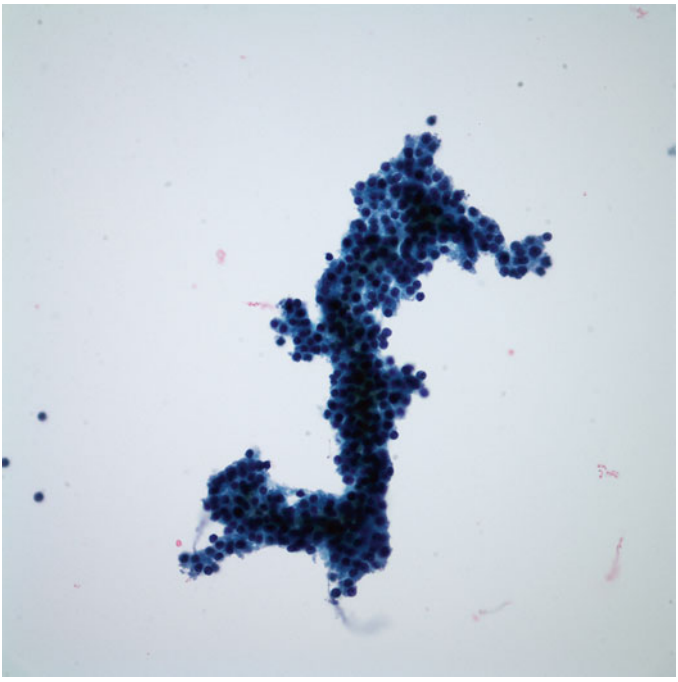

Fig. 20.20 Parathyroid gland cells are arranged as an aggregate of microfollicles. The cells are smaller than the normal thyroid follicular cells (Papanicolaou stain, X400)

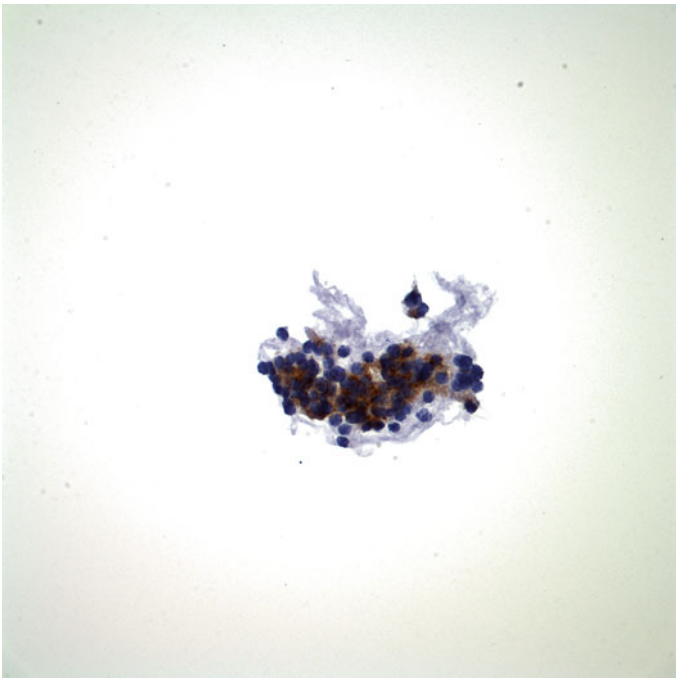

Fig. 20.21 Cells are positive for parathyroid hormone stain

In difficult cases, additional ThinPrep material should be obtained for thyroglobulin and parathyroid hormone (PTH) stains, as staining for PTH helps to confirm the diagnosis of normal parathyroid tissue (Fig. 20.21) [16]. Chemical analysis of the needle rinse solution for PTH can also be helpful in this instance [17].

References

1. Krishnamurthy S, Bedi DG, Caraway NP. Ultrasound-guided fine-needle aspiration biopsy of the thyroid bed. Cancer. 2001;93:199–205.
2. Hay ID, Thompson GB, Grant CS, Bergstralh EJ, Dvorak CE, Gorman CA, Maurer MS, McIver B, Mullan BP, Oberg AL, Powell CC, van Heerden JA, Goellner JR. Papillary thyroid carcinoma managed at the Mayo Clinic during six decades (1940-1999): temporal trends in initial therapy and long-term outcome in 2444 consecutively treated patients. World J Surg. 2002;26:879–85.
3. Mazzaferri EL, Jhiang SM. Long-term impact of initial surgical and medical therapy on papillary and follicular thyroid cancer. Am J Med. 1994;97:418–28.
4. Johnson NA, Tublin ME. Postoperative surveillance of differentiated thyroid carcinoma: rationale, techniques, and controversies. Radiology. 2008;249:429–44.
5. Moser E, Braun S, Büell U, Kirsch CM, Tosch U, Wendt T. Thyroglobulin levels to follow-up patients with treated differentiated thyroid carcinoma. Cancer Detect Prev. 1984;7:79–86.
6. Müller-Gärtner HW, Schneider C. Clinical evaluation of tumor characteristics predisposing serum thyroglobulin to be undetectable in patients with differentiated thyroid cancer. Cancer. 1988;61:976–81.

7. Adhikari LJ, Sciallis AP, Reynolds J, Jenkins S, Smith C, Stan MN, Nassar A. Clinicopathologic predictors of thyroid bed recurrence of differentiated thyroid cancer using ultrasound-guided fine-needle aspiration biopsies. Thyroid. 2013;23:982–8.
8. Rondeau G, Fish S, Hann LE, Fagin JA, Tuttle RM. Ultrasonographically detected small thyroid bed nodules identified after total thyroidectomy for differentiated thyroid cancer seldom show clinically significant structural progression. Thyroid. 2011;21:845–53.
9. Antonelli A, Miccoli P, Ferdeghini M, Di Coscio G, Alberti B, Iacconi P, Baldi V, Fallahi P, Baschieri L. Role of neck ultrasonography in the follow-up of patients operated on for thyroid cancer. Thyroid. 1995;5:25–8.
10. Farrag TY, Agrawal N, Sheth S, Bettegowda C, Ewertz M, Kim M, Tufano RP. Algorithm for safe and effective reoperative thyroid bed surgery for recurrent/persistent papillary thyroid carcinoma. Head Neck. 2007;29:1069–74.
11. Sutton RT, Reading CC, Charboneau JW, James EM, Grant CS, Hay ID. US-guided biopsy of neck masses in postoperative management of patients with thyroid cancer. Radiology. 1988;168:769–72.
12. Shin JH, Han BK, Ko EY, Kang SS. Sonographic findings in the surgical bed after thyroidectomy: comparison of recurrent tumors and nonrecurrent lesions. J Ultrasound Med. 2007;26:1359–66.
13. Renshaw AA. Non-diagnostic rates for thyroid fine needle aspiration are negatively correlated with positive for malignancy rates. Acta Cytol. 2011;55:38–41.
14. Alatli C, Gürkan B, Koçak H, Ozveren A, Dölek S. Fine needle aspiration biopsy (FNAB) in fibrous and non-fibrous soft oral tissue lesions. J Oral Sci. 1999;41:41–5.
15. Zhao L, Gong Y, Wang J, Dawlett M, Huo L, Caraway NP, Guo M. Ultrasound-guided fine-needle aspiration biopsy of thyroid bed lesions from patients with thyroidectomy for thyroid carcinomas. Cancer Cytopathol. 2013;121:101–7.
16. Bishop JA, Owens CL, Shum CH, Ali SZ. Thyroid bed fine-needle aspiration: experience at a large tertiary care center. Am J Clin Pathol. 2010;134:335–9.
17. Owens CL, Rekhtman N, Sokoll L, Ali SZ. Parathyroid hormone assay in fine-needle aspirate is useful in differentiating inadvertently sampled parathyroid tissue from thyroid lesions. Diagn Cytopathol. 2008;36:227–31.

Index

A.J. Adeniran, D. Chhieng, *Common Diagnostic Pitfalls in Thyroid Cytopathology*, DOI 10.1007/978-3-319-31602-4